Aus der Klinik für Radiologie und Nuklearmedizin
der Medizinischen Fakultät
der Otto-von-Guericke-Universität Magdeburg

Interventionell onkologische Therapie mit der interstitiellen 192Iridium HDR- Brachytherapie von Malignomen des Oberbauches. Was wir wissen: Dosiseffekte und Sicherheit, Tumorkontrolle und Prognose, Variabilität und klinische Relevanz.

Habilitationsschrift

zur Erlangung des akademischen Grades

Dr. med. habil.
(doctor medicinae habilitatus)
an der Medizinischen Fakultät
der Otto-von-Guericke-Universität Magdeburg

Vorgelegt von Dr. med. Konrad Mohnike
aus Berlin

Magdeburg 2020

INHALT

1 Vorwort

Gegenstand dieser kumulativen Habilitationsschrift ist der Inhalt der nachfolgend aufgelisteten 29 Publikationen, zu denen 6 Erstautorenschaften, darunter auch eine contributed equally zählen. Damit wird die nach der Habilitationsordnung gegebene Möglichkeit „zur Vorlage publizierter Forschungsergebnisse, die in ihrer Gesamtheit eine einer Habilitationsschrift gleichwertige wissenschaftliche Leistung darstellen“ genutzt. Die empfohlene Anzahl von 10 Publikationen wird aufgrund des konsistenten thematischen Zusammenhangs der genannten Arbeiten überschritten. Die Publikationen wurden nach der Reihenfolge ihre Erwähnung im Text fortlaufend nummeriert.

Diese kumulative Habilitationsschrift umfasst auch Publikationen, die vor der Dissertation entstanden sind. Letztgenannte wurde über ein thematisch anderes Forschungsgebiet angefertigt (Titel: „Mikrostruktur von malignen und benignen Lymphknotenprozessen im sonografischen B-Bild. Eine direkte Korrelation mit der Histomorphologie, vorgelegt 2009“). Die Habilitationsschrift stellt somit den zweiten Forschungsschwerpunkt des Vorlegenden in seiner Gesamtheit dar.

Die vollständige Publikationsliste des Habilitanden wurde diesem Habilitationsantrag in einem separaten Dokument beigefügt. Sie umfasst 50 Publikationen, darunter 8 Erst- sowie 3 Letzt-Autorenschaften.

2 Publikationen dieser kumulativen Habilitationsschrift

(1) Lüdemann L, Wybranski C, Seidensticker M, **Mohnike K**, Kropf S, Wust P, Ricke J. In vivo assessment of catheter positioning accuracy and prolonged irradiation time on liver tolerance dose after single-fraction 192Ir high-dose-rate brachytherapy. Radiat Oncol. 2011 Sep 5;6:107. doi: 10.1186/1748-717X-6-107.

(2) Ricke J, **Mohnike K**, Pech M, Seidensticker M, Rühl R, Wieners G, Gaffke G, Kropf S, Felix R, Wust P. Local response and impact on survival after local ablation of liver metastases from colorectal carcinoma by computed tomography-guided high-dose-rate brachytherapy. Int J Radiat Oncol Biol Phys. 2010 Oct 1;78(2):479-85. doi: 10.1016/j.ijrobp.2009.09.026. Epub 2010 Mar 19.

(3) **Mohnike K**, Wieners G, Schwartz F, Seidensticker M, Pech M, Ruehl R, Wust P, Lopez-Hänninen E, Gademann G, Peters N, Berg T, Malfertheiner P, Ricke J. Computed tomography-guided high-dose-rate brachytherapy in hepatocellular carcinoma: safety, efficacy, and effect on survival. Int J Radiat Oncol Biol Phys. 2010 Sep 1;78(1):172-9. doi: 10.1016/j.ijrobp.2009.07.1700. Epub 2010 Jan 7.

(4) Wieners G*, **Mohnike K***, Peters N, Bischoff J, Kleine-Tebbe A, Seidensticker R, Seidensticker M, Gademann G, Wust P, Pech M, Ricke J. Treatment of hepatic metastases of breast cancer with CT-guided interstitial brachytherapy - a phase II-study. Radiother Oncol. 2011 Aug;100(2):314-9. doi: 10.1016/j.radonc.2011.03.005. Epub 2011 Apr 16.
*** contributed equally to this work**

(5) Omari J, Drewes R, Matthias M, **Mohnike K**, Seidensticker M, Seidensticker R, Streitparth T, Ricke J, Powerski M, Pech M. Treatment of metastatic, imatinib refractory, gastrointestinal stroma tumor with image-guided high-dose-rate interstitial brachytherapy. Brachytherapy. 2019 Jan - Feb;18(1):63-70. doi: 10.1016/j.brachy.2018.09.006. Epub 2018 Oct 29.

(6) Bretschneider T, **Mohnike K**, Hass P, Seidensticker R, Göppner D, Dudeck O, Streitparth F, Ricke J. Efficacy and safety of image-guided interstitial single fraction high-dose-rate brachytherapy in the management of metastatic malignant melanoma. J Contemp Brachytherapy. 2015 Apr;7(2):154-60.

(7) Seidensticker R, Seidensticker M, Doegen K, **Mohnike K**, Schütte K, Stübs P, Kettner E, Pech M, Amthauer H, Ricke J. Extensive Use of Interventional Therapies Improves Survival in Unresectable or Recurrent Intrahepatic Cholangiocarcinoma. Gastroenterol Res Pract. 2016;2016:8732521. doi: 10.1155/2016/8732521. Epub 2016 Feb 4.

(8) Seidensticker M, Wust P, Rühl R, **Mohnike K**, Pech M, Wieners G, Gademann G, Ricke J. Safety margin in irradiation of colorectal liver metastases: assessment of the control dose of micrometastases. Radiat Oncol. 2010 Mar 24;5:24. doi: 10.1186/1748-717X-5-24. PubMed PMID: 20334657;

(9) Pech M, Ricke J, Seidensticker M, Staskiewicz G, Wieners G, **Mohnike K**, Ruhl R, Steinberg J, Wust P, Seidensticker P. Assessment of the tolerance dose of the hepatic reticulo-endothelial system (RES) after single fraction HDR-irradiation: an in-vivo study employing SSPIO. Int J Radiat Biol. 2008 Oct;84(10):830-7.

(10) Ricke J, Seidensticker M, Lüdemann L, Pech M, Wieners G, Hengst S, **Mohnike K**, Cho CH, Lopez Hänninen E, Al-Abadi H, Felix R, Wust P. In vivo assessment of the tolerance dose of small liver volumes after single-fraction HDR irradiation. Int J Radiat Oncol Biol Phys. 2005 Jul 1;62(3):776-84.

(11) Seidensticker M, Seidensticker R, **Mohnike K**, Wybranski C, Kalinski T, Luess S, Pech M, Wust P, Ricke J. Quantitative in vivo assessment of radiation injury of the liver using Gd-EOB-DTPA enhanced MRI: tolerance dose of small liver volumes. Radiat Oncol. 2011 Apr 17;6:40. doi: 10.1186/1748-717X-6-40.

(12) Wybranski C, Seidensticker M, **Mohnike K**, Kropf S, Wust P, Ricke J, Lüdemann L. In vivo assessment of dose volume and dose gradient effects on the tolerance dose of small liver volumes after single-fraction high-dose-rate 192Ir irradiation. Radiat Res. 2009 Nov;172(5):598-606.

(13) Seidensticker M, Burak M, Kalinski T, Garlipp B, Koelble K, Wust P, Antweiler K, Seidensticker R, **Mohnike K**, Pech M, Ricke J. Radiation-induced liver damage: correlation of histopathology with hepatobiliary magnetic resonance imaging, a feasibility study. Cardiovasc Intervent Radiol. 2015 Feb;38(1):213-21.

(14) Rühl R, Lüdemann L, Czarnecka A, Streitparth F, Seidensticker M, **Mohnike K**, Pech M, Wust P, Ricke J. Radiobiological restrictions and tolerance doses of repeated single-fraction hdr-irradiation of intersecting small liver volumes for recurrent hepatic metastases. Radiat Oncol. 2010 May 27;5:44.

(15) Rühl R, Seidensticker M, Peters N, **Mohnike K**, Bornschein J, Schütte K, Amthauer H, Malfertheiner P, Pech M, Ricke J. Hepatocellular carcinoma and liver cirrhosis: assessment of the liver function after Yttrium-90 radioembolization with resin microspheres or after CT-guided high-dose-rate brachytherapy. Dig Dis. 2009;27(2):189-99. doi: 10.1159/000218352. Epub 2009 Jun 22.

(16) Seidensticker M, Seidensticker R, Damm R, **Mohnike K**, Pech M, Sangro B, Hass P, Wust P, Kropf S, Gademann G, Ricke J. Prospective randomized trial of enoxaparin, pentoxifylline and ursodeoxycholic acid for prevention of radiation-induced liver toxicity. PLoS One. 2014 Nov 13;9(11):e112731. doi: 10.1371/journal.pone.0112731. eCollection 2014.

(17) Powerski M, Penzlin S, Hass P, Seidensticker R, **Mohnike K**, Damm R, Steffen I, Pech M, Gademann G, Ricke J, Seidensticker M. Biliary duct stenosis after image-guided high-dose-rate interstitial brachytherapy of central and hilar liver tumors : A systematic analysis of 102 cases. Strahlenther Onkol. 2019 Mar;195(3):265-273.

(18) **Mohnike K**, Wolf S, Damm R, Seidensticker M, Seidensticker R, Fischbach F, Peters N, Hass P, Gademann G, Pech M, Ricke J. Radioablation of liver malignancies with interstitial high-dose-rate brachytherapy : Complications and risk factors. Strahlenther Onkol. 2016 May;192(5):288-96.

(19) Hass P, Steffen IG, Powerski M, **Mohnike K**, Seidensticker M, Meyer F, Brunner T, Damm R, Willich C, Walke M, Karagiannis E, Omari J, Ricke J. First report on extended distance between tumor lesion and adjacent organs at risk using interventionally applied balloon catheters: a simple procedure to optimize clinical target volume covering effective isodose in interstitial high-dose-rate brachytherapy of liver malignomas. J Contemp Brachytherapy. 2019 Apr;11(2):152-161.

(20) Damm R, Streitparth T, Hass P, Seidensticker M, Heinze C, Powerski M, Wendler JJ, Liehr UB, **Mohnike K**, Pech M, Ricke J. Prospective evaluation of CT-guided HDR brachytherapy as a local ablative treatment for renal masses: a single-arm pilot trial. Strahlenther Onkol. 2019 Jul 25.

(21) Omari J, Heinze C, Wilck A, Hass P, Seidensticker M, Seidensticker R, **Mohnike K**, Ricke J, Pech M, Powerski M. Efficacy and safety of CT-guided high-dose-rate interstitial brachytherapy in primary and secondary malignancies of the pancreas. Eur J Radiol. 2019 Mar;112:22-27. doi: 10.1016/j.ejrad.2018.12.020. Epub 2018 Dec 28.

(22) **Mohnike K**, Sauerland H, Seidensticker M, Hass P, Kropf S, Seidensticker R, Friebe B, Fischbach F, Fischbach K, Powerski M, Pech M, Grosser OS, Kettner E, Ricke J. Haemorrhagic Complications and Symptomatic Venous Thromboembolism in Interventional Tumour Ablations: The Impact of Peri-interventional Thrombosis Prophylaxis. Cardiovasc Intervent Radiol. 2016 Dec;39(12):1716-1721.

(23) Damm R, Zörkler I, Rogits B, Hass P, Omari J, Powerski M, Kropf S, **Mohnike K**, Pech M, Ricke J, Seidensticker M. Needle track seeding in hepatocellular carcinoma after local ablation by high-dose-rate brachytherapy: a retrospective study of 588 catheter placements. J Contemp Brachytherapy. 2018 Dec;10(6):516-521. doi: 10.5114/jcb.2018.80626. Epub 2018 Dec 28.

(24) Seidensticker M, Garlipp B, Scholz S, **Mohnike K**, Popp F, Steffen I, Seidensticker R, Stübs P, Pech M, PowerskI M, Hass P, Costa SD, Amthauer H, Bruns C, Ricke J. Locally ablative treatment of breast cancer liver metastases: identification of factors influencing survival (the Mammary Cancer Microtherapy and Interventional Approaches (MAMMA MIA) study). BMC Cancer. 2015 Jul 14;15:517.

(25) Seidensticker R, Damm R, Enge J, Seidensticker M, **Mohnike K**, Pech M, Hass P, Amthauer H, Ricke J. Local ablation or radioembolization of colorectal cancer metastases: comorbidities or older age do not affect overall survival. BMC Cancer. 2018 Sep 10;18(1):882.

(26) **Mohnike K**, Steffen IG, Seidensticker M, Hass P, Damm R, Peters N, Seidensticker R, Schütte K, Arend J, Bornschein J, Streitparth T, Wybranski C, Wieners G, Stübs P, Malfertheiner P, Pech M, Ricke J. Radioablation by Image-Guided (HDR) Brachytherapy and Transarterial Chemoembolization in Hepatocellular Carcinoma: A Randomized Phase II Trial. Cardiovasc Intervent Radiol. 2019 Feb;42(2):239-249.

(27): Pech M, Wieners G, Kryza R, Dudeck O, Seidensticker M, **Mohnike K**, Redlich U, Rühl R, Wust P, Gademann G, Ricke J. CT-guided brachytherapy (CTGB) versus interstitial laser ablation (ILT) of colorectal liver metastases: an intraindividual matched-pair analysis. Strahlenther Onkol. 2008 Jun;184(6):302-6.

(28) Hass P, **Mohnike K**, Kropf S, Brunner TB, Walke M, Albers D, Petersen C, Damm R, Walter F, Ricke J, Powerski M, Corradini S. Comparative analysis between interstitial brachytherapy and stereotactic body irradiation for local ablation in liver malignancies. Brachytherapy. 2019 Sep 12. pii: S1538-4721(19)30461-1.

(29): **Mohnike K**, Neumann K, Hass P, Seidensticker M, Seidensticker R, Pech M, Klose S, Streitparth T, Garlipp B, Benckert C, Wendler JJ, Liehr UB, Schostak M, Göppner D, Gademann G, Ricke J. Radioablation of adrenal gland malignomas with interstitial high-dose-rate brachytherapy : Efficacy and outcome. Strahlenther Onkol. 2017 Aug;193(8):612-619.

3 Einleitung

3.1 Krebs: Inzidenz und Mortalität in Europa und weltweit

Krebs ist weltweit die zweithäufigste Todesursache mit in den vergangenen 100 Jahren drastisch zunehmender Inzidenz und Mortalität[1]. Global stieg die Anzahl der Krebserkrankungen zwischen 2005 und 2015 um 33%, was sowohl mit dem Anwachsen der Weltbevölkerung als auch mit einer gestiegenen Lebenserwartung einhergeht[2]. Die krankheitsspezifische Mortalitätsrate ist in den letzten 20 Jahren hingegen zurückgegangen, was zuvorderst auf die therapeutischen Fortschritte zurückzuführen ist. Dabei ist es keineswegs abwegig anzunehmen, dass auch die Evolution der lokalen Therapieverfahren hieran ihren Anteil hat[3]. Dessen ungeachtet stellen Krebserkrankungen aufgrund ihrer Häufigkeit ein immenses medizinisches und gesundheitspolitisches Problem dar und sind damit auch eine große Herausforderung für die Gesundheitssysteme.
Bemerkenswerterweise wurden für Europa, das einen Anteil von 9% an der Weltbevölkerung hat, immerhin 25% der globalen Krebserkrankungen erfasst. Im Jahr 2018 traten 3,91 Millionen neue Krebsfälle auf und es starben geschätzt 1,93 Millionen Menschen an den Folgen von Krebserkrankungen. Die häufigsten Entitäten waren hierbei Brustkrebs (523.000 Fälle), das kolorektale Karzinom (ca. 500.000 Fälle), Lungenkrebs (ca. 470.000 Fälle) und Pankreaskarzinome (ca. 450.000 Fälle). Bei den krankheitsspezifischen Todesfällen lag das Lungenkarzinom an erster Stelle (ca. 388.000Todesfälle), gefolgt von kolorektalen Karzinomen (ca. 243.000), Brustkrebs (ca. 138.000) und Pankreaskarzinomen (ca. 128.000)[4].

3.2 Evolution der medikamentösen Tumortherapie und des Studiendesigns

Die aktuellen Fortschritte in der medikamentösen Tumortherapie haben auf Grund ihrer teils beeindruckenden Wirksamkeit den Stellenwert der systemischen Behandlung einer Reihe von Tumorentitäten im metastasierten Stadium noch einmal erhöht[5]. Der jüngste Quantensprung war die Einführung immunmodulatorischer Therapeutika[6]. Der inflationäre Aufwuchs von neuen Therapieregimen bei einer Vielzahl von Entitäten macht es bei Studien zu lokalen und lokoregionären Therapiekonzepten zunehmend schwierig, vergleichende Überlegungen mit der systemischen Therapie anzustellen. Zudem ist es anspruchsvoll, entsprechende kombinativ-komparative Studiendesigns aufzulegen, die auch nach dem Abschluss der jeweiligen Studie noch von klinischer Relevanz sind. Auch ist der Erfolg bei allen groß angelegten randomisierten Studien letztlich ungewiss und die Finanzkraft jenseits der Möglichkeiten der Pharmaka-entwickelnden Industrie begrenzt. In jüngster Zeit sind mit auf Untersucher-Ebene erheblichen Anstrengungen verbundene RCT zur ^{90}Yttrium-Radioembolisation in Kombination mit der Standard- medikamentösen Tumortherapie in der

Erstliniensituation bei kolorektalen und hepatozellulären Karzinomen als Negativstudien beendet worden, wenn auch Subgruppenanalysen Anlass zur Hoffnung gaben, dass es einen Platz für die lokale und lokoregionäre Therapie in der Erstliniensituation geben könnte[7-10]. Der Endpunkt Overall survival (OS), also das Gesamtüberleben, sollte zumindest für bestimmte Therapieansätze und Studiendesigns kritisch hinterfragt werden. Die multimodale, Metastasen-gerichtete Therapie erreicht unterhalb der kurativen Erfolge bei einem Gutteil der Patienten inzwischen einen stetig länger werdenden Zeitraum der Palliation, wodurch der notwendige Kohorten-Umfang, der einen Vorteil im OS nachweisen kann, unrealistisch groß wird[11]. Deshalb müssen neue Endpunkte zur Stratifizierung sowie zur Beurteilung des initialen Therapieansprechens definiert werden, die zum Beispiel als Surrogat des Konzeptes der „Deepness-of Response" dienen können[12]. Das könnten etwa Biomarker wie mittels liquid biopsy gewonnene und quantifizierte zirkulierende Tumor-DNA sein[13-17].

3.3 Das Konzept der Oligometastasierung und die lokale Therapie von Metastasen

Das metastasierte Stadium solider Tumoren wird im Allgemeinen immer noch als das systemische Stadium der Erkrankung aufgefasst. Dies ist einerseits die Grundlage für die medikamentöse Tumortherapie. Auf der anderen Seite bleibt die Kuration insbesondere im inoperablen, metastasierten Stadium tatsächlich die Ausnahme und die Anzahl der möglichen Therapien ist begrenzt. Weiterhin muss eine systemische Therapie zwangsläufig mit systemischen Toxizitäten einhergehen, was sowohl die Anwendbarkeit in komorbiden Patienten mit reduziertem Allgemeinzustand einschränkt als auch fast immer zu einer Minderung der Lebensqualität führt[18-20].
Aus diesen und weiteren Gründen ist die Erörterung der lokalen und lokoregionären Ebene der Tumortherapie mit Rückgriff auf das Konzept der Oligometastasierung – des Stadiums zwischen lokaler und systemischer Erkrankung, das trotz (begrenzter) Metastasierung als lokal therapierbar gilt – sinnvoll[21-24] . Dieses Konzept ist anerkannt und hat für alle lokalen Verfahren Relevanz, seien es chirurgische, stereotaktisch-strahlentherapeutische, thermoablative oder interstitiell-brachytherapeutische.

Grundsätzlich sollte bei der Wahl eines Metastasen-gerichteten Verfahrens oder bei lebereigenen Tumoren immer die Therapie gewählt werden, die in Anbetracht der individuellen onkologischen Situation unter Berücksichtigung von Alter, Komorbiditäten und Vortherapien für den Patienten geeignet erscheint und gleichzeitig die beste Tumorkontrolle und Verträglichkeit bietet. Dabei sind die vorliegende Evidenz und die klinische Erfahrung mit einer gegebenen Methode bedeutsam, wobei die Chirurgie einschließlich der Lebertransplantation im Allgemeinen einen angenommenen oder tatsächlichen Evidenzvorsprung besitzt.

Bei einem Teil der Patienten vor allem mit kolorektalen Lebermetastasen werden so Langzeitüberlebensraten erreicht, die an eine Kuration heranreichen, was das Konzept der Oligometastasierung (also der Möglichkeit der Kuration von Patienten im metastasierten Stadium durch Lokaltherapien) grundsätzlich bestätigt[25-28]. Da aber lediglich etwa 20% der Patienten einer solchen Operation zugänglich sind, gibt es einen Bedarf an weiteren, effektiven Lokalverfahren, wenngleich fortgeschrittene Operationstechniken den Anteil der technisch operablen Patienten in den letzten Jahren sukzessive erhöht haben[29,30]. Zudem erleiden bis zu 50-75 % der Patienten nach Resektion von kolorektalen Lebermetastasen ein Rezidiv, wobei ein kurzes Zeitintervall bis zum Auftreten des Rezidivs mit einer schlechteren Prognose verbunden ist[31-35]. Die Genese der postchirurgischen Tumorprogression ist multifaktoriell bedingt. Es gibt Hinweise, dass die Leberregeneration nach chirurgischer Resektion die Tumorprogression begünstigt[36]. Immunantwort, Angiogenese, Lymphangiogenese, die epitheliale- zu- mesenchymale- Transition bzw. das Remodeling der extrazellulären Matrix spielen dabei eine bedeutende Rolle, worauf diverse Antikörper- bzw. Inhibitoren-Therapien abzielen[37]. Diese Phänomene sind für andere lokale Verfahren ebenfalls nicht auszuschließen und bislang nur unzureichend untersucht.

Diese Limitationen und die Möglichkeiten der modernen radiologischen Verfahren führten zur Entwicklung minimal-invasiver Therapien wie der Radiofrequenzablation (RFA), einer thermischen Therapie, bei der über die Reibung gegenläufiger Ionenströme hohe Temperaturen im Tumor erzeugt werden, die zu Zelltod und Nekrose führen. Sie wird neben der interventionell radiologischen Technik auch intraoperativ angewandt. Die RFA ist die am weitesten verbreitete Methode mit der besten Evidenz, daneben existieren die Mikrowellenablation (MWA), Kryoablation und irreversible Elektroporation (IRE) , wobei sich die Kryoablation einen gewissen Stellenwert bei der Ablation von Nierenzellkarzinomen erarbeitet hat[38,39,40]. Unter den lokoregionären Techniken bei leberprädominanter, diffuserer Metastasierung hat wiederum die ^{90}Yttrium-Radioembolisation (RE) in den letzten Jahren zunehmend an Bedeutung gewonnen[7-10].
Eine Langzeit- Beobachtungsstudie zur RFA von kolorektalen Lebermetastasen zeigte beeindruckende Ergebnisse in Bezug auf das Gesamtüberleben bei inoperablen Patienten im Vergleich zu publizierten Ergebnissen nach Chirurgie[41]. In anderen Studien war die Radiofrequenzablation der Resektion deutlich unterlegen, was einerseits an der bekannten Größenlimitation für thermoablative Verfahren liegen mag. Andererseits muss ein Selektionsbias unterstellt werden, da die inoperablen Patienten notwendigerweise das kränkere Patientengut darstellen[42]. Qualitativ hochwertige, prospektiv randomisierte Studien, die eine tatsächliche Vergleichbarkeit der RFA- und chirurgischen Kollektive gewährleisten, sind jedenfalls nicht verfügbar und werden auf Grundlage (vorgeblich?) ethischer Bedenken

teilweise in Statements sogar abgelehnt, wenngleich sie aus wissenschaftlicher, klinischer und ethischer Sicht eigentlich dringend durchgeführt werden müssten[43]. Weiterhin mag man sich vorläufig auf den Standpunkt zurückziehen, dass diese beiden Verfahren in der klinischen Routine weniger in Konkurrenz zueinander stehen als sich vielmehr ergänzen[44-46]. Im frühen und sehr frühen Stadium hepatozellulärer Karzinome ist die RFA vor allem bei Patienten mit Zirrhose ein Standardverfahren, und die CLOCC-Studie hat bei kolorektalen Lebermetastasen und sehr weitgefassten Einschlusskriterien einen signifikanten OS- Vorteil der RFA/OP-Gruppe gegenüber der alleinigen Chemotherapie- Gruppe gezeigt[47-50].
Die RFA und andere thermoablative Lokaltherapien wie die MWA sind im Hinblick auf die Lage und Größe der zu behandelnden Tumoren technisch limitiert. Einerseits erhöht sich die Lokalrezidiv- Rate bei Läsionen über 3 cm deutlich, andererseits ergeben sich durch die Nähe zu großen Gefäßen Kühleffekte, die den therapeutischen Effekt einschränken[42]. Weiterhin kann eine räumliche Beziehung zu thermosensiblen Strukturen wie dem Leberhilus oder der Gallenblase eine RFA unmöglich machen[51,52].

Radiotherapeutische Verfahren können diese Grenzen überwinden.
Eine Strahlentherapie in der Leber, in der Lunge und in anderen Organen kann perkutan ohne einen invasiven Eingriff durch die Stereotaxie (SBRT, stereotactic body radiotherapy) oder Cyberknife- Techniken durchgeführt werden[53,54]. Für die maximale Größe effektiv behandelbarer Läsionen gilt aber – ähnlich wie für die Thermoablation – ein Limit von etwa 4 – 5 cm und die Anzahl gleichzeitig behandelbarer Läsionen ist begrenzt[55,56]. Jenseits dessen scheint die Wirksamkeit der SBRT deutlich zu sinken [57,58].
Eine andere Möglichkeit, Tumoren strahlentherapeutisch zu behandeln, ist die interstitielle Brachytherapie (iBT), bei der eine Punktquelle, zum Beispiel ^{192}Iridium, über Katheter direkt in den Tumor eingeführt wird. In Leber und Lunge wurde die iBT in den frühen 2000er Jahren eingeführt, nachdem CT- basierte 3D- Bestrahlungs-Planungs-Techniken, Mehrschicht-CT und die CT- Fluoroskopie in den 1990er Jahren entwickelt wurden, die eine exakte Applikatoreinlage in parenchymatöse Organe möglich machten [59-62].
Die interstitielle Brachytherapie (iBT) erlaubt bei unerreicht exakter, atemunabhängiger Dosimetrie die Einbringung sehr hoher Dosen als Einzelfraktion, die bis zu 25 Gy am Tumorrand und über 100 Gy im Zentrum des Tumors bedeuten können. Dabei fällt die Dosis zur Peripherie hin stark ab, was häufig eine effektive, tumorizidale Dosis bei Schonung der umgebenden Strukturen auch bei sehr großen und zentral gelegenen Tumoren ermöglicht[63,64].
Derart hohe Einzeldosen (>10-12Gy) zeitigen darüber hinaus zusätzliche therapeutische Effekte. Hier ist die Apoptose-Induktion am Gefäßendothel zu nennen, verbunden mit einem konsekutiven antiangiogenetischem Effekt[65,66]. Gelegentlich können Hypofraktionierungs-

Regime mit Einzeldosen von 10-12 Gy, zum Beispiel bei sehr großen links hepatischen Tumoren mit Nähe zur gastralen Mukosa, sinnvoll sein[67].

Diese überproportionale Effektivität wird durch initiale Studienergebnisse bei verschiedenen Entitäten und Lokalisationen bestätigt [62-64,68-73]. Die lokale Tumorkontrolle in hepatozellulären Karzinomen mit einem Durchmesser bis zu 12 cm und mehr liegt bei >90% der behandelten Metastasen nach 12 Monaten bei einer tumorumschließenden Dosis von 15 Gy. In einer randomisierten Dosiseskalationsstudie zur iBT in kolorektalen Lebermetastasen waren 20-25 Gy Zieldosis mit einer ebenso hohen lokalen Kontrollrate verbunden[70,72]. Diese gute Tumorkontrolle wurde auch extrahepatisch, zum Beispiel bei pulmonalen Neoplasmen unterschiedlicher Herkunft, nachgewiesen [74].

Das Prinzip der bildgeführten Brachytherapie (und der wesentliche Unterschied gegenüber der konventionellen, perkutanen Bestrahlung) ist die exakte, CT- bzw. MRT-gesteuerte Implantation des Katheters in das vorgesehene Zielorgan zur späteren Aufnahme der Strahlenquelle. Tumor und Strahlenquelle sind damit in ihrer Lage zueinander weitestgehend fixiert, was bei Behandlungen im Oberbauch und in der Lunge von besonderem Vorteil ist. Üblicherweise wird in Analgosedierung (Fentanyl und Midazolam, jeweils i. v.) unter CT- oder MR-Fluoroskopie die Positionierung der Brachytherapie- Katheter vorgenommen. Nach Punktion der Malignome wird eine Angiographie-Schleuse und darüber ein Brachytherapie-Katheter eingebracht, der später zur Aufnahme der Quelle dient. Nach Positionierung der Brachytherapie- Katheter wird ein kontrastmittelgestütztes Planungs-CT oder eine MRT akquiriert und an das Bestrahlungsplanungssystem transferiert. Für ein HDR- Brachytherapie-System wird im Allgemeinen eine ^{192}Iridium- Quelle mit 10Ci Aktivität verwendet. Die Bestrahlungszeit beläuft sich- abhängig von der Größe des zu therapierenden Tumorvolumens (Planning- Target- Volume, PTV)- in der Regel auf etwa 10 bis 60 Minuten.

Die Thermoablation und die Stereotaxie sind aus unterschiedlichen Gründen nicht geeignet, in universeller Weise eine Metastasen- gerichtete Therapie zu ermöglichen[42, 51,52 55,56 57,58]. Die interstitielle Brachytherapie erlaubt auf Grund ihrer besonderen Eigenschaften eine unbegrenzte lokale Therapie. Voraussetzung für eine im Sinne des Patienten sichere und erfolgreiche Therapie ist die Patientenselektion, die Wahl der richtigen Dosis sowie die Komplikationskontrolle.

4 Die interstitielle Brachytherapie: Technik

4.1 Implantationstechnik: CT

Die interstitielle Einlage der Brachytherapie-Katheter wird üblicherweise unter Analgosedierung mit lokaler Anästhesie, gelegentlich auch in Allgemeinnarkose durchgeführt. Weit verbreitet ist die Anwendung der CT- Fluoroskopie – an spezialisierten Zentren gibt es auch die MRT-Führung – zur Implantation der langen Angiografie-Schleusen, die zur Aufnahme der Brachytherapie- Katheter dienen[75-78]. Je nach Technik erfolgt die Katheterentfernung mit oder ohne Verschluss des Punktionskanal[60-62,70,79]. Prinzipiell unterscheidet man zwischen der oben beschriebenen Seldinger-Technik und der Direktpunktion, die an einigen Zentren bevorzugt wird[64,80]. Teilweise findet dabei eine virtuelle Vorplanung der Katheter-Lage und der daraus resultierenden Bestrahlungsvolumina unter Berücksichtigung der geplanten Dosis im Tumor und der umgebenden Risikostrukturen statt.
Nach der Vorplanung wird ein (zumeist) natives Planungs-CT akquiriert und anschließend unter CT- Fluoroskopie ein oder mehrere Katheter in das Tumorvolumen implantiert. Bei der Seldinger-Technik wird dabei zunächst nach Entfernen der Nadelseele ein steifer Draht (Amplatz, Boston Scientific) vorgeschoben und über diesen die lange, hydrophile 6F-Angiografie-Schleuse (Terumo, Japan) eingeführt, die den Brachytherapie-Katheter führt. Dieser ist endgeschlossen und verfügt über eine Millimeter-Skala, die für die korrekte Einbringung bis zum Ende der offenen Schleuse ohne Fluoroskopie benötigt wird. Nach Beendigung der Bestrahlung wird zunächst dieser und dann die Schleuse entfernt, wobei während des Rückzugs der Schleuse – ermöglicht durch deren offenes Ende – Gelatine-Schwämmchen-Pfropfen zum Verschließen des Punktionsweges und mithin zur Vermeidung von Blutungskomplikationen eingebracht werden können.
Eine andere, von einigen Kollegen wegen der Einfachheit favorisierte Methode, ist die Direktpunktion mittels 6F- Plastikkathetern mit 200 mm Länge und einer Stahlseele (Nucletron B.V., Veenendaal, The Netherlands, OncoSmart ProGuide Round Needle) mit geschlossenem Ende, die aber keinen Verschluss der Punktionskanäle mit den oben erwähnten Gelatine-Pfropfen erlaubt [64,80]. Die Anzahl der applizierten Katheter ist abhängig von Größe und Form des zu behandelnden Tumors. Im Allgemeinen wird ein Katheter je 1-2 cm Tumordurchmesser implantiert.

4.2 Implantationstechnik: MRT

Bei der Implantation der Katheter im offenen MRT werden dem Interventionalisten auf einem RF-abgeschirmten LCD-Bildschirm interaktive, fluoroskopieähnliche Bilder in allen drei

Raumebenen angezeigt (ca. 1 Bild/s). Damit wird die sichere Katheterimplantation auch in sehr kleine Läsionen ermöglicht. Zuvor wird ein T1- gewichtetes, kontrastmittelverstärktes (Gd-EOB-DTPA, Primovist, Bayer, Germany) Planungs-MRT angefertigt, wobei durch die Hepatozytenspezifität von Primovist üblicherweise keine Aufnahme in die Lebertumoren erfolgt, die entsprechend hypointens zur Darstellung kommen. Die zur Punktion verwendeten Materialen bestehen aus einem Keramik-Skalpell (SLC Ceramic, Deutschland) zur Inzision, einer 18G- MR kompatiblen Punktionsnadel mit einer Länge von 150 bis 200 mm (Invivo, Deutschland) und einem hydrophilen Standard- Angiografie-Draht (Terumo, Japan). Nach Einlage der Katheter wird in den Standard-Brachytherapiekatheter ein Führungsdraht zur Visualisierung eingeführt[78].

4.3 Bestrahlungsplanung: Bildgebung

Nach Katheterimplantation wird eine Planungs-CT, üblicherweise mit Kontrastmittel, angefertigt. Bei der MRT-geführten Implantation wird ein T1- gewichtetes, kontrastmittelverstärktes (Gd-EOB-DTPA, Primovist, Bayer, Germany) Planungs-MRT akquiriert. Ein beiden Fällen werden 3 mm Schichtdicke gewählt, um eine genaue Definition des Zielvolumens und der Katheter- Position zu ermöglichen. In Einzelfällen kann auch eine Ko- Registrierung mit PET (Positronen- Emissions- Tomografie) -Daten notwendig sein, wenn zum Beispiel keine Kontrastmittelgabe im CT möglich ist oder nur die PET- positive Anteile einer partiell nekrotischen Läsion als Zielvolumen definiert werden sollen. Typischerweise wird die Bestrahlung mittels HDR (*high-dose-rate*) -Brachytherapie mit einer ^{192}Iridium- (^{192}Ir) Quelle durchgeführt. Die Bestrahlungsdauer richtet sich nach der Größe des Zielvolumens, der Anzahl der Katheter, der Zieldosis sowie der (mit der Zeit abnehmenden) Aktivität der Quelle und liegt typischerweise zwischen 10 und 60 min.

5 Die interstitielle Brachytherapie: Dosis und Effekt in Tumor, Leber und Risikoorganen

Auch wenn das Konzept von Zielvolumendefinition und Risikoorganen in der ICRU 50-Richtlinie festgelegt wurde, unterscheidet sich die interstitielle Brachytherapie doch von herkömmlichen Bestrahlungsverfahren[81]. Folgerichtig haben Anwender dieser Technik in der Literatur abweichende Definitionen für die Angabe der Zieldosis sowie der Dosis in Risikoorganen entwickelt[62,64,70,72,80].
Hierbei sind zwei Besonderheiten der interstitiellen Brachytherapie zu beachten:

1. Bei der bildgeführten HDR-Brachytherapie sind die Katheter einerseits durch den Gewebsdruck und andererseits durch die Nahtfixierung an der Hautoberfläche im Tumorvolumen sicher fixiert. Dadurch ergeben sich nur geringe Unsicherheiten in Bezug auf die Katheter-Position durch Organbewegungen vor allem durch die Atmung, was hauptsächlich bei Anwendungen in der Leber von enormer Bedeutung ist und einen großen Vorteil gegenüber der perkutanen Bestrahlung darstellt. Daraus folgt, dass – im Gegensatz zur letztgenannten – das klinische Zielvolumen (clinical target volume, CTV) mit dem Planungsvolumen (planning target volume, PTV) nahezu identisch ist, auch wenn Unsicherheiten bis zu 5 mm in der Katheter-Position zum Tumor gegenüber dem Planungs-CT einerseits und dem Zeitpunkt der Bestrahlung andererseits möglich sind **(Publikation 1)**[82]. Dies führt in der Praxis dazu, dass das CTV (=PTV) + 5 mm Sicherheitssaum um das GTV (Gross-Tumor-Volume) im Planungs- CT/oder -MRT markiert wird.

2. Ein weiterer wesentlicher Unterschied zur perkutanen Bestrahlung ist der steile Dosisabfall zur Umgebung hin, da sich die Strahlenquelle im Tumor befindet und somit von innen nach außen bestrahlt wird. Daraus folgt, dass – bei Leberbehandlungen – die Leber das wesentliche Risikoorgan darstellt und sich weitere in unmittelbarer Nähe befinden müssen, um kritische Dosen zu erreichen. Dies kann zum Beispiel bei linkshepatischen oder zentralen Tumoren für den Magen und das Duodenum der Fall sein, weitere relevante Risikoorgane sind der Ductus hepaticus und das Kolon, die Niere und die Haut sowie die Rippen. Für den Magen, das Duodenum und den Ductus hepaticus wurden in Studien Brachytherapie-immanente Grenzdosen ermittelt[67,83-88].

5.1 Individuelle Dosisverschreibung bei Lebermalignomen abhängig von der Tumorhistologie

Frühe Studien zur intraoperativen interstitiellen Brachytherapie kamen zu der Empfehlung von tumorumschließenden Dosen von 15-30 Gy unabhängig von der Histologie der Tumoren[89-91]. Spätere Arbeiten seit 2004 zur nichtoperativen, interventionellen, CT-gesteuerten Brachytherapie von Lebermalignomen arbeiteten genauere Dosisverschreibungen abhängig von der Tumorentität heraus[62,70,72,92]. In einer sowohl explorativen als auch prospektiven sowie randomisierten Dosisfindungsstudie mit 73 Patienten und 199 kolorektalen Lebermetastasen wurden einzeitig minimale Tumordosen am Tumorrand von 15, 20 und 25 Gy appliziert (ein Cross-over bei dosislimitierenden Charakteristika war erlaubt), wobei die Lokalrezidiv-Rate (der primäre Endpunkt, LR) mit der Dosis abnahm. Das mediane Follow-up für die LR mit Bildgebung betrug 15,2 Monate, das Gesamt-Follow-up in Bezug auf das Gesamtüberleben 41 Monate. Dabei handelte es sich überwiegend um multimodal vortherapierte Patienten in der Salvage- Situation mit schlechter Prognose. 58% der Patienten waren synchron lebermetastasiert, 86 bzw. 40% hatten eine first-line bzw. second/third-line Chemotherapie erhalten, 33% eine Leberteilresektion und 21% eine Thermoablation. Die Gesamt-LR betrug für alle Metastasen 25,1% (n=50/199), für den 15 Gy- Arm 35% (n=34/98), für den 20 Gy- Arm 22% (n=15/68) und für den 25 Gy-Arm 3% (n=1/33). Ein Signifikanzlevel mit einem p-Wert unter 0.05 wurde für den 25 Gy- Arm versus 15- bzw. 20- Gy erreicht. Der ermittelte Cut-off-Wert für die D100, also die tatsächliche Dosis, mit der 100% des PTV umschlossen waren und oberhalb derer es keine Lokalrezidive gab, lag bei 23 Gy. Interessanterweise hatte die Tumorgröße in der multivariaten Cox-Regressionsanalyse keinen Einfluss auf die LR.

Die vergleichsweise hohe Cross- over-Rate zeigt einerseits, dass 25 Gy nicht immer erreicht werden können, was dem Umstand geschuldet ist, dass in dieser Studie (repräsentativ für die klinische Situation) auch große bis sehr große Metastasen bis 13,5 cm behandelt wurden. Andererseits belegt das mediane Lokalrezidiv-freie Überleben (LFS) von 25,6 Monaten in der 15 Gy Gruppe (der Median wurde in der 20- und 25- Gy Gruppe nicht erreicht), dass auch mit niedrigen Dosen eine langanhaltende Tumorkontrolle erreicht werden konnte. In der praktischen Konsequenz werden in der klinischen Routine, abhängig von der individuellen Größe sowie der Anzahl und der Verteilung der Metastasen, Zieldosen zwischen 20 und 25 Gy verschrieben. Letztlich beeinflusste in einer multivariaten Analyse das Auftreten eines Lokalrezidivs auch nicht das Gesamtüberleben (Overall survival, OS) und der wiederholte Einsatz der Brachytherapie im Verlauf – sei es bei neu auftretenden Metastasen oder bei Lokalrezidiven – verlängerte das OS signifikant, und zwar stärker als der ebenfalls positive Einfluss einer postinterventionellen Chemotherapie. Angesichts des hohen Anteils an Patienten mit insgesamt schlechter Prognose (58% synchrone Lebermetastasen) ist das

beobachtete mediane OS von 23,4 Monaten, 46,7 Monaten und 56,2 Monaten nach erster Brachytherapie, nach der Erstdiagnose der Lebermetastasen bzw. nach der Erstdiagnose des Primarius bemerkenswert[72] **(Publikation 2)**.

Eine weitere prospektive, explorative Studie zur iBT bei 83 Patienten mit einem hepatozellulären Karzinom (HCC, Child Pugh-Klasse A 64%, Child Pugh-Klasse B 36%; BCLC-Stadium A 61%, B 14%, C 24%) und insgesamt 140 Leberläsionen bei verschriebenen Zieldosen zwischen 15 und 25 Gy beobachtete bei insgesamt 126 Läsionen mit bildgebender Nachsorge 5 Lokalrezidive (4,0%). Der mediane Tumordurchmesser der größten Läsion/Patient betrug 5,2 cm (1-15cm). Es wurde keine Abhängigkeit von der Zieldosis im genannten Bereich von 15 bis 25 Gy nachgewiesen. In der klinischen Routine werden HCC deshalb je nach individueller Tumorcharakteristik mit einer Zieldosis zwischen 15 und 20 Gy behandelt. 114 Läsionen (medianer Tumordurchmesser 3,1 cm, 1-12 cm) wurden dabei einzeitig abladiert, 12 sehr große HCC (medianer Tumordurchmesser 11,3 cm, 6-15 cm) wurden zwei- oder dreizeitig behandelt. Der Lokalrezidiv-freie Anteil der Patienten (LFR) nach 12 Monaten lag bei den kleineren, einzeitig behandelten HCC bei 96% und bei den großen, mehrzeitig behandelten bei 91%. Es konnte also bei einer kleinen Anzahl von Patienten gezeigt werden, dass auch große bis sehr große Tumoren, ggf. mehrzeitig, effektiv behandelt werden können.

Der primäre Endpunkt, die Time-To-Progression (TTP), lag für die kleineren, einzeitig behandelten Läsionen bei 12 Monaten, für die größeren, mehrzeitig behandelten bei 8,4 Monaten. Der mediane Nachbeobachtungszeitraum für das OS betrug 33,8 Monate, das mediane Gesamtüberleben für alle Patienten 19,4 Monate.

Dabei zeigte sich in einer univariaten Analyse eine Abhängigkeit des OS nach Einschluss in die Studie bzw. nach Erstdiagnose des HCC vom CLIP-Score (CLIP-score 0: 46,3 bzw. 58,9 Monate, Clip-score >=3 8,3 bzw. 13,5 Monate) und vom BCLC-Score sowie vom Tumordurchmesser. Multivariat war lediglich der Clip-Score ein signifikanter Faktor.

Ergänzend wurde bei 57 vollständig die Match-Kriterien erfüllenden Paaren eine Matched pair-Analyse der brachytherapierten Patienten gegen eine Kontrollgruppe ohne brachytherapeutische Behandlung durchgeführt, die einen signifikanten Unterschied im OS nach der Erstdiagnose von 37,5 Monaten in der Brachytherapie-Gruppe sowie 18 Monaten in der Kontrollgruppe ergab ($p<0.001$) [70] **(Publikation 3).**

Bei 115 Lebermetastasen von Mammakarzinomen bei 41 Patientinnen mit Zieldosen zwischen 15 und 25 Gy wurde ebenfalls keine Dosisabhängigkeit der LR bei einer LFR von 97%, 93,5 und 93,5% nach 6, 12 und 18 Monaten festgestellt. In der Konsequenz erhalten Patientinnen mit Lebermetastasen eines Mammakarzinoms in der klinischen Routine eine D100 zwischen 15 und 20 Gy. Der mediane Tumordurchmesser betrug 4,6 cm (1,6-11cm). Interessanterweise unterschied sich das mediane Progress-freie Überleben (Progression-

Free-Survival, PFS) zwischen den Patientinnen, die eine zusätzliche Chemotherapie nach der Brachytherapie erhielten, nicht von denen ohne eine solche (8,5 vs. 9 Monate, p>0,05). Auch der Rezeptorstatus (Herceptin, Progesteron, Östrogen) war ohne Einfluss auf das PFS **(Publikation 4)**.

Eine sehr hohe LFR bei einer vergleichsweise niedrigen medianen D100 von 15 Gy konnte in einer retrospektiven Studie bei 40 Metastasen von gastrointestinalen Stromatumoren (GIST, 30 hepatische Metastasen, 10 peritoneale Metastasen) erreicht werden, sie betrug nach 25 Monaten 97,5% (1 Lokalrezidiv). Das mediane PFS bzw. OS lag bei 6,8 bzw. 37,3 Monaten[92] **(Publikation 5).**

Bei 54 Lebermetastasen von Nierenzellkarzinomen (NCC) wurden in einer aktuellen Studie bei einer medianen D100 von 16,1 Gy 4 Lokalrezidive mit einer entsprechenden LFR von 92,6% beobachtet. Das mediane Gesamtüberleben wird mit 51,2 Monaten angegeben[93].

45 Lebermetastasen von duktalen Adenokarzinomen des Pankreas wurden mit einer medianen D100 von 21 Gy behandelt, das Lokalrezidiv-freie Überleben lag hier lediglich bei 3,3 Monaten. Teilweise entwickelten bis zu 3 Metastasen in einem behandelten Patienten ein Lokalrezidiv, das mediane PFS und OS war 3,4 und 8,9 Monate[94].

In der Studie einer anderen Arbeitsgruppe zur gleichen Tumorentität war in 5 von 49 Metastasen bei einer D100 von 18,1 Gy ein Lokalrezidiv zu beobachten (10%), das mediane PFS und OS lag bei 4,9 bzw. 8,6 Monaten[95].

Bei 36 mit iBT behandelten Metastasen (29 Lebermetastasen, 2 pankreatische Metastasen, 5 Lymphknotenmetastasen) in 12 Patienten mit einem Adenokarzinom des Magens wurden insgesamt 4 Lokalrezidive bei eine D100 von 19,9 Gy beobachtet, was einer LFR von 89% bei einem Nachsorgezeitraum von 8,3 Monaten entsprach[96].

Eine mediane D100 von 16,2 Gy führte bei Metastasen von analen Plattenepithelkarzinomen zu einer LFR von 97,4% nach 15,2 Monaten, das PFS und OS lag im Median bei 3,3 bzw. 25,2 Monaten[97].

Bei 52 Lebermetastasen neuroendokriner Tumoren, die mit einer Zieldosis zwischen 15 und 20 Gy ein- oder mehrzeitig behandelt worden waren, wurde bei einer mittleren Tumorgröße von 3,1 cm (max. 11 cm) eine LFR von 92%, 83% und 83% nach 1, 3 und 5 Jahren bei einem PFS von 53%, 43% und 22% nach 1, 2 und 4 Jahren sowie einem OS von 96%, 96% und 53% beobachtet[98].

Bei 52 Patienten mit Lebermetastasen von malignen Melanomen und einer applizierten medianen D100 von 19,9 Gy lag die LFR bei einem Nachsorgezeitraum von 5 Monaten (1-11 Monate) bei 90% (1 Lokalrezidiv)[99] **(Publikation 6).**

Eine interessante Arbeit zur multimodalen, systemischen sowie interventionellen Therapie von intrahepatischen cholangiozellulären Karzinomen (CCC), die sowohl mit lokalen Therapien wie der iBT, aber auch der RFA sowie mit lokoregionären Therapieverfahren wie

der RE, der intraarteriellen Chemotherapie mit 5-FU sowie systemischer Chemotherapie behandelt worden waren, zeigte die iBT (das prädominant eingesetzte Verfahren) bei einer Zieldosis von 20 Gy als Einzige neben der RFA als bestes Ansprechen die Komplettremission (Complete response, CR). Das mediane OS vom Zeitpunkt der Erstdiagnose bzw. vom Zeitpunkt der ersten Intervention wurde mit 33,1 bzw. 16 Monaten ermittelt[100] **(Publikation 7)**.
Die Studie einer anderen Gruppe behandelte 15 Patienten mit einem mittleren Zielvolumen von 131 ml (10-257 ml) und erreichte ein medianes LFS von 10 Monaten bei einem medianen OS von 14 Monaten[101].
Die oben erläuterte Evidenz belegt auch die Wirksamkeit bei großen Tumoren und bei ungünstiger Lage. Dies wird durch Daten aus anderen Arbeitsgruppen gestützt.
Collettini et al. berichteten über die Wirksamkeit der iBT in großen (Tumordurchmesser 5-7 cm) und sehr großen (Tumordurchmesser 7-12 cm) HCC mit einer Leberzirrhose im Child-Pugh A bis B-Stadium, die mittlere Zieldosis betrug 15,8 Gy. Nach einem medianen Nachsorgezeitraum von 12,8 Monaten wurden 2 Lokalrezidive identifiziert (2/30 Patienten mit bildgebendem Follow up, 6,7%), die beide erfolgreich durch eine erneute Brachytherapie behandelt wurden. Das mittlere OS war 15,4 Monate[63].
Tselis et al. behandelten 41 Patienten mit 50 Lebertumoren verschiedener Entitäten und einer Tumorgröße von mehr als 4 cm (medianes CTV 84 cm^3, 38-1348), die eine enge Lagebeziehung zum Leberhilus aufwiesen. Abweichend von den übrigen Arbeitsgruppen verwendeten sie ein Fraktionierungsschema mit ein- bis zweimal täglich applizierten Einzelfraktionen zwischen 4 und 14 Gy bis zu einer medianen physikalischen Dosis von 20 Gy (7-32 Gy). Nach einem medianen FU von 12,4 Monaten betrug die LFR nach 12 Monaten für Lebermetastasen 73%, für lebereigene Tumoren 81%[64].

In vielen Arbeitsgruppen wird die D100, also die minimale Dosis, die 100% des PTV umschließt, als Zieldosis definiert und avisiert, die – auch bedingt durch den steilen Dosisabfall – in gewisser Hinsicht anfällig für Ungenauigkeiten in der CTV-Markierung in der Planungs-Bildgebung ist. Deshalb verwenden andere Arbeitsgruppen die D90 als Zieldosis. Dabei wird die Dosisverteilung zum errechneten mittleren Dosiswert auf der CTV-Oberfläche und der 100% Referenz-Isodose normalisiert[64,80]. Es wird angenommen, dass diese Methode weniger anfällig für oben genannte Ungenauigkeiten in der Zielvolumendefinition im Randbereich und der Berechnungsmatrix der Planungssoftware oder der Anzahl der Haltepunkte der Quelle ist.
Unstrittig ist, dass bei sehr großen Tumoren, bedingt durch dosislimitierende Faktoren wie der Leberexposition oder angrenzender Risikoorgane wie Magen, Duodenum oder der Haut, ein mehrzeitiges Vorgehen sinnvoll sein kann. Eine absolute Grenze hinsichtlich der Tumorgröße ist hier schwer zu ziehen, da die Faktoren Entität (und somit die zu verschreibende Dosis), Lage und ggf. vorliegende weitere Metastasen in die Überlegung mit einbezogen werden

müssen. Die bisherigen Erfahrungen legen ein mehrzeitiges Vorgehen bei Tumoren oberhalb 8-10 cm nahe[64,72,80,83,102]. Normalerweise wird hierbei keine kumulative Dosis für das Gesamtvolumen errechnet, sondern der Praktikabilität halber mehrere Teilvolumina mit der entsprechenden Zieldosis in einem Abstand von 2-4 Wochen behandelt. Dies ist auch vor dem Hintergrund bedeutsam, dass nachweislich einer Studie eine sehr lange Bestrahlungszeit das umgebende, gesunde Leberparenchym überproportional schädigt, und Bestrahlungszeiten von mehr als einer Stunde vermieden werden sollten, wenn auch der Effekt gering zu sein scheint, so tatsächlich vorhanden[82] **(Publikation 1)**.

Bekannt ist, dass die Anzahl und die Entfernung von Mikro-Satellitenmetastasen mit der Größe der Makro-Metastasen zunimmt, und dass das makroskopische Vorhandensein von Satellitenmetastasen, ggf. konfluierend mit der Hauptmetastase, einen negativen prognostischen Faktor darstellt[72,103] **(Publikation 2)**. Auf der anderen Seite sind Mikrometastasen in der Umgebung von makroskopischen Metastasen bildgebend nicht sichtbar. Für kolorektale Lebermetastasen konnte gezeigt werden, dass das Wachstum von makroskopisch nicht sichtbaren Mikrometastasen verhindert werden kann, wenn in 2,1 cm Entfernung vom GTV 15,1 Gy erreicht werden[104] (**Publikation 8).** Dies mag neben der entitätsimmanenten Strahlensensibilität ein weiterer Grund dafür sein, dass Lokalrezidive (die zum Teil vermutlich benachbarten, vordem nicht sichtbaren Mikrometastasen entsprechen) nach der Brachytherapie von kolorektalen Lebermetastasen bei einer D100 von 25 Gy selten sind, da hier 15 Gy in 2 cm Abstand sicher erreicht werden.

Oben wurde die lokale Effektivität mit dem Endpunkt LR ausführlich beschrieben. Dabei konnte, abhängig von den Einschlussbedingungen, prospektiv und retrospektiv eine hohe bis sehr hohe LFR von bis zu >90% nach 12 Monaten gezeigt werden. Nachweisbar war dabei eine Dosisabhängigkeit, wobei die hepatischen Absiedelungen der meisten Entitäten mit 15-20 Gy hervorragend lokal kontrolliert wurden, während die notwendige D100 bei kolorektalen Karzinomen mit mindestens 23 Gy für eine niedrige LR am höchsten ist. Bei diesen sind auch Spätrezidive nach 2 Jahren und mehr auch bei einer entsprechend hohen D100/CTV möglich[72]. Solch hohen einzeitigen Fraktionen sind nicht immer zu erreichen und ein fraktioniertes Vorgehen wegen der oben beschriebenen Dosislimitationen und der individuellen klinischen Situation ist nicht in jedem Falle möglich. Deshalb kommen die Ergebnisse einer weiter unten vorgestellten Studie mit dem primären Endpunkt Komplikationen bei Patienten mit unterschiedlichen Lebermalignomen – da Tumorstadium, Lage, Anzahl und Größe der Lebermalignome bzw. die tatsächlich applizierte D100 kein Kriterium für Ein- oder Ausschluss darstellten und das Patientengut somit weitgehend unselektiert war – der klinischen Situation am nächsten. Hier fand sich eine allgemeine lokale

Kontrollrate nach 12 Monaten von 89%, von 97% in hepatozellulären Karzinomen und bis zu 84% in kolorektalen Lebermetastasen.

5.2 Interventionell-radiologische sowie radio- und tumorbiologische Rationale für die Hypofraktionierung und das Konzept der einzeitigen Bestrahlung

Für die extreme Hypofraktionierung und in der Regel unfraktionierte Durchführung der iBT gibt es interventionsbedingte und radiobiologische Gründe. Erstens konnte zwar kein Zusammenhang zwischen der Komplikationsrate und der Anzahl der Katheter nachgewiesen werden. Zweitens steigt aber sehr wohl – wie bei allen anderen (minimal-) invasiven Verfahren auch – mit der Anzahl der durchgeführten Eingriffe pro Patient das Risiko von Komplikationen[83,105]. Zudem ist eine Fraktionierung mit dem Verbleib der Katheter im Körper des Patienten mit erheblichen Komforteinbußen und Unsicherheiten bzgl. der Konstanz der Katheterlage verbunden, wie klinische Erfahrungen vor allem bei Lokalisationen im Oberbauch zeigen. Außerdem postuliert man eine erhöhte Blutungsgefahr bei Verbleiben der Katheter in Organen des Oberbauches.

Dennoch gibt es Arbeitsgruppen, die hypo- bis hyperfraktionierte Konzepte mit Belassen der Katheter verfolgen. Dieses Konzept findet überwiegend bei Tumoren mit unmittelbarer und breitflächiger Nähe zu Geweben mit geringer Dosistoleranz oder in der wenig bewegungsabhängigen iBT von Hirnmalignomen Anwendung. Bei Behandlungen im Oberbauch werden hingegen, wenn die Tumorgröße oder die Lage es nicht anders erlauben, in üblicherweise 2-3 Eingriffen unterschiedliche Tumorpartitionen behandelt, um in der Summe eine vollständige Abdeckung des gesamten Tumorvolumens zu erreichen. Die Katheter werden dabei nach jeder Sitzung wieder entfernt[106-111].

Einerseits sprechen also Patientenkomfort und Sicherheit für die einzeitige Hypofraktionierung. Andererseits zeitigt die Radiatio mit hohen Einzeldosen (> 10–12 Gy) zusätzliche therapeutische Phänomene, die über die strahlentherapeutischen Effekte mit geringeren Einzeldosen hinausgehen. Hier wird unter anderem eine Apoptose-Induktion am Gefäßendothel postuliert, was einer antiangiogenetischen Wirksamkeit entspricht[65,66]. Einen histopathologischen Vergleich mit der Nekroserate zwischen SBRT und iBT gibt es bislang nicht, zumal auch bei der SBRT vergleichsweise hohe Einzelfraktionen üblich sind. Im Vergleich zur TACE bei hepatozellulären Karzinomen konnte aber ein überproportionaler Nekroseeffekt nach iBT histopathologisch nachgewiesen werden[112].
Diese überproportionale tumorizidale Wirkung der hohen Einzeit-Dosen wird durch die hohe bis sehr hohe LFR bei verschiedenen Entitäten und Lokalisationen im Oberbauch bestätigt, die im Übrigen auch für pulmonale Neoplasien gilt[74,113].

Im Folgenden wird zunächst auf Dosiseffekte im nicht betroffenen Leberparenchym und angrenzenden Geweben eingegangen werden. Dabei wird verdeutlicht werden, dass die oben angegeben hohen Einzelfraktionen, die die hypofraktionierte interstitielle Brachytherapie auszeichnen, routinemäßig und repetitiv anwendbar sind. Die Dosimetrie weist dabei ein hohes Maß an Genauigkeit auf.

5.3 Lebertoleranz und Monitoring des Bestrahlungseffektes

Bei der interstitiellen Brachytherapie von Lebermalignomen stellt die Leber selbst das wichtigste Risikoorgan dar. Allgemein wird (unter der einschränkenden Bedingung einer sonst gesunden Leber und normalen Lebergröße) empfohlen, dass das Volumen, das mit >5Gy exponiert wird, 2/3 des Lebervolumens nicht überschreiten sollte[62,64,88]. Der strahlenbedingte Effekt der unfraktionierten Applikation von 15 bis 25 Gy auf Teilvolumina der Leber ist auf der Basis von iBT-Behandlungen erstmalig anhand von MRT-Daten, histopathologischen Veränderungen und anderen paraklinischen sowie klinischen Parametern untersucht und beschrieben worden. Frühe Arbeiten zur perkutanen Strahlentherapie der Leber zeigten einen klaren Dosiszusammenhang zwischen einer sehr großvolumigen oder Ganzleber- Exposition von 30-55 Gy und der Entwicklung einer RILD (Radiation induced liver disease)[114-119]. Da wegen der erheblichen Atemverschieblichkeit der Leber und des entsprechend notwendigen großen Sicherheitssaums deshalb kaum tumorizidale Dosen bei Lebermalignomen erreicht werden konnten, spielte die perkutane Bestrahlung früher in der Behandlung von Lebermailgnomen kaum eine Rolle, bis Ende der 90- und Anfang der 2000-er Jahre präzisere Techniken entwickelt wurden, die als stereotaktische Bestrahlung bezeichnet werden[120]. Hier wurden bereits Untersuchungen der Leberreaktion nach hypofraktionierter, stereotaktischer Radiatio mit der mehrphasigen, kontrastmittelgestützten CT angestrengt[121]. Die iBT von Lebermalignomen kann in den meisten Fällen als kleinvolumige Leberexposition verstanden werden.

Dabei ist die MRT mit hepatozyten-spezifischem Kontrastmittel eine ausgezeichnete Methode zur Quantifizierung der Lebertoleranz bzw. des Leberparenchym-Schadens. In frühen Arbeiten war dies Gd-BOPTA (Gadobenate dimeglumine, MultiHance, Bracco, U.S.), spätere verwendeten Gd-EOB-DTPA (Gadolinium ethoxybenzyl diethylenetriamine-pentaacetate, Primovist®, Bayer, Germany), das mit einer hepatobiliären Extraktionsrate von >50% dem Gd-BOPTA (3-5%) in der Leberbildgebung überlegen ist[122-126]. Da funktionsfähige Hepatozyten das Kontrastmittel aufnehmen, werden in der T1-gewichteten Sequenz nach etwa 20 min (Gd-EOB-DTPA) bzw. 2 Stunden (Gd-BOPTA) sowohl die meisten Tumore als auch das Lebergewebe mit Funktionsverlust hypointens dargestellt. Entsprechend sind in vivo-Messungen der Lebertoleranz auf die Bestrahlung möglich. Dies wurde für zahlreiche

entsprechende Studien bei einzeitiger und repetitiver iBT genutzt[84,85,87,127]. Auch für die SSPIO-Bildgebung wurde die Toleranzdosis des retikuloendothelialen Systems ermittelt[128]**(Publikation 9)**.

In einer Studie mit Gd-BOPTA, die die Toleranzdosis kleiner Lebervolumina untersuchte, wurden 25 Lebermetastasen mit iBT behandelt. Die Patienten hatten prätherapeutisch eine normale Leberfunktion. Einen Tag vor der Therapie und 3 Tage sowie 6, 12 und 24 Wochen *post interventionem* (p. i.) erfolgte eine Untersuchung der Patienten mit einem Gd-BOPTA-verstärktes MRT. Die Datensätze wurden mit der 3D-Dosimetrie aus der Bestrahlungsplanung fusioniert und mit dem hyperintensen postaktinischen Areal in der T2w- (dem postaktinischen Ödem) bzw. dem entsprechenden hypointensen Areal in der späten T1w-Sequenz (dem behandelten Tumor und ihn umgebendes Leberparenchym mit Funktionseinschränkung entsprechend) korreliert. Dabei stellte sich heraus, dass sich das posttherapeutische Ödem in der T2w zwischen Tag 3 p. i. und 6 Wochen p. i. von der 12,9 Gy Isodosenlinie auf die 9,9 Gy Isodose ausdehnte (Standardabweichung SD 3,3 bzw. 2,6, p=0.006), dann nicht weiter zunahm und nach 24 Wochen auf die 14,7 Gy Isodosenlinie zurückging (SD 4,2, p= 0.002). Das Volumen des hepatozytären Funktionsverlustes lag an Tag 3 p. i. von der 14,9 Gy-Isodosenlinie umschlossen und dehnte sich sich nach 6 Wochen auf die 9,9 Gy- Isodosenlinie aus, es nahm also zu (SD 2,3, p=0.001). Im Gegensatz zum Ödem konnte auch zwischen den MRT-Kontrollen nach 6 bzw. 12 Wochen ein signifikanter Rückgang des Volumens mit hepatozytärem Funktionsverlust zur 11,9 Gy Isodosenlinie beobachtet werden (SD 3,0, p=0.035). Nach 24 Wochen war der Funktionsverlust auf das Volumen, dass von der 15,2 Gy-Isodosenlinie umfasst wurde, zurückgegangen (SD 4,1, p=0.002). Die Ödem provozierende Dosis war initial demnach signifikant geringer als die Dosis, die zu einem Funktionsverlust führte (p<0.001) und vom Volumen her betrachtet ging das Ödem dem Funktionsverlust initial voraus (p=0.001). Kein Zusammenhang wurde zwischen dem Tumorvolumen und der Toleranz des Leberparenchyms gesehen. Auch bestand kein Zusammenhang zwischen der Aktivität der Quelle - also der Dosisleistung - und der Toleranzdosis auf Signifikanzniveau[84] **(Publikation 10).**

Einen ähnlichen Ansatz verfolgte eine spätere Studie mit Gd-EOB-DTPA bei Patienten, die an 23 Lebermetastasen mit der iBT behandelt worden waren. Diese kam zu vergleichbaren Resultaten mit einem Anstieg des Volumens des hepatozytären Funktionsverlustes von der 19,5 Gy Isodosenlinie nach 3 Tagen zu einem Maximum nach 6 Wochen innerhalb des von der 9,4 Gy- Isodosenlinie umfassten Volumens (p<0.001). Nach 12 bzw. 24 Wochen konnte ein Rückgang auf die 11,4 bzw. 14 Gy- Isodosenlinie beobachtet werden (p=0.002). Zwischen der minimalen, einen hepatozytären Funktionsverlust provozierenden Dosis und dem Alter der Patienten, dem Lebervolumen, dem CTV, dem 5- bzw. 10 Gy-Lebervolumen (also dem Anteil der Leber, der mindestens 5 bzw. 10 Gy ausgesetzt war), der Aktivität der Quelle, der

Bestrahlungszeit, der Anzahl der Katheter oder einer früheren Chemotherapie wurde keine Korrelation hergestellt [87] **(Publikation 11)**.

Zumindest in einem Punkt wichen die Ergebnisse in einer Arbeit mit 50 Patienten und 62 Bestrahlungsvolumina von den übrigen in-vivo Studien ab, und zwar insofern, als dass die Grenzdosis für die Lebertoleranz hier signifikant mit dem bestrahlten Volumen indirekt korrelierte, also bei zunehmendem Bestrahlungsvolumen abnahm[88] **(Publikation 12)**.

In einer weiteren Studie wurden die MRT-Signalveränderungen durch Biopsien in den exponierten Leberarealen mit histopathologischen Veränderungen korreliert. Dabei wurden charakteristische Gewebsveränderungen gesucht, die mit einem radiogen induzierten Leberschaden in Zusammenhang stehen, wie die sinusoidale bzw. hepatovenöse Kongestion, eine Vermehrung des perisinusoidalen Retikulinfasernetzes und/oder eine hepatozytäre Atrophie. Dabei fand sich eine exzellente, 100%-ige Korrelation zwischen der fehlenden Aufnahme von Gd-BOPTA und diesen histopathologischen Phänomenen sowie umgekehrt der ungestörten Aufnahme von Gd-BOPTA und einer unauffälligen Histopathologie. Daraus lässt sich schlussfolgern, dass die in-vivo Messung des hepatozytären Funktionsverlustes in der MRT mit hepatozyten-spezifischem Kontrastmittel das Ausmaß des radiogen induzierten Leberschadens mit einer sehr hohen Sicherheit quantifizieren kann[85] **(Publikation 13).**

Letztlich können die Grenzdosen für einzeitige Brachytherapien auf hypofraktionierte, mehrzeitige Brachytherapien über die Ermittlung der biologischen Äquivalentdosis übertragen werden, wie eine diesbezügliche Studie zeigen konnte. Dabei wurden 20 Patienten an identischen oder überlappenden Volumina in 2-4 Fraktionen behandelt, wobei die Funktionsverlust induzierende BED-Grenzdosis 22-24 Gy betrug, was einer Einzeit-Dosis unter Berücksichtigung der Fraktionierung von etwa 10 Gy entsprach, also im Wesentlichen den ermittelten Werten für die einzeitige iBT[129] **(Publikation 14)**.

Die aufgeführten Studien wurden bei Patienten mit normaler Leberfunktion durchgeführt. Zur Evaluierung des Einflusses auf die Leberfunktion durch die Brachytherapie (und die Y90-Radioembolisation) bei Patienten mit einem hepatozellulären Karzinom und einer Leberzirrhose Child A bis B wurden in einer weiteren Arbeit 3 Tage, 6 Wochen und 12 Wochen nach der Intervention leberspezifische Laborparameter bestimmt. Für die 12 brachytherapierten Patienten lag das prätherapeutische Lebervolumen zwischen 708 und 2268 cm^3, das CTV zwischen 3,1 und 72,5 cm^3 (im Mittel 21 cm^3), das 5Gy- Volumen der Leber zwischen 2,6 und 20,3%. Dabei war ein geringgradiger Anstieg der AST und GGT im unmittelbar postinterventionellen Verlauf zu verzeichnen, während die Cholinesterase geringgradig abfiel. Alle relevanten Parameter kehrten nach spätestens 12 Wochen auf die Ausgangswerte zurück.

Innerhalb der Studienbedingungen konnte also gezeigt werden, dass die Brachytherapie auch größerer Volumina und bei kleinen Volumina der Gesamtleber (zum Beispiel nach

Leberteilresektion) für Patienten mit Zirrhose und einer geringen Einschränkung der Leberfunktion sicher möglich war[127] **(Publikation 15)**.

Zusammenfassend lässt sich schlussfolgern, dass die Brachytherapie hinsichtlich der Leberfunktion sicher durchführbar ist, was auch in einer kleinen Population bei Patienten mit geringer Einschränkung der Leberfunktion nachweisbar war. Der temporäre und permanente Funktionsverlust des umgebenden Lebergewebes lässt sich ausgezeichnet mittels MRT mit hepatozyten-spezifischem Kontrastmittel nachweisen, wobei die Veränderungen sehr gut mit den histopathologischen Phänomenen eines radiogen induzierten Leberschadens korrelieren. Durch die Fusion der MRT mit der 3D- Dosimetrie konnte sogar eine gewisse Vorhersagbarkeit des Funktionsverlustes abgeleitet werden, wobei zwischen temporärem und permanentem Funktionsverlust unterschieden werden muss. Die Grenzdosis für den temporären Funktionsverlust, am besten verstanden als temporäre veno-occlusive disease (VOD), erreicht ihr Maximum nach 6 Wochen und entspricht dann im Mittel dem Volumen, das ursprünglich von der 9-10 Gy- Isodosenlinie umfasst worden war. Bis zur 24. Woche p. i. ist ein Rückgang auf die 14-16 Gy Isodosenlinie zu verzeichnen, was im Mittel der Grenzdosis für den permanenten Funktionsverlust entspricht. Insofern bietet sich die 10 Gy- Isodosenlinie als volumetrischer Parameter für den temporären und die 14-16 Gy-Isodosenlinie für den permanenten Funktionsverlust für die präinterventionelle und periinterventionelle dosimetrische Planung an. Einschränkend ist die relative breite interindividuelle Streuung der jeweiligen Grenzdosis anzuführen. Sie weist auf eine individuelle Toleranz des Leberparenchyms hin, die zum Beispiel aus einer Sensibilisierung durch Chemotherapeutika resultieren mag. Da aber mit gewissen Unsicherheiten vorhersagbar ist, welches Volumen temporär bzw. permanent seine Funktion verliert, könnten mit gewissem Recht und unter Berücksichtigung dieser interindividuellen Schwankungen (d.h. einem „Sicherheitszuschlag“ für die erwarteten funktionseingeschränkten Volumina) für die iBT die gleichen Regeln angewandt werden wie für die Leberteilresektion (future- liver- remnant), wohlverstanden als echte „Radiochirurgie“. Letztlich wird in der klinischen Routine weiterhin die V66%/5Gy-Regel (nicht mehr als 66% der Leber werden mit 5Gy oder mehr exponiert) angewandt, ein konservatives Vorgehen, was eine gewisse Bestätigung durch die nur episodisch auftretenden atypischen Formen der RILD erfahren hat. Auf diese wird im Kapitel Komplikationen noch eingegangen werden.

Wegen der sehr guten Quantifizierbarkeit des Dosiseffektes wurde an einem brachytherapierten Patientenkollektiv die leberprotektive Wirkung einer bestimmten Medikamentenkombination (Enoxaparin, Pentoxifyllin und Ursodesoxycholsäure) untersucht. Die Fragestellung ergab sich eigentlich aus den nicht selten beobachteten RILD oder REILD (Radioembolisation- induced- liver- disease) bei der ^{90}Yttrium- Radioembolisation der Leber. Bei dieser ist es aber wegen der deutlich ungenaueren Dosimetrie und der diffuseren

Veränderungen in der MRT unmöglich, einen möglichen Effekt solcher Protektiva zu quantifizieren. In dieser prospektiven randomisierten Studie, die per Protokoll mit 11 Patienten in der Prophylaxegruppe und 11 Patienten in der Kontrollgruppe ohne Prophylaxe analysiert wurde, zeigte sich ein signifikant höherer Lebertoleranz-Grenzwert nach 6 Wochen in der Prophylaxegruppe im Vergleich zur Kontrollgruppe (19,1 versus 14,6 Gy, p=0,011). Das heißt, das Volumen mit temporärem Funktionsverlust war in der Prophylaxegruppe nach 6 Wochen signifikant kleiner, während das Volumen mit hepatozytärem Funktionsverlust nach 12 Wochen in beiden Gruppen vergleichbar war. Ob dies nun damit zusammenhängt, dass die Prophylaxe lediglich in den Wochen 1 bis 8 gegeben wurde oder die Prophylaxe nur einen Einfluss auf die vorübergehend funktionsbeeinträchtigten Hepatozyten hatte, verbleibt Studiendesign bedingt damit unklar. Dennoch sind die Ergebnisse von hoher klinischer Relevanz für die Radioembolisation, da hier die temporären REILD- Ereignisse im Vordergrund stehen und die Prophylaxe Eingang in den klinischen Alltag gefunden hat[86] **(Publikation 16)**. Für die Brachytherapie ist die klinische Bedeutung begrenzt, wird im Einzelfall jedoch bei sehr großen Tumorvolumina nach repetitiver Brachytherapie und/oder Leberzirrhose eingesetzt.

5.4 Dosislimitationen der Gallenwege

Bei der Brachytherapie von zentralen Tumorlokalisationen in der Leber ist die Hepatikusgabel häufig hohen Einzeldosen ausgesetzt. Klinisch entstehen im mittel- bis langfristigen Verlauf nicht selten Veränderungen der angrenzenden Gallenwege im Sinne von unregelmäßigen Erweiterungen, die klinisch nur in der Minderheit zu cholestasetypischen Veränderungen von Klinik und Laborparametern führen. Aus der Fragestellung, inwieweit dies mit der Dosis zu korrelieren wäre und welche tatsächliche klinische Relevanz diese Gallengangs-Veränderungen jenseits der Empirie hätten, leitete sich die folgende Studie ab.
Dabei wurden retrospektiv 102 Patienten mit unterschiedlichen hepatischen Malignomen eingeschlossen, die mit einer maximalen Punktdosis von mindestens 1 Gy auf die zentralen Gallengangstrukturen exponiert waren. 22 Patienten (22%) entwickelten eine morphologische Erweiterung der Gallenwege nach einer medianen Zeit von 17 (3-54) Monaten. 18 von diesen wurden mittels perkutaner oder endoskopischer Drainage (PTCD oder ERC) behandelt. Die mediane Punktdosis der Patienten, die Gallengangs-Erweiterungen aufwiesen, betrug 24,8 Gy (4,4-80) gegenüber eine medianen Punktdosis von 14,2 Gy (1,8-61,7 Gy) bei solchen ohne (p= 0.028). Der ermittelte Cut-off lag bei 20,8 Gy (*p*= 0.028; 59% Sensitivität, 24% Spezifität). Resultierende Abszesse bzw. Cholangitiden waren selten und traten in beiden Gruppen auf, häufiger aber in der Gruppe mit morphologischer Cholestase (4/ 22 vs. 2/ 80; p= 0.029). Das mediane Gesamtüberleben unterschied sich zwischen beiden Gruppen nicht und lag im

Median bei 43 vs. 36 Monaten (p =0.571) für die Patienten mit bzw. ohne Cholestase[130] **(Publikation 17).**

Die breite Streuung der Punktdosen in beiden Gruppen und die niedrige Sensitivität und sehr niedrige Spezifität des berechneten Cut-off machen es schwierig, daraus Empfehlungen für die klinische Routine abzuleiten. Einerseits entwickelten einzelne Patienten bereits ab einer Punktdosis von 4,4 Gy eine morphologische Cholestase, während andere Patienten ungeachtet einer Exposition mit Punktdosen von bis zu 61,7 Gy eine solche nicht entwickelten. Daraus lassen sich vordergründig zwei Erklärungsmuster ableiten: entweder es existieren individuelle Dosistoleranzwerte für die Gallengänge bei jedem Patienten oder die morphologische Cholestase ist weniger eine Folge der Reaktion der gesunden Gallengangswand, sondern Zeichen des Ansprechens auf die Bestrahlung der bereits infiltrierten Gallengangswand, die konsekutiv mit narbigen Veränderungen reagiert. Ersteres ist unwahrscheinlich, da es den bisherigen Erfahrungen von Toleranzdosen in der Strahlentherapie widerspricht, zweiteres ist zumindest denkbar.

Weitere Einflussmöglichkeiten sind die Dauer der Bestrahlung, die Dosisleistung der Quelle oder die Lage der Katheter, die aber in Untersuchungen zur Toleranzdosis des gesunden Leberparenchyms ganz überwiegend keinen Einfluss hatten. Es lässt sich festhalten, dass klinisch relevante Komplikationen bei der Bestrahlung von zentralen Lebertumoren selten sind und bei einer Reihe von Patienten auch sehr hohe Punktdosen auf die zentralen Gallenwegsstrukturen vertragen werden, der Cut-off also wenig geeignet ist, eine entsprechende Patientenselektion durchzuführen. Die ausgezeichnete Behandelbarkeit von zentralen Lebertumoren mittels Brachytherapie als Alleinstellungsmerkmal gegenüber allen anderen lokalen Verfahren einschließlich Chirurgie spricht ebenfalls dafür, das Risiko einer postinterventionellen Cholestase in Abwägung mit dem Patienteninteresse und nach entsprechender Aufklärung in Kauf zu nehmen, zumal sich aus dieser Komplikation keine Verkürzung des Gesamtüberlebens ergab. Weiterhin ist zu überlegen, ob eine prolongierte Steroidprophylaxe, wie sie in der perkutanen Strahlentherapie verwendet wird, sinnvoll sein kann.

5.5 Risikoorgane außerhalb der Leber

5.5.1 Magen und Duodenum

Klinisch bedeutsame Risikoorgane (Organs- at- Risk, OAR) sind Magen und Duodenum. In den ersten Jahren der Anwendung der iBT wurden insbesondere bei linkshepatischen Eingriffen in geringer, aber relevanter Anzahl strahleninduzierte Magen- oder Duodenal-Ulzerationen beobachtet, so dass diesem Aspekt auch wissenschaftlich verstärkt Beachtung geschenkt wurde.

In einer größeren Studie mit 192 Patienten und 343 CT- oder MRT-geführten interstitiellen Brachytherapien verschiedener Entitäten, die im Kapitel Komplikationen ausführlich erörtert wird, erhielten 57 Patienten in 72 Interventionen eine relevante Magen- oder Duodenal-Exposition (Dmax/1cm^3), d.h., auf den am höchsten exponierten Kubikzentimeter Magen- oder Duodenalwand wurden mehr als 1 Gy appliziert. Postinterventionell wurden 3 gastroduodenale Ulzera gesichert (3/72; 4%). Dabei wurde ermittelt, dass Patienten mit Magen-Darm-Ulzerationen, die – lokalisationsbedingt und pathologisch – auf die Bestrahlung zurückzuführen waren, eine signifikant höhere minimale Dosis auf den am höchsten exponierten cm^3 der Magen- bzw. Duodenalwand erhalten hatten als solche ohne (15.8±2.5 vs. 10.0± 4.1 Gy; p= 0.020). Der Cut-off für die Entwicklung von gastroduodenalen Ulzera lag bei 14 Gy[83] **(Publikation 18)**.
Dies bestätigte prinzipiell die Ergebnisse einer früheren Arbeit in einem kleineren Patientenkollektiv (33 Patienten mit iBT im Lebersegment 2 oder 3), die einen Grenzwert für eine symptomatische gastrointestinale Toxizität bzw. die Entwicklung von gastroduodenalen Magen-Darm-Ulzera von 11 bzw. 15,5 Gy ermittelte[67].
Inwieweit eine prä- oder postinterventionelle medikamentöse Tumortherapie, die ulzerogene Substanzen wie Avastin einschließt, die Dosiseffekte verstärkt und zum Risiko beiträgt, ist noch nicht wissenschaftlich untersucht.

In der klinischen Routine werden jedenfalls ab einer relevanten gastroduodenalen Exposition von 8-10 Gy Dmax/1 cm^3 Protonenpumpenhemmer für 3 bis 12 Monate verordnet[83]. Expositionen von über 14-16 Gy werden im Allgemeinen vermieden, was dazu führen kann, dass linkshepatische Tumoren ggf. eine geringere Zieldosis erhalten als empfohlen oder fraktioniert behandelt werden. Es ergeben sich dadurch gelegentlich also Einschränkungen in der unfraktionierten Behandelbarkeit von Lebertumoren in den Segmenten 2 und 3.
Daraus ergab sich die Entwicklung erweiterter Interventionstechniken, um zumindest den Magen vom Leberrand zu distanzieren und damit Abstand zum Bestrahlungsfeld zu schaffen. Zu diesem Zweck ist die interventionelle Einbringung von Okklusionsballons geeignet, wie sie in der Angiografie verwendet werden.

Bei 31 Patienten wurden während der Implantation der Katheter für die iBT auch Okklusionsballons zwischen den Magen und die Leber geschoben. Bei denselben Patienten wurde die Punktdosis ohne diese Ballons an einem anhand der nativen Planungs-CT unmittelbar vor Kathetereinlage, das mit dem 3D- Bestrahlungsplan fusioniert wurde, erstellten virtuellen Plan gegen die tatsächliche Punktdosis am Risikoorgan nach Einlage des Ballons intraindividuell verglichen. Dabei ergab sich – wenig überraschend – für die Planung mit Ballon eine mittlere Dmax/1 cm^3 von 12,6 Gy am Risikoorgan gegenüber 16 Gy ohne Ballon

($p<0.001$). Dieses Studienresultat ist insofern relevant, als dass ohne eine signifikante Reduktion der Punktdosis am Risikoorgan die deutlich invasivere Technik mit Balloneinlage kritisch zu hinterfragen wäre. Gleichzeitig wird aber eine effektive, unfraktionierte Behandlung linkshepatischer Malignome ermöglicht ^{131} **(Publikation 19).**

5.5.2 Die Niere

Nicht selten liegt die Niere bei der iBT des Organs selbst (entweder bei der Ablation von Nierenzellkarzinomen oder den seltenen Nierenmetastasen anderer Primarien), bei der Brachytherapie von Nebennierenmalignomen oder hepatischen Interventionen im Lebersegment 6 im exponierten Bereich. In einer Studie zur anteilig repetitiven iBT von 18 Nierenzellkarzinomen und 2 Nierenmetastasen mit dem primären Endpunkt Nierenfunktionsverlust nach 12 Monaten wurde eine Zieldosis von 15 Gy (bzw. 20 Gy bei Lokalrezidiven) appliziert. 3 Tage, 3 Monate, 6 Monate und 12 Monate nach Brachytherapie wurden unter anderem das Serumkreatinin und die geschätzte glomeruläre Filtrationsrate (eGFR) erhoben. Weiterhin wurde prätherapeutisch sowie 3, 6 und 12 Monaten post interventionem (p. i.) eine ^{99m}Technetium-MAG3-Nierensequenzszintigrafie mit separater Auswertung beider Nieren durchgeführt.

Dabei ergab sich eine mediane Reduktion der eGFR von prätherapeutisch 71ml/min (26-125 ml/min) auf 58 ml/min (23-88 ml) nach 12 Monaten. Zu diesem und keinem anderen Zeitpunkt aber lag der Unterschied auf einem statistischen Signifikanzniveau.

Die mittels Szintigrafie ermittelte tubuläre Extraktionsrate (TER) sank ipsilateral, also in der brachytherapierten Niere, von median 52 ml/min (37-100 ml/min) auf 33 ml/min (5-100 ml/min) nach 12 Monaten, während die kontralaterale TER von median 51 ml/min auf 95 ml/min anstieg, ein statistisches Signifikanzniveau wurde jeweils nicht erreicht. Die Gesamt-TER sank im Median von 156 ml/min (97-340 ml/min) auf 108 ml/min (108-142 ml/min). Eine Patientin mit bilateralen und bilateral behandelten Nierenzellkarzinomen und Diabetes mellitus Typ 2 wurde nach 2,5 Jahren hämodialysepflichtig.

Einschränkend muss gesagt werden, dass aufgrund des Studiendesigns Spätkomplikationen nach über 1 Jahr nicht für die Gesamtheit des Patientenkollektivs erfasst wurden. Allerdings betrug die umfassende Nachsorge mit bildgebenden Verlaufskontrollen im Median 22,5 Monate. Man kann festhalten, dass im 2 bis 3-jährigen Verlauf eine Patientin Hämodialyse-pflichtig wurde, die auf Grund der Bilateralität und des Diabetes hochgradig prädisponiert war. Innerhalb der Limitationen dieser Studie war die iBT also sicher durchführbar, der Funktionsverlust unterhalb des statistischen Signifikanzniveaus^{132} **(Publikation 20)** .

5.5.3 Das Pankreas

Auch das Pankreas ist häufig ein Risikoorgan, entweder auf Grund seiner Nähe zu Bestrahlungsfeldern in Leber, Lymphknoten, Niere oder Nebenniere oder bei der Behandlung von Pankreasläsionen selbst. In einer Studie zur iBT in 13 Patienten mit 13 Pankreasläsionen (8 Metastasen und 5 Primärtumore, davon 2 Lokalrezidive) fand sich bei einem medianen Tumordurchmesser von 3 cm und einer D100 von 15,3 Gy keine Toxizität CTCAE Grad 3 oder höher, lediglich ein Patient entwickelte eine milde akute Pankreatitis, die innerhalb einer Woche spontan abklang[133] **(Publikation 21).**

Für alle anderen Risikoorgane wie die Haut, die Rippen und das Myelon sowie das Kolon werden die Referenz- bzw. Grenzwerte aus den Leitlinien der perkutanen Strahlentherapie, adaptiert an das hypofraktionierte Konzept, übernommen[134].

6 Die interstitielle Brachytherapie: Komplikationen

6.1 Allgemeine prozedurale und radiogene Komplikationen

Aus technischer Sicht kombiniert die hypofraktionierte interstitielle Brachytherapie die minimal-invasive, interventionell-radiologische Punktion einschließlich Kathetereinlage in Seldinger-Technik mit einer besonderen Form der Strahlentherapie.
Diese Strahlentherapie ist in zweierlei Hinsicht besonders: Erstens ist sie nicht, wie sonst in der perkutanen Radiatio angestrebt, konformal mit homogener Dosisverteilung, sondern äußerst inhomogen bei Lage der Quelle im Tumor mit entsprechender Dosiseskalation im Tumorzentrum, aber steilem Dosisabfall zur Peripherie hin. Zweitens werden bei extremer Hypofraktionierung – nämlich der im Normalfall unfraktionierten Behandlung – sehr hohe Einzeldosen zwischen 15 und 25 Gy appliziert.
Nach Abschluss der Behandlung und während der Entfernung der Katheter kann der Punktionskanal nicht – wie bei der Thermoablation – koaguliert werden, weshalb man sich damit behilft, dass die eingeführte lange Angiografie-Schleuse, die den Brachytherapie-Katheter führt, nach Entfernen desselben als Führung für das Stopfen des Punktionskanals mit entsprechend geformten Gelatineschwämmchen-Pfropfen dient. Dies kann Blutungskomplikationen vermeiden. Allerdings wird der andere erhoffte Effekt bei der thermalen Ablation des Stichkanals, nämlich die Abtötung evtuell durch den Eingriff verschleppter Tumorzellen und mithin die Vermeidung von Stichkanalmetastasen, bei der interstitiellen Brachytherapie durch die Bestrahlung des Punktionskanals erzielt (siehe 6.4.).
Deshalb sind die prozeduralen, durch die Invasivität der Intervention bedingten Komplikationen von den strahlentherapeutischen Toxizitäten zu trennen.

Eine umfassende Arbeit hat sich damit beschäftigt. Dabei wurden 192 Patienten in 343 Interventionen mittels interstitieller Brachytherapie in der Leber behandelt. 284 waren CT-geführte Interventionen, 59 MRT-geführte Brachytherapien. Das CTV betrug im Median 36,7 cm^3 (IQR 13-78,8, max. 796 cm^3), das Lebervolumen 1352 cm^3, die Zieldosis 17,3 Gy. Das 5 Gy- Volumen lag median bei 22,5 % (IQR 13,8-34,7, max. 87,9%). Es wurden im Median 4 und bis zu 9 Katheter eingebracht. Die Primärtumoren umfassten kolorektale Karzinome, hepatozelluläre Karzinome, cholangiozelluläre Karzinome, Mammakarzinome, Bronchialkarzinome und andere (43,8%; 26,0%; 8,3%; 6,7%; 4,2%; 10,9%). 34,4% der Tumoren betrugen zwischen 5 und 10 cm im Durchmesser und 6,3% lagen im Durchmesser >10 cm. Dabei handelte es sich überwiegend um multipel vortherapierte Patienten (Chemotherapie 59,4%, dabei mindestens Zweitlinie 39,6%; Leberteilresektion oder atypische Resektion 22,4%, vorherige interventionelle Tumorablationen einschließlich RFA und TACE

26,6%). 26% der Patienten hatten eine Leberzirrhose im Child- Pugh- Stadium A oder B, das mittlere Alter betrug 66,1 Jahre. Nach den CTCAE Kriterien (Common Terminology Criteria for Adverse Events, V. 3.0) erlitten die Patienten bei unter 5% der Eingriffe eine Major-Komplikation Grad 3 oder höher (15/343)[135]. Das waren 5 Grad 3-4 Blutungen, überwiegend mittels Embolisation oder allein durch die Gabe von Erythrozytenkonzentraten behandelt, 1 Aszites Grad 3, 3 gastroduodenale Ulzerationen, 4 Leberabszesse sowie ein hämorrhagischer Gallengangs-Verschluss, der mittels temporärem Stent versorgt wurde. 2 Patienten verstarben innerhalb von 30 Tagen, zum einen verursacht durch eine fulminante Ösophagusvarizen-Blutung, zum anderen durch eine neutropene Sepsis unter Chemotherapie. In früheren Arbeiten wurde rein quantitativ eine höhere 30-Tage-Mortalität bei Patienten mit hepatozellulärem Karzinom und Leberzirrhose gesehen (3,6%, 3/83), als bei Patienten mit kolorektalen Lebermetastasen (0%, 0/73)[70,72].

Unter den Minorkomplikationen waren Pleuraergüsse, Aszites und subkapsuläre Hämatome Grad 2 oder kleiner sowie Pneumothoraces. Eine klassische RILD trat nicht auf. Ein Patient mit einem hepatozellulären Karzinom und Hepatitis C, der 22 Monate nach Leberteilresektion die erste iBT erhielt, entwickelte eine atypische Form der RILD mit Aszites und ikterischem Anstieg der Leberenzyme, das heißt des Bilirubins, der Transaminasen und der alkalischen Phosphatase 7 Wochen nach der letzten von 4 brachytherapeutischen Behandlungen. Unter medikamentöser Therapie, einer RILD- Prophylaxe entsprechend (s.o.), waren die Veränderungen nach 7 Monaten vollständig rückläufig, der Patient verstarb knapp 2 Jahre nach der letzten Brachytherapie. In einer früheren Studie bei 83 Patienten mit einem hepatozellulären Karzinom wurden zwei atypische, mögliche RILD-Fälle beobachtet.

In der Subgruppe, die mittels standardisierter Fragebögen genauer auf somatischen Diskomfort hin untersucht worden waren, traten Übelkeit und Erbrechen Grad 1-2 bei 37% auf. Schwere Schmerzen waren signifikant mit einem Blutungsereignis korreliert (3/5 vs. 4/338, $p<0.001$). Frauen gaben Übelkeit und Schmerzen signifikant häufiger an als männliche Patienten ($p=0.049$ und 0.016).

In dieser Studie traten Major-Blutungen ausschließlich bei Eingriffen bei Patienten mit Leberzirrhose auf (5/89 vs. 0/254, $p= 0.001$) und unter diesen prädominant in der Gruppe mit mittlerer bis schwerer Leberfunktionseinschränkung (Child B 3/13, Child A 2/230, $p<0.001$). Dies bestätigte die Ergebnisse von Pilotstudien bei Patienten mit hepatozellulärem Karzinom bzw. kolorektalen Lebermetastasen[70,72]. Dabei war die prätherapeutische Thrombozytenanzahl ein prädisponierender Faktor auf Signifikanzniveau ($p=0.043$), nicht aber die Anzahl der eingebrachten Katheter, die Prothrombinzeit, eine Portalvenenthrombose oder das Alter. Der Zusammenhang zwischen maximaler Punktdosis (bzw. der Dmax/1cm^3) und der Entwicklung von radiogen induzierten gastroduodenalen Ulzera wurde oben bereits erläutert[83] **(Publikation 18)**.

6.2 Die interstitielle Brachytherapie nach biliodigestiver Anastomose

Es gibt Hinweise, dass das Vorliegen einer biliodigestiven Anastomose die postinterventionelle Abszessrate erhöht, wie dies auch für die TACE und TAE bekannt ist[95,136,137]. Eigene Erfahrungen aus einer noch unveröffentlichten Studie zur iBT bei cholangiozellulären Karzinomen in der Kombination mit medikamentöser Tumortherapie stützen diese Annahme. Ebenso gibt es Hinweise in retrospektiven Studien, dass die ^{90}Yttrium- Radioembolisation (RE) bei biliodigestiver Anastomose diesbezüglich risikoärmer ist[138].

6.3 Die periinterventionelle Thromboseprophylaxe mit niedermolekularen Heparinen: Blutungs- und Thromboserisiko

Das Risiko schwerer Blutungen konnte im Gegensatz zu den dosisabhängigen Effekten der Strahlentherapie initial schwerer prognostiziert werden. Inzwischen gibt es jedoch eine gute Evidenz, die ein individuelles Risikoniveau vor dem Eingriff abzuschätzen erlaubt. In der oben zusammengefassten Studie konnte der Zusammenhang zwischen Leberfunktionseinschränkung bei Leberzirrhose und Blutungsrisiko gezeigt werden.

Bei invasiven Eingriffen an hospitalisierten Patienten mit onkologischen Erkrankungen erhalten diese häufig eine Thromboseprophylaxe mit niedermolekularen Heparinen (NMH). Dies wird mit der Prädisposition dieser Patienten für thrombembolische Ereignisse (*Venous-Thrombembolism*, VTE) begründet, die deutlich über dem bereits erhöhten diesbezüglichen Risiko für nichtonkologische hospitalisierte Patienten liegt[139,140]. Lange wurde postuliert, dass die VTE-bedingte Mortalität und Morbidität durch die NMH-Gabe effektiv gesenkt werden kann[141-143]. Eine aktuellere Metaanalyse unter Einschluss von 16 000 onkologischen und nichtonkologischen Patienten fand allerdings keine signifikante Reduktion von tiefer Beinvenenthrombose, pulmonaler Embolie oder Mortalität[144]. Für die hepatopankreatobiliäre Chirurgie wurde bereits nachgewiesen, dass mit der NMH-Gabe ein erhöhtes Risiko für Blutungen einhergeht[145]. Bedauerlich ist, dass sich auch in aktuellen Leitlinien keine Empfehlung zur Thromboseprophylaxe bei Krebspatienten, die sich einer minimal-invasiven Tumortherapie unterziehen, findet[146].

446 onkologische Patienten wurden in 781 Tumorablationen (iBT n=669, RFA n= 112) mit bzw. ohne periinterventionelle NMH-Gabe (n=260 bzw. n= 521) an Tumorlokalisationen in Leber, Lunge, Niere, Lymphknoten und anderen behandelt. Dabei wurden 63 Blutungsereignisse jedweder Schwere beobachtet, und dies auf Signifikanzniveau häufiger in der Prophylaxegruppe (alle Interventionen 11,66 und 6,26%, p= 0,0127; bei Lebereingriffen 12,73 und 7,1%, p=0.0416). Dabei traten signifikant häufiger Blutungsereignisse nach RFA als nach

der Brachytherapie auf (14,29 versus 7,03%, p=0,0149; bei Lebereingriffen 19,6 versus 7,7%, p= 0,0054). Der Anteil von Patienten mit Thromboseprophylaxe war dabei gleich verteilt (iBT 33%, RFA 34,8%, p= 0.710). Die Anzahl der schweren Blutungen CTCAE- Grad 3 oder höher war um mehr als den Faktor 2,6 in der Prophylaxegruppe erhöht (4,64 und 1,73%, p=0,0243), bei Lebereingriffen um den Faktor 3,3 (5,23 und 1,54%, p=0,028). Die Methode (IBT oder RFA) hatte hier keinen signifikanten Einfluss mehr. Unter den Studienbedingungen war in uni- und multivariaten Datenanalysen die NMH- Gabe der einzige konstant und signifikant mit der Blutungsrate assoziierte Faktor. Die 30- und 90 Tage-Mortalität war unabhängig von der konsekutiven Therapie (angiografische Embolisation oder Chirurgie) bei den Patienten mit schweren Blutungsereignissen massiv erhöht gegenüber den Patienten ohne oder mit nur minderschweren Blutungsereignissen (23,1 und 38,5% bzw. 0,5 und 2,3 %, p<0.0001). Eine postinterventionelle NMH- Gabe erhöhte die Blutungsrate nicht. Weiterhin trat lediglich bei einer Patientin (ohne Prophylaxe) eine symptomatische VTE (Lungenembolie) zwei Monate nach der Brachytherapie auf. Weitere symptomatische thrombotische und thrombembolische Ereignisse wurden nicht beobachtet [105] **(Publikation 22)**.

Aus den Ergebnissen dieser Publikation und der oben aufgeführten **Publikation 18** lassen sich relevante Schlussfolgerungen ableiten:

a) Ein Blutungsereignis CTCAE Grad 3 oder höher ist in Bezug auf die Mortalität die schwerwiegendste Komplikation bei der Brachytherapie oder anderen Tumorablationen wie der RFA, da unabhängig von einer schnellen Versorgung und Stillung der Blutungsquelle häufiger Sekundärkomplikationen, die zum Beispiel aus der Hypovolämie oder einer Infektion des Hämatoms mit konsekutiver Sepsis resultieren, für die hohe Mortalität verantwortlich sind[105].

b) Patienten mit fortgeschrittener Leberzirrhose sind prädisponiert für das Auftreten schwerer Blutungsereignisse.

c) Unabhängig davon ist eine periinterventionelle NMH-Gabe der wichtigste Risikofaktor für eine erhöhte Blutungsrate. Das Morbiditäts- und Mortalitätsrisiko der NMH-Gabe liegt weit über dem Risiko thromboembolischer Ereignisse im interventionell behandelten onkologischen Patientengut mit einer nur kurzen Immobilisationszeit und minimaler Invasivität. Eine solche kann also nicht generell empfohlen werden. Sie ist sogar, wenn nicht weitere thrombogene Komorbiditäten hinzukommen, kontraindiziert.

d) Der Verschluss der Punktionskanäle mit Gelatineschwämmchen-Pfropfen ist effektiv. Es ergibt sich daraus kein Nachteil der iBT gegenüber der RFA, wo die Möglichkeit des thermischen Verschlusses besteht. Im Gegenteil war die Blutungsrate jedweden Grades in einem großen Patientenkollektiv bei Patienten nach iBT geringer als nach RFA[105].

6.4 Das Risiko von Stichkanalmetastasen

Das Risiko der Verschleppung maligner Zellen durch diagnostische oder therapeutische Punktionen ist bekannt und vor allem beim hepatozellulären Karzinom gut untersucht. In einer Metaanalyse unter Einschluss von diagnostischen Punktionen und lokalen Ablationen lag die Rate an extrahepatischen Stichkanalmetastasen (SKM) bei 1,27%[147]. Frühe Arbeiten zur RFA mit einer patienten-basierten SKM-Rate von bis zu 12,5% der Patienten machten die Notwendigkeit der Ablation des Stichkanals deutlich, die sich als effektiv erwies[148]. In aktuellen Arbeiten zur RFA oder Mikrowellenablation (MWA) mit Stichkanalablation konnte die Rate entsprechend auf 0,61-1,6% gesenkt werden[149,150]. Bei der iBT ist die Möglichkeit der thermischen Stichkanalablation nicht gegeben, weshalb die folgende Studie diesem Phänomen Beachtung schenkte.

In 100 Patienten wurden 233 HCC- Läsionen mittels iBT behandelt. Dabei wurden insgesamt 588 Katheter platziert, im Mittel waren das 5,9 Katheter / Patient. Für die Auswertung wurde nach einer Plausibilitätsprüfung auf das Vorliegen von SKM die Bestrahlungsplanungs-Bildgebung einschließlich Dosimetrie mit der Nachsorge-Schnitt-Bildgebung (CT oder MRT) fusioniert. Dabei wurden nach einer mittleren Zeit von 5,5 Monaten (4,8-6,2) 9 Stichkanalmetastasen (7 intrahepatisch, 2 peritoneal) beobachtet, was in einer katheterbasierten Auswertung einer SKM-Rate von 1,5% (1,2% intrahepatisch, 0,3 % extrahepatisch), in der läsionsbasierten Auswertung 3,9% und patientenbasiert 9% entsprach. Dabei war die Verschleppung häufiger bei kleineren HCC-Läsionen zu beobachten, allerdings nicht auf Signifikanzniveau (p=0.09). Leberzirrhose, Ätiologie, Pseudokapsulierung, die Katheterstrecke im Körper, das Vorschieben des Katheters über den Tumor hinaus, die D100 bzw. eine anschließende Sorafenib-Therapie hatten demgegenüber keinen Einfluss. 8 von 9 SKM wurden konsekutiv und erfolgreich mit der iBT behandelt. Es gab keinen Unterschied im medianen Gesamtüberleben bei Patienten mit SKM bzw. ohne (25 vs. 20 Monate).
Ein Alleinstellungsmerkmal dieser Studie ist, dass durch die oben beschriebene Fusionierung der Bildgebung im Verlauf auch intrahepatische SKM identifiziert werden konnten, während die übrigen Studien in diesem Forschungsfeld lediglich die extrahepatische Verschleppung betrachteten. Insofern liegt eine katheterbasierte bzw. patientenbasierte extrahepatische SKM-Rate von 0,2 bzw. 2% – ohne Ablation des Stichkanals – unter oder auf dem Niveau von RFA und MWA. Diese niedrige Rate bestätigt Ergebnisse einer Studie zur iBT von hepatozellulären Karzinomen als Bridging-Therapie vor Lebertransplantation in einer kleineren Kohorte[112]. Unerwünschte Effekte wie Lokalrezidive oder SKM hatten in den bisherigen Studien zur iBT keinen Einfluss auf das Gesamtüberleben. Dies mag – bei lokalisations- und größenmäßig nahezu unbeschränkter Einsetzbarkeit – in der Wiederholbarkeit dieser Technik begründet liegen: nahezu alle SKM in dieser Studie und die

Lokalrezidive in der an anderer Stelle erwähnten Arbeit bei Patienten mit kolorektalen Lebermetastasen wurden erneut mittels Brachytherapie behandelt[72].

In der Konsequenz dieser Analyse werden inzwischen in den meisten Arbeitsgruppen die Punktionskanäle entitätsunabhängig bestrahlt, entweder zeitlich definiert mit einer halben bis einer Sekunde je Haltepunkt oder dosisdefiniert mit etwa 10 Gy in 2-3 mm Abstand um den Katheterverlauf[151] **(Publikation 23)**.

7 Die interstitielle Brachytherapie der Leber: Outcome, multimodale Therapie, prognostische Parameter und der Vergleich zu anderen lokalen Verfahren

7.1 Outcome

Bei der Bewertung jeder lokalen Methode ist die Lokalrezidiv-Rate (LR) das erste Kriterium, mit dem man deren Effektivität bemisst. Das ist im ersten Schritt sinnvoll. Das onkologische Outcome selbst ist aber multifaktoriell bedingt und häufig wenig von diesem Parameter abhängig. Auf Grundlage der bisherigen Evidenz ist anzunehmen, dass eine sehr gute lokale Kontrolle einschließlich großer Tumoren bei den meisten Entitäten gegeben ist, und zwar selbst dann, wenn Lokalrezidive oder Stichkanalmetastasen auftreten (siehe Kapitel 5). Da die iBT in Bezug auf die Tumorlokalisation und -größe sowie in begrenztem Maße auch die Anzahl der Tumoren deutlich geringeren Einschränkungen unterlegen ist als andere lokale Verfahren, ist sie auch wiederholbar. Die onkologische Patientenselektion (vor allem, ob tatsächlich ein oligometastasiertes Stadium vorliegt oder ob ein rascher, lokal nicht kontrollierbarer Progress zu erwarten ist) sowie die Selektion bezgl. der Prädisposition für schwere Komplikationen (siehe Kapitel 5) sind deshalb von entscheidender Bedeutung für die Frage, ob die Therapie im Sinne des Patienten gewinnbringend sein kann. Während bei der Resektion, der Thermoablation und auch der stereotaktischen Bestrahlung in gewissem Maße eine „automatische" Selektion stattfindet, ist vor dem Hintergrund der geringen Limitationen der iBT die Stratifizierung besonders bedeutsam und im Einzelfall schwieriger.

Die Überlebensdaten sind über verschiedene Studien und Arbeitsgruppen hinweg konsistent, auch wenn sie überwiegend retrospektiv erhoben wurden.
Die Ergebnisse einer bereits oben vorgestellten Studie mit 192 Patienten, die mit der iBT behandelt worden waren, kommt mit dem primären Endpunkt Komplikationen der klinischen Situation am nächsten, da Tumorstadium, Lage, Anzahl und Größe der Lebermalignome bzw. die tatsächlich applizierte D100 kein Kriterium für Ein- oder Ausschluss darstellten und das Patientengut somit weitgehend unselektiert war. Das mediane OS lag für alle Patienten bei 20,1 Monaten (medianer Nachsorgezeitraum 20,5 Monate), bei 27,9 Monate für Patientinnen mit einem hepatisch metastasierten Mammakarzinom, bei 21,5 und 21,2 Monaten für hepatisch metastasierte kolorektale Karzinome und hepatozelluläre Karzinome, bei 16,3 Monaten für cholangiozelluläre Karzinome, 8,7 Monaten für hepatisch metastasierte Lungenkarzinome und 24,1 Monate für die anderen, zusammengefassten Entitäten. Das PFS lag im Median bei 5,5 Monaten, von 11,7 Monaten bei hepatozellulären Karzinomen bis zu 2,2 Monaten bei Patienten mit einem Lungenkarzinom[83] **(Publikation 18)**.
Ein begrenzter onkologischer Effekt in Bezug auf die *Outcome*-Parameter LR, PFS und Gesamtüberleben muss, wenn auch bei limitierter Datenlage, für die iBT von

Lebermetastasen des Pankreas, aber auch von Lungenkarzinomen postuliert werden. Allerdings fehlt bei den untersuchten Patientenkohorten eine weiterführende Selektion hinsichtlich des Subtyps und der Prognose. Auf der anderen Seite wurden diese Daten großenteils in der frühen Ära der Antikörpertherapie und vor der Einführung der Checkpoint-Inhibitoren erhoben, so dass sich zukünftig eine andere Sicht ergeben könnte [94,95,152].

7.2 Multimodale Therapie und Prognosefaktoren

Im häufigen Fall eines chronischen onkologischen Verlaufs findet sich die iBT in einem sequenziellen, multimodalen Therapiemanagement wieder. Mehrere Studien haben dies adressiert und prognostische Faktoren evaluiert.

In der MammaMia- Studie von Seidensticker et al. wurden 59 Patientinnen mit einem hepatisch metastasierten Mammakarzinom mittels iBT, RFA oder RE behandelt, eine extrahepatische Metastasierung war kein Ausschlusskriterium. Faktoren mit signifikantem Einfluss auf das Gesamtüberleben (median 21,9 Monate) wurden getrennt betrachtet für solche, die bei Studieneinschluss bekannt waren (A) und solche, die in der Nachsorge evident wurden, wie zum Beispiel Lokalrezidive (B). In (A) hatten der maximale Tumordurchmesser bei Einschluss (Hazard Ratio HR 3,1), das Lebervolumen (HR 2,3) sowie eine stattgehabte Chemotherapie (mindestens Drittlinie, HR 2,5-2,6) einen unabhängigen Einfluss auf das Gesamtüberleben, während dies in (B) der maximale Tumordurchmesser (HR 3,1) sowie die lokale Tumorkontrolle (HR0,29) und das beste Gesamt-Therapieansprechen waren. Weder extrahepatische Metastasen im Allgemeinen noch Knochenmetastasen im Besonderen wiesen einen signifikanten Einfluss auf das Gesamtüberleben auf. Patientinnen mit kleinen Metastasen ohne exzessive systemische Vortherapie profitierten also am meisten, während das Vorliegen einer extrahepatischen Metastasierung ohne prognostischen Wert war. Die lokale Tumorkontrolle dagegen war in dieser Patientenkohorte unter multimodaler Therapie prognostisch bedeutsam[153] **(Publikation 24)**.

Bei 266 Patienten mit kolorektalen Lebermetastasen, die entweder eine iBT, eine RFA oder eine RE erhielten, war interessanterweise eine mittlere bis schwere Niereninsuffizienz der einzige signifikante Einflussfaktor auf das OS. Weder das Alter (Cut-off 70 Jahre) noch Komorbiditäten waren von prognostischer Bedeutung[154] **(Publikation 25)**.

Diese Ergebnisse bestätigen erste Hinweise auf prognostisch relevante Faktoren nach der iBT von kolorektalen Lebermetastasen in einer früheren Studie an 73 Patienten mit 199 Lebermetastasen. Dabei war das Vorhandensein von Satellitenmetastasen der prognostische Faktor für ein verringertes Gesamtüberleben, das Alter (Cut-off 65 Jahre), eine synchrone Lebermetastasierung, die Läsionsgröße, unilobäre vs. bilobäre Lebermetastasierung und die Anzahl der Lebermetastasen hatten keine signifikante Bedeutung. Eine erneute iBT im Verlauf

bei Progress nach erster Brachytherapie verlängerte das Gesamtüberleben bei einer HR von 1,95 (HR systemische Therapie 1,82)[72] **(Publikation 2)**.

Prognostisch bedeutsame Faktoren bei der multimodalen Therapie von 55 Patienten mit einem cholangiozellulären Karzinom, die mittels iBT, RFA, RE und TACE, teilweise in Kombination mit intraarterieller oder intravenöser Chemotherapie, behandelt worden waren, waren bei einem medianen Gesamtüberleben von 33,1 Monaten seit Erstdiagnose und 16 Monaten nach Einschluss in die Studie in einer multivariaten Regressionsanalyse unabhängig voneinander die Anzahl der Tumorläsionen, der Level der Tumormarker CEA und CA 19-9, und das objektive Tumoransprechen[100] **(Publikation 7)**.

In der univariaten Regressionsanalyse bei prospektiv evaluierten 83 Patienten mit einem hepatozellulären Karzinom und einem medianen Gesamtüberleben von 19,4 Monaten nach erster Brachytherapie war dies mit dem CLIP-score, dem BCLC-score und dem Durchmesser der größten Läsion/Patient korreliert, während in der multivariaten Analyse lediglich der CLIP-score auf Signifikanzniveau prädiktiv war. Inzwischen hat sich zur prätherapeutischen Stratifizierung von Patienten mit einem hepatozellulären Karzinom der BCLC- Score durchgesetzt und war dafür auch in einer späteren, randomisierten Studie geeignet, die unten vorgestellt wird[70,102] **(Publikation 3)**.

7.3 Die interstitielle Brachytherapie und die transarterielle Chemoembolisation bei Patienten mit hepatozellulären Karzinomen

7.3.1 Vergleich in einer randomisierten Studie

Frühere Arbeiten haben die hohe lokale Effektivität der iBT auch in großen hepatozellulären Karzinomen nachgewiesen, gleichzeitig aber auf die im Vergleich zu Metastasen höhere Komplikationsrate abgestellt, insbesondere bei Patienten mit fortgeschrittener Leberzirrhose. Diese betreffen vor allem interventionsbedingte Komplikationen wie Blutungen[70,83].
Die transarterielle Chemoembolisation (TACE) ist das therapeutische Standardverfahren für Patienten im BCLC-B Stadium[155]. In randomisierten Studien aus der Jahrtausendwende war für die TACE- Patienten gegenüber solchen mit Best supportive care (BSC) oder Tamoxifen ein signifikanter Überlebensvorteil belegt worden[156].
In einer randomisierten, prospektiven Studie wurden 77 Patienten mit hepatozellulären Karzinomen (HCC) entweder mittels CT-gesteuerter interstitieller Brachytherapie (iBT) oder konventioneller transarterieller Chemoembolisation (cTACE mit Lipiodol und Doxorubicin) nach Randomisation behandelt. Der primäre Endpunkt war die Zeit bis zum lokal nicht mehr beherrschbaren Progress mit der zugeordneten Methode (Time- to- Untreatable-

Progression, TTUP). Sekundäre Endpunkte umfassten die Time- to- Progression (TTP) sowie das Gesamtüberleben (Overall survival, OS). Einschlusskriterien beinhalteten unter anderem ein histologisch (44%) oder (bei Vorliegen einer Leberzirrhose) bildgebend gesichertes HCC (66%) nach den Kriterien der European Association for the Study of the Liver (EASL), Nicht-Resektabilität und eine geschätzte Lebenserwartung von mehr als 16 Wochen[157,158] . Ausschlusskriterien waren eine Portalvenenthrombose (PVT) auf der Tumorseite, extrahepatische Manifestationen, eine Leberzirrhose im Child-Pugh-C Stadium und Zweitkarzinome. Der Therapiearm und die Kontrollgruppe unterschieden sich nicht hinsichtlich zahlreicher Parameter wie dem BCLC- oder Child-Pugh-Stadium, dem Alter, AFP-Level, Tumordurchmesser oder der Anzahl der Läsionen sowie der Ätiologie. Lediglich der prätherapeutische Bilirubinlevel war in der cTACE-Gruppe (18,9µmol/l; IQR 11,4-28,9) signifikant höher als in der iBT- Gruppe (12,2 µmol/l; IQR 9,9-15,7; p=0,007). 84% in der iBT-Gruppe und 88% in der cTACE- Gruppe waren therapienaiv. Nach Erreichen des primären Endpunktes gab es keine Einschränkungen bezüglich weiterer Therapien, so dass 14 Patienten in der cTACE- Gruppe nach Studienende eine iBT erhielten, während bei einem Patienten der iBT-Gruppe nach Studienende eine cTACE durchgeführt wurde (35% vs. 3%, p<0.001). Um ein Bias durch die technisch begründeten unterschiedlichen Abbruchkriterien zu vermeiden, wurden diese bei der Feststellung zum Zeitpunkt des Auftretens zensiert (zum Beispiel die Abbruchkriterien für die cTACE wie eine PVT auf der Tumorseite, arterioportale Shunts; für die iBT unkontrollierter Aszites oder eine schwere Gerinnungsstörung).

Die analysierte Studienpopulation beinhaltete 38 Patienten in der cTACE- Gruppe und 39 Patienten in der iBT- Gruppe (Per- Protocol (PP)- und Intention- to- treat (ITT)-Population cTACE n=40, iBT n= 37).

Der Anteil der Patienten ohne Event für das TTUP lag in der iBT- Gruppe vs. der cTACE-Gruppe nach 1, 2 und 3 Jahren bei 67,5 vs. 55,2%; 56,0 vs. 27,4% und 29,5 vs. 11%, (ITT, HR 0,52, p= 0.021). Die Stratifizierung nach BCLC- Stadien ergab für die Patienten im BCLC-B Stadium einen Vorteil der iBT auf Signifikanzniveau (HR 0,38, p=0.021).

Der Anteil der Patienten ohne Event für das TTP lag in der iBT- Gruppe vs. der cTACE- Gruppe nach 1, 2 und 3 Jahren bei 56,0 vs. 28,2%; 23,9 vs. 6,3% und 15,9 vs. 6,3%, (ITT, HR 0,49, p= 0.008). Die Stratifizierung nach BCLC- Stadien ergab für die Patienten im BCLC-B und C-Stadium einen Vorteil der iBT nahe des Signifikanzniveaus (HR 0,46 bzw. 0,36, p=0.051 bzw. 0,063).

Der Anteil der Patienten ohne Event für das OS lag in der iBT- Gruppe vs. der cTACE- Gruppe nach 1, 2 und 3 Jahren bei 78,4 vs. 67,7%; 62,0 vs. 47,3% und 36,7 vs. 27,0%, (ITT, HR 0,61, p= 0.097). Die Stratifizierung nach BCLC- Stadien ergab keine Unterschiede auf Signifikanzniveau, die Hazard-Ratio in BCLC A, B und C lag bei 0,92, 0,55 und 0,52 (p=0,890; 0,179 und 0,212).

Signifikante Einflussfaktoren in der multivariaten Regressionsanalyse auf das TTUP waren unabhängig voneinander: weibliches Geschlecht (HR 4,21, p<0.001), der iBT- Arm (HR 0,49, p=0,019), der AFP-Level (HR1,13, p=0,001) und ein Child-Pugh B-Stadium (HR 3,81, p=0,036).
Signifikante Einflussfaktoren in der multivariaten Regressionsanalyse auf das TTP waren unabhängig voneinander: der iBT-Arm (HR 0,49, p=0,011) und ein Child-Pugh B-Stadium (HR 3,12, p=0,045).
Signifikante Einflussfaktoren in der multivariaten Regressionsanalyse auf das OS waren unabhängig voneinander: weibliches Geschlecht (HR 3,46, p=0.002), der AFP- Level (HR 1,17, p<0,001) und ein Child-Pugh B- Stadium (HR 5,76, p=0,006).
Für Tumordurchmesser oder Anzahl der Läsionen ergab sich weder in der uni- noch in der multivariaten Datenanalyse ein Einfluss auf die Outcome-Parameter auf Signifikanzniveau.
Bei den schweren Komplikationen Grad 3 oder höher wurden zwischen beiden Therapiearmen in einer interventionsbasierten PP- Analyse (iBT n= 120 Interventionen, cTACE n= 163) keine signifikanten Unterschiede in der Anzahl gesehen[102] **(Publikation 26)**.

Damit zeigte sich ein verlängertes TTUP und TTP für die Patienten im iBT- Arm gegenüber den Patienten im cTACE- Arm mit einer HR von 0,49 (p= 0,019 bzw. 0,011). Vor allem Patienten im BCLC-B Stadium profitierten von der Randomisation in den iBT- Arm, also dem Stadium, wo leitliniengerecht die cTACE empfohlen wird. Dass dieser Vorteil nicht auf das Gesamtüberleben durchschlug, kann einerseits mit den Limitationen dieser Studie zusammenhängen, wobei designbedingt eine größere Anzahl an Patienten aus dem cTACE-Arm nach dem Erreichen des primären Endpunktes eine iBT erhielten. Andererseits wies das eingeschlossene Patientenkollektiv mit Patienten in allen BCLC-Stadien eine relevante Heterogenität auf. Die Aussagekraft ist zudem limitiert durch die insgesamt geringe Patientenanzahl, die aber für eine solche explorative Studie als ausreichend betrachtet werden kann. Eine Pilotstudie hatte in einer Matched-pair-Analyse von HCC- Patienten mit und ohne iBT ein signifikant verlängertes medianes Gesamtüberleben für die Patienten in der iBT-Gruppe ermittelt (37,5 vs. 18 Monate, p<0.001), diese Analyse wurde aber methodisch bedingt retrospektiv durchgeführt[70].
Kein Vorteil für den primären oder die sekundären Endpunkte war für das BCLC-A Stadium zu konstatieren. Einerseits war die cTACE bei limitierter Anzahl und Größe offensichtlich ähnlich effektiv. Andererseits muss hinsichtlich der Einschlusskriterien kritisch angemerkt werden, dass bei kleinen hepatozellulären Karzinomen mit der Radiofrequenzablation eine effektive und leitliniengerechte Methode existiert, die insbesondere bei Tumoren bis zu 2 cm Tumordurchmesser eine gute Tumorkontrolle bietet bei geringerer Hospitalisierung und prozeduraler Morbidität als bei der chirurgischen Resektion[159]. Die häufig postulierte

onkologische Äquivalenz der RFA mit der chirurgischen Resektion von HCC im frühen und sehr frühen Stadium wird allerdings durch aktuellere Metaanalysen bei einer höheren Rezidivrate und geringerem 3 und 5 bzw. 5-Jahres-Überleben der RFA- Patienten auch bei sehr frühen HCC <2cm in Frage gestellt, ein Selektionsbias darf aber vermutet werden[160,161].
Überraschend war das deutlich schlechtere Outcome (ohne Unterscheidung der Gruppen) der weiblichen Patienten sowohl für das TTUP (HR 4,21) als auch für das OS (HR 3,6). Dies steht im Widerspruch zur aktuellen Literatur zumindest für HBV- assoziierte HCC, und sollte Gegenstand weiterer Untersuchungen sein[162]. Der Einfluss des Stadiums der Leberzirrhose war erwartbar hoch (HR 3,81 bzw. 5,76).
Die Ergebnisse dieser ersten, randomisierten Phase II- Studie zur iBT fließen aktuell in die Planung einer größeren Phase-III Studie ein (PI Prof. J. Ricke, München).

7.3.2 Die interstitielle Brachytherapie als Bridging-Therapie vor Lebertransplantation

Vor dem Hintergrund des Mangels an Spenderorganen in Deutschland und der deshalb häufig notwendigen Bridging-Therapie für Patienten mit einem hepatozellulären Karzinom innerhalb (teilweise vor der Brückentherapie auch außerhalb) der Milan-Kriterien auf der Transplantations-Warteliste ist eine Matched-Pair-Analyse interessant[163,164].
Dabei wurden 12 Patienten, die vor einer Lebertransplantation eine iBT als Brückentherapie erhielten, anhand verschiedener Kriterien mit Patienten „gemachted“, die mit der gleichen Intention eine TACE erhielten. Bei der histopathologischen Aufarbeitung nach der Lebertransplantation zeigten die mit der iBT behandelten Läsionen ein überlegenes Tumoransprechen mit einer vollständigen bzw. partiellen Tumornekrose in 33 vs.5% bzw. 58 vs. 36% (p=0,018) gegenüber den Läsionen, die mittels TACE therapiert worden waren.
Die allgemeine Nekrose-Rate lag für die iBT bei 63% (+/-10) und für die TACE bei 22% (+/-7, p=0.002). Unter den beurteilbaren Tumoren mit partieller Nekrose zeigten die hepatozellulären Karzinome, die mittels iBT therapiert worden waren, einen niedrigeren Differenzierungsgrad als die TACE-therapierten (p=0,041). Stichkanalmetastasen wurden nicht beobachtet. In der histologischen Aufarbeitung lagen 100% der iBT-therapierten Patienten innerhalb der Milan-Kriterien (TACE 75%). In einer Subgruppenanalyse der Patienten innerhalb der Milan-Kriterien vor *Bridging*-Therapie erlitt keiner der Patienten nach Transplantation ein Tumorrezidiv.
Die Aussagekraft ist trotz der geringen Anzahl an untersuchten Patienten wegen der histopathologischen Korrelation als nicht zu gering einzuschätzen und der Wert der iBT als Brückentherapie vor Lebertransplantation sollte in größeren, prospektiven Studien überprüft werden[112].

7.4 Die interstitielle Brachytherapie und die thermische Ablation

Die Grenzen der thermischen Ablation sind bekannt[42,51,52]. Die iBT ist in deutlich geringerem Maße limitiert. Ein randomisierter Vergleich zwischen beiden Methoden existiert bisher nicht, da sich die Einschlusskriterien vor allem hinsichtlich der Größe erheblich unterscheiden. Ein mögliches Studienprotokoll wäre gegebenenfalls der randomisierte Vergleich des *Outcomes* bei Patienten mit kolorektalen Lebermetastasen zwischen 3 und 5 cm und limitierter Gesamtanzahl.

Eine frühe Studie hat in einer intraindividuellen, läsionsbasierten Matched-Pair-Analyse die lokale Kontrollrate (LCR) bei 18 Patienten mit 36 kolorektalen Lebermetastasen untersucht, die in verschiedene Metastasen entweder mit laser-induzierter Thermotherapie (LITT, ebenfalls ein thermoablatives Verfahren) oder einer iBT behandelt worden waren.

Dabei war die LCR für die brachytherapierten Läsionen dann signifikant höher, wenn das Matchkriterium Tumorgröße (<= 5cm) außer Acht gelassen wurde, und lag nach 6, 9 und 12 Monaten bei 87%, 80% und 72% für die iBT- Gruppe und 73%, 44% und 36% für die LITT-Gruppe (p=0.04). Eine höhere lokale Kontrollrate war auch für Tumoren <= 5 cm erkennbar, allerdings nicht auf Signifikanzniveau (p=0,23)[165] **(Publikation 27)**.

Dieses Ergebnis überrascht nicht, da die Brachytherapie auch bei Tumoren über 5 cm eine effektive lokale Kontrolle erzielen kann. Interessanterweise wurden diese Patienten noch vor der Dosisfindungsstudie von 2010 behandelt, zu einem Zeitpunkt also, als auch bei kolorektalen Lebermetastasen noch geringere Zieldosen von 15-20 Gy üblich waren[72].

7.5 Die interstitielle Brachytherapie im Vergleich zur Stereotaxie: mehr Dosis für den Tumor, weniger Dosis im Leberparenchym

Die extrakranielle, hypofraktionierte stereotaktische Bestrahlung (SBRT) von Metastasen des Thorax und des Bauchraumes, hat, dem Konzept der Oligometastasierung folgend, in den letzten Jahren an Bedeutung gewonnen.

Sowohl die signifikanten Verbesserungen in der lokalen Tumorkontrolle durch die kranielle Stereotaxie als auch die Einführung der Image Guided RadioTherapy (IGRT) und der Intensity Modulated RadioTherapy (IMRT) haben den Transfer dieser Technik in extrakranielle Indikationen begünstigt. Allerdings sind bei der extrakraniellen Anwendung Unsicherheiten durch Bewegungen, bedingt durch die Atemexkursionen vor allem von Leber und Lunge ein signifikantes Problem. Daraus resultieren anspruchsvolle Anforderungen an Technik und Planung. Die stereotaktische Bestrahlung stellt aber ein elegantes Verfahren der metastasengerichteten Therapie dar, auch wegen des alleinstellenden Vorteils der Nicht-Invasivität. Die Erfahrung mit dieser Technik wächst, was sich an der steigenden Anzahl von Publikationen zur SBRT von Leber- und Lungenmalignomen ablesen lässt[166-171].

Auf der einen Seite bietet die SBRT also eine nicht- invasive Möglichkeit der effektiven Behandlung von Metastasen, interventionell bedingte, periinterventionelle Komplikationen wie Blutungen können hier nicht auftreten[172]. Auf der anderen Seite gehen bei Hypofraktionierung die hohen Dosen mit einer signifikanten Exposition des umgebenden Gewebes einher. Für effektiv behandelbare Läsionen gilt ein Limit von etwa 4-5 cm und die Anzahl gleichzeitig behandelbarer Läsionen ist begrenzt[55,56]. Dies führt dazu, dass die Balance zwischen effektiver Dosis und Sicherheitserwägungen in der klinischen Routine häufig schwierig zu finden ist.

Daten verschiedener Studien zeigen eine Komplikationsrate von CTCAE Grad 3- und Grad 4-Ereignissen mit einer breiten Streuung von 0 bis 78% and 0 bis 25%. Dies schloss gastroduodenale Ulzerationen, Leber-Toxizitäten, Übelkeit/Erbrechen, Ösophagitis und Gallengangs-Stenosen ein[173]. Nach der aktuellen Literaturlage soll eine RILD der Leber im Vergleich zu konventionellen Bestrahlungsmethoden seltener vorkommen, bleibt aber beispielsweise bei der SBRT von hepatozellulären Karzinomen ein klinisches Problem mit Auswirkung auf das Outcome der Patienten[174].

In einer vergleichenden Studie an 85 Patienten und Lebermalignomen verschiedener Entitäten, die mit der iBT behandelt worden waren, wurden post-hoc virtuelle SBRT- Pläne (ebenfalls einzeitige Behandlung) mit derselben Zieldosis zwischen 15 und 20 Gy an der originalen Bestrahlungs-Planungs-CT unter Berücksichtigung der Risikoorgane und gegebenfalls konsekutiver Dosisreduktion erstellt und die dosimetrischen Daten miteinander verglichen (PTV iBT- Planung 34,7 cm^3 (0,5-410) , SBRT- Planung 73,2 cm^3 (6,1-593,4).

Die Abdeckung des PTV mit der Zieldosis wurde in der iBT- Planung signifikant besser erreicht als in der SBRT- Planung. Für die D99.9, also die 99,9%ige Abdeckung des PTV waren das 19,9 +/-0,4 Gy (iBT) vs. 17,5 +/-0,5 Gy (SBRT) bei einer Zieldosis von 20 Gy ($p<0.001$). Das Signifikanzniveau war auch für die 15 Gy-Zieldosis nachweisbar ($p=0.003$). Geradezu extrem ist die Abweichung bei der D90, also der minimalen Abdeckung für 90% des Zielvolumens. Hier erreichte die iBT- Planung bei 15- Gy Zieldosis wegen der heterogenen Dosisverteilung durch die Dosiseskalation im Tumorzentrum und dem steilen Dosisabfall zur Peripherie hin, 24,3 +/- 0,8 Gy gegenüber 16,5 +/- 0,3 Gy in der SBRT- Planung ($p<0.001$), bei 20 Gy Zieldosis waren das 29,2 +/-0,4 Gy (iBT) vs.20,6 +/-0,3 (SBRT, $p<0.001$).

In der Gruppe mit der höheren Zieldosis von 20 Gy war die Leberexposition in der SBRT-Planung signifikant höher als in der iBT- Planung. Das 5 Gy-Volumen (V5Gy) betrug hier 611 +/-43 cm^3 (iBT) vs. 694+/-37 cm^3 (SBRT, $p=0.001$), in Volumenprozent des Gesamtlebervolumens 41,8 +/-2,5% (iBT) vs. 45,9 +/-2,0% ($p=0.007$)[175] **(Publikation 28)**.

In einer früheren vergleichenden Studie wurde der umgekehrte Weg gewählt und virtuelle Brachytherapie- Pläne mit tatsächlich applizierten SBRT- Plänen bei 10 Lebermetastasen verglichen. Im Ergebnis sahen die Autoren keinen Unterschied im mittleren Volumen, das von

100% der Zieldosis erfasst wurde (94,1 vs. 93,9%, p=0,8), das mittlere Volumen, das 150% der Zieldosis erhielt, lag für die iBT bei 63,6%, für die SBRT bei 0%. Die minimale Dosis für das PTV betrug 65,8% für die iBT und 87,4% für die SBRT (p=0,0002). Die mittlere Dünndarmdosis war für die iBT höher als für die SBRT (10,8 vs. 7,1%, p=0.006). Die Autoren schlussfolgerten, dass die iBT- Planung zwar zu einer höheren Dosis im Tumor, aber zu einer schlechteren Abdeckung des Zielvolumens führt[176].

Die Ergebnisse dieser Studie stehen im Widerspruch zu den Resultaten der Studie unserer Arbeitsgruppe. Dies kann mehrere Gründe haben. Erstens ist die Erstellung eines der Realität nahekommenden, virtuellen iBT- Plans ohne interventionell-radiologische Grundkenntnisse über die Möglichkeiten der Kathetereinbringung nur bedingt möglich. Zweitens wird in Teams, die die iBT in der klinischen Routine einsetzen, eben wegen der Heterogenität bzw. Inhomogenität der Dosisverteilung die mittlere Dosis im PTV nicht verwendet, sondern die maximale Punktdosis am Tumorrand (D100 oder D99,9, seltener auch die D90), bei Risikoorganen der am höchsten exponierte Kubikzentimeter (Dmax./1cm^3). Dieses Konzept wurde kürzlich für die SBRT adaptiert[177]. Es ist radiobiologisch gut begründet, hat sich in Studien als sinnvoll erwiesen und wird in der Studie von Pennington ignoriert. Hinzu kommen die verbliebenen Unsicherheiten durch die Atembeweglichkeit der Leber der SBRT, so dass jüngere Studien auf die Bedeutsamkeit der mittleren Dosis im Gross-Tumor-Volume (GTV) und eine darauf abzielende Dosisoptimierung für Tumorkontrolle und Outcome hingewiesen haben[178-181].

Limitationen der Studie unserer Arbeitsgruppe sind, dass die SBRT (virtuell) einzeitig geplant wurde, während in der klinischen Realität ein mehrzeitiges, hypofraktioniertes Schema mit höheren Einzeldosen bevorzugt wird. Zudem wurde die Studie vor Veröffentlichung der ICRU 91 konzipiert und deshalb die SBRT-Planung auf die D99,9 optimiert.

Nichtsdestotrotz bleibt die Nicht-Invasivität ein großer Vorteil der SBRT, und die Effektivität moderner stereotaktischer Konzepte wurde in einer Vielzahl von Lokalisationen nachgewiesen. Man darf auf Grundlage der bisherigen Evidenz annehmen, dass die invasive Brachytherapie ihre Vorteile vor allem bei großen Tumoren und in ihrer Wiederholbarkeit ausspielt.

Eine prospektiv randomisierte, sogar multizentrische vergleichende Studie wird es in absehbarer Zeit nicht geben, da der Verbreitungsgrad der iBT- Technik und das dafür notwendige interventionell-radiologische Know-how noch gering sind. Es wäre wünschenswert, wenn zukünftige Studienkonzepte unter Einschluss dieser beiden und anderer lokal-ablativer Techniken eine Stratifizierung der Patienten adressieren würde.

8 Die interstitielle Brachytherapie bei Malignomen des Oberbauches außerhalb der Leber

In den letzten Jahren wurden eine Reihe von Pilotstudien zur Effektivität und Sicherheit der iBT bei nichthepatischen Malignomen des Oberbauches veröffentlicht.

8.1 Die iBT von Nebennierenmetastasen im Kontext anderer lokaler Verfahren

37 Patienten mit Nebennierenmetastasen (adrenal gland metastases, AGM, mittlerer Tumordurchmesser 5,4 cm, SD +/-2,9) verschiedener Primarien (n= 10 (kolorektal), 7 (Bronchialkarzinom), 6 (Nierenzellkarzinom), 5 (hepatozelluläres Karzinom), 9 (andere)) wurden mit der iBT behandelt. Alle patienten- und behandlungsrelevanten Informationen wurden prospektiv in einer Datenbank erfasst, ebenso die diagnostischen und therapeutischen Informationen des Nachsorgezeitraums. Primärer Endpunkt war die lokale Tumorkontrolle (local- tumor- control, LTC), sekundäre Endpunkte umfassten unter anderem die Time- to- Progression (TTP), die Time- to- untreatable-Progression sowie das Gesamtüberleben (Overall survival, OS). Das Ansprechen wurde nach RECIST 1.1. bewertet. Toxizitäten wurden nach den CTCAE-Kriterien vs. 4.03 erfasst. 36 Patienten erhielten die iBT an einer unilateralen AGM, 1 Patient an bilateralen AGM. 35 Brachytherapien wurden einzeitig durchgeführt, in zwei Metastasen war eine zweizeitige Behandlung im Abstand von 2 Wochen wegen der Tumorgröße erforderlich. Das mittlere CTV betrug 100.7 cm^3 (+/-130), 20 AGM maßen im Durchmesser >4cm (53%), 18 Metastasen waren bis zu 4 cm groß, 14 AGM wurden synchron mit dem Primarius diagnostiziert (38%). Die mediane D100 betrug 15,5 Gy (95% Konfidenzintervall 14,0-16,7), einer biologischen Äquivalentdosis (BED) von 39,8 Gy entsprechend (95% Konfidenzintervall 15,5-73). Bezgl. der Angabe der BED muss einschränkend angemerkt werden, dass das linearquadratische Modell (LQM) für hohe Einzeldosen nicht validiert ist, die BED aber für eine zumindest grobe Vergleichbarkeit mit therapeutischen Effekten in Studien zur stereotaktischen Bestrahlung angegeben wurde. 3 Interventionen wurden von einer Kortison-Substitution begleitet.

Die LTC nach 12 Monaten lag bei 88% und nach 24 Monaten bei 74% (3 Lokalrezidive/37 AGM). 6 AGM zeigten eine Komplettremission (18%/ 33 AGM mit Follow- up) und 25 AGM (75%) eine partielle Remission, einem objektiven Ansprechen (*objective-response-rate*, ORR) von 94% für die AGM mit follow- up (n=33) und 84% für alle AGM (n=37) entsprechend. Die Minor-Komplikationsrate Grad 1-2 lag bei 29% (n=11), die Major-Komplikationsrate bei 3% (n=1, Grad 3- Blutung, die mittels angiografischer Embolisation versorgt wurde). Dabei wurde ein medianes OS von 18,3 Monaten nach Erstdiagnose der AGM beobachtet. Nach der iBT war das OS, TTUP und TTP 11,4, 6,6 und 3,5 Monate. In einer multivariaten

Regressionsanalyse hatten 2 Faktoren Einfluss auf das OS auf Signifikanzniveau: der Tumordurchmesser und synchrone AGM (p= 0,005 und 0,030).
In einer konsekutiven Kaplan-Meier-Analyse war das OS 16,2 und 3,8 Monate für metachrone und synchrone AGM (log rank p< 0,0001) sowie 27,1 und 5,3 Monate für einen Tumordurchmesser <4,0 cm und ≥4,0 cm (log-rank, p= 0,001)[182] **(Publikation 29)**.

Die Evidenz für die lokale Therapie von Nebennierenmetastasen ist schwach und bei der beschriebenen Arbeit unserer Gruppe handelt es sich um eine der größten Einzelstudien bei dieser Entität. Eine Metaanalyse über den Zeitraum von 1990 bis 2012 fand lediglich 45 Studien mit insgesamt 818 Patienten, von denen 178 mit SBRT und 51 mit thermischer Ablation behandelt wurden[183]. Darunter war keine prospektiv randomisierte Studie. Weiterhin sind Studien mit homogenen Patientenkollektiven selten, da sonst prävalenzbedingt keine relevanten Patientenzahlen erreicht werden können.

Die retrospektive Studie einer deutschen Arbeitsgruppe zur SBRT an 33 Patienten mit AGM (medianes Gross-Tumor-Volume [GTV] von 24,15 cm^3, range 8,37-133,44, mediane BED 67,2 Gy, range 42-108,8 Gy) führte in 21 von 31 AGM mit radiologischer Nachsorge zu einem objektiven Ansprechen (67%, davon 4 = 12,9% in kompletter Remission). Lokalrezidive traten in 4/31 AGM auf (12,9%). Das mediane Gesamtüberleben lag bei 11 Monaten, das mediane PFS betrug 4 Monate. In Kaplan-Meier-Analysen wurde eine Korrelation des OS mit der applizierten BED bzw. kurativer vs. palliativer Intention gesehen (p=0.046 bzw. p<0.0001, Test nicht angegeben), Grad 3- Toxizitäten oder höher wurden nicht beobachtet [184].
Eine aktuelle, retrospektive Studie zur SBRT fand bei 31 Patienten mit 33 AGM (mittlerer Tumordurchmesser 3,9 cm, synchrone AGM 15,2 %), die extrahepatisch kontrolliert und adrenal progredient waren, bei einer medianen BED von 112,5 Gy eine lokale Kontroll-Rate von 97 und 93% nach 12 und 24 Monaten, insgesamt wurden 3 Lokalrezidive gezählt. Das mediane Gesamtüberleben betrug 33,5 Monate, Grad 3-Toxizitäten oder höher wurden nicht beobachtet [185].
Eine dritte Studie zur SBRT bei 35 Patienten mit 39 AGM (medianer Tumordurchmesser 2,9 cm, Bereich 0,7-9 cm, 20% Patienten mit synchronen AGM), einem medianen GTV von 19 cm^3 (1,3 -213,2) und einer medianen BED von 72 (30-124,8) zeigte im Ergebnis eine Lokalrezidivrate von 7,6% nach 12 Monaten und 19,2 % nach 3 Jahren. Das mediane OS betrug 19 Monate und korrelierte mit der Tumorgröße (p=0.006). So war das OS bei Patienten mit AGM<2,9 cm 54 Monate und für Patienten mit AGM>= 2,9 cm 11 Monate, Grad 3-Toxizitäten oder höher wurden nicht beobachtet[186].

In diesen Studien zur SBRT bei AGM wurden gute lokale Kontrollraten mit teils längerem medianen OS als in dem Patientenkollektiv der iBT- Studie erzielt. Major-Komplikationen wurden dabei nicht beobachtet, allerdings wurde in einer Pilotstudie zur SBRT von AGM von gastroduodenalen Ulzerationen in 2/18 Patienten berichtet (11%)[187]. Teils wurde eine signifikante Korrelation des OS mit der Tumorgröße angegeben, teils mit der applizierten BED. Die iBT- Kohorte (Major-Komplikationen 3%) umfasste aber deutlich größere Tumoren als die SBRT- Kohorten (mittlerer Tumordurchmesser und CTV 5,4 cm, 100,7 cm^3) und wies weiterhin einen wesentlich höheren Anteil an synchronen AGM (37%) auf. Nach Applikation einer moderaten BED wurde mit einer ORR von 94% eine sehr gute Tumorkontrolle erzielt. Zudem wurden die Daten der iBT- Studie prospektiv dokumentiert. Tumordurchmesser und synchrone AGM waren hochsignifikante Prädiktoren für das OS in unserer Studie. Der Tumordurchmesser war in einer weiteren Studie (SBRT) ebenfalls signifikant mit dem OS korreliert. In einer gepoolten Analyse von 13 Studien mit insgesamt 98 Patienten, deren isolierte AGM bei nichtkleinzelligen Bronchialkarzinomen reseziert worden waren, hatten die Patienten mit synchronen AGM in einer univariaten Abschätzung ein signifikant geringere Gesamtüberlebens-Rate nach 12 und 24 Monaten (49,9 vs. 82,5% und 26,7 vs. 53,7%, p=0.014)[188].

Bei kleinen Tumoren scheint die SBRT unter Berücksichtigung der aktuellen Literaturlage effektiv zu sein und die Möglichkeit schwerer, interventionell bedingter Komplikationen scheidet aus (siehe die Grad- 3 Blutung in der iBT- Kohorte). Der Vergleich der OS-Daten ist aber auf Basis dieser Evidenz nur sinnvoll, wenn hochrelevante Faktoren wie die Tumorgröße und synchrone AGM, aber auch die Anzahl der Tumorlokalisationen einschließlich extrahepatischer Manifestationen (definierend für das oligometastasierte Stadium, multivariat signifikant prädiktiv in der iBT- Kohorte für das TTUP, p=0.032) adressiert werden. Eine zukünftige, gepoolte Metaanalyse zur Radiatio von AGM (einschließlich SBRT und iBT) sollte diese prognostisch bedeutsamen Charakteristika berücksichtigen, um eine sinnvolle Therapiestratifizierung im Hinblick auf die Frage, ob und welche Lokaltherapie bei AGM eingesetzt wird, zu ermöglichen. Festzuhalten bleibt in diesem Zusammenhang, dass keinerlei Evidenz auf einem akzeptablen Niveau für eine bevorzugt chirurgische Therapie auch von isolierten AGM existiert[183].

8.2 iBT bei Nierenmalignomen, Lymphknoten und Pankreas sowie peritonealen Absiedelungen

In einer Pilotstudie zur iBT von 20 Nierenmalignomen (18 primäre Nierenzellkarzinome (NCC) und 2 Metastasen (von kolorektalen bzw. hepatozellulären Karzinomen) wurden bei einer mittleren Tumorgröße von 3,5 cm (1,2 -9,4) und einer D100 von 16,37 +/- 2,38 Gy 3 Lokalrezidive beobachtet, einer primären lokalen Kontrollrate von 85% entsprechend. 2 dieser

Rezidive wurden dosiseskalierend erfolgreich erneut behandelt, was zu einer sekundären lokalen Kontrollrate von 95% führte. Das mediane OS lag bei 27,0 Monaten. Eine periinterventionelle CTCAE Grad 3b-Blutung trat auf. Im Übrigen wurden Sicherheitsaspekte dieser Studie bereits ausführlich in Kapitel 4.5 erörtert[132] **(Publikation 20)**.

13 Patienten mit 13 Pankreasläsionen (8 Metastasen und 5 Primärtumore, davon 2 Lokalrezidive) wurden bei einem medianen Tumordurchmesser von 3 cm und einer D100 von 15,3 Gy mit der iBT behandelt[133] **(Publikation 21).** Bei einem medianen *Follow-up* von 6,7 Monaten (3,2-55,6) entwickelte eine behandelte Läsion ein Lokalrezidiv. Das mediane PFS war 6,2 Monate, das mediane OS 16,2 Monate, für Patienten mit sekundären Pankreasmetastasen waren das 7,4 und 45,6 Monate (Sicherheit Kapitel 4.5).

Eine sehr hohe lokale Kontrollrate bei einer vergleichsweise niedrigen medianen D100 von 15 Gy konnte in einer retrospektiven Studie bei 40 Metastasen von gastrointestinalen Stromatumoren (GIST) erreicht werden, die auch 10 peritoneale Läsionen einschloss.
Sie betrug nach 25 Monaten 97,5% (1 Lokalrezidiv). Das mediane progressfreie Überleben bzw. Gesamtüberleben lag bei 6,8 bzw. 37,3 Monaten[92] **(Publikation 5).**

In einer sehr frühen Studie bei einer heterogenen, hochpalliativen Kohorte von Patienten mit extrahepatischen, extrapulmonalen Malignomen, die unter anderem retroperitoneale Lymphknoten, die Bauchwand unter anderem Lokalisationen einschloss, betrug die lokale Tumorkontrolle immerhin 76,5% nach 6 Monaten bei applizierten Einzeldosen zwischen 6 und 10 Gy in 4 Lokalrezidiven, wobei die dabei applizierten Einzeldosen vergleichsweise gering waren[189].

9 Zusammenfassung

Im globalen Maßstab nahm die Anzahl der neuen Krebserkrankungen zwischen 2005 und 2015 um 33% zu, was vor allem mit der Zunahme der Weltbevölkerung als auch der zunehmenden Lebenserwartung zusammenhängt[2]. Die krankheitsspezifische Mortalitätsrate ist in den letzten 20 Jahren dagegen zurückgegangen, was zuvorderst auf die Fortschritte in der Therapie zurückzuführen ist. Dabei hat auch die Evolution der lokalen Therapieverfahren Anteil an dieser positiven Entwicklung[3].

Die Fortschritte in der medikamentösen Tumortherapie der letzten Jahre haben den Stellenwert der systemischen Behandlung bei einer Reihe von Tumorentitäten im metastasierten Stadium noch einmal erhöht. Ungeachtet dessen hat die metastasengerichtete Tumortherapie in einer Reihe von Studien einen Wirksamkeitsnachweis erzielt. Bei einem Teil der Patienten vor allem mit kolorektalen Lebermetastasen werden nach Resektion der Lebermetastasen Langzeitüberlebensraten erreicht, die an eine Kuration heranreichen. Da aber selbst mit fortgeschrittenen Operationsverfahren lediglich etwa 20-30% (nach neoadjuvanter systemischer Tumortherapie 40-50%) der Patienten einer Operation technisch zugänglich sind, gibt es einen Bedarf an weiteren, effektiven Lokalverfahren [29,30].

Die Möglichkeiten der modernen radiologischen Verfahren führten zur Entwicklung minimalinvasiver Therapien wie der Radiofrequenzablation (RFA), die die am weitesten verbreitete Methode mit der stärksten Evidenz darstellt[41]. Die RFA und andere thermoablative Lokaltherapien wie die Mikrowellenablation MWA sind im Hinblick auf die Lage und Größe der zu behandelnden Tumoren jedoch technisch limitiert[51,52]. Radiotherapeutische Techniken, wie die perkutane stereotaktische Bestrahlung (SBRT) oder die CT- gesteuerte interstitielle Brachytherapie (iBT), können diese Grenzen in unterschiedlicher Weise überwinden, wobei – ähnlich wie bei der Thermoablation – für die perkutane Behandlung eine maximale Größe und Anzahl effektiv behandelbarer Läsionen gilt[55,56]. Jenseits dessen sinkt die Wirksamkeit der SBRT [57,58].

Bei der bildgeführten interstitiellen Brachytherapie wird eine Punktquelle, zum Beispiel ^{192}Iridium, in den Tumor eingeführt. Sie erlaubt bei exakter, atemunabhängiger Dosimetrie die Einbringung sehr hoher Dosen bis zu 25 Gy als Einzelfraktion. Dabei fällt die Dosis zur Peripherie hin stark ab, was im Allgemeinen eine effektive, tumorizidale Dosis bei Schonung der umgebenden Strukturen auch bei sehr großen und zentral gelegenen Tumoren ermöglicht[63,64]. Einerseits sprechen Patientenkomfort und Sicherheit für die einzeitige Hypofraktionierung. Andererseits zeitigt die Radiatio mit hohen Einzeldosen (> 10–12 Gy) zusätzliche therapeutische Phänomene, die über die strahlentherapeutischen Effekte mit geringeren Einzeldosen hinausgehen. Hier wird unter anderem eine Apoptose-Induktion am Gefäßendothel postuliert[65,66]. Komplettremissionen sind nicht die Ausnahme.

Die überproportionale Effektivität wird durch initiale Studienergebnisse bestätigt [62-64,68-73].
In zahlreichen Pilotstudien und in randomisierten Vergleichen konnte bei verschiedenen Entitäten prospektiv und retrospektiv eine hohe bis sehr lokale Tumorkontrolle von bis zu >90% nach 12 Monaten gezeigt werden. Nachweisbar war dabei eine Dosisabhängigkeit, wobei die hepatischen Absiedelungen der meisten Entitäten mit 15-20 Gy hervorragend lokal kontrolliert werden können, während die notwendige D100 bei kolorektalen Karzinomen am höchsten ist. Die interstitielle Brachytherapie ist hinsichtlich der Leberfunktion sicher durchführbar. Klassische RILD sind in eigenen Studien sowie ausweislich der publizierten Daten anderer Arbeitsgruppen nicht beobachtet worden, atypische Fälle mit ikterischem Anstieg der Leberenzyme und Aszites wurden in Einzelfällen berichtet. Das Monitoring des Funktionsverlustes des umgebenden Lebergewebes lässt sich ausgezeichnet mittels MRT mit hepatozytenspezifischem Kontrastmittel durchführen. Die Grenzdosis für den temporären Funktionsverlust nach 6 Wochen beträgt im Mittel 9-10 Gy, das entsprechende Volumen geht nach 24 Wochen auf die 14-16 Gy Isodosenlinie zurück, was der Grenzdosis für den permanenten Funktionsverlust entspricht.
Bei bis zu 5% der Patienten tritt eine Major-Komplikation Grad 3 oder höher auf[135]. Darunter sind interventionelle Komplikationen wie Blutungen, aber auch postaktinische wie gastroduodenale Ulzerationen, und gemischt bedingte wie infektiöse Komplikationen. Nach den Ergebnissen einer Studie prädestiniert eine biliodigestive Anastomose für letztgenannte, was durch eigene Erfahrungen einer noch unveröffentlichten Arbeit gestützt wird.
Es gibt Hinweise auf eine höhere 30-Tage-Mortalität bei Patienten mit hepatozellulärem Karzinom und Leberzirrhose, die sich auch sekundär aus dem erhöhten Blutungsrisiko ableiten lassen (siehe auch unten)[70,72]. Bei großen, zentralen Lebertumoren sind klinisch relevante Komplikationen der Gallenwege selten und in entsprechenden Studien nicht mit einer Verkürzung des Gesamtüberlebens verbunden gewesen. Die ausgezeichnete Behandelbarkeit dieser zentralen Lebertumoren durch die iBT ist ein Alleinstellungsmerkmal gegenüber allen anderen lokalen Verfahren einschließlich der Chirurgie. Klinisch bedeutsame Risikoorgane außerhalb der Leber sind Magen und Duodenum. Hier wurde in mehreren Arbeiten ein Grenzwert für die Entwicklung von postaktinischen gastroduodenalen Magen-Darm-Ulzera zwischen 14 und 16 Gy Dmax/1cm^3 ermittelt. In der klinischen Routine führt dies dazu, dass ab einer relevanten gastroduodenalen Exposition von 8-10 Gy Dmax/1 cm^3 Protonenpumpenhemmer für 3-12 Monate verordnet werden und linkshepatische Tumoren gegebenenfalls mehrzeitig behandelt werden müssen. Ein anderer Ansatz ist es, interventionell Okklusionsballons zwischen Magenwand und Leberrand zu platzieren, die zu einer signifikanten Verringerung der Magenwand- Exposition führen.

Die bildgeführte, interstitielle Brachytherapie ist im Gegensatz zur perkutanen Bestrahlung mit der (minimal-) invasiven Einbringung von Kathetern verbunden, die die (z.B. ^{192}Iridium-) Quelle in den Tumor führen. Das damit verbundene Risiko auch schwerer Blutungen konnte im Gegensatz zu den dosisabhängigen Effekten der Strahlentherapie initial schwerer prognostiziert werden. Inzwischen gibt es jedoch eine gute Evidenz, die ein individuelles Risikoniveau vor dem Eingriff abzuschätzen erlaubt. Es konnte ein signifikanter Zusammenhang zwischen der Leberfunktionseinschränkung bei Leberzirrhose und dem entsprechenden Blutungsrisiko gezeigt werden. Eine andere Arbeit zeigte für Patienten nach iBT oder RFA, dass unter periinterventioneller Thromboseprophylaxe mit niedermolekularen Heparinen (NMH) Blutungsereignisse signifikant häufiger auftraten als ohne. Die Anzahl der schweren Blutungen war in der Prophylaxegruppe um mehr als den Faktor 2,6 (alle Lokalisationen) bzw. 3,3 (Leber) erhöht, und die 30- und 90 Tage-Mortalität war unabhängig von einer zeitnahen Blutungsstillung bei den Patienten mit schweren Blutungsereignissen massiv erhöht. Eine postinterventionelle NMH-Gabe erhöhte die Blutungsrate nicht. Weiterhin trat lediglich bei einer Patientin (ohne Prophylaxe) eine symptomatische Lungenembolie 2 Monate nach der Brachytherapie auf[105]. Eine periinterventionelle NMH-Gabe ist auf Grundlage der Ergebnisse dieser Studie der wichtigste Risikofaktor für eine erhöhte Blutungsrate und zwar noch vor einer Leberfunktionseinschränkung. Das Morbiditäts- und Mortalitätsrisiko der NMH-Gabe liegt weit über dem Risiko thromboembolischer Ereignisse im interventionell behandelten onkologischen Patientengut mit einer nur kurzen Immobilisationszeit und minimaler Invasivität. Eine NMH-Prophylaxe kann also nicht generell empfohlen werden, sie ist sogar, wenn nicht weitere thrombogene Komorbiditäten hinzukommen, kontraindiziert. Weiterhin zeigte sich, dass der Verschluss der Punktionskanäle mit Gelatineschwamm-Pfropfen effektiv ist und sich hierdurch kein Nachteil der iBT- Patienten gegenüber Patienten nach Thermoablation ergibt.

Das Risiko von extrahepatischen Stichkanalmetastasen ist gering, und auch das Auftreten von Lokalrezidiven nach iBT hat keinen Einfluss auf das Gesamtüberleben. In entsprechenden Studien wurde die Brachytherapie in diesen erfolgreich erneut eingesetzt.

Die publizierten Daten zum onkologischen Outcome nach iBT der Leber sind überwiegend gut bis sehr gut, auch eingedenk der Tatsache, dass mehrheitlich Patienten in der Salvage-Situation untersucht wurden. Die Überlebensdaten sind über verschiedene Studien und Arbeitsgruppen hinweg konsistent. Im Median liegt das Gesamtüberleben (OS) entitätsunabhängig bei 20 Monaten. Dabei sind bei einem Teil der Patienten zu einem signifikanten Prozentsatz auch langjährige postinterventionelle Verläufe möglich. Das längste Gesamtüberleben nach iBT zeigten Patienten mit neuroendokrinen Lebermetastasen oder metastasierten gastrointestinalen Stromatumoren sowie hepatisch metastasierte Mammakarzinome. Ein begrenzter onkologischer Effekt muss bis dato, wenn auch bei

limitierter Datenlage, für die iBT von Lebermetastasen des Pankreas, aber auch von Lungenkarzinomen postuliert werden.

Für verschiedene Tumorentitäten wurden bei Patienten nach iBT, aber auch nach einer multimodalen Therapie unterschiedliche, prognostisch bedeutsame Faktoren für das Gesamtüberleben herausgearbeitet.

In einer randomisierten, prospektiven Studie wurden Patienten mit hepatozellulären Karzinomen (HCC) entweder mittels CT-gesteuerter interstitieller Brachytherapie (iBT) oder konventioneller transarterieller Chemoembolisation (cTACE mit Lipiodol und Doxorubicin) nach Randomisation behandelt. Dabei ergab sich ein verlängertes TTUP und TTP für die Patienten im iBT- Arm gegenüber den Patienten im cTACE- Arm. Dass dieser Vorteil numerisch, aber nicht auf Signifikanzniveau auf das Gesamtüberleben durchschlug, kann einerseits mit den Limitationen dieser Studie zusammenhängen, wobei designbedingt eine größere Anzahl an Patienten aus dem cTACE- Arm nach dem Erreichen des primären Endpunktes eine iBT erhielten. Andererseits wies das eingeschlossene Patientenkollektiv eine relevante Heterogenität auf mit Patienten in allen BCLC- Stadien. Kein Vorteil für den primären oder die sekundären Endpunkte war für das BCLC- A Stadium zu konstatieren, was damit begründet werden kann, dass die cTACE bei limitierter Anzahl und Größe offensichtlich ähnlich effektiv war.

Die Ergebnisse dieser ersten, randomisierten Phase II-Studie zur iBT fließen aktuell in die Planung einer größeren Phase-III Studie ein.

Es gibt sehr wenig vergleichende Daten zur interstitiellen Brachytherapie und der Thermoablation bzw. der stereotaktischen Bestrahlung. Eine frühe Studie hat in einer intraindividuellen, läsionsbasierten *Matched-pair*-Analyse eine signifikant höhere lokale Kontrollrate nach iBT im Vergleich zur Thermoablation festgestellt, wenn Tumoren über 5 cm mit einbezogen wurden[165]. Dieses Ergebnis überrascht nicht, da die Brachytherapie – im Gegensatz zur Thermoablation – auch bei Tumoren über 5 cm eine effektive lokale Kontrolle erzielen kann.

In einer Pilotstudie wurden Vorteile der iBT bei der Erreichung der Zieldosis am Tumorrand im Vergleich zu virtuellen SBRT-Plänen festgestellt. Dies steht fraglich im Widerspruch zu einer kleineren Studie einer anderen Arbeitsgruppe, die umgekehrt einen virtuellen iBT- Plan erstellte, aber andere Endpunkte verwendete. Hier sind weitere Untersuchungen erforderlich.

Eine prospektiv randomisierte, sogar multizentrische vergleichende Studie wird es in absehbarer Zeit nicht geben, da der Verbreitungsgrad der iBT- Technik und das dafür notwendige interventionell-radiologische Know-how noch gering sind. Es wäre dennoch wünschenswert, wenn zukünftige Studienkonzepte unter Einschluss dieser beiden und anderer lokalablativer Techniken eine Stratifizierung der Patienten adressieren würde.

Nichtsdestotrotz bleibt die Nicht-Invasivität ein großer Vorteil der SBRT, und die Effektivität moderner stereotaktischer Konzepte wurde in einer Vielzahl von Lokalisationen nachgewiesen. Man darf auf Grundlage der bisherigen Evidenz annehmen, dass die invasive Brachytherapie ihre Vorteile vor allem bei großen Tumoren, kritischen Lokalisationen und in ihrer Wiederholbarkeit ausspielt.

Auch außerhalb der Leber wurden die Effektivität und das Outcome nach iBT in Pilotstudien in Nebennieren- und Nierenmalignomen, peritonealen Metastasen von gastrointestinalen Stromatumoren sowie Pankreaskarzinomrezidiven und Pankreasmetastasen untersucht. Dabei umfasste beispielsweise bei Nebenierenmetastasen die prospektiv dokumentierte iBT-Kohorte deutlich größere Tumoren als in den publizierten SBRT- Kollektiven. Nach Applikation einer moderaten BED wurde mit einem objektiven Ansprechen von 94% der therapierten Läsionen (mit bildgebender Nachsorge) eine sehr gute Tumorkontrolle erzielt. Tumordurchmesser und synchrone AGM waren hier hochsignifikante Prädiktoren für das Gesamtüberleben.

Die interstitielle Brachytherapie hat auf Grund ihrer besonderen Eigenschaften die Potenz, lokale Therapie unbegrenzt zu erlauben. Voraussetzung für eine im Sinne des Patienten sichere und erfolgreiche Therapie ist das interdisziplinäre onkologische Management. Die Patientenselektion, die Wahl der richtigen Dosis – angepasst an die jeweilige Tumorentität und unter Berücksichtigung der Risikoorgane – sowie die Komplikationskontrolle sind dabei nicht nur für die Brachytherapie entscheidende Parameter. Ihr Stellenwert im Reigen der mannigfaltigen lokalen Therapiemöglichkeiten muss in prospektiven Studien weiter erörtert werden. Es bleibt sehr zu wünschen, dass die Verbreitung dieser Technik zunimmt, um multizentrische Studien erst zu ermöglichen. Studiendesign-Vorschläge wurden in dieser Habilitationsschrift gemacht. Bereits auf Grundlage der bisherigen Evidenz zeichnet sich aber die klinische Relevanz ihrer variablen und wenig limitierten Einsetzbarkeit ab.

10 Literaturverzeichnis

1. Ferlay J, Soerjomataram I, Dikshit R, et al. Cancer incidence and mortality worldwide: sources, methods and major patterns in GLOBOCAN 2012. Int J Cancer 2015;136:E359-86.
2. Global Burden of Disease Cancer C, Fitzmaurice C, Akinyemiju TF, et al. Global, Regional, and National Cancer Incidence, Mortality, Years of Life Lost, Years Lived With Disability, and Disability-Adjusted Life-Years for 29 Cancer Groups, 1990 to 2016: A Systematic Analysis for the Global Burden of Disease Study. JAMA Oncol 2018;4:1553-68.
3. Niesen W, Hank T, Buchler M, Strobel O. Local radicality and survival outcome of pancreatic cancer surgery. Ann Gastroenterol Surg 2019;3:464-75.
4. Ferlay J, Colombet M, Soerjomataram I, et al. Cancer incidence and mortality patterns in Europe: Estimates for 40 countries and 25 major cancers in 2018. Eur J Cancer 2018;103:356-87.
5. Falzone L, Salomone S, Libra M. Evolution of Cancer Pharmacological Treatments at the Turn of the Third Millennium. Front Pharmacol 2018;9:1300.
6. Christofi T, Baritaki S, Falzone L, Libra M, Zaravinos A. Current Perspectives in Cancer Immunotherapy. Cancers (Basel) 2019;11.
7. Garlipp B, Gibbs P, Van Hazel GA, et al. Secondary technical resectability of colorectal cancer liver metastases after chemotherapy with or without selective internal radiotherapy in the randomized SIRFLOX trial. Br J Surg 2019.
8. Ricke J, Klumpen HJ, Amthauer H, et al. Impact of combined selective internal radiation therapy and sorafenib on survival in advanced hepatocellular carcinoma. J Hepatol 2019.
9. van Hazel GA, Heinemann V, Sharma NK, et al. SIRFLOX: Randomized Phase III Trial Comparing First-Line mFOLFOX6 (Plus or Minus Bevacizumab) Versus mFOLFOX6 (Plus or Minus Bevacizumab) Plus Selective Internal Radiation Therapy in Patients With Metastatic Colorectal Cancer. J Clin Oncol 2016;34:1723-31.
10. Wasan HS, Gibbs P, Sharma NK, et al. First-line selective internal radiotherapy plus chemotherapy versus chemotherapy alone in patients with liver metastases from colorectal cancer (FOXFIRE, SIRFLOX, and FOXFIRE-Global): a combined analysis of three multicentre, randomised, phase 3 trials. Lancet Oncol 2017;18:1159-71.
11. Ost P, Reynders D, Decaestecker K, et al. Surveillance or Metastasis-Directed Therapy for Oligometastatic Prostate Cancer Recurrence: A Prospective, Randomized, Multicenter Phase II Trial. J Clin Oncol 2018;36:446-53.
12. Aprile G, Fontanella C, Bonotto M, et al. Timing and extent of response in colorectal cancer: critical review of current data and implication for future trials. Oncotarget 2015;6:28716-30.

13. Alunni-Fabbroni M, Ronsch K, Huber T, et al. Circulating DNA as prognostic biomarker in patients with advanced hepatocellular carcinoma: a translational exploratory study from the SORAMIC trial. J Transl Med 2019;17:328.

14. Diehl F, Schmidt K, Choti MA, et al. Circulating mutant DNA to assess tumor dynamics. Nat Med 2008;14:985-90.

15. Iizuka N, Sakaida I, Moribe T, et al. Elevated levels of circulating cell-free DNA in the blood of patients with hepatitis C virus-associated hepatocellular carcinoma. Anticancer Res 2006;26:4713-9.

16. Tokuhisa Y, Iizuka N, Sakaida I, et al. Circulating cell-free DNA as a predictive marker for distant metastasis of hepatitis C virus-related hepatocellular carcinoma. Br J Cancer 2007;97:1399-403.

17. Blackhall F, Frese KK, Simpson K, Kilgour E, Brady G, Dive C. Will liquid biopsies improve outcomes for patients with small-cell lung cancer? Lancet Oncol 2018;19:e470-e81.

18. Funaioli C, Longobardi C, Martoni AA. The impact of chemotherapy on overall survival and quality of life of patients with metastatic colorectal cancer: a review of phase III trials. Journal of chemotherapy 2008;20:14-27.

19. Herman JM, Narang AK, Griffith KA, et al. The quality-of-life effects of neoadjuvant chemoradiation in locally advanced rectal cancer. International journal of radiation oncology, biology, physics 2013;85:e15-9.

20. Hunter KU, Schipper M, Feng FY, et al. Toxicities affecting quality of life after chemo-IMRT of oropharyngeal cancer: prospective study of patient-reported, observer-rated, and objective outcomes. International journal of radiation oncology, biology, physics 2013;85:935-40.

21. Weichselbaum RR, Hellman S. Oligometastases revisited. Nat Rev Clin Oncol 2011;8:378-82.

22. Badakhshi H, Grun A, Stromberger C, Budach V, Boehmer D. Oligometastases: the new paradigm and options for radiotherapy. A critical review. Strahlentherapie und Onkologie : Organ der Deutschen Rontgengesellschaft [et al] 2013;189:357-62.

23. Palma DA, Salama JK, Lo SS, et al. The oligometastatic state - separating truth from wishful thinking. Nat Rev Clin Oncol 2014;11:549-57.

24. Weichselbaum RR, Hellman S. Oligometastases revisited. Nature reviews Clinical oncology 2011;8:378-82.

25. Fong Y, Cohen AM, Fortner JG, et al. Liver resection for colorectal metastases. J Clin Oncol 1997;15:938-46.

26. Kopetz S, Chang GJ, Overman MJ, et al. Improved survival in metastatic colorectal cancer is associated with adoption of hepatic resection and improved chemotherapy. J Clin Oncol 2009;27:3677-83.

27. Robertson DJ, Stukel TA, Gottlieb DJ, Sutherland JM, Fisher ES. Survival after hepatic resection of colorectal cancer metastases: a national experience. Cancer 2009;115:752-9.

28. Simmonds PC, Primrose JN, Colquitt JL, Garden OJ, Poston GJ, Rees M. Surgical resection of hepatic metastases from colorectal cancer: a systematic review of published studies. Br J Cancer 2006;94:982-99.

29. Khatri VP, Chee KG, Petrelli NJ. Modern multimodality approach to hepatic colorectal metastases: solutions and controversies. Surg Oncol 2007;16:71-83.

30. Germer CT. [Hepatic metastases: an interdisciplinary therapy approach is desirable]. Chirurg 2010;81:505-6.

31. Karanjia ND, Lordan JT, Fawcett WJ, Quiney N, Worthington TR. Survival and recurrence after neo-adjuvant chemotherapy and liver resection for colorectal metastases: a ten year study. Eur J Surg Oncol 2009;35:838-43.

32. Malik HZ, Gomez D, Wong V, et al. Predictors of early disease recurrence following hepatic resection for colorectal cancer metastasis. Eur J Surg Oncol 2007;33:1003-9.

33. Saiura A, Yamamoto J, Hasegawa K, et al. Liver resection for multiple colorectal liver metastases with surgery up-front approach: bi-institutional analysis of 736 consecutive cases. World J Surg 2012;36:2171-8.

34. Takahashi S, Konishi M, Nakagohri T, Gotohda N, Saito N, Kinoshita T. Short time to recurrence after hepatic resection correlates with poor prognosis in colorectal hepatic metastasis. Jpn J Clin Oncol 2006;36:368-75.

35. Yamashita Y, Adachi E, Toh Y, et al. Risk factors for early recurrence after curative hepatectomy for colorectal liver metastases. Surg Today 2011;41:526-32.

36. Harun N, Nikfarjam M, Muralidharan V, Christophi C. Liver regeneration stimulates tumor metastases. J Surg Res 2007;138:284-90.

37. Riddiough GE, Fifis T, Muralidharan V, Perini MV, Christophi C. Searching for the link; mechanisms underlying liver regeneration and recurrence of colorectal liver metastasis post partial hepatectomy. J Gastroenterol Hepatol 2019;34:1276-86.

38. Pietropaolo A, Jones P, Aboumarzouk OM, et al. Trends in surgical and ablative treatment of localised renal cell carcinoma: A review of publication trends over 16 years (2000-2015). Arab J Urol 2019;17:120-4.

39. de Baere T, Tselikas L, Yevich S, et al. The role of image-guided therapy in the management of colorectal cancer metastatic disease. Eur J Cancer 2017;75:231-42.

40. Tameez Ud Din A, Tameez-Ud-Din A, Chaudhary FMD, Chaudhary NA, Siddiqui KH. Irreversible Electroporation For Liver Tumors: A Review Of Literature. Cureus 2019;11:e4994.

41. Van Tilborg AA, Meijerink MR, Sietses C, et al. Long-term results of radiofrequency ablation for unresectable colorectal liver metastases: a potentially curative intervention. Br J Radiol 2011;84:556-65.

42. Tanis E, Nordlinger B, Mauer M, et al. Local recurrence rates after radiofrequency ablation or resection of colorectal liver metastases. Analysis of the European Organisation for Research and Treatment of Cancer #40004 and #40983. Eur J Cancer 2014;50:912-9.

43. Morris E, Treasure T. If a picture is worth a thousand words, take a good look at the picture: Survival after liver metastasectomy for colorectal cancer. Cancer Epidemiol 2017;49:152-5.

44. Berber E, Pelley R, Siperstein AE. Predictors of survival after radiofrequency thermal ablation of colorectal cancer metastases to the liver: a prospective study. J Clin Oncol 2005;23:1358-64.

45. Nahum Goldberg S, Dupuy DE. Image-guided radiofrequency tumor ablation: challenges and opportunities--part I. Journal of vascular and interventional radiology : JVIR 2001;12:1021-32.

46. Nakazawa T, Kokubu S, Shibuya A, et al. Radiofrequency ablation of hepatocellular carcinoma: correlation between local tumor progression after ablation and ablative margin. AJR Am J Roentgenol 2007;188:480-8.

47. Cucchetti A, Piscaglia F, Cescon M, et al. An explorative data-analysis to support the choice between hepatic resection and radiofrequency ablation in the treatment of hepatocellular carcinoma. Digestive and liver disease : official journal of the Italian Society of Gastroenterology and the Italian Association for the Study of the Liver 2014;46:257-63.

48. de Lope CR, Tremosini S, Forner A, Reig M, Bruix J. Management of HCC. J Hepatol 2012;56 Suppl 1:S75-87.

49. Ruers T, Punt C, Van Coevorden F, et al. Radiofrequency ablation combined with systemic treatment versus systemic treatment alone in patients with non-resectable colorectal liver metastases: a randomized EORTC Intergroup phase II study (EORTC 40004). Ann Oncol 2012;23:2619-26.

50. Ruers T, Van Coevorden F, Punt CJ, et al. Local Treatment of Unresectable Colorectal Liver Metastases: Results of a Randomized Phase II Trial. J Natl Cancer Inst 2017;109.

51. Kunzli BM, Abitabile P, Maurer CA. Radiofrequency ablation of liver tumors: Actual limitations and potential solutions in the future. World journal of hepatology 2011;3:8-14.

52. Rhim H, Lim HK. Radiofrequency ablation of hepatocellular carcinoma: pros and cons. Gut and liver 2010;4 Suppl 1:S113-8.

53. Scorsetti M, Clerici E, Comito T. Stereotactic body radiation therapy for liver metastases. Journal of gastrointestinal oncology 2014;5:190-7.

54. Scorsetti M, Comito T, Tozzi A, et al. Final results of a phase II trial for stereotactic body radiation therapy for patients with inoperable liver metastases from colorectal cancer. Journal of cancer research and clinical oncology 2014.

55. Dawson LA. Overview: Where does radiation therapy fit in the spectrum of liver cancer local-regional therapies? Seminars in radiation oncology 2011;21:241-6.

56. Scorsetti M, Arcangeli S, Tozzi A, et al. Is stereotactic body radiation therapy an attractive option for unresectable liver metastases? A preliminary report from a phase 2 trial. International journal of radiation oncology, biology, physics 2013;86:336-42.

57. Dawood O, Mahadevan A, Goodman KA. Stereotactic body radiation therapy for liver metastases. Eur J Cancer 2009;45:2947-59.

58. Kirkpatrick JP, Kelsey CR, Palta M, et al. Stereotactic body radiotherapy: a critical review for nonradiation oncologists. Cancer 2014;120:942-54.

59. Ricke J, Wust P, Hengst S, et al. [CT-guided interstitial brachytherapy of lung malignancies. Technique and first results]. Der Radiologe 2004;44:684-6.

60. Ricke J, Wust P, Stohlmann A, et al. CT-guided interstitial brachytherapy of liver malignancies alone or in combination with thermal ablation: phase I-II results of a novel technique. International journal of radiation oncology, biology, physics 2004;58:1496-505.

61. Ricke J, Wust P, Stohlmann A, et al. [CT-Guided brachytherapy. A novel percutaneous technique for interstitial ablation of liver metastases]. Strahlentherapie und Onkologie : Organ der Deutschen Rontgengesellschaft [et al] 2004;180:274-80.

62. Ricke J, Wust P, Wieners G, et al. Liver malignancies: CT-guided interstitial brachytherapy in patients with unfavorable lesions for thermal ablation. Journal of vascular and interventional radiology : JVIR 2004;15:1279-86.

63. Collettini F, Schnapauff D, Poellinger A, et al. Hepatocellular carcinoma: computed-tomography-guided high-dose-rate brachytherapy (CT-HDRBT) ablation of large (5-7 cm) and very large (>7 cm) tumours. European radiology 2012;22:1101-9.

64. Tselis N, Chatzikonstantinou G, Kolotas C, Milickovic N, Baltas D, Zamboglou N. Computed tomography-guided interstitial high dose rate brachytherapy for centrally located liver tumours: a single institution study. European radiology 2013;23:2264-70.

65. Brown JM, Koong AC. High-dose single-fraction radiotherapy: exploiting a new biology? International journal of radiation oncology, biology, physics 2008;71:324-5.

66. Garcia-Barros M, Paris F, Cordon-Cardo C, et al. Tumor response to radiotherapy regulated by endothelial cell apoptosis. Science 2003;300:1155-9.

67. Streitparth F, Pech M, Bohmig M, et al. In vivo assessment of the gastric mucosal tolerance dose after single fraction, small volume irradiation of liver malignancies by computed tomography-guided, high-dose-rate brachytherapy. International journal of radiation oncology, biology, physics 2006;65:1479-86.

68. Collettini F, Singh A, Schnapauff D, et al. Computed-tomography-guided high-dose-rate brachytherapy (CT-HDRBT) ablation of metastases adjacent to the liver hilum. Eur J Radiol 2013;82:e509-14.

69. Mohnike K, Wieners G, Pech M, et al. Image-guided interstitial high-dose-rate brachytherapy in hepatocellular carcinoma. Dig Dis 2009;27:170-4.

70. Mohnike K, Wieners G, Schwartz F, et al. Computed tomography-guided high-dose-rate brachytherapy in hepatocellular carcinoma: safety, efficacy, and effect on survival. International journal of radiation oncology, biology, physics 2010;78:172-9.

71. Pech M, Wieners G, Kryza R, et al. CT-guided brachytherapy (CTGB) versus interstitial laser ablation (ILT) of colorectal liver metastases: an intraindividual matched-pair analysis. Strahlentherapie und Onkologie : Organ der Deutschen Rontgengesellschaft [et al] 2008;184:302-6.

72. Ricke J, Mohnike K, Pech M, et al. Local response and impact on survival after local ablation of liver metastases from colorectal carcinoma by computed tomography-guided high-dose-rate brachytherapy. International journal of radiation oncology, biology, physics 2010;78:479-85.

73. Ricke J, Wust P, Wieners G, et al. CT-guided interstitial single-fraction brachytherapy of lung tumors: phase I results of a novel technique. Chest 2005;127:2237-42.

74. Peters N, Wieners G, Pech M, et al. CT-guided interstitial brachytherapy of primary and secondary lung malignancies: results of a prospective phase II trial. Strahlentherapie und Onkologie : Organ der Deutschen Rontgengesellschaft [et al] 2008;184:296-301.

75. Fischbach F, Bunke J, Thormann M, et al. MR-guided freehand biopsy of liver lesions with fast continuous imaging using a 1.0-T open MRI scanner: experience in 50 patients. Cardiovasc Intervent Radiol 2011;34:188-92.

76. Fischbach F, Thormann M, Seidensticker M, Kropf S, Pech M, Ricke J. Assessment of fast dynamic imaging and the use of Gd-EOB-DTPA for MR-guided liver interventions. J Magn Reson Imaging 2011;34:874-9.

77. Rak M, Konig T, Tonnies KD, Walke M, Ricke J, Wybranski C. Joint deformable liver registration and bias field correction for MR-guided HDR brachytherapy. Int J Comput Assist Radiol Surg 2017;12:2169-80.

78. Ricke J, Thormann M, Ludewig M, et al. MR-guided liver tumor ablation employing open high-field 1.0T MRI for image-guided brachytherapy. European radiology 2010;20:1985-93.

79. Ricke J, Wust P. Computed tomography-guided brachytherapy for liver cancer. Seminars in radiation oncology 2011;21:287-93.

80. Tselis N, Chatzikonstantinou G, Kolotas C, et al. Hypofractionated accelerated computed tomography-guided interstitial high-dose-rate brachytherapy for liver malignancies. Brachytherapy 2012;11:507-14.

81. Bethesda M. ICRU 50 . Prescribing, recording, and reporting photon beam therapy. Bethesda, MD: International Commission on Radiation Units and Measurements Press; 1993. . International Commission on Radiation Units and Measurements Press.

82. Ludemann L, Wybranski C, Seidensticker M, et al. In vivo assessment of catheter positioning accuracy and prolonged irradiation time on liver tolerance dose after single-fraction 192Ir high-dose-rate brachytherapy. Radiat Oncol 2011;6:107.

83. Mohnike K, Wolf S, Damm R, et al. Radioablation of liver malignancies with interstitial high-dose-rate brachytherapy : Complications and risk factors. Strahlentherapie und Onkologie : Organ der Deutschen Rontgengesellschaft [et al] 2016;192:288-96.

84. Ricke J, Seidensticker M, Ludemann L, et al. In vivo assessment of the tolerance dose of small liver volumes after single-fraction HDR irradiation. International Journal of Radiation Oncology Biology Physics 2005;62:776-84.

85. Seidensticker M, Burak M, Kalinski T, et al. Radiation-Induced Liver Damage: Correlation of Histopathology with Hepatobiliary Magnetic Resonance Imaging, a Feasibility Study. Cardiovascular and interventional radiology 2014.

86. Seidensticker M, Seidensticker R, Damm R, et al. Prospective randomized trial of enoxaparin, pentoxifylline and ursodeoxycholic acid for prevention of radiation-induced liver toxicity. PloS one 2014.

87. Seidensticker M, Seidensticker R, Mohnike K, et al. Quantitative in vivo assessment of radiation injury of the liver using Gd-EOB-DTPA enhanced MRI: tolerance dose of small liver volumes. Radiation Oncology 2011;6.

88. Wybranski C, Seidensticker M, Mohnike K, et al. In Vivo Assessment of Dose Volume and Dose Gradient Effects on the Tolerance Dose of Small Liver Volumes after Single-Fraction High-Dose-Rate Ir-192 Irradiation. Radiat Res 2009;172:598-606.

89. Alektiar KM, Zelefsky MJ, Paty PB, et al. High-dose-rate intraoperative brachytherapy for recurrent colorectal cancer. International journal of radiation oncology, biology, physics 2000;48:219-26.

90. Dritschilo A, Harter KW, Thomas D, et al. Intraoperative radiation therapy of hepatic metastases: technical aspects and report of a pilot study. International journal of radiation oncology, biology, physics 1988;14:1007-11.

91. Nag S, Martinez-Monge R, Mills J, et al. Intraoperative high dose rate brachytherapy in recurrent or metastatic colorectal carcinoma. Ann Surg Oncol 1998;5:16-22.

92. Omari J, Drewes R, Matthias M, et al. Treatment of metastatic, imatinib refractory, gastrointestinal stroma tumor with image-guided high-dose-rate interstitial brachytherapy. Brachytherapy 2019;18:63-70.

93. Omari J, Heinze C, Damm R, et al. Radioablation of Hepatic Metastases from Renal Cell Carcinoma With Image-guided Interstitial Brachytherapy. Anticancer Res 2019;39:2501-8.

94. Drewes R, Omari J, Manig M, et al. Treatment of hepatic pancreatic ductal adenocarcinoma metastases with high-dose-rate image-guided interstitial brachytherapy: a single center experience. J Contemp Brachytherapy 2019;11:329-36.

95. Wieners G, Schippers AC, Collettini F, et al. CT-guided high-dose-rate brachytherapy in the interdisciplinary treatment of patients with liver metastases of pancreatic cancer. Hepatobiliary Pancreat Dis Int 2015;14:530-8.

96. Omari J, Drewes R, Orthmer M, Hass P, Pech M, Powerski M. Treatment of metastatic gastric adenocarcinoma with image-guided high-dose rate, interstitial brachytherapy as second-line or salvage therapy. Diagn Interv Radiol 2019;25:360-7.

97. Heinze C, Omari J, Othmer M, et al. Image-guided Interstitial Brachytherapy in the Management of Metastasized Anal Squamous Cell Carcinoma. Anticancer Res 2018;38:5401-7.

98. Schippers AC, Collettini F, Steffen IG, et al. Initial Experience with CT-Guided High-Dose-Rate Brachytherapy in the Multimodality Treatment of Neuroendocrine Tumor Liver Metastases. Journal of vascular and interventional radiology : JVIR 2017;28:672-82.

99. Bretschneider T, Mohnike K, Hass P, et al. Efficacy and safety of image-guided interstitial single fraction high-dose-rate brachytherapy in the management of metastatic malignant melanoma. J Contemp Brachytherapy 2015;7:154-60.

100. Seidensticker R, Seidensticker M, Doegen K, et al. Extensive Use of Interventional Therapies Improves Survival in Unresectable or Recurrent Intrahepatic Cholangiocarcinoma. Gastroenterol Res Pract 2016;2016:8732521.

101. Schnapauff D, Denecke T, Grieser C, et al. Computed tomography-guided interstitial HDR brachytherapy (CT-HDRBT) of the liver in patients with irresectable intrahepatic cholangiocarcinoma. Cardiovasc Intervent Radiol 2012;35:581-7.

102. Mohnike K, Steffen IG, Seidensticker M, et al. Radioablation by Image-Guided (HDR) Brachytherapy and Transarterial Chemoembolization in Hepatocellular Carcinoma: A Randomized Phase II Trial. Cardiovasc Intervent Radiol 2019;42:239-49.

103. Nanko M, Shimada H, Yamaoka H, et al. Micrometastatic colorectal cancer lesions in the liver. Surg Today 1998;28:707-13.

104. Seidensticker M, Wust P, Ruehl R, et al. Safety margin in irradiation of colorectal liver metastases: assessment of the control dose of micrometastases. Radiation Oncology 2010;5.

105. Mohnike K, Sauerland H, Seidensticker M, et al. Haemorrhagic Complications and Symptomatic Venous Thromboembolism in Interventional Tumour Ablations: The Impact of Peri-interventional Thrombosis Prophylaxis. Cardiovasc Intervent Radiol 2016;39:1716-21.

106. Archavlis E, Tselis N, Birn G, Ulrich P, Baltas D, Zamboglou N. Survival analysis of HDR brachytherapy versus reoperation versus temozolomide alone: a retrospective cohort analysis of recurrent glioblastoma multiforme. BMJ Open 2013;3.

107. Chatzikonstantinou G, Zamboglou N, Archavlis E, et al. CT-guided interstitial HDR-brachytherapy for recurrent glioblastoma multiforme: a 20-year single-institute experience. Strahlentherapie und Onkologie : Organ der Deutschen Rontgengesellschaft [et al] 2018;194:1171-9.

108. Karagiannis E, Leczynski A, Tselis N, et al. Inverse planning and inverse implanting for breast interstitial brachytherapy. Introducing a new anatomy specific breast interstitial template (ASBIT). Radiother Oncol 2018;128:421-7.

109. Kolotas C, Roddiger S, Strassmann G, et al. Palliative interstitial HDR brachytherapy for recurrent rectal cancer. Implantation techniques and results. Strahlentherapie und Onkologie : Organ der Deutschen Rontgengesellschaft [et al] 2003;179:458-63.

110. Tselis N, Karagiannis E, Kolotas C, Baghi M, Milickovic N, Zamboglou N. Image-guided interstitial high-dose-rate brachytherapy in the treatment of inoperable recurrent head and neck malignancies: An effective option of reirradiation. Head Neck 2017;39:E61-E8.

111. Tselis N, Kolotas C, Birn G, et al. CT-guided interstitial HDR brachytherapy for recurrent glioblastoma multiforme. Long-term results. Strahlentherapie und Onkologie : Organ der Deutschen Rontgengesellschaft [et al] 2007;183:563-70.

112. Denecke T, Stelter L, Schnapauff D, et al. CT-guided Interstitial Brachytherapy of Hepatocellular Carcinoma before Liver Transplantation: an Equivalent Alternative to Transarterial Chemoembolization? European radiology 2015;25:2608-16.

113. Chatzikonstantinou G, Zamboglou N, Baltas D, Ferentinos K, Bon D, Tselis N. Image-guided interstitial high-dose-rate brachytherapy for dose escalation in the radiotherapy treatment of locally advanced lung cancer: A single-institute experience. Brachytherapy 2019.

114. Burman C, Kutcher GJ, Emami B, Goitein M. Fitting of normal tissue tolerance data to an analytic function. International journal of radiation oncology, biology, physics 1991;21:123-35.

115. Dawson LA, Normolle D, Balter JM, McGinn CJ, Lawrence TS, Ten Haken RK. Analysis of radiation-induced liver disease using the Lyman NTCP model. International journal of radiation oncology, biology, physics 2002;53:810-21.

116. Emami B, Lyman J, Brown A, et al. Tolerance of normal tissue to therapeutic irradiation. International journal of radiation oncology, biology, physics 1991;21:109-22.

117. Kim TH, Panahon AM, Friedman M, Webster JH. Acute transient radiation hepatitis following whole abdominal irradiation. Clin Radiol 1976;27:449-54.

118. Lawrence TS, Robertson JM, Anscher MS, Jirtle RL, Ensminger WD, Fajardo LF. Hepatic toxicity resulting from cancer treatment. International journal of radiation oncology, biology, physics 1995;31:1237-48.

119. Lewin K, Millis RR. Human radiation hepatitis. A morphologic study with emphasis on the late changes. Arch Pathol 1973;96:21-6.

120. Herfarth KK, Debus J, Lohr F, et al. Stereotactic single-dose radiation therapy of liver tumors: results of a phase I/II trial. J Clin Oncol 2001;19:164-70.

121. Herfarth KK, Hof H, Bahner ML, et al. Assessment of focal liver reaction by multiphasic CT after stereotactic single-dose radiotherapy of liver tumors. International journal of radiation oncology, biology, physics 2003;57:444-51.

122. Hamm B, Staks T, Muhler A, et al. Phase I clinical evaluation of Gd-EOB-DTPA as a hepatobiliary MR contrast agent: safety, pharmacokinetics, and MR imaging. Radiology 1995;195:785-92.

123. Kirchin MA, Pirovano GP, Spinazzi A. Gadobenate dimeglumine (Gd-BOPTA). An overview. Invest Radiol 1998;33:798-809.

124. Schuhmann-Giampieri G, Schmitt-Willich H, Press WR, Negishi C, Weinmann HJ, Speck U. Preclinical evaluation of Gd-EOB-DTPA as a contrast agent in MR imaging of the hepatobiliary system. Radiology 1992;183:59-64.

125. Spinazzi A, Lorusso V, Pirovano G, Kirchin M. Safety, tolerance, biodistribution, and MR imaging enhancement of the liver with gadobenate dimeglumine: results of clinical pharmacologic and pilot imaging studies in nonpatient and patient volunteers. Acad Radiol 1999;6:282-91.

126. Spinazzi A, Lorusso V, Pirovano G, Taroni P, Kirchin M, Davies A. Multihance clinical pharmacology: biodistribution and MR enhancement of the liver. Acad Radiol 1998;5 Suppl 1:S86-9; discussion S93-4.

127. Ruhl R, Seidensticker M, Peters N, et al. Hepatocellular carcinoma and liver cirrhosis: assessment of the liver function after Yttrium-90 radioembolization with resin microspheres or after CT-guided high-dose-rate brachytherapy. Dig Dis 2009;27:189-99.

128. Pech M, Ricke J, Seidensticker M, et al. Assessment of the tolerance dose of the hepatic reticulo-endothelial system (RES) after single fraction HDR-irradiation: An in-vivo study employing SSPIO. International Journal of Radiation Biology 2008;84:830-7.

129. Ruhl R, Ludemann L, Czarnecka A, et al. Radiobiological restrictions and tolerance doses of repeated single-fraction hdr-irradiation of intersecting small liver volumes for recurrent hepatic metastases. Radiat Oncol 2010;5:44.

130. Powerski M, Penzlin S, Hass P, et al. Biliary duct stenosis after image-guided high-dose-rate interstitial brachytherapy of central and hilar liver tumors : A systematic analysis of 102 cases. Strahlentherapie und Onkologie : Organ der Deutschen Rontgengesellschaft [et al] 2019;195:265-73.

131. Hass P, Steffen IG, Powerski M, et al. First report on extended distance between tumor lesion and adjacent organs at risk using interventionally applied balloon catheters: a simple procedure to optimize clinical target volume covering effective isodose in interstitial high-dose-rate brachytherapy of liver malignomas. J Contemp Brachytherapy 2019;11:152-61.

132. Damm R, Streitparth T, Hass P, et al. Prospective evaluation of CT-guided HDR brachytherapy as a local ablative treatment for renal masses: a single-arm pilot trial. Strahlentherapie und Onkologie : Organ der Deutschen Rontgengesellschaft [et al] 2019.

133. Omari J, Heinze C, Wilck A, et al. Efficacy and safety of CT-guided high-dose-rate interstitial brachytherapy in primary and secondary malignancies of the pancreas. Eur J Radiol 2019;112:22-7.

134. Pollom EL, Chin AL, Diehn M, Loo BW, Chang DT. Normal Tissue Constraints for Abdominal and Thoracic Stereotactic Body Radiotherapy. Seminars in radiation oncology 2017;27:197-208.

135. Trotti A, Colevas AD, Setser A, et al. CTCAE v3.0: development of a comprehensive grading system for the adverse effects of cancer treatment. Seminars in radiation oncology 2003;13:176-81.

136. Huang SF, Ko CW, Chang CS, Chen GH. Liver abscess formation after transarterial chemoembolization for malignant hepatic tumor. Hepatogastroenterology 2003;50:1115-8.

137. Kim W, Clark TW, Baum RA, Soulen MC. Risk factors for liver abscess formation after hepatic chemoembolization. Journal of vascular and interventional radiology : JVIR 2001;12:965-8.

138. Geisel D, Powerski MJ, Schnapauff D, et al. No infectious hepatic complications following radioembolization with 90Y microspheres in patients with biliodigestive anastomosis. Anticancer Res 2014;34:4315-21.

139. Barbar S, Noventa F, Rossetto V, et al. A risk assessment model for the identification of hospitalized medical patients at risk for venous thromboembolism: the Padua Prediction Score. J Thromb Haemost 2010;8:2450-7.

140. Stein PD, Beemath A, Meyers FA, Skaf E, Sanchez J, Olson RE. Incidence of venous thromboembolism in patients hospitalized with cancer. Am J Med 2006;119:60-8.

141. Anderson FA, Jr., Wheeler HB, Goldberg RJ, Hosmer DW, Forcier A, Patwardhan NA. Physician practices in the prevention of venous thromboembolism. Ann Intern Med 1991;115:591-5.

142. Clagett GP, Anderson FA, Jr., Heit J, Levine MN, Wheeler HB. Prevention of venous thromboembolism. Chest 1995;108:312S-34S.

143. group LGCotTc. Risk of and prophylaxis for venous thromboembolism in hospital patients. Thromboembolic Risk Factors (THRIFT) Consensus Group. BMJ 1992;305(6853):567–74.

144. Spencer A, Cawood T, Frampton C, Jardine D. Heparin-based treatment to prevent symptomatic deep venous thrombosis, pulmonary embolism or death in general medical inpatients is not supported by best evidence. Intern Med J 2014;44:1054-65.

145. Doughtie CA, Priddy EE, Philips P, Martin RC, McMasters KM, Scoggins CR. Preoperative dosing of low-molecular-weight heparin in hepatopancreatobiliary surgery. Am J Surg 2014;208:1009-15; discussion 15.

146. Farge D, Frere C, Connors JM, et al. 2019 international clinical practice guidelines for the treatment and prophylaxis of venous thromboembolism in patients with cancer. Lancet Oncol 2019;20:e566-e81.

147. Stigliano R, Marelli L, Yu D, Davies N, Patch D, Burroughs AK. Seeding following percutaneous diagnostic and therapeutic approaches for hepatocellular carcinoma. What is the risk and the outcome? Seeding risk for percutaneous approach of HCC. Cancer treatment reviews 2007;33:437-47.

148. Llovet JM, Vilana R, Bru C, et al. Increased risk of tumor seeding after percutaneous radiofrequency ablation for single hepatocellular carcinoma. Hepatology 2001;33:1124-9.

149. Yu J, Liang P, Yu XL, Cheng ZG, Han ZY, Dong BW. Needle track seeding after percutaneous microwave ablation of malignant liver tumors under ultrasound guidance: analysis of 14-year experience with 1462 patients at a single center. Eur J Radiol 2012;81:2495-9.

150. Zhong-Yi Z, Wei Y, Kun Y, et al. Needle track seeding after percutaneous radiofrequency ablation of hepatocellular carcinoma: 14-year experience at a single centre. Int J Hyperthermia 2017;33:454-8.

151. Damm R, Zorkler I, Rogits B, et al. Needle track seeding in hepatocellular carcinoma after local ablation by high-dose-rate brachytherapy: a retrospective study of 588 catheter placements. J Contemp Brachytherapy 2018;10:516-21.

152. Pitroda SP, Chmura SJ, Weichselbaum RR. Integration of radiotherapy and immunotherapy for treatment of oligometastases. Lancet Oncol 2019;20:e434-e42.

153. Seidensticker M, Garlipp B, Scholz S, et al. Locally ablative treatment of breast cancer liver metastases: identification of factors influencing survival (the Mammary Cancer Microtherapy and Interventional Approaches (MAMMA MIA) study). BMC Cancer 2015;15:517.

154. Seidensticker R, Damm R, Enge J, et al. Local ablation or radioembolization of colorectal cancer metastases: comorbidities or older age do not affect overall survival. BMC Cancer 2018;18:882.

155. Bruix J, Reig M, Sherman M. Evidence-Based Diagnosis, Staging, and Treatment of Patients With Hepatocellular Carcinoma. Gastroenterology 2016;150:835-53.

156. Llovet JM, Bruix J. Systematic review of randomized trials for unresectable hepatocellular carcinoma: Chemoembolization improves survival. Hepatology 2003;37:429-42.

157. Bruix J, Sherman M, Llovet JM, et al. Clinical management of hepatocellular carcinoma. Conclusions of the Barcelona-2000 EASL conference. European Association for the Study of the Liver. J Hepatol 2001;35:421-30.

158. Bruix J, Sherman M, Practice Guidelines Committee AAftSoLD. Management of hepatocellular carcinoma. Hepatology 2005;42:1208-36.

159. Livraghi T, Meloni F, Di Stasi M, et al. Sustained complete response and complications rates after radiofrequency ablation of very early hepatocellular carcinoma in cirrhosis: Is resection still the treatment of choice? Hepatology 2008;47:82-9.

160. Xu XL, Liu XD, Liang M, Luo BM. Radiofrequency Ablation versus Hepatic Resection for Small Hepatocellular Carcinoma: Systematic Review of Randomized Controlled Trials with Meta-Analysis and Trial Sequential Analysis. Radiology 2018;287:461-72.

161. Yin Z, Jin H, Ma T, Zhou Y, Yu M, Jian Z. A meta-analysis of long-term survival outcomes between surgical resection and radiofrequency ablation in patients with single hepatocellular carcinoma </= 2cm (BCLC very early stage). Int J Surg 2018;56:61-7.

162. Li Y, Xu A, Jia S, Huang J. Recent advances in the molecular mechanism of sex disparity in hepatocellular carcinoma. Oncol Lett 2019;17:4222-8.

163. Bismuth H, Chiche L, Adam R, Castaing D, Diamond T, Dennison A. Liver resection versus transplantation for hepatocellular carcinoma in cirrhotic patients. Ann Surg 1993;218:145-51.

164. Mazzaferro V, Regalia E, Doci R, et al. Liver transplantation for the treatment of small hepatocellular carcinomas in patients with cirrhosis. N Engl J Med 1996;334:693-9.

165. Pech M, Wieners G, Kryza R, et al. CT-guided brachytherapy (CTGB) versus interstitial laser ablation (ILT) of colorectal liver metastases - An intraindividual matched-pair analysis. Strahlentherapie Und Onkologie 2008;184:302-6.

166. Andratschke N, Alheid H, Allgauer M, et al. The SBRT database initiative of the German Society for Radiation Oncology (DEGRO): patterns of care and outcome analysis of stereotactic body radiotherapy (SBRT) for liver oligometastases in 474 patients with 623 metastases. BMC Cancer 2018;18:283.

167. Boda-Heggemann J, Jahnke A, Chan MKH, et al. In-vivo treatment accuracy analysis of active motion-compensated liver SBRT through registration of plan dose to post-therapeutic MRI-morphologic alterations. Radiother Oncol 2019;134:158-65.

168. Gkika E, Strouthos I, Kirste S, et al. Repeated SBRT for in- and out-of-field recurrences in the liver. Strahlentherapie und Onkologie : Organ der Deutschen Rontgengesellschaft [et al] 2019;195:246-53.

169. Han S, Yin FF, Cai J. Evaluation of dosimetric uncertainty caused by MR geometric distortion in MRI-based liver SBRT treatment planning. J Appl Clin Med Phys 2019;20:43-50.

170. Ibragimov B, Toesca DAS, Yuan Y, Koong AC, Chang DT, Xing L. Neural Networks for Deep Radiotherapy Dose Analysis and Prediction of Liver SBRT Outcomes. IEEE J Biomed Health Inform 2019;23:1821-33.

171. Scorsetti M, Comito T, Clerici E, et al. Phase II trial on SBRT for unresectable liver metastases: long-term outcome and prognostic factors of survival after 5 years of follow-up. Radiat Oncol 2018;13:234.

172. Rieber J, Streblow J, Uhlmann L, et al. Stereotactic body radiotherapy (SBRT) for medically inoperable lung metastases-A pooled analysis of the German working group "stereotactic radiotherapy". Lung Cancer 2016;97:51-8.

173. Thomas TO, Hasan S, Small W, Jr., et al. The tolerance of gastrointestinal organs to stereotactic body radiation therapy: what do we know so far? Journal of gastrointestinal oncology 2014;5:236-46.

174. Sanuki N, Takeda A, Oku Y, et al. Influence of liver toxicities on prognosis after stereotactic body radiation therapy for hepatocellular carcinoma. Hepatol Res 2015;45:540-7.

175. Hass P, Mohnike K, Kropf S, et al. Comparative analysis between interstitial brachytherapy and stereotactic body irradiation for local ablation in liver malignancies. Brachytherapy 2019.

176. Pennington JD, Park SJ, Abgaryan N, et al. Dosimetric comparison of brachyablation and stereotactic ablative body radiotherapy in the treatment of liver metastasis. Brachytherapy 2015;14:537-42.

177. Wilke L, Andratschke N, Blanck O, et al. ICRU report 91 on prescribing, recording, and reporting of stereotactic treatments with small photon beams : Statement from the DEGRO/DGMP working group stereotactic radiotherapy and radiosurgery. Strahlentherapie und Onkologie : Organ der Deutschen Rontgengesellschaft [et al] 2019;195:193-8.

178. Andratschke N, Parys A, Stadtfeld S, et al. Clinical results of mean GTV dose optimized robotic guided SBRT for liver metastases. Radiat Oncol 2016;11:74.

179. Baumann R, Chan MKH, Pyschny F, et al. Clinical Results of Mean GTV Dose Optimized Robotic-Guided Stereotactic Body Radiation Therapy for Lung Tumors. Front Oncol 2018;8:171.

180. Stera S, Balermpas P, Chan MKH, et al. Breathing-motion-compensated robotic guided stereotactic body radiation therapy : Patterns of failure analysis. Strahlentherapie und Onkologie : Organ der Deutschen Rontgengesellschaft [et al] 2018;194:143-55.

181. Zhao L, Zhou S, Balter P, et al. Planning Target Volume D95 and Mean Dose Should Be Considered for Optimal Local Control for Stereotactic Ablative Radiation Therapy. International journal of radiation oncology, biology, physics 2016;95:1226-35.

182. Mohnike K, Neumann K, Hass P, et al. Radioablation of adrenal gland malignomas with interstitial high-dose-rate brachytherapy : Efficacy and outcome. Strahlentherapie und Onkologie : Organ der Deutschen Rontgengesellschaft [et al] 2017;193:612-9.

183. Gunjur A, Duong C, Ball D, Siva S. Surgical and ablative therapies for the management of adrenal 'oligometastases' - A systematic review. Cancer Treat Rev 2014;40:838-46.

184. Burjakow K, Fietkau R, Putz F, Achterberg N, Lettmaier S, Knippen S. Fractionated stereotactic radiation therapy for adrenal metastases: contributing to local tumor control with low toxicity. Strahlentherapie und Onkologie : Organ der Deutschen Rontgengesellschaft [et al] 2019;195:236-45.

185. Scouarnec C, Pasquier D, Luu J, et al. Usefulness of Stereotactic Body Radiation Therapy for Treatment of Adrenal Gland Metastases. Front Oncol 2019;9:732.

186. Toesca DAS, Koong AJ, von Eyben R, Koong AC, Chang DT. Stereotactic body radiation therapy for adrenal gland metastases: Outcomes and toxicity. Adv Radiat Oncol 2018;3:621-9.

187. Holy R, Piroth M, Pinkawa M, Eble MJ. Stereotactic body radiation therapy (SBRT) for treatment of adrenal gland metastases from non-small cell lung cancer. Strahlentherapie und Onkologie : Organ der Deutschen Rontgengesellschaft [et al] 2011;187:245-51.

188. Gao XL, Zhang KW, Tang MB, Zhang KJ, Fang LN, Liu W. Pooled analysis for surgical treatment for isolated adrenal metastasis and non-small cell lung cancer. Interact Cardiovasc Thorac Surg 2017;24:1-7.

189. Wieners G, Pech M, Rudzinska M, et al. CT-guided interstitial brachytherapy in the local treatment of extrahepatic, extrapulmonary secondary malignancies. European radiology 2006;16:2586-93.

11 Eidesstattliche Versicherung

gemäß der Habilitationsordnung der Medizinischen Fakultät der Otto- von- Guericke-Universität Magdeburg

Hiermit erkläre ich, Konrad Mohnike, geboren am 24.01.1976 in Berlin, dass

- keine staatsanwaltschaftlichen Ermittlungsverfahren gegen mich anhängig sind,

- weder früher noch gleichzeitig ein Habilitationsverfahren an einer in- oder ausländischen Hochschule/Universität durchgeführt oder angemeldet wurde bzw. welchen Ausgang ein durchgeführtes Habilitationsverfahren hatte,

- die vorgelegte Habilitationsschrift ohne fremde Hilfe verfasst, die beschriebenen Ergebnisse selbst gewonnen wurden, sowie die verwendeten Hilfsmittel, die Zusammenarbeit mit anderen Wissenschaftlerinnen oder Wissenschaftlern und technischen Hilfskräften und die Literatur vollständig angegeben sind,

- bei der Abfassung der Habilitationsschrift keine Rechte Dritter verletzt wurden,

- mir die geltende Habilitationsordnung bekannt ist.

Ich übertrage der Medizinischen Fakultät der Otto-von-Guericke-Universität Magdeburg das Recht, weitere Kopien meiner Habilitationsschrift herzustellen und zu vertreiben.

(Dr. med. Konrad Mohnike)

12 Danksagung

Mi, seit wir uns kennen, trage ich dieses Habilitationsvorhaben wie eine Monstranz vor mir her. Dass du das ausgehalten hast, für deine stete Unterstützung, deinen Rat und für alles andere – aber nicht nur dafür – danke ich dir, ich liebe dich.
Liv und Ivar, meine Arbeit stand oft zwischen uns. Danke dafür, dass Ihr mir nicht nachtragt, dass ich nicht immer so für euch da war, wie ein Vater es für seine Kinder sein sollte. Ich liebe euch.

Mein ärztliches und wissenschaftliches Denken wurde maßgeblich von meinen Lehrern Prof. Dr. med. Jens Ricke und Prof. Dr. med. Maciej Pech geprägt, denen ich nicht nur deshalb sehr viel zu verdanken habe.
Die Zusammenarbeit mit den klinischen Fächern war in meiner Zeit als Assistenz-, Fach- und Oberarzt stets gewinnbringend. Hier möchte ich Prof. Dr. med. Peter Malfertheiner, ehemals Direktor der Klinik für Gastroenterologie, Hepatologie und Infektiologie, Prof. Dr. med. Günther Gademann, ehemals Direktor der Klinik für Strahlentherapie und Prof. Dr. med. Hans Lippert, ehemals Direktor der Klinik für Allgemein-, Viszeral- und Gefäßchirurgie, besonders hervorheben. Ebenso möchte ich meinen Kollegen und Freunden der Uniklinik Magdeburg aus verschiedenen Fächern danken, mit denen ich forschen und arbeiten durfte, hier vor allem: Max und Ricarda Seidensticker, Kerstin Schütte, Nils Peters, Ludwig von Rohden, Peter Hass, Marino Venerito, Maciej Powerski, Alexander Link, Björn Friebe, Tina Streitparth, Robert Damm, Frank und Katharina Fischbach, Patrick Stübs, Christoph Benckert, Jan Bornschein, Gero Wieners, Claudia Pambor und nicht zuletzt Klaus Mohnike.

Meiner Schwester Katharina und Nils Peters möchte ich für ihre sorgfältige und intelligente Durchsicht der Arbeit danken. Patrick, danke für die vielen inspirierenden Gespräche über Epidemiologie und Statistik und die schönen Seiten des Lebens!
Martin und Familie haben mich während der Niederschrift im Häuschen an der Ostsee mit Essen und guten abendlichen Gesprächen versorgt. Ihr wart großartig.

Meine Eltern Antje Mohnike, Nephrologin, und Wolfgang Mohnike, Nuklearmediziner, waren und sind mir stets Maßstab vieler Dinge, ich danke euch.

Sophie, schön, dass du wieder da bist!

13 Originale der Publikationen

RADIATION ONCOLOGY

RESEARCH Open Access

In vivo assessment of catheter positioning accuracy and prolonged irradiation time on liver tolerance dose after single-fraction ^{192}Ir high-dose-rate brachytherapy

Lutz Lüdemann[1*†], Christian Wybranski[2†], Max Seidensticker[2], Konrad Mohnike[2], Siegfried Kropf[3], Peter Wust[1] and Jens Ricke[2]

Abstract

Background: To assess brachytherapy catheter positioning accuracy and to evaluate the effects of prolonged irradiation time on the tolerance dose of normal liver parenchyma following single-fraction irradiation with ^{192}Ir.

Materials and methods: Fifty patients with 76 malignant liver tumors treated by computed tomography (CT)-guided high-dose-rate brachytherapy (HDR-BT) were included in the study. The prescribed radiation dose was delivered by 1 - 11 catheters with exposure times in the range of 844 - 4432 seconds. Magnetic resonance imaging (MRI) datasets for assessing irradiation effects on normal liver tissue, edema, and hepatocyte dysfunction, obtained 6 and 12 weeks after HDR-BT, were merged with 3D dosimetry data. The isodose of the treatment plan covering the same volume as the irradiation effect was taken as a surrogate for the liver tissue tolerance dose. Catheter positioning accuracy was assessed by calculating the shift between the 3D center coordinates of the irradiation effect volume and the tolerance dose volume for 38 irradiation effects in 30 patients induced by catheters implanted in nearly parallel arrangement. Effects of prolonged irradiation were assessed in areas where the irradiation effect volume and tolerance dose volume did not overlap (mismatch areas) by using a catheter contribution index. This index was calculated for 48 irradiation effects induced by at least two catheters in 44 patients.

Results: Positioning accuracy of the brachytherapy catheters was 5-6 mm. The orthogonal and axial shifts between the center coordinates of the irradiation effect volume and the tolerance dose volume in relation to the direction vector of catheter implantation were highly correlated and in first approximation identically in the T1-w and T2-w MRI sequences ($p = 0.003$ and $p < 0.001$, respectively), as were the shifts between 6 and 12 weeks examinations ($p = 0.001$ and $p = 0.004$, respectively). There was a significant shift of the irradiation effect towards the catheter entry site compared with the planned dose distribution ($p < 0.005$). Prolonged treatment time increases the normal tissue tolerance dose. Here, the catheter contribution indices indicated a lower tolerance dose of the liver parenchyma in areas with prolonged irradiation ($p < 0.005$).

Conclusions: Positioning accuracy of brachytherapy catheters is sufficient for clinical practice. Reduced tolerance dose in areas exposed to prolonged irradiation is contradictory to results published in the current literature. Effects of prolonged dose administration on the liver tolerance dose for treatment times of up to 60 minutes per HDR-BT session are not pronounced compared to effects of positioning accuracy of the brachytherapy catheters and are therefore of minor importance in treatment planning.

* Correspondence: lutz.luedemann@charite.de
† Contributed equally
[1]Department of Radiation Therapy, Charité Medical Center, Berlin, Germany
Full list of author information is available at the end of the article

1 Background

Single-fraction ^{192}Ir high-dose-rate brachytherapy (HDR-BT) of the liver is an ablation technique which has shown promising results with respect to safety and efficacy in the treatment of nonresectable primary and secondary liver malignancies [1-3]. HDR-BT provides steep dose gradients at the surface of the target volume due to the low γ-ray energy of ^{192}Ir and use of a point source, and thus can be used to treat several malignancies in one session or recurrent malignancies sequentially without seriously impairing the functional hepatic reserve [4]. To prevent recurrence at the tumor margins, catheter placement and dwell positions of the ^{192} Ir point source have to be carefully planned [5]. The accuracy of dose application is predominantly dependent on catheter positioning. Computed tomography (CT) was used to monitor catheter implantation, and 3D CT datasets acquired in breath-hold were used for treatment planning. For irradiation patients were transferred from the CT unit to the brachytherapy unit. Dislocation of catheters during patient transfer might be a potential source of error with respect to correct dose application at the target site. Additionally, the liver is an elastic organ and could be deformed between catheter implantation and irradiation.

The treatment of larger tumors with an ^{192}Ir point source requires the implantation of approximately 1 catheter for each 1 - 2 cm of tumor diameter. The contributions of several catheters with numerous dwell positions to the planned dose in a large part of the target volume lead to regional prolongation of irradiation. Several authors describe an increased normal tissue dose tolerance for prolonged radiation therapy or pulsed dose rate (PDR) radiation therapy [6,7] even if the total irradiation time is less than one hour [8].

The present study aims at addressing two methodical aspects of HDR-BT: First, to investigate the limits of catheter positioning accuracy and its clinical importance. Second, to investigate if effects of prolonged irradiation times on the tolerance dose of normal liver parenchyma are important for clinical practice and may have to be taken into account in treatment planning.

2 Methods

Study population

In this study we retrospectively analyzed irradiation effects on normal liver tissue in 50 consecutive patients who underwent CT-guided single-fraction HDR-BT as part of a clinical phase II study prospectively assessing local tumor control. In 50 HDR-BT sessions a total of 76 solid primary or secondary liver tumors were treated (1 - 4 malignant tumors per session). The study was approved by the local ethics committee. Written informed consent was obtained from all patients.

Interventional technique

The interventional technique has been described in detail elsewhere [9]. In brief, a T2-weighted (T2-w) respiratory-triggered ultrafast turbo spin echo (UTSE) and a T1-weighted (T1-w) breath-hold gradient echo (GRE) sequence with administration of the hepatocyte-specific contrast agent gadobenate dimeglumine (Gd-BOPTA (Multihance), Bracco, Princeton, NJ) were acquired to delineate primary and secondary liver lesions (see Follow-up section below). The brachytherapy catheters were positioned using CT guidance (Somatom 4, Siemens, Erlangen, Germany), i.e., CT scans were acquired continuously during the interventional procedure with an image reconstruction rate of 12 per second to monitor actual catheter location. They were placed in 6F angiographic sheaths (Radiofocus, Terumo, Japan), which were implanted in Seldinger technique within the tumors. The angiographic sheaths were sutured to the skin. After catheter positioning, a spiral CT scan of the liver (matrix size, 512 × 512; slice thickness, 5 mm; increment, 5 mm) enhanced by intravenous administration of iodine contrast medium (100 ml Ultravist 370; flow, 1 ml/s; start delay, 80s) was acquired in breath-hold technique for treatment planning. Four catheters were implanted on average per HDR-BT session (range, 1 - 11 catheters).

Treatment planning and irradiation

Treatment was planned using the BrachyVision software package, version 7.1 (Varian Medical Systems, Palo Alto, CA). The dwell positions and irradiation times were optimized to ensure delivery of the prescribed dose to the entire clinical target volume (CTV), see Figure 1. The 24-channel HDR afterloading system (Gammamed 12i, Varian, Charlottesville, VA) employed a ^{192}Ir source (nominal source strength, 370GBq). A dose of 15, 20, or 25Gy was prescribed, which was planned to enclose the lesion (clinical target volume). Compromises were necessary if organs of risk such as the stomach, small intestine, or a large bile duct were very close to the target. No upper limit was defined for the dose within the tumor volume. To preserve liver function after irradiation, one third of the liver parenchyma should receive a dose of less than 5Gy. The effective irradiation time needed to apply the target dose with all catheters was corrected according to the actual ^{192} Ir source strength. We usually limit the maximum irradiation time to 60 minutes to increase patient comfort. The catheters were then sequentially connected to the afterloading system according to the prescribed enumeration, and irradiation was started at the most distant dwell position in each catheter. All dwell positions within one catheter were sequentially irradiated without any delay. An interval of

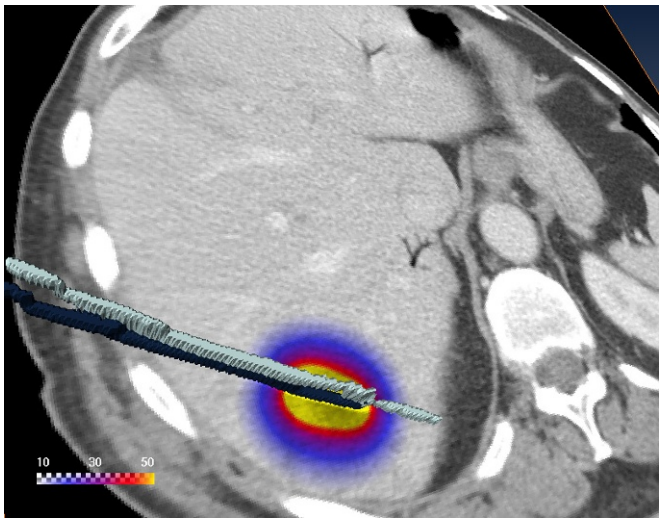

Figure 1 Geometry. The 3D visualization shows a CT slice with the calculated dose in Gy overlayed. The dose is applied using two catheters. The two catheters were visualized in 3D using surface rendering of the catheters labeled in the CT scan.

approx. 2 - 3 minutes was required for connecting each catheter. Manual sequential connection of the catheters was necessary because only a single adapter was available for connecting the catheters to the afterloader. The exposure times were in the range of 844 - 4432 seconds.

Follow-up

A total of 161 MRI examinations were performed 6 ± 2 weeks and 12 ± 2 weeks after HDR-BT. The MRI protocol comprised the following sequences (Gyroscan NT Intera, Philips, The Netherlands) [10]: T2-w respiratory-triggered UTSE (echo time/repetition time (TE/TR), 90/2100 ms; echo train length (ETL), 21; slice thickness, 8 mm, acquired in interleaved mode with no gap) with fat suppression to assess the extent of interstitial edema and T1-w breath-hold GRE (TE/TR 5/30 ms; flip angle,30°; slice thickness, 8 mm, acquired in, interleaved mode with no gap) 2 h after intravenous injection of 15 ml gadobenate dimeglumine (Gd-BOPTA (Multihance), Bracco, Princeton, NJ). The hepatocyte-specific contrast agent gadobenate dimeglumine allowed visualization of the extent of hepatocyte dysfunction. The underlying mechanism of intracellular uptake is a polyspecific organic anionic transport [11-13].

Image registration

Merging of the 3D dosimetry data calculated by BrachyVision with the corresponding follow-up MRI scans was accomplished using an independent image registration implementation within the 3D visualization software Amira 3.1 (Mercury Computer Systems, Berlin, Germany). The image voxel-property-based registration method allowed affine transformation (12 degrees of freedom: 3

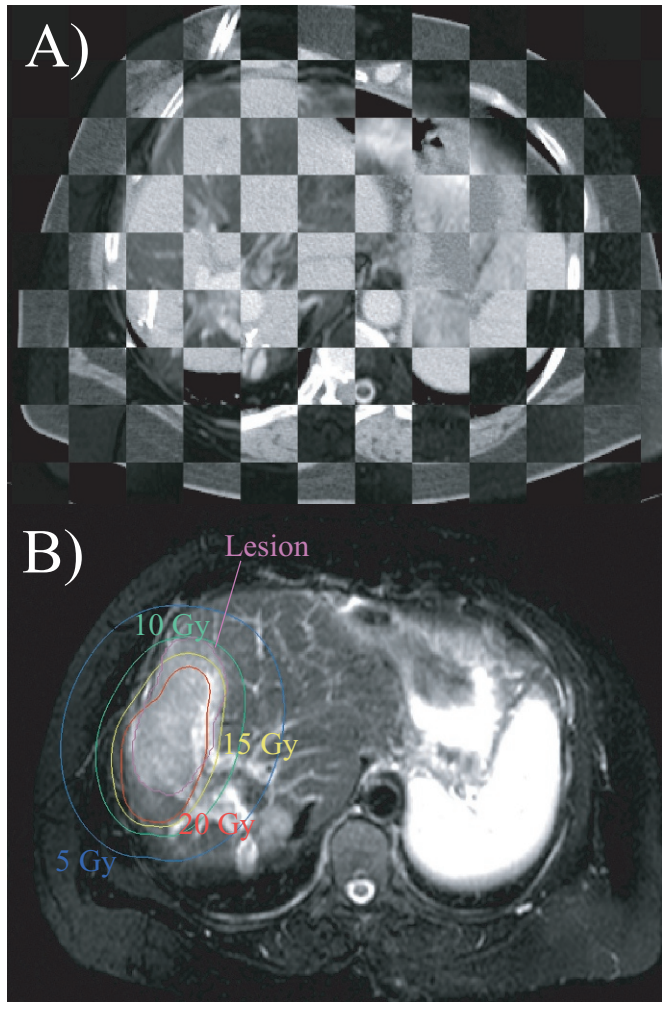

Figure 2 Image registration. A) T2-w image coregistered with the planning CT. Note that only the liver was coregistered and therefore good matching of the images was only achieved for the liver. B) T2-w image showing segmented lesion and isodoses at 12-week follow-up. A prononounced shift of the irradiation effect with respect to the planned dose distribution as shown in this example was typically not found.

rotations, 3 translations, 3 scalings, and 3 shears) by exploring the normalized mutual information (NMI) [14], see Figure 2A. The liver including a 1-cm margin was segmented in the treatment planning CT. The segmented data served as reference for registration to optimize registration accuracy for the liver. Registration accuracy was validated using intrahepatic vessel bifurcations as landmarks. Three to four landmarks were set in the CT and MRI image data of ten patients. Distances between the landmarks in the coregistered images (CT vs. MRI) were determined using the differences between the absolute positions determined with Amira. A total of 120 coregistered landmark combinations were evaluated.

Calculation of normal liver tissue tolerance dose

The borders of hyperintensity on T2-w images (interstitial edema) and hypointensity on late Gd-BOPTA-

enhanced T1-w images (hepatocyte dysfuntion) around the irradiated liver tumors were outlined, see Figure 2B. The volume of each irradiation effect was determined. As the next step, we used this volume to calculate the 3D-isodose, which was confined to the liver and encompassed a corresponding volume (± 1%). The calculated isodose was taken as a surrogate for the tolerance dose of normal liver tissue assuming consistency between an observed radiation effect and the dose applied [9]. The volume encompassed by the isodose surface will be referred to as tolerance dose volume in the following. The mismatch areas between both volumes were investigated in detail for the effect of prolonged irradiation time, see Figure 3.

Measurement of lesion volume shift in relation to planned volume

Potential inaccuracies of the treatment planning procedure or catheter dislocation were analyzed by calculating the shift between the center coordinates of the irradiation effect volume and the tolerance dose volume using the coordinate system of the planning CT. Only those brachytherapies were evaluated in which the catheters were implanted unidirectionally, i.e., in parallel (n = 38).

The direction vector of an implanted catheter was calculated from the coordinates of the catheter skin entry site and the catheter tip in the treatment planning CT. If more than one catheter was implanted, an average coordinate from the coordinates of the entry sites and of the catheter tips was calculated. The direction vector of catheter implantation was converted into a unit vector $\vec{e}$ with unit length 1 *cm*.

The shift vector $\vec{S}$ describing the shift between the irradiation effect volume and the tolerance dose volume was calculated from the center coordinates of both volumes. The scalar product of the unit vector and the shift vector, $S_{axial} = \vec{e} \cdot \vec{S}$, was taken as a measure of the shift between irradiation effect volume and tolerance dose volume axial to the direction vector of catheter implantation. It serves as a surrogate for catheter dislocation within the catheter track. The vector product of both vectors, $S_{ortho} = |\vec{e} \times \vec{S}|$, provides a measure of the orthogonal shift between the center coordinates of the irradiation effect volume and the tolerance dose volume in relation to the direction vector of catheter implantation. Since movement of the brachytherapy catheters within the liver is limited to the catheter track the orthogonal shift results mainly from methodical limitations of image registration due to local liver deformation. The vector product thus serves as an additional surrogate for registration inaccuracy.

An asymmetry coefficient of the scalar and vector product was calculated to differentiate between a systematic shift and registration inaccuracy:

$$AC_S = \frac{|S_{axial}| - S_{ortho}}{0.5(|S_{axial}| + S_{ortho})} \quad (1)$$

A positive value of the asymmetry coefficient indicates a shift predominantly parallel to the direction vector of the implanted catheter, whereas a negative value indicates a shift predominantly orthogonal to the direction vector of the implanted catheter.

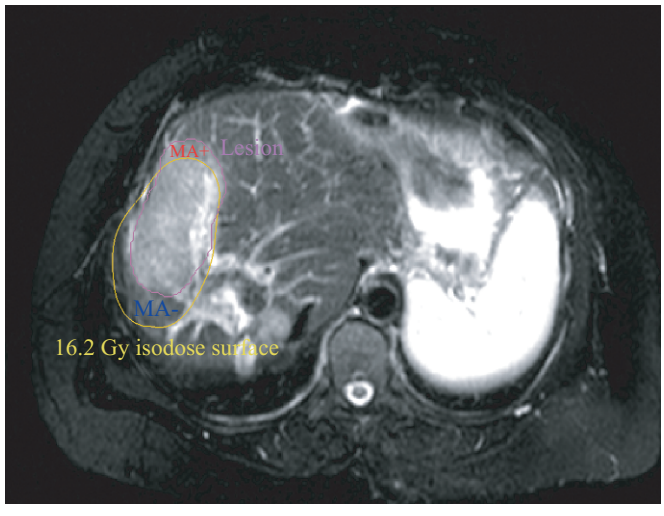

Figure 3 Mismatch areas. T2-w image showing segmented irradiation effect and 16.2Gy isodose encompassing the corresponding tolerance dose volume. A very pronounced shift of the irradiation effect with respect to the isodoses is shown to illustrate the likely maximum inaccuracy of catheter positioning. Mismatch areas in which we observed a dose response at doses smaller than the tolerance dose of the total irradiation effect are indexed with "*MA+*" and mismatch areas in which we did not observe a dose response at doses higher than the tolerance dose of the total irradiation effect are indexed with "*MA-* ".

Evaluation of prolonged irradiation time

Irradiation took up to 4432 seconds (≈ 74 minutes) using multiple catheters with numerous dwell positions of the ^{192}Ir source. Therefore, in areas with significant dose contribution of several catheters, dose delivery time was prolonged and may be characterized as pulsed dose administration. The effects of regionally longer, pulsed irradiation were investigated in areas where the extent of hepatocyte dysfunction and edema was not consistent with the applied dose. Only radiation effects induced by at least 2 brachytherapy catheters were assessed (n = 48).

We used a boolean tool implemented in Amira 3.1 to identify nonoverlapping areas of the irradiation effect volume and the corresponding tolerance dose isovolume (confined to the liver). These areas will be referred to as mismatch areas in the following. Mismatch areas where edema or hepatocyte dysfunction occurred at doses

smaller than the tolerance dose of the total irradiation effect are indexed with '"MA+". Conversely, mismatch areas in which edema or hepatocyte dysfuntion did not manifest at doses exceeding the tolerance dose of the total irradiation effect are indexed with "MA-", see Figure 3. The '"MA+" and "MA-" mismatch areas by definition have identical volumes.

A comprehensive description of the time course of irradiation in brachytherapy is difficult since multiple catheters with numerous dwell positions contribute to dose fractionation in each voxel. First, the total voxel dose, D_{tot} (x,y,z), depends on the voxel position. Second, the dose contribution of each catheter, $D_i(x, y, z)$, depends on the voxel position, (x,y,z), where i is the catheter number. Third, each voxel is irradiated with a different dose administration scheme, D_{tot} $(x,y,z) = \Sigma_n$ $D_i(x,y,z)$, where n is the number of catheters. The BrachyVision software allows separation of the total dose map, D_{tot} (x,y,z), into n separate dose maps, $D_i(x,y,z)$, for each catheter $\boldsymbol{i}$, see Figure 4. We calculated a total of 202 separate treatment plans using the treatment planning system to determine the contribution of each catheter to the total of 48 irradiation effects. To estimate the prolongation of irradiation by the ^{192}Ir HDR source we calculated a catheter contribution index, $I_P(x, y,z)$, that uses the number of dose contribution pulses:

$$|I_P(x,y,z)| = n - \sum_{i=1}^{n} \sqrt{\left(2 \cdot \frac{D_i(x,y,z)}{D_{tot}(x,y,z)} - 1\right)^2} \qquad (2)$$

The irradiation of a single voxel is prolonged as the number of dose-contributing catheters increases. Therefore, the catheter contribution index increases with the number of contributing catheters. In case of a single contributing catheter, $I_P = 0$. In case of two equally contributing catheters, $D_i / D_{tot} = 0.5$, and $I_P = 2.0$. I_P is always in the range between 0 and 2. The separate treatment plans were combined in a voxelwise approach using an arithmetic module implemented in Amira 3.1, see Figure 5.

Catheter contribution index $I_P(x,y,z)$ was then averaged over the 3D maps of the mismatch areas, $I_P(MA+)$ and $I_P(MA-)$. We calculated an asymmetry coefficient with the following formula

$$AC_I = \frac{I_P(MA+) - I_P(MA-)}{0.5(I_P(MA+) + I_P(MA-))} \qquad (3)$$

to compare the averaged catheter contribution indices $I_P(MA+)$ and $I_P(MA-)$ calculated using Eq. 2. A value of the asymmetry coefficient > 0 indicates that the catheter contribution index in "MA+" is higher than in "MA-", vice versa a value of the asymmetry coefficient < 0

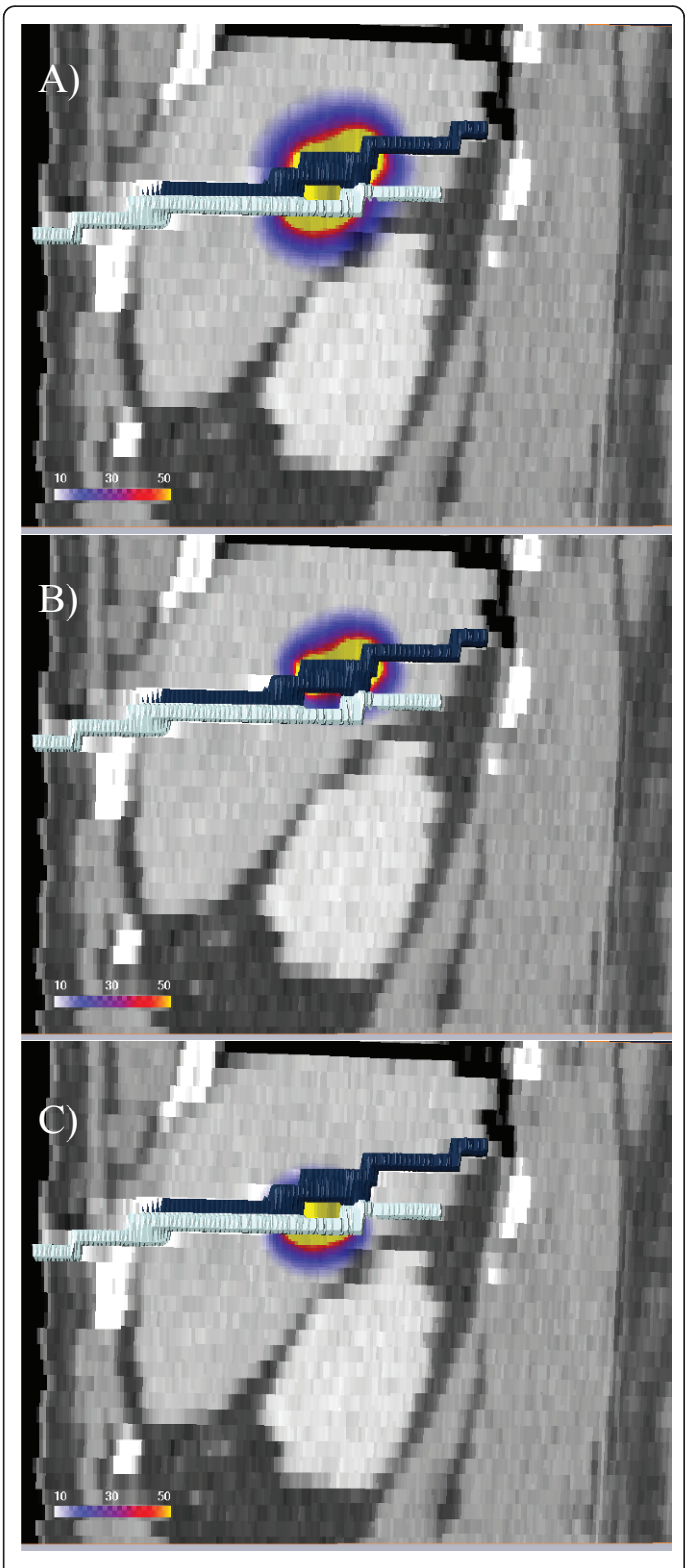

Figure 4 Dose separation. The 3D visualization shows a coronal CT reconstruction with the calculated dose in Gy overlayed using the patient in Fig. 1. The dose is applied using two catheters. The two catheters were visualized in 3D using surface rendering of the catheters labeled in the CT scan. A) Total dose, D_{tot} , overlayed. B) Dose applied by the cranial catheter, D_1. C) Dose applied by the caudal catheter, D_2 .

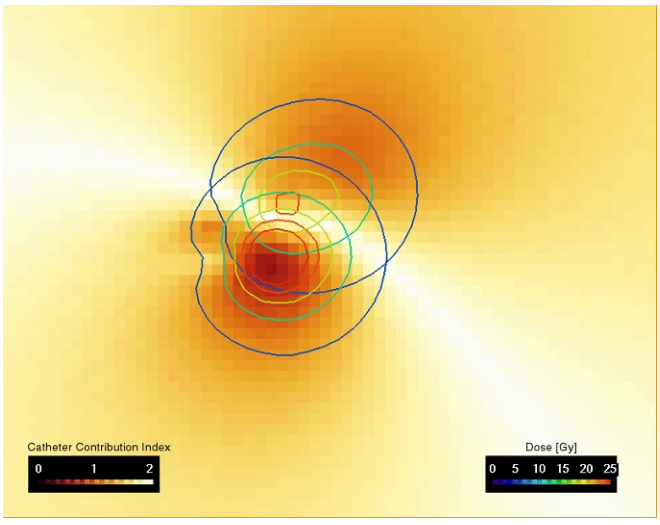

Figure 5 Catheter contribution index. The image showing the separated isodoses of two catheters for the patient in Fig. 1 and Fig. 4. The separated doses of the cranial and caudal catheter (Fig. 4) are used to calculate the catheter contribution index (Eq. 2) shown in color coding. In case of two equally contributing catheters, D_i/D_{tot} = 0.5 and I_P = 2.0. I_P is always in the range between 0 and 2.

indicates that the catheter contribution index in "MA+" is lower than in "MA-".

Statistical analysis

The Generalized Estimating Equation (GEE) model was employed to statistically assess limits of catheter positioning accuracy and the effects of prolonged irradiation times on the tolerance dose of normal liver parenchyma. For a dataset consisting of repeated measurements (2 MRI sequences, 2 follow-up dates) of a variable of interest, a GEE model allows the correlation of outcomes within one individual to be estimated and taken into appropriate account in the equation which generates the regression coefficients and their standard errors [15,16]. The GEE model was calculated with SAS, Version 9.1 (SAS Institute Inc., Cary, NC, USA). A $p < 0.05$ was considered significant.

3 Results

The validation of image registration accuracy using landmarks yielded a mean deviation of 2.64 mm (25% quartile width (Q_{25}): 0.28 mm, 75% quartile width (Q_{75}): 4.51 mm). Thus registration accuracy proved to be sufficient for evaluating catheter positioning accuracy. A total of 161 MRI examinations of 62 irradiation effects were performed 6 and 12 weeks after HDR-BT. Table 1 shows the mean volume and threshold dose of hepatocyte dysfunction (T1-w images) and interstitial edema (T2-w images) and corresponding liver tolerance doses as well as the standard deviation between the examinations at 6 and 12 weeks (6W and 12W).

Table 1 Normal liver tissue tolerance dose and volume of irradiation effect

	6w T1-w	12w T1-w	6w T2-w	12w T2-w
n =	44	36	48	33
Dose/Gy	13.7 ± 4.8	16.7 ± 5.0	14.3 ± 6.2	16.6 ± 6.4
Volume/ cm^3	190.3 ± 158.6	127.2 ± 118.8	190.0 ± 166.4	157.0 ± 143.5

Mean normal liver tissue tolerance dose and volume (± standard deviation) for interstitial edema assessed by hyperintensity on T2-w images and hepatocyte dysfunction assessed by hypointensity on T1-w images six/twelve weeks (6w and 12w) after HDR-BT (n: number of MRI examinations evaluated).

A total of 96 follow-up MRI examinations of 30 patients with 38 irradiation effects were assessed to analyze methodical limitations of catheter positioning accuracy. Only patients with unidirectionally implanted, i.e., nearly parallel, catheters were included in the evaluation. The median number of catheters inserted was 2 (Q_{25}:1, Q_{75}: 3 catheters; range: 1-8 catheters).

Table 2 presents the axial, orthogonal, and total shifts (in mm) between the center coordinates of the irradiation effects and tolerance dose volumes in relation to the direction vectors of catheter implantation. The mean axial shift of hepatocyte dysfunction (T1-w images) was -5. 3 ± 5.4 mm and of interstitial edema (T2-w images) -5. 6 ± 6.0 mm in plane, indicating a shift of the irradiation effect volume against the corresponding tolerance dose volume in the direction of the catheter entry sites. The orthogonal shift as a surrogate for registration inaccuracy due to liver deformation was 4.0 ± 2.5 mm on T1-w images and 4.6 ± 2.6 mm on T2-w images.

The orthogonal and axial shifts between the center coordinates of the irradiation effect volume and the tolerance dose volume in relation to the direction vector of catheter implantation were highly correlated in the T1-w and T2-w MRI sequences ($p = 0.003$ and $p < 0.001$, respectively), as were the shifts between 6 and 12 weeks examinations ($p = 0.001$ and $p = 0.004$, respectively).

The asymmetry coefficient of the orthogonal and axial shifts of the center coordinates of the irradiation effect

Table 2 Shift between irradiation effect and planned dose distribution

	T1-w	T2-w
n =	47	49
Axial shift/mm	-5.3 ± 5.4	-5.6 ± 6.0
Orthogonal shift/mm	4.0 ± 2.5	4.6 ± 2.6
Total shift/mm	7.7 ± 4.4	8.4 ± 4.4
AC_S	1.14 ± 0.43	1.04 ± 0.49

Mean axial, orthogonal, and total shift between center coordinates of the irradiation effect and planned dose distribution in relation to the direction vector of catheter implantation for T1-w and T2-w MRI data. Both follow-up dates, 6w and 12w, were evaluated together. A negative value of the axial shift indicates a shift into the direction of the catheter entry site. T1-w = hepatocyte dysfunction, T2-w = interstitial edema, n = number of MR examinations assessed.

and corresponding tolerance dose volume in relation to the direction vector of catheter implantation, AC_S, was 1.14 ± 0.43 for hepatocyte dysfunction and 1.04 ± 0.49 for interstitial edema, indicating that the axial shift as a surrogate for catheter dislocation within the catheter track was predominant ($p < 0.005$). The asymmetry coefficient was significantly affected by the MRI sequence used ($p = 0.014$) but not by the change in the irradiation effect volume between the 6-week and 12-week examinations ($p = 0.48$).

A total of 129 follow-up MRI examinations of 44 patients with 48 irradiation effects were assessed to analyze the effect of prolonged irradiation time on the tolerance dose of normal liver parenchyma. All irradiation effects were induced by at least 2 brachytherapy catheters. The median number of catheters per irradiation effect was 4 (Q_{25}: 3; Q_{75}: 6 catheters; range: 2-11 catheters). The average time for complete application of the radiation dose was 1865 ± 758 seconds (range: 844 - 4432 seconds).

The volumes of the mismatch areas, "MA+" and "MA-", averaged over the 6-week and 12-week follow-up MRI examinations and T1-w and T2-w acquisitions, was 40.6 ± 28.9 cm^3 (23.5 ± 10.1%). The differences between the mismatch area volumes with regard to 6-week and 12 week follow-up examinations and T1-w and T2-w MRI are small, see Table 3. The average dose in "MA+" is approximately 12Gy 6 weeks and 14Gy 12 weeks after the intervention. The average dose in "MA-", is approximately 22-23Gy 6 weeks and 28Gy 12 weeks post intervention, see Table 3. The difference between the average doses in the mismatch areas is significant ($p < 0.0001$). The values for the catheter contribution indices in the mismatch areas, $I_P(MA+)$ and $I_P(MA-)$, as well as the asymmetry coefficients of the catheter contribution indices in the mismatch areas, AC_I, with respect to hepatocyte dysfunction and interstitial edema and the corresponding follow-up dates are displayed in Table 3. The mean of AC_I is > 0 in each subgroup, indicating that the catheter contribution index in "MA+" is slightly higher than in "MA-". $I_P(MA+)$ and $I_P(MA-)$ are significantly affected by the volume loss of the irradiation effect between the 6-week and 12-week follow-up examinations and consecutive shifts of the mismatch areas towards the high dose regions of the dose plan ($p = 0.0014$). There is no significant difference between $I_P(MA+)$ and $I_P(MA-)$ with respect to hepatocyte dysfunction and interstitial edema ($p = 0.9$).

Table 3 Mean dose, deviation of mean dose from normal liver tissue tolerance dose, and dose protraction in mismatch areas

	6W T1-w	12W T1-w	6W T2-w	12W T2-w
n	35	27	40	27
$D(MA+)$/Gy	12.0 ± 4.3	14.1 ± 4.4	11.8 ± 5.4	14.0 ± 6.3
$D(MA-)$/Gy	23.2 ± 11.9	28.5 ± 11.0	22.2 ± 11.6	27.7 ± 15.1
$\Delta D(MA+)$/Gy	-2.1 ± 2.8	-3.2 ± 1.9	-2.1 ± 4.3	-3.0 ± 3.1
$\Delta D(MA-)$/Gy	9.1 ± 7.5	11.2 ± 6.8	8.3 ± 6.6	10.7 ± 8.8
$I_P(MA+)$	1.67 ± 0.33	1.69 ± 0.26	1.67 ± 0.31	1.70 ± 0.27
$I_P(MA-)$	1.45 ± 0.39	1.35 ± 0.37	1.45 ± 0.37	1.39 ± 0.36
AC_I	0.17 ± 0.28	0.25 ± 0.27	0.16 ± 0.26	0.23 ± 0.22
V (*MA* +/*MA*-)/cm^3	42.0 ± 26.7	38.2 ± 31.2	40.8 ± 29.2	43.0 ± 33.1
V (*MA* +/*MA*-)/%	21.8 ± 11.1	23.9 ± 7.8	23.1 ± 0.8	27.0 ± 9.0

$D(MA+)$, $D(MA-)$: Average dose in mismatch areas; "*MA*+" for response at doses smaller than the tolerance dose and "*MA*-" for missing response at doses exceeding the tolerance dose.

$\Delta D(MA+)$, $\Delta D(MA-)$: Difference between the average dose in "*MA*+"and "*MA*-" and corresponding tolerance dose of the irradiation effect.

$I_P(MA+)$, $I_P(MA-)$: Catheter contribution index in "*MA*+" and "*MA*-".

AC_I : Asymmetry coefficient between the catheter contribution indices in "*MA* +" and "*MA*-".

V (*MA* +/*MA*-): Volume of the mismatch areas "*MA*+" and "*MA*-" in percent and absolute value which is per definition identical for both areas.

Errors are given as standard deviation.

4 Discussion

In this study, we sought to assess two methodical aspects of HDR-BT: first, limits of catheter positioning accuracy and, second, effects of prolonged irradiation on the tolerance dose of normal liver parenchyma. The mean shift between the center coordinates of the irradiation effect volume and corresponding tolerance dose volume in relation to the direction vector of catheter implantation is ≈ - 5 mm in plane, indicating a shift of the irradiation effect in the direction of the catheter entry site. The shift is within the slice thickness of 5 mm of the treatment planning CT but larger than could be explained by registration inaccuracy, which is ≈ 3 mm, and inaccuracy due to local liver deformation in the follow-up images, resulting in an overall registration inaccuracy of ≈ 4-5 mm.

Determination of catheter positioning accuracy might be limited by the delineation of the brachytherapy catheters in the treatment planning CT since applicator geometry is entered manually. Partial volume effects in the treatment planning datasets could be a potential source of error in the treatment planning procedure, especially for catheters in oblique direction, since correct placement of the starting point of the catheter is dependent on conspicuity of the catheter tip.

Another limitation is the dislocation of catheters between acquisition of the planning CT and irradiation. Although the angiographic sheaths containing the catheters were secured to the skin by suture, retraction of the brachytherapy catheters within the catheter tracks might potentially occur due to patient movement, e.g., when the patient is transferred from the CT unit to the brachytherapy unit, and liver movement during respiration. However, the extent of the shift between an irradiation

effect and the center of the planned dose distribution does not suggest a significant dislocation of the brachytherapy catheters within the catheter tracks.

The systematic shift between the irradiation effect volume and planned dose distribution has to be considered in treatment planning when defining the CTV to avoid underdosage of the tumor periphery. In our institution, the CTV comprises the tumor volume visible on contrast-enhanced CT scans plus a 5-mm safety margin. With regard to treatment planning, we conclude that a slice thickness exceeding 3 mm potentially impairs catheter positioning accuracy. We furthermore propose that it would be beneficial to increase the safety margin of the CTV in the direction of the catheter tips from 5 to 10 mm to avoid underdosage and consecutive recurrence at the tumor margin. The amount of mismatch (Table 3) between planned dose distribution and irradiation effect volume is determined by the registration accuracy or possibly by biological effects but does not allow to assess the reproducibility of the CTV. Two studies evaluated the accuracy of target positioning in extracranial stereotactic radiotherapy (ESRT) using special patient fixation. For mobile soft tissue targets, such as liver metastasis, Wulf et al. [17] reported mean target deviations of 0.9 ± 4.5 mm, 0. 9 ± 3.0 mm, and 3.4 ± 3.2 mm in the craniocaudal, anteroposterior, and lateral directions, respectively, when breathing control was applied. The mean 3D deviation of the targets was 6.1 ± 4.6 mm.

For single-fraction therapy, Herfarth et al. [18] reported mean target set-up deviations between treatment planning and treatment of 4. 0 ± 2.5 mm, 2.2 ± 1. 8 mm, and 2.2 ± 1.7 mm in the craniocaudal, anteroposterior, and lateral directions, respectively. The mean 3D deviation of the targets was 5.7 ± 2.5 mm.

The total in-plane deviation of the target location in our study was slightly higher, 4-6 ± 2-6 mm. However, we determined the effective positioning accuracy by comparing the shift between the irradiation effect in follow-up MRI and planned dose distribution. The authors quoted above compared treatment planning images with control CT datasets acquired before treatment [17,18] and did not evaluate the treatment effect.

Based on metric analysis of target mobility and set-up inaccuracy in the CT simulation prior to or during treatment, safety margins for defining the planning target volume (PTV) of about 5 mm in axial and 5 - 10 mm in craniocaudal direction are commonly added to the CTV in ESRT of lung and liver tumors [19]. In contrast to the present study, Wulf et al. evaluated the reproducibility of the CTV of lung and liver tumors within the planning target volume (PTV) over the entire course of hypofractionated treatment in CT simulation prior to application of each fraction [19]. The mean volume ratio of the PTV to the CTV was 2.2 ± 0.6 in liver targets. The authors showed that especially liver tumors with a CTV exceeding 100 cm^3 were susceptible to target deviation exceeding the standard safety margins for PTV definition. They suggested to increase the PTV by adding a larger safety margin to ensure adequate target dose deposition in these CTVs. In brachytherapy, the applicator moves to a certain extent together with the target and there is no need to increase the safety margin for larger tumors.

Catheter dislocation in brachytherapy was mainly investigated in fractionated HDR brachytherapy of the prostate, which differs from the technique used here in that a much larger number of catheters are implanted for more than one day. Imaging techniques (cone beam CT and CT) were used to assess catheter dislocation between the first and second fraction, i.e., over 24 hours. Foster et al. found a mean catheter displacement of 5. 1 mm, resulting in a significantly ($p < 0.01$) decreased mean prostate V_{100} (volume receiving 100Gy or more) from 93.8% to 76.2% [20]. Five patients had maximum catheter displacement exceeding 10 mm. Simnor et al. found a mean movement in caudal direction relative to the prostate base between the first and second fraction of 7. 9 mm (range 0-21 mm). Planning target volume dose $D_{90\%}$ was reduced without movement correction by a mean of 27.8% [21]. Kim et al. found an average (range) magnitude of craniocaudal catheter displacement of 2.7 mm (- 6.0 to 13.5 mm) using bone markers and 5.4 mm (-3.75 to 18.0 mm) using the center of two gold markers [22]. Catheter dislocation in fractionated HDR brachytherapy of the prostate is in the same range as in the present study but, because of the much more complex irradiation geometry, the impact on dose coverage is much larger.

We assessed the effect of prolonged irradiation times on the tolerance dose of normal liver tissue to determine its relevance for treatment planning. A catheter contribution index served as a surrogate for prolonged pulsed dose administration in nonoverlapping areas of the irradiation effect volume and the corresponding tolerance dose volume. The catheter contribution index was slightly but significantly higher in “MA+” than in “MA-”, indicating a prolongation of dose application in “MA+” compared to “MA-”. Based on published data, we would have expected to find an increased tolerance dose of the liver parenchyma in areas irradiated for a longer time, i. e., by several catheters [6,7], even if the overall irradiation time is less than one hour [8]. However, we found a decreased tolerance dose of the liver parenchyma in areas where the radiation dose was applied by several catheters for a prolonged period of time.

We hypothesize that the effects of prolonged irradiation on the tolerance dose of normal liver tissue might have been obscured by other factors. For instance,

biological effects such as reactive inflammatory changes may mimic irradiation effects, or scarring of the liver tissue induced by catheter insertion may cause retraction of the irradiation effect towards the catheter entry site. Furthermore, we propose that inaccuracies in the positioning of the brachytherapy catheters are more pronounced in areas where several catheters contribute to the total irradiation dose and that the total applied effective dose in "MA+" was higher than would have been expected from the treatment plan. Since steep dose gradients are an inherent quality of interstitial HDR-BT, the shift of active dwell positions of one or several catheters towards the tumor periphery would be sufficient to significantly increase the applied dose outside the CTV. As the number of catheters increases, the probability of a dose shift due to slight inaccuracy in catheter positioning likely increases as well.

We conclude that the effects of prolonged irradiation time are of minor importance for interstitial HDR-BT compared to other factors such as positioning accuracy of brachytherapy catheters and do not have to be taken into account in treatment planning in HDR-BT if the total irradiation time does not significantly exceed one hour.

The study has several limitations. Obviously one key issue of the study is the registration accuracy. The validation of registration accuracy was based on corresponding vessel bifurcations identified in the planning CT and follow-up MR images by an experienced radiologist [23,24]. We applied affine registration, allowing 12 degrees of freedom, which compensates for whole organ deformation and yielded an accuracy of ≈ 3 mm with respect to vessel bifurcations within the central parts of the liver, comparable to other studies [25,26]. Affine registration has been proven to be precise and robust for liver registration [25-27]. However, local liver deformation resulting from compression by adjacent organs (such as the stomach), different respiration levels, or the implanted catheters in the treatment planning CT data might not be sufficiently compensated for. To adequately compensate for these effects a finite element model-based deformable image registration would have been superior [23,24]. We tried to compensate for the limitations of affine registration by restricting the registration to the liver [25]. Using this procedure, we achieved a registration accuracy with a mean deviation of 2.64 mm, which was smaller than that of the nonrigid registration used by Elhawary et al. [28], for which the authors reported a mean target registration error of. 4.1 mm and a mean 95^{th}-percentile Hausdorff distance of 3. 3 mm.

Second, the catheter contribution index has to be considered a rough simplification, merely providing a first estimate of the effect of prolonged dose administration. Dose administration was considered highly prolonged if the index was 2 (meaning that each catheter of the brachytherapy implant contributed < 50% of the irradiation dose in the mismatch area). It was considered fairly prolonged if the value was between 1 and 2 (indicating that more than 25% of the total irradiation dose in the mismatch area was applied by more than 1 catheter), and nonprolonged if the value was ≤ 1 (meaning that 75% or more of the total irradiation dose in the mismatch area was applied by 1 catheter only). Nevertheless, the tool is sufficient to rule out practically relevant effects of prolonged dose administration in HDR-BT in vivo.

5 Conclusions

In conclusion, positioning accuracy of brachytherapy catheters is sufficiently precise with approx. 5-6 mm. Accuracy was within the 5-mm slice thickness of the treatment planning CT. Thus positioning accuracy is potentially affected by inaccuracy in the delineation of the brachytherapy catheters during treatment planning due to partial volume effects in the planning CT. Retraction of the catheters within the catheter tracks during transfer of the patient from the CT unit to the brachytherapy unit might occur; however, this retraction is not pronounced. Therefore, CT-guided HDR-BT can be safely performed, even if CT and brachytherapy are not performed in the same unit. Effects of prolonged irradiation times on the tolerance dose of normal liver tissue are negligible compared to positioning accuracy of brachytherapy catheters and do not have to be taken into account in treatment planning if the total irradiation time does not significantly exceed one hour.

6 Competing interests

The authors declare that they have no competing interests.

7 Authors' contributions

LL, CW: data analysis, manuscript preparation.
PW, JR: study coordination, study design.
MS, KM: data acquisition.
SK: data analysis
All authors read and approved the final manuscript.

Author details
[1]Department of Radiation Therapy, Charité Medical Center, Berlin, Germany. [2]Department of Radiology and Nuclear Medicine, Otto von Guericke University, Magdeburg, Germany. [3]Department of Biometrics and Medical Informatics, Otto von Guericke University, Magdeburg, Germany.

Received: 16 May 2011 Accepted: 5 September 2011
Published: 5 September 2011

References

1. Ricke J, Mohnike K, Pech M, Seidensticker M, Rühl R, Wieners G, Gaffke G, Kropf S, Felix R, Wust P: **Local response and impact on survival after local**

ablation of liver metastases from colorectal carcinoma by computed tomography-guided high-dose-rate brachytherapy. *Int J Radiat Oncol Biol Phys* 2010, **78(2)**:479-485.
2. Mohnike K, Wieners G, Schwartz F, Seidensticker M, Pech M, Ruehl R, Wust P, Lopez-Hänninen E, Gademann G, Peters N, Berg T, Malfertheiner P, Ricke J: **Computed tomography-guided high-dose-rate brachytherapy in hepatocellular carcinoma: safety, efficacy, and effect on survival.** *Int J Radiat Oncol Biol Phys* 2010, **78**:172-179.
3. Wieners G, Mohnike K, Peters N, Bischoff J, Kleine-Tebbe A, Seidensticker R, Seidensticker M, Gademann G, Wust P, Pech M, Ricke J: **Treatment of hepatic metastases of breast cancer with CT-guided interstitial brachytherapy - A phase II-study.** *Radiother Oncol* 2011.
4. Rühl R, Lüdemann L, Czarnecka A, Streitparth F, Seidensticker M, Mohnike K, Pech M, Wust P, Ricke J: **Radiobiological restrictions and tolerance doses of repeated single-fraction hdr-irradiation of intersecting small liver volumes for recurrent hepatic metastases.** *Radiat Oncol* 2010, **5**:44-44.
5. Seidensticker M, Wust P, Rühl R, Mohnike K, Pech M, Wieners G, Gademann G, Ricke J: **Safety margin in irradiation of colorectal liver metastases: assessment of the control dose of micrometastases.** *Radiat Oncol* 2010, **5**:24-24.
6. Hall EJ: **Weiss lecture. The dose-rate factor in radiation biology.** *Int J Radiat Biol* 1991, **59(3)**:595-610.
7. Fowler JF, Van Limbergen EF: **Biological effect of pulsed dose rate brachytherapy with stepping sources if short half-times of repair are present in tissues.** *Int J Radiat Oncol Biol Phys* 1997, **37(4)**:877-883.
8. Pop LA, Millar WT, van der Plas M, van der Kogel AJ: **Radiation tolerance of rat spinal cord to pulsed dose rate (PDR-) brachytherapy: the impact of differences in temporal dose distribution.** *Radiother Oncol* 2000, **55(3)**:301-315.
9. Wybranski C, Seidensticker M, Mohnike K, Kropf S, Wust P, Ricke J, Lüdemann L: **In vivo assessment of dose volume and dose gradient effects on the tolerance dose of small liver volumes after single-fraction high-dose-rate 192Ir irradiation.** *Radiat Res* 2009, **172(5)**:598-606.
10. Ricke J, Seidensticker M, Lüdemann L, Pech M, Wieners G, Hengst S, Mohnike K, Cho CH, Hanninen EL, Al-Abadi H, Felix R, Wust P: **In vivo assessment of the tolerance dose of small liver volumes after single-fraction HDR irradiation.** *Int J Radiat Oncol Biol Phys* 2005, **62(3)**:776-84.
11. Clement O, Siauve N, Cuenod CA, Vuillemin-Bodaghi V, Leconte I, Frija G: **Mechanisms of action of liver contrast agents: impact for clinical use.** *J Comput Assist Tomogr* 1999, **23(Suppl 1)**:S45-52.
12. Kirchin MA, Pirovano GP, Spinazzi A: **Gadobenate dimeglumine (Gd-BOPTA). An overview.** *Invest Radiol* 1998, **33(11)**:798-809.
13. de Haen C, Ferla RL, Maggioni F: **Gadobenate dimeglumine 0.5 M solution for injection (MultiHance) as contrast agent for magnetic resonance imaging of the liver: mechanistic studies in animals.** *J Comput Assist Tomogr* 1999, **23(Suppl 1)**:S169-79.
14. Rohlfing T, West JB, Beier J, Liebig T, Taschner CA, Thomale UW: **Registration of functional and anatomical MRI: accuracy assessment and application in navigated neurosurgery.** *Comput Aided Surg* 2000, **5(6)**:414-25.
15. Burton P, Gurrin L, Sly P: **Extending the simple linear regression model to account for correlated responses: an introduction to generalized estimating equations and multi-level mixed modelling.** *Stat Med* 1998, **17(11)**:1261-91.
16. Zeger SL, Liang KY: **Longitudinal data analysis for discrete and continuous outcomes.** *Biometrics* 1986, **42**:121-30.
17. Wulf J, Hadinger U, Oppitz U, Olshausen B, Flentje M: **Stereotactic radiotherapy of extracranial targets: CT-simulation and accuracy of treatment in the stereotactic body frame.** *Radiother Oncol* 2000, **57(2)**:225-36.
18. Herfarth KK, Debus J, Lohr F, Bahner ML, Fritz P, Hoss A, Schlegel W, Wannenmacher MF: **Extracranial stereotactic radiation therapy: set-up accuracy of patients treated for liver metastases.** *Int J Radiat Oncol Biol Phys* 2000, **46(2)**:329-35.
19. Wulf J, Hadinger U, Oppitz U, Thiele W, Flentje M: **Impact of target reproducibility on tumor dose in stereotactic radiotherapy of targets in the lung and liver.** *Radiother Oncol* 2003, **66(2)**:141-50.
20. Foster W, Cunha JA, Hsu IC, Weinberg V, Krishnamurthy D, Pouliot J: **Dosimetric impact of interfraction catheter movement in high-dose rate prostate brachytherapy.** *Int J Radiat Oncol Biol Phys* 2011, **80**:85-90.
21. Simnor T, Li S, Lowe G, Ostler P, Bryant L, Chapman C, Inchley D, Hoskin PJ: **Justification for inter-fraction correction of catheter movement in fractionated high dose-rate brachytherapy treatment of prostate cancer.** *Radiother Oncol* 2009, **93(2)**:253-258.
22. Kim Y, Hsu IC, Pouliot J: **Measurement of craniocaudal catheter displacement between fractions in computed tomography-based high dose rate brachytherapy of prostate cancer.** *J Appl Clin Med Phys* 2007, **8(4)**:2415-2415.
23. Brock KK, Dawson LA, Sharpe MB, Moseley DJ, Jaffray DA: **Feasibility of a novel deformable image registration technique to facilitate classification, targeting, and monitoring of tumor and normal tissue.** *Int J Radiat Oncol Biol Phys* 2006, **64(4)**:1245-1254.
24. Voroney JP, Brock KK, Eccles C, Haider M, Dawson LA: **Prospective comparison of computed tomography and magnetic resonance imaging for liver cancer delineation using deformable image registration.** *Int J Radiat Oncol Biol Phys* 2006, **66(3)**:780-791.
25. van Dalen JA, Vogel W, Huisman HJ, Oyen WJ, Jager GJ, Karssemeijer N: **Accuracy of rigid CT-FDG-PET image registration of the liver.** *Phys Med Biol* 2004, **49(23)**:5393-5405.
26. Carrillo A, Duerk JL, Lewin JS, Wilson DL: **Semiautomatic 3-D image registration as applied to interventional MRI liver cancer treatment.** *IEEE Trans Med Imaging* 2000, **19(3)**:175-185.
27. Christina Lee WC, Tublin ME, Chapman BE: **Registration of MR and CT images of the liver: comparison of voxel similarity and surface based registration algorithms.** *Comput Methods Programs Biomed* 2005, **78(2)**:101-114.
28. Elhawary H, Oguro S, Tuncali K, Morrison PR, Tatli S, Shyn PB, Silverman SG, Hata N: **Multimodality non-rigid image registration for planning, targeting and monitoring during CT-guided percutaneous liver tumor cryoablation.** *Acad Radiol* 2010, **17(11)**:1334-1344.

doi:10.1186/1748-717X-6-107
Cite this article as: Lüdemann *et al.*: In vivo assessment of catheter positioning accuracy and prolonged irradiation time on liver tolerance dose after single-fraction ^{192}Ir high-dose-rate brachytherapy. *Radiation Oncology* 2011 **6**:107.

ELSEVIER

Int. J. Radiation Oncology Biol. Phys., Vol. 78, No. 2, pp. 479–485, 2010

0360-3016/$–see front matter

doi:10.1016/j.ijrobp.2009.09.026

CLINICAL INVESTIGATION **Liver**

LOCAL RESPONSE AND IMPACT ON SURVIVAL AFTER LOCAL ABLATION OF LIVER METASTASES FROM COLORECTAL CARCINOMA BY COMPUTED TOMOGRAPHY–GUIDED HIGH-DOSE-RATE BRACHYTHERAPY

Jens Ricke, M.D.,* Konrad Mohnike, M.D.,* Maciej Pech, M.D.,* Max Seidensticker, M.D.,* Ricarda Rühl, M.D.,* Gero Wieners, M.D.,* Gunnar Gaffke, M.D.,* Siegfried Kropf, Ph.D.,† Roland Felix, M.D.,‡ and Peter Wust, M.D.‡

*Klinik für Radiologie und Nuklearmedizin and †Institut für Biometrie und Medizinische Informatik, Universitätsklinikum Magdeburg, Magdeburg, Germany; and ‡Klinik für Strahlentherapie, Charité Berlin, Berlin, Germany

Purpose: To determine local tumor control after CT-guided brachytherapy at various dose levels and the prognostic impact of extensive cytoreduction in colorectal liver metastases.
Methods and Materials: Seventy-three patients were treated on a single-center prospective trial that was initially designed to be randomized to three dose levels of 15 Gy, 20 Gy, or 25 Gy per lesion, delivered in a single fraction. However, because there was a high rate of cross-over of subjects from higher to lower dose levels, this study is better understood as a prospective trial with three dose levels. No upper size limit for the metastases was applied. We assessed time to local progression, progression-free survival, and overall survival.
Results: According to safety constraints cross-over was performed. The final assignment was $n = 98$, $n = 68$, and $n = 33$ in the 15-Gy, 20-Gy, and 25-Gy groups, respectively. Median diameter of the largest tumor lesion in each patient was 5 cm (range, 1–13.5 cm). Estimated mean local recurrence-free survival for all lesions was 34 months (median not reached). The group assigned to 15 Gy after cross-over displayed 34 local recurrences out of 98 lesions; 20 Gy, 15 out of 68 lesions; 25 Gy, 1 out of 33 lesions. The difference between the 25-Gy and the 20-Gy or 15-Gy group was significant ($p < 0.05$). Repeated local tumor ablations were the most prominent factor for increased survival and dominated additional systemic antitumor treatments.
Conclusions: Local tumor control after CT-guided brachytherapy of colorectal liver metastases demonstrated a strong dose dependency. The role of extensive minimally invasive tumor ablation in metastatic colorectal cancer needs to be further established. © 2010 Elsevier Inc.

Liver metastases, Local ablation, Brachytherapy, Colorectal carcinoma.

INTRODUCTION

Tremendous advances have been shown recently by the introduction of various new active agents for the treatment of metastatic colorectal cancer (1–3). However, despite the introduction of these new treatments, the 5-year survival rate for metastatic colorectal cancer remains just 10% (4).

Surgical resection of liver metastasis is often limited, despite the fact that 25–35% of patients have the liver as their sole site of disease and could be considered potentially to have regionally confined metastasis (5). The evidence for a benefit of surgical resection is based on retrospective studies only, and the advantage of resection has also been called into question by some investigators owing to a proposed lead time bias and extreme patient selection (6–8). However, surgical resection of liver metastases has been adopted as the standard of care, also on the basis of the observation that long-term survival or cure is usually limited to these patients.

In advanced colorectal cancer the goal of therapy is to eliminate cancer, reduce cancer burden, stabilize cancer, or slow cancer progression (9). Percutaneous ablative therapies achieve substantial tumor kill by directly applying chemicals, temperature changes, or radiation to solid tumors, and they are most widely accepted for their application in the treatment of liver tumors (10–14). These image-guided ablation techniques offer the advantage of reduced morbidity and mortality, as well as lower procedural costs when compared with traditional surgical methods. They can also be performed on an outpatient basis, repeated over time, or combined with other anticancer treatments. Their intention usually is

Reprint requests to: Jens Ricke, M.D., Department of Radiology and Nuclear Medicine, Universitätsklinikum Magdeburg AöR, Leipzigerstrasse 44, 39120 Magdeburg, Germany. Tel: (+49) 391-67-13030; Fax: (+49) 391-67-13029; E-mail: jens.ricke@med.ovgu.de

Conflict of interest: none.

Acknowledgment—The authors thank Mrs. C. Besseler for coordinating patient follow-up and for maintaining the database of this study.

Received June 18, 2009, and in revised form Aug 10, 2009. Accepted for publication Aug 10, 2009.

palliative, even though some investigators claim curative potential on the basis of retrospective data (15).

A new ablation technique has been introduced recently overcoming the size limit of approximately 4 to 5 cm that usually applies for thermal tumor ablation by radiofrequency ablation or laser. This new technique, referred to as CT-guided brachytherapy, merges image-guided intervention with high-dose-rate interstitial irradiation. It has been proven not to be affected by cooling effects, and it has demonstrated safety and efficacy in various locations of the body (16–18). The aim of the present study is to prove the effectiveness of CT-guided brachytherapy in providing local tumor control in surgically nonresectable colorectal liver metastases at various dose levels. We additionally tried to define the impact of extensive local tumor ablation of liver metastases on overall survival (OS). This study is based on a single-center trial, initially designed to be prospectively randomized. However, because a high rate of cross-over events from higher to lower dose levels occurred, the trial data are better understood as a prospective trial with three dose levels.

METHODS AND MATERIALS

Patients

Patients with histologically confirmed colorectal carcinoma and metastatic disease limited to the liver were eligible to participate in this study. Absence of extrahepatic disease was confirmed by clinical evaluation and diagnostic imaging, including abdominal and chest CT. No upper size limit for the liver lesions was applied. We excluded patients with ≥10 lesions, patients with >3 lesions ≥5 cm, and patients with 4–10 lesions and ≥2 lesions exceeding 3 cm. Additional eligibility criteria included preserved liver function with bilirubin >3 mg/dL, a prothrombin time >50%, preserved hematologic function with a platelet count of >50,000/mm^3, Karnofsky index ≥70%, and Eastern Cooperative Oncology Group status 0–2.

Study design

The primary endpoint of this prospective single-center, Phase III trial was time to local progression (TLP; ''local tumor control'') after applying CT-guided brachytherapy. Patients were randomly assigned to receive minimal tumor-enclosing doses of 15 Gy, 20 Gy, or 25 Gy (as D100, *i.e.,* the dose enclosing the target volume). A cross-over to lower the applied target doses to 20 Gy or 15 Gy was performed if (*1*) the calculated irradiation time exceeded 60 min, if (*2*) more than two thirds of normal liver parenchyma received >5 Gy, if (*3*) stomach, duodenum, or colon received >15 Gy per 1-mL surface, or if (*4*) gallbladder received >20 Gy per 1-mL surface. The true dose delivered was reassessed immediately after end of treatment using the contrast-enhanced planning CT. Secondary endpoints included progression-free survival (PFS) and OS. All patients were open for additional medical treatment, such as chemotherapy, even though adjuvant therapy was not generally recommended. Patient surveillance was continued after the primary endpoint had been reached, with patients receiving standard medical care or repeated local tumor ablations in case of tumor progression if at all applicable. No dose level was predefined in these patients. However, repeated brachytherapy treatments followed the same dose constraints with respect to risk organs as applied in the study protocol.

We additionally performed an independent analysis of patients from the time point of *any* tumor progression. We assessed the influence of various treatment strategies applied, such as repeated tumor ablation, chemotherapy, or best care.

No protective measures against radiation hepatitis, such as cortisone or anticoagulants, were applied. Adverse events related to the procedure, as well as late toxic effects, were graded according to the National Cancer Institute Common Toxicity Criteria, version 2. Patients underwent a clinical examination and laboratory tests before the first intervention and 3 days, 6 weeks, and every 3 months after intervention. At these time points imaging procedures were performed, including contrast-enhanced MRI (gadolinium ethoxybenzyl diethylenetriaminepentaacetic acid; Primovist, Bayer Schering, Berlin, Germany) and additional abdominal and chest CT upon suspected tumor progression by rising carcinoembryonic antigen levels or other clinical evidence.

The study protocol was written in conformance with the declaration of Helsinki and approved by the local ethics committee. All patients provided written, informed consent.

Interventional and irradiation technique

The technique of CT-guided brachytherapy has been described in detail elsewhere (16). Positioning of the brachytherapy catheters was performed with fluoroscopy CT (Siemens, Erlangen, Germany). For treatment planning purposes, a spiral CT of the liver (slice thickness, 5 mm; increment, 5 mm) enhanced by i.v. application of iodide contrast media (100 mL Ultravist 370; flow, 1 mL/s; start delay, 80 s) was acquired with breathhold technique immediately after positioning of the brachytherapy applicators in the tumor volume. Practically, one catheter per 1 to 2-cm tumor diameter was applied.

The high-dose-rate afterloading system (Gammamed; Varian Medical Systems, Charlottesville, VA) used a ^{192}Ir source of 10 Ci. The source diameter was <1 mm. The duration of the irradiation was typically 20–40 min.

For treatment planning, Varian Brachyvision software was used. The relative coordinates of the catheters as well as the tumor boundaries including a safety margin of 5 mm were determined manually in the three-dimensional CT dataset after being transferred in the treatment planning unit. A dose exposure of 5 Gy to more than two thirds of the liver served as a prospective constraint. Fifteen grays per milliliter organ surface was defined as the maximum exposure to stomach, duodenum, or colon, as well as 8 Gy/mL to the spinal cord. The organ surface was specified by outlining the organ in the treatment planning system. After irradiation, a gastric prophylaxis (pantoprazole 1 × 40 mg/d for 3 months and magaldrate H_2O-free on demand) was prescribed if the gastric or duodenal mucosa was calculated to have received more than 10 Gy/mL.

Assessments

Local tumor control (*i.e.,* stable disease, partial or complete remission) after brachytherapy treatment was determined by contrast-enhanced MRI (gadolinium ethoxybenzyl diethylenetriaminepentaacetic acid) and defined as any of the following: (*1*) absence of symmetric lesion growth ≥25% compared with baseline starting at 3 months after irradiation, or (*2*) absence of asymmetric lesion growth at any time during follow-up. Any suspected tumor recurrence was best differentiated from hepatic parenchyma necrosis in late contrast-enhanced T1-weighted images (120 min after irradiation). Partial response was defined as a lesion volume loss ≥50%, and complete response was defined as lesion disappearance. Response criteria for nonirradiated lesions followed the Response Evaluation Criteria In Solid Tumors. Progression-free survival was measured from the first intervention to the date of the first assessment showing progression.

Statistical methods

The accrual goal was 60 lesions per study arm to provide a statistical power of 80% at a significance level of 0.05. An interim analysis was performed when an unexpectedly high rate of cross-over events occurred, and the study was closed thereafter. We decided to emphasize the analysis of dose levels as assigned after cross-over, and we added data on intent-to-treat as well as an analysis of treatments as effectively applied (*i.e.,* D100).

Time to local progression, PFS, and OS were estimated using the Kaplan-Meier method and compared using the log–rank, Breslow and Tarone-Ware tests. Repeated local treatments of a study lesion were excluded from lesion-based analysis. For lesion-based analysis and limited to TLP we enhanced the Cox proportional hazards model with a robust sandwich estimate to exclude bias by patients displaying more than one lesion. In addition, we performed a Cox regression with and without a competing risk analysis (*e.g.,* risk of death before observation of local recurrence). We assessed the association of TLP with the dose applied after cross-over, lesion size, lesion shape (oligonodular or presence of satellite metastases vs. round), and number of lesions.

Progression-free survival and OS were assessed on the basis of patient only, without reference to the doses applied. We used a standard Cox proportional hazards model with respect to lesion size, lesion shape, number of lesions, unilobar vs. bilobar tumor spread, synchronous vs. metachronous disease, salvage chemotherapy during follow-up, and repeated tumor ablation.

Definitions

We introduced two categories of lesion appearance on MRI or CT: round or oligonodular. ''Round lesions'' were defined by an almost symmetric or spheroid shape with a regular margin; ''oligonodular lesions'' were defined by an irregular shape, such as piled clouds. Satellite lesions had their isocenter within 1 cm of the originating liver metastasis. The category ''oligonodular lesion'' included radiologically visible satellite lesions.

Patient characteristics

Between January 2003 and January 2006, 73 patients with 199 colorectal liver metastases were randomly assigned to CT-guided brachytherapy with a minimal target dose of 15 Gy ($n = 64$ metastases), 20 Gy ($n = 67$), and 25 Gy ($n = 68$). According to safety constraints or excessive irradiation time, cross-over was performed from the 20-Gy or 25-Gy arm to the 15-Gy or 20-Gy arm in 38 lesions. Hence, the final assignment to the dose levels was as follows: 15 Gy ($n = 98$), 20 Gy ($n = 68$), and 25 Gy ($n = 33$). The effective treatment applied per each treatment arm (average D100) was 12.8 Gy in the 15-Gy group, 15.7 Gy in the 20-Gy group, and 18.8 Gy in the 25-Gy group.

Patients presented with one to eight lesions (mean, 2.2; median, 2). The lesion size ranged from 1 to 13.5 cm (mean, 3.6 cm; median, 3.1 cm). The mean and the median diameter of the largest tumor lesion in each patient was 4.9 and 5 cm, respectively. The median (range) lesion size per dose group as assigned after cross-over was 3.2 (1–13.5), 3.1 (1–9.6), and 3.0 (1–6) cm for the 15-Gy, 20-Gy, and 25-Gy groups, respectively. The median (range) tumor size per intent-to-treat had been 4 (1–11.3), 3.2 (1.2–9.6), and 2.5 (1–7.2) cm, respectively.

Table 1 displays further disease- and treatment-specific details. All patients had no evidence of extrahepatic disease at randomization.

Table 1. Demographic and clinical characteristics of the patients ($n = 73$)

Age (y), mean (range)	63.6 (28-86)
Male sex (%)	67.1
Time since diagnosis (mo), mean (95% CI)	20.3 (16.0–24.7)
Metachronous liver disease (%)	42.5
Synchronous liver disease* (%)	57.5
Previous chemotherapy (%)	
First line	86
Second or third line	39.7
Liver resection (%)	32.9
Previous thermal ablation (RFA, laser) (%)	20.5

Abbreviations: ECOG = eastern cooperative oncology group performance status; RFA = radiofrequency ablation.

* Diagnosis of liver metastases within 6 months after diagnosis of the primary tumor.

Local tumor control

Local tumor recurrence was observed in 50 of 199 lesions (25.1%). According to the Kaplan-Meier method, the estimated mean TLP for all lesions was 34 months (median not reached).

The patient group assigned to 15 Gy after cross-over displayed 34 local recurrences out of 98 lesions; 20 Gy, 15 recurrences out of 68 lesions; 25 Gy, 1 recurrence out of 33 lesions. The difference between the 25-Gy and the 20-Gy or 15-Gy group was significant ($p < 0.05$). The mean (median) local recurrence-free survival was 27.1 (25.6) months in the 15-Gy group, 31.1 (median not reached) months in the 20-Gy group, and 46.4 (median not reached) months in the 25-Gy group. The Kaplan-Meier curve for local recurrence-free survival is displayed in Fig. 1.

Per intent to treat, the 15-Gy group displayed 22 local recurrences out of 64 lesions; 20 Gy, 20 recurrences out of 67 lesions; 25 Gy, 8 recurrences out of 68 lesions (Fig. 2). Dose groups as intended to treat displayed mean (median) local recurrence-free survival of 26.5 (22.5) months in the 15-Gy group, 27.3 (median not reached) months in the 20-Gy group, and 42.3 (median not reached) months in the 25-Gy group. The difference between the 25-Gy and the 20-Gy or 15-Gy group was significant ($p < 0.05$). The Kaplan-Meier curve for local recurrence-free survival is displayed in Fig. 2.

At univariate analysis, dose assigned after cross-over, the dose effectively applied (D100), lesion shape (oligonodular displaying higher frequencies of local tumor recurrence after ablation), and tumor diameter had a significant impact on TLP ($p < 0.05$).

Multivariate analysis revealed significantly improved local tumor control with an increase of the D100, or with round vs. oligonodular shape ($p < 0.001$). Lesion size did not have a significant impact on local tumor control anymore. Adding a competing risk analysis, only lesion shape remained as a significant prognostic factor for TLP. Per dose assigned after cross-over, lesion shape and dose level remained as significant prognostic factors for TLP in a multivariate analysis including the competing risk analysis. Per intent to treat, only lesion shape had a prognostic impact. When lesion shape was omitted from the multivariate analysis, lesion size and dose level had a significant influence on TLP. This was true for the D100, the dose as assigned after cross-over, as well as for the intent-to-treat dose level ($p < 0.05$). The hazard ratios applying the D100 were 1.176 (lesion size) and 0.923 (D100); applying the dose as assigned after cross-over, 1.186 (lesion size) and 0.856 (dose as assigned); applying the intent-to-treat dose level, 1.169 (lesion size) and 0.919 (intent-to-treat dose).

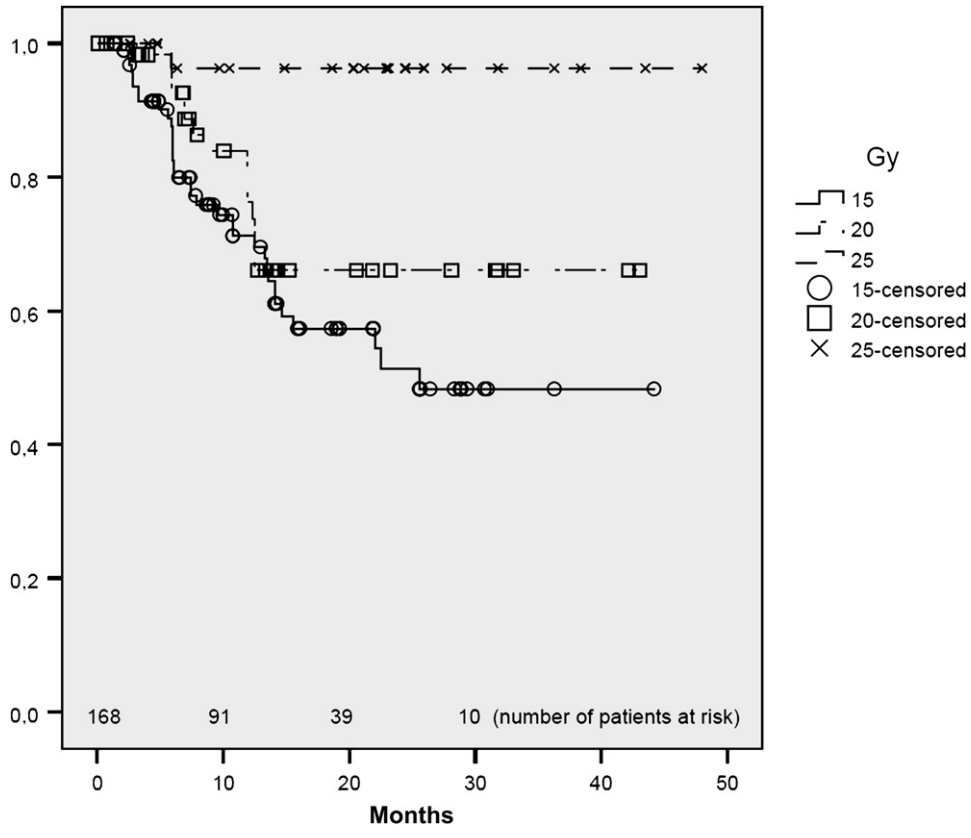

Fig. 1. Time to local progression (dose as assigned after cross-over).

Treatment-related complications and toxicity

Treatment of 199 lesions was performed in 124 single sessions. There was no perioperative or 30-day mortality. We observed six major complications: occult bleeding (n = 2, 2.5%) treated symptomatically with blood infusion of 1000 mL each; symptomatic gastric ulcer (n = 2, 2.5%) rated as radiation induced after treatment of left lobe locations; recurrent pleural effusion (n = 1, 1%) treated by pleurodesis; and anaphylactic reaction to iodide contrast media (n = 1, 1%) treated symptomatically.

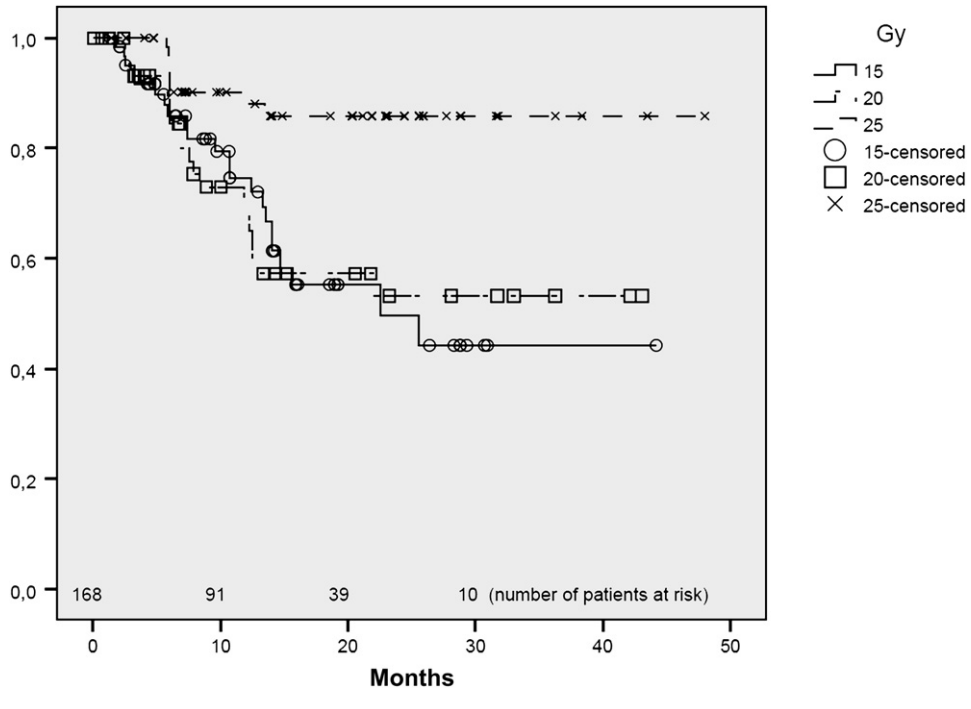

Fig. 2. Time to local progression (dose per intent-to-treat).

Table 2. Multivariate analysis: variables investigated as potential predictors for PFS and OS after first local ablation

	PFS (log–rank/Cox)		OS (log–rank/Cox)	
Variable	*p*	HR	*p*	HR
Age (<65, 65+)	0.776	1.077	0.522	0.835
Lesion size*	0.188†; 0.02‡	1.082†; 1.270‡	0.760	1.020
Synchronous disease (yes/no)	0.085	0.620	0.244	0.710
Lesion shape (round, oligonodular)	0.036†; 1.228‡	1.966†; 1.701‡	0.013†; 2.323‡	0.014†; 2.976‡
Unilobar or bilobar disease	0.706	1.150	0.295	1.530
Total no. of liver lesions	0.907	0.989	0.442	0.911
Local recurrence	N/A	N/A	0.924	0.972

Abbreviations: PFS = progression-free survival; OS = overall survival; HR = hazard ratio.
* Largest lesion at the time of first local ablation.
† Includes local recurrence.
‡ Excludes local recurrence.

Additional treatments after first tumor progression

Fifty-three patients received additional brachytherapy of hepatic tumor recurrences. Twenty-seven patients received a single treatment, 23 patients two local treatments, 2 patients three local treatments, and 1 patient four additional liver brachytherapies. The doses applied ranged from 10 to 25 Gy (mean, 18.5 Gy; median, 20 Gy). Systemic chemotherapy treatments in case of tumor progression were applied in 46 of 67 patients with tumor progression. Twelve of 46 patients qualified for additional targeted therapies. The mean duration of chemotherapy after progression was 7 months (range, 1–17 months). All but 4 patients had received at least first-line chemotherapy before trial inclusion.

PFS and OS

The median duration of follow-up was 15.2 months (including MRI for assessment of local recurrence). For survival, patients were followed 41 months at median (18 still alive). Mean and median PFS was 8.6 and 6 months for all patients, respectively. When local tumor recurrences were excluded, the mean PFS was 10.5 months.

Mean (median) OS after first ablation, first diagnosis of liver metastases, and first diagnosis of the primary tumor were 27.9 (23.4), 53.5 (46.7), and 65 (56.2) months, respectively.

A patient-based multivariate analysis using the Cox proportional hazards model was used to determine the impact of variables associated with PFS or OS after first ablation. Dose levels did not play any role in these analyses. The variables considered were postprogression therapy (chemotherapy, repeated local ablations), age (<65, ≥65 years), lesion size, synchronous disease (yes/no), lesion shape (round vs. oligonodular or presence of satellite metastases), unilobar or bilobar disease, and total number of liver lesions.

A significant association of decreasing OS was apparent for an oligonodular lesion shape or the incidence of satellite lesions. The incidence of local tumor recurrence after first local tumor ablation did not influence OS on a patient-based analysis. Oligonodular shape was associated with a decrease of PFS only if local tumor progression of the study lesion was included. Excluding local recurrences, only an increasing tumor diameter of the initial lesion was significantly related to a decrease of PFS (Table 2).

Variables significantly increasing OS were repeated brachytherapy and chemotherapy in case of tumor progression after the first successful study treatment. Repeated local tumor ablations were the most prominent factor for increased survival and dominated additional systemic antitumor treatments (Table 3). Best outcomes were observed with multimodality regimens combining local and systemic treatments after first progression after local ablation. According to the Kaplan-Meier method, median OS after first tumor progression ($n = 67$) was 11.1 months in patients with no further local or systemic therapy; 26.3 months in patients with brachytherapy and systemic chemotherapy; 19.3 months with chemotherapy only; and 22.2 months with brachytherapy only. Differences in survival between patients receiving combined local and systemic treatments vs. patients with either local or systemic treatment proved to be significant ($p < 0.05$).

DISCUSSION

Computed tomography–guided brachytherapy has been validated for safety and efficacy in previous trials in colorectal metastases, including studies in tumors for which common thermal ablation techniques have lacked appropriateness, such as in tumors >5 cm or tumors adjacent to risk structures (*e.g.,* liver hilum and hepatic bifurcation) (17). The inherent value of this technique is its ubiquitous availability, the ease and cost-effectiveness of its use, and the applicability in almost any region of the human body (18). In contrast to stereotactic external-beam irradiation, the method is independent from patient movements or target motion, such as through breathing. Lesion size may also be a limitation in stereotactic irradiation (19, 20). Our study was primarily designed to evaluate the duration of local response after brachytherapy treatment of colorectal liver metastases. Our

Table 3. Multivariate analysis: variables investigated as potential predictors for OS after first local ablation and further progression ($n = 67$)

	OS (log–rank/Cox)	
Variable	*p*	HR
Systemic chemotherapy	0.049	1.818
Further local ablations	0.032	1.952
Extent of progression*	0.067	1.302

Abbreviations: OS = overall survival; HR = hazard ratio.
* Intrahepatic solitary vs. intrahepatic disseminated or extrahepatic spread.

results show a clear dose dependency, with no local recurrences observed if the minimum dose in the target (the true D100) exceeded 20.4 Gy. However, the frequent cross-over between the study arms with dose reduction to a prescription of 20 Gy or 15 Gy indicates some limitations of this method. In large tumors, excessive irradiation time and unpredictable risks when irradiating very large volumes hamper the delivery of >20 Gy in a single fraction. However, in future this problem may be overcome by simply treating large tumor volumes intermittently. In effect, tumors >8 cm (for example) could be treated in two or more sessions, or fractionated irradiation schemes may be applied. In concordance with the literature, we encountered no symptomatic radiation hepatitis despite very large or multiple tumors treated in individual patients (21).

Data on the clinical value of minimally invasive tumor ablation techniques as an adjunct in oncologic treatment strategies are scarce, and the future role of minimally invasive tumor ablation in different tumor types is unclear today. With respect to colorectal carcinoma, surgical resection has proven prognostic advantages, and it also offers a chance for long-term survival or cure. However, advances in surgical techniques have expanded the indications for liver surgery. As a consequence, risk factors such as anatomic or nonanatomic resections result in an increasing proportion of patients with positive resection margins after liver surgery. Surprisingly, a positive margin after re-resection did not alter the patients' prognosis in a study by Welsh *et al*. (22), whereas patients with R1 resection at the time of their first liver surgery demonstrated a significantly lower OS compared with R0 resection. The investigators conclude that patients with recurrent liver metastases should be considered for repeat resection, despite the increased risk of an involved margin. Compared with the patients recruited by Welsh *et al*. (22), our own study patients represented a cohort with poorer prognosis, with 33% after liver resection, and 86%, 40%, and 21% of patients after first-, second-, or third-line chemotherapy, respectively. The indication for local tumor ablation was truly palliative, with extensive cytoreduction often performed in a salvage situation. Still, the rate of complications was quite low, and patient discomfort was usually minimal, despite tumor dimensions reaching up to 13.5 cm in diameter. In this rather dismal study cohort, the local recurrence rate was 25% for all lesions and <5% if a minimal dose of 25 Gy was prescribed (this prescription led to an average dose of 18.8 Gy delivered, *i.e.,* D100). This compares to 8.8% R1 resection in the total surgical study cohort of Welsh *et al*. (22) and 17.9% in cases of re-resection, or 35% R1 resection in patients with extended anatomic and nonanatomic resection (22). We conclude that in patients with an increased risk of a positive resection margin at liver resection, minimally invasive tumor ablation should be considered. According to Welsh *et al*. (22) these risks include bilobar disease, multiple tumors (three or more), large tumors (>10 cm), extended anatomic or nonanatomic resections, and re-resection.

Extensive cytoreduction by interstitial irradiation or thermal techniques in combination with systemic therapies is intriguing but has not yet been validated. Data from randomized trials are still not available. In our study cohort, both repeated local tumor ablations and further chemotherapies had a positive impact on the prognosis, with local ablations dominating systemic therapies. We propose that this positive impact of CT-guided brachytherapy resulted from the extensive tumor load that was effectively treated in each single session. However, most favorable survival outcomes were achieved by the combination of local ablative measures with further systemic therapies. It remains unclear, though, whether a patient selection bias was at least in part responsible for these results. Nevertheless, our data strongly support the initiation of randomized study protocols designed to assess survival after concepts combining local tumor ablation with systemic or targeted therapies.

Three variables proved to influence local tumor control: minimum dose delivered to the target volume, lesion shape, and lesion size. However, larger lesions were associated with lower doses, thus increasing the risk for local recurrence. Whereas round lesions with a regular outer rim displayed favorable local control rates, oligonodular lesions frequently led to recurrent tumor growth during follow-up. Irregular lesion shape has been discussed previously as a sign of greater aggressiveness as well as an indicator for increased microsatellite presence within 1 cm of the tumor (23, 24). We recommend that in lesions displaying oligonodular shape, the dose prescription should be 25 Gy to cover radiographically invisible microsatellites through the dose gradient reaching beyond the macroscopic tumor margin. If this dose is not applicable, treatment of such lesions may be intermittent, or fractionated regimens should be used. At this time no data are available on fractionated regimens, and safe devices that could be kept in place for an extended period, such as 2 or 3 days, need to be developed.

In summary, local tumor control after CT-guided brachytherapy of colorectal liver metastases demonstrated a strong dose dependency. No recurrences were observed if the true dose delivered exceeded 23 Gy. However, we frequently observed underdosing as compared with the prescribed dose levels, and treatment planning has to be revised carefully in the clinical setting. Repeated local ablations were the most dominant factor for survival in patients with advanced colorectal cancer. The role of extensive minimally invasive tumor ablation in the treatment of metastatic colorectal cancer needs to be established in randomized trials.

REFERENCES

1. Hurwitz H, Fehrenbacher L, Novotny W, *et al*. Bevacizumab plus irinotecan, fluorouracil, and leucovorin for metastatic colorectal cancer. *N Engl J Med* 2004;350:2335–2342.
2. Giantonio BJ, Levy DE, O'Dwyer PJ, *et al*. A phase II study of high-dose bevacizumab in combination with irinotecan, 5-fluorouracil, leucovorin, as initial therapy for advanced colorectal

cancer: Results from the Eastern Cooperative Oncology Group study E2200. *Ann Oncol* 2006;17:1399–1403.
3. Cunningham D, Humblet Y, Siena S, *et al*. Cetuximab monotherapy and cetuximab plus irinotecan in irinotecan-refractory metastatic colorectal cancer. *N Engl J Med* 2004;351:337–345.
4. Jemal A, Siegel R, Ward E, *et al*. Cancer statistics, 2008. *CA Cancer J Clin* 2008;58:71–96.
5. Steele G, Ravikumar TS. Resection of hepatic metastases from colorectal cancer: Biologic perspective. *Ann Surg* 1989;210: 127–138.
6. Norstein J, Silen W. Natural history of liver metastases from colorectal carcinoma. *J Gastrointest Surg* 1997;1:398–407.
7. Silen W. Hepatic resection for metastases from colorectal carcinoma is of dubious value. *Arch Surg* 1989;124:1021–1022.
8. Adson MA. Resection of liver metastases—when is it worthwhile? *World J Surg* 1987;11:511–520.
9. Yothers G. Toward progression-free survival as a primary end point in advanced colorectal cancer. *J Clin Oncol* 2007;25: 5153–5154.
10. Goldberg SN, Grassi CJ, Cardella JF, *et al*. Image-guided tumor ablation: Standardization of terminology and reporting criteria. *J Vasc Interv Radiol* 2005;16:765–778.
11. Xiao YY, Tian JL, Li JK, *et al*. CT-guided percutaneous chemical ablation of adrenal neoplasms. *AJR Am J Roentgenol* 2008; 190:105–110.
12. Gillams AR, Lees WR. Radiofrequency ablation of lung metastases: Factors influencing success. *Eur Radiol* 2009;18:672–677.
13. Curley SA. Radiofrequency ablation versus resection for resectable colorectal liver metastases: Time for a randomized trial? *Ann Surg Oncol* 2008;15:11–13.
14. Zhang YJ, Liang HH, Chen MS, *et al*. Hepatocellular carcinoma treated with radiofrequency ablation with or without ethanol injection: A prospective randomized trial. *Radiology* 2007;244: 599–607.
15. Vogl TJ, Straub R, Eichler K, *et al*. Colorectal carcinoma metastases in liver: Laser-induced interstitial thermotherapy-local tumor control rate and survival data. *Radiology* 2004;230: 450–458.
16. Ricke J, Wust P, Stohlmann A, *et al*. CT-guided interstitial brachytherapy of liver malignancies alone or in combination with thermal ablation: Phase I-II results of a novel technique. *Int J Radiat Oncol Biol Phys* 2004;58:1496–1505.
17. Ricke J, Wust P, Wieners G, *et al*. Liver malignancies: CT-guided interstitial brachytherapy in patients with unfavorable lesions for thermal ablation. *J Vasc Interv Radiol* 2004;15: 1279–1286.
18. Wieners G, Pech M, Rudzinska M, *et al*. CT-guided interstitial brachytherapy in the local treatment of extrahepatic, extrapulmonary secondary malignancies. *Eur Radiol* 2006;16:2586–2593.
19. Dawson L, Jaffray D. Advances in image guided radiation therapy. *J Clin Oncol* 2007;25:938–946.
20. Shirato H, Shimizu S, Kitamura K, *et al*. Four-dimensional treatment planning and fluoroscopic real-time tumor tracking radiotherapy for moving tumor. *Int J Radiat Oncol Biol Phys* 2000;48:435–442.
21. Ricke J, Seidensticker M, Lüdemann L, *et al*. In vivo assessment of the tolerance dose of small liver volumes after single-fraction HDR irradiation. *Int J Radiat Oncol Biol Phys* 2005; 62:776–784.
22. Welsh FK, Tekkis PP, ÓRourke T, *et al*. Quantification of risk of a positive (R1) resection margin following hepatic resection for metastatic colorectal cancer: An aid to clinical decision-making. *Surg Oncol* 2008;17:3–13.
23. Shirabe K, Takenaka K, Gion T, *et al*. Analysis of prognostic risk factors in hepatic resection for metastatic colorectal carcinoma with special reference to the surgical margin. *Br J Surg* 1997;84:1077–1080.
24. Yokoyama N, Shirai Y, Ajioka Y, *et al*. Immunohistochemically detected hepatic micrometastases predict a high risk of intrahepatic recurrence after resection of colorectal carcinoma liver metastases. *Cancer* 2002;94:1642–1647.

Int. J. Radiation Oncology Biol. Phys., Vol. 78, No. 1, pp. 172–179, 2010

0360-3016/$–see front matter

ELSEVIER

doi:10.1016/j.ijrobp.2009.07.1700

CLINICAL INVESTIGATION **Liver**

COMPUTED TOMOGRAPHY–GUIDED HIGH-DOSE-RATE BRACHYTHERAPY IN HEPATOCELLULAR CARCINOMA: SAFETY, EFFICACY, AND EFFECT ON SURVIVAL

Konrad Mohnike, M.D.,* Gero Wieners, M.D.,* Franziska Schwartz, M.D.,* Max Seidensticker, M.D.,* Maciej Pech, M.D.,* Ricarda Ruehl, M.D.,* Peter Wust, M.D.,† Enrique Lopez-Hänninen, M.D.,‡ Günther Gademann, M.D.,§ Nils Peters, M.D.,§ Thomas Berg, M.D.,¶ Peter Malfertheiner, M.D.,† and Jens Ricke, M.D.*

*Klinik für Radiologie und Nuklearmedizin, Otto von Guericke University, Magdeburg, Germany; †Klinik für Gastroenterologie und Hepatologie, Otto von Guericke University, Magdeburg, Germany; ‡Klinik für Strahlentherapie, Charité Universitätsmedizin, Berlin, Germany; §Klinik für Radiologie und Nuklearmedizin, Martin-Luther-Krankenhaus, Berlin, Germany; ||Klinik für Strahlentherapie, Otto von Guericke University, Magdeburg, Germany; and ¶Medizinische Klinik mit Schwerpunkt Hepato-Gastroenterologie, Charité Universitätsmedizin, Berlin, Germany

Purpose: To determine the saftety and efficacy of computed tomography (CT)–guided brachytherapy in hepatocellular carcinoma (HCC).
Methods and Materials: A total of 83 patients were recruited, presenting with 140 HCC- lesions. Treatment was performed by CT-guided high-dose-rate (HDR) brachytherapy with an iridium—192 source. The primary endpoint was time to progression; secondary endpoints included local tumor control and overall survival (OS). A matched-pair analysis with patients not receiving brachytherapy was performed. Match criteria included the Cancer of the Liver Italian Program (CLIP) score, alpha-fetoprotein, presence, and extent of multifocal disease. For statistical analysis, Kaplan-Meier and Cox regression were performed.
Results: Mean and median cumulative TTP for all patients (n = 75) were 17.7 and 10.4 months. Five local recurrences were observed. The OS after inclusion reached median times of 19.4 months (all patients), 46.3 months (CLIP score, 0), 20.6 months (CLIP score, 1) 12.7 months, (CLIP score, 2), and 8.3 months (CLIP score, ≥3). The 1— and 3—year OS were 94% and 65% (CLIP score, 0), 69% and 12% (CLIP score, 1), and 48% and 19% (CLIP score, 2), respectively. Nine complications requiring intervention were encountered in 124 interventions. Matched-pair analysis revealed a significantly longer OS for patients undergoing CT-guided brachytherapy.
Conclusion: Based on our results the study treatment could be safely performed. The study treatment had a beneficial effect on OS in patients with advanced HCC,with respect to (and depending on) the CLIP score and compared with OS in a historical control group. A high rate of local control was also observed, regardless of applied dose in a range of 15 to 25 Gy. © 2010 Elsevier Inc.

Liver malignancies, Hepatocellular carcinoma, Radiotherapy, Local ablation.

INTRODUCTION

In European studies, 5-year survival rates up to 51% have been shown for hepatocellular carcinoma (HCC) suitable for resection (1). Unfortunately, 70% to 80% are not candidates for resection because of advanced cirrhosis, multiple lesions, or diffuse tumor growth and comorbidity. Liver transplantation is the only potentially curative option at present, with 5-year post-transplantation survival rates of up to 70% for patients with limited disease. Apart from the shortage of organs available for transplantation, the number of patients qualified for transplantation is restricted by the Milan criteria (solitary lesion ≤5 cm or three or fewer lesions with diameter ≤3 cm) (2).

The established treatment of choice is transarterial chemoembolization (TACE), frequently in combination with thermoablative techniques (3–5), resulting in 3-year OS rates of up to 47% in some studies (6). Effectiveness and feasibility are limited by factors such as advanced-stage cirrhosis and portal vein thrombosis (PVT). Thermal ablation is usually performed by radiofrequency ablation in tumors up to 5 cm; this method has shown 2—year survival rates of 61% to 98% in randomized controlled trials (RCTs) (7–9).

Reprint requests to: Jens Ricke, M.D., Dept. of Radiology and Nuclear Medicine, Otto von Guericke University, Leipziger Str. 44, 39120 Magdeburg, Germany. Tel: 0049 391/6713030; Fax: 0049 391/6713029; E-mail: ricke@med.ovgu.de

This work was funded exclusively by the University of Magdeburg.
Conflict of interest: none.
Received June 10, 2009, and in revised form July 12, 2009. Accepted for publication July 15, 2009.

Recently, a randomized controlled trial comparing radiofrequency ablation, TACE, and combined TACE and radiofrequency ablation treatment in large tumors showed prolonged survival in favor of combined treatment (3). Stereotactic irradiation has been described, either alone or in combination with TACE (10). There is also some experience with proton-beam therapy (11–16). The precision of these percutaneous techniques, despite technical advantages such as respiration-gated irradiation, are potentially limited by patient or breathing motion.

Recently, computed tomography (CT)–guided brachytherapy of liver tumors has been introduced, a local radioablative high-dose-rate (HDR) brachytherapy technique in which an iridium—192 source is temporarily inserted through catheters placed under CT guidance. The therapeutic effect of this new technique is not influenced by cooling of surrounding large vessels and patient movement, and the method is not limited by tumor size or PVT. It requires facilities that are widely available, and it is comparatively inexpensive (17–22).

In this prospective series of 83 patients examining safety and preliminary efficacy, we sought to determine the efficacy of CT-guided brachytherapy in the treatment of nonresectable HCC. In addition, in a matched-pair analysis, we compared OS in the study cohort with OS in a historical control group given other or no treatments.

METHODS AND MATERIALS

Patients

From November 2002 to July 2007, 83 patients (17 female and 66 male), presenting with 140 lesions of HCC, were registered in the study. Most patients presented with relapse after various pretreatments, including liver resection. Of the patients, 18 had no previous treatment. We consecutively included patients with four or fewer tumor nodules visible in either contrast-enhanced MRI or CT. All patients had been rated unesectable by visceral surgeons due to extensive tumor spread or increased operative risk or patients had refused surgery. No upper limit was placed upon the tumor diameter. Patients without a clearly defined tumor margin in MRI or CT and patients presenting with hepatic impairment in Child-Pugh Class C were excluded. Further inclusion criteria included an ECOG performance status of 0 to 2, Karnofsky index >70%, platelet count >50,000, prothrombin time of at least 50%, and bilirubin <50 μmol/l. Ascites and portal vein occlusion were not exclusion criteria. Decision was made in interdisciplinary consensus.

All 83 patients were included in the assessment of OS. Eight patients were lost to detailed follow-up (*i.e.,* dates of death were recorded but without further information). Hence, TTP and local recurrence-free survival were estimated on the basis of 75 patients and 126 lesions for which at least the first MRI follow-up examination after 6 weeks was performed. In 48 cases, diagnosis was confirmed by histopathology. The remaining 35 cases were diagnosed according to the criteria of the Consensus Conference of the European Association for the Study of Liver Disease (23). Six patients presented with limited extrahepatic disease at the time of intervention (see Results); in 1 of these patients, extrahepatic CT-guided brachytherapy to a metastasis of the abdominal wall was also performed. Details of patient characteristics including Child-Pugh stage, Cancer of the Liver Italian Program (CLIP), and Barcelona Clinic Liver-Cancer [classification] (BCLC) score are shown in Table 1, and details of lesions and treatment in Table 2.

Study design

The central aim of this trial was to assess the safety and efficacy of CT-guided brachytherapy in the treatment of HCC. The endpoint of the primary was time-to progression (TTP). Secondary endpoints were overall survival (OS) and local tumor control. We extended our analysis by a matched-pair analysis comparison of the study cohort with a ''standard care'' control group with respect to OS. The study protocol was written in conformance with the Declaration of Helsinki and approved by the local ethics committee. All patients provided written informed consent to participate.

Interventional and irradiation technique

The technique of CT-guided brachytherapy has been described in detail elsewhere (24, 25). Briefly, we performed irradiation by the HDR brachytherapy technique, using a 10—Ci iridium—192 source. Positioning of the brachytherapy catheters was performed by fluoroscopy CT. After positioning of the catheters, a three-dimensional, contrast-enhanced CT dataset with a slice thickness of 5 mm was acquired and transferred to the treatment planning unit (Patients 1–24, Abacus; Patients 25–61, BrachyVision [both by Varian Medical Systems, Palo Alto, California]; Patients 62–83, Plato [Nucletron B.V., Veenendaal, the Netherlands]). The coordinates of the catheters in three dimensions and the tumor margin were determined manually based on contrast-enhanced CT (Fig. 1). For analgesia/sedation, fentanyl, and midazolam were used according to individual requirement.

Dose

To preserve the liver parenchyma, dosing was adjusted such that not more than two-thirds of the normal liver tissue received an exposure of >5 Gy. The maximum exposure was limited to 15 Gy per 1 ml for the stomach and intestine and 8 Gy per 1 ml for the spinal cord. If exposure of the gastric wall or duodenal mucosa was >10 Gy/ml of the organ at risk, then proton-pump inhibitors were prescribed (pantoprazol 40 mg *q.d.* for 3 months).

The target dose was defined as the minimum dose taken up by the visible tumor margin. In the 114 lesions treated in a single session, we prescribed minimum target doses between 15 and 25 Gy, with lower doses in cases in which the tumor volume was large or where adjacent structures were at risk of high exposure. Two patients refused repeated sessions for personal reasons and received a total of 12 Gy (for final assignment to dose levels, see Results). The dose to the tumor was reduced if the stomach or intestine was exposed to >15 Gy/ 1 ml, or if more than two thirds of the hepatic parenchyma received >5 Gy.

Twelve patients with very large tumors (median diameter, 11.3 cm) were treated in a multiple-session approach at intervals of 2 weeks, with the target volume divided into regions. Dose levels assigned were 12 Gy ($n = 6$) or 15 Gy ($n = 6$) applied to each region, and potential dose overlap in the tumor volume was ignored. Because of extensive overlap of irradiation fields and because of the large overall treatment volumes, no higher doses were administered to these patients (for their treatment and lesion characteristics of these patients, see Results).

Assessments

We performed contrast-enhanced MRI after 6 weeks and then every 3 months after the intervention, to assess local tumor control of every single treated lesion, defined as either of the following: (a)

Table 1. Patient characteristics (N = 83)

Child-Pugh class	A: 53 (64%)	B: 30 (36%)	
CLIP score at the time of inclusion	0: 17 (21%)	1: 26 (31%)	
	2: 25 (30%)	3: 11 (13%)	
	4: 2 (2%)	5: 2 (2%)	
BCLC score	A: 51 (61%)	B: 12 (14%)	C: 20 (24%)
Diameter of the patient's largest lesion (cm)	Mean, 5.8; median, 5.2		
	Range, 1–15		
Diameter of the patient's largest lesion (cm) according to the CLIP score (0, 1, 2, 3, and more points)	0: 5.0 cm (range, 1.0–12.0)		
	1: 4.4 cm (range, 1.2–10.0)		
	2: 5.4 cm (range, 1.7–10.7)		
	≥3: 7.0 cm (range, 2.0–15.0 cm)		
Patients displaying more than one lesion	43 (52%)		
Disease confirmed by histopathology	48 (58%)		
Known extrahepatic cancer disease at the time of intervention	Abdominal wall: 1 (1%) Lung: 4 (5%)		
	Bones: 1 (1%)		
Age (y)	Mean 67.6; range, 43.3–85.5		
Previous liver resection	18 (22%)		

Abbreviations: BCLC Barcelona Clinic Liver-Cancer [classification]; CLIP = Cancer of the Liver Italian Program.

absence of symmetric lesion growth ≥20% compared with baseline, starting 3 months after irradiation (taking into account the postradiation edema peaking 6 weeks after radiotherapy (26), or (b) absence of asymmetric lesion growth during follow-up. Time to progression (TTP) was assessed according to the modified RECIST (Response Criteria In Solid Tumors) criteria (27) and defined as the time from the first CT-guided brachytherapy to the date of the first assessment showing intrahepatic progression, *i.e.,* local progressions of the treated lesions and/ or occurrence of new lesions, or extrahepatic progression. Overall survival (OS) was defined in two ways: from the first diagnosis of HCC to the date of death, and from inclusion (and first CT-guided brachytherapy) to the date of death. Each follow-up visit also included clinical examinations and assessment of laboratory variables (*i.e.,* liver enzymes, bilirubin, and alpha-fetoprotein).

Statistical methods

Time to local progression, TTP, and OS including matched-pair analysis were estimated by the Kaplan-Meier method and compared by using the log-rank, Breslow, and Tarone-Ware tests. Repeated local treatments of a study lesion were excluded from lesion-based analysis of local tumor control. The Cox proportional hazards model was used to assess the association of survival with BCLC and CLIP scores (28–30), lesion size, total number of liver lesions, multifocal disease, and minimum dose at the tumor margin.

For matched-pair analysis, a local data base of 256 HCC patients presenting at our institution from 2002 to 2006 was searched. Match criteria were CLIP score, alpha-fetoprotein (0–30; 30–100; 100–200; 200–400; >400 mg/l), and presence (1 and 2 or more) and extent of multifocal disease (fewer than three vs. three or more lesions). We exclusively considered fuel-matched pairs for analysis, achieved for 57 of 83 patients in the original study cohort. We assessed OS of the matched patients, and we also stratified the patients into subgroups according to CLIP score and the number of nodules (multifocal disease or single lesion). Characteristics of the treatment and control group are shown in Table 3.

RESULTS

TTP and OS

Median follow-up including MRI to assess TTP was 9.6 months (range, 1.2–58.4 months). Median TTP for all patients (n=75) was 10.4 months (Fig. 2); for the single-session treatment, these were respectively 12 months, and for multiple-session treatment (with larger tumor burden, as discussed above) 8.4 months. In univariate Cox regression, higher CLIP and BCLC scores (p = 0.008 and 0.034, respectively) were significantly associated with a decreasing TTP. The association with diameter of the largest lesion (p = 0.449) was statistically insignificant, whereas that with multifocal disease suggested a tendency of association, albeit without statistical significance (p = 0.06).

Median OS was estimated for all 83 patients. A total of 60 patients had died at the time of analysis for OS. Median follow-up for OS for the 23 patients alive was 33.8 months after inclusion and 42.0 months after first diagnosis of HCC. Median OS after inclusion (and first CT-guided brachytherapy) was 19.4 months (Fig. 3), with cumulative 1-year and 3-year survival rates of 64% and 25%, respectively. Our data revealed strong dependence upon the CLIP score (Fig. 4). According to the CLIP score at the time of inclusion, median OS after inclusion was 46.3 months (CLIP score, 0), 20.6 months (CLIP score, 1), 12.7 months (CLIP score, 2), and 8.3 months (CLIP score, ≥3). The 1— and 3—year OS were 94% and 65% (CLIP score 0), 69% and 12% (CLIP score 1) and 48% and 19% (CLIP score 2), respectively. Median OS after the date of diagnosis of the HCC was 58.9 months for CLIP score 0 (CLIP score, 1: 39.9 months; CLIP score, 2: 23.5 months; CLIP score, ≥3: 13.5 months). The 1— and 3—year OS were 94% and 86% (CLIP score, 0), 89% and 59% (CLIP score, 1), and 76% and 40% (CLIP score, 2), respectively. In a univariate Cox regression, OS was significantly associated with the CLIP and BCLC score as well as with the diameter of the largest lesion. No significant correlation was found with age, multifocal disease or Child-Pugh stage. When the CLIP and BCLC scores and the diameter of the largest lesion were included in a multivariate model, the CLIP score proved to be the only predictor ($p < 0.02$).

Matched-pair analysis

We identified 57 pairs of patients meeting all match criteria (see Methods and Materials) The treatment characteristics of

Table 2. Lesion and treatment characteristics

All lesions (lesions, N = 126)	
Tumor diameter (cm)	Mean, 4.4; median, 3.4; 95% CI, 3.8–5.0; SD, 3.3; range, 1–15
Dose at the tumor margin, no. of lesions	12 Gy, n = 8; 15 Gy, n = 64; 20 Gy, n = 36; 25 Gy, n = 18
Local recurrences	12 Gy, n = 1; 15 Gy, n = 2; 20 Gy, n = 2; 25 Gy, n = 0
Mean MRI follow-up (mo)	12.0
1-Year cumulative local control rate	95%
Single-session treatments (lesions: N = 114)	
Tumor diameter (cm)	Mean, 3.7; median, 3.1 95% CI, 3.3–4.2; SD, 2.5; range, 1–12
Dose at the tumor margin, no. of lesions	12 Gy, n = 2; 15 Gy, n = 58; 20 Gy, n = 36; 25 Gy, n = 18
Local recurrences	12 Gy, n = 0; 15 Gy, n = 2; 20 Gy, n = 2; 25 Gy, n = 0
1-Year cumulative local control rate	96%
Multiple-session treatments (lesions N = 12)	
Tumor diameter (cm)	Mean, 10.9; median, 11.3; 95% CI, 8.9–12.8; SD, 3.1; range, 6–15
Dose at the tumor margin, no. of lesions	12 Gy, n = 6; 15 Gy, n = 6
Local recurrences	12 Gy, n = 1; 15 Gy, n = 0
1-Year cumulative local control rate	91%

Abbreviation: MRI = magnetic resonance imaging.

both the treatment and the control group are shown in Table 4. In the treatment group, 41 patients presented in Child-Pugh Class A and another 16 in Child-Pugh Class B; in the control group these were 45 and 12 patients, respectively. The median tumor diameter of the largest lesion was 5.2 cm in the treatment group and 5.0 cm in the control group. At the time of analysis, 38 patients in the treatment group had died compared with 39 in the control group. Whereas the treatment group displayed a median OS after first diagnosis of 37.5 months, respectively, the control group showed a median OS of 18 months (Fig. 5). The difference was significant ($p < 0.0001$), and results favoring the treatment group remained significant in all analyses of subgroups according to CLIP score (Table 4).

Local tumor control

In all, five local tumor progressions were observed in all 126 lesions. The 1—year cumulative local control rate was 95% for all lesions. Of the 12 lesions treated in two or three sessions rather than a single session, one lesion (12-Gy minimum dose) relapsed. Four of 114 lesions treated in a single session relapsed. In univariate and multivariate analysis of the single- and multiple-session treatments, neither tumor diameter nor minimum dose at the tumor margin had a significant influence on local recurrence–free survival.

Fig. 1. Contrast-enhanced planning computed tomography, with catheters guiding the source, the planning target volume, and the isodose lines of the treatment plan.

Complications

We performed 124 CT-guided brachytherapy sessions with 83 patients with one to three lesions (mean, 1.5 lesions) per treatment. Complications requiring intervention (n=9) were five bleeding events, three abscesses, and one radiation-induced gastric ulcer. Eight of these nine complications proved to be reversible. One treatment-related death was encountered after hemorrhage and consecutive multiorgan failure after delayed detection of injury to the intercostal artery (0.8%). All other bleedings (n = 4) were embolized successfully by an endovascular method. The three abscesses were all treated successfully by percutaneous drainage and antibiotics. A radiation-induced gastric ulcer was treated symptomatically by administration of a proton-pump inhibitor. Three patients died within the 30 days following the intervention; two of these deaths

Table 3. Patient and treatment characteristics of the control and treatment groups

	Control group, no. of patients	Treatment group, no. of patients*
Median age, y (range)	67.3 (44.3–85.3)	66.7(43.3–84.0)
Gender	M/W: 42/15	M/W: 45/12
Treatment		
Liver resection	8	13
TACE	26	21
Thermoablation	0	11
Systemic chemotherapy	8	4
PEI	5	2
SIRT	2	0
Liver transplantation†	2	4
No (other) treatment	6	18
Unknown	5	0

Abbreviations: M = men; PEI = percutaneous ethanol injection; SIRT = yttrium—90 selective internal radiotherapy; TACE = transarterial chemoembolization; W = women.

* Treatments other than CT-guided brachytherapy.

† Date of liver transplantation was assigned as ‘‘censored’’ in both groups.

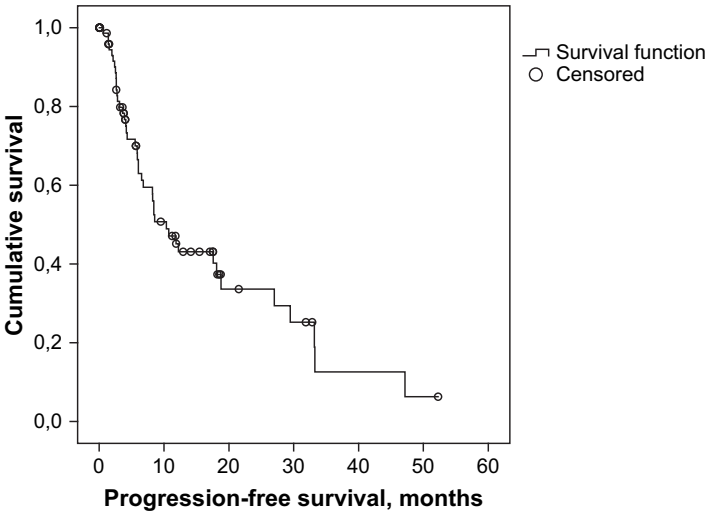

Fig. 2. Time to progression in study patients.

were caused by uncontrolled variceal bleeding not related to our intervention, and the third was caused by a fatal lung embolism 15 days after the intervention, to which it was considered unrelated. The 30—day mortality was thus 4 of 83 patients (4.9%) and the perioperative mortality 1 of 83 patients (1.2%).

Liver function after treatment

We found no evidence for radiation-induced liver disease (RILD) in our patient group. However, 2 patients showed impaired liver function within the 4 months after brachytherapy without evidence of hepatic tumor progression, not meeting the criteria for RILD (minimum twofold increase in anicteric elevation of alkaline phosphatase and nonmalignant ascites or fivefold increase of elevated transaminases over pretreatment levels).

One patient, initially in Child-Pugh Class B, developed progressive ascites and an anicteric elevation of liver enzymes starting 2 months after treatment of a single lesion 6 cm in diameter. The patient died 7 months after the first treatment. Another patient, initially Child-Pugh Class A, developed a reversible icteric elevation of liver enzymes 6 weeks after the last of four brachytherapy sessions, spread over 14 months, in which six different lesions had been treated. However, in neither case was more than two thirds of the liver exposed to a dose of >5 Gy.

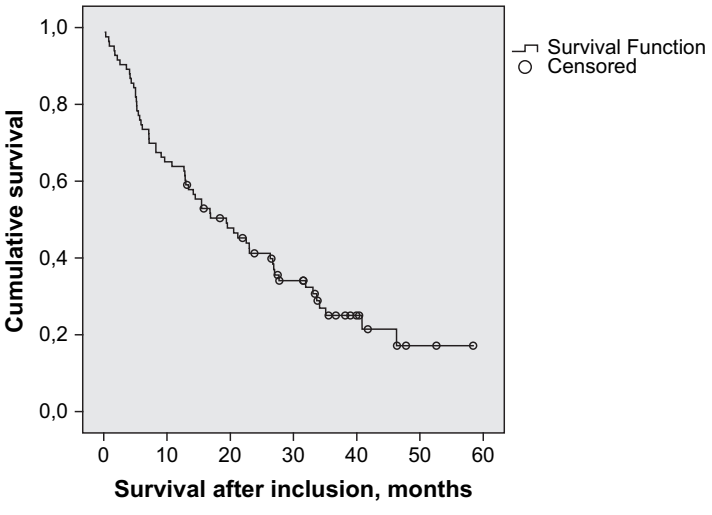

Fig. 3. Overall survival in study patients after computed tomography–guided brachytherapy.

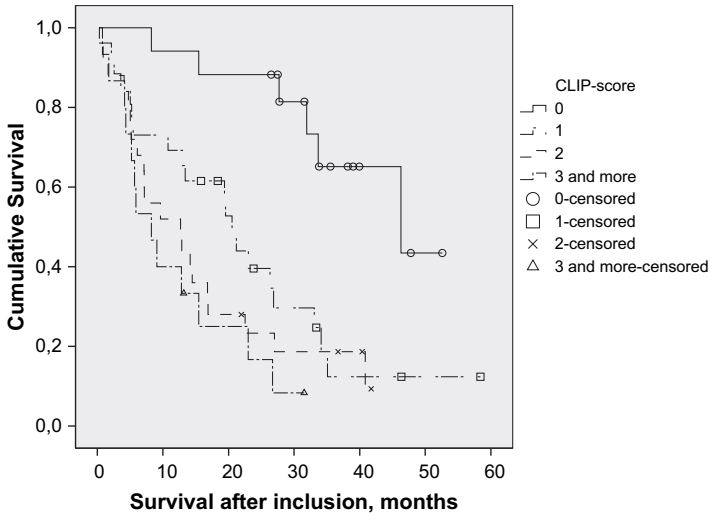

Pairwise Comparisons

		0	1	2	3 and more
		Sig.	Sig.	Sig.	Sig.
Log Rank	0		,001	,000	,000
	1	,001		,328	,050
	2	,000	,328		,444
	3	,000	,050	,444	
Breslow	0		,001	,000	,000
	1	,001		,190	,072
	2	,000	,190		,523
	3	,000	,072	,523	
Tarone-Ware	0		,001	,000	,000
	1	,001		,220	,056
	2	,000	,220		,485
	3	,000	,056	,485	

Fig. 4. Overall survival in study patients after computed tomography–guided brachytherapy according to Cancer of the Liver Italian Program (CLIP) score.

DISCUSSION

Treatment of unresectable hepatocellular carcinoma remains a therapeutic challenge but seems worthwhile, given the poor prognosis for untreated tumors (31). Hepatocellular carcinoma is clinically chemotherapy resistant to numerous cytotoxic agents. Immunotherapy has also so far failed to improve survival (32–35). Recently, promising results have been obtained for sorafenib, an oral multikinase inhibitor of vascular endothelial growth factor

Table 4. Matched-pair analysis (Kaplan-Meier) according to the CLIP score

	Overall survival (mo)				
	Treatment group		Control group		
CLIP score	Median	95% CI	Median	95% CI	*p* (log rank)
0–1	42.3	33.0–51.5	26.7	21.8–31.5	0.000
2	22.8	12.8–32.7	5.0	2.8–7.2	0.003
≥3	18.3	7.8–28.9	3.8	2.6–4.9	0.007
All	37.5	24.0–51.0	18.1	9.4–26.8	0.000

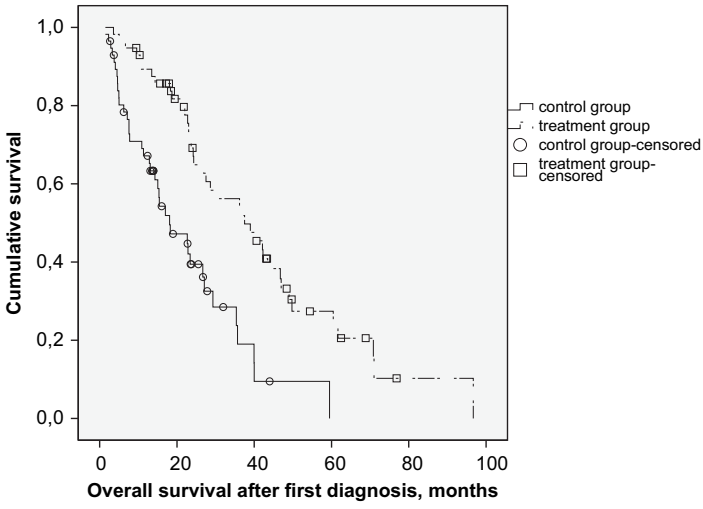

Pairwise Comparisons

	AL	control group Sig.	treatment group Sig.
Log Rank (Mantel-Cox)	control group treatment group	,000	,000
Breslow (Generalized Wilcoxon)	control group treatment group	,000	,000
Tarone-Ware	control group treatment group	,000	,000

Fig. 5. Overall survival in study patients after first diagnosis of hepatocellular carcinoma (matched pairs analysis).

receptor and platelet-derived growth factor (36). Hepatocellular carcinoma rarely gives rise to extrahepatic metastases; therefore local ablative techniques cause maximum damage to the tumor while preserving the organ function and thus are the only currently available tumor-specific therapy. In a recent analysis based on 5,317 patients receiving various treatments, local ablation was associated with a 5-year survival rate of 20% (37). As mentioned above, thermal ablative techniques are of limited value in highly vascularized and large HCC, and their therapeutic effect is hampered by the close proximity of large vessels or risk-prone structures such as the liver hilum. Lesions often exceeding 4 to 5 cm in diameter at the time of diagnosis, which places another limitation upon thermal ablation. Up to now, experience in radiotherapy of hepatocellular carcinoma in particular is limited. Early trials of whole-liver irradiation showed a low response rate and OS, and also a very high toxicity rate of up to 60% to 80%. More recently, 3D conformal radiotherapy has allowed increasing radiation doses without increasing complication rates. This has resulted in an OS of 15.2 months with 21% and 9% of patients developing Grade 3 and 4 toxicity (respectively) in a Phase II trial with concomitant hepatic arterial floxuridine (38). Nevertheless, studies have revealed the radiosensitivity of HCC. In our study population, outcome was predicted by clinical scoring systems rather than tumor size. The CLIP score was the best predictor of overall survival and time to progression, although BCLC has been shown to be an accurate predictor of survival in other studies (39). The best outcome regarding overall survival was obtained for patients with a CLIP score of 0, with a 65% surviving 3 years after inclusion. Although tumors were quite large, with a median of 5 cm (range, 1 to 12 cm), the outcome was comparable to 3-year survival rates after RFA of lesions of majoritarian ≤3 cm (40), revealing the effectiveness of CT-guided brachytherapy regardless of tumor size in contrast to thermal ablation. Matched-pair analysis revealed a highly significant impact of performing CT-guided brachytherapy on OS compared with patients receiving conventional therapy. We found no significant dose dependence for doses between 15 and 25 Gy. Very high local tumor control rates were achieved with moderate and well-tolerated doses of 15 Gy applied at the tumor margin; therefore, the great majority of lesions can be treated effectively in a single session. In view of a median OS, TTP and theoretical time to local progression of 19.4, 10.4, and 47.2 months and regarding the impact of the CLIP-score, causes of death were the underlying cirrhosis and/or intra- or extrahepatic progression outside of the treated nodule, rather than local tumor progression.

In general, a limited effect on OS was seen in very large tumors that were treated in several sessions, even though there were long-term survivors with very large tumors treated solely by CT-guided brachytherapy. Combined therapy could prolong OS in these patients, as suggested by trials combining TACE and radiotherapy (3). Irradiation in combination with sorafenib could also be a reasonable approach because of its radiosensitizing potential (41, 42).

The frequency of irreversible treatment-related events was very low, and reversible events occurred at an acceptable frequency. In cirrhotic patients with HCC, complications from interventional procedures are in general more frequent than in other similar indication (*e.g.,* colorectal liver metastases; personal data) not associated with cirrhosis, as shown for RFA by other authors (43–45). We consider cirrhotic patients to be at high risk because of their liver function impairment and the relatively high portion of patients with coagulation disorders. Altogether, and especially considering the comorbidity of cirrhotic patients, it can be concluded that CT-guided brachytherapy is reasonably safe if patients are monitored carefully, especially for the first 24 hours after intervention. The impact on liver function is low, because of the steep decrease in dose outside the target volume.

CONCLUSION

In summary, our results suggest that CT-guided brachytherapy is an effective and safe method for treating patients with advanced HCC, most of whom will, at the same time, have cirrhosis. A substantial improvement in TTP and OS was seen in the prospectively recruited patients, and this was significantly higher compared with a historical control group in a retrospective matched-pair analysis. Future studies should investigate the combination of local irradiation techniques and sorafenib.

REFERENCES

1. Jaeck D, Bachellier P, Oussoultzoglou E, *et al*. Surgical resection of hepatocellular carcinoma. Post-operative outcome and long-term results in Europe: An overview. *Liver Transpl* 2004;10(2 Suppl. 1):S58–S63.
2. Mazzaferro V, Regalia E, Doci R, *et al*. Liver transplantation for the treatment of small hepatocellular carcinomas in patients with cirrhosis. *N Engl J Med* 1996;334:693–699.
3. Cheng BQ, Jia CQ, Liu CT, *et al*. Chemoembolization combined with radiofrequency ablation for patients with hepatocellular carcinoma larger than 3 cm: A randomized controlled trial. *J Am Med Assoc* 2008;299:1669–1677.
4. Helmberger T, Dogan S, Straub G, *et al*. Liver resection or combined chemoembolization and radiofrequency ablation improve survival in patients with hepatocellular carcinoma. *Digestion* 2007;75:104–112.
5. Llovet JM, Bruix J. Systematic review of randomized trials for unresectable hepatocellular carcinoma: Chemoembolization improves survival. *Hepatology* 2003;37:429–442.
6. Vogl TJ, Naguib NN, Nour-Eldin NE, *et al*. Review on transarterial chemoembolization in hepatocellular carcinoma: Palliative, combined, neoadjuvant, bridging, and symptomatic indications. *Eur J Radiol* 2009;72:505–516.
7. Lopez PM, Villanueva A, Llovet JM. Systematic review: Evidence-based management of hepatocellular carcinoma—an updated analysis of randomized controlled trials. *Aliment Pharmacol Ther* 2006;23:1535–1547.
8. Sutherland LM, Williams JA, Padbury RT, *et al*. Radiofrequency ablation of liver tumors: A systematic review. *Arch Surg* 2006;141:181–190.
9. Llovet JM, Sala M, Bruix J. *Nonsurgical treatment of hepatocellular carcinoma*. Liver Transpl 2000;6(6 Suppl. 2):S11–S15.
10. Hawkins MA, Dawson LA. Radiation therapy for hepatocellular carcinoma: From palliation to cure. *Cancer* 2006;106:1653–1663.
11. Mizumoto M, Tokuuye K, Sugahara S, *et al*. Proton beam therapy for hepatocellular carcinoma adjacent to the porta hepatis. *Int J Radiat Oncol Biol Phys* 2008;71:462–467.
12. Hata M, Tokuuye K, Sugahara S, *et al*. Proton beam therapy for aged patients with hepatocellular carcinoma. *Int J Radiat Oncol Biol Phys* 2007;69:805–812.
13. Hata M, Tokuuye K, Sugahara S, *et al*. Proton beam therapy for hepatocellular carcinoma patients with severe cirrhosis. *Strahlenther Onkol* 2006;182:713–720.
14. Hata M, Tokuuye K, Sugahara S, *et al*. Proton beam therapy for hepatocellular carcinoma with limited treatment options. *Cancer* 2006;107:591–598.
15. Hata M, Tokuuye K, Sugahara S, *et al*. Proton beam therapy for hepatocellular carcinoma with portal vein tumor thrombus. *Cancer* 2005;104:794–801.
16. Chiba T, Tokuuye K, Matsuzaki Y, *et al*. Proton beam therapy for hepatocellular carcinoma: A retrospective review of 162 patients. *Clin Cancer Res* 2005;11:3799–3805.
17. Peters N, Wieners G, Pech M, *et al*. CT-guided interstitial brachytherapy of primary and secondary lung malignancies: Results of a prospective phase II trial. *Strahlenther Onkol* 2008; 184:296–301.
18. Wieners G, Pech M, Rudzinska M, *et al*. CT-guided interstitial brachytherapy in the local treatment of extrahepatic, extrapulmonary secondary malignancies. *Eur Radiol* 2006;16: 2586–2593.
19. Ricke J, Wust P, Wieners G, *et al*. CT-guided interstitial single-fraction brachytherapy of lung tumors: Phase I results of a novel technique. *Chest* 2005;127:2237–2242.
20. Ricke J, Wust P, Wieners G, *et al*. Liver malignancies: CT-guided interstitial brachytherapy in patients with unfavorable lesions for thermal ablation. *J Vasc Interv Radiol* 2004; 15:1279–1286.
21. Ricke J, Hildebrandt B, Miersch A, *et al*. Hepatic arterial port systems for treatment of liver metastases: Factors affecting patency and adverse events. *J Vasc Interv Radiol* 2004;15:825–833.
22. Ricke J, Wust P, Stohlmann A, *et al*. CT-guided interstitial brachytherapy of liver malignancies alone or in combination with thermal ablation: Phase I–II results of a novel technique. *Int J Radiat Oncol Biol Phys* 2004;58:1496–1505.
23. Bruix J, Sherman M, Llovet JM, *et al*. Clinical management of hepatocellular carcinoma. Conclusions of the Barcelona–2000 EASL conference. European Association for the Study of the Liver. *J Hepatol* 2001;35:421–430.
24. Ricke J, Wust P, Stohlmann A, *et al*. [CT-guided brachytherapy. A novel percutaneous technique for interstitial ablation of liver metastases]. *Strahlenther Onkol* 2004;180:274–280.
25. Ricke J, Wust P, Stohlmann A, *et al*. CT-guided interstitial brachytherapy of liver malignancies alone or in combination with thermal ablation: Phase I–II results of a novel technique. *Int J Radiat Oncol Biol Phys* 2004;58:1496–1505.
26. Ricke J, Seidensticker M, Ludemann L, *et al*. In vivo assessment of the tolerance dose of small liver volumes after single-fraction HDR irradiation. *Int J Radiat Oncol Biol Phys* 2005; 62:776–784.
27. Therasse P, Arbuck SG, Eisenhauer EA, *et al*. New guidelines to evaluate the response to treatment in solid tumors. European Organization for Research and Treatment of Cancer, National Cancer Institute of the United States, National Cancer Institute of Canada. *J Natl Cancer Inst* 2000;92:205–216.
28. Grieco A, Pompili M, Caminiti G, *et al*. Prognostic factors for survival in patients with early-intermediate hepatocellular carcinoma undergoing non-surgical therapy: Comparison of Okuda, CLIP, and BCLC staging systems in a single Italian centre. *Gut* 2005;54:411–418.
29. Llovet JM, Bruix J. Prospective validation of the Cancer of the Liver Italian Program (CLIP) score: A new prognostic system for patients with cirrhosis and hepatocellular carcinoma. *Hepatology* 2000;32:679–680.
30. Llovet JM, Bru C, Bruix J. Prognosis of hepatocellular carcinoma: The BCLC staging classification. *Semin Liver Dis* 1999;19:329–338.
31. Okuda K, Ohtsuki T, Obata H, *et al*. Natural history of hepatocellular carcinoma and prognosis in relation to treatment. Study of 850 patients. *Cancer* 1985;56:918–928.
32. Oquinena S, Inarrairaegui M, Vila JJ, *et al*. Spontaneous regression of hepatocellular carcinoma: Three case reports and a categorized review of the literature. *Dig Dis Sci* 2009;54:1147–1153.
33. Randolph AC, Tharalson EM, Gilani N. Spontaneous regression of hepatocellular carcinoma is possible and might have implications for future therapies. *Eur J Gastroenterol Hepatol* 2008;20:804–809.
34. Sibartie V, Moriarty J, Crowe J. Spontaneous regression of hepatocellular carcinoma. *Am J Gastroenterol* 2008;103:1050–1051.
35. Cho YK, Kim JK, Kim MY, *et al*. Systematic review of randomized trials for hepatocellular carcinoma treated with percutaneous ablation therapies. *Hepatology* 2009;49:453–459.
36. Llovet JM, Ricci S, Mazzaferro V, *et al*. Sorafenib in advanced hepatocellular carcinoma. *N Engl J Med* 2008;359:378–390.
37. Schwarz RE, Smith DD. Trends in local therapy for hepatocellular carcinoma and survival outcomes in the US population. *Am J Surg* 2008;195:829–836.
38. Ben-Josef E, Normolle D, Ensminger WD, *et al*. Phase II trial of high-dose conformal radiation therapy with concurrent hepatic artery floxuridine for unresectable intrahepatic malignancies. *J Clin Oncol* 2005;23:8739–8747.
39. Cillo U, Vitale A, Grigoletto F, *et al*. Prospective validation of the Barcelona Clinic Liver Cancer staging system. *J Hepatol* 2006;44:723–731.

40. Cho YK, Kim JK, Kim MY, *et al*. Systematic review of randomized trials for hepatocellular carcinoma treated with percutaneous ablation therapies. *Hepatology* 2009;49: 453–459.
41. Dawson LA. The evolving role of radiation therapy in hepatocellular carcinoma. *Cancer Radiother* 2008;12:96–101.
42. Plastaras JP, Kim SH, Liu YY, *et al*. Cell cycle dependent and schedule-dependent antitumor effects of sorafenib combined with radiation. *Cancer Res* 2007;67:9443–9454.
43. Cheung TT, Ng KK, Poon RT, Fan ST. Tolerance of radiofrequency ablation by patients of hepatocellular carcinoma. *J Hepatobiliary Pancreat Surg* 2009;16:655–660.
44. Buell JF, Thomas MT, Rudich S, *et al*. Experience with more than 500 minimally invasive hepatic procedures. *Ann Surg* 2008;248:475–486.
45. Kong WT, Zhang WW, Qiu YD, *et al*. Major complications after radiofrequency ablation for liver tumors: Analysis of 255 patients. *World J Gastroenterol* 2009;15:2651–2656.

Radiotherapy and Oncology 100 (2011) 314–319

Contents lists available at ScienceDirect

Radiotherapy and Oncology

journal homepage: www.thegreenjournal.com

Phase II trial

Treatment of hepatic metastases of breast cancer with CT-guided interstitial brachytherapy – A phase II-study

Gero Wieners [a,1], Konrad Mohnike [a,1], Nils Peters [a,b], Joachim Bischoff [c], Anke Kleine-Tebbe [e], Ricarda Seidensticker [a], Max Seidensticker [a], Günther Gademann [b], Peter Wust [d], Maciej Pech [a], Jens Ricke [a,*]

[a] Klinik für Radiologie und Nuklearmedizin; [b] Universitätsklinikum für Strahlentherapie; [c] Universitätsfrauenklinik, Otto-von-Guericke-University Magdeburg, Germany; [d] Charité Zentrum für Tumormedizin, Klinik für Strahlentherapie; [e] Charité Zentrum für Tumormedizin, Interdisziplinäres Brustzentrum, Campus Virchow Klinikum, Germany

ARTICLE INFO

Article history:
Received 16 February 2009
Received in revised form 8 February 2011
Accepted 13 March 2011
Available online 16 April 2011

Keywords:
Brachytherapy
CT-guided intervention
Breast cancer
Liver metastases

ABSTRACT

Purpose: The aim of the study was the evaluation of feasibility, safety and effectiveness of interstitial brachytherapy for the treatment of hepatic metastases of breast cancer.

Materials and methods: Forty-one consecutive patients with 115 unresectable hepatic metastases of breast cancer were included in this phase-II-trial. They were treated in 69 interventions of CT-guided-interstitial-brachytherapy of the liver. Brachytherapy was applied as a single fraction high-dose-irradiation (15–25 Gy (Gray)) using a ^{192}Ir-source of 10 Ci. Nineteen patients presented systemically pretreated extrahepatic tumors. Primary endpoints were complications, local tumor control and progression-free survival.

Results: The median tumor diameter was 4.6 cm (1.5–11 cm). The median irradiation time per intervention was 26.5 min (range: 7–47 min). The applied median minimal dose at the CTV (clinical target volume) margin was 18.5 Gy (12–25 Gy). In 69 interventions and during the postinterventional period, one major complication (symptomatic post-interventional bleeding) (1.5%) and six minor complications occurred (8.7%). The median follow-up time was 18 months (range: 1–56). After 6, 12 and 18 months, local tumor control was 97%, 93.5% and 93.5%, intra- and extrahepatic progression free survival was 53%, 40% and 27%, and overall survival was 97%, 79% and 60%, respectively.

Conclusion: CT-guided-brachytherapy is safe and effective for the treatment of liver metastases of breast cancer.

In Germany breast cancer is one of the most frequent malignomas with an incidence of approximately 51,000 patients and 19,000 diagnosis related deaths per year [1].

Liver metastases are a general crucial problem for morbidity and mortality [2,3]. In contrary to liver metastases of colorectal cancer a curative surgical resection is not possible in patients with breast cancer, owing to the systemic nature of the disease [3,4]. However, findings of several studies have shown that surgical treatment of hepatic metastases from breast cancer may prolong survival in certain patients [4–7]. In the recent past minimal invasive image guided therapies such as radio-frequency-ablation (RFA) and interstitial laser therapy (ILT) were established as therapeutic alternatives with promising results [8]. However, for both of these thermo ablative therapies, the general limitations for an effective treatment are tumor sizes greater than 4–5 cm, hyperperfused tumors and location, e.g. thermosensitive structures or bigger vessels with a resulting cooling effect or proximity to bile ducts in the liver hilus, which might cause complications such as jaundice [9]. This could hamper tumor destruction and induce a higher risk of incomplete tumor ablation [10,11].

We introduced a technique for brachytherapy of solid tumors by applying CT-guidance and 3D CT-data for dose planning. Ideally, local irradiation is performed as a high dose, single fraction brachytherapy under tomographic guidance (CT or MRI). The individual irradiation planning using the 3D data set of spiral CT or MRI after percutaneous placement for brachytherapy catheters optimizes the therapeutic success by exact dose application and coverage of target volume. The method is independent of inherent patient motion such as respiration. This exact dosimetry minimizes possible complications by preventing damage to structures at risk around the target volume. Initial data suggest that this method is as safe and effective as thermal ablation such as RFA or ILT in the treatment of liver and even safer in lung tumors [12,13]. In addition, no known restrictions exist with respect to the maximum tumor size or cooling effects of tumor perfusion or adjacent blood vessels for CT-guided brachytherapy [14–16].

* Corresponding author. Address: Klinik für Radiologie und Nuklearmedizin, Otto-von-Guericke-University Magdeburg, Leipzigerstr. 44, 39120 Magdeburg, Germany.
E-mail address: jens.ricke@med.ovgu.de (J. Ricke).

[1] These authors contributed equally to this work.

0167-8140/$ - see front matter © 2011 Elsevier Ireland Ltd. All rights reserved.
doi:10.1016/j.radonc.2011.03.005

The results of CT guided brachytherapy in treatment of liver metastases of breast cancer are reported in this study. Primary endpoints were complication rate, local tumor control and progression-free survival.

Materials and methods

Patient population

The study population comprised 41 consecutive patients with hepatic metastases of breast cancer. Median age was 55 years (range: 34–82 years). Preinterventional treatment of the patients included first line ($n = 7$), second line ($n = 9$), third line ($n = 11$), fourth line ($n = 8$), fifth line ($n = 4$) chemotherapy and two patients with unknown preinterventional chemotherapy ($n = 2$). One hundred fifteen liver malignomas were treated in 69 interventions with CT-guided interstitial high-dose-rate (HDR) brachytherapy. All patients were determined not to be candidates for surgical resection by interdisciplinary consensus and had been rated unresectable by visceral surgeons, due to relative or absolute contraindications.

Twelve patients had pretreated bone metastases (29%), two patients had pretreated metastases in the bone and lung or lymph nodes, and five patients had pretreated metastases in the lung ($n = 3$; 7.3%) or lymph nodes ($n = 2$; 4.9%). Pretreatments consisted of systemic chemotherapies, hormonal treatment, and radiation therapy and bisphosphonates in case of bone metastases. In total 19 patients presented extrahepatic tumor manifestations (46.3%). Eligibility criteria consisted of: ECOG-PS 0-2 (Eastern Cooperative Oncology Group Performance Status Scale), erythrocytes $>3.3 \times 10^{12}$/l, thrombocytes $>50 \times 10^{9}$/l, leucocytes $>3 \times 10^{9}$/l, hemoglobin >10 g/dl, prothrombin time > 50% and partial thromboplastin time (PTT) <50 s, as well as absence of infection. Written informed consent was obtained from all patients. The study was approved by the local ethics committee.

Intervention

The technique of CT-guided brachytherapy has been described in detail in the literature [17]. We used Fluoroscopy CT guidance (Somatom Plus 4, Siemens, Germany; Toshiba Aquillion 16 slice, Japan) for applicator positioning in the tumor.

Immediately after catheter placement, a spiral CT of the liver was acquired for 3D treatment planning. For sedation and pain management during the intervention an initial dose of 75 μg fentanyl and 1 mg midazolam i.v. was administered. Additional pain medication was titrated in increments of 25 μg fentanyl or 0.5 mg midazolam i.v. as needed. To prevent postinterventional bleeding at the puncture site, Gelfoam (Gelaspon, Chauvin ankerpharm, Germany) was applied through each brachytherapy sheath during removal.

Radiation properties and treatment planning

The irradiation plan and the irradiation were performed by a physicist and radiooncologist using the treatment planning unit BrachyVision (Varian medical systems, Charlottesville, VA). The dosage calculations implemented in BrachyVision conform to the recommendations of the AAPM TG43 [18]. BrachyVision performs its volume optimization using the Nelder–Mead Simplex optimization method [19,20]. A 10 Ci (Curie) ^{192}Iridium afterloading with a radiation source diameter <1 mm was used. The target dose enclosing the lesion was applied as a single fraction. Dose gradients follow the inverse square law, for typical treatment doses fall off to clinical irrelevant numbers in 10–20 mm distance. To preserve liver function after irradiation at least one-third of the liver had to receive less than 5 Gy. Careful delineation of the clinical target volume was performed in every CT slice with the afterloading catheters in place (Fig. 1).

Intention of radiation treatment planning was a complete (100%) confinement of the CTV with the prescribed target dose. Inside the CTV high dose inhomogeneties were regularly seen ranging from the minimal applied dose (D100) at the margin of the CTV to maximum doses of several hundred Gray in the smallest volumes next to the applicator. For a typical treatment average doses of 80–150 Gy for the CTV and a V5 of the liver of several hundred milliliters were seen.

Follow up

MRI was performed 3 days, 6 weeks and every 3 months after the intervention. The MR parameters were T2-weighted ultra turbo spin echo (UTSE; TE/TR 90/2100) with and without fat suppression, T1-weighted gradient echo (GRE; TE/TR 5/30, flip angle 30°) plain, dynamic sequences and sequences 20 min post i.v. injection of 0.1 ml/kg Gd-EOB-DTPA (Primovist, Bayer-Schering Healthcare). Baseline and follow up visits concluded of a clinical examination, assessment of adverse events and serological and hematological parameters including indicators of the liver function: AST, ALT, AP, GGT, bilirubin, PCHE, albumin and PT.

Statistical analysis

Statistical analysis was calculated using the Wilcoxon test, the Kaplan–Meier method and the Log-rank test.

Results

Interventional procedure, irradiation and complications of brachytherapy

The median tumor diameter was 4.4 cm (1–11 cm). Between one and six lesions were treated during each session (41×1 lesion, 14×2, 7×3, 2×4, 1×5 and 2×6). According to the tumor size and configuration between 1 and 11 brachytherapy applicators were positioned (median: 4). The applied median minimal irradiation dose at the CTV-margin was 18.5 Gy (12–25 Gy). If surrounding structures or organs, e.g. stomach or intestines were inside the region of high dose irradiation, the tumor surrounding the dose had to be reduced to avoid side effects. The maximum dose applied to stomach or duodenum was 15 Gy per 1 ml organ volume. The minimal tumor surrounding dose was then 2×12 Gy, 22×15 Gy, 1×18 Gy, 29×20 Gy and 15×25 Gy according to D100, i.e. 100% of the CTV receiving the respective dose. Patient characteristics are listed in Table 1.

The median irradiation time was 26.5 min (range: 7–47 min). 30 day mortality was 0%. Minor complications were fever and shivering ($n = 2$), subcapsular hematoma ($n = 1$), hepatic bleeding through the puncture site ($n = 2$) and postinterventional jaundice ($n = 1$) which resolved without therapeutic intervention (total: 8.6%). One major complication in 69 interventions (1.4%) was observed. This patient experienced a symptomatic post interventional blood loss through the puncture site requiring a blood transfusion of 1000 cc. The patient recovered without further intervention. During follow up laboratory tests frequently documented a mild and asymptomatic increase of AST, ALT as well as serum bilirubin, GammaGT and AP immediately after the intervention. No changes were recorded for liver function parameters, such as PCHE, PT or serum albumin. No postinterventional radiation induced liver disease (RILD) was found during long term follow up.

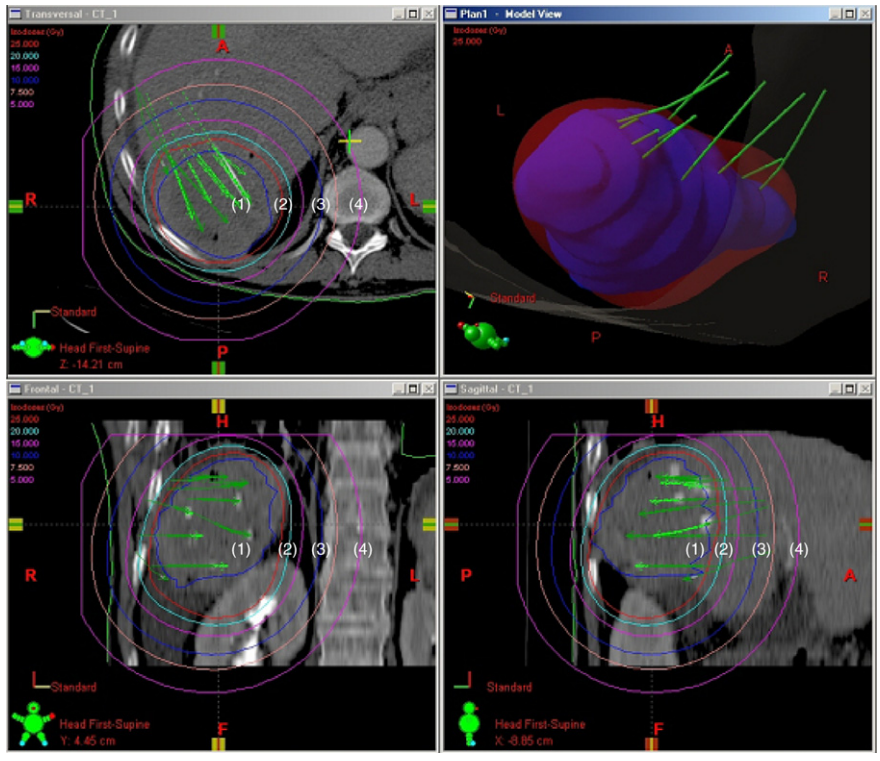

Fig. 1. Screen shot of the BrachyVision software: outlined clinical target volume (CTV) in the liver (segment 6 and 7) with implanted brachytherapy catheters in the axial planning CT (top left) and 3D-model of target-volume (top right) with the minimal surrounding irradiation dose of 20 Gy for this tumor manifestation. In between these catheters irradiation dose elevations up to 300–400 Gy can be calculated and visualized virtually with the BrachyVision software (Varian medical systems, Charlottesville, VA). Coronal and sagittal reconstruction lower left and right. (1 = target volume; 2 = 20 Gy isodose; 3 = 10 Gy isodose; 4 = 5 Gy isodose).

Therapeutic response

The median follow up time was 18 months (range: 1–56 months). According to the Kaplan–Meier method, local tumor control after 6, 12 and 18 months was 97%, 93.5% and 93.5%, (Fig. 2)respectively. At 6, 12 and 18 months, systemic progression free survival was 53%, 40% and 27%, (Fig. 2)respectively. Twenty-four patients (58.5%) showed intrahepatic tumor progression, eight patients intra- and extrahepatic progression (19.5%) and three patients just extrahepatic progression (7.3%) during follow up. The mean time to progression was 8.1 months (range: 1.3–33 months). Overall survival was 97%, 79% and 60%, respectively (Fig. 2). No clear dose dependency was observed. Whereas 3 out of 20 patients receiving 12 and 15 Gy suffered from local recurrence after 6 and 11 months, two other patients experienced local failures with 20 Gy and 25 Gy after 21 and 3 months, respectively.

During follow up, 17 patients (41%) were treated repeatedly with interstitial brachytherapy only in response to intrahepatic progression or local tumor recurrence. Five other patients received a combination of systemic chemotherapy and interstitial brachytherapy upon intrahepatic progression. All other patients with intra- and/or extrahepatic progression received further systemic chemotherapy only.

A comparison of patient groups with a different extent of preinterventional treatment showed a significant difference in their overall survival. However, local tumor control was not significant between these patients. Mean time to progression was unfavorable in the strongly pretreated group of the fourth and fifth line preinterventional chemotherapy with 4 and 5.2 months, respectively. The mean time to progression was 7.3, 9 and 14 months for the three other groups (first, second and third line chemotherapy) with a total of 27 patients (Table 2). Adjuvant chemotherapy was administered in 14 patients only (34%). Mean time to progression for the patient group with adjuvant chemotherapy was 8.5 months (range: 3–20 months). In comparison, the mean time to progression for the patient group without adjuvant chemotherapy was 9 months (range: 1.4–33 months, not significant). No significant difference in the time to progression occured between patients with positive or negative receptor status (herceptin ($p = 0.352$), estrogen ($p = 0.31$) and progesterone receptors ($p = 0.681$)). In a subgroup analysis of patients with positive estrogen receptor status and preinterventional chemotherapy line not more than "third line", a significantly longer time to progression ($p = 0.038$) was evident. Another subgroup analysis of HER 2 receptor positive patients ($n = 14$) demonstrated that patients who received herceptin post intervention ($n = 8$) displayed a prolonged time to progression as compared to HER 2 receptor positive patients who did not receive herceptin ($n = 6$). However, this difference did not prove to be significant, but a tendency is indicated. There was also no significant difference in the time to progression for patients with or without pretreated bone metastases.

Discussion

CT-guided brachytherapy has been described in the literature as safe and effective for the treatment of primary or secondary tumors in liver, lung and also for extrahepatic or extrapulmonary tumors [12–15,17,21–23].

In this study, interstitial brachytherapy as a palliative treatment for hepatic metastases from breast cancer were examined for effectiveness, safety and technical success. Local tumor control after brachytherapy of 115 lesions was quite satisfactory (Fig. 2). No dose dependency of local tumor control was observed if a minimal dose of 15 Gy was applied. However, in case of local recurrence, due to the relative independence of brachytherapy to the size of

Table 1
Patient characteristics (– = negative receptor status; + = positive receptor status; ++ = highly positive receptor status).

Pat. Num.	Age	Extrahep. metastases	Estrogen receptor	Progesterone receptor	HER 2 receptor)	Liver metastases (first brachytherapy)	Localization (liver segment)	CTV volume (ml)	Number of catheters	Surrounding dose (CTV)	Complications	Adjuvant chemotherapy	Progress local/ intrahepatic/ extrahepatic
1	36,4	Bone	+	+	++	2	3/5	127	7	25	No	No	N/Y/N
2	49,1	Bone	+	+	–	1	Central	6	1	15	No	No	N/Y/N
3	75,7	No	–	–	++	1	7	204	5	20	No	No	N/Y/N
4	57,1	No	–	–	–	1	5	163,4	7	25	No	No	N/Y/N
5	51	Bone	–	–	–	1	4/5/8	69	4	15	Symp. bleeding	No	N/N/N
6	36,9	Bone	+	–	–	1	Central	212	5	20	No	No	N/Y/Y
7	53,5	Bone	+	–	–	1	Central	10,8	2	20	No	No	N/Y/N
8	58,8	No	+	+	++	3	2 + 3/5/6	44	6	15	No	No	N/N/N
9	55	Lung	+	+	++	1	8	153	5	15	Jaundice	No	Y/Y/Y
10	50,6	No	+	+	++	1	5	31	3	12	Subcap. hematoma	Yes	N/N/N
11	52	No	+	+	–	1	Central	4,5	1	20	No	Yes	Y/Y/N
12	42	Lung	+	+	–	1	4/5/8	392,7	11	12	No	Yes	N/Y/N
13	55,3	No	+	+	–	1	4	8,7	1	20	No	No	N/N/Y
14	69,5	No	+	+	–	2	4	10,9	2	20	No	No	N/Y/Y
15	51,9	No	–	+	–	1	7	26,9	3	20	No	No	N/N/N
16	81,6	No	–	–	–	1	7/8	217	7	20	No	No	N/Y/N
17	60,9	Lung	+	+	–	2	3/7	127,9	5	15	No	Yes	N/Y/N
18	63,5	No	–	–	–	5	1/3/4/7	74	7	15	No	Yes	N/Y/N
19	66,5	No	–	–	–	1	6/7	251	10	15	Fever	No	Y/Y/N
20	67,1	Bone/lung	+	–	–	2	6/7	22	3	15	No	Yes	N/N/Y
21	44,7	Lung	–	–	++	1	Central	93	5	20	No	No	N/Y/N
22	52,7	No	–	+	–	2	4/8	26	4	15	No	Yes	N/Y/N
23	61,2	No	–	–	++	2	1/7	103	5	25	No	No	N/Y/N
24	65,6	No	+	+	–	6	1/3/5/8	49	5	15	No	No	N/Y/N
25	48,2	Bone/lymph nodes	–	–	–	3	1/2/5	45	5	20	No	No	N/Y/N
26	65	Lymph nodes	+	+	++	1	Central	33	3	20	No	No	N/Y/N
27	53,8	Bone	–	–	++	1	2/3	103	5	15	No	No	Y/Y/Y
28	68,2	Bone	+	–	–	1	7	128	5	20	No	No	N/Y/N
29	60,3	Bone	–	–	–	1	2	39	3	20	No	No	N/Y/Y
30	69,7	Bone	–	–	++	1	6	154	7	15	Shivering	Yes	N/Y/N
31	64,4	No	+	–	–	2	3/8	102	9	12	Asymp. bleeding	No	N/Y/N
32	38,6	No	–	–	–	3	3/4/7	132	4	15	No	No	N/Y/N
33	52,8	No	+	+	–	1	8	25	2	25	Asymp. bleeding	No	N/Y/N
34	51,8	Bone	+	+	++	2	8	18	2	20	No	No	N/Y/N
35	54,5	No	+	+	–	3	4/7	77	6	15	No	Yes	N/Y/N
36	41	Bone	+	–	–	2	4/8	33	4	15	No	No	N/Y/N
37	43,5	Bone	+	+	++	1	5	29	3	15	No	Yes	N/Y/Y
38	60,3	No	+	–	++	1	3	42	4	25	No	No	N/Y/N
39	62,6	No	–	–	–	1	Central	49	5	15	No	Yes	N/N/N
40	53,2	No	–	–	–	2	5/6	28	4	20	No	Yes	N/N/N
41	56,5	No	–	–	++	2	3/8	12	2	20	No	No	N/Y/Y

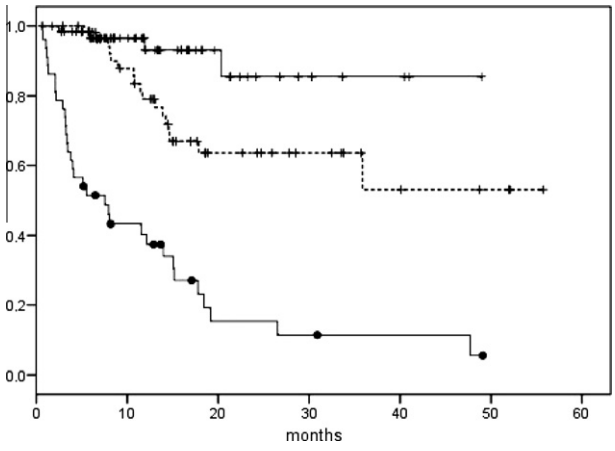

Fig. 2. This graphic demonstrates local tumor control (+), progression free survival (●) and overall survival (—+—) in the Kaplan–Meier method. Local tumor control of 115 intrahepatic metastases of mamma carcinoma treated by interstitial brachytherapy. According to the Kaplan–Meier method local tumor control after 6, 12 and 18 months the local tumor control was 97%, 93.5% and 93.5%. After 6, 12 and 18 months progression free survival was 53%, 40% and 27%. Overall survival after 6, 12 and 18 months was 97%, 79% and 60%, respectively.

the tumor volume treated and the low impact on liver function, CT-guided brachytherapy could be repeated [14,15].

Local tumor control for laser ablation (ILT) as another local treatment option for hepatic metastases of mamma carcinoma is also quite satisfactory and varies in the literature between 83% and 92% after 10–17 months [8,16,24]. Compared to thermal ablation, CT-guided brachytherapy has proven to be advantageous with respect to tumor size and tumor perfusion [14]. Furthermore, most authors believe that RFA or ILT is limited to approximately 4–5 cm if complete tumor ablation is intended [8,16]. For brachytherapy, the maximum limit for effective tumor ablation has not yet been determined, although treatment of tumor sizes of up to 15 cm have been reported [21]. Additionally, in thermal ablation large blood vessels adjacent to the tumor or strong tumor perfusion account for adverse cooling effects, potentially prohibiting complete tumor ablation [25].

A different technique of brachytherapy was described by Kettenbach et al. [26]. Brachytherapy catheters were introduced under MR-image guidance, which is comparable to the approach under CT-fluoroscopy. For the treatment planning they used conventional X-ray with marked wires and transferred these image data in their planning systems. In this study as described, immediately after catheter placement, a spiral CT of the liver was performed for 3D treatment planning to know the exact catheter position in the CTV. In comparison to Kettenbach et al. the treatment planning for the CTV and the organs at risk in this study seems to be more precise, which might explain the difference to their conclusion that MR-guided brachytherapy is feasible for liver metastases with diameter of less than 3 cm. However, they concluded also further developments of their technique were necessary for a promising therapy.

Stereotactic body radiation therapy (SBRT) has been described in the literature as a feasible technique for local irradiation of liver metastasis [27–29]. Current protocols state doses of 60 Gy in three fractions (a 20 Gy), maximum numbers of three metastases and a maximum diameter of 6 cm. Whereas applied nominal doses in Brachytherapy are lower (20 versus 60 Gy), the actual average doses can be much higher due to dose inhomogeneity and very high doses in central, possibly hypoxic, tumor areas. This might be an explanation for the lower nominal doses required for local tumor control compared to SBRT. The stated doses indicate the D100, thus specifying the minimal dose covering 100% of the planning target volume. To compare equitably with dose prescriptions of other methods (for example SBRT, where dose prescriptions in standard protocols are covering 80–90% of the PTV), D90 of treated patients becomes relevant. For a standard treatment with a D100 of 15 Gy, D90 averages to 21.1 Gy (range 18–23.6 Gy).

The size of a metastasis is not a limiting factor for image guided brachytherapy. In this study lesions up to 11 cm were successfully treated. Also, several lesions can be easily treated in a single session. The steep dose gradient in contrast to SBRT facilitates sparing of healthy liver tissue. All local recurrences in this study occurred in marginal regions of comparably large lesions, which further supports the idea of beneficial effects of higher central doses.

Owing to the systemic nature of the disease, progression-free survival (Fig. 2) was 53%, 40% and 27% in our patients after 6, 12 and 18 months, respectively. Overall survival after 6, 12 and 18 months was 97%, 79% and 60%, respectively (Fig. 2). However, previous studies have proven more favorable outcomes for survival in breast cancer patients with resection of their hepatic metastases [4,30,31]. In these patients, overall survival after 1, 3 and 5 years was 77–94%, 50–66%, and 31–42%, respectively as compared to patient groups with rather diffuse metastastic disease demonstrating 1-year survival rates of only 27.6% [30]. Vlastos et al. described a 5-year-survival rate of 61% for patients with isolated liver metastases. He postulated that patients should fit specific preinterventional criteria for improved survival, like stabile disease under preinterventional chemotherapy, no extrahepatic tumor and fewer than four intrahepatic metastases [32]. In contrary to this study, in our study also patients in advanced tumor stages were included. In contrast also to common surgical approaches our only restrictions were the absence of disseminated metastastic disease such as patients with diffuse liver metastases or extrahepatic disease dominating liver disease. We also included true salvage patients who had undergone up to the fifth line preinterventional chemotherapy (Table 2). We believe that this rather unfavorable patient selection explains the difference in the overall survival as compared to surgical resection. We, however, believe that in light of this poor patient selection survival data are promising.

We found that even for advanced tumor stages, interstitial brachytherapy is a helpful option or complement in the treatment of liver metastases, and it might be life-extending with a good

Table 2
Comparison of groups with different preinterventional chemotherapy lines.

Preinterventional chemotherapy	Number of patients	Number of metastases treated by brachytherapy	Adjuvant chemotherapy	Mean follow up in months (range)	Mean time to progression in months (range)	Type of progression (intrahepatic/ extrahepatic/both)	Local recurrence	Survival after 12/18/ 24 months in %
First line	7	25	1	20 (6–52)	9 (1.4–19.4)	3/0/1	1	100/100/100
Second line	9	22	5	21 (5.5–52)	7.3 (2–28)	5/1/2	0	75/45/45
Third line	11	24	6	19 (3–36)	14 (1.5–33)	7/1/2	1	89/78/78
Fourth line	8	30	1	19.2 (4.5–56)	4 (2–6)	5/0/2	3	80/60/60
Fifth line	4	11	1	9.2 (5.3–14.6)	5.2 (2–10)	3/0/1	0	25/0/0

*Two patients are missing as no data of preinterventional chemotherapies were available.

quality of life as a palliative treatment option for patients, who are not suitable to resection. There is clear evidence, that it can be applied safely with a small rate of severe adverse events. In 69 interventions only one major complication occured. A radiation induced liver disease (RILD) was not observed. Previous studies on CT-guided brachytherapy have also demonstrated a very small number of major complications in the treatment of patients with secondary liver malignancies [12–14]. Given that, minimal invasive tumor ablation by brachytherapy or thermal methods represents an indication for local tumor ablation even with extrahepatic tumor spread [14–16,31,33]. A limitation of this study might be the short follow-up period in the present cohort of 18 months.

In conclusion, CT-guided brachytherapy proved to be a safe and effective treatment for liver metastases of breast cancer as a palliative treatment option for patients who are not suitable for surgical resection. Further studies should target the ideal point in time for local tumor ablation in oncological treatment concepts for metastastic breast cancer. In light of favorable outcomes after extensive minimal-invasive cytoreduction, best candidates for combined local and systemic therapies still need to be identified.

Financial disclosure

There was no financial agreement, compensation, payment or financial interests of the authors which influenced the results of this study in any kind.

Conflict of interest statement

None of the authors has any conflict of interest in any kind concerning this scientific paper.

Acknowledgment

This work has been supported by the European Commission Leonardo da Vinci Grant.

References

[1] Ferlay J. Globocan. International Agency for Research on Cancer. World Health Organisation, Genf. 2001.
[2] Fumoleau P. Treatment of patients with liver metastases. Anticancer Drugs 1996;2:21–3.
[3] Vogl TJ, Muller PK, Mack MG, et al. Liver metastases: interventional therapeutic techniques and results, state of the art. Eur Radiol 1999;9:675–84.
[4] Bathe OF, Kaklamanos IG, Moffat FL, et al. Metastasectomy as a cytoreductive strategy for treatment of isolated pulmonary and hepatic metastases from breast cancer. Surg Oncol 1999;8:35–42.
[5] Adam R, Salmon R, Elias D, et al. Breast cancer liver metastases (BCLM): what may be the role of surgery combined with chemotherapy? J Clin Oncol ASCO Annual Meeting 2007;25:1039.
[6] Thelen A, Benckert C, Jonas S, et al. Liver resection for metastases from breast cancer. J Surg Oncol 2008;1:25–9.
[7] Adam R, Aloia T, Krissat J, et al. Is liver resection justified for patients with hepatic metastases from breast cancer? Ann Surg 2006;244:897–907.
[8] Mack MG, Straub R, Eichler K, et al. Breast cancer metastases in liver: laser-induced interstitial thermotherapy – local tumor control rate and survival data. Radiology 2004;233:400–9.
[9] Rhim H. Percutaneous radiofrequency ablation therapy for patients with hepatocellular carcinoma during occlusion of hepatic blood flow: comparison with standard percutaneous radiofrequency ablation therapy. Cancer 2003;98:433–4.
[10] Pech M, Werk M, Beck A, et al. Comparison of different MRI sequences with and without application of gadolinium-bopta as follow up after LITT. Fortschr Röntgenstr 2004;176:550–5.
[11] Ruhl R, Ricke J. Image-guided micro-therapy for tumor ablation: from thermal coagulation to advanced irradiation techniques. Onkologie 2006;29:219–24.
[12] Ricke J, Wust P, Wieners G, et al. CT-guided interstitial single-fraction brachytherapy of lung tumors: phase I results of a novel technique. Chest 2005;127:2237–42.
[13] Ricke J, Wust P, Hengst S, et al. CT-guided interstitial brachytherapy of lung malignancies. Technique and first results. Radiologe 2004;44:684–6.
[14] Ricke J, Wust P, Stohlmann A, et al. CT-guided interstitial brachytherapy of liver malignancies alone or in combination with thermal ablation: phase I–II results of a novel technique. Int J Radiat Oncol Biol Phys 2004;58:1496–505.
[15] Ricke J, Wust P, Wieners G, et al. Liver malignancies: CT-guided interstitial brachytherapy in patients with unfavorable lesions for thermal ablation. J Vasc Interv Radiol 2004;15:1279–86.
[16] Livraghi T, Goldberg SN, Solbiati L, et al. Percutaneous radio-frequency ablation of liver metastases from breast cancer: initial experience in 24 patients. Radiology 2001;220:145–9.
[17] Ricke J, Seidensticker M, Ludemann L, et al. In vivo assessment of the tolerance dose of small liver volumes after single-fraction HDR irradiation. Int J Radiat Oncol Biol Phys 2005;62:776–84.
[18] Nath R, Anderson LL, Luxton G, et al. Dosimetry of interstitial brachytherapy sources: recommendations of the AAPM Radiation Therapy Committee Task Group No. 43. American Association of Physicists in Medicine. Med Phys 1995;22:209–34.
[19] Lagarias JC, Reeds JA, Wright MH, et al. Convergence properties of the Nelder–Mead simplex method in low dimensions. Siam J Opt 1998;9:112–47.
[20] Olsson DM, Nelson LS. Nelder–Mead Simplex procedure for function minimization. Technometrics 1975;17:45–51.
[21] Wieners G, Pech M, Rudzinska M, et al. CT-guided interstitial brachytherapy in the local treatment of extrahepatic, extrapulmonary secondary malignancies. Eur Radiol 2006;16:2586–93.
[22] Bergk A, Wieners G, Weich V, et al. CT-guided brachytherapy of hepatocellular carcinoma in liver cirrhosis – a novel therapeutic approach. J Hepatol 2005;42:89.
[23] Streitparth F, Pech M, Böhmig M, et al. In vivo assessment of the gastric mucosal tolerance dose after single fraction, small volume irradiation of liver malignancies by computed tomography-guided, high-dose-rate brachytherapy. Int J Radiat Oncol Biol Phys 2006;65:1479–86.
[24] Trubenbach J, Schmidt D, Pereira PL. Percutaneous treatment of liver metastases. Zentralbl Chir 2003;128:920–7.
[25] Kolotas C, Roddiger S, Strassmann G, et al. Palliative interstitial HDR brachytherapy for recurrent rectal cancer. Implantation techniques and results. Strahlenther Onkol 2003;179:458–63.
[26] Kettenbach J, Pokrajac B, Schamp S, et al. MRI-assisted brachytherapy of nonresectable liver metastases. Preliminary technical and clinical experiences. Radiologe 2001;41:56–63.
[27] Herfarth KK, Debus J, Lohr F, et al. Stereotactic single-dose radiation therapy of liver tumors: results of a phase I/II trial. J Clin Oncol 2001;19:164–70.
[28] Schefter TE, Kavanagh BD, Timmerman RD, et al. A phase I trial of stereotactic body radiation therapy (SBRT) for liver metastases. Int J Radiat Oncol Biol Phys 2005;62:1371–8.
[29] Rusthoven KE, Kavanagh BD, Burri SH, et al. Multi-institutional phase I/II trial of stereotactic body radiation therapy for lung metastases. J Clin Oncol 2009;27:1579–84.
[30] Thelen A, Benckert C, Jonas S, et al. Liver resection for metastases from breast cancer. J Surg Oncol 2008;97:25–9.
[31] Lubrano J, Roman H, Tarrab S, et al. Liver resection for breast cancer metastasis: does it improve survival? Surg Today 2008;38:293–9.
[32] Vlastos G, Smith D, Singletary E, Mirza N, Tuttle T, Popat R, et al. Long term survival after an aggressive surgical approach in patients with breast cancer hepatic metastases. Ann Surg Oncol 2004;11:869–74.
[33] Wyld L, Gutteridge E, Pinder SE, et al. Prognostic factors for patients with hepatic metastases from breast cancer. Br J Cancer 2003;89:284–90.

ELSEVIER

BRACHYTHERAPY

Brachytherapy 18 (2019) 63–70

Gastrointestinal Oncology

Treatment of metastatic, imatinib refractory, gastrointestinal stroma tumor with image-guided high-dose-rate interstitial brachytherapy

Jazan Omari[1], Ralph Drewes[1,*], Manig Matthias[1], Konrad Mohnike[2], Max Seidensticker[3], Ricarda Seidensticker[3], Tina Streitparth[3], Jens Ricke[3], Maciej Powerski[1], Maciej Pech[1,4]

[1]*Department of Radiology and Nuclear Medicine, Otto-von-Guericke University, Magdeburg, Germany*
[2]*Diagnostisch Therapeutische Zentrum (DTZ), Berlin, Germany*
[3]*Klinik und Poliklinik für Radiologie, Klinikum der Universität München, München, Germany*
[4]*2nd Department of Radiology, Medical University of Gdansk, Gdansk, Poland*

ABSTRACT

PURPOSE: Evaluation of efficacy and safety of CT- or MRI-guided high-dose-rate interstitial brachytherapy (iBT) in the treatment of advanced, imatinib refractory, metastatic gastrointestinal stroma tumors (GISTs) was the objective of this retrospective study.

METHODS AND MATERIALS: A cumulative number of 40 unresectable metastases (30 hepatic, 10 peritoneal) were treated with iBT in 10 selected patients with histologically proven GISTs. Six patients had peritoneal disease, and 5 patients were even progressing under sunitinib (second line)—thus iBT was applied as a salvage maneuver. IBT uses an interstitially introduced ^{192}iridium source in a high-dose-rate irradiation regime to destroy vital cells in a single fraction. Response to treatment was assessed clinically and with acquisition of MRI/CT every 3 months.

RESULTS: Local tumor control was reached in 97.5% of all treated metastases during a median time of 25 months—only one local relapse was observed during followup. The median diameter of the irradiated lesions was 2.4 cm (range 0.6–11.2 cm); a median dose of 15 Gy (range 6.7–21.96 Gy) was applied. The median progression-free survival after iBT was 6.8 (range 3.0–20.2) months; the median overall survival was 37.3 months (range 11.4–89.7). Two major complications (Common Terminology for Adverse Events grade 3) occurred following the intervention: local hemorrhage and pneumothorax, successfully dealt with by angiographic embolization and pleural drainage, respectively.

CONCLUSIONS: In selected patients with metastatic, imatinib refractory GISTs, iBT safely enables high rates of local tumor control and presents an alternative, anti-neoplastic treatment option even in a salvage situation.

Keywords: GIST; Interstitial brachytherapy; Local ablation; Local tumor control; Salvage; TKI resistance

Introduction

Gastrointestinal stroma tumors (GISTs) are the most common type of mesenchymal tumors in the gastrointestinal tract with a yearly incidence of 1–2/100000 and account for 1–3% of all GI tract neoplasms, following gastric and colorectal cancer (1). GISTs arise from the interstitial cells of Cajal in the lamina muscularis mucosae, which physiologically function as pacemakers of the gastrointestinal motility. Reported incidences of distant metastases from GISTs ranges between 23% and 47%, thereof 20–60% in the liver; 50% of these patients have peritoneal disease (2,3). About 15–20% of patients with GIST have metastatic disease at diagnosis.

Overactivation or gain-of-function mutations in the KIT and PDGFRA genes, which code for tyrosine kinase receptors, are responsible for proliferation and survival of GIST tumor cells. According to a gene analysis study, KIT mutations occur in 75–80% and PDGFRA mutations in 7% of patients (4). GISTs without the aforementioned mutations are referred to as wild-type malignancies and account for

Received 2 July 2018; received in revised form 12 September 2018; accepted 25 September 2018.

Conflict of interest: No author has any conflict of interest to declare.

* Corresponding author. Department of Radiology and Nuclear Medicine, Otto-von-Guericke University, Leipziger Strasse 44, 9120 Magdeburg, Germany. Tel.: +49 391 6713030; fax: +49 391 6713029.

E-mail address: ralph.drewes@med.ovgu.de (R. Drewes).

1538-4721/$ - see front matter
https://doi.org/10.1016/j.brachy.2018.09.006

about 15% of these tumors. Since its introduction, the tyrosine kinase inhibitor (TKI) imatinib serves as the backbone of metastatic GIST therapy—up to 80% of patients show an initial response to treatment (5,6). Mutations of a KIT exon 11 have been demonstrated to be associated with better progression free survival (PFS) and overall survival (OS) than mutations of KIT exon nine or wild-type GISTs. (7) KIT exon nine mutations have been identified as the most important adverse prognostic factor for risk of progression and death. (7) Resistance to imatinib is often a result of secondary gene mutations, developed typically 18–24 months after initial successful systemic therapy in more than 50% of all cases. Therefore, the median time of recurrence is around 2 years. Primary TKI resistance is defined as the evidence of disease progression during the first 6 months of imatinib treatment, and secondary resistance is defined as tumor progression after 6 months of initial tumor response or stable disease. Before treatment with TKI agents, the prognosis for patients with metastatic GIST was poor with a median overall survival of less than 2 years (8). The OS for limited metastatic GISTs under imatinib treatment has been described in different trials; a median overall survival of 57, 53, and 45 months was reported in three studies (9).

Although international guidelines currently do not primarily recommend a surgical approach for extensive metastatic GISTs, the combination of systemic therapy (Imatinib) with metastasis resection shows a tendency to prolong survival in highly selected patients. (10) In cases of limited metastatic disease, guidelines suggest treatment of progressing lesions with resection or ablation while continuing systemic TKI treatment. (7) However, evidence based on prospective, randomized trials with unselected patients is still lacking. Besides, few patients are prospects for surgery because of tumor dissemination or general condition/comorbidities.

Radiofrequency ablation (RFA), either intraoperative or transcutaneous, is an alternative method to achieve tumor control, which had been applied to other tumor entities and was evaluated for patients with hepatic GIST metastases by a few reports with a low number of patients. (2,11,12).

An alternative local ablative measure to RFA is interstitial brachytherapy (iBT), which is based on the application of internal radiation in contrast to thermal ablation methods like RFA. IBT employs ^{192}Iridium, a highly active, gamma-radiation emitting radionuclide, which is transiently installed inside the target lesion. CT- or MRI-guided iBT has been proven to be a safe and effective procedure to treat primary or secondary liver and extrahepatic tumor entities by several investigators in the past. (13–16).

To our knowledge, no study has assessed the efficacy of image-guided high-dose-rate (HDR) iBT in the treatment of metastatic GISTs. The purpose of this retrospective study was to evaluate safety and efficacy of iBT application for the treatment of metastatic GISTs in a collective of 10 patients with 40 GIST metastases.

Methods and materials

Patient characteristics

Ten patients with histologically proven GISTs and a cumulative number of 40 unresectable metastases received treatment with iBT in our department between August 2009 and February 2016 and were enrolled in our retrospective study. Every patient was in a metastatic and progressive stage of disease at the time of referral to our department. Our study was approved by the local ethics committee.

Study design and eligibility criteria

Local tumor control (LTC) was the primary endpoint of this retrospective study; overall safety of iBT was the secondary endpoint.

Each individual patient's case with GIST was discussed at an interdisciplinary board of oncologists, interventional radiologists, and visceral surgeons who determined the indication for iBT for each patient individually.

The inclusion criteria were (1) resection impossible or unfavorable because of risk or (in case of liver metastases) loss of liver function, (2) patient unwilling to undergo surgery, (3) oligometastatic/controllable disease extent ($\leq$5 metastatic lesions on initial investigation), and (4) adequate coagulation parameters (thrombocytes $>$ 50000/nl, prothrombin $>$50%, partial thromboplastin time $<$ 50 s). Exclusion criteria were correspondingly (1) lack of consent and (2) uncontrollable tumor spread.

Interventional technique and irradiation

Preliminaries

Before the local ablation procedure took place, a whole-body contrast enhanced CT, and in case of hepatic tumor involvement, a Gb-EOB-DTPA–enhanced MRI (Primovist, Bayer Pharma, Leverkusen, Germany) was acquired for staging and treatment planning purposes. Laboratory parameters and physical status were checked preintervention with iBT.

Procedure

In a first step, local anesthesia (lidocaine) as well as intravenous analgesia (fentanyl) and sedation (midazolam) were administered, adapted to the individual weight, discomfort, and pain level of each patient. In the next step, the target lesions were punctured using an 18-gauge needle under CT-fluoroscopic guidance (Toshiba, Aquilion, Japan) or real time 1.0 T MRI (Panorama 1.0 T, open MR system, Philips Healthcare). After this, a flexible 6-french catheter sheath (Radifocus, Terumo, Tokyo, Japan) was placed applying the Seldinger's technique over a stiff angiography guidewire (Amplatz, Boston Scientific, Marlborough, USA). In a last step, the 6-french afterloading catheter (Afterloadingkatheter, Primed Medizintechnik Gmbh,

Halberstadt, Germany) was introduced, and the extracorporal catheter ending transiently fixated to the skin with a cutaneous suture and sterile bandages. The angulation and number of catheters were determined individually in consideration of organs at risk in close proximity and target lesion size. Finally, to confirm correct catheter positioning and to plan the following irradiation, a CT scan in breath-holding technique or a gadolinium-enhanced MRI was acquired. The clinical target volume (CTV) and the adjacent organs at risk (e.g. gastrointestinal tract) were highlighted by the interventional radiologist in every CT or MRI slice.

Irradiation design and dosimetric analysis

Design

Detailed and individual treatment strategy was planned using the acquired data set and the software system Oncentra (Nucletron, Elekta Ab, Stockholm, Sweden), an integral part of the HDR-afterloading system. The three-dimensional coordinates (x, y, z) of each inserted catheter's tip and exit at the tumor margin were determined and transferred into the treatment planning system. The calculated isodose lines were controlled in every slice and if necessary adjusted depending on the target lesion margins. Each target lesion's boundary was established individually for every inserted catheter. An example of the interventional technique is illustrated in Fig. 1.

Irradiation

The HDR brachytherapy/afterloading system (Nucletron, Elekta Ab, Stockholm, Sweden) applied an ^{192}Iridium source with a nominal activity of 10 Ci or 370 GBq, which was administered as a single fraction irradiation. The applied reference dose of 12 Gy was defined as the anticipated minimum dose to enclose the target lesion entirely and was installed in a single fraction. Even higher doses were possible and certain at the tumor center. A security margin of 5 mm surrounding the target lesion defining the CTV was incorporated to prevent new peripheral tumor incidences. Before radiation planning, the inserted brachytherapy catheters are fixated to the skin; hence, they maintain position and stay intratumoral even during body movement or respiration; therefore, in this case, PTV is equal to CTV. Organs at risk, such as the proximal gastrointestinal tract (empiric dose $<$ 14 Gy/mL), (17) in close proximity to the target lesions were taken into consideration and the irradiation dose correspondingly adjusted.

Catheter removal

Finally, after the irradiation was completed, the catheters were removed, and the punctures sites sealed by insertion of gelfoam or injection of fibrin tissue glue. Patients stayed

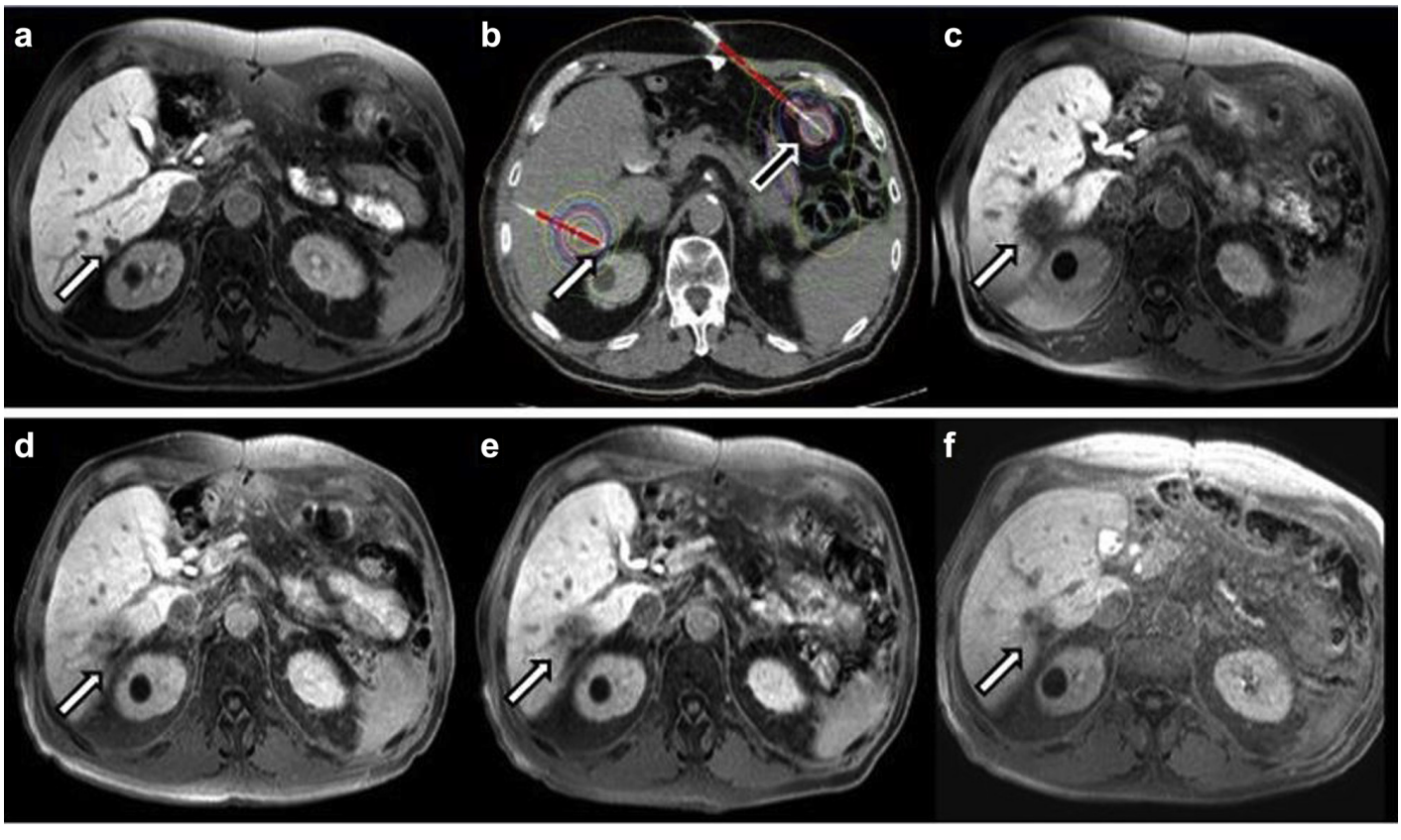

Fig. 1. (a): Baseline Gd-EOB-DTPA enhanced T1w MRI. White arrow indicates gastrointestinal stroma tumor metastasis in liver segment 6. (b) Demonstrates inserted brachytherapy catheters in the liver lesion (white arrow) and in a second extrahepatic peritoneal lesion (black arrow). Lines represent isodoses with red line showing 12 Gy. (c–f): Followup and local control documentation of hepatic lesion 3 (c), 6 (d), 9 (e), and 30 (f) months after iBT. Note the Gd-EOB-DTPA enhancement defect (dark rim around lesion) after iBT in (c) and recovery in (d-f). (For interpretation of the references to color in this figure legend, the reader is referred to the Web version of this article.)

in our postinterventional observation unit for a short period of time before transfer to the ward.

Followup

Schedule

Evaluation of response to iBT treatment was done every 3 months after local ablation procedure; a contrast-enhanced whole-body CT and a Gb-EOB-DTPA–enhanced liver MRI in case of liver involvement as well as a clinical and laboratory checkup were performed.

Adverse events

Potential adverse events associated with the local therapy were recorded and defined corresponding to the "Common Terminology for Adverse Events" (CTCAE) version 4.03 and according to the guidelines of the Society of Interventional Radiology (18).

Definitions of local tumor control rates (primary endpoint) and remission criteria

Definition

LTC after brachytherapy was defined corresponding to the Choi Criteria for GISTs categories as stable disease, partial remission, and complete remission. An increase in diameter >20% during followup was deemed to be progressive disease.

Pitfalls

Assessment of tumor response in routine followup examinations had to be done meticulously because of two crucial factors: (1) radiation hepatitis can often mimic tumor growth, (2) GIST metastases not only change in size but also in density; a typical described progression pattern addressed in the Choi criteria is a lesion becoming partially hyperdense ("nodule within the mass").

Statistical methods

The study was retrospective. Local tumor control as primary endpoint and OS as well as progression-free survival were calculated (from the time of each patient's first local therapy) by employment of the Kaplan–Meier method with SPSS version 22 (SPSS, version 22.0, SPSS, Chicago, Illinois). The secondary endpoint, safety, was evaluated descriptively.

Results

Ten patients with histologically proven GISTs were treated with iBT in our institution between August 2009 and February 2016. The median patient age at the time of diagnosis was 58.5 (range 37–68) years with a male to female ratio of 9:1 (Table 1).

The primary GIST site was six in the stomach, three in the small intestines, and one in the rectum. The mutational status of our patients is unknown; no genetic analysis has been performed. Eight patients had resection of the primary before referral to our institute. Recurrence operation, partial hepatectomy, and whipple operation were performed in 1 patient each. Before the local treatment, every patient underwent the first line therapy with imatinib. Five patients

Table 1
Patient characteristics

Total number of patients	10
Patient sex	
Men	9
Women	1
Age at time of diagnosis	
Median	58.5
Range	37–68
Primary tumor localization	
Stomach	6
Small intestines	3
Rectum	1
Metastases (cumulative)	
Liver	30
Peritoneal	10
Metastases timeframe	
Metachronous	6
Synchronous	4
Lesion size (cm)	
Median	2.4 (Q_1 = 1.5, Q_3 = 3.7)
Range	0.6–11.2
Irradiation dose (iBT) (Gy)	
Median	15.0 (Q_1 = 12.2, Q_3 = 16.4)
Range	6.7–22.0
Irradiation time (iBT) (min)	
Median	28.5 (Q_1 = 17.5, Q_3 = 40.3)
Range	2.3–69.3
Number of catheters/lesion	
Median	1
Range	1–11
Local tumor control (LTC)	39/40 (97.5%)
Median time (month)	25
Followup time (month)	
Median	24.6 (Q_1 = 7.9, Q_3 = 41.1)
Range	2.3–92.9
Time to progression (month)	
Median	6.8 (Q_1 = 5.5, Q_3 = 8.0)
Range	3.0–20.2
Overall survival after iBT (month)	
Median	37.3 (Q_1 = 20.6, Q_3 = 47.3)
Range	11.4–89.7
OS from time of diagnosis (month)	
Median	107 (Q_1 = 65.8, Q_3 = 160.3)
Range	41–203
Previous treatment (before iBT)	
First line (Imatinib)	10 (100%)
Second line (Sunitinib)	5 (50%)
Resection	8 (80%)
iBT image guidance	
CT	34
MRI	6
Time of hospitalization (days)	
Median	4
Range	3–6

received second line therapy with sunitinib. TKI systemic therapy was continued in 7 patients after the local therapy and before disease progression.

Treatment characteristics

The locations of GIST metastases were as follows: 30 hepatic and 10 peritoneal. Most patients' metastases were treated in several iBT sessions (an overview is given in table 2). The median target lesion diameter was 2.4 cm (range 0.6–11.2). CT guidance was used in 34 interventions, and MRI guidance was used in 6. A median of one (n = 1) catheter was placed into each tumor (range 1–11 catheters). The prescribed minimal tumor reference dose was 12 Gy. In some cases, the nominal dose had to be adjusted because of tumor size or proximity of organs at risk, which led to a median applied dose of 15.0 (range 6.7–22.0 Gy). Total irradiation time varied between 2.3 and 69.3 min with a median of 28.5 min. The time of hospitalization ranged from 3 to 6 days with a median of 4 days. Two patients experienced a major adverse event (CTCAE grade 3): local hepatic hemorrhage, which was dealt with successfully by embolization in digital subtraction angiography and prolonged hospitalization (4 days); pneumothorax, which required a pleural drain. The location of the treated tumor in the single case of pneumothorax was liver segment VIII, and because of the pericapsular locus, a needle forerun was needed to minimize the risk of potential liver hematoma. Furthermore, the access was impeded by a deep sulcus/recessus, which was punctured during catheter placement resulting in a pneumothorax.

Elevated inflammatory parameters (CTCAE grade 1) were observed in 3 patients, who consequently received postinterventional antibiotics; no sign of abscess or any other focus in imaging or followup examinations was seen. One patient was given antibiotics as a precaution; no sign of infection was detected after iBT.

Local tumor control, overall survival, progression-free survival

LTC was achieved in 97.5% of all treated lesions over a median time of 25 months in the Kaplan–Meier analysis; only one relapse was noticed during followup (Fig. 2). The median progression-free survival was 6.8 (range 3.0–20.2) months (Fig. 3), and the median overall survival 37.3 (range 11.4–89.7) months (Fig. 4). The current OS status of all patients with GIST in the collective: 6 dead and 4 alive.

Table 2
iBT intervention overview

Patient	Number of iBT interventions	Treated metastases	Time interval between iBTs (months)
1	2	1/2	10
2	3	1/1/1	8/4
3	2	1/2	9
4	3	1/1/1	0,5/1
5	2	1/3	0,5
6	6	3/1/2/2/3/2	22/17/15/15/0,5
7	1	1	-
8	2	1/1	7
9	2	1/3	4
10	2	2/1	1

Discussion

The treatment of metastatic GISTs remains challenging to this date, especially in the case of hepatic involvement or peritoneal disease, which are the most common sites of relapse occurrences (19). International guidelines like European Society for Medical Oncology and National Comprehensive Cancer Network (NCCN) from 2018 differentiate between widespread and limited progressive disease. (7,20) TKI dose escalation and change of therapeutic regimen (second line) with an imaging followup to reassess treatment response and evaluate further options are recommended for widespread progression. However, for metastatic GISTs that show limited disease progression, a more aggressive approach is suggested (NCCN, European Society for Medical Oncology); TKI should be continued, and progressing lesions should be considered for treatment with resection, RFA, or (chemo) embolization. In the case of even further disease progression despite imatinib or sunitinib, regorafenib treatment or other options like antineoplastic agents or clinical trials can be attempted.

The role of surgery in metastatic or recurrent disease is controversial, and meticulous case selection is crucial. The potential benefit is difficult to anticipate and quantify. Raut *et al.*, some of the first investigators to publish results of surgically treated metastatic GISTs in the imatinib era,

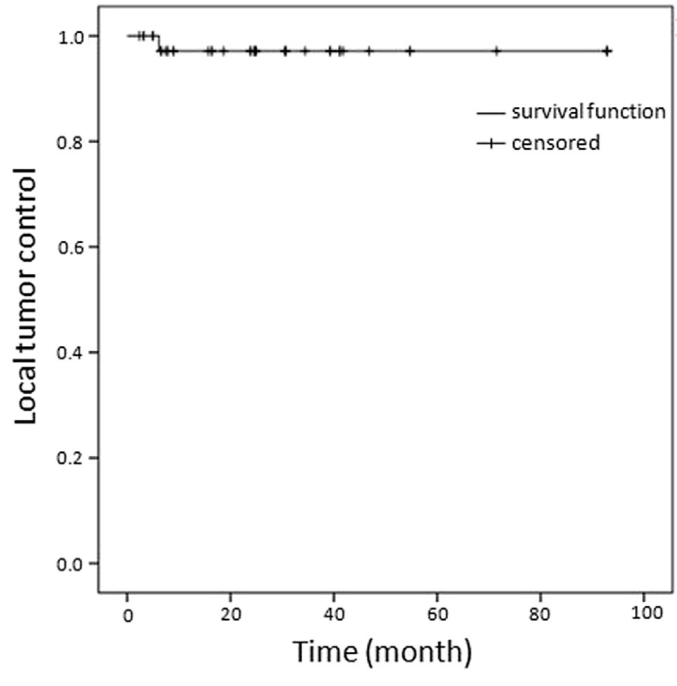

Fig. 2. Local tumor control after iBT of gastrointestinal stroma tumor metastases.

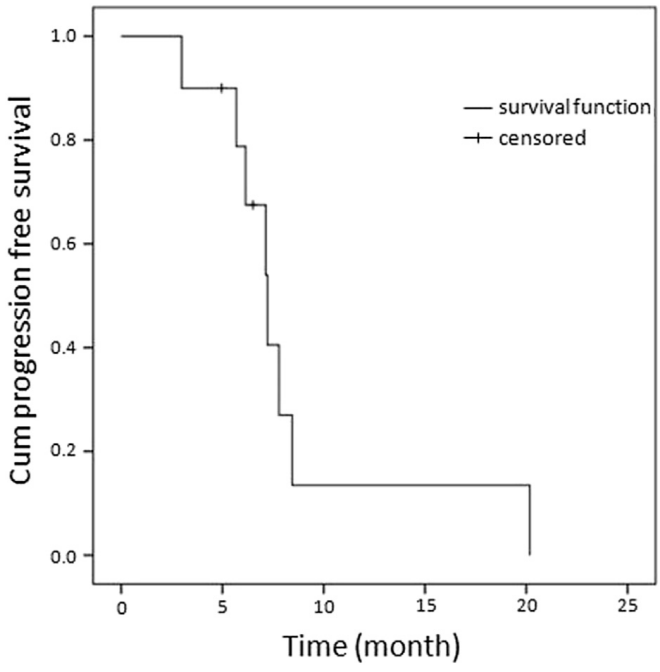

Fig. 3. Progression-free survival (calculated from the time of iBT) of patients with metastatic gastrointestinal stroma tumor after treatment with iBT.

reported an OS of 29.8 months and a median PFS of 7.7 months for patients with limited disease progression (n = 32). (21) Similar, subsequent, retrospective studies confirmed those observations. The EORTC-STBSG collaborative study (n = 239), the largest series of patients treated at high-volume centers in Europe, with different disease extent patients groups reported a median OS of 1.5 years from time of metastasectomy in the patient group progressing at the time of surgery (22).

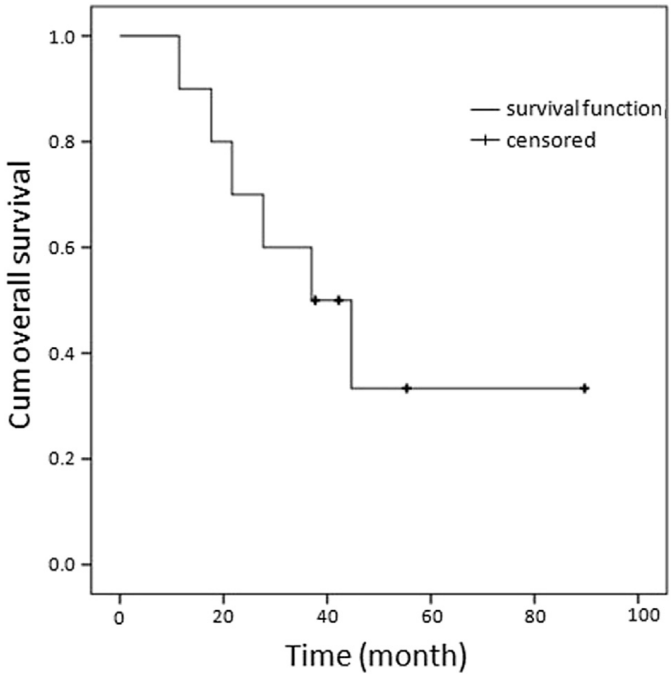

Fig. 4. Graph shows overall survival (calculated from the time of iBT) of patients with metastatic gastrointestinal stroma tumor ablated with iBT.

If complete resection is not feasible, one main goal and indication of either local ablation or surgery in a limited progression setting refractory to imatinib is to minimize tumor clone selection with secondary mutations, which otherwise cements TKI resistance and consequently hinders further systemic treatment. The greater the number of tumor cells exposed to TKI treatment and the higher the tumor growth rate (mitotic counts), the higher the chance of molecular evolution and secondary TKI resistance. Secondary TKI resistance following tumor clone outgrowth and selection is one of the major difficulties in metastatic GIST treatment. Xia et al. came to the conclusion that patients with poor imatinib response show improved survival after resection of liver metastases and reported a 3-year survival rate of 89.5%, indicating a benefit of cytoreduction. (23) However, intra-/perioperative tumor rupture bears a considerable risk of tumor cell spillage into the peritoneal cavity and consecutive potential for development of peritoneal carcinomatosis. Furthermore, the NCCN guidelines point out that incomplete resections (R1 or even R2) are frequent and complication rates are high; therefore, careful selection of eligible patients is advised. Finally, the lack of any randomized, prospective data precludes an unequivocal or general recommendation for surgery.

Local ablation therapy, however, presents a promising and alternative treatment option, applicable as a standalone measure or combined with surgery. In the study by Sun Yoon *et al.,* combined intraoperative RFA with surgery in highly selected patients, resecting large lesions and carefully ablating smaller ones to preserve as much liver function as possible; (19) 24 patients were treated with intraoperative RFA; 5-year OS rate of 87.7% and two major complications (biliary stricture and hepatic abscess) were reported. The high survival and low recurrence rates of that study have been attributed to the highly selected patient cohort: RFA inclusion criteria with a tumor size <3 cm, an exact intraoperative positioning and the pre and postoperative imatinib therapy. Pawlik *et al.* treated metastatic GISTs with intraoperative radiofrequency ablation and reported a median OS of 47.2 months. (24).

In contrast to RFA, the application of iBT to metastatic GISTs as an internal, high-dose single fraction radiation method has not been explored so far. IBT has been tested and validated on different primary and secondary liver tumor entities by few researchers in the past (13,15,16). Liver malignancies originating from hepatocellular carcinoma and colorectal cancer were some of the first entities treated with iBT; local tumor control rates of 95% and 88% after 12 months were reported.

Corresponding to these figures, the results of our study (Figs. 2–4, Table 1) demonstrate a high local tumor control rate of 97.5% over a median time of 25 months, a mOS of 37 months, and a PFS of 6.8 months (calculated after iBT) for our patients despite being in an advanced, progressive stage. Median OS from the time of GIST diagnosis was 107 months; at that time 4 patients already had synchronous

metastases. Half of our patients were even progressing while receiving second line therapy (sunitinib) and 6 of 10 patients had peritoneal disease; thus iBT was applied as a salvage maneuver with the intention to delay further progression. Demetri *et al.* demonstrated in a randomized controlled trial that the median PFS for patients with imatinib-refractory metastatic GISTs treated with sunitinib is 24.6 weeks. (25) In summary, taking the salvage situation of our patient collective into consideration, the OS and PFS results are at least similar or even better than those of comparable surgical or RFA data.

In contrast to the rather conventional, external fractionated EBRT, whose role is currently limited to rare cases of GIST bone metastasis according to guidelines, brachytherapy applies a highly active ^{192}Iridium radionuclide to metastatic lesions internally. It decays by emitting gamma (γ) radiation at an activity of around 10 Ci or 370 GBq. Commonly known restrictions of thermal ablation measures like RFA do not apply to brachytherapy. There are no general limits to tumor size, no cooling effects from nearby vessels, and fewer restrictions concerning adjacent risk structures. The issue of potential needle-track metastasis was addressed specifically by radiation of the interventional access as a precaution.

The occurrence and severity of peri and postinterventional complications were low. Two major adverse events (Grade 3), a local hepatic hemorrhage treated with embolization and a pneumothorax requiring a pleural drain, were recorded. Time of hospitalization was not overly prolonged in these cases; both patients stayed in our ward for 4 days. According to literature, major adverse events (Grade 3 and 4) after iBT are observed in 3% of cases and are usually dealt with by angiographic embolization in case of active hemorrhage. (26,27) In comparison, a prospective cohort study, where cytoreductive surgery was performed on patients with sunitinib therapy, 15% of patients experienced a major complication (Grade III). (28).

Short term, postinterventional hospitalization was a safety precaution to monitor potential and occult hemorrhage or other side effects. Patients could usually be discharged after 48 h.

TKI therapy after iBT was discontinued in 3 patients for unknown reasons. Besides, duration of TKI administration after local therapy is also unknown in our patient collective. Early TKI cancellation at any given time is known to bear a high risk of recurrences and certainly has a significant impact on PFS and OS. (29).

Limitations of this study, equal to other data assessing different therapeutic options for metastatic GISTs, are the low patient number and the retrospective nature. The lack of genetic analysis and therefore missing mutational status was considered another limitation. However, recent research indicates that, contrary to general expectation, mutational status does not have a significant prognostic influence concerning a surgical or local ablative approach; (30) cytoreduction through surgery or ablation is assumed to have a countering effect on the negative impact of KIT exon nine mutations. Nevertheless, the potential gain of cytoreduction for TKI refractory patients is still far from understood.

There is an urgent need for a prospective randomized trial with a large patient collective and a control group to validate promising therapeutic options for metastatic GISTs like brachytherapy.

The success of local ablation methods in selected patients in general should be considered an incentive for wider application. Patients with metastatic GIST, especially those who are not eligible for extensive surgery, might benefit particularly not only because of direct cytoreduction but also because of lower risk of tumor clone selection and development of secondary TKI resistance.

Conclusion

The results of our study confirm the overall safety of the image-guided HDR iBT procedure. This local ablation method enables excellent rates of local tumor control for metastatic GIST lesions—even in a salvage situation—and indicates prolonged survival in selected patients ineligible for surgery.

References

[1] Joensuu H, Fletcher C, Dimitrijevic S, *et al*. Management of malignant gastrointestinal stromal tumours. *Lancet Oncol* 2002;3:655–664.

[2] Yamanaka T, Takaki H, Nakatsuka A, *et al*. Radiofrequency ablation for liver metastasis from gastrointestinal stromal tumor. *J Vasc Interv Radiol* 2013;24:341–346.

[3] Unalp HR, Derici H, Kamer E, *et al*. Gastrointestinal stromal tumours: outcomes of surgical management and analysis of prognostic variables. *Can J Surg* 2009;52:31–38.

[4] Corless CL, Schroeder A, Griffith D, *et al*. PDGFRA mutations in gastrointestinal stromal tumors: frequency, spectrum and in vitro sensitivity to imatinib. *J Clin Oncol* 2005;23:5357–5364.

[5] Verweij J, Casali PG, Zalcberg J, *et al*. Progression-free survival in gastrointestinal stromal tumours with high-dose imatinib: randomised trial. *Lancet* 2004;364:1127–1134.

[6] An HJ, Ryu M-H, Ryoo B-Y, *et al*. The effects of surgical cytoreduction prior to imatinib therapy on the prognosis of patients with advanced GIST. *Ann Surg Oncol* 2013;20:4212–4218.

[7] von Mehren M, Randall RL, Benjamin RS, *et al*. Soft tissue sarcoma, version 2.2018, NCCN clinical practice guidelines in oncology. *J Natl Compr Canc Netw* 2018;16:536–563.

[8] Dematteo RP, Heinrich MC, El-Rifai WM, *et al*. Clinical management of gastrointestinal stromal tumors: before and after STI-571. *Hum Pathol* 2002;33:466–477.

[9] Call J, Walentas CD, Eickhoff JC, *et al*. Survival of gastrointestinal stromal tumor patients in the imatinib era: life raft group observational registry. *BMC Cancer* 2012;12:90.

[10] Shi Y-N, Li Y, Wang L-P, *et al*. Gastrointestinal stromal tumor (GIST) with liver metastases: an 18-year experience from the GIST cooperation group in North China. *Medicine (Baltimore)* 2017;96:e8240.

[11] Dileo P, Randhawa R, Vansonnenberg E, *et al*. Safety and efficacy of percutaneous radio-frequency ablation (RFA) in patients (pts) with metastatic gastrointestinal stromal tumor (GIST) with clonal

evolution of lesions refractory to imatinib mesylate (IM). *J Clin Oncol* 2004;22:9024.

[12] Jones RL, McCall J, Adam A, *et al*. Radiofrequency ablation is a feasible therapeutic option in the multi modality management of sarcoma. *Eur J Surg Oncol* 2010;36:477−482.

[13] Ricke J, Wust P, Wieners G, *et al*. Liver malignancies: CT-guided interstitial brachytherapy in patients with unfavorable lesions for thermal ablation. *J Vasc Interv Radiol* 2004;15:1279−1286.

[14] Lüdemann L, Wybranski C, Seidensticker M, *et al*. In vivo assessment of catheter positioning accuracy and prolonged irradiation time on liver tolerance dose after single-fraction 192Ir high-dose-rate brachytherapy. *Radiat Oncol* 2011;6:107.

[15] Tsalpatouros A, Baltas D, Kolotas C, *et al*. CT-based software for 3-D localization and reconstruction in stepping source brachytherapy. *IEEE Trans Inf Technol Biomed* 1997;1:229−242.

[16] Collettini F, Poellinger A, Schnapauff D, *et al*. CT-guided high-dose-rate brachytherapy of metachronous ovarian cancer metastasis to the liver: initial experience. *Anticancer Res* 2011;31:2597−2602.

[17] Streitparth F, Pech M, Böhmig M, *et al*. In vivo assessment of the gastric mucosal tolerance dose after single fraction, small volume irradiation of liver malignancies by computed tomography-guided, high-dose-rate brachytherapy. *Int J Radiat Oncol Biol Phys* 2006; 65:1479−1486.

[18] Ahmed M, Solbiati L, Brace CL, *et al*. Image-guided tumor ablation: standardization of terminology and reporting criteria–a 10-year update. *J Vasc Interv Radiol* 2014;25:1691−1705.e4.

[19] Yoon IS, Shin JH, Han K, *et al*. Ultrasound-guided intraoperative radiofrequency ablation and surgical resection for liver metastasis from malignant gastrointestinal stromal tumors. *Korean J Radiol* 2018;19: 54−62.

[20] Casali PG, Abecassis N, Bauer S, *et al*. Gastrointestinal stromal tumours: ESMO-EURACAN Clinical Practice Guidelines for diagnosis, treatment and follow-up. *Ann Oncol* 2018;29(Suppl 4):iv68−iv78.

[21] Raut CP, Posner M, Desai J, *et al*. Surgical management of advanced gastrointestinal stromal tumors after treatment with targeted systemic therapy using kinase inhibitors. *J Clin Oncol* 2006;24:2325−2331.

[22] Bauer S, Rutkowski P, Hohenberger P, *et al*. Long-term follow-up of patients with GIST undergoing metastasectomy in the era of imatinib – analysis of prognostic factors (EORTC-STBSG collaborative study). *Eur J Surg Oncol* 2014;40:412−419.

[23] Xia L, Zhang M-M, Ji L, *et al*. Resection combined with imatinib therapy for liver metastases of gastrointestinal stromal tumors. *Surg Today* 2010;40:936−942.

[24] Pawlik TM, Vauthey J-N, Abdalla EK, *et al*. Results of a single-center experience with resection and ablation for sarcoma metastatic to the liver. *Arch Surg* 2006;141:537−543. discussion 543-544.

[25] Demetri GD, van Oosterom AT, Garrett CR, *et al*. Efficacy and safety of sunitinib in patients with advanced gastrointestinal stromal tumour after failure of imatinib: a randomised controlled trial. *Lancet* 2006; 368:1329−1338.

[26] Bretschneider T, Ricke J, Gebauer B, *et al*. Image-guided high-dose-rate brachytherapy of malignancies in various inner organs - technique, indications, and perspectives. *J Contemp Brachytherapy* 2016;8:251−261.

[27] Mohnike K, Neumann K, Hass P, *et al*. Radioablation of adrenal gland malignomas with interstitial high-dose-rate brachytherapy : efficacy and outcome. *Strahlenther Onkol* 2017;193:612−619.

[28] Yeh C-N, Wang S-Y, Tsai C-Y, *et al*. Surgical management of patients with progressing metastatic gastrointestinal stromal tumors receiving sunitinib treatment: a prospective cohort study. *Int J Surg* 2017;39:30−36.

[29] The ESMO/European Sarcoma Network Working Group. Gastrointestinal stromal tumours: ESMO Clinical Practice Guidelines for diagnosis, treatment and follow-up. *Ann Oncol* 2014;25:iii21−iii26.

[30] Ford SJ, Gronchi A. Indications for surgery in advanced/metastatic GIST. *Eur J Cancer* 2016;63:154−167.

Clinical Investigations

Original paper

Efficacy and safety of image-guided interstitial single fraction high-dose-rate brachytherapy in the management of metastatic malignant melanoma

Tina Bretschneider, MD[1], Konrad Mohnike, MD[1], Peter Hass, MD[2], Ricarda Seidensticker, MD[1], Daniela Göppner, MD[3], Prof. Oliver Dudeck[1], Florian Streitparth, MD[4], Prof. Jens Ricke[1]

[1]Department of Radiology and Nuclear Medicine, University of Magdeburg, [2]Department of Radiation Therapy, University of Magdeburg, [3]Department of Dermatology and Venerology, University of Magdeburg, [4]Department of Radiology, Charite, Humboldt-University, Berlin, Germany

Abstract

Purpose: Computed tomography (CT) or magnetic resonance imaging (MRI) guided brachytherapy provides high tumor control rates in hepatocellular carcinoma (HCC) and colorectal liver metastases. In contrast to thermal ablation methods such as radiofrequency ablation (RFA), much less restrictions apply with respect to tumor location or size. In this study, we determined the efficacy and safety of CT- or MRI-guided brachytherapy in metastatic melanoma.

Material and methods: Fifty-two metastases of malignant melanoma in 14 patients were included in this retrospective study. Local tumor control and safety were evaluated as primary and secondary endpoints. Furthermore, we evaluated overall survival and progression free survival. Tumor locations were liver (n = 31), lung (n = 15), adrenal (n = 3), lymph nodes (n = 2), and kidney (n = 1). Treatment planning was performed using three-dimensional CT or MRI data acquired after percutaneous applicator positioning under CT or open MRI guidance. Subsequently, single fraction high-dose-rate (HDR) brachytherapy was applied using a ^{192}Iridium source. Clinical and cross-sectional follow-up were performed every 3 months post intervention.

Results: The median diameter of treated lesions was 1.5 cm (range: 0.7-10 cm). Doses between 15 and 20 Gy were applied (median dose: 19.9 Gy). The mean irradiation time ranged between 7-45 minutes. After treatment, there was one patient with a cholangitis. After a median follow up of five months, the median local tumor control was 90%. The median overall survival of the patients was 8 months. The median progression free survival of the patients was 6 months.

Conclusion: Image-guided HDR brachytherapy is a safe and effective treatment procedure in metastatic malignant melanoma.

J Contemp Brachytherapy 2015; 7, 2: 154-160
DOI: 10.5114/jcb.2015.51095

Key words: brachytherapy, CT- and MRI-guided intervention, high-dose-rate, malignant melanoma, metastases.

Purpose

Patients with distant unresectable metastases of malignant melanoma have an impaired prognosis despite treatment strategies using combined chemotherapies or targeted drugs [1,2]. With distant metastases, median survival is 6-8 months with a 5-year survival rate of approximately 10% [2]. An important role in the treatment of advanced, unresectable metastases of malignant melanoma should be the reduction of clinical symptoms by reduction of the tumour volume, and therefore the improvement of quality of life. Due to the limited efficacy of systemic treatments, visceral, lung, or lymph node metastases may quickly become symptomatic despite being locally confined. At present, local treatment options such as surgery, or local tumour ablation do not play an important role because the evidence on their prognostic impact is rare. These treatment options currently are limited to highly selected patients. Patients with visceral metastases are considered to be less qualified for local treatments than patients displaying lung metastases only or in combination with metastatic lymph nodes [3-5]. Regarding local ablation techniques, thermal ablation such as radiofrequency ablation (RFA) is limited by a size restriction of 3-5 cm and a close proximity to risk organs [6,7]. Furthermore, a location near blood vessels decreases the effectivity of thermal ablation due to consecutive heat sink effects [6,7]. Beside percutaneous treatments like RFA, also transarterial chemoembolization (TACE) was analyzed in the treatment of liver metastases of melanoma [8].

Address for correspondence: Prof. Jens Ricke, Department of Radiology and Nuclear Medicine, University Otto-von-Guericke Magdeburg, Leipzigerstrasse 44, 39120 Magdeburg, Germany, phone: +49 39167 13030, fax: +49 39167 13029, e-mail: Jens.Ricke@med.ovgu.de

Received: 28.10.2014
Accepted: 26.01.2015
Published: 30.04.2015

Recently, computed tomography (CT)-guided brachytherapy has been introduced, which may overcome some of the aforementioned limitations. Whereas local tumour control in hepatocellular carcinoma (HCC) and colorectal carcinoma is > 90% after 1 year despite tumour sizes up to 15 cm, cooling effects or proximity to risk organs play no or just a minor role [9]. However, no data has been published evaluating the efficacy of high-dose-rate (HDR) brachytherapy on visceral or other malignant melanoma metastases. In this study described herein, we assessed safety and efficacy of image-guided HDR brachytherapy in patients with metastases of malignant melanoma.

Material and methods

Patient characteristics

Between February 2007 and April 2012, 14 patients with malignant melanoma with an overall amount of 52 unresectable metastases were included in this retrospective study. There were 37 visceral metastases, including 31 hepatic metastases, 4 lesions located in the adrenal gland and kidney, and 2 lymph node metastases. In addition, 15 pulmonary metastases were treated. No patient with pulmonary lesions had a history of previous lung surgery. All the patients who underwent lung treatments had a clinically fully compensated lung function. The patient population comprised 12 men and 2 women; the median age was 66 years (range: 50-81 years) (Table 1). All patients had been pretreated with systemic chemotherapy or chemo-immunological treatment. In detail, eight patients were pretreated with interferon alpha. After treatment with interferon alpha, six patients showed a progressive disease. Furthermore, one patient who was pretreated with interferon alpha finished the therapy because of side effects. Four patients were treated with Dacarbazine and three patients received Fotemustine. All patients displayed tumor progression at the time of referral to our institution for local treatment.

Study design and eligibility criteria

In this retrospective study, primary endpoint was the local tumor control and secondary endpoint was the safety of CT- or magnetic resonance imaging (MRI)-guided HDR brachytherapy. The indication for the HDR brachytherapy was determined for all patients in an interdisciplinary consensus of dermatologists, oncologists, visceral surgeons, and interventional radiologists. The inclusion criteria for performing image-guided brachytherapy were technically unresectable tumor due to its location or due to e.g. reduced liver function or low residual tissue, medical contraindication for resection or comorbidities, and denial of operation. In case of pulmonary lesions, we performed pulmonary function tests before the treatment to secure sufficient lung capacity. A Karnofsky Index ≥ 70% as well as appropriate coagulation parameters (thrombocytes > 100,000/nl, prothrombin > 50%, partial thromboplastin time < 50 s), and liver parameters (bilirubin < 30 µmol/l) qualified for the treatment. The administration of anticoagulants like coumarin derivatives and inhibitors of platelet aggregation were discontinued 7 days prior to intervention and changed to low-dose heparin if necessary. The exclusion criteria for performing brachytherapy were a diffuse uncontrollable tumor spread.

Interventional technique and irradiation

The detailed methodology of CT-guided brachytherapy has been described elsewhere [10]. In brief, placement of the brachytherapy applicators was performed under guidance of a Fluoroscopy-CT (Toshiba, Japan) (for metastasis with a diameter > 20 mm) or an open MRI at 1.0 T (Panorama HFO, Philips Healthcare, Best, The Netherlands) for smaller liver lesions (Fig. 1A-D). Thirty lesions were treated under CT guidance, twenty-two metastases under open MRI guidance. After adequate patient positioning, puncture of the lesion was performed employing an 18-gauge needle. An angiography sheath of 6 F diameter (Radiofocus, Terumo^{TM}, Tokyo, Japan) was inserted over a stiff angiography guide wire (Amplatz, Boston Scientific, Boston, USA). Finally, 16-gauge brachythera-

Table 1. Patient characteristics

	Value
Total number of patients	14
Sex	
Men	12
Women	2
Age (years)	
Median	66
Range	50-81
Metastases (*n*)	52
Hepatic	31
Pulmonary	15
Adrenal	3
Retroperitoneal lymph nodes	2
Kidney	1
Type of metastases (*n*)	
Synchronous	–
Metachronous	14
Tumor size (cm)	
Median	1.5
Range	0.7-10
Previous treatment	
Interferon alpha	7
Dacarbazin	4
Fotemustine	3
Median follow-up (month)	5

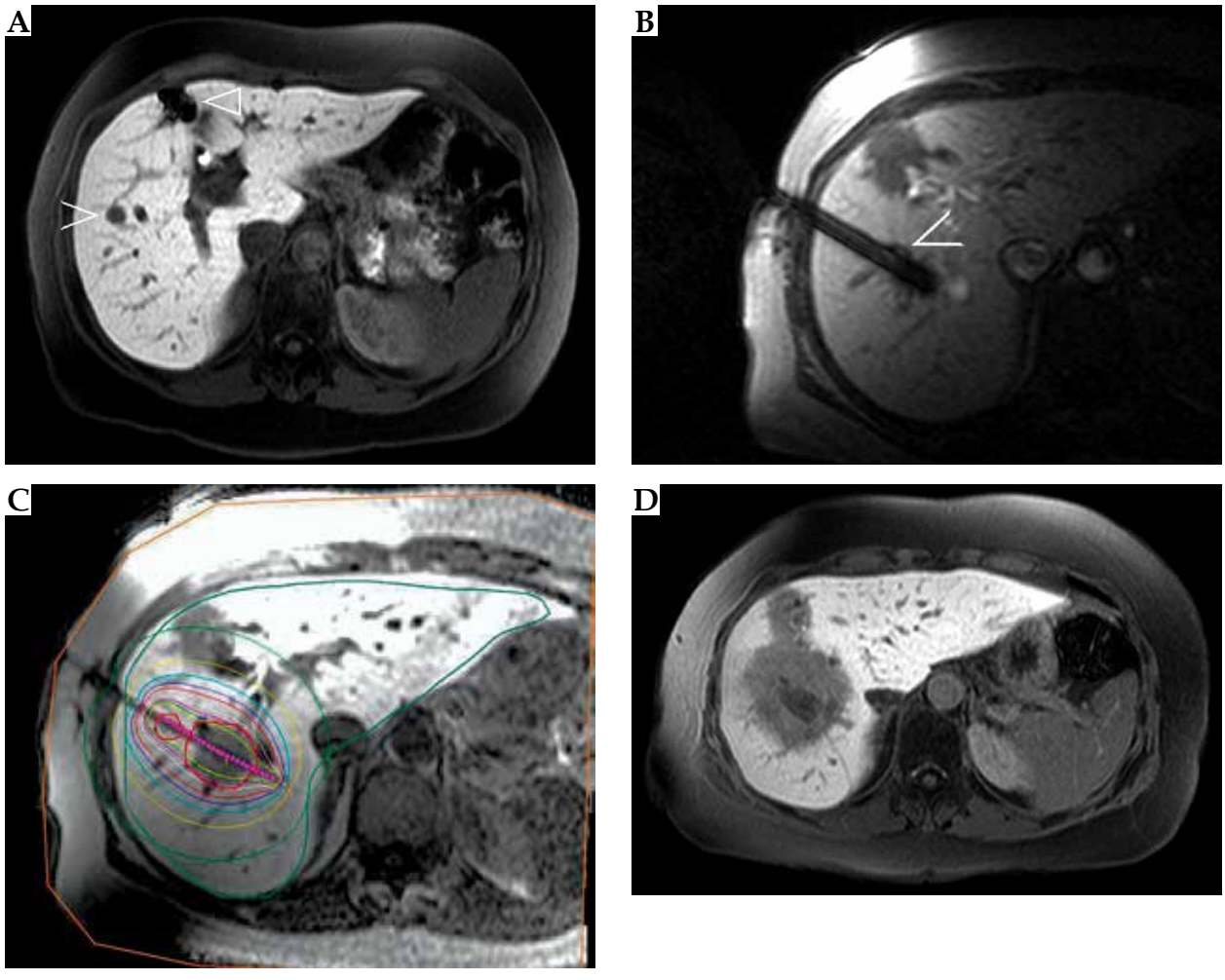

Fig. 1. Local tumor control in a 58-year-old female patient with histological proven malignant melanoma metastases. **A)** Preoperative axial contrast-enhanced liver magnetic resonance imaging (MRI) (liver specific contrast agent Gd-EOB-DTPA) shows two metastases in segment V in the right liver lobe (open arrow), former partial resection of the liver segment IV (outlined arrow). **B)** Both metastases were treated by open MRI high-dose-rate brachytherapy using one catheter. **C)** Treatment planning and dosimetric analysis, tumor encircling isodoses (red line indicates 20 Gy). **D)** Follow-up contrast-enhanced liver MRI at 3 months shows the shrinking ablation zone with local control of the treated lesions

py catheters (Nucletron, Elekta AB, Stockholm, Sweden) were placed in the sheaths. For treatment planning purposes, a contrast-enhanced CT in breathhold technique was acquired after placement of the catheters. The HDR afterloading system (Nucletron, Elekta AB, Stockholm, Sweden) used a ^{192}Iridium source of 10 Ci. The source diameter was < 1 mm. In mean 2 applicators were inserted (range 1-5).

Treatment planning and dosimetric analysis

Treatment planning was performed using the software system Oncentra (Nucletron, Elekta AB, Stockholm, Sweden) integrated in the HDR-afterloading system. Firstly, a careful delineation of the target volume was performed in every CT/MRI slice with the afterloading catheters in place. Secondly, the relative coordinates (x, y, z) of the catheters were determined, considering the tip and the exit at the margin of the tumor, and transferred into the planning system. The given boundary of the target was individually addressed for every catheter by specifying the distance to the reference point. A reference dose of 15-20 Gy was prescribed in our patients, which was by definition identical to the minimum dose enclosing the lesion, and applied as a single dose. The anatomic optimization routine of the planning software was employed with the specified set of reference points. Isodose lines relative to the target contours were controlled and matched slice by slice by varying input parameters of the planning system. We considered dose limitations in treatment planning for treated tumors adjacent to organs at risk (OAR), such as the gastric wall or duodenum for tumors in the left liver lobe (< 15 Gy/ml), or the spinal canal (10 Gy/ml) for treated retroperitoneal lymph node metastases, adrenal gland, or kidney.

All procedures were performed under local anesthesia. Midazolam and fentanyl *i.v.* were given for sedation and analgesia according to the individual discomfort level of each patient during the intervention. For catheter re-

trieval, gelfoam or fibrin tissue glue was injected through each brachytherapy sheath during removal.

Follow up and safety assessment

Clinical visits, supplemented by CT or MRI, were performed after 6 weeks and then every 3 months after treatment. We included standard laboratory tests. Therapy-related adverse events were defined according to the guidelines of the Society of Interventional Radiology (SIR) [11]. Liver toxicity after CT/MRI-guided HDR brachytherapy was assessed according to the definition of radiation-induced liver disease (RILD), characterized by the occurrence of ascites accompanied by elevated alkaline phosphatase levels or by a serum bilirubin level of ≥ 3 mg/dl, and ascites 1-2 months after HDR brachytherapy with an absence of tumor progression or bile duct obstruction [12]. There was no need for lung tests in the follow up period because no clinical symptoms were shown.

Definitions of remission criteria and local control rates

Local tumor control after CT or MRT-guided brachytherapy was defined according to RECIST 1.1 response criteria and classified either as stable disease (SD), partial (PR), or complete remission (CR) of the treated lesion. Any increase > 20% in diameter of a singular lesion was interpreted as progressive disease (PD). However, restrictions apply for lung and liver follow up. Since in both, lung and liver tissue adjacent to the target volume, focal radiation pneumonitis or radiation hepatitis may mimic tumor growth. For liver tumors, we therefore limited tumor measurements to hepatobiliary phase imaging > 20 min. post *i.v.* application of gadoxetic acid (Primovist®). For lung tumors, we measured tumor response not in comparison to the baseline, but to the first follow up examination in order to compensate for lung tissue alterations adjacent to the clinical target volume.

Statistical methods

All results were analyzed in a non-randomized and retrospective approach. To evaluate the local tumor control, the overall survival and the progression free survival statistical analysis was performed employing the Kaplan-Meier method with SPSS version 19 (SPSS, version 19.0; SPSS, Chicago, Illinois). The secondary endpoint safety was evaluated descriptively.

Results

Treatment characteristics

The median diameter of the metastases was 1.5 cm (range: 0.7-10 cm). There were 5 lesions with a maximum tumor diameter between 5 and 10 cm, which were treated with 5 or 6 catheters. Metastases with a maximum tumor diameter of 2 to 5 cm received 1 or 2 catheters depending on the geometrical position of the first catheter implanted, or depending on specifics of adjacent critical organs. Patients with tumor < 2 cm received a single applicator per lesion only. All lesions were treated once by a single fraction HDR brachytherapy. The prescribed minimal tumor dose (D_{100}) was 20 Gy. However, in some patients, the minimal dose had to be lowered to spare adjacent risk structures. The applied minimal doses inside the clinical target volume (CTV) ranged from 15 to 20 Gy (median dose D_{100}: 19.9 Gy). A complete coverage of the tumor with 20 Gy was applied in 15 pulmonary and 21 hepatic lesions. In the adrenal gland and in the retroperitoneum, a dose of 15 Gy was given. Total irradiation time ranged between 7 and 45 min. The mean hospital stay of the patients was 4 days (range: 3-13).

Adverse events

Three of fourteen patients (21%) showed slight side effects like sickness and emesis. One of the three patients had an allergic reaction, which was treated successfully with Fenestil® and Tagamet®. Five of fourteen patients (35%) described unspecific abdominal pain after the image-guided brachytherapy, in the ultrasound control no associated reasons could be found. The symptoms regressed spontaneously. We encountered no intraoperative bleeding complications. Two small pneumothoraces regressed spontaneously after the treatment of pulmonary metastases. One patient with a central liver metastasis developed cholangitis 3 weeks after HDR brachytherapy as well as abdominal pain in the right epigastrium and an increase of liver parameters. He was successfully treated with endoscopically guided stent implantation and *i.v.* antibiosis.

Local tumor control, overall survival, and progression free survival

According to Response Evaluation Criteria in Solid Tumors Criteria (RECIST 1.1), one of the treated lesions exhibited complete remission, 19 partial response, 30 treated metastases showed stable disease, and two progressive disease after a median follow up of five months (1-11 months). Local tumor control was 90% in the Kaplan-Meier analysis (Fig. 2). All patients showed a progressive disease elsewhere during the follow-up period. The median overall survival of the 14 patients with metastatic malignant melanoma after HDR brachytherapy was 8 months (Fig. 3). The median progression free survival (PFS) of the 14 patients was 6 months (Fig. 4).

Discussion

In metastatic malignant melanoma, tumor resection or image-guided ablation must be considered a palliative treatment option, not a curative approach. Due to macroscopically undetectable tumor spreading, progression free survival after these interventions is usually limited [4,5]. The effect of debulking, i.e. the reduction of the unresectable tumor mass, either by surgery or radiation is so far unknown due to the lack of prospective randomized data. However, in a retrospective data, long-term survivors have been described after liver and lung surgery specifically in ocular rather than cutaneous melanoma [3-5]. In pulmonary metastases of malignant melanoma, a number of factors have proven to be predictive for sur-

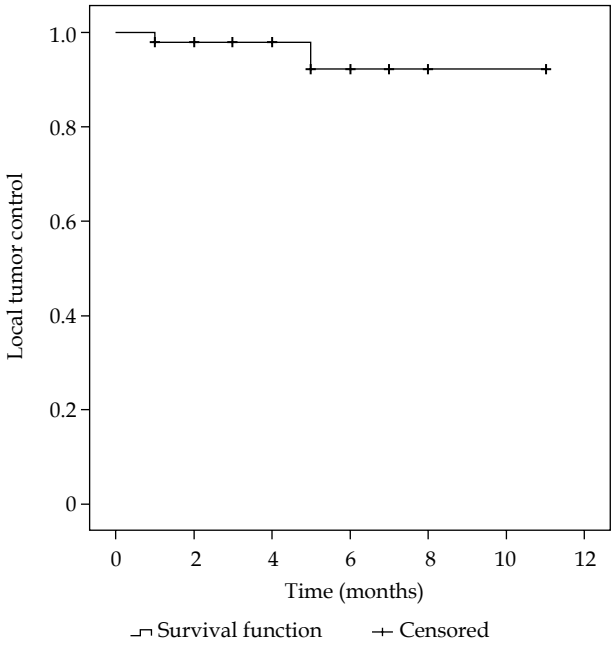

Fig. 2. Graph shows the local tumor control after image-guided high-dose-rate brachytherapy; two patients experienced local tumor progression 1 and 5 months after the treatment

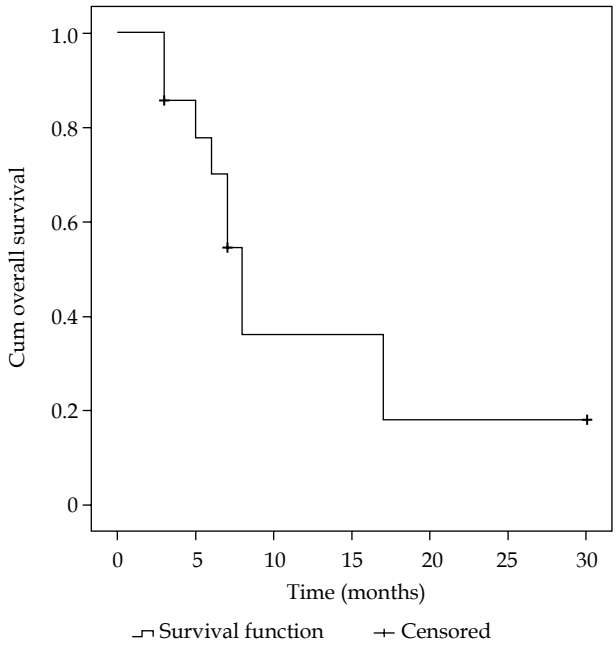

Fig. 3. Overall survival of all patients with metastatic malignant melanoma treated with high-dose-rate brachytherapy

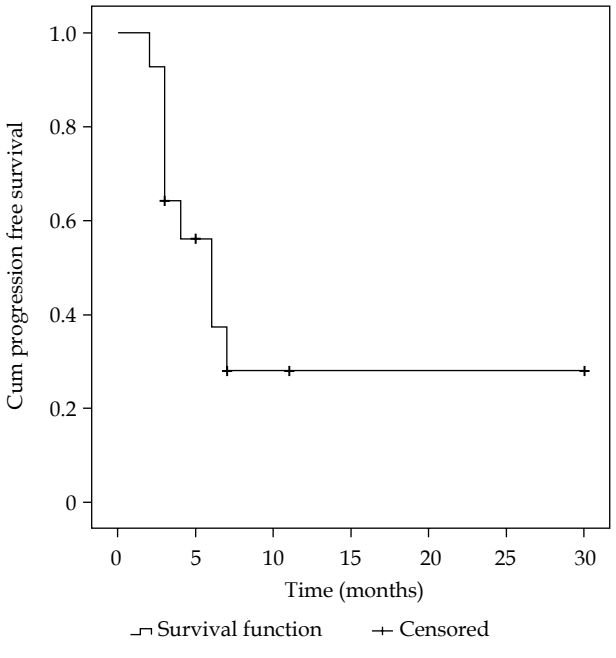

Fig. 4. Progression-free survival of all patients with metastatic malignant melanoma treated with high-dose-rate brachytherapy

vival, including site of primary lesion, histological type, lymph node status, disease-free interval, number of metastases, and the presence of extra-thoracic metastases [4]. Based on these data, surgical resection or local ablation of lung metastases has been adopted in the treatment algorithm in many centers, even in patients displaying minor additional non-visceral tumor implants.

The objective of surgery or local ablation in metastatic melanoma is symptom relief such as pain or organ compression, e.g. jaundice caused by obstruction of the bile duct. Few studies reported the application of image-guided local ablation by radiofrequency ablation (RFA), or laser induced thermotherapy (LITT), with limited efficacy in tumor larger 5 cm and in proximity to critical organs [6,7,13]. That includes bile duct in the liver hilum, large liver vessels that lead to cooling effects, and therefore incomplete ablation, lung hilum, proximity of gut or tubular structures (ureter) and more. Image-guided HDR brachytherapy, a technique that has been so far predominately evaluated in metastatic colorectal as well as hepatocellular carcinoma (HCC) [9,14], renders a new minimally invasive approach unharmed by those restrictions. In contrast to thermal ablation, tumor size, cooling effects of large vessels, or proximity to risk organs such as liver or lung hilum, bile duct or intestines do not limit its efficacy [10,15-17].

In the study described herein, we report only one major complication after MRI-guided brachytherapy of a central localization in the liver with a presentation of cholangitis. Other than this, the treatments were well tolerated with just one minor pneumothorax in another patient, which disappeared without treatment. Even though the applicator sizes are similar in RFA, LITT, and image-guided brachytherapy, mechanical damage, such as pneumothorax, seems to be more frequent in cases, in which thermal ablation techniques are used, with a reported frequency of 30% to 50% [18]. In addition, the instantaneous thermal effect holds, at least theoretically, a higher risk of acute complications and, by formation of necrotic cavities, a higher risk of late adverse effects [18].

Thus, advantages in favor of brachytherapy exist with respect to conformity and control of dose distribution, which becomes especially important when treating adjacent to risk structures [16].

Melanoma is widely believed to be a radio-resistant tumor, a misunderstanding that has led to the limited use of radiotherapy for its treatment [19]. Reason for this relative radiation resistance was the large shoulder referred to the linear-quadratic (LQ) model. Actually malignant melanoma is not radio-resistant, which was shown in local control rates after radiation *in vivo* [20]. A promising local control means, in a few cases, an improvement in the quality of life and, occasionally, an extended overall survival. Regarding visceral metastases, most experiences were collected in the treatment of bone and brain metastases [21]. For a lasting effect, minimal cumulative- and partial dose, or rather biologic equivalent dose (BED) is required. Konefal *et al*. suggested that the increase of dose is useful in treating cutaneous metastases, but in case of side effects, it is dispensable in treating visceral metastases [22]. A randomized study from Overgaard *et al*. showed an increasing efficacy in single doses > 4 Gy [23], analysis from Olivier showed a significantly higher efficacy in high doses > 30 Gy and BEDs > 39 Gy [24].

Recently, Stinauer *et al*. reviewed 17 patients with 28 metastatic melanoma lesions, treated with a single body radiation therapy [25]. A higher dose per fraction and higher single fraction equivalent dose (SFED) were significantly correlated with a better local control. The authors concluded that an aggressive stereotactic body radiation therapy with SFED ≥ 45 Gy is effective for controlling metastatic melanoma [25].

However, the use of higher doses shows limitations regarding the radiation tolerance of the adjacent structures (OAR). A possibility to apply such effective BED is the use of stereotactic body radiation therapy (SBRT). Different strategies (e.g. 4D-CT, gating, tracking) provide a reduction of the planning target volume (PTV), resulting in a significant decrease in exposure of normal tissue. Meanwhile SBRT is, due to a connotatively figure of retro- and prospective analyses, a widely used and accepted method for several tumors even in curative intention, e.g. treatment of early-stage non-small-cell-lung-cancer, primary and secondary liver malignancies [26-29]. Several authors considered limitations in case of liver treatment. According to Rusthoven, liver-SBRT requires a well-defined quantity and size of lesions [30]. Although these specifications are arguable, certainly there are constrictions mostly due to adjacent organs and structures. In contrast, interstitial brachytherapy enables treatment of larger tumors due to the steep dose gradients and a constant catheter position, latter enabling a lesser PTV.

In the present study, we achieved a local tumor control of 90% after a median follow up of 5 months. Amersi *et al*. showed local recurrences for tumors larger than 3 cm in 29% of melanoma lesions treated with RFA [25]. Not only the size of the treated lesions, also the number of ablated lesions (> 3, < 3) was related to the appearance of recurrence. However, the diagnosis melanoma was a predictive factor for developing local recurrence in an univariate analysis when compared to other diagnosis such as colorectal, breast or neuroendocrine primary. Most likely the comparatively aggressive tumor biology of melanoma is responsible for earlier and more frequent detection of tumor recurrence [31].

There are also promising results in the literature regarding the treatment of malignant melanoma in the nasal cavity and choroidal melanoma by using brachytherapy [32,33]. In this case report, a patient with choroidal melanoma was successfully treated with brachytherapy, achieving tumor control for 12 years [33].

After the treatment with HDR brachytherapy, we achieved a median overall survival of 8 months. Over the last decades, only two systemic treatments were approved in the therapy of metastatic melanoma until 2010: Dacarbazin and Vindesine. The reached prolongation of median overall survival was limited to 6-10 months [34]. Similar rates of remission or survival were reached with the treatment of interferon-alpha and interleukin-2. With the introduction of new target therapies like Ipilimumab and BRAF-inhibitors Vemurafenib, two new effective options are available. Diverse phase II studies showed a prolongation of overall survival up to 15 months [35]. In the future, the combination of target therapies and local ablative options, such as image-guided HDR brachytherapy, could be a promising strategy. We achieved a median progression-free survival of 6 months, which is comparable to the literature. As mentioned, the introduction of target therapies like BRAF-inhibitors in combination with MEK inhibitors may prolong the progression-free survival [34,35].

Several limitations to our study need to be acknowledged. The first weakness of this study is the retrospective nature and the short follow up period. However, the results of this investigation show that HDR brachytherapy can be safely used for local tumor control in selected patients. To identify appropriate candidates for local ablation with the intention to prolong survival, a prospective comparative trial is needed, i.e. to assess the combination of local ablation plus systemic treatments versus systemic treatment alone. In such a study format, HDR brachytherapy would just be one out of a set of tools for local tumor treatment, supplemented by RFA, SBRT, TACE, Y90 radioembolisation, surgery, and others. A thoughtful, interdisciplinary consideration of local and systemic treatment options will in future be mandatory for optimal treatment success in each patient with metastatic melanoma.

We conclude that for patients in a palliative and non-curable stadium, image-guided single high-dose-rate brachytherapy is a promising alternative and well-tolerated treatment, which can be used in most tumor locations, and may therefore be considered specifically in metastases causing symptoms or metastases at risk to cause complications. Treatment rationale should be the reduction of clinical symptoms by reduction of the tumor volume, and therefore the improvement of quality of life.

Disclosure

Authors report no conflict of interest.

References

1. Garbe C, Hauschild A, Volkenandt M et al. Evidence-based and interdisciplinary consensus-based German guidelines: systemic medical treatment of melanoma in the adjuvant and palliative setting. *Melanoma Res* 2008; 18: 152-160.
2. Ahn HJ, Na II, Park YH et al. Role of adjuvant chemotherapy in malignant mucosal melanoma of the head and neck. *Oral Oncol* 2010; 46: 607-611.
3. Pawlik TM, Zozri D, Abdalla EK et al. Hepatic resection for metastatic melanoma: distinct patterns of recurrence and prognosis for ocular versus cutaneous disease. *Ann Surg Oncol* 2006; 13: 712-720.
4. Neuman HB, Patel A, Hanlon C et al. Stage-IV melanoma and pulmonary metastases: factors predictive of survival. *Ann Surg Oncol* 2007; 14: 2847-2853.
5. Schuhan C, Muley T, Dienemann H et al. Survival after pulmonary metastatectomy in patients with malignant melanoma. *Thorac Cardiov Surg* 2011; 59: 158-162.
6. Curley SA, Iuzzo F. Radiofrequency ablation of primary and metastatic hepatic malignancies. *Int J Clin Oncol* 2002; 7: 72-81.
7. Galandi D, Antes G. Radiofrequency thermal ablation versus other interventions for hepatocellular carcinoma. *Cochrane Database Syst Rev* 2002; 3: CD003046.
8. Huppert PE, Fierlbeck G, Pereira P et al. Transarterial chemoembolization of liver metastases in patients with uveal melanoma. *Eur J Radiol* 2010; 74: 38-44.
9. Mohnike K, Wieners G, Schwartz F et al. Computed tomography-guided high-dose-rate brachytherapy in hepatocellular carcinoma: safety, efficacy, and effect on survival. *Int J Radiat Oncol Biol Phys* 2010; 78: 172-179.
10. Ricke J, Wust P, Stohlmann A et al. CT-guided interstitial brachytherapy of liver malignancies alone or in combination with thermal ablation: phase i/ii results of a novel technique. *Int J Radiat Oncol Biol Phys* 2004; 58: 1496-1505.
11. Goldberg SN, Grassi CJ, Cardella JF et al. For the Society of Interventional Radiology Technology Assessment Committee and the International Working Group on Image-guided Tumor Ablation (2009): Standardization of terminology and reporting criteria. *J Vasc Interv Radiol* 2009; 20: 377-390.
12. Gil-Alzugaray B, Chopitea A, Iñarrairaegui M et al. Prognostic factors and prevention of radioembolization-induced liver disease. *Hepatology* 2013; 57: 1078-1087.
13. Pech M, Werk M, Beck A et al. System continuity and energy distribution in laser-induced thermo therapy (LITT). *Fortschr Röntgenstr* 2002; 174: 754-760.
14. Ricke J, Mohnike K, Pech M et al. Local response and impact on survival after local ablation of liver metastases from colorectal carcinoma by computed tomography-guided high dose rate brachytherapy. *Int J Radiat Oncol Biol Phys* 2010; 78: 479-485.
15. Wieners G, Pech M, Rudzinska M et al. CT-guided interstitial brachytherapy in the local treatment of extrahepatic, extrapulmonary secondary malignancies. *Eur Radiol* 2006; 16: 2586-2593.
16. Streitparth F, Pech M, Böhmig M et al. In vivo assessment of the gastric mucosal tolerance dose after single fraction, small volume irradiation of liver malignancies by computed tomography-guided, high-dose-rate brachytherapy. *Int J Radiat Oncol Biol Phys* 2006; 65: 1479-1486.
17. Collettini F, Singh A, Schnapauff D et al. Computed-tomography-guided high-dose-rate brachytherapy (CT-HDRBT) ablation of metastases adjacent to the liver hilum. *Eur J Radiol* 2013; 82: 509-514.
18. Holsten N, Stier A, Weigel C et al. Laser-induced thermotherapy (LITT) of lung metastases: description of a miniaturized applicator, optimization, and initial treatment of patients. *Fortschr Röntgenstr* 2003; 175: 393-400.
19. Zygogianni A, Kyrgias G, Kouvaris J et al. Melanoma: the radiotherapeutic point of view; review of the current literature. *Rev Recent Clin Trials* 2011; 6: 127-133.
20. Seegenschmiedt MH, Keilholz L, Altendorf-Hofmann A et al. Palliative radiotherapy for recurrent and metastatic malignant melanoma: prognostic factors for tumour response and long-term outcome: a 20-years' experience. *Int J Radiat Oncol Biol Phys* 1999; 44: 607-618.
21. Samlowski WE, Watson GA, Wang M et al. Multimodality treatment of melanoma brain metastases incorporating stereotactic radiosurgery (SRS). *Cancer* 2007; 109: 1855-1862.
22. Konefal JB, Emami B, Pilepich MV et al. Analysis of dose fractionation in the palliation of metastases from malignant melanoma. *Cancer* 1988; 61: 243-246.
23. Overgaard J, von der Maase H, Overgaard M et al. A randomized study comparing two high-dose per fraction radiation schedules in recurrent or metastatic malignant melanoma. *Int J Radiat Oncol Biol Phys* 1985; 11: 1837-1839.
24. Olivier KR, Schild SE, Morris CG et al. A higher radiotherapy dose is associated with more durable palliation and longer survival in patients with metastatic melanoma. *Cancer* 2007; 110: 1791-1795.
25. Stinauer MA, Kavanagh BD, Schefter TE et al. Stereotactic body radiation therapy for melanoma and renal cell carcinoma: impact of single fraction equivalent dose on local control. *Radiat Oncol* 2011; 6: 34.
26. Almaghrabi MY, Supiot S, Paris F et al. Stereotactic body radiation therapy for abdominal oligometastases: a biological and clinical review. *Radiat Oncol* 2012; 7: 126.
27. Chang DT, Swaminath A, Kozak M et al. Stereotactic body radiotherapy for colorectal liver metastases: a pooled analysis. *Cancer* 2011; 117: 4060-4049.
28. Sharma DN, Thulkar S, Sharma S et al. High-dose-rate interstitial brachytherapy for liver metastases: first study from India. *J Contemp Brachytherapy* 2013; 5: 70-75.
29. Potters L, Kavanagh B, Galvin JM et al. American Society for Therapeutic Radiology and Oncology (ASTRO) and American College of Radiology (ACR) practice guidelines for the performance of stereotactic body radiation therapy. *Int J Radiat Oncol Biol Phys* 2010; 76: 326-332.
30. Rusthoven KE, Kavanagh BD, Cardenes H et al. Multi-institutional phase I/II trial of stereotactic body radiation therapy for liver metastases. *J Clin Oncol* 2009; 27: 1572-1578.
31. Amersi FF, McElrath-Garza A, Ahmad A et al. Long-term survival after radiofrequency ablation of complex unresectable liver tumours. *Arch Surg* 2006; 141: 581-588.
32. Scepanovic D, Paluga M, Rybnikarova M et al. Brachytherapy as a treatment for malignant melanoma of the nasal cavity and nasopharynx – case report. *J Contemp Brachytherapy* 2013; 5: 157-163.
33. Correa-Pérez ME, Saornil MA, García-Álvarez C et al. Bilateral episcleral brachytherapy in simultaneous choroidal melanoma and circumscribed hemangioma. *J Contemp Brachytherapy* 2013; 5: 250-257.
34. Eigentler TK, Caroli UM, Radny P et al. Palliative therapy of malignant melanoma: a systemic review of 41 randomized clinical trials. *Lancet Oncol* 2003; 4: 748-759.
35. Sosman JA, Kim KB, Schuchter L et al. Survival in BRAF V600-mutant advanced melanoma treated with vemurafenib. *N Engl J Med* 2012; 366: 707-714.

Hindawi Publishing Corporation
Gastroenterology Research and Practice
Volume 2016, Article ID 8732521, 13 pages
http://dx.doi.org/10.1155/2016/8732521

Research Article

Extensive Use of Interventional Therapies Improves Survival in Unresectable or Recurrent Intrahepatic Cholangiocarcinoma

Ricarda Seidensticker,[1,2,3] Max Seidensticker,[1,2,3] Kathleen Doegen,[1] Konrad Mohnike,[1,2,3] Kerstin Schütte,[2,4] Patrick Stübs,[2,5] Erika Kettner,[1,2] Maciej Pech,[1,3] Holger Amthauer,[1,3] and Jens Ricke[1,2,3]

[1]*Klinik für Radiologie und Nuklearmedizin, Universitätsklinikum Magdeburg, Leipziger Strasse 44, 39120 Magdeburg, Germany*
[2]*Zentrum für Gastrointestinale Tumoren (ZeGIT), Universitätsklinikum Magdeburg, Leipziger Strasse 44, 39120 Magdeburg, Germany*
[3]*Deutsche Akademie für Mikrotherapie (DAfMT), Leipziger Strasse 44, 39120 Magdeburg, Germany*
[4]*Klinik für Gastroenterologie, Hepatologie und Infektiologie, Universitätsklinikum Magdeburg, Leipziger Strasse 44, 39120 Magdeburg, Germany*
[5]*Klinik für Allgemein-, Viszeral- und Gefäßchirurgie, Universitätsklinikum Magdeburg, Leipziger Strasse 44, 39120 Magdeburg, Germany*

Correspondence should be addressed to Ricarda Seidensticker; ricarda.seidensticker@med.ovgu.de

Received 12 October 2015; Accepted 20 December 2015

Academic Editor: Mohamad H. Imam

Aim. To assess the outcomes of patients with unresectable intrahepatic cholangiocellular carcinoma (ICC) treated by a tailored therapeutic approach, combining systemic with advanced image-guided local or locoregional therapies. *Materials and Methods*. Treatment followed an algorithm established by a multidisciplinary GI-tumor team. Treatment options comprised ablation (RFA, CT-guided brachytherapy) or locoregional techniques (TACE, radioembolization, i.a. chemotherapy). *Results*. Median survival was 33.1 months from time of diagnosis and 16.0 months from first therapy. UICC stage analysis showed a median survival of 15.9 months for stage I, 9 months for IIIa, 18.4 months for IIIc, and 13 months for IV. Only the number of lesions, baseline serum CEA and serum CA19-9, and objective response (RECIST) were independently associated with survival. Extrahepatic metastases had no influence. *Conclusion*. Patients with unresectable ICC may benefit from hepatic tumor control provided by local or locoregional therapies. Future prospective study formats should focus on supplementing systemic therapy by classes of interventions ("toolbox") rather than specific techniques, that is, local ablation leading to complete tumor destruction (such as RFA) or locoregional treatment leading to partial remission (such as radioembolization). This trial is registered with German Clinical Trials Registry (Deutsche Register Klinischer Studien), DRKS-ID: DRKS00006237.

1. Introduction

Peripheral or intrahepatic cholangiocellular carcinoma (ICC) is a rare neoplasm. However, its incidence and mortality have been reported to be increasing worldwide [1]. Prognosis is poor, with a 5-year survival below 5%, including patients who do undergo tumor resection. However, surgical treatment currently represents the only potentially curative therapy. Unfortunately only 20% of patients are eligible for resection because of disease spread, anatomic location, inadequate hepatic reserve, or limiting comorbidities [2–5].

Median survival for patients with untreated unresectable ICC has been reported as 3–6 months [5, 6]. Furthermore, systemic intravenous (i.v.) chemotherapy (ivCTX) has only limited benefit. Although modern chemotherapy regimens have improved survival considerably in recent years, median survival is still less than one year for, for example, gemcitabine plus cisplatin [7].

Several palliative therapeutic options exist for patients with unresectable ICC. The goals of palliative therapy are to control local tumor growth, to relieve symptoms, and to improve and preserve quality of life. Thus, local-ablative

treatment options are gaining attention, as results from studies analyzing radiofrequency ablation (RFA) and ^{90}Y-radioembolization (RE), high dose rate brachytherapy (HDR-BT), intra-arterial chemotherapy (iaCTX), and transarterial chemoembolization (TACE) have been encouraging [8–12].

However, most of these studies included patients with intrahepatic and extrahepatic cholangiocarcinoma or gallbladder cancer and involved only a small number of patients, so that definitive conclusions are sometimes difficult to draw.

Since 2006, we have treated patients with unresectable or recurrent ICC by different local therapies (alone or in combination) according to a therapy algorithm that was established after thorough discussion in a multidisciplinary team (GI board) involving surgeons, gastroenterologists, medical oncologists, and interventional radiologists. Data from these patients treated according to this algorithm were prospectively collected in an institutional database.

In the study described herein we present the clinical outcomes of this patient-tailored therapeutic approach, combining systemic and image-guided local or locoregional therapies for the treatment of intrahepatic cholangiocarcinoma in nonsurgical candidates.

2. Materials and Methods

This study was compliant with the ethical guidelines of the 1975 Declaration of Helsinki and was approved by our Institutional Review Board (positive vote assigned by "Ethikkommission der Medizinischen Fakultät der Otto-von-Guericke-Universität Magdeburg" at 7-16-2013); written informed consent to scientific use of data was obtained before therapy. All clinical data were obtained from the prospectively maintained institutional ICC database.

The study was registered at DRKS (Deutsche Register Klinischer Studien DRKS00006237).

2.1. Patients. From March 2006 to June 2012 (last follow-up performed in March 2013), 75 consecutive patients with unresectable ICC were referred to our multidisciplinary GI board and received treatment recommendations with local or locoregional treatments often supplementary to systemic treatments. All of these patients were not surgical candidates due to advanced tumor stage, comorbidities, or refused resection. From this cohort, 20 patients were excluded from analysis: 10 were lost to follow-up within the first two months (most of them initially referred from distant centers) and 10 presented with a secondary malignoma (3 of those with an additional extrahepatic cholangiocellular carcinoma, i.e., Klatskin tumor). Thus, 55 patients were analyzed. Patient and tumor characteristics at the time of first local or locoregional therapy are summarized in Table 1.

Palliative treatment options were part of the aforementioned multidisciplinary treatment algorithm. The algorithm is outlined in detail in Figure 1. Image-guided techniques comprised RFA (radiofrequency ablation), TACE (conventional chemoembolization), HDR-BT (CT-guided interstitial high dose rate brachytherapy), RE (^{90}Y-radioembolization), iaCTX (intra-arterial chemotherapy), and ivCTX (intravenous chemotherapy).

Factors guiding the treatment allocation included stage and specific morphological properties of the disease (tumor size, number of lesions, and preexisting extrahepatic metastases) as well as liver function and performance status.

All 55 patients analyzed have been treated with at least one local or locoregional treatment option at our clinic. Patients were reassessed with clinical examination and CT or MR imaging every 3 months thereafter. According to that restaging patients were entered in the treatment algorithm again if disease progression was present. As a consequence, 37 out of 55 patients received one type of ablative or locoregional therapy, whereas another 18 patients received a combination of additional image-guided therapies. With 21 patients presenting after previous, often multiple chemotherapy lines, 16 patients received systemic treatments after the first local/locoregional intervention. All treatment details after inclusion as well as tumor-targeted prior treatments are outlined in detail in Table 1.

2.2. Evaluation and Staging. Diagnosis of ICC was based on biopsy. Pretreatment assessment consisted of demographics, presence or absence of cirrhosis, biliary obstruction and portal invasion, extrahepatic metastases, and prior treatments. Diagnostic imaging was performed by magnetic-resonance imaging (MRI) and/or triphasic computerized tomography (CT).

Staging was performed at the time of first diagnosis as baseline staging and again at the time of the first interventional therapy at our institution by the TNM classification adapted from the 6th edition of the staging manual of the UICC/AJCC [13]. Lymph nodes were considered to be metastatic when they were larger than 1 cm in short-axis diameter [14].

The treatment algorithm groups patients according to six potential treatments (Figure 1). Patients with single tumors ($n \leq 4$) received HDR-BT, TACE, or RFA in the absence of portal vein thrombosis (PVT). In case of PVT, only HDR-BT or RFA were applicable. Concomitant chemotherapy was recommended in patients with biologically aggressive tumors (disease free interval < 12 months) specifically in chemotherapy-naïve patients. In patients with biologically favorable tumors with disease free interval ≥ 12 months, an ECOG > 1, and/or previous chemotherapies further chemotherapies immediately after complete ablative or locoregional treatment were not recommended.

Patients with multinodular ($n > 4$) or diffuse disease received radioembolization or iaCTX with 5-fluorouracil/leucovorin (5-FU/LV) when bilirubin was less than 30 μmol/L. If bilirubin was 30–50 μmol/L, iaCTX was preferred alone or in combination with HDR-BT or RFA (depending on the likelihood for reliable, technically safe complete tumor destruction). Patients with bilirubin above 50 μmol/L and those with diffuse peritoneal carcinomatosis were not eligible for any local-ablative or locoregional therapy and received ivCTX or best supportive care only. All treatment recommendations were issued by the multidisciplinary gastrointestinal oncology team in consensus.

Table 1: Patients' characteristics.

Demographics and disease history		%/(range)
Total *N*	55	100%
Sex		
Male	28	50.9%
Female	27	49.1%
Age, year		
Median	67.3	(34.0–82.6)
≤65	25	45.5%
>65	30	54.5%
Months from diagnosis to 1st therapy		
Median	10	(0.8–64.4)
Karnofsky index, $n = 47$		
Median	70	(60–100)
60	9	16.4%
70	13	23.4%
80	14	25.6%
90	17	31.0%
100	2	3.6%
ECOG index, $n = 47$		
Median	1	(0–2)
0	19	34.6%
1	27	49.0%
2	9	16.4%
Prior liver-directed treatment (*n*)		
Any	21	38.2%
Resection	15	27.3%
Intraoperative RFA	3	5.5%
TACE	2	3.6%
RFA	1	1.8%
Prior chemotherapy (*n*)		
Yes	21	38.2%
No	34	61.8%
Prior chemotherapy lines (*n*)		
One	17	30.9%
Two	2	3.6%
>two	2	3.6%
Median	1	(1–5)
Prior chemotherapy agents (*n*)		
Gemcitabine	19	34.5%
Oxaliplatin	12	21.8%
Capecitabine	8	14.5%
5-FU/FA	4	7.3%
Cisplatin	3	5.5%
Others*	9	16.4%
T-stage (*n*)		
T1	21	38.2%
T2	12	21.8%
T3	21	38.2%
T4	1	1.8%

Table 1: Continued.

Demographics and disease history		%/(range)
Overall tumor stage (UICC**) (*n*) at first diagnosis		
Stage I	17	30.9%
Stage II	3	5.5%
Stage IIIa	3	5.5%
Stage IIIb	0	0%
Stage IIIc	21	38.2%
Stage IV	5	9.1%
No information available	6	10.9%
Overall tumor stage (UICC**) (*n*) at first local therapy in Magdeburg		
Stage I	11	20.0%
Stage II	5	9.1%
Stage IIIa	3	5.5%
Stage IIIb	0	0%
Stage IIIc	22	40.0%
Stage IV	14	25.5%
CEA		
Median, range [ng/mL]	2.6	(0.3–391.7)
Elevated, >3.4 ng/mL (*n*)	23	41.8%
Not elevated (*n*)	32	58.2%
CA 19–9		
Median, range [U/mL]	66	(0.6–72.9)
Elevated, >39.9 U/mL (*n*)	34	61.8%
Not elevated (*n*)	21	38.2%
Tumor load		
Median, range (%)	8	(2–80)
Tumor size		
Median, range (mm)	45	(14–189)
Extent of disease (*n*)		
Bilobar	32	58.2%
Unilobar	23	41.8%
Extrahepatic metastases (*n*)		
All	36	65.5%
Lymph node metastases	32	58.2%
Peritoneal metastases	8	14.5%
Pulmonary metastases	5	9.1%
Bone metastases	2	3.6%
Concomitant liver disease (*n*)		
Vascular infiltration	21	38.2%
Cirrhosis	20	36.4%
Biliary obstruction	18	32.7%
Portal vein thrombosis	10	18.2%
Ascites	7	12.7%
Therapies and combinations of therapies (*n*)		
HDR-BT	19	34.5%
RE	5	9.1%
TACE	2	3.6%
RFA	1	1.8%
HDR-BT & ivCTX	11	20.0%
HDR-BT & iaCTX	6	10.9%
HDR-BT & RE	3	5.5%
HDR-BT & RFA	2	3.6%

Table 1: Continued.

Demographics and disease history		%/(range)
HDR-BT & iaCTX & ivCTX	2	3.6%
HDR-BT & RE & ivCTX	2	3.6%
TACE & ivCTX	1	1.8%
RE & iaCTX	1	1.8%

*Irinotecan ($n = 1$), taxotere ($n = 1$), bevacizumab ($n = 1$), erlotinib ($n = 1$), mitomycin C ($n = 1$), cetuximab ($n = 2$), and sorafenib ($n = 2$).
**Acc. to UICC Edition 6, stage I disease is a solitary tumor without vascular involvement; stage II disease is a solitary tumor with vascular invasion or multiple tumors <5 cm; stage IIIa disease is multiple tumors >5 cm with or without vascular invasion; stage IIIb disease is perforation of the peritoneum or infiltration of adjacent organs; stage IIIc disease is any tumor with regional lymph node metastasis; and stage IV disease is any tumor with distant metastasis.

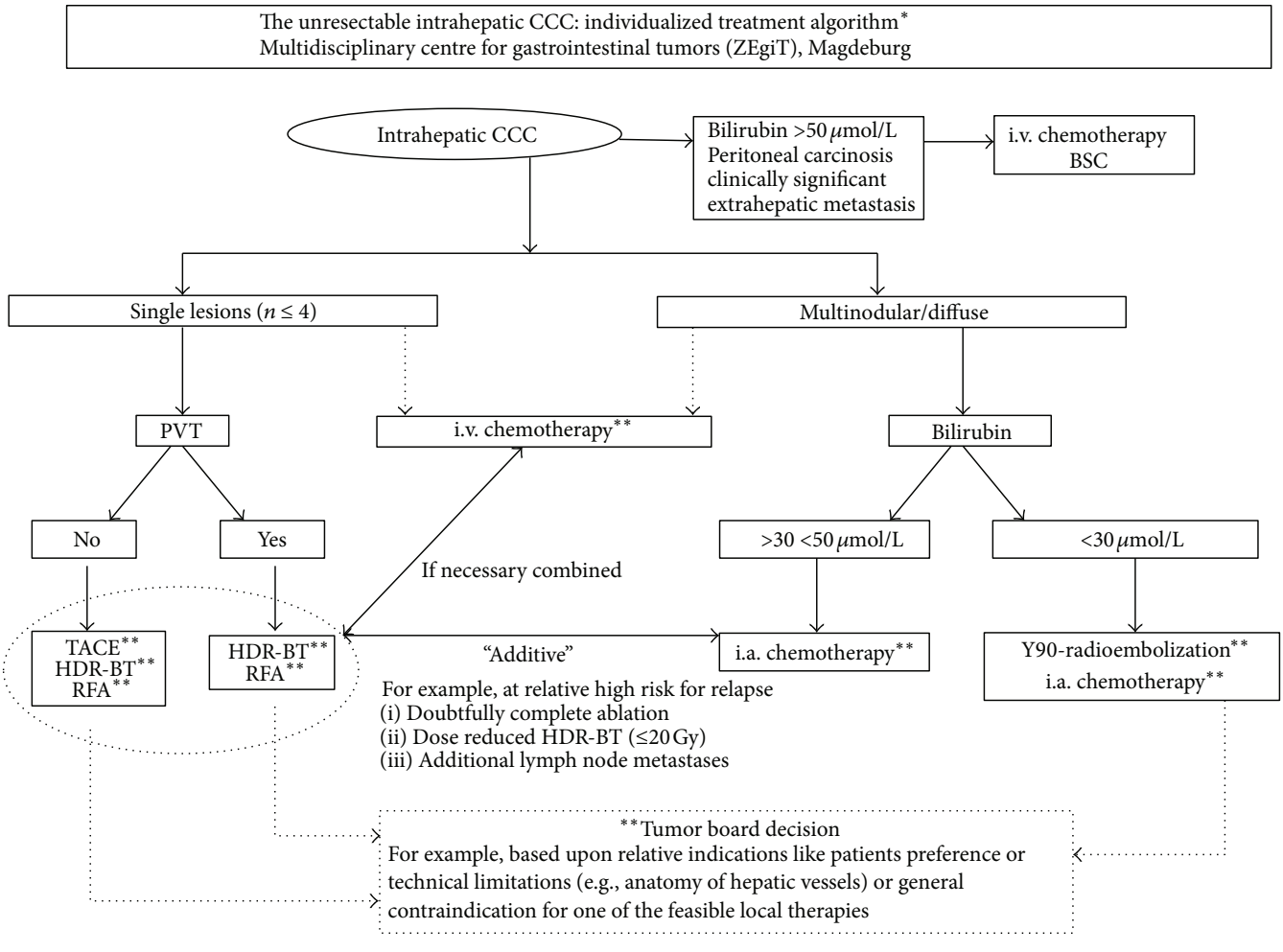

Figure 1: Algorithm for the treatment of intrahepatic cholangiocellular carcinoma. CCC, cholangiocellular carcinoma; HDR-BT, image-guided HDR brachytherapy; TACE, transarterial chemoembolization; RFA, radiofrequency ablation; i.a., intra-arterial; i.v., intravenous; BSC, best supportive care; PVT, portal venous thrombosis.

Complications were classified following CTCAE v4.0, with minor (CTCAE Grades 1 and 2) or major complications (CTCAE Grades 3 and 4).

2.3. Local-Ablative Therapies

2.3.1. Radiofrequency Ablation (RFA). RFA is an ablative technique intending complete local tumor destruction. RFA was performed under CT or MRI guidance using a radiofrequency applicator, which can be expanded stepwise to cover an area of maximum diameter 5 cm and a 150 W RF generator (Starburst Semi-Flex; AngioDynamics, Mountain View, CA) [15, 16]. The RFA protocol was always completed according to the manufacturer's instructions; completeness of ablation was confirmed by MRI 24 hours after RFA.

2.3.2. Image-Guided HDR Brachytherapy (HDR-BT). The technique of HDR-BT has been described in detail elsewhere [9, 17]. As an ablative technique, its intention is complete and durable local tumor destruction. In brief, liver malignancies

are treated with high dose rates of iridium-192 in an afterloading technique after percutaneous positioning of the brachytherapy catheters under CT or MRI control. The prescribed minimum dose for the clinical target volume is 20 Gy. Specifically in patients where RFA is not feasible owing to larger tumor sizes (>5 cm) or adjacent, potentially cooling structures such as larger vessels, HDR-BT is a useful option [18–20].

2.3.3. Radioembolization (RE) with Yttrium-90 Microspheres. Radioembolization with ^{90}Y-labeled resin microspheres has been shown to be effective in unresectable ICC and tumor metastases of the liver [21, 22]. Its intended effect was partial remission of diffuse hepatic tumor spread rather than complete tumor ablation.

The principle of RE is based on the dual blood supply of the liver from the portal vein and the hepatic artery, so delivery of the radioactive microspheres via the hepatic artery results in high dose local irradiation with only minor effects on normal liver tissue. All patients underwent pretreatment mesenteric angiography and ^{99}Tc-macroaggregated albumin scanning to minimize the risk of nontarget embolisation [19, 23]. A detailed account of the treatment protocol has been published previously [22]. The median dose was 1.63 GBq (range 0.9–2.55 GBq).

2.3.4. Transarterial Chemoembolization (TACE). The intended effect of TACE was partial remission of limited hepatic tumor spread beyond the technical capabilities of local ablation such as through RFA or CT-guided brachytherapy. TACE was conducted by standard techniques with an emulsion of doxorubicin and cisplatin in lipiodol (1 mL contains 0.5 mL lipiodol and 2.5 mg each of doxorubicin and cisplatin) until stasis in tumor feeding arteries was achieved. No additional embolization particles were administered. TACE was performed every 6 weeks. After three sessions tumor response was assessed by CT and/or MRI and, depending on outcome, TACE was either continued or interrupted [19, 24, 25].

2.3.5. Intra-Arterial Chemotherapy (iaCTX). iaCTX was performed on an outpatient basis. Chemotherapy was delivered through a microcatheter-port system into the hepatic artery, implanted via the common femoral artery as described elsewhere [26]. This method potentially decreases systemic side effects (e.g., nausea and vomiting) and may optimize the chemotoxic effects of the drugs in the hepatic malignancy [27, 28].

Intra-arterial chemotherapy consisted of daily infusions of fluorouracil (5-FU) 600 mg/mÂš and folinic acid 170 mg/mÂš on days 1–5, repeated on day 22.

Nine patients (16%) received a median of 6 cycles (range 4–23 cycles) of intra-arterial 5-FU chemotherapy.

2.3.6. Intravenous Chemotherapy (ivCTX). Lacking a well-defined therapeutic standard until 2010, various ivCTX regimens have been administered following protocols including monotherapy or combinations of cisplatin, gemcitabine, oxaliplatin, 5-FU/FA, and capecitabine [7, 29, 30]. Since 2010 the standard first-line therapy was gemcitabine combined with cisplatin [7]. In our study, sixteen patients received ivCTX in combination with their local therapy. The median number of chemotherapeutic cycles was 5 (range 1–12). Thirteen patients (24%) received one line of ivCTX, two (4%) received a second line, and one (2%) received a third line. Patients who had been treated with ivCTX only are not part of this analysis.

2.4. Follow-Up/Clinical Assessments. At imaging follow-up, usually every three months after the intervention, clinical assessment and laboratory tests (blood counts, liver function tests, and tumor markers (carbohydrate antigen 19-9 (CA 19-9) and carcinoembryonic antigen (CEA))) were routinely performed.

Patients diagnosed with progressing ICC during follow-up were reassessed by the multidisciplinary treatment decision algorithm and treated again accordingly. Patients were followed until death or censored at the last known clinical follow-up.

2.5. Imaging Analysis. Patients were examined every three months by liver MRI using the liver-specific contrast agent gadoxetic acid (Gd-EOB-DTPA, Primovist, Bayer Healthcare, Berlin, Germany) or triphasic contrast-enhanced CT with iopremol 300 (Imeron 300, Bracco Imaging, SpA, Milan, Italy) of the abdomen. Every six months a chest X-ray was conducted and once a year a multislice CT of the thorax. Response was assessed applying the RECIST 1.1 criteria [31].

2.6. Statistical Analysis. Descriptive statistics were calculated for quantitative variables; frequency counts by category were calculated for qualitative variables; 95% confidence intervals are presented where appropriate. p values were considered significant if <0.05. The primary study endpoint was overall survival (estimated from the date of first interventional therapy at our institution and additionally from the date of first diagnosis), analyzed by the Kaplan-Meier method and compared between different groups by a log-rank test.

The following prognostic factors for influencing patient survival were evaluated: patient's age and sex, time interval from first diagnosis to first local therapy at our institution, performance status at the time of first local therapy at our institution (Karnofsky and ECOG), prior resection, prior chemotherapies, prior local therapies, tumor load, tumor number, tumor size and tumor stage (according to UICC), extrahepatic metastasis, vascular infiltration, portal vein invasion, biliary obstruction, ascites, cirrhosis, elevated tumor marker levels (CEA and CA 19-9), best response, and therapy-associated complications.

Several prognostic factors were grouped for analysis of differences in survival. These are listed below (Table 3).

Univariate and multivariate Cox regression analyses were performed to identify factors associated with the patients' survival. Only factors showing significance ($p < 0.05$) in the univariate model were included in the multivariate analysis.

Statistical analyses were performed with SPSS (version 21, IBM, Chicago, IL, USA).

Table 2: Treatment characteristics and cumulative toxicities analysis: only Grade 3-4 toxicities are reported (CTCAE version 4.0).

Treatment characteristics	HDR-BT	RE	RFA	TACE	ivCTX	iaCTX
Patients (*n*)	45	11	3	3	16	9
Karnofsky index, median (range)	80 (60–100)	80 (60–90)	90 (60–90)	70 (70)	70 (60–100)	90 (80–90)
ECOG index, median (range)	1 (0–2)	1 (0–2)	0 (0–2)	1 (1-1)	1 (0–2)	0 (0-1)
Number of days hospitalized, median (range)	4 (1–11)	4 (3–5)	5 (4–6)	4 (3–6)	0	0
Total number of treatments/chemotherapeutic cycles (*n*)	101	20	3	12	64	43
Median number of treatments/chemotherapeutic cycles per patient (range)	1 (1–5)	1 (1–4)	3 (1-1)	4 (3–5)	5 (1–12)	6 (4–23)
Median RE-dose delivered (GBq), median (range)	—	1.63 (0.9–2.55)	—	—	—	—
Best response	CR	PR	CR	PD	SD	PR
Adverse events acc. CTCAE (highest grade recorded)	3	2	2	1	3	2
Abscess (*n*)	1	—	—	—	—	—
Shivering* (*n*)	1	—	—	—	—	—
Hematoma subcapsular (*n*)	1	—	—	—	—	—
Anemia (*n*)	—	—	—	—	1	—
Thrombopenia (*n*)	—	—	—	—	1	—
Neutropenia (*n*)	—	—	—	—	1	—
Anorexia (*n*)	—	—	—	—	1	—
Fatigue (*n*)	—	—	—	—	2	—
Pain (*n*)	—	—	—	—	1	—
Diarrhea (*n*)	—	—	—	—	1	—
Rash (*n*)	—	—	—	—	1	—

Data are expressed as absolute number of events (*n*).
CR, complete response; PR, partial response; SD, stable disease; PD, progressive disease. CTCAE, common toxicity criteria of adverse events.
*Shivering due to radiation effects during HDR-BT with the need for abruption of the intervention.

3. Results

3.1. Patient Population. Table 1 summarizes the patient and tumor characteristics in the current study.

At the time of first interventional treatment, 58% of the patients suffered from bilobar tumor spread, the median tumor size was 45 mm, and 65% presented with extrahepatic metastasis (lymph node metastasis ($n = 32$), single peritoneal nodules ($n = 8$), and pulmonary ($n = 5$) and bone metastasis ($n = 2$)).

Forty-two patients (76%) underwent prior therapies before local intervention at our institution, 21 (38%) had undergone liver-directed therapy, and another 21 patients (38%) had received ivCTX.

3.2. Treatment Characteristics and Complication Rates. Treatment characteristics and Grade 3-4 treatment-related toxicities of all 55 patients are summarized in Table 2.

For 101 sessions of HDR brachytherapy, 3 (3%) Grade 3 events (no Grade 4) were reported. Of 16 patients who received ivCTX combined with a local therapy, 9 (56%) suffered from Grade 3 toxicities (no Grade 4). Patients receiving iaCTX, TACE, RE, or RFA did not report any Grade 3 or 4 toxicity. No patient suffered from severe liver decompensation.

3.3. Best Tumor Response. Of 55 patients, 8 (15%) showed complete remission, 21 (38%) partial remission, 8 (15%) stable disease, and 18 (33%) progressive disease. The best response for each type of therapy is shown along with the treatments in Table 2.

3.4. Follow-Up and Overall Survival. Median follow-up time was 11.7 months (range 0.9–51.1). Forty-three of the 55 (78.2%) patients died during the follow-up period. The median number of follow-up visits was 3 (range: 1–15). The median overall survival period was 33.1 months (95% CI 16.5–49.8 months) from the time of first diagnosis and 16.0 months (95% CI 8.8–32.2 months) from the time of first local therapy at our institution (Figures 2(a) and 2(b)). A subgroup analysis by UICC stage showed a median survival of 15.9 months (95% CI 11.9–19.9 months) for patients with stage I disease, 9

Table 3: Cox regression analysis of the prognostic factors of the patient survival period.

Variables	Univariate analysis			Multivariate analysis		
	HR	95% CI	p	HR	95% CI	p
Age (≤65 years versus >65 years)	0.83	0.45–1.53	0.551			
Sex (male versus female)	1.17	0.64–2.12	0.615			
Previous resection (no versus yes)	0.73	0.37–1.43	0.358			
UICC at first therapy (stage I versus stages II–IV)	1.20	0.96–1.50	0.133			
Lobar spread of disease (unilobar versus bilobar)	1.47	0.78–2.76	0.237			
Extrahepatic metastasis (no versus yes)	1.55	0.78–3.09	0.211			
Tumor load (≤10% versus >10%)	1.81	0.99–3.31	0.055			
Number of lesions (1 versus >1)	2.44	1.27–4.71	**0.008**	2.85	1.43–5.65	**0.003**
Portal vein thrombosis (no versus yes)	1.43	0.62–3.30	0.407			
Vascular infiltration (no versus yes)	1.20	0.65–2.24	0.560			
Ascites (no versus yes)	1.49	0.66–3.35	0.314			
Liver cirrhosis (no versus yes)	1.25	0.67–2.34	0.493			
Biliary obstruction (no versus yes)	1.02	0.53–1.97	0.950			
ECOG index (0 versus 1–4)	1.23	0.66–2.30	0.511			
CA19–9 (≤39.9 U/mL versus >39.9 U/mL)	1.93	1.01–3.68	**0.047**	2.05	0.99 – 4.22	**0.052**
CEA (≤3.4 ng/mL versus >3.4 ng/mL)	2.30	1.23–4.31	**0.009**	1.89	0.97 – 3.72	**0.025**
Objective response (CR + PR versus SD + PD)	2.43	1.28–4.60	**0.006**	2.84	1.41 – 5.72	**0.003**
Complications (no versus yes)	1.06	0.68–1.67	0.796			
Tumor size (≤50 mm versus >50 mm)	1.35	0.74–2.46	0.328			
Tumor size (≤100 mm versus >100 mm)	1.22	0.60–2.50	0.585			

HR, hazard ratio; CI, confidence interval; objective response categories, see Table 2.

months (95% CI 0.8–17.2 months) for patients with stage IIIa, 18.4 months (95% CI 8.1–28.7 months) for patients with stage IIIc, and 13 months (95% CI 6–18.9 months) for patients with stage IV. Only 5 patients were in stage II when they received first local therapy and, of these, 3 were still alive and therefore censored at the time of analysis. There was no significant difference in survival between the various stages.

3.5. Factors Related to Patients' Survival Period. The following variables were found to be significant in the univariate analysis (Table 3) and were entered into the multivariate Cox regression model: number of tumor lesions, the tumor markers carcinoembryonic antigen (CEA) and carbohydrate antigen 19-9 (CA 19-9), and objective response. The multivariate analysis showed that these parameters were independent factors associated with duration of survival after therapy. According to the Kaplan-Meier analysis, factors identified as influencing median overall survival (after first local treatment) were number of tumors (1 versus ≥2), 34 versus 12.3 months, $p = 0.006$; elevated CA 19-9 levels (normal versus above normal), 23.2 versus 15.9 months, $p = 0.043$; elevated CEA levels (normal versus above normal),

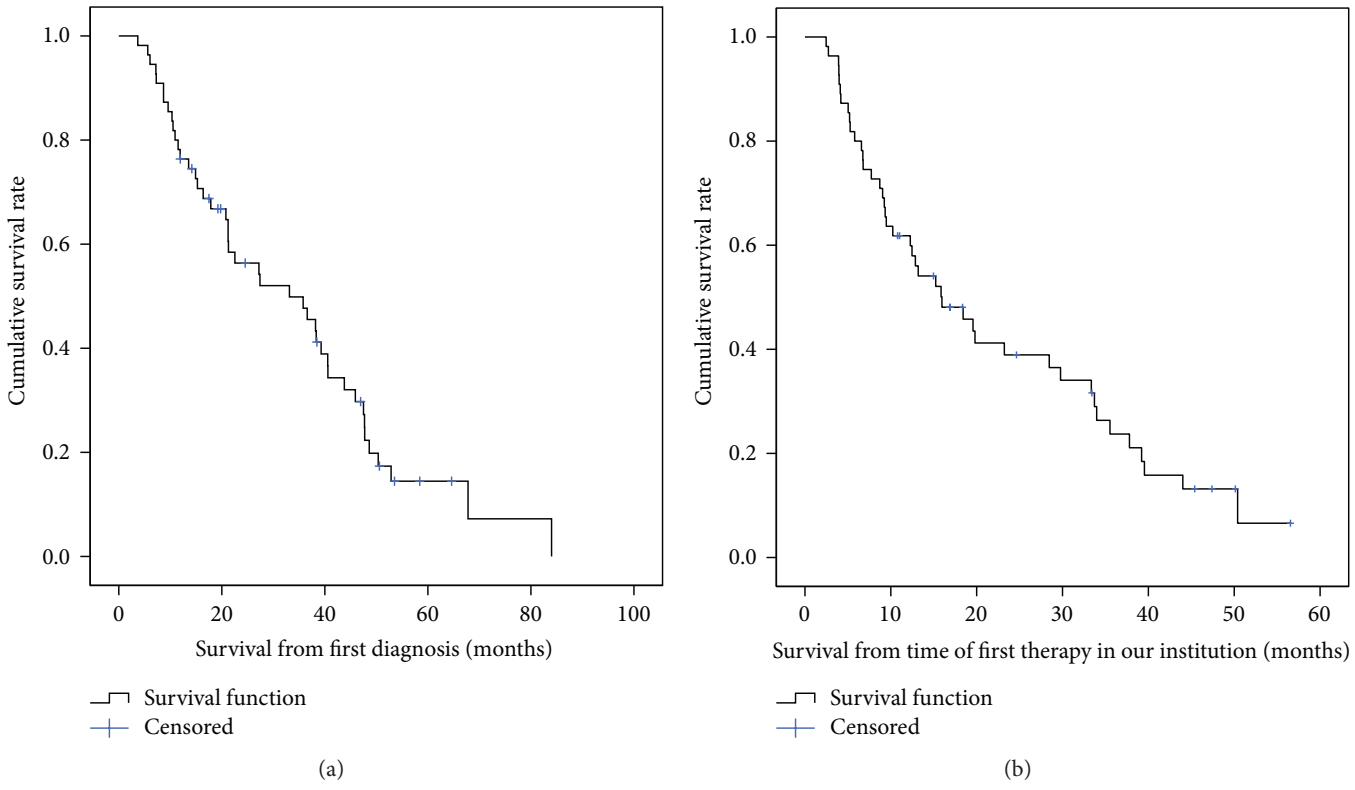

Figure 2: Overall survival rate in all patients from time of first diagnosis (a) and from time of first therapy at our institution (b). Median overall survival from time of first diagnosis: 33.1 months (95% CI 16.5–49.8 months). Median overall survival from time of first therapy at our institution: 16.0 months (95% CI 8.8–32.2 months).

29.8 versus 9.1 months, $p = 0.007$ (the upper normal limits were taken to be 39.9 U/mL for CA 19-9 and 3.4 ng/mL for CEA); and objective response according to RECIST, 29.8 versus 9.3 months, $p = 0.005$. Corresponding survival curves are shown in Figures 3(a)–3(d).

4. Discussion

ICC (intrahepatic cholangiocarcinoma of the mass-forming type) is a uniformly fatal disease with a poor prognosis when detected at an advanced stage. Unfortunately most patients present with unresectable disease because of the absence of symptoms until late in disease progression. Published data concerning systemic or local therapy options are limited. Furthermore, most studies fail to provide a clear profile of their patients in respect of tumor stage or metastatic disease and often comprise heterogeneous study populations including patients with Klatskin tumors, ampullary carcinoma, and gallbladder carcinoma. Therefore, direct comparison with systemic or standard locoregional therapy approaches is sometimes difficult.

We sought to investigate the outcome of a patient-tailored therapy course, including all modalities of minimally invasive oncology, applied alone or in combination, singly or repeatedly, following an interdisciplinary treatment algorithm for patients with mass-forming ICC only. In our study the clinical stage of patients was well described, and tumor disease was staged according to the UICC tumor node metastasis (TNM) classification system.

Our study showed a median survival of 16 months from first local therapy and 33.1 months from first diagnosis, which is higher than that found in most of the earlier studies examining different locoregional therapies. Kiefer et al. [12] reported a median survival of 15 months from chemoembolization and 20 months from diagnosis. In their study 62 patients with heterogeneous tumor entities were treated, 37 with histologically proven ICC and 25 with poorly differentiated adenocarcinoma of unknown primary origin; 49% of the patients presented with UICC (TNM) stage IIIa and 24% with stage IV, comparable to our study where 40% of patients presented with stage IIIc and 25% with stage IV. Survival data concerning different UICC stages are unfortunately not reported.

In a study conducted by Park et al. 72 patients (61% stage IIIa/IIIb and 19% stage IV) with untreated, unresectable ICC received TACE as first-line therapy. Survival after diagnosis was measured and compared with that of patients who received supportive therapy only [10]. Median survival was shorter than in our study: 12.2 months for the TACE group and 3.3 months for the "supportive treatment" group.

Another study assessing survival after RE was published by an Australian group in 2010. In that study, 25 patients underwent RE in advanced ICC: 60% had >25% tumor burden, 48% showed extrahepatic metastasis, and 76% had previous antitumor treatments. Seven patients (26%) underwent ivCTX after RE. The median survival after diagnosis of ICC was 20.4 months and after RE 9.3 months, but for 13

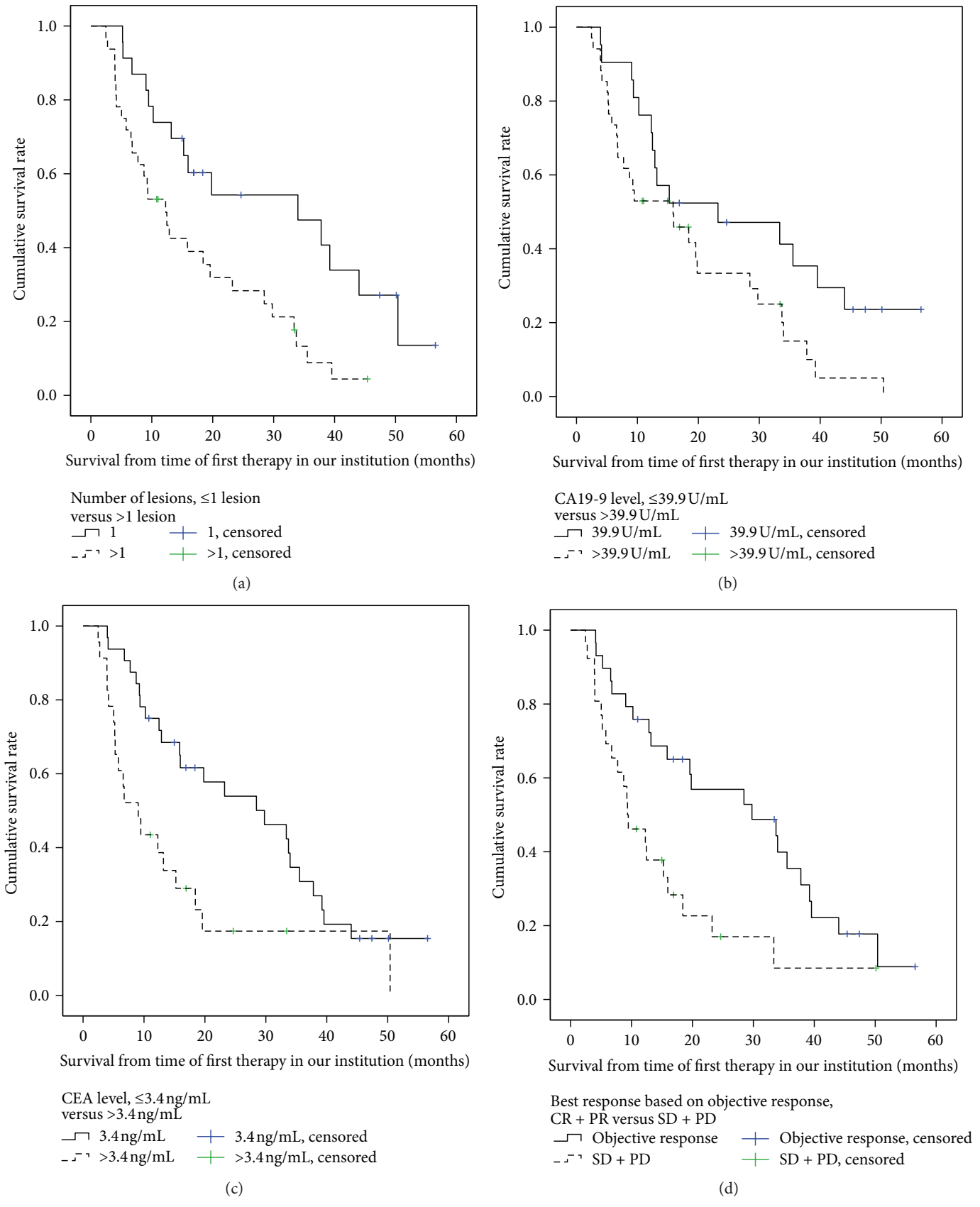

Figure 3: Overall survival rate in all patients according to influencing factors (derived from Cox model, Table 3). (a) Overall survival rates with regard to number of lesions (≤1 lesion versus >1 lesion), with a median overall survival of 34 and 12.3 months, $p = 0.006$. (b) Overall survival rates with regard to CA 19-9 level (≤39.9 U/mL versus >39.9 U/mL) with a median overall survival of 23.2 and 15.9 months, $p = 0.043$. (c) Overall survival rates with regard to CEA level (≤3.4 ng/mL versus >3.4 ng/mL), with a median overall survival of 29.8 and 9.1 months, $p = 0.007$. (d) Overall survival rates with regard to best response (objective response (CR and PR) versus stable and progressive disease (SD + PD)), with a median overall survival of 29.8 and 9.3 months, $p = 0.005$.

patients with hepatic disease only a median survival of 16.3 months was achieved [8].

Excellent results have been reported for 13 patients with 17 unresectable but small ICC (10 tumors < 3 cm, 5 tumors 3–5 cm, and 2 tumors > 5 cm) treated by RFA in an early tumor stage (8 stage I, 3 stage II, 1 stage IIIb, and 1 stage IV). They presented a median overall survival period of 38.5 months [11].

Schnapauff et al. evaluated outcomes after repeated interstitial HDR-BT (27 sessions) in 15 patients with unresectable ICC who did not show extrahepatic metastasis and suffered from limited hepatic disease only (<5 lesions), revealing a median survival of 11 months and 21 months after primary diagnosis [9].

Recently, results of a larger-scale randomized phase III trial of systemic therapy were published, comparing "gemcitabine alone" with "gemcitabine plus cisplatin" in a heterogeneous group of 410 patients with locally advanced or metastatic cholangiocarcinoma, gall-bladder cancer, or ampullary cancer. In that study the gemcitabine-cisplatin combination resulted in a significantly prolonged median overall survival of 11.7 months, compared with 8.1 months in the gemcitabine monotherapy group [7].

In summary, comparing our results with those from other studies on local-ablative therapies on ICC, we can conclude a comparatively long overall survival of our patient cohort, even though the stage of disease was mostly advanced according to UICC. Overall survival in our study cohort was substantially longer than in recent ivCTX-only studies [7]. However, since a significant proportion of our patients were already heavily pretreated with various treatments (including ivCTX) when receiving a first locoregional treatment of the liver, a selection bias towards a favorable tumor biology cannot be ruled out. However, irrespective of this potential bias, we were able to show an overall survival from first diagnosis that was comparable to that after surgical resection with curative intent (median survival of 27–36 months) [32–34].

In the present study 65% (36/55) of the patients had extrahepatic metastases (Table 1) before first treatment at our institution. In agreement with Gusani et al. [35] who reported the treatment outcome of ICC after TACE, we found that median survival after therapy did not differ significantly between patients with liver-only disease and patients suffering from extrahepatic metastasis as well. Similar findings have emerged from other studies on TACE and radioembolization of ICC [8, 12]. Additionally, overall survival was not affected by the UICC stage at the time of treatment at our institution. Regarding tumor characteristics, only the number of ICC lesions had an influence on survival (1 versus >1 lesion, $p = 0.006$). We claim that all these results indicate a pivotal change in the management and treatment of patients with advanced ICC disease. The importance of local tumor control as the main palliative goal has to be emphasized, regardless of extrahepatic metastases and stage of disease. This assumption is underlined by the finding that objective tumor response (liver only) was one of the independent factors influencing survival, with 29.8 months for OR and 9.3 months for SD/PD ($p = 0.005$). Obviously, prevention of liver failure due to progression of intrahepatic tumor (a frequent cause of mortality) is of utmost importance. According to our and others' results, effective suppression of liver tumors may prolong the survival period even in patients with advanced local disease and extrahepatic metastasis. We strongly believe that these findings should further promote clinical trials of local or locoregional therapies and that these may become a key modality in the treatment of nonresectable ICC in future.

Besides objective response and the number of ICC manifestations, only elevation of serum tumor markers CA 19-9 and CEA beyond normal levels showed a negative influence on survival. This might represent a more active tumor biology in patients with elevated tumor markers. Other factors included in our analysis (patient age and gender, prior liver-directed therapies, tumor size and stage, unilobar or bilobar tumor spread, portal vein thrombosis, vascular invasion, biliary obstruction, ascites, cirrhosis, therapy-related complications, ECOG status, Karnofsky index, and time from primary diagnosis to first local therapy) did not appear to affect outcome.

5. Conclusion

Our results show that patients with unresectable ICC of the mass-forming type may benefit from hepatic tumor control by local or locoregional therapies even with presence of extrahepatic spread. If local or locoregional therapies were deemed favorable by clinical means, therapeutic recommendations for a specific technique were driven by technical strengths or limitations of a given modality. As such, future prospective study formats should focus on supplementing systemic therapy by classes of interventions ("toolbox") rather than specific techniques, that is, local ablation leading to complete tumor destruction (such as RFA) or locoregional treatment leading to partial remission (such as radioembolization or TACE).

Abbreviations

ICC:	Intrahepatic cholangiocellular carcinoma
CTCAE:	National Cancer Institute Common Toxicity Criteria
95% CI:	95% confidence interval
CEA:	Carcinoembryonic antigen
CA 19-9:	Carbohydrate antigen 19-9
RECIST:	Response evaluation criteria in solid tumors
i.v.:	Intravenous
IvCTX:	Intravenous chemotherapy
RFA:	Radiofrequency ablation
RE:	^{90}Y-radioembolization
HDR-BT:	High dose rate brachytherapy
IaCTX:	Intra-arterial chemotherapy
TACE:	Transarterial chemoembolization
UICC:	Union for International Cancer Control
ECOG:	Eastern Cooperative Oncology Group
MRI:	Magnetic-resonance imaging
CT:	Computerized tomography
PVT:	Portal vein thrombosis

5-FU/FA: 5-Fluorouracil/leucovorin
TNM: Tumor node metastasis.

Conflict of Interests

All authors disclose that there is not any actual or potential conflict of interests related to the publication of this paper. Jens Ricke receives consulting fees, advisory arrangements, and research grants from SIRTEX Medical Limited and BAYER Healthcare. Maciej Pech receives consulting fees, speakers' bureau, research, and travel grants from SIRTEX Medical Limited. Ricarda Seidensticker, Max Seidensticker, and Holger Amthauer receive research and travel grants from SIRTEX Medical Limited.

Authors' Contribution

Ricarda Seidensticker and Max Seidensticker contributed equally to this work.

References

[1] B. Blechacz and G. J. Gores, "Cholangiocarcinoma: advances in pathogenesis, diagnosis, and treatment," *Hepatology*, vol. 48, no. 1, pp. 308–321, 2008.

[2] J. Yamamoto, T. Kosuge, T. Takayama et al., "Surgical treatment of intrahepatic cholangiocarcinoma: four patients surviving more than five years," *Surgery*, vol. 111, no. 6, pp. 617–622, 1992.

[3] M. J. Lieser, M. K. Barry, C. Rowland, D. M. Ilstrup, and D. M. Nagorney, "Surgical management of intrahepatic cholangiocarcinoma: a 31-year experience," *Journal of Hepato-Biliary-Pancreatic Surgery*, vol. 51, no. 1, pp. 41–47, 1998.

[4] K. M. Chu, E. C. Lai, S. Al-Hadeedi et al., "Intrahepatic cholangiocarcinoma," *World Journal of Surgery*, vol. 213, pp. 301–306, 1997.

[5] S. A. Khan, H. C. Thomas, B. R. Davidson, and S. D. Taylor-Robinson, "Cholangiocarcinoma," *The Lancet*, vol. 366, no. 9493, pp. 1303–1314, 2005.

[6] S. C. Cunningham, M. A. Choti, E. C. Bellavance, and T. M. Pawlik, "Palliation of hepatic tumors," *Surgical Oncology*, vol. 16, no. 4, pp. 277–291, 2007.

[7] J. Valle, H. Wasan, D. H. Palmer et al., "Cisplatin plus gemcitabine versus gemcitabine for biliary tract cancer," *The New England Journal of Medicine*, vol. 362, no. 14, pp. 1273–1281, 2010.

[8] A. Saxena, L. Bester, T. C. Chua, F. C. Chu, and D. L. Morris, "Yttrium-90 radiotherapy for unresectable intrahepatic cholangiocarcinoma: a preliminary assessment of this novel treatment option," *Annals of Surgical Oncology*, vol. 17, no. 2, pp. 484–491, 2010.

[9] D. Schnapauff, T. Denecke, C. Grieser et al., "Computed tomography-guided interstitial HDR brachytherapy (CT-HDRBT) of the liver in patients with irresectable intrahepatic cholangiocarcinoma," *CardioVascular and Interventional Radiology*, vol. 35, no. 3, pp. 581–587, 2012.

[10] S.-Y. Park, J. H. Kim, H.-J. Yoon, I.-S. Lee, H.-K. Yoon, and K.-P. Kim, "Transarterial chemoembolization versus supportive therapy in the palliative treatment of unresectable intrahepatic cholangiocarcinoma," *Clinical Radiology*, vol. 66, no. 4, pp. 322–328, 2011.

[11] J. H. Kim, H. J. Won, Y. M. Shin, K.-A. Kim, and P. N. Kim, "Radiofrequency ablation for the treatment of primary intrahepatic cholangiocarcinoma," *American Journal of Roentgenology*, vol. 196, no. 2, pp. W205–W209, 2011.

[12] M. V. Kiefer, M. Albert, M. McNally et al., "Chemoembolization of intrahepatic cholangiocarcinoma with cisplatinum, doxorubicin, mitomycin C, ethiodol, and polyvinyl alcohol," *Cancer*, vol. 117, no. 7, pp. 1498–1505, 2011.

[13] L. Sobin, M. K. Gospodarowicz, and C. Wittekind, *TNM Classification of Malignant Tumours*, Wiley-Liss, New York, NY, USA, 6th edition, 2002.

[14] Y. C. Yoon, K. S. Lee, Y. M. Shim, B.-T. Kim, K. Kim, and T. S. Kim, "Metastasis to regional lymph nodes in patients with esophageal squamous cell carcinoma: CT versus FDG PET for presurgical detection prospective study," *Radiology*, vol. 227, no. 3, pp. 764–770, 2003.

[15] S.-Y. Park, J. H. Kim, H. J. Won, Y. M. Shin, and P. N. Kim, "Radiofrequency ablation of hepatic metastases after curative resection of extrahepatic cholangiocarcinoma," *American Journal of Roentgenology*, vol. 197, no. 6, pp. W1129–W1134, 2011.

[16] G. Carrafiello, D. Laganà, E. Cotta et al., "Radiofrequency ablation of intrahepatic cholangiocarcinoma: preliminary experience," *CardioVascular and Interventional Radiology*, vol. 33, no. 4, pp. 835–839, 2010.

[17] J. Ricke, P. Wust, A. Stohlmann et al., "CT-guided interstitial brachytherapy of liver malignancies alone or in combination with thermal ablation: phase I-II results of a novel technique," *International Journal of Radiation Oncology Biology Physics*, vol. 58, no. 5, pp. 1496–1505, 2004.

[18] R. Rühl and J. Ricke, "Image-guided micro-therapy for tumor ablation: from thermal coagulation to advanced irradiation techniques," *Onkologie*, vol. 29, no. 5, pp. 219–224, 2006.

[19] A. H. Mahnken, P. Bruners, and R. W. Günther, "Techniques of interventional tumor therapy," *Deutsches Arzteblatt*, vol. 105, no. 38, pp. 646–653, 2008.

[20] G. Wieners, M. Pech, B. Hildebrandt et al., "Phase II feasibility study on the combination of two different regional treatment approaches in patients with colorectal 'liver-only' metastases: hepatic interstitial brachytherapy plus regional chemotherapy," *CardioVascular and Interventional Radiology*, vol. 32, no. 5, pp. 937–945, 2009.

[21] R.-T. Hoffmann, P. M. Paprottka, A. Schön et al., "Transarterial hepatic yttrium-90 radioembolization in patients with unresectable intrahepatic cholangiocarcinoma: factors associated with prolonged survival," *CardioVascular and Interventional Radiology*, vol. 35, no. 1, pp. 105–116, 2012.

[22] R. Seidensticker, T. Denecke, P. Kraus et al., "Matched-pair comparison of radioembolization plus best supportive care versus best supportive care alone for chemotherapy refractory liver-dominant colorectal metastases," *CardioVascular and Interventional Radiology*, vol. 35, no. 5, pp. 1066–1073, 2012.

[23] O. N. Kucuk, C. Soydal, S. Lacin, E. Ozkan, and S. Bilgic, "Selective intraarterial radionuclide therapy with Yttrium-90 (Y-90) microspheres for unresectable primary and metastatic liver tumors," *World Journal of Surgical Oncology*, vol. 9, article 86, 2011.

[24] J. H. Kim, H.-K. Yoon, K.-B. Sung et al., "Transcatheter arterial chemoembolization or chemoinfusion for unresectable intrahepatic cholangiocarcinoma: clinical efficacy and factors influencing outcomes," *Cancer*, vol. 113, no. 7, pp. 1614–1622, 2008.

[25] T. J. Vogl, S. Zangos, K. Eichler et al., "Radiological diagnosis and intervention of cholangiocarcinomas (CC)," *Fortschr Röntgenstr*, vol. 184, no. 10, pp. 883–892, 2012.

[26] J. Ricke, B. Hildebrandt, A. Miersch et al., "Hepatic arterial port systems for treatment of liver metastases: factors affecting patency and adverse events," *Journal of Vascular and Interventional Radiology*, vol. 15, no. 8, pp. 825–833, 2004.

[27] M. Cantore, A. Mambrini, G. Fiorentini et al., "Phase II study of hepatic intraarterial epirubicin and cisplatin, with systemic 5-fluorouracil in patients with unresectable biliary tract tumors," *Cancer*, vol. 103, no. 7, pp. 1402–1407, 2005.

[28] T. J. Vogl, S. Zangos, K. Eichler, J. B. Selby, and R. W. Bauer, "Palliative hepatic intraarterial chemotherapy (HIC) using a novel combination of gemcitabine and mitomycin C: results in hepatic metastases," *European Radiology*, vol. 18, no. 3, pp. 468–476, 2008.

[29] J. R. A. Skipworth, S. W. M. Olde Damink, C. Imber, J. Bridgewater, S. P. Pereira, and M. Malagó, "Review article: surgical, neo-adjuvant and adjuvant management strategies in biliary tract cancer," *Alimentary Pharmacology and Therapeutics*, vol. 34, no. 9, pp. 1063–1078, 2011.

[30] M. Fuchs and W. Schepp, "Is there a nonsurgical therapeutic approach to cholangiocellular carcinomas?" *Chirurg*, vol. 77, no. 4, pp. 341–351, 2006.

[31] E. A. Eisenhauer, P. Therasse, J. Bogaerts et al., "New response evaluation criteria in solid tumours: revised RECIST guideline (version 1.1)," *European Journal of Cancer*, vol. 45, no. 2, pp. 228–247, 2009.

[32] I. Endo, M. Gonen, A. C. Yopp et al., "Intrahepatic cholangiocarcinoma: rising frequency, improved survival, and determinants of outcome after resection," *Annals of Surgery*, vol. 248, no. 1, pp. 84–96, 2008.

[33] S. Yedibela, R. Demir, W. Zhang, T. Meyer, W. Hohenberger, and F. Schönleben, "Surgical treatment of mass-forming intrahepatic cholangiocarcinoma: an 11-year western single-center experience in 107 patients," *Annals of Surgical Oncology*, vol. 16, no. 2, pp. 404–412, 2009.

[34] R. Dhanasekaran, A. W. Hemming, I. Zendejas et al., "Treatment outcomes and prognostic factors of intrahepatic cholangiocarcinoma," *Oncology Reports*, vol. 29, no. 4, pp. 1259–1267, 2013.

[35] N. J. Gusani, F. K. Balaa, J. L. Steel et al., "Treatment of unresectable cholangiocarcinoma with gemcitabine-based transcatheter arterial chemoembolization (TACE): a single-institution experience," *Journal of Gastrointestinal Surgery*, vol. 12, no. 1, pp. 129–137, 2008.

RADIATION ONCOLOGY

RESEARCH Open Access

Safety margin in irradiation of colorectal liver metastases: assessment of the control dose of micrometastases

Max Seidensticker*[1], Peter Wust[2], Ricarda Rühl[1], Konrad Mohnike[1], Maciej Pech[1], Gero Wieners[1], Günther Gademann[3] and Jens Ricke[1]

Abstract

Backround: Micrometastases of colorectal liver metastases are present in up to 50% of lesions. In this study we sought to determine the threshold dose for local control of occult micrometastases in patients undergoing CT (computed tomography)-guided brachytherapy of colorectal liver metastases.

Materials and methods: Nineteen patients demonstrated 34 local tumor recurrences originating from micrometastases after CT-guided brachytherapy of 27 colorectal liver metastases. We considered a local tumor recurrence as originating from a micrometastasis if tumor regrowth occurred adjacent to a formerly irradiated lesion and the distance of the 3D isocenter of the new lesion was ≤ 23.5 mm from the previous tumor margin. Follow-up MRI was fused with the planning-CT and dosimetry data. Two reviewers independently indicated the dose exposure at the isocenter of the micrometastases. Statistical analysis included an analysis of variance (ANOVA) using backward selection. 95% tolerance intervals with coverage of 87.5 and 75% of the data of the normal distribution were calculated.

Results: The median distance of the micrometastases to the margin of the originating colorectal metastases was 8.75 mm (1-21 mm). Dose exposure at the isocenter was 12.25 Gy (7-19.8) in median. We stratified according to the distance from the isocenter to the initial tumor margin: ≤ 9 mm, > 9-15 mm and > 15 mm. The median dose in the according isocenters was 13.18, 11.6 and 11.85 Gy. The threshold dose failing to prevent micrometastasis growth was sigificantly higher in a subgroup of lesions with ≤ 9 mm distance as compared to > 15 mm (13.18 vs 11.85 Gy). Adjuvant chemotherapy correlated with greater distance of micrometastasis growth to the tumor but not with the threshold dose.

Conclusion: To prevent loss of local tumor control by continuous growth of micrometastases a threshold dose of 15,4 Gy (single fraction) should be delivered at a distance of 21 mm to the gross tumor margin.

Backround

For the treatment of liver metastases from colorectal carcinoma, surgery as well as percutaneous image guided tumor ablation have demonstrated favourable results with respect to an improvement of the patient's prognosis [1-7]. Both the surgical as well as the minimal, or, in case of percutaneous irradiation, non-invasive approach require a safety margin around the target to reduce the risk of a recurrence and to gain a better prognosis [1,8-12]. Recent publications have drawn attention to the presence of radiologically invisible micrometastases or microsatellites, respectively (in the following we apply the term micrometastases). These micrometastases directly originate from and are found frequently adjacent to colorectal liver metastases [12-16].

Occult tumor cell nests such as micrometastases play a significant role in recurrent tumor growth after local tumor treatments. A histopathologic study of 31 liver specimen after liver resection of colorectal metastases demonstrated micrometastases deriving from neighbouring macrometastases in 56% of the cases. The mean distance between micrometastasis and originating

* Correspondence: max.seidensticker@med.ovgu.de
[1] Klinik für Radiologie und Nuklearmedizin, Universitätsklinikum Magdeburg, Otto-von-Guericke-Universität Magdeburg, Germany
Full list of author information is available at the end of the article

macrometastases was 7.5 mm (SD (standard deviation) 8 mm) [13]. Hence, treatment planning in liver metastases irradiation must not only consider the radiologically visible tumor bulk, but also the extension of subclinical disease around the gross tumor. Radiobiologically, local control of low cell densities is required. The according dose will be lower than control doses for gross tumor volumes [17,18]. Considering the distance subclinical micrometastases may have from the gross tumor volume, knowledge about the control dose for micrometastases helps to reduce the clinical target volume specifically in irradiation techniques with steep dose gradients.

In the study described herein we retrospectively analyzed recurrent tumor growth after CT-guided brachytherapy of colorectal liver metastases. We included only patients displaying tumor recurrences identified as originating from micrometastases around the initial target lesion. The aim of this study was to determine the threshold dose for local control of micrometastases of colorectal liver metastases.

Materials and methods

Patient identification

We included 19 patients (female, $n_{patients}$ = 8; male, $n_{patients}$ = 11) with a mean age of 64 years (range 49-86 years). All patients displayed nodular tumor regrowth ($n_{lesions}$ = 34) during follow up after CT-guided brachytherapy of 27 colorectal liver metastases. These tumor recurrences were classified as originating from micrometastases *(for definition of micrometastases see standard of reference)*. Primary tumor site was colon in 11 and rectum in 8 patients. After CT-guided brachytherapy, 4 patients had received chemotherapy (FOLFIRI (×1), irinotecan (×2), FU/FA (×1)) as adjuvant treatment. All other patients did not receive systemic treatment in the time interval between local treatment and confirmation of tumor regrowth.

Standard of reference and definitions

Colorectal liver metastases were confirmed by histopathology prior to the initial CT guided brachytherapy. Tumor burden prior to therapy was assessed by MRI (magnetic resonance imaging) based volumetry. Diagnosis of local tumor recurrence during follow up was confirmed by tumor growth in contrast enhanced MRI. No biopsy was taken from these tumor recurrences. We considered a local tumor recurrence to be originating from a micrometastasis if all of the following applied:

a) the new lesion occurred adjacent to a previously treated lesion.

b) the new lesion had a nodular shape applying a asymmetrical appearance in conjunction with the original, pretreated lesion.

c) The 3D isocenter of the new lesion was ≤ 23.5 mm from the initial margin of the metastasis before brachytherapy (adapted from histopathological studies by Nanko et al [13]) (figure 1).

Eligibility criteria

We excluded patients presenting a symmetric tumor regrowth of the irradiated metastasis or patients with disseminated new intrahepatic tumor deposits.

Interventional technique CT-guided brachytherapy

The technique of CT-guided brachytherapy has been described elsewhere [19]. The placement of the brachytherapy applicators was performed at a Fluoroscopy CT (Siemens, Erlangen, Germany). For treatment planning purposes, a spiral CT of the liver (slice thickness: 5 mm; increment: 5 mm) enhanced by intravenous administration of iodide contrast media (100 ml Ultravist 370, flow: 3 ml/s; start delay: 80 s) was acquired using breathhold technique after positioning of the brachytherapy catheters in the tumor.

Depending on tumor geometry and lesion size, a median of 4 catheters was used in our patients (range: 2 - 20 catheters).

The 3D CT data set acquired after catheter positioning was transferred to the treatment planning unit (BrachyVision®, Varian Medical Systems, Charlottesville, VA, USA).

A Radiooncologist defined the CTV (clinical target volume) including a safety margin of 2 mm in the 3D CT data. Threshold doses for local control of colorectal liver

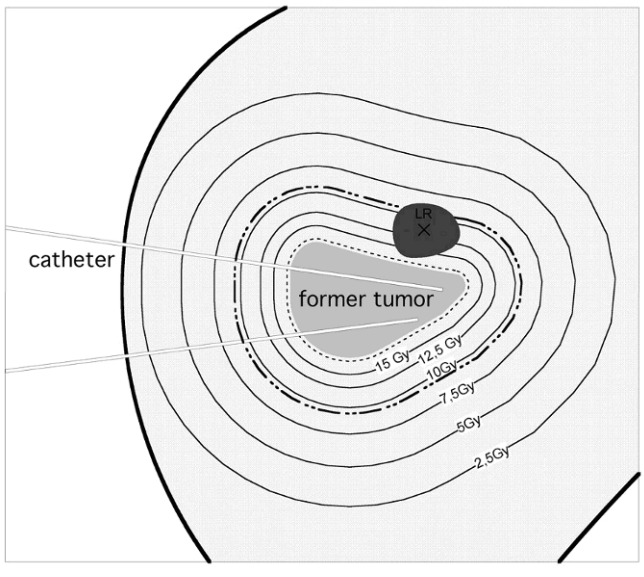

Figure 1 Scheme of a follow-up MRI merged with the initial dosimetry displaying a tumor recurrence of a micrometastasis (LR). The black cross in LR marks the 3D isocenter. The dashed line describes the CTV around the colorectal liver metastasis which had been treated initially. The bold dashed line outlines 23.5 mm distance from the initial tumor margin.

metastases using this approach have been published recently [5]. No image fusion of MRI pre treatment with planning CT was performed since in all patients tumor conspicuity on CT was sufficient for treatment planning. The prescribed and applied minimal dose inside the CTV was 15 Gy at median (12 to 25 Gy).

The high dose rate afterloading system employed a ^{192}Iridium source of 10 Ci (Gammamed®, Varian Medical Systems, Charlottesville, VA, USA). The source diameter was < 1 mm. Dwell positions were located every 5 mm. Dwell times were corrected automatically according to the actual source strength. The true mean duration of the irradiation was 2018 seconds (range: 1088 to 4666 seconds). Normalized to 10 Ci according to the actual source strength the theoretical duration would have been 1633 seconds (range: 639 to 3825 seconds). A single dose rate can not be calculated due to variable catheter geometries and differing distances of tumor tissue to the catheters. According to the irradiation time and the known minimal dose at the tumor margin a minimal dose rate can be calculated ranging from 11-84 Gy/h (mean 43).

MRI Baseline and Follow-up

All patients underwent MRI (Gyroscan NT 1.5T, Philips, Best, The Netherlands) of the liver 1 day prior to brachytherapy and in follow up 6 weeks and every 3 months after treatment. The MRI protocol consisted of the following sequences: T2-w UTSE (T2-weighted ultrafast spinecho) (TE/TR (time to echo/timo to repetition) 90/2100 ms) with and without fat suppression, T1-w GRE (T1-weighted gradient recalled echo) (TE/TR 5/30 ms, flip angle 30°) pre-contrast, 20 s post intravenous administration of 15 ml Gd-BOPTA (Gadobenate dimeglumine, Multihance®, Bracco, Princeton, USA), and 2 h post injection of intravenous Gd-BOPTA. The slice thickness was 5 mm (T1-w sequences) and 8 mm (T2-w sequences) acquired in interleaved mode with no gap applied.

Tumor assessment and image registration

Plain T1-w GRE sequences were used to determine the location and the size of nodular local tumor recurrences [20]. Image fusion of the MRI sequence showing the regrowth of the micrometastases with the former treatment plan was performed by BrachyVision®. The algorithm employs a rigid local semi-automated point based 3D-3D image registration. Match points were defined on corresponding landmarks such as branches of the portal vein to enable fusion of MR and planning CT/dosimetry data. Landmarks were restricted to the liver and chosen as close to the lesion as possible, i.e. limited to the identical liver lobe. As a result of this procedure, BrachyVision® simultaneously displayed the treatment plan as well as the anatomical structures of the MRI with a maximum deviation of < 5 mm (figure 2).

One radiologist and one radiooncologist (reader 1 and 2) evaluated the combined MRI/dosimetry data independently. The reviewers individually calculated the largest diameter of the recurrent tumor mass, its 3D-isocenter coordinates ("center of the recurrent mass") as well as the dose at this respective point. In addition, they measured the distance of the 3D isocenter to the initial tumor margin prior to the first brachytherapy. By image fusion of MRI (T1-w GRE pre contrast) 1 day prior to treatment with follow up MRI visible tumor as origin of the recurrent tumor mass could be excluded.

Statistical analysis

Results of continuous data are displayed as medians and ranges, results of frequency data as counts and percentages. For the analysis, independence between lesions within the same patient was assumed as the treatment was applied locally and not systemic, so that the treatment of one lesion did not affect a second lesion and any micrometastasis with this second lesion.

The agreement between the two readers evaluating the applied dose was measured by the intra-class correlation coefficient based on a linear model.

For two-group comparisons of the medians two-sided Wilcoxon rank sum tests were used. Measured doses were assumed to be normally distributed. Therefore t-Tests were used to test for pairwise differences in doses. We used a mixed linear model to account for the repeated measurements of doses for each lesion by the two readers. Independence was used as working correlation matrix.

Important independent factors to explain the variation of the measured dose in the center of the recurrent mass were evaluated by an analysis of variance (ANOVA) using backward selection to select significant factors. Based on the final model, 97.5% upper tolerance limits with coverage of 87.5% and 75% were calculated. The maximum upper tolerance limit (incuding 87.5% or 75% of the data, respectively) for all combinations of significant factors were used to define the "insufficient doses to prevent micrometastasis growth". The tolerance intervals were extrapolated to a maximum distance of 23 mm from the limit of the primary lesion as the data only contained data up to 21 mm. p-values below 0.05 were regarded as statistically significant.

Calculations were performed using R software (version 2.7.1, R Development Core Team (2008)) and SAS® 9.2 (SAS-Institute, Cary, NY).

Results

The mean diameter of the colorectal metastases treated by CT-guided brachytherapy was 4.5 cm (range 1.5-11 cm), the volume 50 ccm (range 3-630 ccm). The shape of the respective metastases was oligonodular (asymmetric

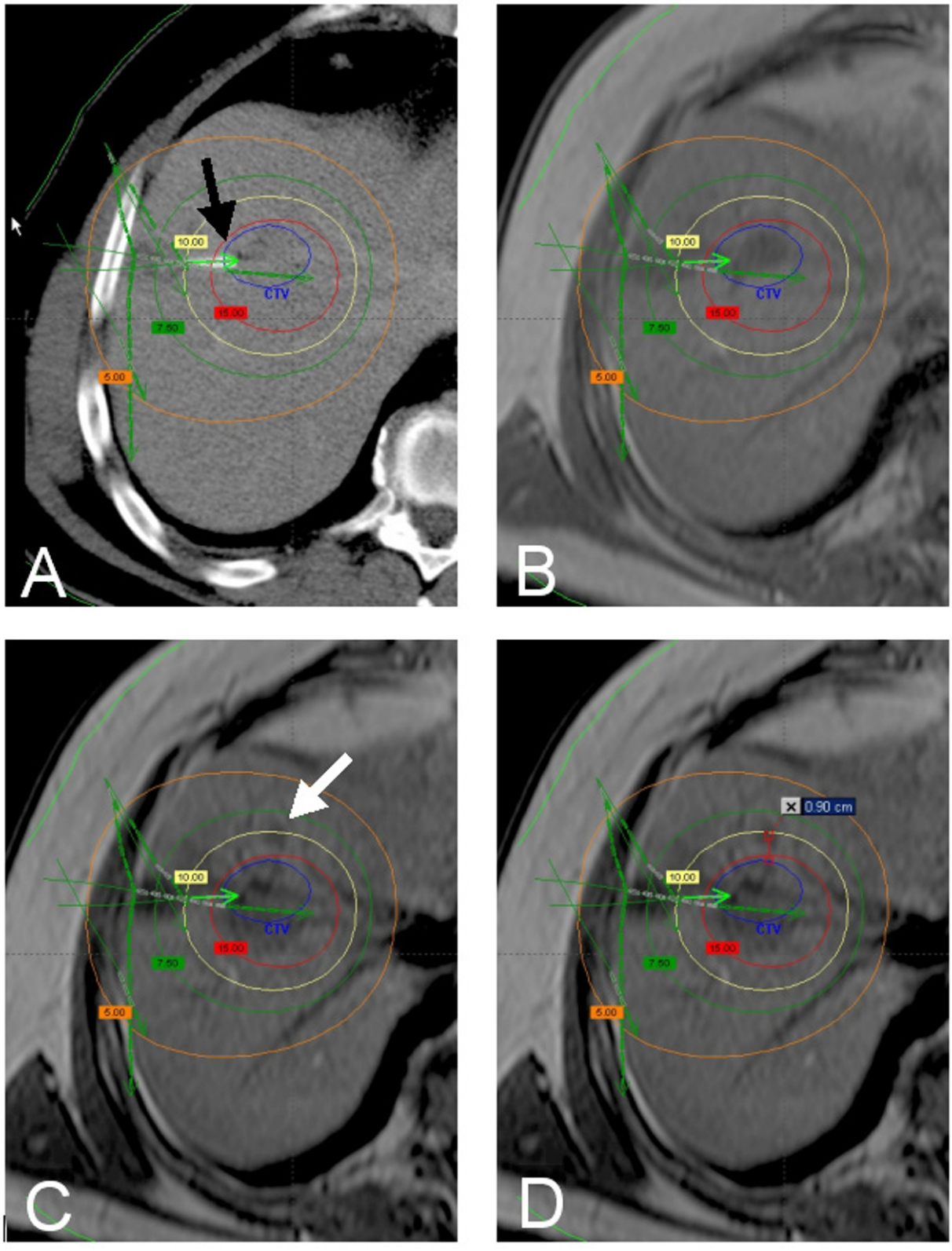

Figure 2 A: planning CT with overlayed dosimetry (BrachyVision®) showing a colorectal liver metastasis in segment 8. One catheter tip is displayed directly (black arrow), more catheters in other levels of the liver are indicated by green arrows. Verification of correct definition of the CTV was performed by image fusion of the planning CT with a MR scan (T1 GRE without contrast media) obtained 3 days prior to treatment (B). Local recurrence (white arrow) 6 months after treatment (MR, T1 GRE without contrast media, C). The distance of the 3D isocenter of the local recurrence from the initial tumor margin is 9 mm. Thus, the local tumor recurrence meets the criteria for micrometastasis growth (D). The dose initially applied in the center of the micrometastasis was 10.9 Gy.

confluent) versus round (regular spheroid) in 32% and 68% of lesions, respectively. The minimal dose at the tumor margin applied during CT-guided brachytherapy was 15 Gy (range 12-25 Gy). The activity factor of the ^{192}Iridium source was 1.17 (range 0.97-1.83).

Recurrent tumor categorized as micrometastasis growth was depicted at a mean follow up of 6 months (range 3-22 months) with 88% of all lesions occuring within 12 months.

Local tumor recurrences from micrometastases displayed a mean axial diameter of 1.5 cm (range 0.8-2.4 cm), the mean tumor volume was 1.76 ccm (0.27-7.23 ccm).

The distance of the 3D isocenter of the micrometastases to the margin of the originating colorectal metastases was 8.75 mm (range 1-21 mm, Q25: 3 mm, Q75: 15 mm).

The dose in the 3D-isocenter of the micrometastases was 12.95 Gy (Reader 1: 7.33-18.75 Gy, Q25: 10.93 Gy, Q75: 13.47 Gy) and 12.25 Gy (Reader 2: 7-19.8 Gy, Q25: 10.5 Gy, Q75: 13.5 Gy) (figure 3).

The interobserver-correlation was 0.86 (figure 4). Since the interobserver-correlation yielded this very high agreement, a cumulative evaluation was performed during further analyses.

We stratified tumor recurrences from micrometastases according to the distance from the 3D-isocenter to the initial tumor margin: ≤ 9 mm (n = 18), > 9-15 mm (n = 8) and > 15 mm (n = 8). The median dose across readers in the according isocenters was 13.18 Gy, 11.6 Gy and 11.85 Gy, respectively (figure 5). Significant pairwise differences between the groups were only found for distances ≤ 9 mm as compared to > 15 mm for the assessments across readers (p = 0.0442).

Stratification of the tumor recurrence from micrometastases according to a history of adjuvant chemotherapy (yes/no) after initial irradiation showed a significantly higher distance of the 3D-isocenter to the originating metastases when adjuvant chemotherapy was applied (p = 0.0038) (figure 6). However, despite the influence of adjuvant chemotherapy regarding the distance of the isocenter, lower dose levels at greater distances as a result of the dose gradient failed to reach significance (p > 0.05).

Results of the ANOVA analysis are displayed in table 1. Upper 97.5% tolerance limits were calculated with coverage of 87.5% and 75% of the data. In essence, doses indicated refer to the threshold doses avoiding tumor growth from micrometastases in 87.5% or 75% of the cases. The Maximum upper 97.5% tolerance limit with coverage of 87.5% for the distance of 21 was 15.4 Gy: 87.5% of the doses in the isocenters of the micrometastases with a dis-

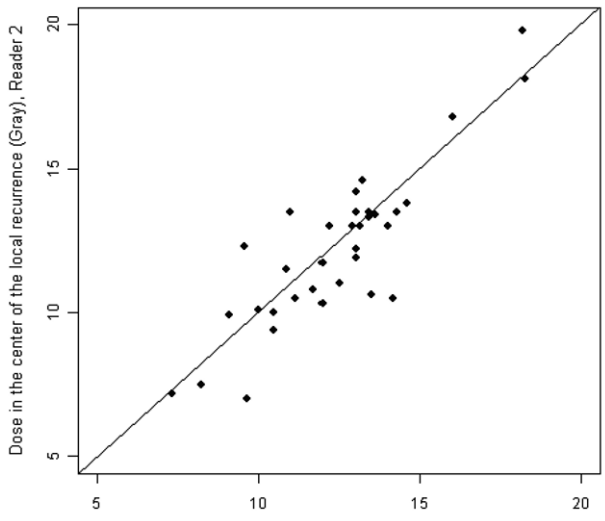

Figure 4 Intra-class correlation for comparison of the readers demonstrating a very high interobserver correlation (0.86).

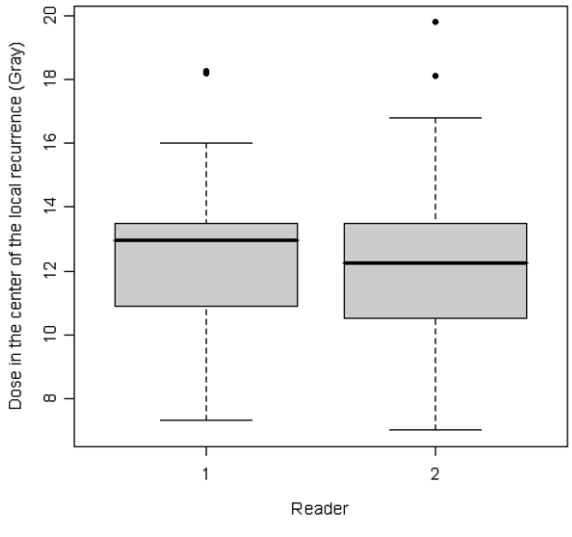

Figure 3 Boxplot of the point dose at the center of each micrometastasis as indicated by both readers.

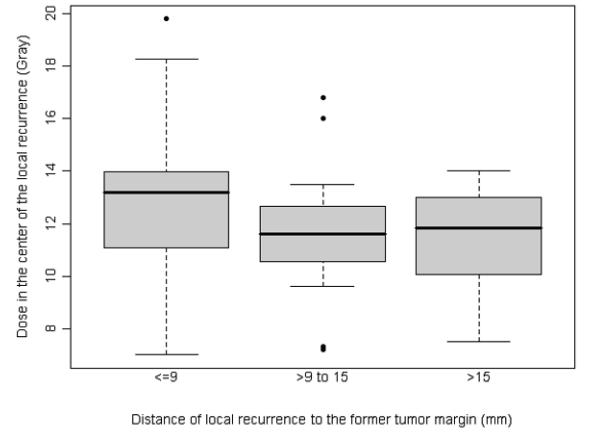

Figure 5 Boxplot of the dose at the 3D isocenter of each micrometastasis grouped according to the distance to the margin of the originating metastases across readers. The difference between the doses measured in the group ≤ 9 mm (in median 13.18 Gy) and > 15 mm (in median 11.85 Gy) was significant (p = 0.0442).

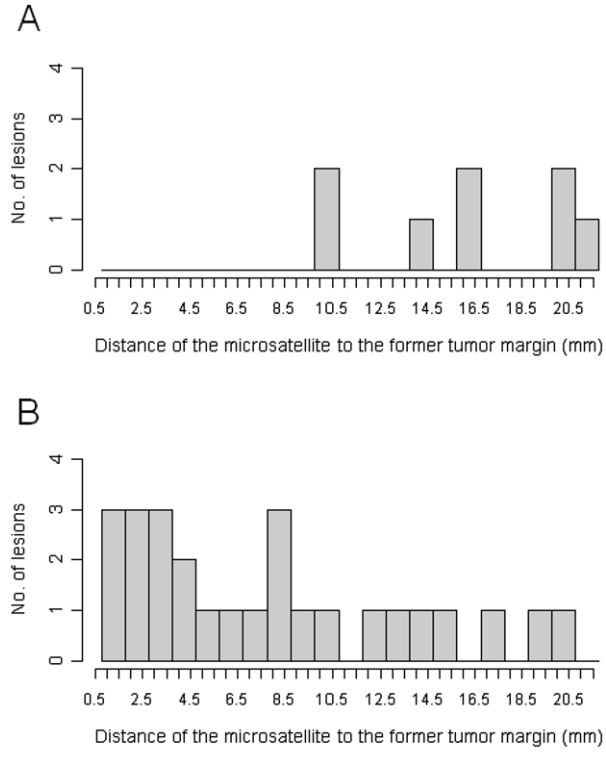

Figure 6 Distance of the micrometastases to the former tumor margin stratified by history of adjuvant chemotherapy (yes: figure 6 A, no: figure 6 B), whereas tumor growth occurred in significantly greater distance from the originating metastasis when adjuvant chemotherapy was applied (p = 0.0038)— related lower dose levels failed to reach statistical significance (p > 0.05).

tance of < 21 mm to the initial tumor margin were less than 15.4 Gy. Thus < 15.4 Gy at a distance of < 21 mm was insufficient to avoid tumor growth from micrometastases in 87.5% of the cases.

As independent factors the distance between the isocenter and the initial tumor margin (the higher the distance the lower the dose, p = 0.0004) as well as the geometry of the initial liver lesion (oligonodular shape was associated with a higher threshold dose, p = 0.009) significantly influenced the threshold doses for micrometastasis growth. The size of the irradiated colorectal liver metastases showed no influence on the threshold dose.

Discussion

In surgical and local treatment of colorectal liver metastases the margin status is consistently related to prognosis after treatment. Numerous authors have investigated the significance of margin status for resection of colorectal liver metastases [1,8-12]. Although the existence of positive margins is shown to account for a high rate of local recurrences, practical guidelines for the extent of a safety margin are not fully understood. Surgical studies dedicated to this issue have demonstrated a lower rate of local tumor recurrences in patients resected with a safety margin > 1 cm margin [9,12]. In a study of Wray et al. in 112 patients undergoing liver resection with a safety margin < 1 cm 45% developed a local tumor recurrence [9].

These clinical observations are supported by histopathological findings. Previous authors have described a direct invasion of cancer cells into bile duct and lymphatic vessels inducing satellite lesions in close distance [12,13]. The frequency of such lesions termed micrometastases or microsatellites is influenced by distance to the macrometastases, presence of a pseudocapsule, lymphocyte infiltration separating metastases and neighbouring liver parenchyma, and the morphologic type of the lesion (round vs. oligonodular) [13,14,21,22]. Histopathologically, micrometastases were depicted more often with the confluent nodular (oligonodular) morphology [22]. A recent study has proven a negative impact of oligonodular lesion shape on local progression free survival in colorectal cancer patients undergoing irradiation therapy (CT-guided brachytherapy) of liver metastases [5]. These findings suggest that the presence of micrometastases frequently found in oliginodular lesions may at least in part be responsible for early local failures.

Hence, the presence of radiologically occult micrometastases around colorectal liver metastases has to be considered when delineating the clinical target volume for local irradiation. Nanko et al. [13] described the mean distance of micrometastases to the margin of the radiologically visible macrometastases of 7.5 mm ± 8 mm. An explanation for this high standard deviation was not stated by the authors; however, a low number of micrometastases at a larger distance to the initial tumor margin might have been causative. Assuming an underlying Gaussian distribution 95% of the micrometastases were found in a distance of < 23,5 mm. This calculation led to our definition of micrometastasis regrowth, with asymmetrical, nodular growth at a total distance of ≤ 23.5 mm from the initial tumor margin after brachytherapy. In our study, the mean distance from the 3D isocenter of the micrometastases to the former tumor border was 9.6 mm ± 6.5 mm (median: 8,75 mm). This finding correlates closely with the histopathological data published by Nanko et al. of 7.5 mm ± 8 mm and it supports the validity of our definition of micrometastases [13].

Furthermore, both histopathology by Nanko et al. as well as our own data describe a higher rate of micrometastases in close proximity to the tumor margin (74 and 53% ≤ 9 mm, respectively) [13]. In addition, the cell density in these nearby lesions has been described to be higher than at greater distance [13,16]. Wakai et al described a tenfold higher cell densitiy of the micrometastases in the close zone of ≤ 10 mm around the tumor compared to the distant zone > 10 mm [16]. Radiobiologically, a higher radiation dose is needed to achieve complete cell kill in areas of higher tumor cell density [17,18].

Table 1: Results of the ANOVA analysis

Distance of the local recurrence to the former tumor margin (mm)	Maximum upper 97.5% tolerance limit with coverage of 87.5% (Gy)	Maximum upper 97.5% tolerance limit with coverage of 75% (Gy)
1	18.66	17.56
2	18.49	17.40
3	18.32	17.23
4	18.16	17.06
5	17.99	16.90
6	17.82	16.73
7	17.66	16.57
8	17.49	16.41
9	17.33	16.24
10	17.17	16.08
11	17.01	15.92
12	16.85	15.76
13	16.69	15.59
14	16.53	15.43
15	16.37	15.27
16	16.22	15.11
17	16.06	14.96
18	15.90	14.80
19	15.75	14.64
20	15.60	14.48
21	15.45	14.33
22	15.30	14.17
23	15.15	14.01

Maximum upper 97.5% tolerance limits with coverage of 87.5% and 75%. 87.5% means that 87.5% of the data (dose measured in the center of the micrometastasis) are below the upper limit of the tolerance interval (with a confidence of 97.5%).
The Maximum upper 97.5% tolerance limit with coverage of 87.5% for the distance of 21 mm was 15.4 Gy: 87.5% of the doses in the isocenters of the micrometastases with a distance of < 21 mm to the initial tumor margin were less than 15.4 Gy. Thus < 15.4 Gy at a distance of < 21 mm was insufficient to avoid tumor growth from micrometastases in 87.5% of the cases.

The histopathological proof of higher cell density of micrometastases at close proximity may well explain our own finding that micrometastases located nearby the macrometastases occurred despite marginally increased doses (table 1 and figure 5).

The inherent advantage of computed tomographic guidance for interstitial irradiation of liver malignancies is the accuracy of the dose administration whereas external beam liver radiotherapy is hampered by a discrepancy between planned and radiated target, mainly due to breathing movements of the organ (up to 10 mm in craniocaudal direction) [23,24]. Therefore, the PTV in external beam liver radiotherapy exceeds the CTV substantially [3]. In CT-guided brachytherapy the catheters are positioned and fixed inside the tumor. Hence, organ motion is not a limiting factor and the CTV and PTV are theoretically not different. An implementation of the gained data regarding the threshold dose of micrometastases in treatment planning of CT guided brachytherapy of colorectal liver metastases seems feasible whereas in external beam liver radiotherapy an additional extension of the radiated field will cumber at least the therapy of big metastases.

With respect to the methodology used, some aspects need to be discussed. First, although performing a locally focused 3D-3D registration of the liver CT and MRI the deviation was up to 5 mm. This mismatch in image registration of CT and MRI of the liver is in good congruence to other studies [25,26]. Due to different modalities and possible organ distortion between the image studies a small registration error is not avoidable. The direction of registration mismatch is variable and not systemetical, thus we do believe that the margin as calculated by us accounts for this deviation.

Second, our determination of the 3D isocenter of a micrometastasis as its primary location was based on the assumption of centrifugal tumor growth [27-30]. Simulated three-dimensional tumor growth dynamics of brain tumors by Kansal et al. revealed spherical growth even if multiple cell strains participated in growth [31].

Third, statistical analysis by ANOVA was used to determine the threshold doses failing to prevent micrometastasis growth after brachytherapy. In consequence, our assumptions are limited to the negative proof in lesions displaying treatment failure. The positive affirmation, i.e. the dose assuring micrometastasis control could not be tested since micrometastases were occult at the time of the initial treatment. However, the consistency of the data drawn from the negative proof in this study is extremely high. As can be seen in table 1, an increasing distance of the isocenter of the micrometastases from the originating metastases corresponds to a quite discrete linear dose decline for both the 87.5% and the 75% interval. Stratification in micrometastases at a distance of < 9 mm, 9-15 mm and > 15 mm revealed significance for the threshold dose only for nearby lesions compared to the very distanced lesions, a phenomenon which we attribute to the decreasing cell density of remote micrometastases as has been proven by histopathology [13,16]. In contrast to this, in CT-guided brachytherapy the dose gradient outside the CTV typically shows a strong decline to approximately 25% of the dose at a distance of 2 cm [32]. We conclude that our results gained by employing the negative proof are statistically very consistent and thus demonstrated their validity for the determination of the threshold dose to prevent recurrent micrometastasis growth.

In summary, micrometastases are frequent in patients with colorectal liver metastases. According to histopathological results, micrometastases may be encountered in up to 50% of metastases with a predominance in lesions displaying an oligonodular shape. To prevent loss of local tumor control by continuous growth of micrometastases after single fractioned irradiation of colorectal liver metastases, we recommend to deliver a dose of at least 15,4 Gy at a distance of 21 mm to the gross tumor margin. Adjuvant chemotherapy had a positive impact on the development of tumor growth from micrometastases.

Competing interests

The authors declare that they have no competing interests.

Authors' contributions

MS participated in the study design and drafted the manuscript; PW participated in the design of the study; RR performed image fusion and screened patients for inclusion; KM performed image fusion and screened patients for inclusion; MP served as reader; GW performed image fusion and screened patients for inclusion; GG served as reader; JR conceived of the study and paticipated in its design and coordination. All authors read and approved the final manuscript.

Acknowledgements

This research was not financially supported.

Special thanks to Carsten Schwenke (SCOSSiS Statistical Consulting) for his support regarding statistical analysis.

Author Details

[1]Klinik für Radiologie und Nuklearmedizin, Universitätsklinikum Magdeburg, Otto-von-Guericke-Universität Magdeburg, Germany, [2]Klinik für Strahlenheilkunde, Charité Universitätsmedizin Berlin, Campus Virchow Klinikum, Germany and [3]Klinik für Strahlentherapie, Universitätsklinikum Magdeburg, Otto-von-Guericke-Universität Magdeburg, Germany

Received: 23 December 2009 Accepted: 24 March 2010
Published: 24 March 2010

References

1. Scheele J, Stang R, Altendorf-Hofmann A, Paul M: **Resection of colorectal liver metastases.** *World J Surg* 1995, **19:**59-71.
2. Herfarth KK, Debus J, Lohr F, Bahner ML, Rhein B, Fritz P, Hoss A, Schlegel W, Wannenmacher MF: **Stereotactic single-dose radiation therapy of liver tumors: results of a phase I/II trial.** *J Clin Oncol* 2001, **19:**164-170.
3. Wulf J, Hadinger U, Oppitz U, Thiele W, Ness-Dourdoumas R, Flentje M: **Stereotactic radiotherapy of targets in the lung and liver.** *Strahlenther Onkol* 2001, **177:**645-655.

4. Siperstein AE, Berber E, Ballem N, Parikh RT: **Survival after radiofrequency ablation of colorectal liver metastases: 10-year experience.** *Ann Surg* 2007, **246:**559-565.
5. Ricke J, Mohnike K, Pech M, Seidensticker M, Rühl R, Wieners G, Gaffke G, Kropf S, Felix R, Wust P: **Local response and impact on survival after local ablation of liver metastases from colorectal carcinoma by CT-guided HDR-brachytherapy.** *Int J Radiat Oncol Biol Phys* 2010 in press.
6. Adam R, Avisar E, Ariche A, Giachetti S, Azoulay D, Castaing D, Kunstlinger F, Levi F, Bismuth F: **Five-year survival following hepatic resection after neoadjuvant therapy for nonresectable colorectal.** *Ann Surg Oncol* 2001, **8:**347-353.
7. Vogl TJ, Straub R, Eichler K, Sollner O, Mack MG: **Colorectal carcinoma metastases in liver: laser-induced interstitial thermotherapy--local tumor control rate and survival data.** *Radiology* 2004, **230:**450-458.
8. Ambiru S, Miyazaki M, Isono T, Ito H, Nakagawa K, Shimizu H, Kusashio K, Furuya S, Nakajima N: **Hepatic resection for colorectal metastases: analysis of prognostic factors.** *Dis Colon Rectum* 1999, **42:**632-639.
9. Wray CJ, Lowy AM, Mathews JB, Park S, Choe KA, Hanto DW, James LE, Soldano DA, Ahmad SA: **The significance and clinical factors associated with a subcentimeter resection of colorectal liver metastases.** *Ann Surg Oncol* 2005, **12:**374-380.
10. Fong Y, Fortner J, Sun RL, Brennan MF, Blumgart LH: **Clinical score for predicting recurrence after hepatic resection for metastatic colorectal cancer: analysis of 1001 consecutive cases.** *Ann Surg* 1999, **230:**309-318.
11. Nagashima I, Oka T, Hamada C, Naruse K, Osada T, Muto T: **Histopathological prognostic factors influencing long-term prognosis after surgical resection for hepatic metastases from colorectal cancer.** *Am J Gastroenterol* 1999, **94:**739-743.
12. Shirabe K, Takenaka K, Gion T, Fujiwara Y, Shimada M, Yanaga K, Maeda T, Kajiyama K, Sugimachi K: **Analysis of prognostic risk factors in hepatic resection for metastatic colorectal carcinoma with special reference to the surgical margin.** *Br J Surg* 1997, **84:**1077-1080.
13. Nanko M, Shimada H, Yamaoka H, Tanaka K, Masui H, Matsuo K, Ike H, Oki S, Hara M: **Micrometastatic colorectal cancer lesions in the liver.** *Surg Today* 1998, **28:**707-713.
14. Okano K, Yamamoto J, Kosuge T, Yamamoto S, Sakamoto M, Nakanishi Y, Hirohashi S: **Fibrous pseudocapsule of metastatic liver tumors from colorectal carcinoma. Clinicopathologic study of 152 first resection cases.** *Cancer* 2000, **89:**267-275.
15. Isono T, Miyazaki M, Nakajima T, Okui K, Kondo Y: **Clinicopathological significance of intrahepatic micrometastases in hepatic metastatic carcinomas.** *Nippon Geka Gakkai Zasshi* 1990, **91:**1778-1783.
16. Wakai T, Shirai Y, Sakata J, Valera VA, Korita PV, Akazawa K, Ajioka Y, Hatakeyama K: **Appraisal of 1 cm hepatectomy margins for intrahepatic micrometastases in patients with colorectal carcinoma liver metastasis.** *Ann Surg Oncol* 2008, **15:**2472-2481.
17. Buffa FM, Fenwick JD, Nahum AE: **An analysis of the relationship between radiosensitivity and volume effects in tumor control probability modeling.** *Med Phys* 2000, **27:**1258-1265.
18. Buffa FM, West C, Byrne K, Moore JV, Nahum AE: **Radiation response and cure rate of human colon adenocarcinoma spheroids of different size: the significance of hypoxia on tumor control modelling.** *Int J Radiat Oncol Biol Phys* 2001, **49:**1109-1118.
19. Ricke J, Wust P, Stohlmann A, Beck A, Cho CH, Pech M, Wieners G, Spors B, Werk M, Rosner C, *et al.*: **CT-guided interstitial brachytherapy of liver malignancies alone or in combination with thermal ablation: phase I-II results of a novel technique.** *Int J Radiat Oncol Biol Phys* 2004, **58:**1496-1505.
20. Pech M, Spors B, Wieners G, Warschewske G, Beck A, Cho C, Fischbach F, Ricke J: **Comparison of different MRI sequences with and without application of Gd-BOPTA as follow-up after LITT.** *Rofo* 2004, **176:**550-555.
21. Okano K, Maeba T, Moroguchi A, Ishimura K, Karasawa Y, Izuishi K, Goda F, Usuki H, Wakabayashi H, Maeta H: **Lymphocytic infiltration surrounding liver metastases from colorectal cancer.** *J Surg Oncol* 2003, **82:**28-33.
22. Yasui K, Hirai T, Kato T, Torii A, Uesaka K, Morimoto T, Kodera Y, Yamamura Y, Kito T, Hamajima N: **A new macroscopic classification predicts prognosis for patient with liver metastases from colorectal cancer.** *Ann Surg* 1997, **226:**582-586.
23. Herfarth KK, Debus J, Lohr F, Bahner ML, Fritz P, Hoss A, Schlegel W, Wannenmacher MF: **Extracranial stereotactic radiation therapy: set-up accuracy of patients treated for liver metastases.** *Int J Radiat Oncol Biol Phys* 2000, **46:**329-335.
24. Wulf J, Hadinger U, Oppitz U, Thiele W, Flentje M: **Impact of target reproducibility on tumor dose in stereotactic radiotherapy of targets in the lung and liver.** *Radiother Oncol* 2003, **66:**141-150.
25. Lange T, Wenckebach TH, Lamecker H, Seebass M, Hunerbein M, Eulenstein S, Gebauer B, Schlag PM: **Registration of different phases of contrast-enhanced CT/MRI data for computer-assisted liver surgery planning: evaluation of state-of-the-art methods.** *Int J Med Robot* 2005, **1:**6-20.
26. Wybranski C, Seidensticker M, Mohnike K, Kropf S, Wust P, Ricke J, Ludemann L: **In vivo assessment of dose volume and dose gradient effects on the tolerance dose of small liver volumes after single-fraction high-dose-rate 192Ir irradiation.** *Radiat Res* 2009, **172:**598-606.
27. Bru A, Albertos S, Subiza JL, Garcia-Asenjo JL, Bru I: **The universal dynamics of tumor growth.** *Biophysical Journal* 2003, **85:**2948-2961.
28. Freyer JP, Sutherland RM: **A reduction in the in situ rates of oxygen and glucose consumption of cells in EMT6/Ro spheroids during growth.** *J Cell Physiol* 1985, **124:**516-524.
29. Laird AK: **Dynamics of Tumor Growth.** *British Journal of Cancer* 1964, **18:**490-502.
30. Turner GA, Weiss L: **Some effects of products from necrotic regions of tumours on the in vitro migration of cancer and peritoneal exudate cells.** *Int J Cancer* 1980, **26:**247-254.
31. Kansal AR, Torquato S, Harsh GR IV, Chiocca EA, Deisboeck TS: **Simulated brain tumor growth dynamics using a three-dimensional cellular automaton.** *J Theor Biol* 2000, **203:**367-382.
32. Ricke J, Wust P, Stohlmann A, Beck A, Cho CH, Pech M, Wieners G, Spors B, Werk M, Rosner C, *et al.*: **CT-Guided brachytherapy. A novel percutaneous technique for interstitial ablation of liver metastases.** *Strahlenther Onkol* 2004, **180:**274-280.

doi: 10.1186/1748-717X-5-24
Cite this article as: Seidensticker *et al.*, Safety margin in irradiation of colorectal liver metastases: assessment of the control dose of micrometastases *Radiation Oncology* 2010, **5**:24

Int. J. Radiat. Biol., Vol. 84, No. 10, October 2008, pp. 830–837

informa
healthcare

Assessment of the tolerance dose of the hepatic reticulo-endothelial system (RES) after single fraction HDR-irradiation: An *in-vivo* study employing SSPIO

MACIEJ PECH[1], JENS RICKE[1], MAX SEIDENSTICKER[1], GRZEGORZ STASKIEWICZ[1], GERO WIENERS[1], KONRAD MOHNIKE[1], RICARDA RÜHL[1], JOHANNES STEINBERG[2], PETER WUST[2], & PETER SEIDENSTICKER[3]

[1]*Universitätsklinik Magdeburg, Klinik für Radiologie und Nuklearmedizin, Magdeburg,* [2]*Charite Berlin – Virchowklinikum, Klinik für Strahlenheilkunde, Berlin, and* [3]*Bayer-Schering AG, Berlin, Germany*

(Received 6 January 2008; revised 6 June 2008; accepted 22 July 2008)

Abstract

Purpose: To prospectively assess a dose-response relationship for the hepatic reticulo-endothelial system (RES) after small volume single fraction irradiation of liver parenchyma *in vivo*.

Materials and methods: Twenty-five liver tumors were treated by computed tomography (CT)-guided interstitial brachytherapy. Magnetic resonance imaging (MRI) was performed 1 day before and 3 days, 6, 12 and 24 weeks after therapy. MR-sequences included T2-w Turbo Spin Echo (TSE) enhanced by hepatic RES targeted Standard Superparamagnetic Iron Oxide (SSPIO). All MRI data sets were merged with three dimensional (3D) dosimetry data and evaluated by two radiologists. We estimated the threshold dose for either edema or function loss as the D90. A match-pair analysis was performed with another 25 liver tumors, which were treated the same but had MRI follow-up using the hepatocyte specific MRI contrast media Gadobenate dimeglumine (Gd-BOPTA).

Results: Three days post brachytherapy the D90 for hepatic RES function loss reached the 18.3 Gray (Gy) isosurface (Standard Deviation (SD) 7.7). At 6 weeks, the respective zone had increased significantly to the 12.9 Gy isosurface (SD 4.4). After 12 and 24 weeks, the dysfunction of liver volume decreased significantly to the 15 Gy and 20.4 Gy isosurface respectively (SD 7.1 and 10.0). Comparison to the hepatocyte function loss indicates a higher minimal threshold dose of the hepatic RES.

Conclusion: Hepatic RES demonstrated a high regenerative capacity and a higher minimal threshold dose than hepatocytes. Temporary function loss was found from the 13 Gy isosurface.

Keywords: *Brachytherapy, dosimetry-radiation, liver*

Introduction

The radiotherapy of liver malignancies has made considerable advances within the last few years. Percutaneous stereo-tactical approaches such as brachytherapy procedures and transarterial application of open isotopes such as Yttrium90 have made an impact in clinical treatment (Herfarth et al. 2001, Stubbs et al. 2001, Ricke et al. 2004, Herfarth et al. 2004, Welsh et al. 2006). The dose tolerance assessment of intact liver parenchyma for the determination of the compatibility of such a procedure is essentially based on knowledge published in 1991 (Emami et al. 1991). A dose limiting value was established with arithmetical models for the development of radiation-induced hepatitis. Detailed knowledge of hepatic subsystems such as the reticulo-endothelial system (RES) and it's vulnerability for dose exposure was unknown, and until now, not examined *in vivo*.

This dose response relationship is important in individual treatment strategies for patients with larger tumor volumes, after liver resection or with multiple and recurrent lesions requiring repetitive irradiations.

The purpose of the study is to assess the dose threshold with an *in vivo* model for the sensitivity of

Correspondence: Dr Maciej Pech, Universitätsklinik Magdeburg, Klinik für Radiologie und Nuklearmedizin, Leipziger Strasse 44, Magdeburg, 39120 Germany. E-mail: maciej.pech@med.ovgu.de

ISSN 0955-3002 print/ISSN 1362-3095 online
DOI: 10.1080/09553000802389660

the RES in the liver and a comparison to the hepatocyte function after irradiation. We examined patients treated with Computed Tomography (CT)-guided brachytherapy of liver malignancies (Ricke et al. 2004). Magnetic Resonance Tomography (MRI) is a sensitive tool for the detection of edema during follow up after irradiation. Adding the RES directed contrast agent Standard Superparamagnetic Iron Oxide (SSPIO, Resovist®, Bayer Schering, Berlin, Germany) or the hepatocyte directed contrast agent Gadobenate dimeglumine (Gd-BOPTA, Multihance®, Bracco, Princeton, NJ, USA) to the MRI examination enables the visualization of eventual function loss of the hepatic RES and hepatocytes with a high contrast to noise ratio (Stark et al. 1988, Kopp et al. 1997, Muller et al. 1999, Rohlfing et al. 2000, Schnorr et al. 2006). The clinical end-point is SSPIO and Gd-BOPTA-enhanced MRI visualization of the loss of phagocytosis of the RES and the loss of hepatocyte function, respectively.

Materials and methods

Twenty-one patients with 25 malignancies were included in this prospective study. Either to patients wish or due to technical irresectability or extrahepatic tumor spread surgical options were refused. All patients were scheduled to receive High Dose Radiation (HDR) single fraction brachytherapy. The institutional ethical committee approved the study. Written informed consent was obtained from all patients.

The patient population was comprised of 11 men and 10 women; the mean age was 66 years (range: 52–79). Primary malignancies were colo-rectal carcinoma in 15 patients, breast cancer in four, hepatocellular carcinoma (HCC) in four and Gastrointestinal Stromal Tumor (GIST) in two. One day prior to the intervention and 3 days, 6, 12 and 24 weeks after we assessed the following laboratory parameters: prothrombin time (PT), bilirubin, aspartate aminotransferase (AST), alanine aminotransferase (ALT), alkaline phosphatase (AP), albumin, ammonia (NH_3), international Normalized ration (INR) and C-reactive protein (CRP). No patient presented evidence of liver function degradation prior to therapy. All patients demonstrated a Karnofsky score higher than 80%. All patients with a HCC suffered an underlying cirrhosis, all of Child-Pugh score A. Elevations of liver function tests in the follow-up were graded according to the common toxicity criteria of the Radiation Therapy and Oncology Group (RTOG).

The technique of CT-guided brachytherapy has been described in the literature (Ricke et al. 2004). We used fluoroscopy CT guidance for brachytherapy applicator placement (Siemens, Erlangen, Germany). For treatment planning purposes, a spiral CT of the liver (slice thickness: 5mm; increment: 5 mm) enhanced by i.v. application of iodide contrast media (100 ml Ultravist 370 (Bayer Schering, Berlin, Germany) flow: 1ml/s; start delay: 80s) was acquired in breath-hold technique after positioning of the brachytherapy catheters in the tumor. Each patient received three catheters on the average (range: 1–8 catheters).

We used 10 Ci (Curie)^{192}Iridium afterloading with a radiation source diameter < 1 mm. Dwell positions were located every 5 mm. Treatment planning was performed using the software system Abacus 3.0 integrated in the controller of the HDR-afterloading system (Gammamed, Varian, Charlottesville, VA, USA). The relative coordinates (x, y, z) of the catheters were determined in the CT dataset and transferred manually in the treatment planning system. A reference dose of 15–25 Gray (Gy) enclosing the lesion (clinical target volume) was prescribed in our patients and applied as a single dose. No maximum dose constraints were given inside the tumor volume. To preserve liver function after irradiation, at least one-third of the liver parenchyma had to receive < 5 Gy. The irradiation time was between 20 and 40 minutes.

A total of 76 MRI examinations were performed in 21 patients, 3 days, 6, 12 and 24 weeks after tumor ablation (Gyroscan NT® 1.5T, Philips, Best, The Netherlands). Missing MRI scans were most from week 24 ($n = 6$). The MRI protocol comprised of the following sequences: T2-w breathing-triggered Ultra Short Turbo Spin Echo (UTSE) (Echo Time (TE)/ Repetition Time (TR) 90/2100 ms) with and without fat suppression, T1-w breath-hold Gradient Recalled Echo (GRE) (TE/TR 5/30 ms, flip angle 30°) pre contrast, 20s post i.v. application of 0.9 or 1.4 ml of SSPIO and T2-w breathing-triggered UTSE (TE/ TR 90/2100 ms) with and without fat suppression with SSPIO 10 min. post i.v. application. The slice thickness was 8 mm acquired in interleafed mode with no gap applied.

The technique of image fusion and volumetry has been described in the literature (Ricke et al. 2005). Volumetry of the liver, the tumor, or the liver and tumor volume receiving more than 10 Gy were performed by using the Digital Imaging and Communication in Medicine (DICOM) CT data acquired after applicator positioning and a proprietary viewing and image processing software (Jive X, VISUS TT, Bochum, Germany).

To merge dosimetry data calculated for CT-guided brachytherapy with the MRI data acquired in this study, the isodose plan was three dimensional (3D) digitized. We performed 3D interpolation using a cubic shape function for continuous isodose values. In the next step, this data was merged with the

CT data set acquired for treatment planning. Finally, the data set containing the CT and the dosimetry was merged with each MRI acquired prior to therapy and during the six months follow up. Typically, MRI and CT are acquired in different breath-hold phases. In our study, CT was acquired as a single breath-hold sequence and a breath-triggered technique was used for T2-w UTSE. A complete image fusion between CT and different MRI sequences would therefore require an elastic 3D image transformation. In our study we evaluated only radiation effects on the liver. MRI data was limited to liver parenchyma and a surrounding margin of approximately 2 cm. The reduced image was merged with the CT-dosimetry data set using anisoscalar image fusion. The registration routine of the algorithm has been described by Studholme et al. (1997). It is based on normalized mutual information (Studholme et al. 2005). We used a modified independent implementation within the 3D visualization software Amira® (Visage Imaging Inc., Carlsbad, CA, USA). The image fusion accuracy of the liver was found to always be better than 5 mm for the liver surface

Two radiologists evaluated independently the combined MRI and dosimetry data. On the T2-w as well as the T2-w SSPIO enhanced images, the reviewers indicated the border of hyperintensity on T2-w images (edema) or hyperintensity on T2-w images with SSPIO (loss of hepatic RES function) around the irradiated liver tumor (referred to as 'pseudolesion' in the following) (Figures 1 & 2).

Figure 1. Contrast enhanced CT after CT-guided positioning of two brachytherapy catheters (arrows) in a metastasis of a colorectal carcinoma. Second Lesion (arrow head) near resection margin after right hemihepatectomy displays a thermal necrosis after radiofrequency ablation.

Amira® software calculated a dose-volume histogram based on the total 3D data set (Figure 3). As a result, we determined the percentage of each pseudolesion covered by a specific dose and higher. We assumed a 10% error of the overall methodology, including fusion mismatches. Hence, we estimated the threshold dose for either edema or function loss as the D_{90}, i.e., the dose achieved in at least 90% of the pseudolesion volume.

To determine intraobserver variations and to establish the reliability of the image fusion process, four randomly selected patients underwent image fusion as well as the review process repeatedly in two sessions separated by one week. A Kendall W test was applied to establish significance for intra- as well as interobserver variations.

The t-test and the Spearman correlation were applied to evaluate the dynamics of the pseudolesion development over time. We tested a chemotherapy treatment as well as the ^{192}Iridium source activity as independent factors influencing the hepatic tissue tolerance.

To compare hepatic RES function with hepatocyte function loss, we performed a match-pair analysis with another 25 liver tumors in 25 patients, which were treated the same but radiation damage was evaluated with hepatocyte-targeted contrast agent Gd-BOPTA instead of SSPIO in the MRI follow-up. Match criteria were tumor histology, tumor volume, absence of functional liver disease in non cirrhotic patients and Child Pugh score A in the patients suffering a HCC in cirrhosis. Image fusion and statistical analysis were applied in the same manner as previously described.

Results

Figure 4 demonstrates the development of edema or hepatic RES function loss over time. Between three days and six weeks, the extension of the edema increased significantly from the 12.9 Gy isosurface to 9.9 Gy (Standard Deviation (SD) 3.3 and 2.6, respectively; $p = 0.006$). No significant change was detected between 6 and 12 weeks (11.1 Gy, SD 2.6; $p = 0.281$). After 24 weeks, the edematous tissue had significantly shrunk to the isosurface of 14.7 Gy (SD 4.2; $p = 0.002$).

Three days after brachytherapy, the D_{90} for hepatic RES function loss was 18.3 Gy isosurface (SD 7.7). At six weeks, the respective zone had increased significantly to the 12.9 Gy isosurface (SD 4.4; $p = 0.001$). The dysfunctional volume had decreased to the 15.0 Gy isosurface between 6 and 12 weeks (SD 7.1; $p = 0.073$). After 24 weeks, the volume decreased further to the 20.3 Gy isosurface (SD 10; $p = 0.118$).

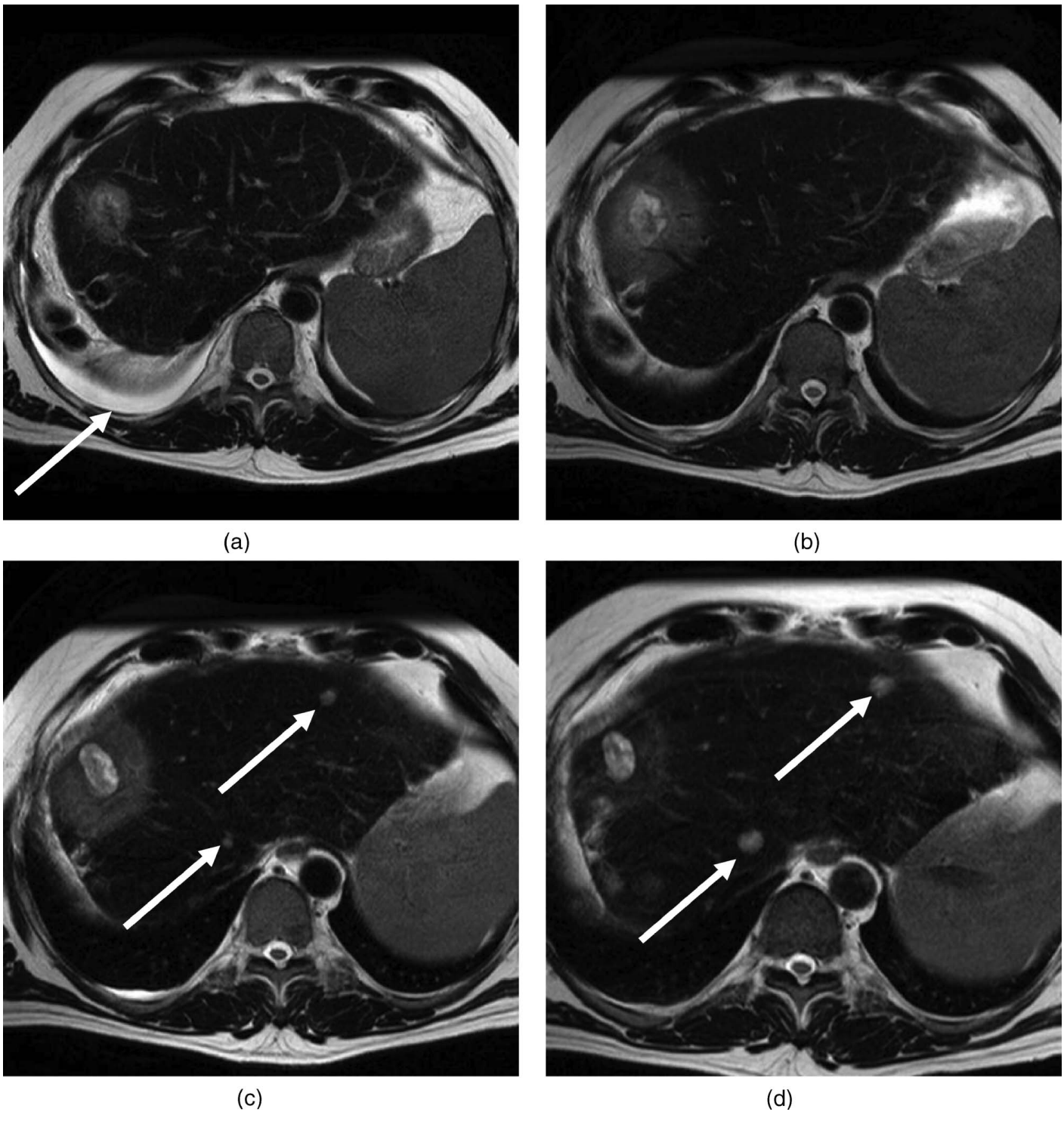

Figure 2. MRI acquired 3 days (a), 6 weeks (b), 12 weeks (c) and 24 weeks (d) after brachytherapy. T2-w TSE post i.v. application of SSPIO. Development of a hyperintense rim around the tumor lesion through diminished uptake of contrast agent indicating hepatic RES dysfunction. Note in figure (a) a small pleural effiusion (arrow) after treatment and in figures (c & d) a manifestation of new metastasis (arrows) under chemotherapy and no progression of the treated metastasis after CT-guided brachytherapy. No further local treatment of the new liver metastases was performed due to multiple intra- and extrahepatic tumor deposits.

The minimal dose causing edema was significantly less than the dose causing the hepatic RES function loss ($p < 0.001$) three days post brachytherapy. No differences between the doses were noted at six weeks ($p = 0.9$). At 12 and 24 weeks, edema again occurred in areas of less dose exposure when compared to areas of hepatic RES function loss (both $p = 0.02$).

Interobserver and intraobserver correlation as determined by the Kendall W test were highly significant with a coefficient of 0.93 and 0.94 respectively (both $p < 0.001$).

The average target volume was 65 ml (range: 1–329 ml). There was no correlation between the target volume and the threshold tolerance of adjacent hepatic tissue.

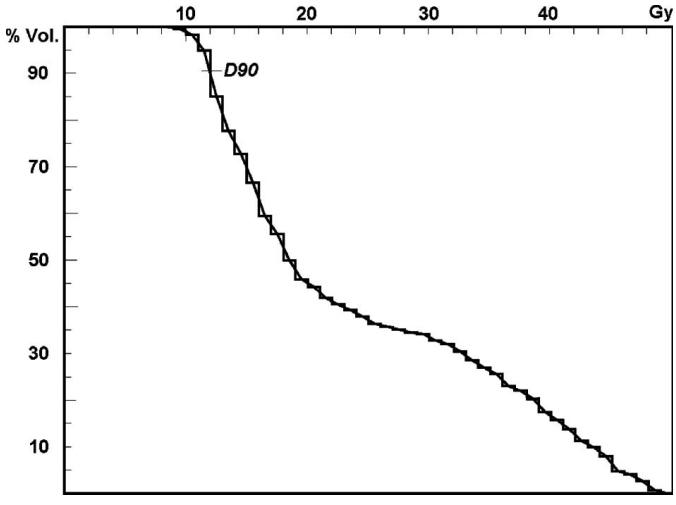

Figure 3. Patient No. 11. Dose-volume histogram day 3 post brachytherapy demonstrating the dose distribution in the edema. D_{90} is 12 Gy.

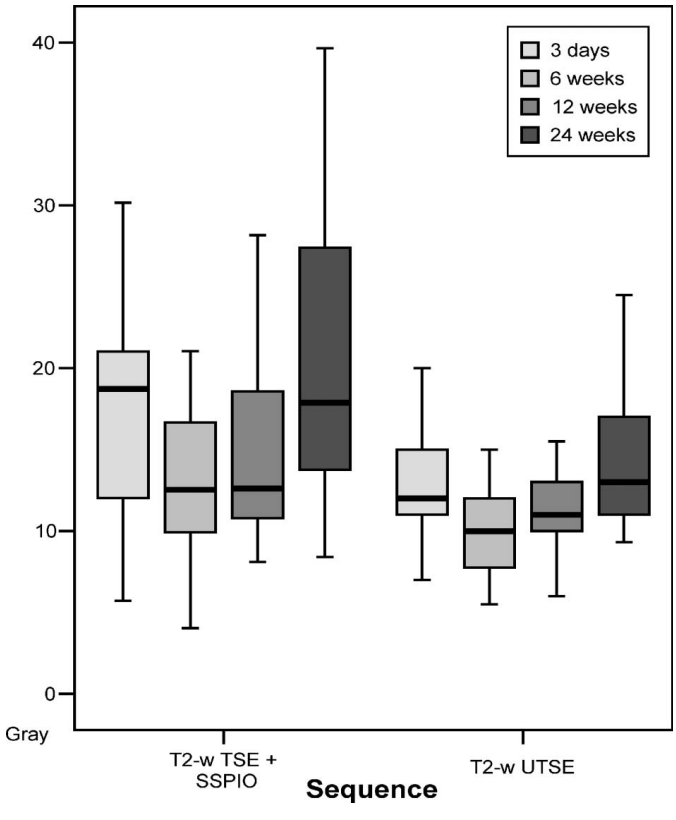

Figure 4. Development of edema (T2-w UTSE) depending on time versus dose exposition and development of the area of hepatic RES function loss (T2-w, TSE + SSPIO). Error bars indicate the standard error of the mean for each $n = 25$ independent experiments.

The source factor of the ^{192}Iridium afterload varied between 0.91 and 1.76 (median 1.19). We found no correlation between the dose tolerance of the liver tissue and the source factor. We found no correlation between the dose tolerance of the liver tissue and the history of chemotherapy or diagnosis of liver cirrhosis.

All patients included in this study demonstrated no significant sustained degradation of liver function after CT-guided brachytherapy: Grade 1 toxicities were recorded in 40% ($n = 10$) in the SSPIO group and in 56% ($n = 12$) in the Gd-BOPTA group 3 days after radiotherapy. Grade 2 were seen in 12% ($n = 3$) and in 20% ($n = 5$) 3 days after radiation therapy, respectively. Increased liver function tests resolved to baseline level after 6 weeks in all cases and stayed normal.

Figure 6 depicts the results of the match-pair analysis between hepatocyte and hepatic RES function loss development over time. A significant difference of threshold doses for hepatocyte or hepatic RES function loss was found at six weeks with hepatic RES being more resistant or higher regenerative against dose exposure ($p = 0.008$).

Discussion

Several therapies have been developed and evaluated clinically within the last few years for the treatment of primary or secondary liver malignancies. These techniques include percutaneous stereotactic irradiation as fractionated treatment and catheter based CT-guided brachytherapy as a one time treatment (Herfarth et al. 2001, Ricke et al. 2004, Herfarth et al. 2004).

An exact knowledge of the hepatic dose tolerance is required for the therapy plan in both techniques. End-point of the data in the literature is usually the onset of a symptomatic radiation induced hepatitis (RILD). The size of the irradiated volume in relation to non-exposed, thus yet functional parenchyma is of considerable importance for the development of clinical signs of RILD. Emami arithmetically calculated 30 Gy as a threshold dose for fractionated irradiation treatment of the whole liver and 50 Gy for the partial liver (Emami et al. 1991). The α/β model was used with a value of 2 for the liver parenchyma. Lawrence et al. reported a threshold dose of 45 Gy. Yamasaki et al. describe a focal liver reaction in 73% of patients treated with 48 Gy and in 86% treated with 72.8 Gy (Lawrence et al. 1995, Yamasaki et al. 1995). These data describe the threshold dose of the whole liver function to irradiation and allow no differentiation of the threshold dose of the cell types within the liver. No in vivo studies on the threshold dose of hepatic RES, neither to fractionated nor to single fractioned irradiation is present.

Previous authors describe small volume stereotactic irradiation or CT-guided brachytherapy, employing the end-point 'function loss of hepatocytes' by using a hepatocyte target contrast medium threshold of 15 Gy (Ricke et al. 2005), and for the end-point 'signal breakdown of the liver tissue in CT' of also 15 Gy (Herfarth et al. 2003). The development of a clinically comprehensible radiation-induced hepatitis was not decisive in two

publications, but changes in the liver imaging by means of contrast media enhanced MRI or non-contrast CT as a surrogate parameter were considered (Herfarth et al. 2003, Ricke et al. 2005).

Comparable to the data on hepatocyte threshold dose by Ricke et al. we were able to show a dynamic in the development of the function loss of hepatic RES with a maximum after 6 weeks and a partial regeneration in the following 18 weeks (Ricke et al. 2005).

The understanding of the hepatic reaction to irradiation is particularly of great importance when larger tumor volumes or multiple tumors distributed throughout the liver cause cumulative effects within large or overlapping treatment volumes.

At present, the development of radiation-induced liver disease or a hepatocyte function loss is still unsolved. Endothelial cells are primarily targeted which lead to erythrocyte accumulation and the impression of a veno-occlusive pathology in the sinusoids, as displayed by a biopsy taken from a non-study subject one year after CT-guided brachytherapy (Figure 5) (Fajardo & Berthrong 1978, Fajardo & Colby 1980, Cromheecke et al. 2000). The dose tolerance of hepatocytes with the endpoint cell death appears to be considerably higher and does not correlate with the function loss of a given liver volume after irradiation treatment (Alati et al. 1988). Experimental studies on hepatic radiation injury using clonogenic assay show that the endothelial lining of venules and sinusoids is far more sensitive to radiation than hepatocytes. Studies on the D_0, the dose of irradiation that reduces the number of *in vitro* confluent cells in culture to 37%, of hepatocytes and non-parenchymal cells indicate that endothelium has a greater radiosensitivity than hepatocytes. (Jirtle et al. 1981, Johnson et al. 1982, Rubin 1984). No *in vitro* studies directed solely on the dose tolerance of the RES of the liver are present.

Furthermore the question must be addressed whether the loss of a large-volume of hepatic RES may cause any clinical symptoms after irradiation treatment, or whether the loss of the large RES volume is tolerated without function loss. Previous data suggests that early hepatic RES and stellate cell activation together with congestive changes plays an important role in radiation induced liver injury and ensuing fibrosis (Sempoux et al. 1997). In our study the results the loss of the hepatic RES function correlated clearly with the parameters for the hepatocyte function. The match pair analysis showed a significant difference with dose threshold increase for the hepatic RES function only after six weeks (Figure 6). The reason for this isolated mismatch remains unclear and may well result from statistical errors.

Some restrictions apply to our study. The maximum error caused by the fusion technique employed for MRI follow-up images and CT-dosimetry never exceeded 5 mm. However, a systematic error in dose computation in our 21 patients occurred, it would probably have little impact on the statistical result of our findings. The image fusion software uses voxel-based registration to perform an aniso-scalar adaptation of the CT-dosimetry images to the follow up MRI. However, voxel-based techniques working directly on the image grey-values have recently been shown to be far superior to other

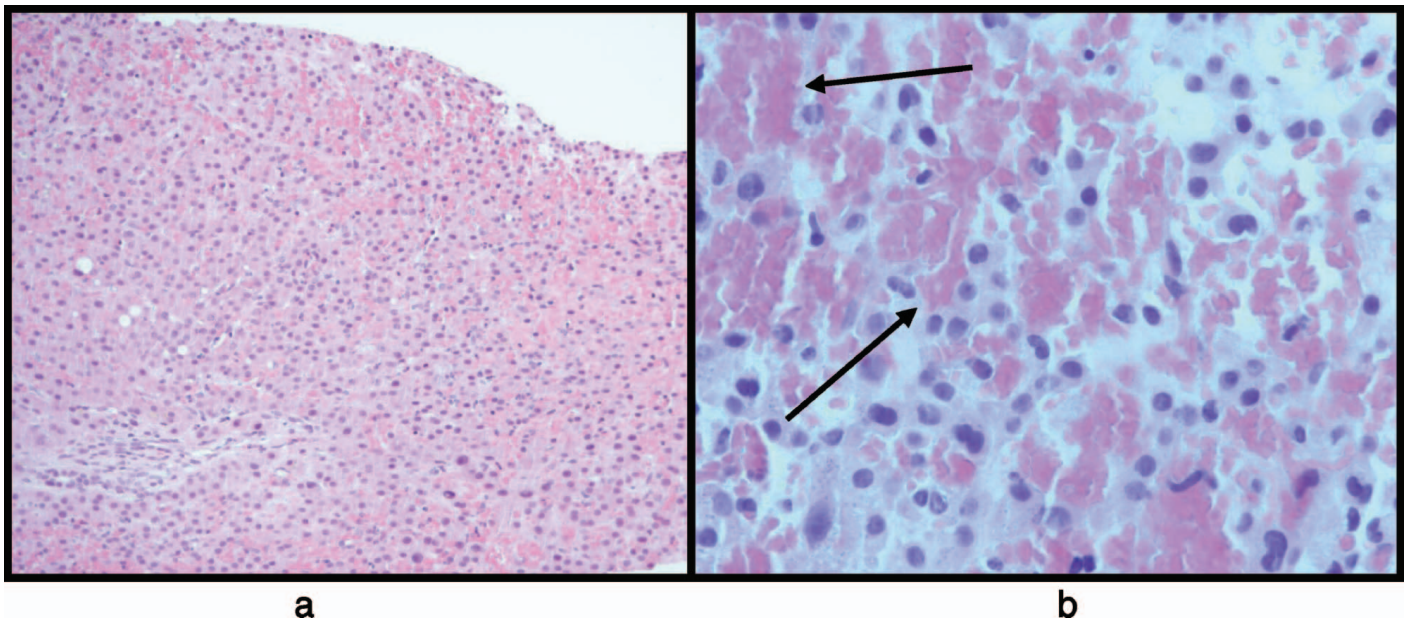

Figure 5. (a) Liver (hematoxylin-eosin, ×100). Histologic section acquired by liver biopsy one year after single-fraction irradiation by CT-guided brachytherapy. Exposure approximately 14–16 Gy. (b) Sinusoids shows erythrocyte accumulation and the impression of a veno-occlusive pathology (arrow) (×400). Patient did not belong to study group.

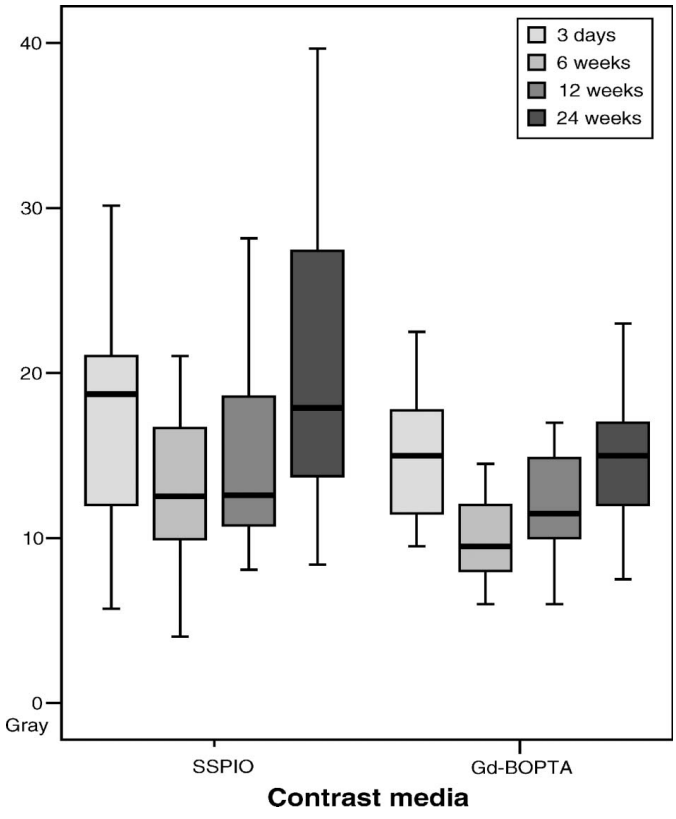

Figure 6. Development of hepatocyte function loss (Gd-BOPTA) depending on time versus dose exposure and demarcation of the area of hepatic RES function loss (SSPIO). Error bars indicate the standard error of the mean for each $n = 25$ independent experiments.

methods such as surface-based registration (West et al. 1999, Rohlfing et al. 2000). Intraobserver as well as interobserver correlation was excellent and significant.

Additionally an error due to variably predamaged liver tissue by chemotherapy or by underlying liver cirrhosis can be discussed. However, as mentioned above, at least no correlation of the calculated threshold dose and the history of chemotherapy or diagnosis of liver cirrhosis could be found.

SSPIO, a polycrystalline superparamagnetic iron oxide particulate coated with dextran. After intravenous administration, particles are cleared by the RES, including the Kupffer cells in the liver, which account for 80% of the clearance of the injected dose. The clearance induces a strong decrease in the liver signal by creating local field inhomogeneities (Saini et al. 1987, Weissleder et al. 1989, Majumdar et al. 1990, Ferrucci & Stark 1990, Stubbs et al. 2001). With *in vivo* MR imaging in animals as well as humans, liver signal blackening shows a reversal toward normal baseline tissue characteristics over 3–7 days (Saini et al. 1987, Stark et al. 1988). However, shortly after injection a blunted decline in signal intensity in irradiated areas is indicative of decreased Kupffer cell extraction of this particular contrast agent. Since we use SSPIO enhanced MRI as a surrogate marker for RES function, it should be discussed whether an assumed radiation induced VOD as underlying pathology could influence the accumulation of SSPIO by hindered blood flow in the irradiated liver tissue. This could lead to an underestimation of the threshold dose of the RES. The main question is, on which mechanism the loss of the iron phagocytosis is based on, relative to the reported values in the irradiated area. Particularly the high similarity of the dose values in comparison with the hepatocyte function loss after irradiation treatment raises the question, whether similar mechanisms for the function failure of both systems are responsible. More exact knowledge is needed as to whether a direct cytotoxic damage of the hepatic RES or whether for the hepatocytes a pseudo venous-occlusion disease initiates the loss of function in the irradiated area.

Given the fact that the meaning of the function loss of hepatic RES is still unclear, the most important result of our study is the finding that a circumscribed function loss of the hepatic REC corresponded well with the functional status of the hepatocytes. Interestingly the sensitivity of the hepatic RES to radiation exposure does not exceed the sensitivity of hepatocytes or their function and show, as well as hepatocytes, a regenerative potential after irradiation. The implementation of the assumed threshold dose of hepatic RES and hepatocytes in treatment planning can afford a higher safety in single fractioned radiotherapy of the liver.

Nevertheless, the clinical consequences of an isolated hepatic RES function loss in large liver volumes are unclear.

Declaration of interest: The authors report no conflicts of interest. The authors alone are responsible for the content and writing of the article.

References

Alati T, Van Cleeff M, Strom SC, Jirtle RL. 1988. Radiation sensitivity of adult human parenchymal hepatocytes. Radiation Research 115(1):152–160.

Cromheecke M, Konings AW, Szabo BG, Hoekstra HJ. 2000. Liver tissue tolerance for irradiation: experimental and clinical investigations. Hepatogastroenterology 47(36):1732–1740.

Emami B, Lyman J, Brown A, Coia L, Goitein M, Munzenrider JE, Shank B, Solin LJ, Wesson M. 1991. Tolerance of normal tissue to therapeutic irradiation. International Journal of Radiation Oncology, Biology & Physics 21(1):109–122.

Fajardo LF, Berthrong M. 1978. Radiation injury in surgical pathology. Part I. American Journal of Surgery Pathology 2(2):159–199.

Fajardo LF, Colby TV. 1980. Pathogenesis of veno-occlusive liver disease after radiation. Archives of Pathology & Laboratory Medicine 104(11):584–588.

Ferrucci JT, Stark DD. 1990. Iron oxide-enhanced MR imaging of the liver and spleen: Review of the first 5 years. American Journal of Roentgenology 155(5):943–950.

Herfarth KK, Debus J, Lohr F, Bahner ML, Rhein B, Fritz P, Hoss A, Schlegel W, Wannenmacher MF. 2001. Stereotactic single-dose radiation therapy of liver tumors: Results of a phase I/II trial. Journal of Clinical Oncology 19(1):164–170.

Herfarth KK, Debus J, Wannenmacher M. 2004. Stereotactic radiation therapy of liver metastases: update of the initial phase-I/II trial. Frontiers in Radiation Therapy in Oncology 38:100–105.

Herfarth KK, Hof H, Bahner ML, Lohr F, Hoss A, van Kaick G, Wannenmacher M, Debus J. 2003. Assessment of focal liver reaction by multiphasic CT after stereotactic single-dose radiotherapy of liver tumors. International Journal of Radiation Oncology, Biology & Physics 57(2):444–451.

Jirtle RL, Michalopoulos G, McLain JR, Crowley J. 1981. Transplantation system for determining the clonogenic survival of parenchymal hepatocytes exposed to ionizing radiation. Cancer Research 41(9 Pt 1):3512–3518.

Johnson LK, Longenecker JP, Fajardo LF. 1982. Differential radiation response of cultured endothelial cells and smooth myocytes. Analytical and Quantitative Cytology 4(3):188–198.

Kopp AF, Laniado M, Dammann F, Stern W, Gronewaller E, Balzer T, Schimpfky C, Claussen CD. 1997. MR imaging of the liver with Resovist: safety, efficacy, and pharmacodynamic properties. Radiology 204(3):749–756.

Lawrence TS, Robertson JM, Anscher MS, Jirtle RL, Ensminger WD, Fajardo LF. 1995. Hepatic toxicity resulting from cancer treatment. International Journal of Radiation Oncology, Biology & Physics 31(5):1237–1248.

Majumdar S, Zoghbi SS, Gore JC. 1990. Pharmacokinetics of superparamagnetic iron-oxide MR contrast agents in the rat. Investigative Radiology 25(7):771–777.

Muller RD, Vogel K, Neumann K, Hirche H, Barkhausen J, Stoblen F, Henrich H, Langer R. 1999. SPIO-MR imaging versus double-phase spiral CT in detecting malignant lesions of the liver. Acta Radiologica 40(6):628–35.

Ricke J, Seidensticker M, Ludemann L, Pech M, Wieners G, Hengst S, Mohnike K, Cho CH, Lopez HE, Al Abadi H, Felix R, Wust P. 2005. In vivo assessment of the tolerance dose of small liver volumes after single-fraction HDR irradiation. International Journal of Radiation Oncology, Biology & Physics 62(3):776–784.

Ricke J, Wust P, Stohlmann A, Beck A, Cho CH, Pech M, Wieners G, Spors B, Werk M, Rosner C, Hanninen EL, Felix R. 2004. CT-guided interstitial brachytherapy of liver malignancies alone or in combination with thermal ablation: phase I-II results of a novel technique. International Journal of Radiation Oncology, Biology & Physics 58(5): 1496–1505.

Rohlfing T, West JB, Beier J, Liebig T, Taschner CA, Thomale UW. 2000. Registration of functional and anatomical MRI: Accuracy assessment and application in navigated neurosurgery. Computer Aided Surgery 5(6):414–425.

Rubin P. 1984. The Franz Buschke lecture: Late effects of chemotherapy and radiation therapy: A new hypothesis. International Journal of Radiation Oncology, Biology & Physics 10(1):5–34.

Saini S, Stark DD, Hahn PF, Wittenberg J, Brady TJ, Ferrucci TJ, Jr., 1987. Ferrite particles: a superparamagnetic MR contrast agent for the reticuloendothelial system. Radiology 162(1 Pt 1): 211–216.

Schnorr J, Wagner S, Abramjuk C, Drees R, Schink T, Schellenberger EA, Pilgrimm H, Hamm B, Taupitz M. 2006. Focal liver lesions: SPIO-, gadolinium-, and ferucarbotran-enhanced dynamic T1-weighted and delayed T2-weighted MR imaging in rabbits. Radiology 240(1):90–100.

Sempoux C, Horsmans Y, Geubel A, Fraikin J, Van Beers BE, Gigot JF, Lerut J, Rahier J. 1997. Severe radiation-induced liver disease following localized radiation therapy for biliopancreatic carcinoma: Activation of hepatic stellate cells as an early event. Hepatology 26(1):128–134.

Stark DD, Weissleder R, Elizondo G, Hahn PF, Saini S, Todd LE, Wittenberg J, Ferrucci JT. 1988. Superparamagnetic iron oxide: clinical application as a contrast agent for MR imaging of the liver. Radiology 168(2):297–301.

Stubbs RS, Cannan RJ, Mitchell AW. 2001. Selective internal radiation therapy (SIRT) with 90Yttrium microspheres for extensive colorectal liver metastases. Hepatogastroenterology 48(38):333–337.

Studholme C, Drapaca C, Cardenas V. 2005. Intensity robust viscous fluid deformation based morphometry using regionally adapted mutual information. Conference Proceedings of the IEEE Engineering & Medical Biological Society 1:470–473.

Studholme C, Hill DL, Hawkes DJ. 1997. Automated three-dimensional registration of magnetic resonance and positron emission tomography brain images by multiresolution optimization of voxel similarity measures. Medicine & Physics 24(1):25–35.

Weissleder R, Stark DD, Engelstad BL, Bacon BR, Compton CC, White DL, Jacobs P, Lewis J. 1989. Superparamagnetic iron oxide: Pharmacokinetics and toxicity. American Journal of Roentgenology 152(1):167–173.

Welsh JS, Kennedy AS, Thomadsen B. 2006. Selective Internal Radiation Therapy (SIRT) for liver metastases secondary to colorectal adenocarcinoma. International Journal of Radiation Oncology, Biology & Physics 66(2 Suppl):S62–S73.

West J, Fitzpatrick JM, Wang MY, Dawant BM, Maurer CR, Jr., Kessler RM, Maciunas RJ. 1999. Retrospective intermodality registration techniques for images of the head: surface-based versus volume-based. IEEE Transactions in Medical Imaging 18(2):144–150.

Yamasaki SA, Marn CS, Francis IR, Robertson JM, Lawrence TS. 1995. High-dose localized radiation therapy for treatment of hepatic malignant tumors: CT findings and their relation to radiation hepatitis. American Journal of Roentgenology 165(1):79–84.

Int. J. Radiation Oncology Biol. Phys., Vol. 62, No. 3, pp. 776–784, 2005

0360-3016/05/$–see front matter

ELSEVIER

doi:10.1016/j.ijrobp.2004.11.022

CLINICAL INVESTIGATION **Liver**

IN VIVO ASSESSMENT OF THE TOLERANCE DOSE OF SMALL LIVER VOLUMES AFTER SINGLE-FRACTION HDR IRRADIATION

Jens Ricke, M.D.,* Max Seidensticker, M.S.,* Lutz Lüdemann, Ph.D.* Maciej Pech, M.D.,* Gero Wieners, M.D.,* Susanne Hengst, M.D.,* Konrad Mohnike,* Chie Hee Cho, M.D.,* Enrique Lopez Hänninen, M.D.,* Hussain Al-Abadi,† Roland Felix, M.D.,* and Peter Wust, M.D., Ph.D.*

*Klinik für Strahlenheilkunde and †Klinik für Allgemein-, Viszeral-, und Transplantationschirurgie, Charité Campus Virchow-Klinikum, Humboldt-University Medical School, Berlin, Germany

Purpose: To prospectively assess a dose–response relationship for small volumes of liver parenchyma after single-fraction irradiation.

Methods and Materials: Twenty-five liver metastases were treated by computed tomography (CT)-guided interstitial brachytherapy. Magnetic resonance imaging was performed 1 day before and 3 days and 6, 12, and 24 weeks after therapy. MR sequences included T1-w gradient echo (GRE) enhanced by hepatocyte-targeted gadobenate dimeglumine. All MRI data sets were merged with 3D dosimetry data and evaluated by two radiologists. The reviewers indicated the border of hyperintensity on T2-w images (edema) or hypointensity on T1-w images (loss of hepatocyte function). Based on the total 3D data, a dose–volume histogram was calculated. We estimated the threshold dose for either edema or function loss as the D_{90}, i.e., the dose achieved in at least 90% of the pseudolesion volume.

Results: Between 3 days and 6 weeks, the extension of the edema increased significantly from the 12.9 Gy isosurface to 9.9 Gy (standard deviation [SD], 3.3 and 2.6). No significant change was detected between 6 and 12 weeks. After 24 weeks, the edematous tissue had shrunk significantly to 14.7 Gy (SD, 4.2). Three days postbrachytherapy, the D_{90} for hepatocyte function loss reached the 14.9 Gy isosurface (SD, 3.9). At 6 weeks, the respective zone had increased significantly to 9.9 Gy (SD, 2.3). After 12 and 24 weeks, the dysfunction volume had decreased significantly to the 11.9 Gy and 15.2 Gy isosurface, respectively (SD, 3 and 4.1).

Conclusions: The 95% interval from 7.6 to 12.2 Gy found as the minimal hepatocyte tolerance after 6 weeks accounts for the radiobiologic variations found in CT-guided brachytherapy, including heterogeneous dose rates by variable catheter arrays. **© 2005 Elsevier Inc.**

CT-guided intervention, Dosimetry, Hepatocyte function, High-dose-rate brachytherapy, Liver.

INTRODUCTION

Irradiation of liver malignancies has evolved as an effective treatment sparing liver surgery in selected patients. Both stereotactic irradiation and image-guided brachytherapy have been described recently with most promising results (1, 2).

The tolerance dose of the liver ranges from 30 Gy to the whole organ to 50 Gy to approximately one-third of the total liver volume. For external radiotherapy, the clinical end-points are liver failure and/or severe hepatitis. If the irradiated volume of normal liver tissue is reduced down to ~100 mL or less, the tolerated doses are much higher—in principle, without any upper limit with respect to the clinical end-points mentioned. In these cases, the options for the irradiated liver tissue are either destruction (above a certain dose) or recovery to normal function (below this level). The threshold dose corresponds to the survival curves of the target cells, probably the hepatocytes, which are difficult to determine. The knowledge of a dose–response relationship might not be important if only one or a few lesions are irradiated using a high-precision technique. However, in clinical practice this knowledge is essential for individual treatment strategies for patients with larger tumor volumes, after liver resection, or with multiple and recurrent lesions requiring repetitive irradiations. In these situations, the post-therapeutic liver function must be preestimated, and the prospective boundary between intact and malfunctioning liver tissue is crucial.

In our study, we employed computed tomography (CT)-guided brachytherapy of liver malignancies to determine the

Reprint requests to: Jens Ricke, M.D., Klinik für Strahlenheilkunde, Charité Campus Virchow-Klinikum, Humboldt-University Medical School, Augustenburgerplatz 1, 13353 Berlin, Germany. Tel: (+49) 30-4505-57001; Fax: (+49) 30-4505-57901; E-mail: jens.ricke@charite.de

Received Mar 23, 2004, and in revised form Sep 8, 2004. Accepted for publication Nov 8, 2004.

tolerance doses of small liver volumes. This technique uses a fluoroscopy CT for catheter positioning and 3D CT data sets for dose planning. Because the CT data are acquired after percutaneous positioning of the catheters inside the tumor, patient motion does not disturb the dose distribution in the clinical target volume, and therefore no safety margin is required to compensate for positioning errors (2). During follow-up to irradiation, magnetic resonance imaging (MRI) is a sensitive measure for detecting edema. Adding the hepatocyte-directed contrast agent gadobenate dimeglumine (Gd-BOPTA) to the MR examination enables the visualization of eventual function loss of liver parenchyma (3–6). By applying image fusion, the isodose lines calculated for interstitial irradiation can be projected onto the respective MRI scans. In the study described herein, we employed these techniques to assess the tolerance dose of small volumes of liver parenchyma after single-fraction high-dose-rate (HDR) brachytherapy.

METHODS AND MATERIALS

Twenty-five patients were included in this prospective study. All patients were scheduled to receive HDR single-fraction brachytherapy of one liver malignancy each. The local ethics committee approved the study. Written informed consent was obtained from all patients.

The patient population was comprised of 14 men and 11 women; the mean age was 66 years (range, 41–86 years). Primary malignancies were colorectal carcinoma in 17, breast cancer in 3, hepatocellular carcinoma in 2, and other tumors in 3 (urothelial carcinoma, cholangiocarcinoma, cervical carcinoma).

One day before the intervention and 6, 12, and 24 weeks after we assessed the following laboratory parameters: prothrombin time (PT), bilirubin, aspartate aminotransferase (AST), alanine aminotransferase (ALT); alkaline phosphatase (AP), albumin, ammonia (NH), International Normalized ratio (INR), and C-reactive protein (CRP). No patient presented evidence of liver function degradation before therapy. All patients demonstrated a Karnofsky performance score higher than 80%.

Twelve out of 25 patients had received chemotherapy or other cytotoxic adjuvant before brachytherapy. In all but 1 patient, chemotherapy had been terminated at least 6 weeks before tumor ablation. Postintervention, 2 patients received chemotherapy starting after 4–8 weeks, and 3 patients after 3–6 months.

The technique of CT-guided brachytherapy has been described elsewhere (2). The placement of the brachytherapy applicators was performed with a fluoroscopy CT (Siemens, Erlangen, Germany). For treatment planning purposes, a spiral CT of the liver (slice thickness: 5 mm, increment: 5 mm), enhanced by i.v. application of iodide contrast media (100 mL Ultravist 370, flow: 1 mL/s; start delay: 80 s), was acquired using the breath-hold technique after the brachytherapy catheters were positioned in the tumor. Three catheters on average were used in our patients (range, 1–8 catheters).

The HDR afterloading system (Gammamed, Varian, Charlottesville, VA) employed a ^{192}Ir source of 10 Ci. The source diameter was $<$1 mm. Dwell positions were located every 5 mm. Treatment planning was performed using the software system Abacus 3.0 (Abacus Concepts, Berkeley, CA) integrated in the controller of the HDR-afterloading system. The relative coordinates (x, y, z) of the catheters were determined in the CT data set and transferred manually into the treatment planning system. A reference dose of 15, 20, or 25 Gy, which was aimed to enclose the lesion (clinical target volume), was prescribed in our patients and applied as a single dose. Compromises were necessary if risk organs such as the stomach, small intestine, or a large bile duct nearly touched the target. No maximum dose constraints were given inside the tumor volume. To preserve liver function after irradiation, we prescribed a dose of $<$5 Gy to one-third of the liver parenchyma. The irradiation time was typically 20–40 min.

A total of 100 MRI examinations were performed in 25 patients 1 day before and 3 days and 6, 12, and 24 weeks after tumor ablation. The MRI protocol was comprised of the following sequences: T2-w breathing-triggered UTSE (TE/TR 90/2,100 ms) with and without fat suppression, T1-w breath-hold gradient echo (GRE) (TE/TR 5/30 ms, flip angle 30°) precontrast, 20 s post i.v. application of 15 mL Gd-BOPTA, and 2 h post injection of i.v. Gd-BOPTA (Multihance; Bracco, Princeton, NJ). The slice thickness was 8 mm, acquired in interleafed mode with no gap applied.

Gadobenate dimeglumine is an octadentate chelate of the paramagnetic ion gadolinium. Its kinetic properties resemble those of conventional iodinated contrast media and can be described by a bi-exponential function comprising a distribution phase and an elimination phase (3). Studies have shown that this agent differs from other available gadolinium chelates in that it distributes not only to the extracellular fluid space, but also is selectively taken up only by functioning hepatocytes and excreted into the bile by the so-called canalicular multispecific organic anion transporter shared with bilirubin (4–6). However, whereas the biliary excretion rate is 55% in rats and 25% in rabbits, respectively, it is only 3–5% in humans, with these results being constant and reproducible (6). This level of uptake is sufficient to bring about specific, long-lasting enhancement of MR signal intensity in normal liver parenchyma.

Volumetrics of the liver, of the tumor, or of the liver and tumor volume receiving more than 10 Gy were performed by using the DICOM CT data acquired after applicator positioning and a proprietary viewing and image processing software (Jive X; VISUS TT, Bocham, Germany).

To merge dosimetry data calculated during CT-guided brachytherapy with the MRI data acquired in this study, the isodose plan was 3D digitized. We performed a 3D interpolation using a cubic shape function for continuous isodose values. In the next step, these data were merged with the CT data set acquired for treatment planning. Finally, the data set containing the CT and the dosimetry was merged with each MRI acquired before therapy and during the 6 months of follow-up. Typically, MRI and CT are acquired in different breath-hold phases. In our study, CT was acquired as a single breath-hold sequence, T1-w GRE were acquired as breath-hold sequences, and T2-w UTSE employed a breath-triggered mode. A complete image fusion between CT and different MRI sequences would therefore require an elastic 3D image transformation. In our study we evaluated radiation effects on only the liver, so MRI data were reduced to contain just liver parenchyma and a surrounding margin of approximately 2 cm. The reduced image was merged with the CT/dosimetry data set by employing anisoscalar image fusion. The registration routine of the algorithm has been described by Studholme *et al.* (7). It is based on normalized mutual information (8). We employed a modified independent implementation within the 3D visualization software Amira (Mercury Computer Systems, Berlin, Germany) (9) (Figs. 1, 2). The image fusion accuracy of the liver was found to always be better than 5 mm for the liver surface.

Two radiologists evaluated the combined MRI and dosimetry

data. On any of the T2-w as well as the T1-w late Gd-BOPTA enhanced images, the reviewers indicated the border of hyperintensity on T2-w images (edema) or hypointensity on T1-w images (loss of hepatocyte function) around the irradiated liver tumor (referred to as "pseudolesion" in the following) (Figs. 3, 4). Based on the total 3D data set, Amira software calculated a dose–volume histogram (Fig. 5). As a result, we determined the percentage of each pseudolesion covered by a specific dose and higher. We assumed a 10% error of the overall methodology, including fusion mismatches. Hence, we estimated the threshold dose for either edema or function loss as the D_{90}, i.e., the dose achieved in at least 90% of the pseudolesion volume. To ensure the appropriateness of our approach and to verify the results of the dose–volume histograms, we determined the volume of each pseudolesion in relation to the intrahepatic 10 Gy isodose surface as an additional descriptor of the hepatic tolerance doses.

To determine intraobserver variations and to establish the reliability of the image fusion process, 4 randomly selected patients underwent image fusion, as well as the review process, repeatedly in three sessions separated by 1 week. A Kendall W test was applied to establish significance for intra- as well as interobserver variations.

The Wilcoxon test and the Pearson correlation were applied to evaluate the dynamics of the pseudolesion development over time. We tested a history of chemotherapy as well as the ^{192}Ir source activity as independent factors influencing the hepatic tissue tolerance.

RESULTS

Figures 6a and 6b display the dynamics of the minimal dose exposure provoking either edema or hepatocyte function loss. Between 3 days and 6 weeks, the extension of the edema increased significantly from the 12.9 Gy isosurface to 9.9 Gy (standard deviation [SD], 3.3 and 2.6, respectively; $p = 0.006$). No significant change was detected between 6 and 12 weeks (11.1 Gy, SD, 2.6; $p = 0.281$). After 24 weeks, the edematous tissue had significantly shrunk to the isosurface of 14.7 Gy (SD, 4.2; $p = 0.002$).

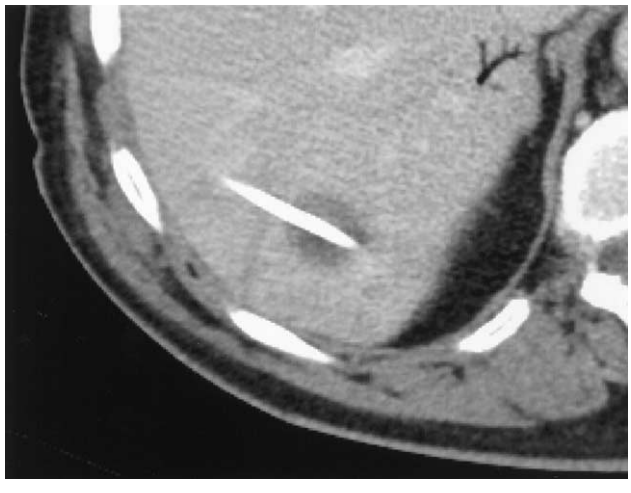

Fig. 1. Contrast-enhanced computed tomography (CT) after CT-guided positioning of a brachytherapy catheter in a metastasis of a colorectal carcinoma.

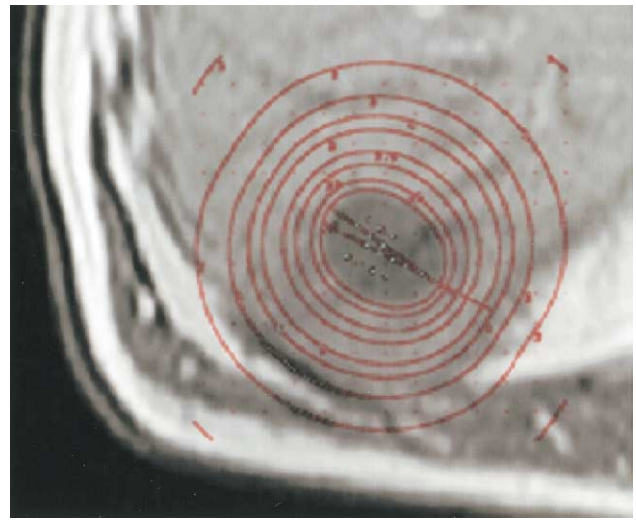

Fig. 2. Magnetic resonance imaging acquired 3 days after brachytherapy. Plain T1-w gradient echo. Image fusion with the 3-dimensional dosimetry.

Three days after brachytherapy, the D_{90} for hepatocyte function loss was the 14.9 Gy isosurface (SD, 3.9). At 6 weeks, the respective zone had increased significantly to the 9.9 Gy isosurface (SD, 2.3; $p = 0.001$). Between 6 and 12 weeks, the dysfunction volume had decreased significantly to the 11.9 Gy isosurface (SD, 3.0; $p = 0.035$). After 24 weeks, the volume decreased further to the 15.2 Gy isosurface (SD, 4.1; $p = 0.002$).

Figures 7a and 7b illustrate the development of the volume of edema or hepatocyte function loss in relation to the 10 Gy isosurface postbrachytherapy. Between 3 days and 6 weeks, edema volume increased significantly ($p = 0.014$). After 12 weeks, edema volume did not change significantly ($p > 0.05$). After 6 weeks, a decrease was highly significant ($p < 0.001$).

The relative volume of hepatocyte function loss increased significantly between 3 days and 6 weeks ($p < 0.001$). After 12 weeks, the decline of the volume with hepatocyte function loss was significant compared with that at 6 weeks ($p = 0.006$), and again comparing that at 12 and 24 weeks ($p < 0.001$).

At 3 days postbrachytherapy, the minimal dose leading to edema was significantly less than the dose provoking the hepatocyte function loss ($p < 0.001$). No differences between the doses were noted at 6 weeks ($p = 0.9$). At 12 and 24 weeks, edema again occurred in areas of less dose exposition compared with hepatocyte function loss (both $p = 0.02$).

When comparing the extent of the relative volume of the edema to the relative volume of hepatocyte function loss, again edema preceded function loss significantly 3 days postirradiation ($p = 0.001$). No differences in the relative volumes of edema vs. hepatocyte function loss were noted 6, 12, and 24 weeks postbrachytherapy ($p > 0.05$).

The average target volume was 40 mL (range, 7–124

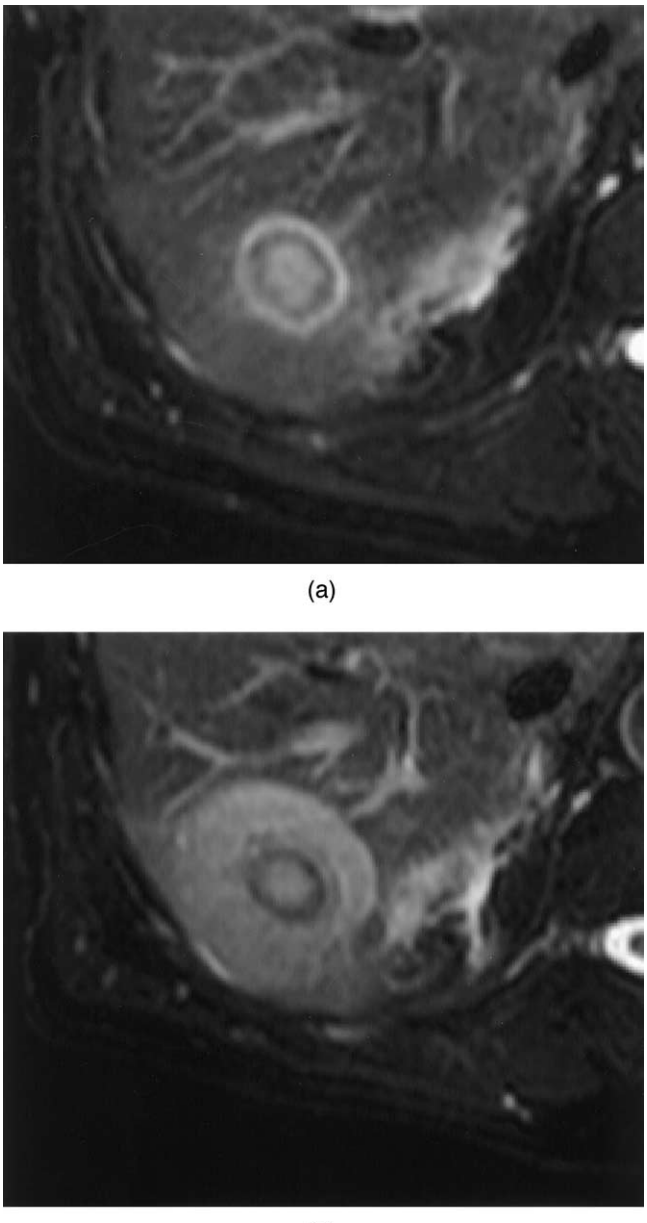

Fig. 3. Magnetic resonance imaging acquired (a) 3 days and (b) 6 weeks after brachytherapy. T2-w UTSE showing the development of (hyperintense) edema around the lesion.

mL). We found no correlation between the target volume and the threshold tolerance of adjacent hepatic tissue.

The source factor of the ^{192}Ir afterloader varied between 0.96 and 1.88 (median, 1.29). We found no correlation between the dose tolerance of the liver tissue and the source factor.

No correlation was found between the dose tolerance and pretreatment with chemotherapy.

All patients included in this study demonstrated normal liver function parameters before CT-guided brachytherapy. No patient developed symptoms of acute or late chronic liver dysfunction.

Interobserver and intraobserver correlations as determined by the Kendall W test were highly significant with a coefficient of 0.99 and 0.97, respectively (both $p < 0.001$).

DISCUSSION

The tolerance doses of the entire liver or of large portions of the liver to external irradiation are well understood in the literature. However, the effect of single radiation doses to small volumes of hepatic parenchyma has not yet been clearly defined. Tolerance doses of small-sized liver parenchyma must be considered if radioablative treatments, using either brachytherapy or extracranial radiosurgery, are per-

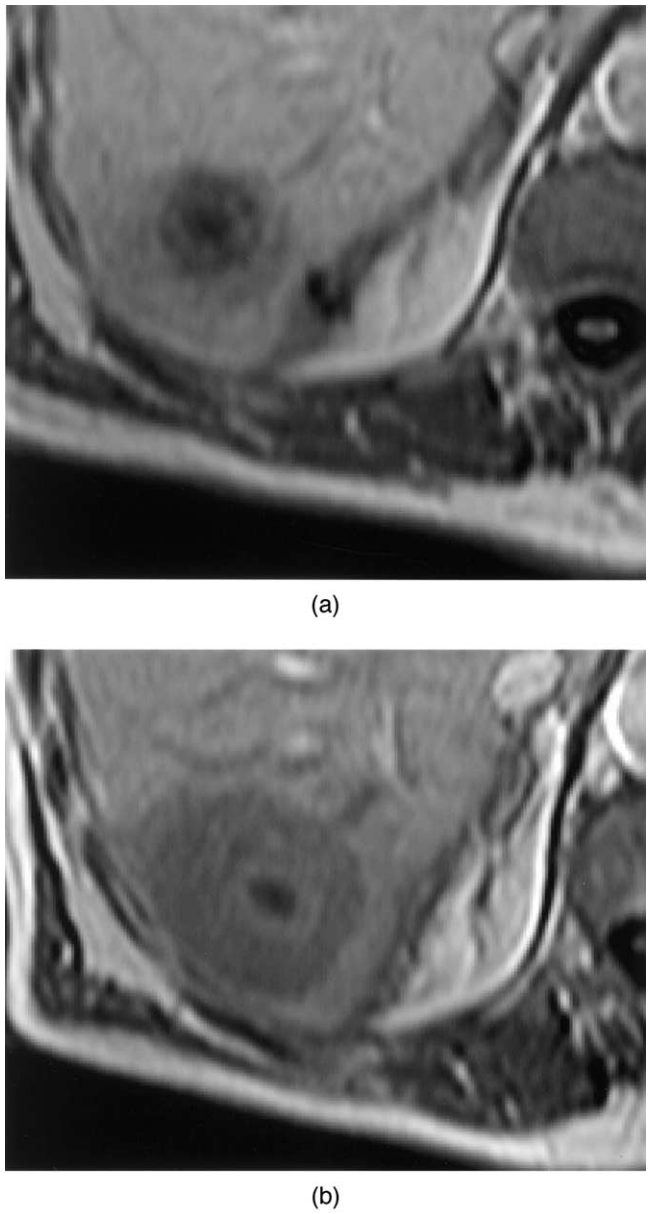

Fig. 4. Magnetic resonance imaging acquired (a) 3 days and (b) 6 weeks after brachytherapy. T1-w gradient echo 2 h post i.v. application of gadobenate dimeglumine. Development of a hypointense rim around the tumor lesion through diminished uptake of contrast agent, indicating hepatocyte dysfunction.

formed, in particular in a single patient displaying a variety of lesions.

Until today, the experience with single high-dose exposure to the liver is limited, and the dosimetry usually is not accurate. Intraoperative single-fraction irradiation is commonly performed without image guidance, delivering just the surgeon's estimate as to what extent liver parenchyma has been exposed to irradiation (10, 11). Stereotactic percutaneous irradiation usually is delivered as a fractionated treatment employing the linear-quadratic model to recalculate and compare the doses with respect to a conventional scheme. Furthermore, the accuracy of the dose plan in percutaneous treatment is hampered by inherent patient motion such as breathing (12, 13). Herfarth *et al.* reported an additional positioning error of 2–3 mm for intrahepatic targets when applying a stereotactic frame (14). Considering the steep dose gradients in stereotactic irradiation, even these 2–3 mm contribute to a significant uncertainty in dose estimation.

The inherent advantage of tomographic guidance for interstitial irradiation is the accuracy of the dose administration. In our study we employed CT-guided brachytherapy, where the catheters are positioned and fixed inside the tumor. Hence, patient motion is no limiting factor (15). The accuracy of the dosimetry for the actual treatment is as high as the accuracy of the treatment planning system and the point source approximation, respectively. In our case, the treatment planning system used the Meisberger polynomial and anisotropy correction. The accuracy of the dose absorbed in water is typically <2–3% (16–19).

Some limitations may apply with respect to the follow-up MRI data used to establish threshold doses for hepatocyte function loss or edema. First, the image fusion software employs voxel-based registration to perform an anisoscalar adaptation of the CT/dosimetry images to the follow-up MRI. However, voxel-based techniques working directly on the image gray values have recently been shown to be far superior to other methods such as surface-based registration

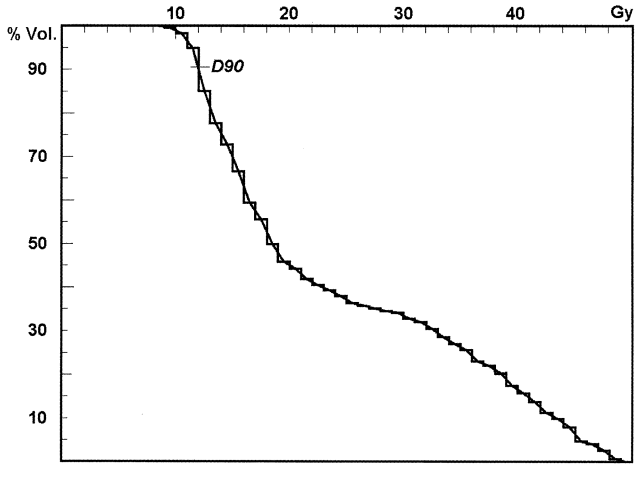

Fig. 5. Patient 15: dose–volume histogram 3 days postbrachytherapy demonstrating the dose distribution in the edema. D_{90} is 12 Gy.

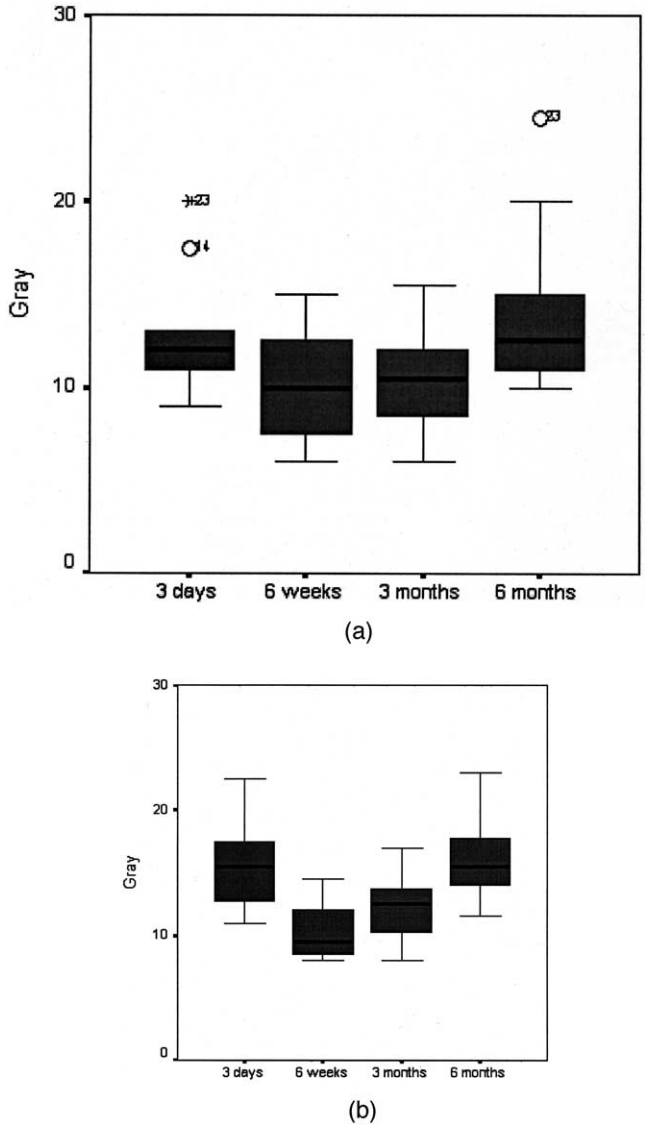

Fig. 6. (a) Development of edema dependent on time vs. dose exposition. (b) Development of the area of hepatocyte function loss.

(9, 20). Second, the determination of the outer border of either edema or signal void after Gd-BOPTA was performed manually by two radiologists. Intraobserver as well as interobserver correlation was excellent; however, owing to these uncertainties of the overall system, we presumed a 10% error by extracting the D_{90} from the dose–volume histograms (Fig. 5). To ensure greater reliability of our study results, we additionally performed a lesion volume–based analysis with the intrahepatic 10 Gy isodose margin as reference. As can be seen in Figs. 6a, 6b, 7a, and 7b, both methods generated very similar results with respect to the development of either hepatocyte function loss or edema postirradiation.

Gadobenate dimeglumine is a hepatocyte-targeted contrast agent. The underlying mechanism for intracellular uptake is a polyspecific organic anionic transport. The absence of this transport mechanism is closely correlated to the

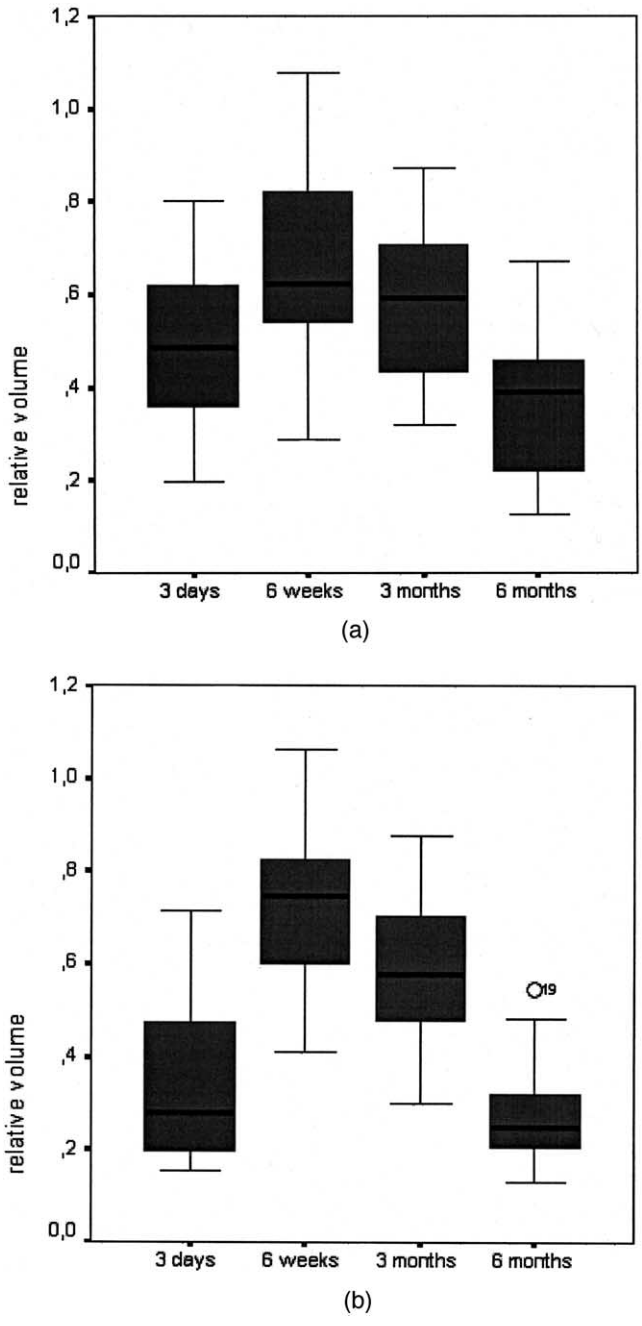

Fig. 7. (a) Development of the edema volume around the irradiated tumor relative to the 10 Gy isodose (liver parenchyma only). (b) Development of the area of hepatocyte function loss around the irradiated tumor relative to the 10 Gy isodose (liver parenchyma only).

functional state of a hepatocyte, i.e., in case of hepatitis (21–24). In the first few minutes after i.v. administration, the behavior of Gd-BOPTA resembles that of the standard MRI interstitial contrast agent Gd-DTPA. Approximately 2 h postadministration, it reaches a peak uptake in functional hepatocytes only.

In our study, the predominant early tissue reaction to irradiation was edema. Three days posttreatment, the diminished uptake of Gd-BOPTA, indicating hepatic function loss, was limited to areas of higher-dose exposure. After 6 weeks, differences in the extent of dose exposure leading to edema or hepatocyte function loss had vanished. The greatest volume of function loss or edema was found after 6 weeks to 3 months. Six months postirradiation, the relevant areas resolved significantly, and the volumes of edema or hepatocyte function loss were not different from those 3 days posttreatment. We conclude that after a single radiation dose, the acute function loss transforms into an irreversible damage at a dose exposure of more than 15 Gy. At a dose exposure between 10 and 15 Gy, hepatic dysfunction is reversible through hepatic regeneration or intracellular repair mechanisms. The peak dysfunctional volume is reached between 6 and 12 weeks. This has to be considered when a series of radioablations is planned in a patient because of oligotopic metastatic disease. Below 10 Gy dose exposure, no functional degradation is detectable in the MRI scans. It should be noted that we found considerable standard deviations for the dose thresholds. Furthermore, we did not investigate late toxicity (>6 months) in this study. However, in 10 patients undergoing MRI up to 18 months follow-up, we did not see additional chronic liver damage compared with the status 6 months postirradiation. In none of our imaging studies did we see fibrotic changes or considerable hypertrophy of the uninvolved liver, presumably because just minor portions of healthy liver had been exposed to higher doses. We extracted a limited number of cytology specimens by core biopsy, enabling us to assess cellular changes of small volumes of liver postirradiation. Even areas that had been exposed to high doses did not show high amounts of fibroblasts or lymphatic cells that would have indicated a strong fibrotic activity. In contrast, frequent polyploidism of hepatocytes demonstrated a high regenerative activity weeks after high-dose exposure (Figs. 8a, 8b).

The lowest threshold dose found in our study to impair hepatocyte function was 9.9 Gy (SD, 2.3 Gy) at 6 weeks postirradiation (no significant changes to 3 months). Herfarth *et al.* published a study applying stereotactic single-fraction irradiation to liver malignancies, with the data on hepatocyte tolerance derived from follow-up contrast-enhanced CT (25). The authors observed a focal reaction at a dose minimum of 13.7 Gy (range, 8.9–19.2 Gy). However, Herfarth *et al.* did not perform an image fusion of the CT used for treatment planning and the follow-up scans but instead relied on volumetric measurements. These measurements determined the relative volume of the whole liver in the follow-up CTs. The focal reaction after irradiation as visible on CT does not necessarily correspond to a hepatocyte function loss. The authors concede potential underestimation of larger parts of the reacting volumes because of the limitations of contrast-enhanced CT and therefore potential overestimation of the calculated threshold volume (25). We believe that this lower threshold dose of the early hepatic reaction demonstrated in our study is a result of the higher sensitivity of MRI to soft tissue changes compared with CT. This hypothesis is supported by the fact that

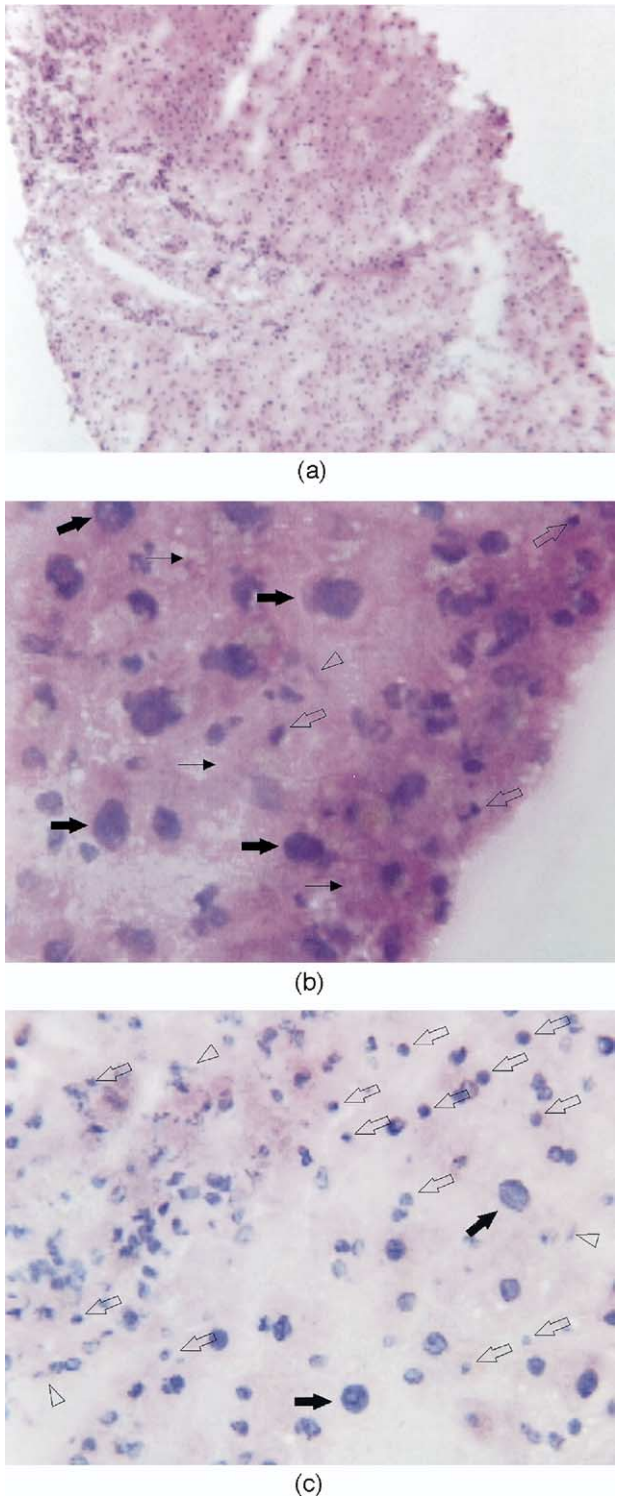

Fig. 8. (a) Liver (hematoxylin-eosin, 100×). Histologic section acquired by liver biopsy 6 weeks after single-fraction irradiation showing typical hepatic architecture with portal tract and hepatic vein. (b, c) Exposure to 10–12 Gy (b, 600×) and 18–20 Gy (c, 400×). (b) In the low-dose area, strong regenerative activity with multiple polyploid hepatocytes (thick arrows) and only a negligible trend to fibrosis with just a minor portion of lymphatic cells (open arrows) or fibroblasts (open arrowheads). Some of the necrotic areas are indicated by thin arrows. (c) After high-dose exposure, multiple lymphatic cells and a few fibroblasts (open arrowheads) as predecessors of fibrosis, along with only a minor portion of polyploid hepatocytes.

Herfarth *et al.* (25) found the earliest visible changes on CT 2 months after treatment. In our study, conventional T2-w sequences demonstrated edema just 3 days postirradiation, and diminished Gd-BOPTA uptake in T1-w sequences indicated hepatocyte function loss as early.

Further literature data on the hepatic tolerance dose are inconclusive and commonly derived from focal reactions detected on follow-up CT after fractionated irradiation. Lawrence *et al.* (26) reported a threshold dose of 45 Gy; Yamasaki *et al.* (27) reported a focal liver reaction in 73% of patients treated with 48 Gy and 86% treated with 72.8 Gy. Formally, these fractionated tolerance doses correspond to single-fraction doses of 13.5 up to 17.5 Gy, respectively, according to the linear-quadratic model and an assumed α/β of 3 Gy for liver tissue. Again, the use of a CT follow-up most likely led to an underestimation of the hepatic response to irradiation.

Dose rate is an important factor determining the dose tolerance of human tissues (28). In an HDR system, the dose rate changes significantly depending on the catheter or implant location as the source moves along the dwell positions. Biologic effects vary in points receiving the same cumulative dose. In a study evaluating the effects of dose rate in an HDR-brachytherapy model, Manning *et al.* demonstrated increased cell kill ratios in locations exposed to a sudden dose peak compared with locations with dose distribution delivered continuously over the total irradiation time (29). The variations in bioeffects were more obvious in tissues such as liver with low α/β values, varying strongly with a tissue's specific repair capacity. In our study applying CT-guided brachytherapy for liver tumor ablation, we do not consider the total irradiation time to be an important factor for cell kill inside the target volumes. In contrast to current dose uniformity constraints in percutaneous radiotherapy, we did not apply upper dose limits, resulting in considerable dose inhomogeneities inside the tumor (30–35). However, the relatively high spread found in our study for the tolerance dose of hepatic tissue most likely has its origin in variations of the dose rate that contribute to the uncertainty of an isoeffect predominantly in boundary locations. To predict a most accurate dose tolerance to an HDR irradiation, a time factor compensating for the temporal distribution of the dose administration is probably useful (36).

HDR sources typically decay by one half-life period before replacement. In our study we did not find a significant correlation between threshold dose and source activity. However, we believe that the time variations in dose application resulting from variable catheter positions in each patient and additionally the small study population may have covered this correlation.

In contrast to our study, previous studies have demonstrated a dose–volume tolerance for radiation-induced liver disease when the Lyman-Kutcher-Burman normal tissue complication probability model was applied in patients receiving percutaneous liver irradiation (37, 38). Whereas these considerations deal with the integrity of

the whole organ, we investigated the radiation effect on a cellular level. Dawson *et al.* (38) as well as Cheng *et al.* (37) evaluated clinical signs of radiation-induced liver disease (hepatitis) in patients where extensively higher volumes of the liver had been exposed to irradiation as compared to our study.

We conclude that the 95% interval from 7.6 to 12.2 Gy found as the threshold dose to induce an early loss of function in liver tissue after 6 weeks accounts for the inherent radiobiologic variations found in CT-guided brachytherapy, including the influence of heterogeneous dose rates delivered by variable catheter arrays. These dose limits should be addressed when assessing the remaining liver capacity in patients with extensive tumors, repeated radioablations, or diminished hepatic reserve capacity after surgery.

REFERENCES

1. Herfarth KK, Debus J, Lohr F, *et al.* Stereotactic single-dose radiation therapy of liver tumors: Results of a phase I/II trial. *J Clin Oncol* 2001;19:164–170.
2. Ricke J, Wust P, Stohlmann A, *et al.* CT-guided interstitial brachytherapy of liver malignancies alone or in combination with thermal ablation: Phase I/II results of a novel technique. *Int J Radiat Oncol Biol Phys* 2004;58:1496–1505.
3. de Haen C, Lorusso V, Tirone P. Hepatic transport of gadobenate dimeglumine in TR-rats. *Acad Radiol* 1996;3:S452–S454.
4. Kirchin MA, Pirovano GP, Spinazzi A. Gadobenate dimeglumine (Gd-BOPTA). An overview. *Invest Radiol* 1998;33:798–809.
5. Spinazzi A. Safety, tolerance, biodistribution, and MR imaging enhancement of the liver with gadobenate dimeglumine: Results of clinical pharmacologic and pilot imaging studies in nonpatient and patient volunteers. *Acad Radiol* 1999;6:282–291.
6. de Haen C, Gozzini L. Soluble-type hepatobiliary contrast agents for MR imaging. *J Magn Reson Imaging* 1993;3:179–186.
7. Studholme C, Hill DLG, Hawkes DJ. Automated three-dimensional registration of magnetic resonance and positron emission tomography brain images by multiresolution optimization of voxel similarity measures. *Med Phys* 1997;24:25–35.
8. Studholme C, Hill DLG, Hawkes DJ. An overlap invariant entropy measure of 3D medical alignment. *Pattern Recognition* 1999;32:71–86.
9. Rohlfing T, West JB, Beier J, Liebig T, Taschner CA, Thomale UW. Registration of functional and anatomical MRI: Accuracy assessment and application in navigated neurosurgery. *Comput Aided Surg* 2000;5:414–425.
10. Thomas DS, Nauta RJ, Rodgers JE, *et al.* Intraoperative high-dose rate interstitial irradiation of hepatic metastases from colorectal carcinoma. Results of a phase I-II trial. *Cancer* 1993;71:1977–1981.
11. Dritschilo A, Harter KW, Thomas D, *et al.* Intraoperative radiation therapy of hepatic metastases: Technical aspects and report of a pilot study. *Int J Radiat Oncol Biol Phys* 1988;14:1007–1011.
12. Minohara S, Endo M, Kanai T, Kato H, Tsujii H. Estimating uncertainties of the geometrical range of particle radiotherapy during respiration. *Int J Radiat Oncol Biol Phys* 2003;56:121–125.
13. Brock KK, McShan DL, Ten Haken RK, Hollister SJ, Dawson LA, Balter JM. Inclusion of organ deformation in dose calculations. *Med Phys* 2003;30:290–295.
14. Herfarth KK, Debus J, Lohr F, *et al.* Extracranial stereotactic radiation therapy: Set-up accuracy of patients treated for liver metastases. *Int J Radiat Oncol Biol Phys* 2000;46:329–335.
15. Ricke J, Wust P, Stohlmann A, *et al.* CT-guided brachytherapy: A new technique for interstitial ablation of liver malignancies. *Strahlenther Onkol* 2004;180:281–288.
16. Podgorsak MB, DeWerd LA, Paliwal BR, Ho AK, Sibata CH. Accuracy of the point source approximation to high dose-rate Ir-192 sources. *Med Dosim* 1995;20:177–181.
17. Cho SH, Muller-Runkel R, Hanson WF. Determination of the tissue attenuation factor along two major axes of a high dose rate (HDR) 192Ir source. *Med Phys* 1999;26:1492–1497.
18. Gromoll C, Karg A. Determination of the dose characteristics in the near area of a new type of 192Ir-HDR afterloading source with a pinpoint ionization chamber. *Phys Med Biol* 2002;47:875–887.
19. Cheung YC, Yu PK, Young EC, *et al.* The electron-dose distribution surrounding an 192Ir wire brachytherapy source investigated using EGS4 simulations and GafChromic film. *Appl Radiat Isot* 1997;48:985–990.
20. West J, Fitzpatrick JM, Wang MY, *et al.* Retrospective intermodality registration techniques for images of the head: Surface-based versus volume-based. *IEEE Trans Med Imaging* 1999;18:144–150.
21. Pastor CM, Planchamp C, Pochon S, *et al.* Kinetics of gadobenate dimeglumine in isolated perfused rat liver: MR imaging evaluation. *Radiology* 2003;229:119–125.
22. Lorusso V, Arbughi T, Tirone P, de Haen C. Pharmacokinetics and tissue distribution in animals of gadobenate ion, the magnetic resonance imaging contrast enhancing component of gadobenate dimeglumine 0.5 M solution for injection (MultiHance). *J Comput Assist Tomogr* 1999;23:S181–189.
23. Marzola P, Maggioni F, Vicinanza E, Dapra M, Cavagna FM. Evaluation of the hepatocyte-specific contrast agent gadobenate dimeglumine for MR imaging of acute hepatitis in a rat model. *J Magn Reson Imaging* 1997;7:147–152.
24. de Haen C, La Ferla R, Maggioni F. Gadobenate dimeglumine 0.5 M solution for injection (MultiHance) as contrast agent for magnetic resonance imaging of the liver: Mechanistic studies in animals. *J Comput Assist Tomogr* 1999;23:S169–179.
25. Herfarth KK, Hof H, Bahner ML, *et al.* Assessment of focal liver reaction by multiphasic CT after stereotactic single-dose radiotherapy of liver tumors. *Int J Radiat Oncol Biol Phys* 2003;57:444–451.
26. Lawrence TS, Robertson JM, Anscher MS, Jirtle RL, Ensminger WD, Fajardo LF. Hepatic toxicity resulting from cancer treatment. *Int J Radiat Oncol Biol Phys* 1995;31:1237–1248.
27. Yamasaki SA, Marn CS, Francis IR, Robertson JM, Lawrence TS. High-dose localized radiation therapy for treatment of hepatic malignant tumors: CT findings and their relation to radiation hepatitis. *AJR Am J Roentgenol* 1995;165:79–84.
28. Arnfield MR, Lin PS, Manning MA, *et al.* The effect of high-dose-rate brachytherapy dwell sequence on cell survival. *Int J Radiat Oncol Biol Phys* 2002;52:850–857.
29. Manning MA, Zwicker RD, Arthur DW, Arnfield M. Biologic treatment planning for high-dose-rate brachytherapy. *Int J Radiat Oncol Biol Phys* 2001;49:839–845.
30. Zwicker RD, Schmidt-Ullrich R. Dose uniformity in a planar interstitial implant system. *Int J Radiat Oncol Biol Phys* 1995;31:149–155.

31. Saw CB, Suntharalingam N. Reference dose rates for single- and double-plane 192Ir implants. *Med Phys* 1988;15:391–396.
32. Paul JM, Philip PC, Brandenburg RW, Koch RF. Comparison between continuous and discrete sources in the Paris system of implants. *Med Phys* 1989;16:414–424.
33. Paul JM, Koch RF, Philip PC. Uniform analysis of dose distribution in interstitial brachytherapy dosimetry systems. *Radiother Oncol* 1988;13:105–125.
34. Barendsen GW. Parameters of linear-quadratic radiation dose-effect relationships: Dependence on LET and mechanisms of reproductive cell death. *Int J Radiat Biol* 1997;71:649–655.
35. Barendsen GW, Van Bree C, Franken NA. Importance of cell proliferative state and potentially lethal damage repair on radiation effectiveness: Implications for combined tumor treatments. *Int J Oncol* 2001;19:247–256.
36. Barendsen GW. Dose fractionation, dose rate and iso-effect relationships for normal tissue responses. *Int J Radiat Oncol Biol Phys* 1982;8:1981–1997.
37. Cheng JC, Wu JK, Huang CM, *et al.* Radiation-induced liver disease after three-dimensional conformal radiotherapy for patients with hepatocellular carcinoma: Dosimetric analysis and implication. *Int J Radiat Oncol Biol Phys* 2002;54:156–162.
38. Dawson LA, Normolle D, Balter JM, McGinn CJ, Lawrence TS, Ten Haken RK. Analysis of radiation-induced liver disease using the Lyman NTCP model. *Int J Radiat Oncol Biol Phys* 2002;53:810–821.

RADIATION ONCOLOGY

RESEARCH Open Access

Quantitative in vivo assessment of radiation injury of the liver using Gd-EOB-DTPA enhanced MRI: tolerance dose of small liver volumes

Max Seidensticker[1*], Ricarda Seidensticker[1], Konrad Mohnike[1], Christian Wybranski[1], Thomas Kalinski[2], Sebastian Luess[1], Maciej Pech[1], Peter Wust[3] and Jens Ricke[1]

Abstract

Backround: Hepatic radiation toxicity restricts irradiation of liver malignancies. Better knowledge of hepatic tolerance dose is favourable to gain higher safety and to optimize radiation regimes in radiotherapy of the liver. In this study we sought to determine the hepatic tolerance dose to small volume single fraction high dose rate irradiation.

Materials and methods: 23 liver metastases were treated by CT-guided interstitial brachytherapy. MRI was performed 3 days, 6, 12 and 24 weeks after therapy. MR-sequences were conducted with T1-w GRE enhanced by hepatocyte-targeted Gd-EOB-DTPA. All MRI data sets were merged with 3D-dosimetry data. The reviewer indicated the border of hypointensity on T1-w images (loss of hepatocyte function) or hyperintensity on T2-w images (edema). Based on the volume data, a dose-volume-histogram was calculated. We estimated the threshold dose for edema or function loss as the D_{90}, i.e. the dose achieved in at least 90% of the pseudolesion volume.

Results: At six weeks post brachytherapy, the hepatocyte function loss reached its maximum extending to the former 9.4Gy isosurface in median (i.e., ≥9.4Gy dose exposure led to hepatocyte dysfunction). After 12 and 24 weeks, the dysfunctional volume had decreased significantly to a median of 11.4Gy and 14Gy isosurface, respectively, as a result of repair mechanisms. Development of edema was maximal at six weeks post brachytherapy (9.2Gy isosurface in median), and regeneration led to a decrease of the isosurface to a median of 11.3Gy between 6 and 12 weeks. The dose exposure leading to hepatocyte dysfunction was not significantly different from the dose provoking edema.

Conclusion: Hepatic injury peaked 6 weeks after small volume irradiation. Ongoing repair was observed up to 6 months. Individual dose sensitivity may differ as demonstrated by a relatively high standard deviation of threshold values in our own as well as all other published data.

Backround

Irradiation of liver malignancies has evolved as an effective treatment alternative to liver surgery in selected patients. Both external radiotherapy as well as image guided brachytherapy have been described in the literature with promising results [1-4]. One of the few limiting factors is the tolerance dose of the surrounding liver parenchyma.

Literature of quantitative in vivo data of the hepatic tolerance to irradiation is limited [5-8]. However, such knowledge is essential for the treatment strategy in patients with multiple or large tumors or in situations with a small parenchymal reserve after liver resection.

Previous studies on the tolerance dose of the liver are mainly based on fractionated large volume liver irradiation with the clinical endpoint of radiation induced liver disease (RILD). This status may occur if more than 30 - 55 Gy are applied, depending on the irradiated liver volume [6,7,9-14]. These doses lead to a decline of the total organ function causing clinical symptoms.

* Correspondence: max.seidensticker@med.ovgu.de
[1]Klinik für Radiologie und Nuklearmedizin, Universitätsklinikum Magdeburg, Otto-von-Guericke-Universität Magdeburg, Germany
Full list of author information is available at the end of the article

However, this does not necessarily reflect the inherent radiosensitivity of the liver and even less the intrinsic radiosensitivity of hepatocytes or the liver functioning units.

Computed tomography (CT)-guided brachytherapy of liver malignancies utilizes CT fluoroscopy for catheter positioning and three dimensional (3D) CT-data sets for dose planning. During follow up after irradiation, magnetic resonance imaging (MRI) may be used as a sensitive method to detect edema as well as liver function loss by employing hepatocyte-directed contrast agents. By applying image fusion of follow up MRI with the treatment planning CT, the isodoses calculated for interstitial irradiation can be displayed in the MRI scans, indicating the exact dose distribution at any given time point during follow up. In a precursor study, we utilized this approach along with the hepatocyte directed contrast agent Gadobenate dimeglumine (Gd-BOPTA). We determined a median threshold dose of 9.9 Gy after six weeks as the minimal tolerance dose of small volume liver parenchyma to single fraction high dose rate (HDR) brachytherapy over time [8].

However, Gd-BOPTA displays only a small biliary excretion of only 6%. In contrast, Gadolinium ethoxybenzyl diethylenetriamine-pentaacetate (Gd-EOB-DTPA), a second generation hepatocyte directed contrast agent, has shown vast improvements over Gd-BOPTA in liver contrast through biliary excretion rates of >50% [15-18]. By employing Gd-EOB-DTPA in the study described herein we sought to determine the hepatic tolerance dose to small volume single fraction high dose irradiation as primary endpoint. As secondary endpoints we searched for factors of influence on the threshold dose (history of chemotherapy, irradiated volume etc.) and we intended to gain a more accurate assessment of dose thresholds specifically in light of the relatively high standard deviation in the precursor study employing Gd-BOPTA. As with Gd-BOPTA, surrogate for local liver function was a diminished uptake of the contrast agent in liver parenchyma, and image fusion with dosimetry data determined the respective threshold doses.

Material and methods

Patient identification

Twenty-three patients were included in this study. All patients were scheduled to receive a CT guided HDR single fraction brachytherapy of one liver malignancy each. Follow-up MRI employed Gd-EOB-DTPA. The study was approved by the institutional ethics committee.

The patient population comprised of 12 men and 11 women. The mean age was 66 years (30-84 years). All patients demonstrated a Karnofsky score greater than 80%. All liver tumors were metastastic, and liver cirrhosis was exclusion criteria. The primary tumors were: 10 colorectal, 8 breast, 3 renal cell, 1 gastric and 1 non small cell lung cancer (Table 1).

Eligibility criteria

In addition to patients with clinical signs of liver cirrhosis we excluded patients who had previously undergone radiotherapy of the liver. To avoid confounding radiosensitizing effects or toxicities, systemic chemotherapy was paused for at least 14 days prior and post brachytherapy (Table 1).

Interventional technique and follow up

The technique of CT-guided brachytherapy has been described in detail elsewhere [3,4]. In brief, placement of the brachytherapy applicators was performed under CT fluoroscopy. For treatment planning purposes, a spiral CT of the liver (slice thickness: 5 mm; increment: 5 mm) enhanced by intravenous administration of iodide contrast media (100 ml Ultravist 370, Bayer Schering Pharma, Berlin, Germany, flow: 1 ml/s; start delay: 80s) was acquired after positioning of the brachytherapy catheters in the tumor. A median of three catheters was used in our patients (range: 1 - 7 catheters).

The planning CT data set was digitally transferred to the treatment planning unit (BrachyVision®, Varian Medical Systems, Charlottesville, VA, USA). A radiologist defined the Clinical Target Volume (CTV) in the planning CT data set (Figure 1b). An one day prior to treatment obtained MRI of the liver was taken visually into account to avoid underestimation of the tumor size. To fulfill dosimetry planning in a timely manner, no registration of pre-treatment MRI with planning CT was performed due to patient safety and patient comfort. Based on literature and on own, yet unpublished data, the prescribed minimal dose inside the CTV was 15 to 20 Gy [4]. The true D100 applied was 14.3 to 21.2 (median 20Gy). The CTV ranged from 0.8 ml to 340.4 ml (median 20.5 ml), the volume (tumor plus liver parenchyma) which was exposed to more than 10 Gy ranged from 14.7 - 689 ml (median 137.7 ml) (Table 1).

The high dose rate afterloading system employed a ^{192}Iridium source of 10Ci (Gammamed®, Varian medical systems, Charlottesville, VA, USA). The source diameter was < 1 mm. Dwell positions were located every 5 mm. Dwell times were corrected automatically according to the actual source strength. The median duration of irradiation was 1154 seconds (range: 250 to 3762 seconds).

The calibration factor used to compensate for the decay of the ^{192}Iridium source ranged from 0.88 to 1.65 (median 1.36) relative to 10Ci.

Baseline MRI (Gyroscan NT® 1.5T, Philips, Best, The Netherlands) was obtained in all patients one day prior

Table 1 Patient identification and previous cancer therapies

Patient	Age -yr	Primary Tumor site	Treatment date (months after first diagnosis)	Liver Volume -ccm	CTV -ccm	With ≥10 Gy irradiated Liver Volume -ccm	Chemotherapy prior to brachytherapy	Chemotherapy during follow-up	Liver resection or local treatment prior to brachytherapy
1	84	Colon	79	1063	66.7	249.5	n/a	none	Right hemihepatectomy, RFA
2	69	Gastric	16	1720	340.4	689	CAP+DOC, CAP	none	none
3	66	Lung	10	2135	30.6	205	none	GEM	RFA
4	66	Colon	13	1296	3.64	19	FOLFOX	none	none
5	66	Breast	83	1206	2.7	79.5	TAM, END+EPI+5FU/FA, EXE	EXE	none
6	63	Breast	18	1301	41.5	277.7	VP 16+JM8, DOC	GEM, DOC+CAP	none
7	72	Colon	30	1499	23.1	141	5FU/FA, FOLFOX	none	Wedge resection S4
8	30	Breast	12	1334	9.2	90.6	DOC+EPI, TAM+LEU, VIN+ Anti-Her-2/neu, 5FU/FA	CAP	none
9	61	Breast	n/a	1406	15.1	91.3	none	none	Wedge resection S4
10	70	Colon	14	2672	20.5	181	5FU/FA	none	none
11	58	Colon	49	1531	36.4	236	5FU/FA, FOLFIRI, FOLFOX	none	none
12	69	Colon	43	1610	100.7	381.6	FOLFIRI, FOLFOX, 5FU/FA, Anti-EGFR +CPT11	Anti-EGFR +CPT11	none
13	61	Colon	n/a	1350	123.6	327.6	FOLFOX+Anti-VEGF, 5FU/FA,	FOLFOX	Right hemihepatectomy, RFA
14	72	Renal	n/a	1170	1.7	49.4	none	none	Wedge resection, RFA
15	55	Colon	56	1484	58.5	370	FOLFIRI, FOLFOX	none	Right hemihepatectomy
16	62	Colon	20	1247	4.9	104.5	FOLFOX	none	none
17	56	Renal	6	822	30.5	137.7	none	SOR	none
18	55	Colon	22	1170	7.3	145	CAP+L-OHP, CAP+L-OHP+ Anti-VEGF	none	Right hemihepatectomy
19	69	Breast	34	1073	10.1	60.1	EPI+DOC, Anti-Her-2/neu +CAP+VIN, SDX 105, DOC	none	none
20	53	Breast	125	1054	0.8	22.2	VP 16+CAR, DOC+ADR, TAM, EXE, LET, 5FU/FA +CTX+EPI, FUL, GEM	none	none
21	52	Breast	16	1650	7.1	102	VP 16+JM8, LET	CAP	none
22	76	Renal	156	930	2.9	14.7	none	none	Wedge resection, RFA
23	77	Breast	80	1503	28.9	100.7	CAP	none	none

Abbreviations: Bendamustine (SDX 105), Bevacizumab (Anti-VEGF), Capecitabine (CAP), Carboplatin (JM8), Cetuximab (Anti-EGFR), Cyclophosphamide (CTX), Docetaxel (DOC), Doxorubicin (ADR), Endoxane (END), Epirubicin (EPI), Etoposide (VP 16), Exemestan (EXE), 5-Fluorouracil (5FU), Folic acid (FA), 5-Fluorouracil/Folic acid +Irinotecan (FOLFIRI), 5-Fluorouracil/Folic acid +Oxaliplatin (FOLFOX), Fulvestrant (FUL), Gemcitabine (GEM), Irinotecan (CPT 11), Letrozole (LET), Leuprorelin (LEU), Oxaliplatin (L-OHP), Sorafenib (SOR), Tamoxifen (TAM), Trastuzumab (Anti-Her-2/neu), Vinorelbine (VIN).

Combined applications are marked by +. Comma marks indicate sequential chemotherapeutic regimens.

Clinical Target Volume (CTV), Radiofrequency Ablation (RFA)

to therapy. During follow-up, MRI was performed at 3 days, 6, 12 and 24 weeks after treatment. The MRI protocol consisted of the following sequences: T2-weighted (T2-w) ultrafast spinecho (UTSE) (time to echo (TE)/ time to repetition (TR) 90/2100 ms) with and without fat suppression, T1-weighted (T1-w) gradient echo (GRE) (TE/TR 5/30 ms, flip angle 30°) pre-contrast, 20s, 60s and 120s post intravenous administration of 0.025 mmol/kg bodyweight Gd-EOB-DTPA (Primovist®, Bayer Schering Pharma, Berlin, Germany), and 20 minutes post injection of intravenous Gd-EOB-DTPA. The slice thickness was 5 mm (T1-w) and 8 mm (T2-w) acquired in interleafed mode with no gap applied.

Gd-EOB-DTPA

We used the diminished uptake of the hepatocyte specific contrast agent Gd-EOB-DTPA as a surrogate marker for the functioning state of the liver parenchyma. Gd-

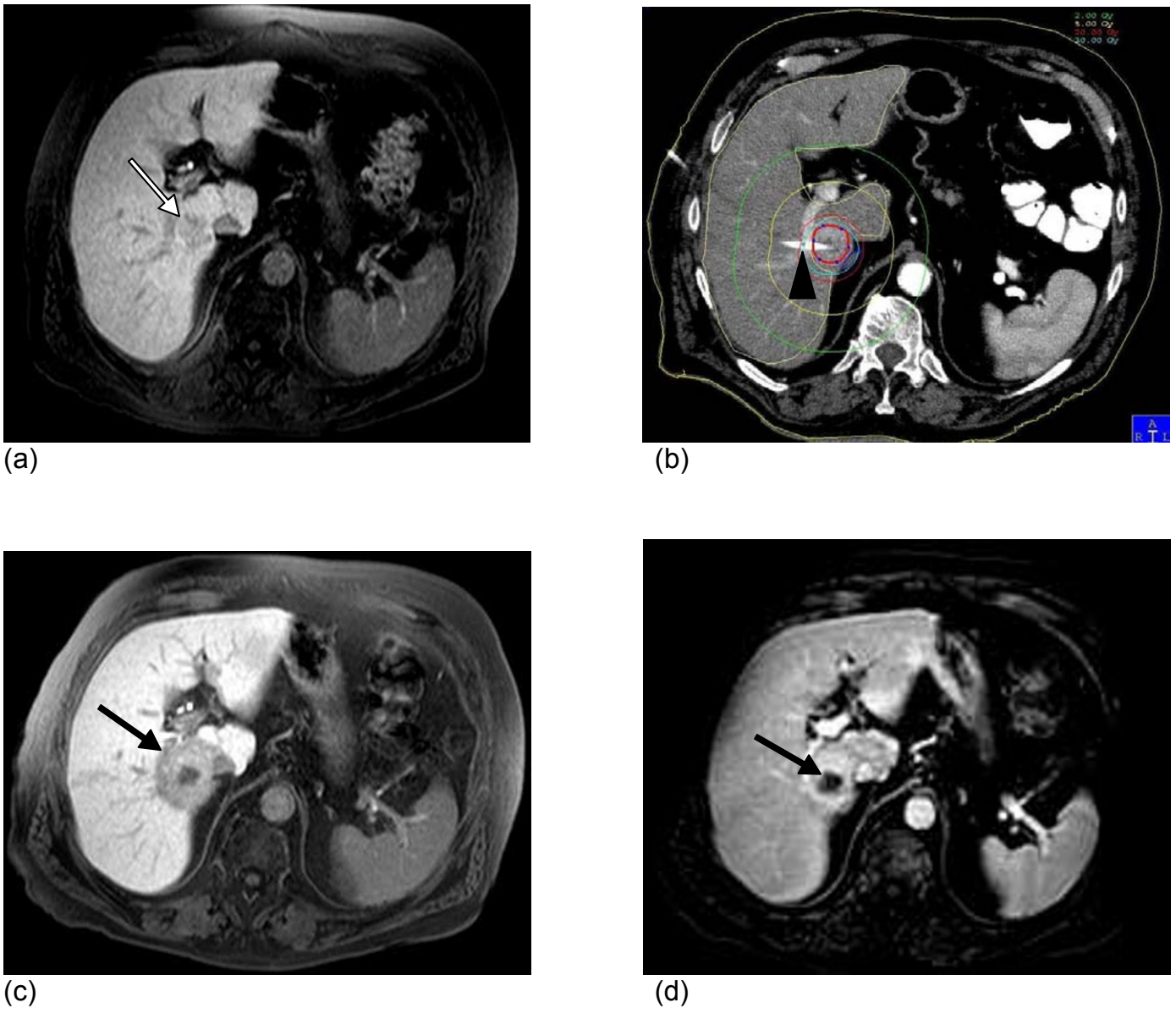

Figure 1 Illustration of CT guided brachytherapy and post interventional hepatic dysfunction in MRI. (a) Baseline MRI. T1-w GRE 20 minutes post i.v. application of Gd-EOB-DTPA. Colorectal liver metastasis in segment 6/7 (white arrow). (b) Contrast-enhanced computed tomography (CT) after CT-guided positioning of one brachytherapy catheter (truncated, black arrowhead) in the metastasis. The red line resembles the 15Gy isodose. (c) MRI 6 weeks after treatment. T1-w GRE 20 minutes post i.v. application of Gd-EOB-DTPA. Signal void around the tumor indicates hepatocyte dysfunction of liver parenchyma (black arrow). No evidence of tumor regrowth in (d): T1-w GRE dynamic scan 60s after application of the contrast dye shows shrinkage resulting from tumor necrosis after irradiation (black arrow).

EOB-DTPA is a newly developed water soluble MR contrast agent containing a lipophilic moiety. Like other gadolinium contrast media, the contrast function is basically determined by the paramagnetic gadolinium ion leading to a high T1 relaxivity. Unlike common MRI contrast agents (e.g. Gd-DTPA), Gd-EOB-DTPA is distributed not only to the extracellular fluid space, but taken up by the organic anion transporting polypeptide (OATP) of the hepatocytes. It is excreted via the canalicular multispecific organic anion transporter (cMOAT/mrp2) following a linear, concentration dependent mechanism [19-22]. Animal studies have shown a biliary excretion rate of 63-80% and 32-34% in rats and simians, respectively. Biodistribution studies in humans reveal a dose independent biliary (41.6-51.2%) and renal (43.1-53.2%) elimination and an enterohepatic recirculation of approximately 4%. Enhancement during the distribution phase of the contrast agent mainly depends on the vascularity, while enhancement on delayed images 20 minutes after administration is characterized by the selective uptake of the contrast agent by the hepatocytes. Non-hepatic tissue (e.g. liver metastases) shows no contrast enhancement on delayed images [15,17,21,23-26] (Figure 1a + c). The signal intensity of

liver parenchyma on the delayed images correlates with the functioning state of the according hepatocytes with a decreased signal intensity in dysfunctional liver parenchyma [27]. Thus a MRI based volumetric assessment of liver parenchyma damage is possible.

Image registration

Quantitative analysis of hepatocellular dysfunction and edema in areas exposed to focal high dose rate brachytherapy was performed using T1-w GRE 20 minutes post intravenous administration of Gd-EOB-DTPA and T2-w UTSE with fat suppression, respectively. Follow-up imaging was performed at four follow-up time-points (3 days, 6, 12 and 24 weeks after brachytherapy) leading to a total number of 92 MRI scans in 23 patients.

For image fusion of the follow-up MRI scans with the according treatment plan (based on the planning CT data set), MRI data was transferred to the treatment planning system. BrachyVision® offers an isoscalar local semi-automated point based 3D-3D image registration. Match points were defined on corresponding landmarks such as branches of the portal vein to enable fusion of MR and planning CT/dosimetry data. Landmarks were restricted to liver structures.

A linear interpolation was performed automatically by BrachyVision® to match the varying slice thicknesses of T2-w MRI (8 mm) and CT (5 mm). As a result of this procedure, BrachyVision® simultaneously displayed the treatment plan as well as the anatomical structures of the MRI scan (Figure 2a -c). The absolute registration error was always less than 5 mm. A retrospective registration of pre-treatment MRI with planning CT/dosimetry to obtain the CTV as basline in MRI was deemed inappropriate due to a possible additional registration error. As already stated the tumor extent in pre treatment MRI was respected in dosimetry planning.

Quantitative analysis

On all of the T1-w late Gd-EOB-DTPA as well as the T2-w enhanced images an experienced GI Radiologist digitally outlined the border of hypointensity on T1-w images (loss of hepatocyte function as displayed by diminished Gd-EOB-DTPA uptake) or hyperintensity on T2-w images (edema) around the irradiated liver tumor (referred to as "pseudolesion (including the irradiated tumor)" in the following). Pre-existing peritumoral changes could be excluded on the pre treatment MRI. Based on the total 3D data set of these volumes, the Brachyvision® software calculated a dose-volume histogram. As a result, we determined the percentage of each pseudolesion receiving a specific dose. We specified the threshold dose for either edema or function loss as the D_{90}, i.e. the dose achieved in at least 90% of the pseudolesion volume (Figure 3).

As an additional descriptor, we determined the volume of each pseudolesion in relation to the former intrahepatic 10Gy isodose volume. This additional volumetric approach was performed as an independent verification of the previously described methodology.

Laboratory analysis

One day prior to the intervention and during follow up we assessed the following laboratory parameters: bilirubin, aspartate aminotransferase, alanine aminotransferase, alkaline phosphatase, albumin, international normalized ratio, and cholinesterase. Laboratory parameters were graded according to the 'Common Terminology Criteria for Adverse Events' (CTCAE version 4.02, National Cancer Institute, USA).

No patient presented evidence of liver function degradation prior to therapy.

Factors of influence

Following factors were recorded and tested for influence on the minimal dose provoking edema or hepatocyte function loss (i.e. the dose at 6 weeks): patient age, the liver volume, the clinical target volume, the liver volume which was exposed with more than 5Gy or 10Gy, the source factor, the irradiation time, the number of catheters applied, history of chemotherapy.

Statistical analysis

Results of continuous data are displayed as medians and ranges and/or lower and upper quartile, results of frequency data as counts and percentages.

For two-group comparisons of the medians two-sided Wilcoxon rank sum tests were used. Correlations were evaluated using a two sided Pearson correlation test.

A $p < 0.05$ was considered to be statistically significant.

For statistical analysis the software 'Statistical Package for the Social Sciences' (IBM SPSS, Version 17.0, Somers, NY, USA) was used.

Results

The registration error of the landmarks after image fusion of the planning CT to the follow-up MRI was as follows: in median 0.95 mm (0.53-1.5), 1.82 mm (0.22-2.91), 1.79 mm (0.81-2.91) and 2.04 mm (0.85-5) for the T1 weighted sequences at 3 days, 6, 12 and 24 weeks, respectively. For the T2 weighted images, the registration error was in median 0.98 mm (0.59-1.3), 1.75 mm (0.79-3.65), 1.89 mm (0.81-3.89) and 1.98 mm (0.98-3.53), respectively.

Figure 4a + b display the development of hepatocyte dysfunction or hepatic edema in correlation to the isodose distribution. Three days after brachytherapy, the D_{90} for hepatocyte function loss reached a median of 19.5Gy (7.4-53.1, Q_{25}: 16.9, Q_{75}: 21.1), i.e. doses

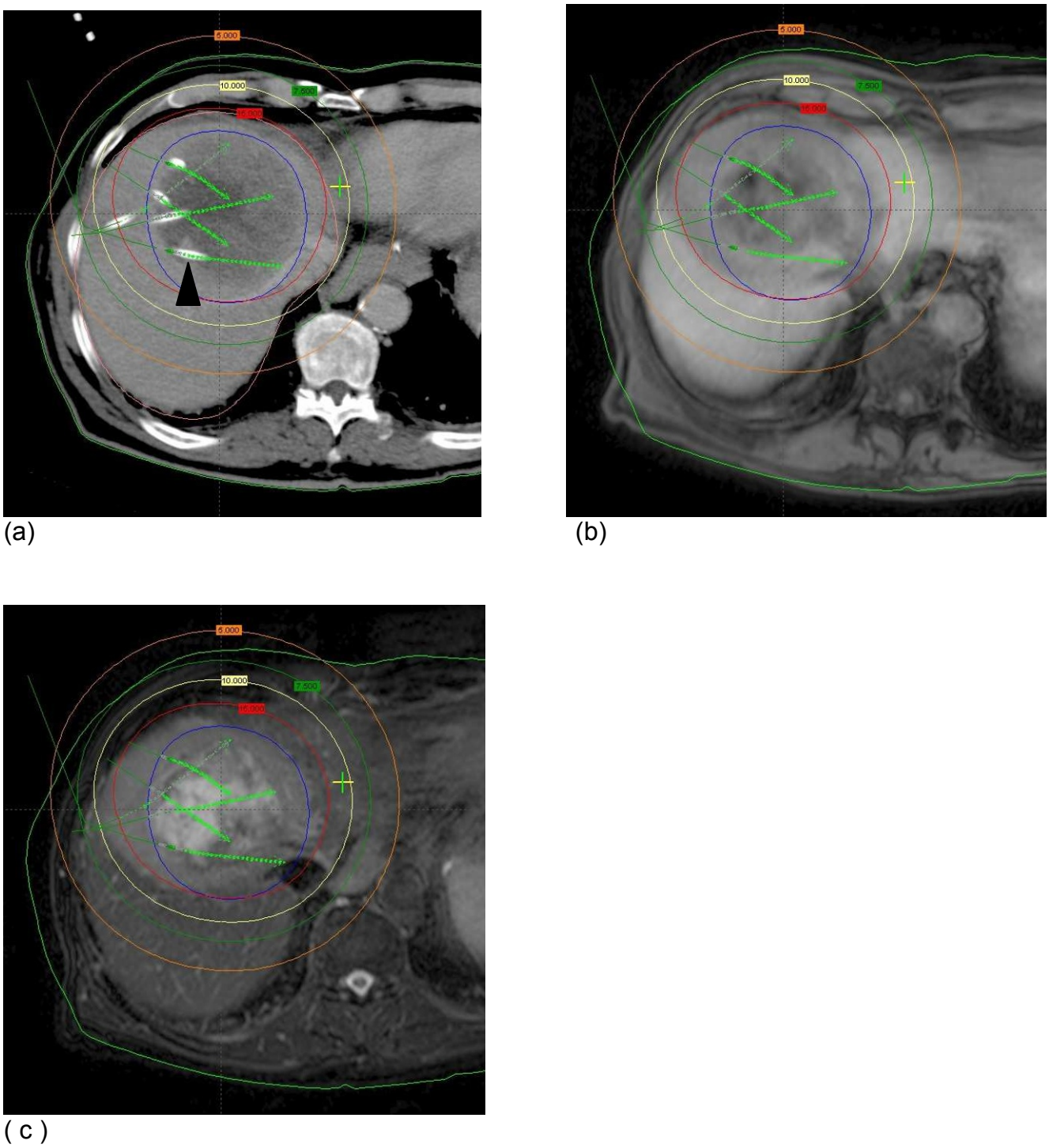

Figure 2 Image fusion of planning CT/dosimetry and follow-up MRI. (a) Contrast-enhanced CT after CT-guided positioning of 5 brachytherapy catheters in a colorectal metastasis (one catheter is labeled with a black arrowhead, the other catheter positions in cranial or caudal planes are indicated by green arrows). Isodoses lines the CTV (blue circle) after dosimetry with BrachyVision® (b + c). MRI 3 months after brachytherapy: T1-w gradient echo 20 minutes post i.v. application of Gd-EOB DTPA (b) and T2-w UTSE FS (c) showing image fusion with the treatment planning CT.

≥19.5Gy provoked a state of hepatocyte dysfunction. At six weeks, the isosurface had increased significantly to a median of 9.4 Gy (6.4-16.6, Q_{25}: 8.5, Q_{75}: 11.7; $p < 0.001$), i.e. protracted toxic effects lowered the threshold dose for hepatic dysfunction to 9.4Gy. Between 6 and 12 weeks, the dysfunctional volume had decreased significantly to a median of 11.4Gy (7.8-20.2, Q_{25}: 9, Q_{75}: 14.5; $p = 0.002$). After 24 weeks, the isosurface decreased further to a median of 14 Gy (7.9-24.7, Q_{25}: 10.5, Q_{75}: 17.6; $p = 0.002$).

Between three days and 6 weeks, the extension of the edema increased significantly from the 19.1Gy (7.8-33.8,

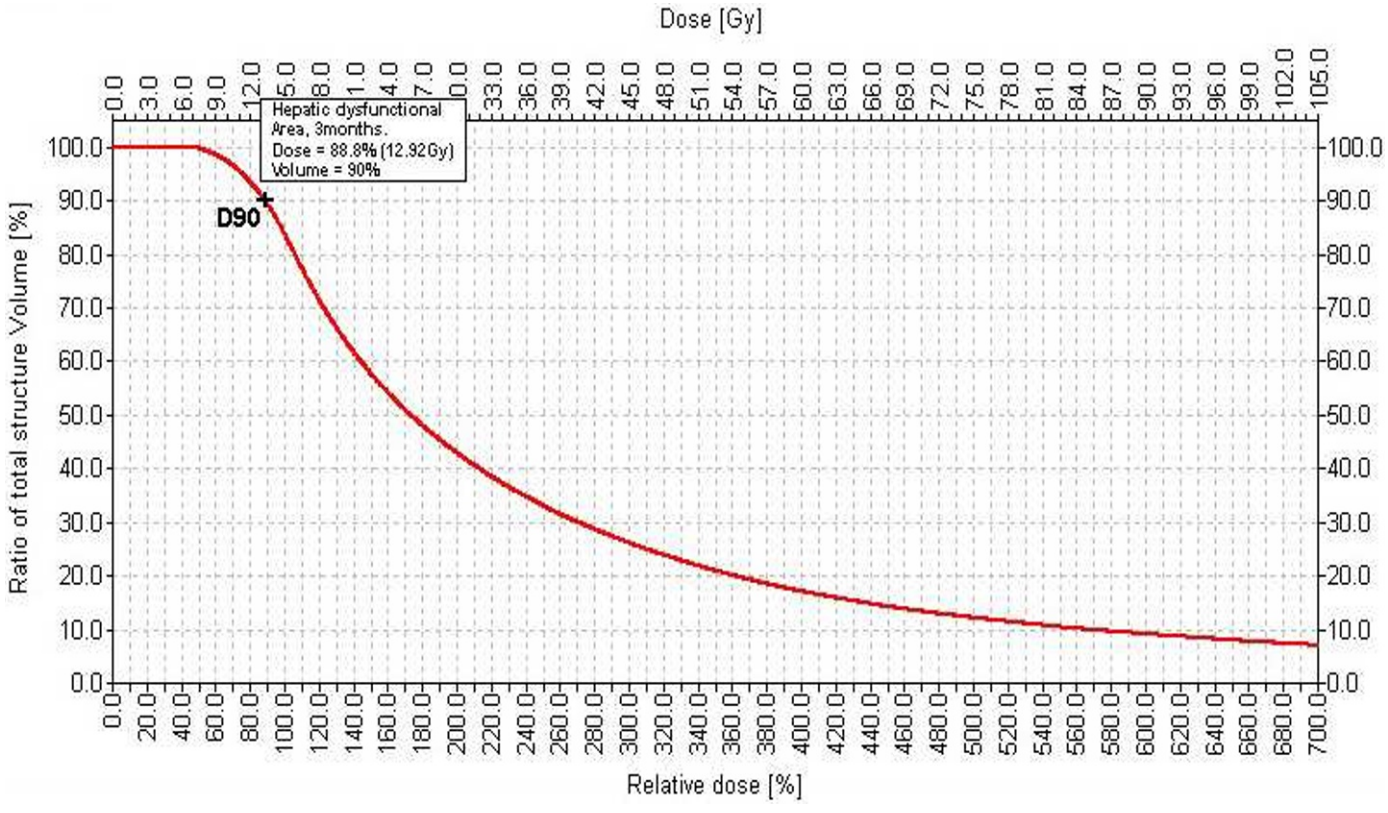

Figure 3 Dose-Volume-Histogram of nonfunctioning liver volume. Dose volume histogram of nonfunctioning liver volume in a patient 3 months after HDR brachytherapy. (D90: the dose applied to at least 90% of the volume, in this case 12.92 Gy.)

Q_{25}: 12.3, Q_{75}: 22.7) isosurface to 9.2Gy at median (5.9-17.4, Q_{25}: 6.8, Q_{75}: 10.9; $p < 0.001$). After this peak a significant decrease occurred between 6 and 12 weeks (median 11.3Gy, 7.4-18.4, Q_{25}: 9.3, Q_{75}: 13.1; $p = 0.002$). After 24 weeks, the edematous tissue isosurface shrank to a median of 11.8 Gy (7.9-24.3, Q_{25}: 9.3, Q_{75}: 14.8; $p = 0.018$).

At three days post brachytherapy, the minimal dose leading to edema tended to be less compared to the dose provoking focal hepatocyte function loss ($p = 0.055$). No differences between the doses provoking focal hepatic dysfunction or edema were noted at 6, 12 and 24 weeks ($p = 0.158$, 0.212 and 0.128, respectively).

Figure 5a + b illustrate the development of the volume of focal hepatocyte function loss or edema post brachytherapy in correlation to the liver volume which was exposed with more than 10Gy. The relative volume of hepatocyte function loss increased significantly between three days and 6 weeks ($p < 0.001$) with an extend to 81% of the 10Gy volume in median after 6 weeks (Q_{25}: 61%, Q_{75}: 100%). After 12 weeks, the decline of the volume with hepatocyte function loss was significant compared to 6 weeks (58%, Q_{25}: 43%, Q_{75}: 76%; $p < 0.001$), and again after 24 weeks when compared to 12 weeks (36%, Q_{25}: 27%, Q_{75}: 51%; $p < 0.001$). Between three days and 6 weeks, edema volume increased significantly (6 weeks: 91%, Q_{25}: 63, Q_{75}: 116%; $p < 0.001$). From week 6 to week 12, edema volume shrank significantly (68%, Q_{25}: 54%, Q_{75}: 91%; $p = 0.001$) and continued to week 24 with a significant decrease (48%, Q_{25}: 31%, Q_{75}: 60%; $p < 0.001$). At all time points the size of the edema volume surmounted the size of the volume of hepatocyte dysfunction in relation to the 10 Gy volume ($p < 0.05$).

We found no statistical correlation between the minimal dose provoking edema or hepatocyte function loss (i.e. the dose at 6 weeks) and: patient age, the liver volume, the clinical target volume, the liver volume which was exposed with more than 5Gy or 10Gy, the source factor, the irradiation time, the number of catheters applied, or a history of chemotherapy.

No patient included in this study demonstrated a severe impairment of liver function as measured by the above named laboratory parameters before CT guided brachytherapy. No severe acute or late toxicity were observed after CT guided brachytherapy. Liver function tests graded according to the 'common terminology criteria for adverse events' (CTCAE) version 4.02 never exceeded grade 2 toxicities during follow up.

Discussion

Quantitative data on the radiation threshold dose of hepatic tissue is scarce compared to other late-responding

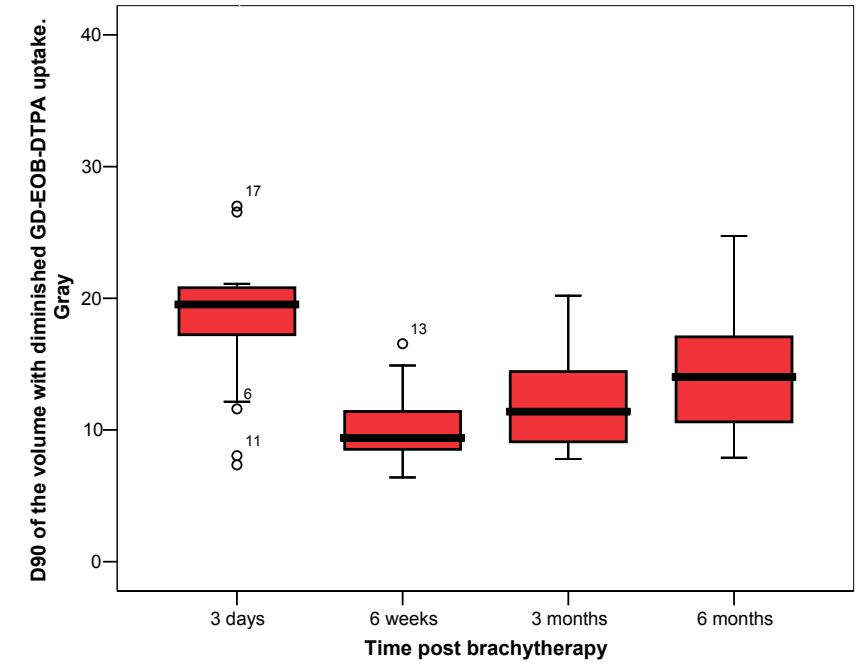

(a)

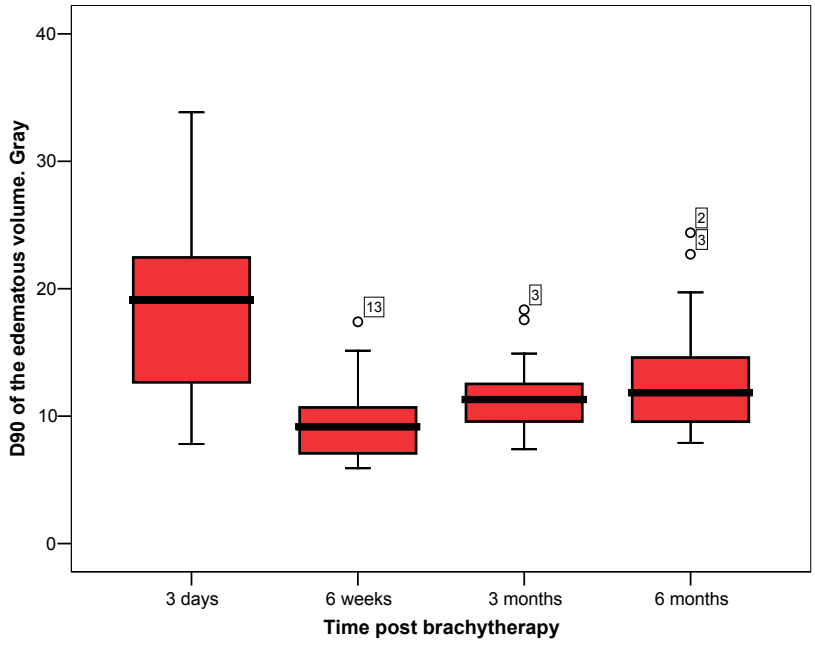

(b)

Figure 4 Boxplot of threshold doses of hepatocyte function loss and edema over time. (a) Hepatocyte function loss over time relative to dose exposition. (b) Development of the according edema.

tissues. In this study we used regional uptake of the hepatocyte specific MRI contrast media Gd-EOB-DTPA as a surrogate parameter for hepatic function after HDR irradiation of small liver volumes. Thus we were able to determine the hepatocyte tolerance dose in vivo. Small volumes of hepatic parenchyma irradiated with more than 9.4Gy revealed a non functioning state after six weeks. After six months, recovery of hepatic parenchyma led to a threshold dose of 14 Gy for hepatic dysfunction.

The histological appearance of radiation induced liver disease indicates that endothelial injury and subsequent obstruction of centrilobular venules and sinusoids are

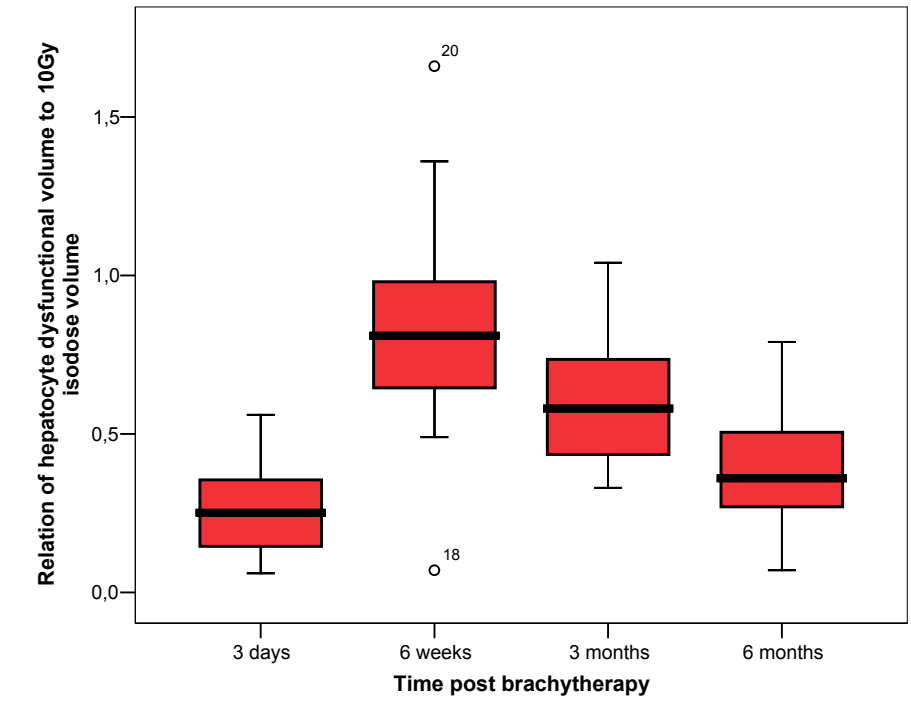

(a)

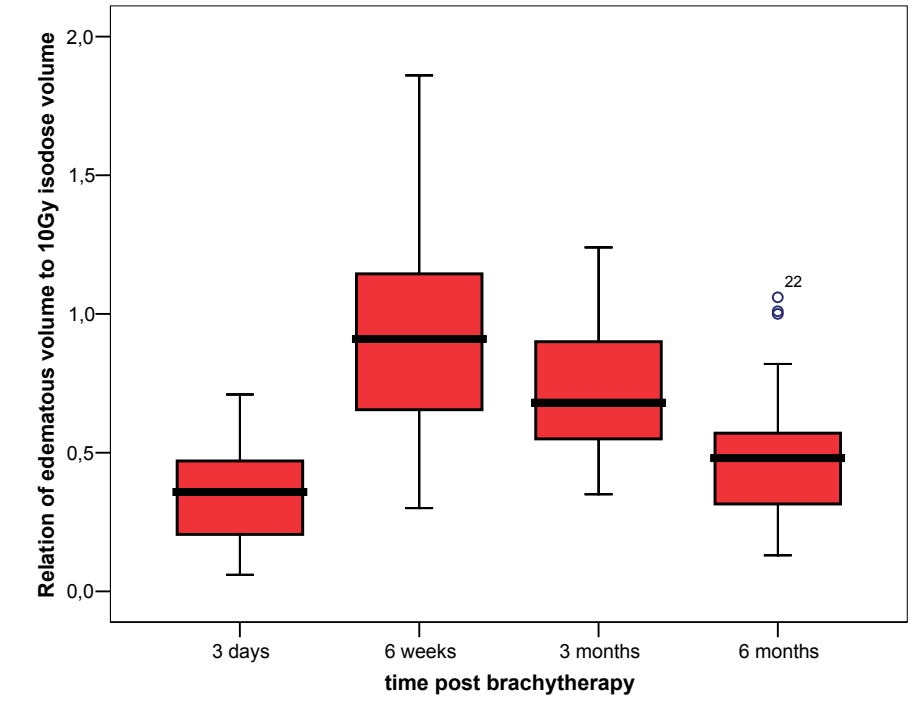

(b)

Figure 5 Boxplot of volume of hepatocyte function loss and edema over time. Development of hepatic function loss (a) and edema (b) around the irradiated tumor relative to the 10 Gy isodose volume (liver parenchyma only).

the key events in the pathogenesis of radiation injury of the liver. Larger veins are frequently spared [7,12,13,28]. The pathological lesion resembles veno-occlusive disease, frequently seen after total body irradiation in induction therapy prior to bone marrow transplantation [29-31]. This initial injury is followed by a wide, edematous subendothelial zone, resembling deposits of fibrin-related aggregates and fragmented red cells in the

subendothelial zone. Early deposition of fibrinogen is frequently found without platelet accumulation. These aggregates, as well as the intramural entrapment of fluid and cellular debris, progressively occlude the hepatic venous outflow by intraluminal sinusoidal fibrous material, subendothelial collagen fibers and foamy cells [7,13,28] (Figure 6). Experimental studies on hepatic radiation injury support the theory that the endothelial lining of venules and sinusoids is far more sensitive to radiation than hepatocytes [32-34].

However, changes of uptake of a hepatocyte specific contrast media illuminate the final path of the radiation injury, i.e. these changes visualize areas of a dysfunctional hepatic system, not necessarily individual hepatocyte dysfunction [27]. The model does not differentiate whether parenchymal (hepatocytes) or non-parenchymal cells (endothelial-, Kupffer- and Ito-cells) play the key role in the development of focal hepatic dysfunction. Hence, our model must be interpreted as the reaction of a liver functioning unit to irradiation.

Therapeutic irradiation of liver malignancies is restricted by hepatic tolerance with the clinical endpoint liver function loss. In total or large volume irradiation of the liver, major complications such as RILD have frequently been described [6,7,10,11]. However, the parallel functional structure of the liver may cover a loss of extensive liver volume without clinical symptoms such as after hepatectomy. A comparison between data of total or large volume liver irradiation using the clinical endpoint RILD or liver failure has to be differentiated from small volume irradiation as executed in our study. CT-guided brachytherapy as well as stereotactic irradiation of liver malignancies are locally circumscribed radiotherapies designed to spare healthy liver parenchyma. In a clinical setting, a relatively small rim of liver parenchyma around the CTV is exposed to high irradiation doses. This limited loss of functioning hepatic tissue is generally tolerated well without any impairment of the whole organ function as seen by unchanged liver function parameters during follow-up [35]. However,

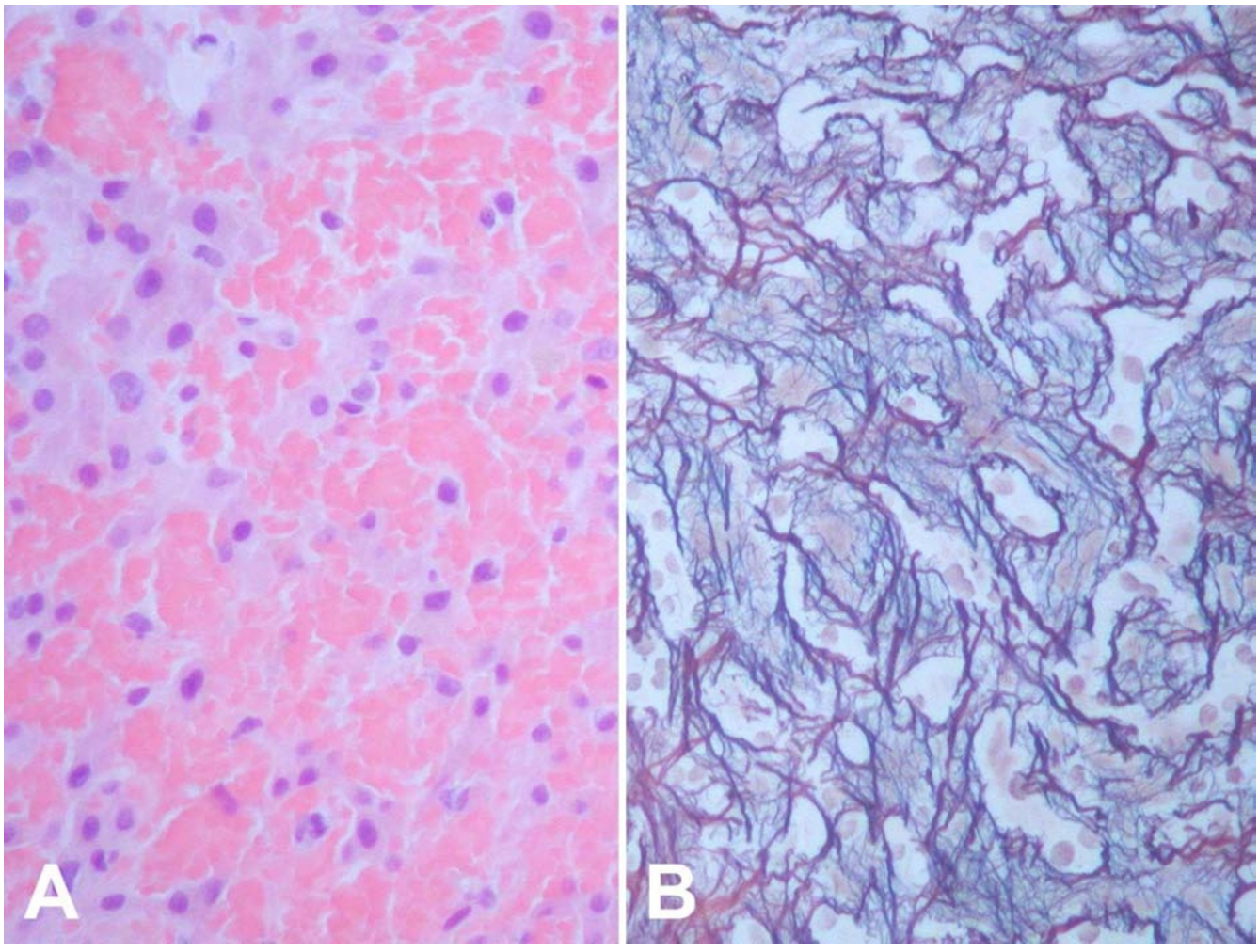

Figure 6 Histological specimen: liver tissue after radiation exposure. Liver biopsy in an area exposed to approximately 20 Gy two months earlier. Severe sinusoidal congestion with atrophy of hepatocytes (A) and increased perisinusoidal reticulin deposition (B). Hematoxylin-eosin (A) and Gomori's silver stain (B), original magnification: x200. Biopsy was taken to rule out local recurrence.

caution should be exercised if the total volume of unexposed liver is small such as

- in patients scheduled for synchronous multifocal irradiation of liver malignancies because of overlapping isodoses of the single lesions.
- in patients scheduled for irradiation of a large tumor volume in small livers.
- in patients scheduled for irradiation with a history of partial liver resection because of a potentially small residual parenchymal volume.
- In patients with chronic and/or degenerative liver diseases (such as cirrhosis).

An increase of the incidence of clinical RILD has been observed in total liver irradiation when doses 30-55Gy are delivered applying conventional fractionation schemes [6,7,10-14,28]. These fractionated tolerance doses translate into single-fraction doses of 11.25 up to 14Gy, respectively, according to the linear-quadratic model and an assumed α/β of 3Gy for liver tissue [11]. These threshold values correspond well to our own data on focal liver dysfunction after single fraction small volume irradiation and correspond well to observed clinical significant hepatic injury after doses as low as 10Gy in patients undergoing a single fractioned total body or abdominal irradiation and chemotherapy prior to bone marrow transplantation [29,30,36]. However, an unequal dose rate of the different approaches has to be considered.

The reaction of small liver volumes to irradiation has also been studied by other groups. Herfarth et al. examined hepatic tolerance after applying stereotactic single-fraction irradiation to liver malignancies with data derived from follow-up contrast-enhanced CT. The authors observed a focal reaction at a dose minimum of mean 13.7Gy (range 8.9 -19.2Gy) [5]. In principle, contrast enhanced CT will most likely demonstrate the venous outflow occlusion after radiation exposure. This approach visualizes the underlying pathophysiological change provoking focal liver function degradation. Consequently, the results of this workgroup match well with the data derived from our model applying hepatocyte directed contrast agent in MRI, visualizing the effect of venous outflow occlusion with distraction of a liver function unit as described above. It remains questionable whether the higher standard deviation of their results may be explained by a smaller sensitivity of the CT model as compared to MRI [5,8].

In the present study we not only sought to add further data on hepatic dose tolerance, but to improve the study concept applied previously that had used the first generation hepatocyte-directed contrast agent Gd-BOPTA [8]. While the pharmacodynamics of Gd-BOPTA are similar to those of Gd-EOB-DTPA, the pharmacokinetics differ significantly. The biliary excretion rate of Gd-BOPTA is just 0.6 to 4% compared to 41.6 to 51.2% in Gd-EOB-DTPA [15-18]. This results in a higher signal-to-noise-ratio in Gd-EOB-DTPA and consequently to a better demarcation of liver lesions and non-functional parenchyma. The results presented in this study determining the threshold dose of hepatocytes support the data from the precursor study using Gd-BOPTA [8]. Apart from the different hepatocyte specific contrast agent used (Gd-BOPTA vs. Gd EOB DTPA) in MRI follow up, the design of these two studies was similar. The minimal tolerance dose to high dose irradiation in the precursor study was determined with 9.5Gy in median (6-14.5, Q_{25}: 8, Q_{75}: 12) after six weeks (n = 25), compared to 9.4Gy in median (6.4-16.6, Q_{25}: 8.5, Q_{75}: 11.7) in the present study. Both studies showed a strong recuperation of dysfunctional liver parenchyma after six months with a residual non-functioning liver parenchyma in areas irradiated with formerly more than 15.2Gy in median (7.5-23, Q_{25}: 12, Q_{75}: 18) and 14 Gy in median (7.9-24.7, Q_{25}: 10.5, Q_{75}: 17.6) at present [8].

However, we did not reach our goal to decrease the relatively high variation from the precursor study employing Gd-BOPTA, despite the superior imaging properties of Gd-EOB-DTPA. We attribute this failure to the fact that individual differences in hepatic dose tolerance do not preferably reflect flaws of the imaging model, but rather unknown factors of individual predisposition. In other words, data derived from different models (including CT or MR imaging) consistently shows deviations of individual hepatic dose tolerance to small volume single fraction irradiation.

Conclusion

In summary, our study supports previous data on hepatic tolerance doses after single fraction, high dose rate small volume irradiation. We conclude that the threshold dose to induce a focal loss of liver function is about 10 Gy after 6 weeks. We confirmed previously observed strong recuperation with a threshold dose of 14 Gy after 6 months. These results should be considered specifically in cases where more than one liver lesion shall be irradiated, or in patients with a history of focal liver irradiation. Further investigation is warranted to assess the correlation between deminished uptake of Gd-EOB-DTPA in the affected liver volume and clinical symptoms as liver function degradation before routine use of Gd-EOB-DTPA can be recommended in this matter.

List of abbreviations

RILD: Radiation Induced Liver Disease; CT: Computed Tomography; 3D: Three Dimensional; MRI: Magnetic Resonance Imaging; Gd-BOPTA: Gadobenate dimeglumine; HDR: High Dose Rate; Gd-EOB-DTPA: Gadolinium ethoxybenzyl

diethylenetriaminepentaacetate; CTV: Clinical Target Volume; T2-w: T2-weighted; UTSE: Ultrafast Spinecho; TE: Time to Echo; TR: Time to Repetition; T1-w: T1-weighted; GRE: Gradient Echo.

Author details
[1]Klinik für Radiologie und Nuklearmedizin, Universitätsklinikum Magdeburg, Otto-von-Guericke-Universität Magdeburg, Germany. [2]Institut für Pathologie, Universitätsklinikum Magdeburg, Otto-von-Guericke-Universität Magdeburg, Germany. [3]Klinik für Strahlentherapie, Charité Universitätsmedizin Berlin, Campus Virchow Klinikum, Germany.

Authors' contributions
MS and RS participated in the study design and drafted the manuscript; KM performed image fusion and screened patients for inclusion; CW participated in the design of the study; TK performed histological staining and corrected the manuscript; SL performed image fusion and screened patients for inclusion; MP served as reader; PW participated in study design; JR conceived of the study and paticipated in its design and coordination. All authors read and approved the final manuscript.

Conflict of interest
JR receives grants for consulting and research from Bayer Healthcare. No stock holder or shares. All other authors: there is no actual or potential conflicts of interest, sources of financial support, corporate involvement, patent holdings, etc. for each author to report.

Received: 20 December 2010 Accepted: 17 April 2011
Published: 17 April 2011

References

1. Herfarth KK, Debus J, Lohr F, Bahner ML, Rhein B, Fritz P, Hoss A, Schlegel W, Wannenmacher MF: **Stereotactic single-dose radiation therapy of liver tumors: results of a phase I/II trial.** *J Clin Oncol* 2001, **19**:164-170.
2. Kavanagh BD, Schefter TE, Cardenes HR, Stieber VW, Raben D, Timmerman RD, McCarter MD, Burri S, Nedzi LA, Sawyer TE, *et al*: **Interim analysis of a prospective phase I/II trial of SBRT for liver metastases.** *Acta Oncol* 2006, **45**:848-855.
3. Ricke J, Wust P, Stohlmann A, Beck A, Cho CH, Pech M, Wieners G, Spors B, Werk M, Rosner C, *et al*: **CT-guided interstitial brachytherapy of liver malignancies alone or in combination with thermal ablation: phase I-II results of a novel technique.** *Int J Radiat Oncol Biol Phys* 2004, **58**:1496-1505.
4. Ricke J, Mohnike K, Pech M, Seidensticker M, Rühl R, Wieners G, Gaffke G, Kropf S, Felix R, Wust P: **Local response and impact on survival after local ablation of liver metastases from colorectal carcinoma by CT-guided HDR-brachytherapy.** *Int J Radiat Oncol Biol Phys* 2009.
5. Herfarth KK, Hof H, Bahner ML, Lohr F, Hoss A, van Kaick G, Wannenmacher M, Debus J: **Assessment of focal liver reaction by multiphasic CT after stereotactic single-dose radiotherapy of liver tumors.** *Int J Radiat Oncol Biol Phys* 2003, **57**:444-451.
6. Kim TH, Panahon AM, Friedman M, Webster JH: **Acute transient radiation hepatitis following whole abdominal irradiation.** *Clin Radiol* 1976, **27**:449-454.
7. Lawrence TS, Robertson JM, Anscher MS, Jirtle RL, Ensminger WD, Fajardo LF: **Hepatic toxicity resulting from cancer treatment.** *Int J Radiat Oncol Biol Phys* 1995, **31**:1237-1248.
8. Ricke J, Seidensticker M, Ludemann L, Pech M, Wieners G, Hengst S, Mohnike K, Cho CH, Lopez HE, Al Abadi H, *et al*: **In vivo assessment of the tolerance dose of small liver volumes after single-fraction HDR irradiation.** *Int J Radiat Oncol Biol Phys* 2005, **62**:776-784.
9. Burman C, Kutcher GJ, Emami B, Goitein M: **Fitting of normal tissue tolerance data to an analytic function.** *Int J Radiat Oncol Biol Phys* 1991, **21**:123-135.
10. Dawson LA, Normolle D, Balter JM, McGinn CJ, Lawrence TS, Ten Haken RK: **Analysis of radiation-induced liver disease using the Lyman NTCP model.** *Int J Radiat Oncol Biol Phys* 2002, **53**:810-821.
11. Emami B, Lyman J, Brown A, Coia L, Goitein M, Munzenrider JE, Shank B, Solin LJ, Wesson M: **Tolerance of normal tissue to therapeutic irradiation.** *Int J Radiat Oncol Biol Phys* 1991, **21**:109-122.
12. Lewin K, Millis RR: **Human radiation hepatitis. A morphologic study with emphasis on the late changes.** *Arch Pathol* 1973, **96**:21-26.
13. Reed GB Jr, Cox AJ Jr: **The human liver after radiation injury. A form of veno-occlusive disease.** *Am J Pathol* 1966, **48**:597-611.
14. De Bari B, Pointreau Y, Rio E, Mirabel X, Mornex F: **Normal tissue tolerance to external beam radiation therapy: liver.** *Cancer Radiother* 2010, **14**:344-349.
15. Hamm B, Staks T, Muhler A, Bollow M, Taupitz M, Frenzel T, Wolf KJ, Weinmann HJ, Lange L: **Phase I clinical evaluation of Gd-EOB-DTPA as a hepatobiliary MR contrast agent: safety, pharmacokinetics, and MR imaging.** *Radiology* 1995, **195**:785-792.
16. Kirchin MA, Pirovano GP, Spinazzi A: **Gadobenate dimeglumine (Gd-BOPTA). An overview.** *Invest Radiol* 1998, **33**:798-809.
17. Schuhmann-Giampieri G, Schmitt-Willich H, Press WR, Negishi C, Weinmann HJ, Speck U: **Preclinical evaluation of Gd-EOB-DTPA as a contrast agent in MR imaging of the hepatobiliary system.** *Radiology* 1992, **183**:59-64.
18. Spinazzi A, Lorusso V, Pirovano G, Taroni P, Kirchin M, Davies A: **Multihance clinical pharmacology: biodistribution and MR enhancement of the liver.** *Acad Radiol* 1998, **5(Suppl 1)**:S86-S89.
19. Clement O, Muhler A, Vexler V, Berthezene Y, Brasch RC: **Gadolinium-ethoxybenzyl-DTPA, a new liver-specific magnetic resonance contrast agent. Kinetic and enhancement patterns in normal and cholestatic rats.** *Invest Radiol* 1992, **27**:612-619.
20. Oude Elferink RP, Jansen PL: **The role of the canalicular multispecific organic anion transporter in the disposal of endo- and xenobiotics.** *Pharmacol Ther* 1994, **64**:77-97.
21. Pascolo L, Cupelli F, Anelli PL, Lorusso V, Visigalli M, Uggeri F, Tiribelli C: **Molecular mechanisms for the hepatic uptake of magnetic resonance imaging contrast agents.** *Biochem Biophys Res Commun* 1999, **257**:746-752.
22. van Montfoort JE, Stieger B, Meijer DK, Weinmann HJ, Meier PJ, Fattinger KE: **Hepatic uptake of the magnetic resonance imaging contrast agent gadoxetate by the organic anion transporting polypeptide Oatp1.** *J Pharmacol Exp Ther* 1999, **290**:153-157.
23. Muhler A, Weinmann HJ: **Biodistribution and excretion of 153Gd-labeled gadolinium ethoxybenzyl diethylenetriamine pentaacetic acid following repeated intravenous administration to rats.** *Acad Radiol* 1995, **2**:313-318.
24. Reimer P, Rummeny EJ, Shamsi K, Balzer T, Daldrup HE, Tombach B, Hesse T, Berns T, Peters PE: **Phase II clinical evaluation of Gd-EOB-DTPA: dose, safety aspects, and pulse sequence.** *Radiology* 1996, **199**:177-183.
25. Schuhmann-Giampieri G: **Liver contrast media for magnetic resonance imaging. Interrelations between pharmacokinetics and imaging.** *Invest Radiol* 1993, **28**:753-761.
26. Weinmann HJ, Schuhmann-Giampieri G, Schmitt-Willich H, Vogler H, Frenzel T, Gries H: **A new lipophilic gadolinium chelate as a tissue-specific contrast medium for MRI.** *Magn Reson Med* 1991, **22**:233-237.
27. Ryeom HK, Kim SH, Kim JY, Kim HJ, Lee JM, Chang YM, Kim YS, Kang DS: **Quantitative evaluation of liver function with MRI Using Gd-EOB-DTPA.** *Korean J Radiol* 2004, **5**:231-239.
28. Fajardo LF, Colby TV: **Pathogenesis of veno-occlusive liver disease after radiation.** *Arch Pathol Lab Med* 1980, **104**:584-588.
29. Jacobs P, Miller JL, Uys CJ, Dietrich BE: **Fatal veno-occlusive disease of the liver after chemotherapy, whole-body irradiation and bone marrow transplantation for refractory acute leukaemia.** *S Afr Med J* 1979, **55**:5-10.
30. Shulman HM, McDonald GB, Matthews D, Doney KC, Kopecky KJ, Gauvreau JM, Thomas ED: **An analysis of hepatic venocclusive disease and centrilobular hepatic degeneration following bone marrow transplantation.** *Gastroenterology* 1980, **79**:1178-1191.
31. Shulman HM, Gown AM, Nugent DJ: **Hepatic veno-occlusive disease after bone marrow transplantation. Immunohistochemical identification of the material within occluded central venules.** *Am J Pathol* 1987, **127**:549-558.
32. Geraci JP, Mariano MS: **Radiation hepatology of the rat: parenchymal and nonparenchymal cell injury.** *Radiat Res* 1993, **136**:205-213.
33. Jirtle RL, Michalopoulos G, McLain JR, Crowley J: **Transplantation system for determining the clonogenic survival of parenchymal hepatocytes exposed to ionizing radiation.** *Cancer Res* 1981, **41**:3512-3518.
34. Johnson LK, Longenecker JP, Fajardo LF: **Differential radiation response of cultured endothelial cells and smooth myocytes.** *Anal Quant Cytol* 1982, **4**:188-198.

35. Ruhl R, Seidensticker M, Peters N, Mohnike K, Bornschein J, Schutte K, Amthauer H, Malfertheiner P, Pech M, Ricke J: **Hepatocellular carcinoma and liver cirrhosis: assessment of the liver function after Yttrium-90 radioembolization with resin microspheres or after CT-guided high-dose-rate brachytherapy.** *Dig Dis* 2009, **27**:189-199.
36. Farthing MJ, Clark ML, Sloane JP, Powles RL, McElwain TJ: **Liver disease after bone marrow transplantation.** *Gut* 1982, **23**:465-474.

doi:10.1186/1748-717X-6-40
Cite this article as: Seidensticker *et al.*: Quantitative in vivo assessment of radiation injury of the liver using Gd-EOB-DTPA enhanced MRI: tolerance dose of small liver volumes. *Radiation Oncology* 2011 **6**:40.

RADIATION RESEARCH **172**, 598–606 (2009)
0033-7587/09 $15.00

DOI: 10.1667/RR1773.1

In Vivo Assessment of Dose Volume and Dose Gradient Effects on the Tolerance Dose of Small Liver Volumes after Single-Fraction High-Dose-Rate ^{192}Ir Irradiation

Christian Wybranski,[a] Max Seidensticker,[a] Konrad Mohnike,[a] Siegfried Kropf,[c] Peter Wust,[b] Jens Ricke[a] and Lutz Lüdemann[b,1]

[a] *Department of Radiology and Nuclear Medicine, Otto von Guericke University, Magdeburg, Germany;* [b] *Department of Radiation Therapy, Charité Medical Center, Berlin, Germany; and* [c] *Department of Biometrics and Medical Informatics, Otto von Guericke University, Magdeburg, Germany*

Wybranski, C., Seidensticker, M., Mohnike, K., Kropf, S., Wust, P., Ricke, J. and Lüdemann, L. *In Vivo* Assessment of Dose Volume and Dose Gradient Effects on the Tolerance Dose of Small Liver Volumes after Single-Fraction High-Dose-Rate ^{192}Ir Irradiation. *Radiat. Res.* 172, 598–606 (2009).

The aim of this study was to assess the dependence of the normal liver tissue threshold dose on the volume exposed and the catheter geometry-dependent dose gradients for single-fraction high-dose-rate brachytherapy of malignant liver lesions. A total of 50 patients with malignant liver tumors treated with CT-guided high-dose-rate ^{192}Ir brachytherapy were included. Dose planning was performed using a three-dimensional CT data set acquired after percutaneous applicator positioning. Magnetic resonance imaging (MRI), performed 6 and 12 weeks after therapy, was analyzed retrospectively. All MRI data sets were merged with 3D dosimetry data. The border of hyperintensity on T2-weighted images (edema) and of hypointensity on T1-weighted images (impaired hepatocyte function) were analyzed to assess the radiation effect. The threshold isodose surface of the volume exposed was calculated from the 3D dosimetry data. The relationships between irradiated volume and threshold isodose surface as well as dose gradient and threshold isodose surface were evaluated over time. The median threshold dose of the volume exposed, characterized by hepatocyte dysfunction and edema, was ≈13 Gy 6 weeks after irradiation and ≈16 Gy at 12 weeks. We found a significant correlation between the normal liver tissue threshold dose and volume exposed ($P < 0.0001$). The 12-week threshold dose was estimated between ≈14 Gy for 500 cm^3, ≈16 Gy for 100 cm^3, and ≈18 Gy for 10 cm^3 of irradiated volume. The results indicate that the dose gradient has no effect on the threshold liver dose. There was a significant shift of the threshold doses from regions of lower to regions of higher-dose exposure in the course of follow-up ($P < 0.0001$). Thus the normal liver tissue threshold dose is dependent on the volume exposed but not on the dose gradient.

[1] Address for correspondence: Charité Medical Center, Department of Radiation Therapy, CVK, Augustenburger Platz 1, Berlin 13353, Germany; e-mail: lutz.luedemann@charite.de.

INTRODUCTION

High-precision irradiation techniques such as stereotactic body radiotherapy (SBRT) and computed tomography (CT)-guided single-fraction high-dose-rate brachytherapy have shown promising results with regard to safety and efficacy in the treatment of unresectable malignant liver tumors (*1–4*). Both techniques are based on conformal avoidance of normal liver tissue adjacent to the irradiated tumor and steep dose gradients at the margins of the target volume.

Structural damage of the perifocal normal liver tissue is regularly observed after irradiation and suggests considerable variations of the calculated threshold doses (*2, 3, 5, 6*). A previous prospective study of the dose–response relationship of liver parenchyma after high-dose-rate ^{192}Ir brachytherapy revealed irreversible structural damage of perifocal normal liver tissue at doses of more than 15 Gy and reversible hepatic dysfunction at doses between 10 and 15 Gy. The peak dysfunctional volume was reached between 6 and 12 weeks after irradiation (*6*). In that study the D_{90} covering 90% of the edema/functionally impaired volume was employed, which was based on superimposition of the dose distribution on the MR images. Accurate image registration was attempted. However, even a small registration error might lead to over- or underestimation of the D_{90}, especially when small lesions are irradiated. In the present study we sought to avoid the uncertainties associated with the use of standard image fusion algorithms. Our basic assumption in the present study was that the isodose surface corresponds to the threshold isosurface D_{100} of the volume exposed.

In high-dose-rate ^{192}Ir brachytherapy, the steepness of the dose gradients of the iridium source, which depends on the irradiated volume and catheter geometry, might affect the threshold dose of normal tissue encompassed in the clinical target volume (CTV). Therefore, the purpose of this study was to assess the threshold dose

dependence of normal perifocal liver tissue on the volume exposed and the steepness of the average dose gradients produced by the geometrical array of the catheters and the dwell position of the iridium point source.

METHODS

Study Population

In this study we retrospectively analyzed the perifocal normal liver tissue reactions in 50 consecutive patients who underwent CT-guided single-fraction high-dose-rate ^{192}Ir brachytherapy of one to four malignant liver tumors between December 2002 and October 2004 as part of a clinical phase II study prospectively assessing local tumor control after CT-guided brachytherapy in Berlin, Germany. The study was approved by the local ethics committee in Berlin. Written informed consent was obtained from all patients. The patient population comprised 31 men and 19 women. The median age of the patients was 63 years (range: 35–86 years). All patients had fully preserved liver function, as assessed by the serum parameters bilirubin and transaminases. Patients with hepatocellular carcinoma and/or signs of cirrhosis were excluded. A total of 76 solid liver tumors were ablated in 50 brachytherapy treatments. The lesions treated included six cholangiocellular carcinomas and 70 metastases from other primary solid malignancies (colorectal carcinoma, 55; breast cancer, four; neuroendocrine tumor, two; lung cancer, three; ovarian cancer, two; pancreatic cancer, schwannoma, cervical carcinoma, urinary bladder cancer, one each). Thirty-four patients were treated for solitary liver lesions, and 16 patients were treated for multiple liver lesions (two lesions in nine patients, three in four patients, and four in three patients).

Study End Points

The volume dependence of the threshold dose was assessed for all volumes exposed. Since the peak extension of the volume exposed was observed 6–12 weeks postirradiation on follow-up magnetic resonance imaging (MRI) (*6*), only the MRI data sets acquired at 6 and 12 weeks were evaluated in the present study. The decrease in the volume exposed was calculated in absolute terms (cm^3) and as a percentage change from the T1-weighted and/or T2-weighted image data sets acquired at the two follow-up times after the intervention. Additionally, the dose gradient dependence of the threshold dose, resulting from the geometric array of the dwell positions, was examined for all volumes exposed using at least two brachytherapy catheters.

Interventional Technique and Irradiation

The technique of CT-guided brachytherapy has been described in detail previously (*4, 7*). In brief, a T2-weighted respiratory-triggered fast spin echo and a T1-weighted breath-hold gradient echo sequence with administration of the hepatocyte-specific contrast agent gadobenate dimeglumine (Gd-BOPTA; Multihance; Bracco, Princeton, NJ) were acquired to delineate primary and secondary liver lesions (see Follow-up section below). The brachytherapy catheters were positioned using fluoroscopy CT guidance (Somatom 4, Siemens, Erlangen, Germany). We did not apply strict geometric constraints for catheter placement. Distances between catheters or between the catheter and the outer rim of the CTV were chosen to be between 1 and 2 cm to ensure adequate coverage of the CTV. After catheter positioning, a spiral CT of the liver (slice thickness, 5 mm; increment, 5 mm) enhanced by intravenous administration of iodine contrast medium (100 ml Ultravist 370; flow, 1 ml/s; start delay, 80 s) was acquired in breath-hold technique for treatment planning. Four catheters were used on average (range, 1–11 catheters). The high-dose-rate afterloading system (Gammamed, Varian, Charlottesville, VA) employed a ^{192}Ir source (source strength, 370 GBq = 10 Ci). The source diameter was <1 mm. Dwell positions inside the brachytherapy catheters were located every 5 mm. Nominal dwell times were corrected automatically according to the actual source strength.

Treatment Planning

Treatment was planned using the BrachyVision software package, version 7.1 (Varian Medical Systems, Palo Alto, CA). The dose calculation formalism used by BrachyVision complies with the recommendations of the AAPM (American Association of Physicists in Medicine) TG-43 report (*8*) for brachytherapy implant sources. The CTV was delineated on each axial slice of the planning CT data set. According to the study protocol of the clinical phase II trial, each patient was randomized to receive a minimum dose of 15, 20 or 25 Gy inside the CTV. No maximum intralesional dose constraints applied. The dose was administered in a single fraction.

Follow-up

A total of 161 MRI examinations were performed 6 ± 2 weeks and 12 ± 2 weeks after the intervention. The MRI protocol comprised the following sequences (Gyroscan NT Intera, Philips, The Netherlands): T2-weighted respiratory-triggered fast spin echo (FSE) (TE/TR 90/2100 ms, echo train length 21) with fat suppression to assess the extent of edema and T1-weighted breath-hold gradient echo (GRE) (TE/TR 5/30 ms, flip angle 30°) 2 h after i.v. injection of 15 ml gadobenate dimeglumine (Gd-BOPTA; Multihance; Bracco, Princeton, NJ). The slice thickness of the axial images was 8 mm, acquired in interleaved mode with no gap. The hepatocyte-specific contrast agent gadobenate dimeglumine allowed visualization of the extent of hepatocyte dysfunction. The signal intensity enhancement of functionally unimpaired liver parenchyma has been shown to last for at least 2 h (*9–11*). MRI examinations of poor image quality (e.g., motion artifacts in T1-weighted breath-hold sequences) were excluded from the evaluation.

Image Registration

Merging of the 3D dosimetry data calculated by BrachyVision with the respective follow-up MRI scans was accomplished using an independent image registration implementation within the 3D visualization software Amira 3.1 (Mercury Computer Systems, Berlin, Germany) (*12*). We used a voxel-property-based image registration method allowing affine transformation (12 degrees of freedom: three rotations, three translations, three scalings and three shears). Introduction of image scaling and shearing allowed correction for first-order liver deformations. Registration optimization was based on a normalized mutual information (NMI) similarity measure, which has been shown to provide high accuracy for liver registration (*13*). Cropping of the image data to contain liver parenchyma and a small surrounding margin approximately 1 cm wide was performed as a preprocessing step. The average error of image registration within the liver was <5 mm for the liver surface and prominent intrahepatic anatomic structures, e.g., bifurcation of large vessels (see Fig. 1).

Segmentation of the Perifocal Irradiation Effect

An experienced GI radiologist (>10 years in liver CT and MRI) evaluated the merged planning CT and MRI data and outlined the borders of hyperintensity on T2-weighted images (edema) and hypointensity on late Gd-BOPTA-enhanced T1-weighted images (functionally impaired hepatocytes) around the irradiated liver tumors. Perifocal hepatic tissue damage after conformal irradiation was assumed to be attributable to veno-occlusive disease (VOD) (*5, 14, 15*), characterized by severe congestion of the afferent sinusoids and centrilobular veins and hepatocyte dysfunction (*16, 17*).

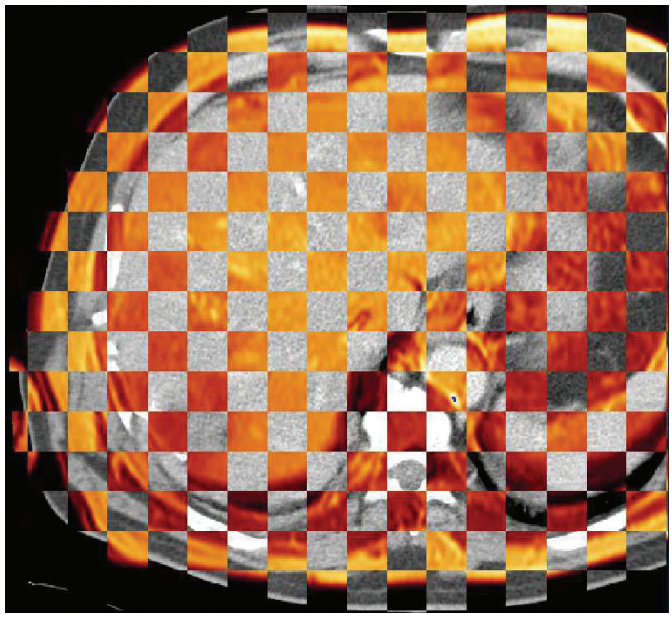

FIG. 1. T1-weighted image (color encoded) coregistered with the planning CT. Note that only livers were coregistered. Therefore, a good matching result was achieved only for livers.

Therefore, we treated functionally impaired hepatocytes and edema as two different qualities of the volumes exposed.

Calculation of the Threshold Isosurface

We performed volumetry of each volume exposed (edema and impaired hepatocyte function). As the next step, we used this volume to calculate the 3D isodose volumes (confined to the liver) corresponding to the volume of edema and the volume of functional impairment of the hepatocytes with a maximum deviation of $\leq 1\%$. Our assumption was that this isodose surface corresponded to the threshold isosurface D_{100} of the volume exposed (see Fig. 2).

The relationship between the volume exposed and the threshold dose was visualized using PAW, version 2.13/08 (CERN, Switzerland) to create a phenomenological parameter-dependent model curve. To evaluate the influence of volume effects on the regeneration of the exposed volumes between 6 and 12 weeks after intervention, we calculated the absolute and relative decreases in volume (in cm^3 and%) for all patients with a T1-weighted and/or a T2-weighted follow-up MRI at both follow-up times.

Calculation of the Dose Gradients

Dose uniformity and dose gradients of an ^{192}Ir brachytherapy implant depend on the dwell positions and dwell times of the source as well as the catheter positions (*18, 19*). We assessed the relationship between the threshold isosurface of the volume exposed and the catheter geometry-dependent average dose gradient of the brachytherapy implant for all volumes exposed using at least two brachytherapy catheters.

Since no dose uniformity constraints were applied in our study, dose gradients differed considerably on the threshold isosurface. We used a voxel-based approach to calculate the average of the norm of the dose gradient vector in 3D, $|\nabla D(x,y,z)|$, for each D_{100}. We segmented part of the 3D dosimetry data encompassing the D_{100} by ± 2 Gy to comprise a sufficient quantity of voxels for calculation. To exclude the inverse square relationship between the average dose gradient and the threshold isosurface as confounder, we calculated the average dose gradient for a reference isodose surface in each MRI data set as an additional descriptor of the dose–gradient relationship.

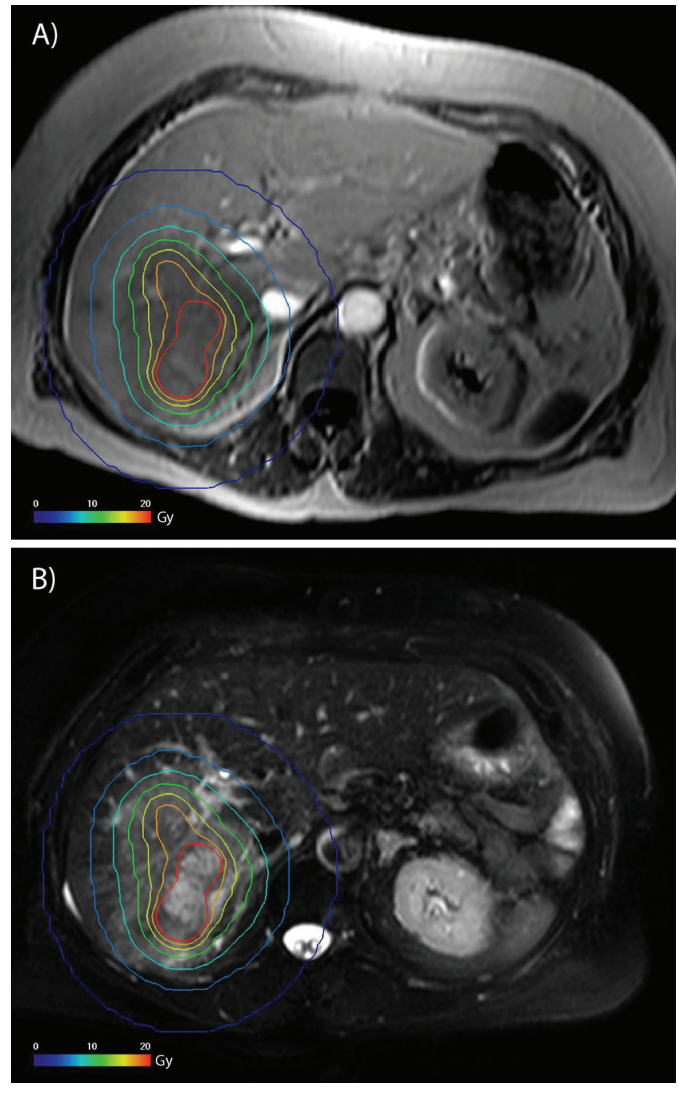

FIG. 2. Overlay of the isodoses on the T1-weighted image (panel A) and on T2-weighted (panel B) images. Note the mismatch between the isodose surface and the effect of the radiation response in the MR images. Due to the isovolumetric approach first-order errors resulting from this mismatch have no effect on the results.

The corresponding median threshold isosurfaces of all patients for each MRI sequence (T2-weighted and T1-weighted) and follow-up date (6 and 12 weeks postirradiation) served as reference isodose surfaces.

Statistical Analysis

The linear relationship between the exposed volume at the 6-week follow-up and absolute and relative volume decreases in the course of follow-up was evaluated using Pearson's correlation coefficient r. Only patients who underwent a T1 and/or a T2-weighted follow-up MRI examination at both follow-up times after the intervention were included in this statistical analysis. Pearson's correlation coefficient r was calculated using SPSS, version 12.0 (SPSS Inc., Chicago, IL).

The dependence of the liver tissue threshold dose on the irradiated volume and dose gradients generated by the iridium source was assessed using a Generalized Estimating Equation (GEE) model. For a data set consisting of repeated measurements (two MRI sequences, two follow-up dates) of a variable of interest, a GEE model allows the

TABLE 1
Volume of Hyperintensity on T2-Weighted Images (edema) and Hypointensity on T1-Weighted Images 2 h after i.v. Gd-BOPTA (hepatocyte dysfunction) 6 and 12 Weeks after Irradiation

	T1-weighted		T2-weighted	
	6 weeks	12 weeks	6 weeks	12 weeks
n	44	36	48	33
Median (cm^3)	134.1	104.0	141.5	110.5
Q_{25} (cm^3)	69.9	34.8	58.9	45.3
Q_{75} (cm^3)	295.7	166.0	273.3	205.0
Minimum (cm^3)	14.2	8.7	4.4	8.4
Maximum (cm^3)	568.4	499.4	607.1	536.0

Note. *n*: number of MRI examinations evaluated; Q_{25}: 25% quartile width; Q_{75}: 75% quartile width.

TABLE 2
Threshold Dose for Hepatic Dysfunction/Edema as Assessed by Hypointensity on T1-Weighted Images 2 h after i.v. Gd-BOPTA/Hyperintensity on T2-Weighted Images 6 and 12 Weeks after Irradiation

	T1-weighted		T2-weighted	
	6 weeks	12 weeks	6 weeks	12 weeks
n	44	36	48	33
Median (cm^3)	134.1	104.0	141.5	110.5
Q_{25} (cm^3)	69.9	34.8	58.9	45.3
Q_{75} (cm^3)	295.7	166.0	273.3	205.0
Minimum (cm^3)	14.2	8.7	4.4	8.4
Maximum (cm^3)	568.4	499.4	607.1	536.0

Note. *n*: number of MRI examinations evaluated; Q_{25}: 25% quartile width; Q_{75}: 75% quartile width.

correlation of outcomes within one individual to be estimated and taken into appropriate account in the equation, which generates the regression coefficients and their standard errors (*20, 21*). The GEE model was calculated with SAS, version 9.1 (SAS Institute Inc., Cary, NC). A $P < 0.05$ was considered significant.

RESULTS

A total of 62 exposed volumes were observed in 50 patients after interstitial brachytherapy of 76 solid liver tumors. The volume dependence of the threshold dose was assessed for all exposed volumes. Of the 50 patients, 23 patients had a T1-weighted follow-up MRI and 26 patients had a T2-weighted follow-up MRI at both follow-up times (6 and 12 weeks after intervention). The absolute volume decreases (in cm^3) and the relative volume changes (in %) between the two follow-up dates with respect to hepatocyte dysfunction and edema were calculated considering just these 49 patients. Forty-eight of the 62 volumes exposed using at least two implanted brachytherapy catheters were assessed for the relationship between the threshold isosurface and the catheter geometry-dependent average dose gradient of the brachytherapy implant.

For all exposed volumes included in the analysis, volumetry data and the extent of the threshold isosurfaces for hepatocyte dysfunction (T1-weighted hypointense images) and edema (T2-weighted hyperintense images) 6 and 12 weeks after intervention are presented in Tables 1 and 2. The median volume of hepatocyte dysfunction decreased from 134.1 cm^3 at week 6 to 104.5^3 at week 12 (22.4%). The median edema volume decreased from141.5 cm^3 at week 6 to 110.5 cm^3 at week 12 (21.9%).

The GEE model was applied to investigate the correlation between threshold dose, MRI volume, MRI sequence and follow-up date. We found a significant correlation between the threshold dose and the exposed volume ($P < 0.0001$). The calculated threshold isosurfaces were affected significantly by the dynamics of the MRI volumes between 6 and 12 weeks after intervention ($P = 0.003$). No significant difference between the MRI sequences used was found ($P = 0.227$).

Considering only the patients with both a T1- and a T2-weighted follow-up MRI at both examination dates after intervention, we found a significant linear relationship between the exposed volume at the 6-week follow-up and the absolute volume decrease (in cm^3) between 6 and 12 weeks after intervention with respect to hepatocyte dysfunction ($P = 0.015$) and edema ($P = 0.002$). However, no significant linear relationship was found between the exposed volume at 6 weeks and relative volume changes (in %) between 6 and 12 weeks after intervention with respect to hepatocyte dysfunction ($P = 0.72$) and edema ($P = 0.43$).

Figure 3 displays the correlation between the threshold dose D_{100} of the visible radiation effect and the MRI volume. The relationship is nonlinear and was therefore investigated in more detail. A phenomenological parameter-dependent model was found to fit the relationship between the D_{100} and exposed volume and can be described by the following equation:

$$D_{100}(V) = D_{0;V} - D_{1;V} \cdot V + D_{2;V} - exp^{(D_{3;V})}, \quad (1)$$

where V represents the volume exposed, $D_{100}(V)$ the threshold dose of the visible radiation effect, and $D_{i,V}$, $i = 0,1,2,3$ fitting parameters. The fitting parameters are given in Table. 3. Equation (1) consists of an exponential term predominant at small volumes and a linear term predominant at larger volumes. Since no significant differences between the observed threshold isosurfaces of hepatocyte dysfunction and edema were found, the T1- and T2-weighted data were fitted simultaneously for either follow-up date. The fitting parameters $D_{1;2;3;V}$ for 6- and 12-week follow-up varied independently. Only the parameter $D_{0;V}$ was allowed to differ between T1- and T2-weighted investigations for each follow-up time (see Table 3). The dose–volume curve shown in Fig. 3 was

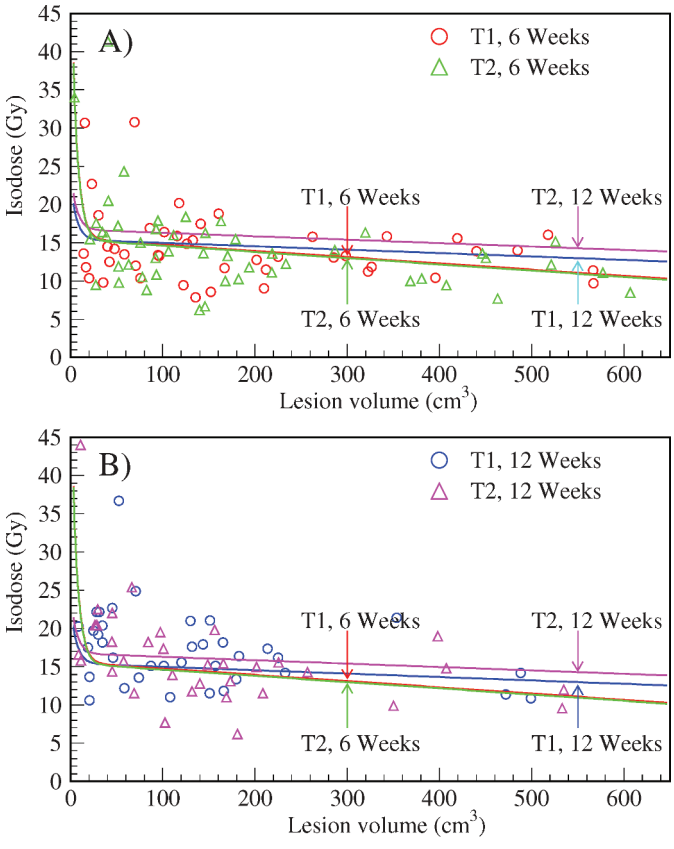

FIG. 3. Threshold doses for hepatic dysfunction/edema as assessed by hypointensity on T1-weighted images 2 h after i.v. Gd-BOPTA/hyperintensity on T2-weighted images 6 (panel A) and 12 (panel B) weeks after irradiation in relation to lesion volume. The fits are plotted in both figures for better intercomparison.

flattened out between weeks 6 and 12, indicating that the dose–volume effect is reduced 12 weeks after intervention.

Threshold doses of hepatocyte dysfunction and edema were calculated using the phenomenological-parameter-dependent model (Eq. 1). According to Eq. (1), $D_{0,V}$ provides a basic isodose threshold of 15.5 Gy for edema and hepatocyte dysfunction at 6 weeks and 15.4 Gy and 16.7 Gy for edema and hepatocyte dysfunction, respectively, at 12 weeks (Table 3). The threshold dose decreased by 0.0082 Gy/cm^3 at 6 weeks and 0.0045 Gy/cm^3 at 12 weeks for volumes larger than 50 cm^3 ($D_{1,V}$). A selection of threshold doses derived from Eq. (1) for different MRI volumes at 6 and 12 weeks postirradiation are presented in Table 4.

TABLE 3
Fitting Parameters of Eq. (1) Describing the Dose–Volume Effect

	$D_{0,V}$ (Gy)	$D_{1,V}$ (Gy/cm^3)	$D_{2,V}$ (Gy)	$D_{3,V}$ (1/cm^3)
6 weeks				
T1-weighted	15.57	0.00816	39.89	0.1689
T2-weighted	15.43			
12 weeks				
T1-weighted	15.43	0.00445	7.96	0.1601
T2-weighted	16.74			

The relationship between the threshold isosurface dose and the catheter geometry-dependent average dose gradient of the brachytherapy implant was assessed for 48 of the 62 MRI volumes, which were induced by at least two brachytherapy catheters. The GEE model was applied to investigate correlations between threshold isosurface dose, average dose gradient, MRI sequence and follow-up date. We found a significant correlation between the threshold isosurface dose and average dose gradient ($P < 0.0001$), which is shown in Fig. 4. With regard to this result, there was no significant difference between hepatocyte dysfunction and edema ($P = 0.76$), whereas the calculated threshold isosurfaces were significantly affected by the dynamics of the exposed volumes during follow-up ($P = 0.002$). In first approximation, this finding indicates an inverse square law-dependent dose gradient effect, which is expressed by a linear correlation between dose and gradient for a point source. The curve was best fitted with a nonlinear approach, $D(x,y,z) = 8.59 + (|\nabla D(x,y,z)| - 2.88)^{0.898}$ for $|\nabla D(x,y,z)| > 2.88$. Figure 4 displays the corresponding curve differs only slightly from the linear approach.

We did not find a significant correlation between the threshold isosurface dose and average dose gradient on the corresponding median threshold isosurface ($P = 0.36$), shown in Fig. 5. There was no significant difference between hepatocyte dysfunction and edema ($P = 0.76$). Again this statistical analysis revealed a significant change in the calculated threshold isosurfaces between 6 and 12 weeks after intervention ($P = 0.0025$).

DISCUSSION

In the present study, we investigated how irradiated volumes and catheter geometry-dependent dose gradients influence radiation effects on normal hepatic parenchyma. Hepatocyte dysfunction was assessed as non-uptake of the hepatocyte-selective contrast agent Gd-BOPTA 2 h after i.v. injection on T1-weighted MR images. In addition, development of interstitial edema was assessed on T2-weighted MR images. The MR images revealed a significant volume effect. The volume-corrected isodose threshold described by the parameter $D_{0;V} \approx 16$ Gy (Table 3) was found to be nearly independent of the follow-up time and MRI method used. This indicates that liver shrinkage (*6*) had no effect during the follow-up times investigated here. The threshold dose of the perifocal normal hepatic parenchyma was not dependent on the steepness of the average dose gradient of the brachytherapy implant.

VOD has been identified as the pathological correlate of hepatic tissue damage after liver irradiation (*16, 22*). It has been suggested as the underlying cause of morphological alterations of perifocal hepatic paren-

TABLE 4
Effective Threshold Isodoses, D_{100}, Hepatic Dysfunction/Edema as Assessed by Hypointensity on T1-Weighted Images 2 h after i.v. Gd-BOPTA/Hyperintensity on T2-Weighted Images 6 and 12 Weeks after Irradiation

	T1-weighted		T2-weighted	
V (cm^3)	6 weeks (Gy)	12 weeks (Gy)	6 weeks (Gy)	12 weeks (Gy)
10	22.9	17.0	22.7	18.3
50	15.2	15.2	15.0	16.5
100	14.8	15.0	14.6	16.3
500	11.5	13.2	11.4	14.5

Notes. The data were obtained with Eq. (1) for different irradiated volumes at week 6 and week 12 (see Fig. 3). A dose–volume effect is clearly apparent.

chyma after conformal irradiation (*5, 14, 15*). VOD is characterized by severe congestion of afferent sinusoids and centrilobular veins by erythrocytes and extensive deposits of fibrin as well as functional impairment and atrophy of hepatocytes. Functional impairment and atrophy of hepatocytes were found to occur secondary to hypoxia and nutritional deficits caused by obstruction of small branches of hepatic veins (*16, 22*). It typically occurs 4–8 weeks after the completion of irradiation.

Recent *in vitro* and *in vivo* studies have stressed the influence of radiation-induced early interdependent biological mechanisms in nonparenchymal and parenchymal liver cells of the liver sinusoids in the development of radiation-induced liver disease (*23–26*). We propose that the dose–volume effect observed in our study is a phenomenon based on the interdependent amplification of radiation-induced microvascular injury and inflammatory response.

Radiation-generated free radicals lead to apoptosis, altered expression of adhesion molecules, and up-regulation of proinflammatory cytokines like IL-1β, IL-6 and TNFα in endothelial cells (*25–27*). Increased vascular permeability due to disruption of the endothelial cell barrier allows inflammatory cells and their metabolic products to enter the liver parenchyma around the hepatic veins easily. Proinflammatory cytokines secreted by the endothelium not only attract inflammatory cells but also lead to increased parenchymal damage, facilitated by a radiation-induced transient down-regulation of hepatoprotective genes in hepatocytes (*24*). Transient susceptibility of hepatocytes to TNFα-mediated apoptosis has been proposed as an initial step toward radiation-induced liver disease and liver fibrosis (*23*). The proinflammatory cytokines secreted by the endothelial cells further induce expression of multiple proinflammatory chemokines in the hepatocytes adjacent to the hepatic veins. The increased chemokine expression potentially perpetuates hepatic damage through activation and attraction of neutrophils, T lymphocytes and natural killer cells in the irradiated area (*26*).

Impaired hepatic blood flow in the irradiated area leads to hypoxia and nutritional deficits of the hepatocytes. Subsequent shunting of portal venous blood into collaterals and anastomoses between afferent and efferent vessels might additionally aggravate parenchymal dysfunction in the irradiated area independent of the functional status of the hepatocytes (*28*).

Regeneration is indicated by systematic reduction of the exposed volume between week 6 and week 12 by

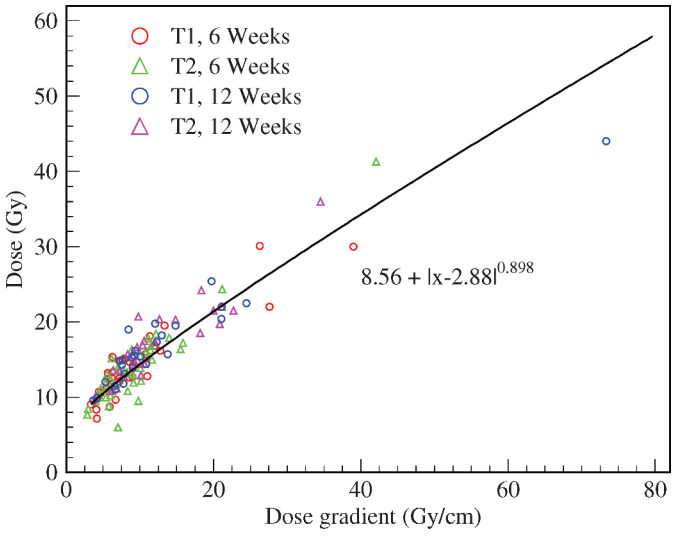

FIG. 4. Dose gradient relationship: Correlation between D_{100} isosurface and the corresponding average dose gradient. The curve is fitted with a nonlinear approach. The fitting parameters are printed next to the graph.

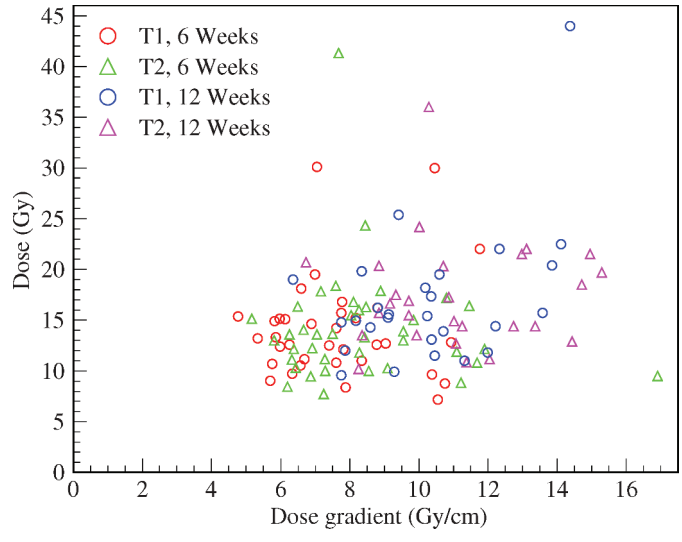

FIG. 5. Dose gradient relationship: Correlation between D_{100} isosurface and dose gradient on the corresponding reference isodose surface. The reference isodose surface was chosen based on MRI sequence (T2- and T1-weighted) and follow-up time (6 and 12 weeks postirradiation).

30.1 cm^3 = 22.4% and 31.0 cm^3 = 21.9%, respectively (see Table 1). The dose–volume curve in Fig. 3 flattened out between weeks 6 and 12, indicating that the dose–volume effect is reduced in the course of follow-up. The threshold dose range was reduced from ≈11–23 Gy at week 6 to ≈13–18 Gy at week 12 (see Table 4). This may be a result of repair and regeneration in the transitional zone between functionally damaged and morphologically normal liver tissue between 6 and 12 weeks after irradiation.

Cytology specimens extracted from the exposed volumes by core biopsy ≈6 weeks after high-dose-rate ^{192}Ir brachytherapy in our previous study confirmed high regenerative activity with multiple polyploid hepatocytes and only a minor portion of lymphatic cells and fibroblasts in areas that had been exposed to low doses (10–12 Gy). Multiple lymphatic cells and fibroblasts as predecessors of fibrosis and only a minor amount of polyploid hepatocytes were observed in areas of high-dose exposure (18–20 Gy) (*6*). We found a significant linear relationship between the exposed volume 6 weeks after intervention and the absolute volume decrease (in cm^3) between 6 and 12 weeks after intervention. No significant linear relationship was found between the exposed volume at 6 weeks and relative volume changes (in %) between 6 and 12 weeks after intervention. We therefore conclude that hepatic regeneration is not impaired in a volume-dependent manner.

The volume effect on the liver tissue threshold dose was relatively consistent for exposed volumes >100 cm^3; however, we found a considerable standard deviation for the threshold doses in exposed volumes <100 cm^3. Interindividual differences in the radiosensitivity of normal liver tissue probably become more evident if the irradiated volume is small and might account for the variable standard deviation of the threshold doses observed in the current study and our previous prospective assessment of the dose–response relationship for small volumes of liver parenchyma after single-fraction high-dose-rate ^{192}Ir brachytherapy (*6*).

The threshold doses determined in this study differ from those calculated in our previous study. In our previous study we found that the average extent of both edema and hepatocyte dysfunction for the D_{90} corresponded to the 9.9 ± 2.6- and 9.9 ± 2.3-Gy isodose surface, respectively, 6 weeks after irradiation (±SD). At 12 weeks, the extent decreased to the 11.1 ± 2.6- and 11.9 ± 3.0-Gy isodose surface for edema and hepatocyte dysfunction, respectively (*6*).

There are two possible explanations for this difference: First, the threshold dose and exposed volume correlated significantly (see Table 4). In our previous study we did not calculate the threshold doses separately for different irradiated volume sizes. The difference might therefore be attributable to the fact that exposed volumes were not taken into account in the earlier study. Second, in our previous study we used dose–volume histograms to calculate the D_{90} threshold isosurface (covering 90% of the exposed volume) based on overlap of the 3D dosimetry data with the fused MR images.

Although accurate image registration was attempted, small registration errors of a few millimeters could have led to over- or underestimation of the D_{90}, especially for small lesions. In the present study, calculation of the D_{100} threshold isosurface was based on volumetry of exposed volumes on fused MR images. First-order misregistration errors have no impact on the results if the lesion is completely surrounded by liver tissue because only the lesion volume is used for threshold estimation. Registration is necessary only to exclude dose contributions from outside the liver and for quality assurance; thus the impact of image fusion uncertainties on the calculated threshold isosurface was minimized, especially for small irradiated volumes, resulting in a more accurate estimate.

In the present study, liver dysfunction volumes between 14 and 568 cm^3 and edema volumes between 4 and 607 cm^3 were determined for analysis of the threshold isodose. The distance between the boundary separating functionally intact and functionally impaired hepatocytes and the radiation source increased with the size of the irradiated volume. At a large distance, the dose distribution of a point source can be assumed to decrease in first order according to the inverse square law with the distance, r, from the point source, $D(x;y;z) \propto 1/r^2$. As follows, the dose gradient decreases with inverse cubic law, i.e. $|\nabla D(x;y;z)| \propto 1/r^3$, which means $D(x;y;z) \propto |\nabla D(x;y;z)|^{(2/3)}$. At small distances from the radiation source, the source can no longer be regarded as a point source and dose and dose gradient are not correlated by $D(x;y;z) \propto |\nabla D(x;y;z)|^{(2/3)}$. The exponent found in the present study, 0.898, differs from the exponent that would be expected for a point source, 0.666 (Fig. 4). The difference between a point source and the dose gradient actually measured is attributable mainly to catheter geometry and dwell positions. To exclude the intrinsic relationship between the threshold isosurface of the exposed volume and the corresponding average dose gradient as confounder based on the distance r from the point source, we calculated the average dose gradient at the corresponding median threshold isosurface. We found no correlation between the threshold isosurface of the exposed volume and the average dose gradient at the corresponding median threshold isosurface, indicating that there is no significant threshold dose dependence on the steepness of the average dose gradients produced by the geometrical array of the catheters in the ^{192}Ir point source. Therefore, we conclude that high-dose-rate ^{192}Ir brachytherapy can be applied safely without the need to consider catheter geometry as long as all catheters are placed properly inside the tumor volume. This holds true for the catheter

distribution used in our study patients (i.e., distance of 1 to 2 cm between the catheters or between the catheters and the border of the CTV).

We used a voxel property-based image registration method based on an NMI similarity measure to perform affine registration of the CT/dosimetry images and the follow-up MR images. The NMI similarity measure has been shown to yield robust and accurate registration results for liver images (*13*). Introduction of image scaling and shearing allowed correction for first-order liver deformations. Nevertheless, elastic registration would have enabled correction of all liver deformations between the imaging modalities used. Volumetry of each exposed volume in the fused MR images was performed. The volumes determined in this way served to calculate the threshold isosurface of the 3D dosimetry data (confined to the liver) for an exposed volume of identical size. This reduced under- and overestimation of the threshold dose resulting from registration errors.

Our method has some limitations with respect to the determination of the volume and dose gradient dependence of the threshold dose of perifocal normal liver tissue. First, the outer borders of edema in the T2-weighted images and area of functionally impaired hepatocytes in the T1-weighted Gd-BOPTA-enhanced MR images were outlined manually in each slice. Thus low contrast between the exposed volume and morphologically unaffected normal liver tissue was a potential source of error for the determination of the liver tissue threshold dose. Second, calculation of the threshold dose of the perifocal normal tissue reaction was based on the assumption of a relatively consistent relationship between the distribution of isodoses and biological effects within an individual. This assumption has been tested for high-dose-rate ^{192}Ir brachytherapy in experimental investigations (*29, 30*). Third, we used a highly simplified approach to examine the relationship between the liver tissue threshold dose and dose gradients produced by the ^{192}Ir implants. Calculation of an average dose gradient resulted in loss of spatial information on dose gradient inhomogeneity and precluded intraindividual comparison of regions irradiated with different dose gradients. Additionally, a slice thickness of 8 mm was used to acquire the images during breathhold. A slice thickness of 8 mm results in a significant partial volume effect. This might have an impact on small lesions and result in under- or overestimation of lesion size. As the lesion becomes larger, the partial volume effect is reduced.

The threshold dose of the structural damage of the perifocal normal liver tissue must be considered if brachytherapy is performed in patients with unfavorable preconditions such as multiple liver lesions or diminished hepatic reserve capacity after surgical resection. Available data on the threshold dose of normal liver parenchyma for highly conformally irradiated malignancies shows considerable variations (*2, 3, 5, 6*). To the best of our knowledge, our study is the first to demonstrate a volume dependence of the normal liver tissue threshold dose after single-fraction irradiation on a structural level. The volume dependence of the normal liver tissue threshold dose has to be taken into consideration for individual treatment planning, especially if several larger malignant tumors are irradiated in patients with diminished hepatic reserve capacity. The catheter geometry-dependent average dose gradient of the brachytherapy implant did not correlate with the liver tissue threshold dose. This indicates that high-dose-rate ^{192}Ir brachytherapy can be used safely without the need for strict geometrical catheter placement restrictions as long as all catheters are placed properly inside the tumor volume and the catheter distribution applied in our study patients is used.

In conclusion, the normal liver tissue threshold dose proved to be dependent on the irradiated volume. The long-term tolerance dose (>12 weeks) is expected in the range of 15 Gy for volumes <100 cm^3 and lower (11.5–14 Gy) for volumes >300 cm^3. This has to be taken into consideration for individual treatment planning for patients with a diminished hepatic reserve capacity. No effect of the steepness of the average dose gradient was found.

ACKNOWLEDGMENT

The authors received no outside funding for this study.

Received: March 10, 2009; accepted: July 8, 2009

REFERENCES

1. K. K. Herfarth, J. Debus, F. Lohr, M. L. Bahner, B. Rhein, P. Fritz, A. Hoss, W. Schlegel and M. F. Wannenmacher, Stereotactic single-dose radiation therapy of liver tumors: results of a phase I/II trial. *J. Clin. Oncol.* **19**, 164–170 (2001).
2. J. Wulf, M. Guckenberger, U. Haedinger, U. Oppitz, G. Mueller, K. Baier and M. Flentje, Stereotactic radiotherapy of primary liver cancer and hepatic metastases. *Acta Oncol.* **45**, 838–847 (2006).
3. T. E. Schefter, B. D. Kavanagh, R. D. Timmerman, H. R. Cardenes, A. Baron and L. E. Gaspar, A phase I trial of stereotactic body radiation therapy (SBRT) for liver metastases. *Int. J. Radiat. Oncol. Biol. Phys.* **62**, 1371–1378 (2005).
4. J. Ricke, P. Wust, A. Stohlmann, A. Beck, C. H. Cho, M. Pech, G. Wieners, B. Spors, M. Werk and R. Felix, CT-guided interstitial brachytherapy of liver malignancies alone or in combination with thermal ablation: phase I–II results of a novel technique. *Int. J. Radiat. Oncol. Biol. Phys.* **58**, 1496–1505 (2004).
5. K. K. Herfarth, H. Hof, M. L. Bahner, F. Lohr, A. Hoss, G. van Kaick, M. Wannenmacher and J. Debus, Assessment of focal liver reaction by multiphasic CT after stereotactic single-dose radiotherapy of liver tumors. *Int. J. Radiat. Oncol. Biol. Phys.* **57**, 444–451 (2003).

6. J. Ricke, M. Seidensticker, L. Lüdemann, M. Pech, G. Wieners, S. Hengst, K. Mohnike, C. H. Cho, E. L. Hanninen and P. Wust, *In vivo* assessment of the tolerance dose of small liver volumes after single-fraction HDR irradiation. *Int. J. Radiat. Oncol. Biol. Phys*. **62**, 776–784 (2005).
7. J. Ricke, P. Wust, G. Wieners, A. Beck, C. H. Cho, M. Seidensticker, M. Pech, M. Werk, C. Rosner and R. Felix, Liver malignancies: CT-guided interstitial brachytherapy in patients with unfavorable lesions for thermal ablation. *J. Vasc. Interv. Radiol*. **15**, 1279–1286 (2004).
8. R. Nath, L. L. Anderson, G. Luxton, K. A. Weaver, J. F. Williamson and A. S. Meigooni, Dosimetry of interstitial brachytherapy sources: recommendations of the AAPM Radiation Therapy Committee Task Group No. 43. *Med. Phys*. **22**, 209–234 (1995).
9. O. Clement, N. Siauve, C. A. Cuenod, V. Vuillemin-Bodaghi, I. Leconte and G. Frija, Mechanisms of action of liver contrast agents: impact for clinical use. *J. Comput. Assist. Tomogr*. **23** (Suppl. 1), S45–S52 (1999).
10. M. A. Kirchin, G. P. Pirovano and A. Spinazzi, Gadobenate dimeglumine (Gd-BOPTA). An overview. *Invest. Radiol*. **33**, 798–809 (1998).
11. C. de Haen, R. L. Ferla and F. Maggioni, Gadobenate dimeglumine 0.5 M solution for injection (MultiHance) as contrast agent for magnetic resonance imaging of the liver: mechanistic studies in animals. *J. Comput. Assist. Tomogr*. **23** (Suppl. 1), S169–S179 (1999).
12. T. Rohlfing, J. B. West, J. Beier, T. Liebig, C. A. Taschner and U. W. Thomale, Registration of functional and anatomical MRI: accuracy assessment and application in navigated neurosurgery. *Comput. Aided. Surg*. **5**, 414–425 (2000).
13. A. Carrillo, J. L. Duerk, J. S. Lewin and D. L. Wilson, Semiautomatic 3-D image registration as applied to interventional MRI liver cancer treatment. *IEEE Trans. Med. Imaging* **19**,175–185 (2000).
14. S. Y. Chiou, R. C. Lee, K. H. Chi, J. C-H. Cheng, J. H. Chiang and C. Y. Chang, The triple-phase CT image appearance of post-irradiated livers. *Acta Radiol*. **42**, 526–531 (2001).
15. M. Krix, C. Plathow, M. Essig, K. Herfarth, J. Debus, H-U. Kauczor and S. Delorme, Monitoring of liver metastases after stereotactic radiotherapy using low-MI contrast-enhanced ultrasound—initial results. *Eur. Radiol*. **15**, 677–684 (2005).
16. T. S. Lawrence, J. M. Robertson, M. S. Anscher, R. L. Jirtle, W. D. Ensminger and L. F. Fajardo, Hepatic toxicity resulting from cancer treatment. *Int. J. Radiat. Oncol. Biol. Phys*. **31**, 1237–1248 (1995).
17. L. Felipe, The pathology of ionizing radiation as defined by morphologic patterns. *Acta Oncol*. **44**, 13–22 (2005).
18. R. D. Zwicker and R. Schmidt-Ullrich, Dose uniformity in a planar interstitial implant system. *Int. J. Radiat. Oncol. Biol. Phys*. **31**, 149–155 (1995).
19. R. D. Zwicker, D. W. Arthur, B. D. Kavanagh, R. Mohan and R. K. Schmidt-Ullrich, Optimization of planar high-dose-rate implants. *Int. J. Radiat. Oncol. Biol. Phys*. **44**, 1171–1177 (1999).
20. S. L. Zeger and K. Y. Liang, Longitudinal data analysis for discrete and continuous outcomes. *Biometrics* **42**, 121–130 (1986).
21. P. Burton, L. Gurrin and P. Sly, Extending the simple linear regression model to account for correlated responses: an introduction to generalized estimating equations and multi-level mixed modelling. *Stat. Med*. **17**, 1261–1291 (1998).
22. G. B. Reed, Jr. and A. J. Cox, Jr., The human liver after radiation injury. A form of veno-occlusive disease. *Am. J. Pathol*. **48**, 597–611 (1966).
23. H. Christiansen, B. Saile, K. Neubauer-Saile, S. Tippelt, M. Rave-Frank, R. M. Hermann, J. Dudas, C. F. Hess, H. Schmidberger and G. Ramadori, Irradiation leads to susceptibility of hepatocytes to TNF-alpha mediated apoptosis. *Radiother. Oncol*. **72**, 291–296 (2004).
24. H. Christiansen, D. Batusic, B. Saile, R. M. Hermann, J. Dudas, M. Rave-Frank, C. F. Hess, H. Schmidberger and G. Ramadori, Identification of genes responsive to gamma radiation in rat hepatocytes and rat liver by cDNA array gene expression analysis. *Radiat. Res*. **165**, 318–325 (2006).
25. H. Christiansen, N. Sheikh, B. Saile, F. Reuter, M. Rave-Frank, R. M. Hermann, J. Dudas, A. Hille, C. F. Hess and G. Ramadori, X-irradiation in rat liver: consequent upregulation of hepcidin and downregulation of hemojuvelin and ferroportin-1 gene expression. *Radiology* **242**, 189–197 (2007).
26. F. Moriconi, H. Christiansen, D. Raddatz, J. Dudas, R. M. Hermann, M. Rave-Frank, N. Sheikh, B. Saile, C. F. Hess and G. Ramadori, Effect of radiation on gene expression of rat liver chemokines: *in vivo* and *in vitro* studies. *Radiat. Res*. **169**, 162–169 (2008).
27. J. W. Denham and M. Hauer-Jensen, The radiotherapeutic injury—a complex 'wound'. *Radiother. Oncol*. **63**, 129–145 (2002).
28. J. P. Geraci, M. S. Mariano and K. L. Jackson, Hepatic radiation injury in the rat. *Radiat. Res*. **125**, 65–72 (1991).
29. M. A. Manning, R. D. Zwicker, D. W. Arthur and M. Arnfield, Biologic treatment planning for high-dose-rate brachytherapy. *Int. J. Radiat. Oncol. Biol. Phys*. **49**, 839–845 (2001).
30. M. R. Arnfield, P. S. Lin, M. A. Manning, D. W. Arthur, B. D. Kavanagh, R. D. Zwicker and R. K. Schmidt-Ullrich, The effect of high-dose-rate brachytherapy dwell sequence on cell survival. *Int. J. Radiat. Oncol. Biol. Phys*. **52**, 850–857 (2002).

Cardiovasc Intervent Radiol (2015) 38:213–221
DOI 10.1007/s00270-014-0872-7

TECHNICAL NOTE

Radiation-Induced Liver Damage: Correlation of Histopathology with Hepatobiliary Magnetic Resonance Imaging, a Feasibility Study

Max Seidensticker · Miroslaw Burak · Thomas Kalinski · Benjamin Garlipp · Konrad Koelble · Peter Wust · Kai Antweiler · Ricarda Seidensticker · Konrad Mohnike · Maciej Pech · Jens Ricke

Received: 2 December 2013 / Accepted: 27 January 2014 / Published online: 8 March 2014

Abstract
Purpose Radiotherapy of liver malignancies shows promising results (radioembolization, stereotactic irradiation, interstitial brachytherapy). Regardless of the route of application, a certain amount of nontumorous liver parenchyma will be collaterally damaged by radiation. The functional reserve may be significantly reduced with an impact on further treatment planning. Monitoring of radiation-induced liver damage by imaging is neither established nor validated. We performed an analysis to correlate the histopathological presence of radiation-induced liver damage with functional magnetic resonance imaging (MRI) utilizing hepatobiliary contrast media (Gd-BOPTA).
Methods Patients undergoing local high-dose-rate brachytherapy for whom a follow-up hepatobiliary MRI within 120 days after radiotherapy as well as an evaluable liver biopsy from radiation-exposed liver tissue within 7 days before MRI were retrospectively identified. Planning computed tomography (CT)/dosimetry was merged to the CT-documentation of the liver biopsy and to the MRI. Presence/absence of radiation-induced liver damage (histopathology) and Gd-BOPTA uptake (MRI) as well as the dose applied during brachytherapy at the site of tissue sampling was determined.
Results Fourteen biopsies from eight patients were evaluated. In all cases with histopathological evidence of radiation-induced liver damage ($n = 11$), no uptake of Gd-BOPTA was seen. In the remaining three, cases no radiation-induced liver damage but Gd-BOPTA uptake was seen. Presence of radiation-induced liver damage and absence of Gd-BOPTA uptake was correlated with a former high-dose exposition.
Conclusions Absence of hepatobiliary MRI contrast media uptake in radiation-exposed liver parenchyma may indicate radiation-induced liver damage. Confirmatory studies are warranted.

M. Seidensticker (✉) · R. Seidensticker · K. Mohnike · M. Pech · J. Ricke
Klinik für Radiologie und Nuklearmedizin, Universitätsklinik Magdeburg, Leipziger Strasse 44, 39120 Magdeburg, Germany
e-mail: max.seidensticker@med.ovgu.de

M. Burak
Department of Diagnostic Imaging and Interventional Radiology, Pomeranian Medical University, 1, Unii Lubelskiej St, 71-252 Szczecin, Poland

T. Kalinski
Institut für Pathologie, Universitätsklinik Magdeburg, Leipziger Strasse 44, 39120 Magdeburg, Germany

B. Garlipp
Klinik für Allgemein-, Viszeral- und Gefäßchirurgie, Universitätsklinik Magdeburg, Leipziger Strasse 44, 39120 Magdeburg, Germany

K. Koelble
Fachbereich Medizin der, Abteilung für Neuropathologie, Philipps Universität Marburg, Baldingerstrasse, 35043 Marburg, Germany

P. Wust
Klinik für Radioonkologie und Strahlentherapie, Charité Universitätsmedizin Berlin, Campus Virchow-Klinikum, Augustenburger Platz 1, 13353 Berlin, Germany

K. Antweiler
Institut für Biometrie und Medizinische Informatik, Universitätsklinik Magdeburg, Leipziger Strasse 44, 39120 Magdeburg, Germany

Keywords Radiation-induced liver disease · Hepatobiliary contrast media · Gd-BOPTA · Gd-EOB-DTPA

Introduction

Radiotherapy of liver malignancies has been demonstrated to be an effective treatment modality in selected patients. External radiotherapy as well as ^{90}Y-radioembolization and image-guided brachytherapy have been described in the literature with promising results [1, 3, 14, 24, 33, 37]. One of the few factors limiting the use of liver-directed radiotherapy (regardless of the route) is the relatively low tolerance dose of the liver parenchyma, leading to an either focal or generalized liver parenchymal damage, which if a certain volume of the liver is affected might lead to a reduction of the functional liver capacity, a so-called radiation (or radioembolization)-induced liver disease (RILD or REILD) [4, 7, 15, 22, 29, 32, 36]. Reliable prediction and avoidance of substantial radiation-induced liver damage is not always possible. The "gold standard" for the diagnosis of a radiation-induced liver damage remains histopathology with evidence of veno-occlusive disease [8, 22, 27, 38].

Functional MRI using organ-specific contrast agents might serve as a new method to visualize radiation-induced liver damage. The so-called hepatobiliary contrast agents (gadobenate dimeglumine (Gd-BOPTA) and gadoxetate disodium (Gd-EOB-DTPA)) differ from other available gadolinium chelates in that they distribute not only to the extracellular fluid space but also are selectively and actively taken up by functioning hepatocytes and excreted into the bile [6, 19, 25, 26, 34, 35, 41]. The uptake of the hepatobiliary contrast media in functionally altered liver parenchyma is significantly reduced. This also seems to be true for radiation-induced liver damage, because a loss of uptake of hepatobiliary contrast media is described in the liver parenchyma adjacent to the clinical target volume after local radiotherapy [23, 29, 36, 42].

We therefore sought to determine the correlation of hepatobiliary MRI findings with histopathological evidence of radiation-induced liver damage in patients undergoing local high-dose-rate brachytherapy of liver tumors in a feasibility study.

Materials and Methods

Patients, Inclusion and Exclusion Criteria

Patients were identified from our institutional database using the following inclusion criteria: (1) secondary liver malignancy, (2) computed tomography-guided interstitial high-dose-rate brachytherapy (CTGB), (3) available liver biopsy of a liver region with radiation exposure after CTGB (within 120 days), and (4) available magnetic resonance imaging (MRI) of the liver using hepatobiliary contrast media within 7 days before liver biopsy. Patients displaying histopathological evidence of liver cirrhosis or no evaluable liver parenchyma in the biopsy specimen were excluded (Fig. 1). In total, eight patients (patients characteristics see Table 1) with 14 evaluable liver biopsies from radiation-exposed liver regions were identified.

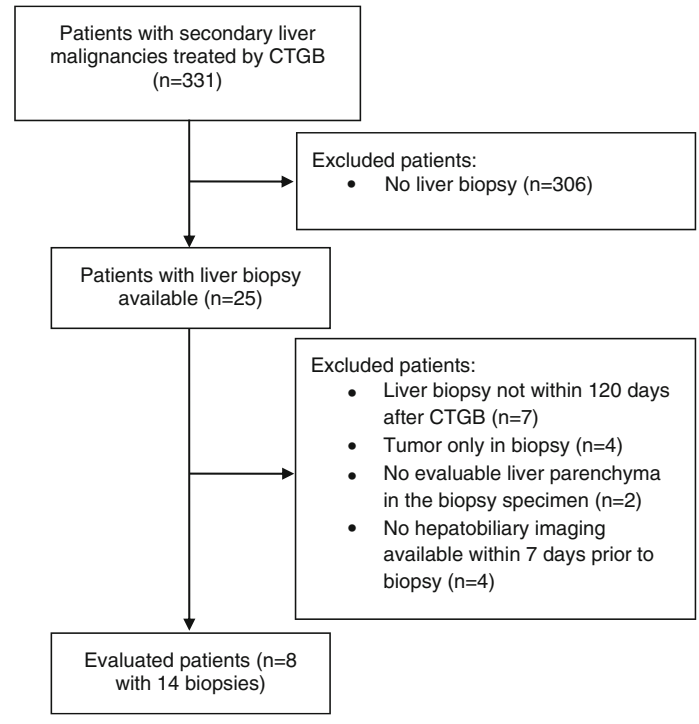

Fig. 1 Patient enrolment

The local ethics committee approved this retrospective study; written, informed consent for general anonymized data processing, including acquired tissue samples was available from all patients. Most of the patients with colorectal metastases were part of a prospective trial on the effectiveness of CTGB [28].

Radiotherapy

All patients underwent CTGB. The technique has been described previously [28]. Briefly, the placement of the introducer sheaths (6F Radiofocus, Terumo, Tokio, Japan) with the brachytherapy applicators (Lumencath, Nucletron, Veenendaal, The Netherlands) inside was performed using computed tomography (CT) fluoroscopy (Siemens, Erlangen, Germany) using Seldinger technique. For treatment planning purposes, a spiral multislice CT of the liver enhanced by intravenous application of iodide contrast media was acquired. According to the defined course of the catheters, the clinical target volume and the predefined

Table 1 Patient characteristics and histopathological and imaging findings; biopsy-based evaluation

Sex (f/m)	4/10
Age (year, mean, range)	64 (55–72)
Primary tumor (*n*)	
CRC	10
Breast	1
GIST	3
Median time interval MRI to biopsy (d, range)	1 (1–3)
Median time interval CTGB to biopsy (d, range)	35 (24–77)
Time from CTGB to biopsy, graded (<30 d/30–60 d/60–120 d) (*n*)	6/6/2
Mean dose at biopsy site (Gy, SD)	20.8 (8.4)
Dose at biopsy site, graded (≤10 Gy/10–20 Gy/>20 Gy) (*n*)	1/5/8
Uptake of Gd-BOPTA at biopsy site (yes/no)	3/11
Presence of radiation-induced liver damage at biopsy site (yes/no)	11/3
Other histopathological findings (*n* (with/without concomitant presence of radiation-induced liver damage))	
Fat depositions	4 (3/1)
Focal necrosis	6 (6/0)
Focal fibrosis	4 (2/2)
History of chemotherapy (yes/no)	14/0
Platinum containing chemotherapy, all cases (yes/no)	6/8
Platinum containing chemotherapy, in cases with radiation-induced liver damage only (yes/no)	6/5
Median time interval from last chemotherapy to MRI (mo, range)	3 (2–17)

minimum dose at the tumor margin (15–20 Gy, delivered as a single fraction) the planning software (Brachyvision, Varian Medical Systems, Charlottesville, VA) calculated a dosimetry. The high-dose-rate afterloading system (Gammamed, Varian Medical Systems) employed a Iridium-192 source.

Liver Biopsy and Histopathological Evaluation

In all patients, analyzed core biopsies were part of liver sample sets obtained after CTGB to exclude a local recurrence/new tumor close to the former tumor margin. Biopsies were taken 35 days (median; range 24–77 days) after CTGB. Core biopsies were obtained under CT fluoroscopic (Siemens) guidance with a 16 or 18G biopsy needle (Quick-Core, Cook Group Inc., Bloomington, IN), throw length 20 mm. The location of the biopsy was documented by CT. Standard hematoxylin-eosin as well as Gomori stain was used for this analysis (Fig. 2H,I). All specimens were evaluated by two independent pathologists for presence or absence of radiation-induced liver damage (defined as presence of sinusoidal and hepatic vein congestion, increased perisinusoidal reticulin network, and coexistence of atrophy of hepatocytes; rating: yes/no) [8, 22, 27, 38]. Other pathological findings were recorded (e.g., tumor, fibrosis, necrosis, fat deposits). In case of divergent opinions of the reviewers, the decision was made by consensus. However, initial interrater reliability was 92.9 % with a Cohen's kappa of 0.811, which resembles an almost perfect agreement [21].

Magnetic Resonance Imaging

In all patients MRI (Gyroscan NT® 1.5T, Philips, Best, The Netherlands) employing Gd-BOPTA (Multihance, Bracco, Princeton, NJ) was performed 1–3 days (median 1) before liver biopsy. The MRI protocol consisted of the following sequences: axial T2-weighted (T2-w) ultrafast spin-echo (UTSE) (time to echo (TE)/time to repetition (TR) 90/2100 ms) with and without fat suppression, axial T1-weighted (T1-w) gradient echo (GRE) (TE/TR 5/30 ms, flip angle 30°) without fat suppression precontrast, 20, 60, and 120 s post intravenous administration of 0.1 mL/kg bodyweight Gd-BOPTA (in median 7 mL), and 2-h post injection of i.v. Gd-BOPTA. The slice thickness was 5–8 mm. For the image registration, the axial T1-w GRE sequence 2 h after intravenous application of Gd-BOPTA was used.

Image Registration

Image registration of the CT documentation of the site of the liver biopsy with the contrast-enhanced planning CT (including the dosimetry) was performed using the treatment planning software BrachyVision (semiautomated point based 2D–3D image registration). Match points were defined on corresponding landmarks of the liver ($n = 3$–4) by an experienced radiologist to enable fusion of biopsy CT with planning CT/dosimetry data. As a result of this procedure, BrachyVision simultaneously displayed the treatment plan as well as the anatomical structures of the biopsy CT allowing a dose measurement at the site of biopsy (Fig. 1A–C). Image registration of the CT documentation of the site of the liver biopsy with the hepatobiliary phase MRI (T1-w GRE) was executed using an independent image registration implementation within the 3D-visualization software Amira 3.1 (Mercury Computer Systems, Berlin, Germany) [30]. Again, a semiautomated point-based 2D–3D image registration was performed according to defined landmarks in the liver (Fig. 2D–F). Dose measurements and Gd-BOPTA uptake evaluation

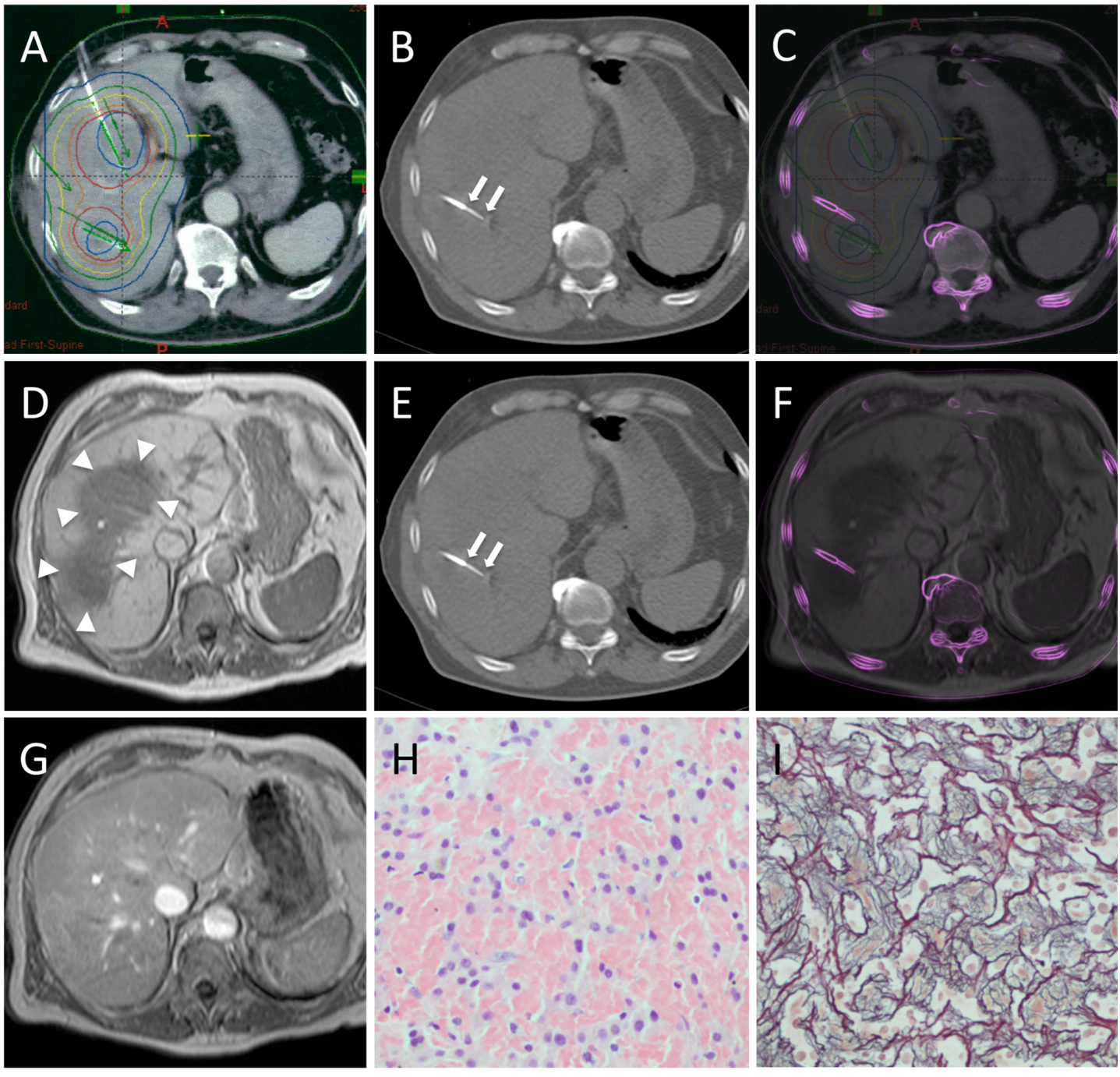

Fig. 2 Patient example of the image workup. Image fusion of the planning-CT/dosimetry (**A**) with the CT documentation of the CT-guided liver biopsy (**B**) leading to a fused image data set of A and B, displayed in an overlay modus (**C**). **A** *Blue circles* resemble the clinical target volumes, *red circles* resemble the 15-Gy isodose, *orange circles* the 10-Gy isodose. Brachytherapy catheters in-plane are superimposed by *light green arrows*, catheters positioned in other levels are indicated by *dark green arrows*. **B** Biopsy was taken 32 days after brachytherapy (**A**). The throw of the biopsy needle is marked by an arrow at the beginning and at the end. **C** Fusion of **A** and **B**. The CT documentation of the CT-guided liver biopsy is superimposed and colored transparent magenta. The former applied dose at the center of biopsy was calculated within mean 18 Gy. **D-F** Image fusion of the hepatobiliary MRI (**D**) with the CT documentation of the CT-guided liver biopsy (**E**) leading to a merged image data set of **D** and **E**, displayed in an overlay modus (**F**). **D** T1-w GRE 2 h after application of Gd-BOPTA, acquired 1 day before biopsy. *Dark grey areas* in the liver (marked by *white arrowheads*) indicate an absent uptake of the hepatocyte specific Gd-BOPTA in contrast to the remaining liver parenchyma. Note that the geometry of the absent Gd-BOPTA uptake region is in good concordance with the overall isodose geometry from the dosimetry (resembling approximately the 12 Gy isodose). **F** Fusion of **D** and **E**. The CT documentation of the CT-guided liver biopsy is superimposed and colored transparent magenta. Clearly visible: no Gd- BOPTA uptake at the site of biopsy. **G** displays the correspondent (to **D**) T1-w GRE 60 s after application of Gd-BOPTA: no relevant other finding (e.g., tumor) is present at the site of biopsy. **H** and **I** Procured histological specimen: severe sinusoidal and hepatic vein congestion with atrophy of hepatocytes and increased perisinusoidal reticulin network (H: hematoxylin-eosin stain; I: Gomori stain, original magnification ×200)

The formerly applied dose at the site of biopsy was measured in the centre of the biopsy core. The range was 6–35 Gy [mean 20.8 Gy, standard deviation (SD) 8.4]. Two experienced MRI GI radiologists (blinded for the histopathology results) independently evaluated the presence or absence of Gd-BOPTA uptake at the site of biopsy sampling (on the merged images, rating: yes/no). To avoid uptake misinterpretation (underlying anatomical structures, tumor), all other obtained MRI sequences (although not merged) were available to the reviewers (Fig. 2). In case of divergent reviewer opinions the decision was made by consensus. However, as with histopathology, initial inter-rater reliability was 92.9 % with a Cohen's kappa of 0.811 [21].

Statistics

Statistical analysis was performed using SPSS (SPSS 21, IBM, Chicago, IL). Measurements in different regions of the same patient were regarded as independent. Cross-tables were used to display the association of histopathological and MRI findings. The confidence interval according to Clopper-Pearson was calculated to estimate the congruence of histopathology and MRI. *T* test was performed to analyze the relation of formerly applied dose and histopathology/MRI findings. A $p < 0.05$ was regarded as statistical significant.

Results

Patient characteristics and biopsy-based results of the histopathological analysis, the dose determination at the site of tissue sampling, and the uptake characteristics of Gd-BOPTA at the sampling site are summarized in Table 1. Radiation-induced liver damage was seen in 11 of the 14 biopsies.

In all cases of histopathological evidence of radiation-induced liver damage, no uptake of Gd-BOPTA was detected at the site of tissue sampling. Conversely, in all cases without radiation-induced liver damage, Gd-BOPTA uptake at MRI was preserved (Table 2). The Clopper-Pearson 95 % confidence interval (CI) reaches from 76.8 to 100 % for concordance of histopathology and MRI and from 71.5 to 100 % for the sensitivity to detect a radiation-induced liver damage by MRI.

The association of the degree of former radiation exposure (graded: ≤10 Gy/10–20 Gy/> 20 Gy) and resulting radiation-induced liver damage and loss of Gd-BOPTA uptake is displayed in Tables 3 and 4. After exposure to >20 Gy radiation-induced liver damage and loss of Gd-BOPTA were seen in all cases, whereas cases with or without radiation-induced liver damage/Gd-BOPTA uptake were seen if prior radiation exposure was ≤20 Gy. However, statistical testing revealed a significant lower dose exposition (continuous values) in cases with preserved Gd-BOPTA uptake or absent radiation-induced liver damage (mean exposure: 10.7 Gy) compared with cases with lost Gd-BOPTA uptake or radiation-induced liver damage (mean exposure: 23.5 Gy; $p = 0.012$). A clinically overt RILD was not observed in any of the patients.

Table 2 Cross-table, presence of radiation-induced liver damage, and uptake of Gd-BOPTA at the site of tissue sampling

Presence of radiation-induced liver damage	Uptake of Gd-BOPTA		Total
	Yes	No	
Yes	0	11	11
No	3	0	3
Total	3	11	14

Cross-table of findings of histopathology and hepatobiliary MRI. A perfect congruence of histopathology and hepatobiliary MRI can be seen

Table 3 Cross-table, presence of radiation-induced liver damage and dose (Gy) at the site of tissue sampling

Presence of radiation-induced liver damage	Dose (Gy) at the site of tissue sampling			Total
	≤10	>10 and ≤20	>20 Gy	
Yes	0	3	8	11
No	1	2	0	3
Total	1	5	8	14

Cross-table of the degree of former radiation-exposure (graded (≤10 Gy/10–20 Gy/>20 Gy)) at the site of biopsy and radiation-induced liver damage (yes/no). An increasing rate of presence of radiation-induced liver damage can be seen with increasing radiation-exposure

Discussion

To our knowledge, no systematic study focusing on the correlation of histopathological presence of radiation-induced liver damage after radiotherapy with hepatobiliary MRI findings has been published to date. We were able to show that in our small patient cohort radiation-induced liver damage in radiation-exposed liver parenchyma is significantly associated with a loss of uptake of the hepatocyte-specific MRI contrast media Gd-BOPTA. The concordance was perfect with absence of Gd-BOPTA uptake demonstrated in all cases with and in no case without radiation-induced liver damage.

Functional MRI using hepatocyte-specific contrast agents is increasingly being evaluated as a method to

Table 4 Cross-table, uptake of Gd-BOPTA and dose (Gy) at the site of tissue sampling

Uptake of Gd-BOPTA	Dose (Gy) at the site of tissue sampling			Total
	≤10 Gy	>10 and ≤20 Gy	>20 Gy	
Yes	1	2	0	3
No	0	3	8	11
Total	1	5	8	14

Cross-table of the degree of former radiation-exposure (graded (≤10 Gy/10–20 Gy/> 20 Gy)) and Gd-BOPTA uptake (yes/no), both at the site of biopsy. An increasing rate of absence of Gd-BOPTA uptake can be seen with increasing radiation-exposure

determine the liver capacity noninvasively [42]. According to our results, liver MRI employing hepatocyte-specific contrast media also might serve as a new method to visualize radiation-induced liver damage. The hepatobiliary contrast agents Gd-BOPTA and Gd-EOB-DTPA are selectively taken up (through an organic-anion-transporter-polypeptide, mainly OATP1B1 and 3) by functioning hepatocytes and excreted into the bile by the adenosine-triphosphate-dependent-multidrug-resistance-protein 2 [5, 19, 25, 26, 34, 35, 41]. Regarding Gd-BOPTA, the biliary excretion rate is 3–5 % in humans [5, 41]. The biliary excretion rate of Gd-EOB-DTPA in humans is even higher with approximately 50 % [25, 35]. However, with both contrast media the level of uptake is sufficient to bring about specific, long-lasting enhancement of MR signal intensity in normal liver parenchyma.

Significant damage to the hepatocyte results in a reduced or absent uptake of both of these agents [23, 26, 34, 42]. This also seems to be true for significantly radiation-exposed liver parenchyma for which a reduced uptake of the hepatobiliary contrast agents Gd-BOPTA and Gd-EOB-DTPA has been demonstrated [29, 36, 43]. Besides direct damage to the hepatocyte by irradiation, the radiation-induced liver damage is mainly determined by the low radiation tolerability of nonparenchymal cells, particularly venous and sinusoidal endothelial cells, which results in the early development of venous and sinusoidal congestion [11]. However, this endothelial damage is followed by a thrombogenic state, inducing additional and substantial hepatocyte damage [8, 22, 27].

We see a potential clinical use of these results for the following purposes in patient management (and use them already in our daily practice): to support the diagnosis of clinically suspected radiation-induced liver disease; to optimize treatment planning in repeat liver-directed radiotherapy (to visualize the functional remnant liver parenchyma); to evaluate the topographic concordance between treatment planning and distribution of radiation effects as early therapy control [44].

Additionally, the indication of the functional state of the hepatocyte after radiation-exposure may provide a possibility to determine the tolerance of hepatic tissue to irradiation quantitatively. Studies on quantitative in vivo data of the hepatic tolerance to irradiation are sparse and frequently biased by the volume function of exposed liver parenchyma [4, 7]. Reports of hepatic tolerance after whole organ irradiation also are rare [9, 16, 40]. New approaches use surrogates (contrast-enhanced computed tomography (CT), hepatobiliary MRI) to determine the functionality of the liver parenchyma after focal radiotherapy [15, 29, 36, 43]. Notably, a correlation of imaging findings with histopathology of radiation-induced liver damage was not investigated in these cited studies. However, all these studies indicate that a relevant parenchymal damage can be expected if a single dose of approximately >10 Gy or a fractionated dose of approximately >30 Gy (2 Gy/d) is applied to the liver. However, the interindividual heterogeneity of hepatic tolerance to irradiation remains high, most probably due to prior exposition to potentially hepatotoxic chemotherapeutic agents [9, 36, 40]. Based on the structure of the presented analysis and the low sample size, we cannot provide reliable data on quantitative liver tolerance. Nevertheless, we found a significant association of applied dose and the presence of radiation-induced liver damage with a high rate of radiation-induced liver damage after exposition to a single fraction of >10 Gy.

There is reason to believe that our results obtained from CTGB treatment can be transferred to other radiation treatment methods for liver malignancies, such as ^{90}Y-radioembolization. During CTGB, the liver parenchyma is exposed to single doses of high-dose-rate radiation, with a liver damage starting to develop already at doses of approximately 10 Gy [29, 36, 43]. Radiation exposure of liver tissue is characterized by a slope-factor alpha/beta equal to 2 Gy. This translates into a conventional fractionation scheme of 5 × 2 Gy with a total threshold dose (EQ) of approximately 30 Gy. This dose pattern is quite similar to ^{90}Y-radioembolization. Here, a high-radiation dose of upto 200 Gy is directed at metastases by intra-arterial injection of ^{90}Y-microspheres. A steep fall-off of dose around the ^{90}Y-microsphere-accumulating lesions is observed, ideally with a mean dose of 15 Gy in the remaining liver tissue and—if occurring at all—parenchymal damage exclusively at the interface of tumor and parenchyma [2, 18]. However, depending on the embolized volume, the tumor-to-liver distribution ratio of the spheres, and the number and spatial distribution of metastases, the volume of liver tissue exposed to >30 Gy and more may be considerable. The resulting focal or generalized radioembolization-induced liver damage may lead to clinically overt REILD in upto 22.7 %, especially in patients with preexisting liver damage [2, 10, 12, 17, 18, 20, 32, 37]. Clearly, the time factor with ^{90}Y-radioembolization is different. However, for cells with a typical repair constant

(μ) of 0.1–1 h-1, we have calculated that nominal doses of ^{90}Y-radioembolization are equal or slightly below the corresponding standard doses EQ, indicating that the dose ranges associated with ^{90}Y-radioembolization and CTGB are comparable if recalculated with respect to the standard fractionation. Moreover, a reduced uptake of Gd-EOB-DTPA in liver regions exposed to >30 Gy after ^{90}Y-radioembolization was presented recently [13]. Because imaging of the actual distribution of the ^{90}Y-microspheres is hampered by properties and low resolution of post therapeutic bremsstrahlung imaging, the identification of hepatic parenchymal injury induced by implantation of ^{90}Y-microspheres is appealing in terms of quality assurance, patient management and, most importantly, identification of patients at risk for REILD.

As a limitation of our study the low sample size (8 patients, 14 biopsies) has to be discussed. In order to minimize confounders, we excluded patients with an underlying liver cirrhosis (reduced contrast agent uptake), patients with a long time period between brachytherapy and biopsy (>120 days) (after that a radiation-induced liver damage is unlikely) and patients with a delay of more than 7 days between biopsy and hepatobiliary MRI (to avoid a morphological bias between imaging and histopathology). Thus, while certainly reducing the number of evaluable patients, we believe that the strict application of these criteria for inclusion and exclusion of patients increased the homogeneity of the cohort and therefore improved the overall quality of this analysis. However, the study concept remains exploratory. A confirmatory study is needed to verify these findings (i.e., prospective hepatobiliary MRI and collection of liver tissue samples within a defined time span after CTGB, for example in patients who require repetitive interventions due to lesion number or new lesions).

Finally, interference of sinusoidal-obstruction-syndrome (SOS) after platinum containing chemotherapy with histopathological and imaging findings should be discussed [31, 39]. In contrast to SOS, the geometry and the distribution of the uptake loss of hepatobiliary contrast media after CTGB is focal, homogenous, and circumferential around the clinical target volume, as shown in our example (Fig. 2D) and described in the literature as well [29, 36]. Thus, we believe that we can exclude underlying SOS as a confounder to our results.

Conclusions

We were able to show that loss of hepatobiliary MRI contrast media uptake in patients undergoing liver-directed radiotherapy may indicate the presence of radiation-induced liver damage as determined by histopathology. We believe that, if confirmed in larger studies, this finding has an impact on treatment follow-up and further treatment planning after radiotherapy of the liver, as well as on further research on liver reaction to radiotherapy.

Conflict of interest None in context of the presented study for all authors. Possible Coi outside study matter: Max Seidensticker: reports to receive research grants by SIRTEX medical and Bayer Healthcare and honoraria by Bayer Healthcare. Miroslaw Burak: no conflict of interest. Thomas Kalinski: no conflict of interest. Benjamin Garlipp: reports to receive lecture fees by SIRTEX medical. Konrad Koelble: no conflict of interest. Peter Wust: no conflict of interest. Kai Antweiler: no conflict of interest. Ricarda Seidensticker: reports to receive research grants by SIRTEX medical and Bayer Healthcare and honoraria by Bayer Healthcare. Konrad Mohnike: no conflict of interest. Maciej Pech: no conflict of interest. Jens Ricke: reports to receive research grants by SIRTEX medical, Bayer Healthcare and Siemens.

References

1. Boda-Heggemann J, Dinter D, Weiss C, Frauenfeld A, Siebenlist K, Attenberger U, Ottstadt M, Schneider F, Hofheinz RD, Wenz F, Lohr F (2012) Hypofractionated image-guided breath-hold SABR (stereotactic ablative body radiotherapy) of liver metastases–clinical results. Radiat Oncol 7:92
2. Campbell AM, Bailey IH, Burton MA (2001) Tumour dosimetry in human liver following hepatic yttrium-90 microsphere therapy. Phys Med Biol 46(2):487–498
3. Cosimelli M, Golfieri R, Cagol PP, Carpanese L, Sciuto R, Maini CL, Mancini R, Sperduti I, Pizzi G, Diodoro MG, Perrone M, Giampalma E, Angelelli B, Fiore F, Lastoria S, Bacchetti S, Gasperini D, Geatti O, Izzo F (2010) Multi-centre phase II clinical trial of yttrium-90 resin microspheres alone in unresectable, chemotherapy refractory colorectal liver metastases. Br J Cancer 103(3):324–331
4. Dawson LA, Normolle D, Balter JM, McGinn CJ, Lawrence TS, Ten Haken RK (2002) Analysis of radiation-induced liver disease using the Lyman NTCP model. Int J Radiat Oncol Biol Phys 53(4):810–821
5. de Haen C, Gozzini L (1993) Soluble-type hepatobiliary contrast agents for MR imaging. J Magn Reson Imaging 3(1):179–186
6. de Haen C, Lorusso V, Tirone P (1996) Hepatic transport of gadobenate dimeglumine in TR-rats. Acad Radiol 3(Suppl 2):S452–S454
7. Emami B, Lyman J, Brown A, Coia L, Goitein M, Munzenrider JE, Shank B, Solin LJ, Wesson M (1991) Tolerance of normal tissue to therapeutic irradiation. Int J Radiat Oncol Biol Phys 21(1):109–122
8. Fajardo LF, Colby TV (1980) Pathogenesis of veno-occlusive liver disease after radiation. Arch Pathol Lab Med 104(11):584–588
9. Farthing MJ, Clark ML, Sloane JP, Powles RL, McElwain TJ (1982) Liver disease after bone marrow transplantation. Gut 23(6):465–474
10. Fox RA, Klemp PF, Egan G, Mina LL, Burton MA, Gray BN (1991) Dose distribution following selective internal radiation therapy. Int J Radiat Oncol Biol Phys 21(2):463–467
11. Geraci JP, Mariano MS (1993) Radiation hepatology of the rat: parenchymal and nonparenchymal cell injury. Radiat Res 136(2):205–213
12. Gil-Alzugaray B, Chopitea A, Inarrairaegui M, Bilbao JI, Rodriguez-Fraile M, Rodriguez J, Benito A, Dominguez I,

D'Avola D, Herrero JI, Quiroga J, Prieto J, Sangro B (2013) Prognostic factors and prevention of radioembolization-induced liver disease. Hepatology 57(3):1078–1087
13. Grosser OS, Conrad S, Steffen IG, Seidensticker M, Ulrich G, Nultsch M, Furth C, Ricke J, Amthauer H (2012) Therapievalidierung der yttrium-90-radioembolisation durch Bestimmung der Dosisverteilung in einem softwareassistierten workflow. Nuklearmedizin 51:A84
14. Herfarth KK, Debus J, Lohr F, Bahner ML, Rhein B, Fritz P, Hoss A, Schlegel W, Wannenmacher MF (2001) Stereotactic single-dose radiation therapy of liver tumors: results of a phase I/II trial. J Clin Oncol 19(1):164–170
15. Herfarth KK, Hof H, Bahner ML, Lohr F, Hoss A, van Kaick G, Wannenmacher M, Debus J (2003) Assessment of focal liver reaction by multiphasic CT after stereotactic single-dose radiotherapy of liver tumors. Int J Radiat Oncol Biol Phys 57(2):444–451
16. Jacobs P, Miller JL, Uys CJ, Dietrich BE (1979) Fatal veno-occlusive disease of the liver after chemotherapy, whole-body irradiation and bone marrow transplantation for refractory acute leukaemia. S Afr Med J 55(1):5–10
17. Kennedy AS, McNeillie P, Dezarn WA, Nutting C, Sangro B, Wertman D, Garafalo M, Liu D, Coldwell D, Savin M, Jakobs T, Rose S, Warner R, Carter D, Sapareto S, Nag S, Gulec S, Calkins A, Gates VL, Salem R (2009) Treatment parameters and outcome in 680 treatments of internal radiation with resin 90Y-microspheres for unresectable hepatic tumors. Int J Radiat Oncol Biol Phys 74(5):1494–1500
18. Kennedy AS, Nutting C, Coldwell D, Gaiser J, Drachenberg C (2004) Pathologic response and microdosimetry of (90)Y microspheres in man: review of four explanted whole livers. Int J Radiat Oncol Biol Phys 60(5):1552–1563
19. Kirchin MA, Pirovano GP, Spinazzi A (1998) Gadobenate dimeglumine (Gd-BOPTA). An overview. Invest Radiol 33(11):798–809
20. Lam MG, Abdelmaksoud MH, Chang DT, Eclov NC, Chung MP, Koong AC, Louie JD, Sze DY (2013) Safety of 90Y radioembolization in patients who have undergone previous external beam radiation therapy. Int J Radiat Oncol Biol Phys 87(2):323–329
21. Landis JR, Koch GG (1977) The measurement of observer agreement for categorical data. Biometrics 33(1):159–174
22. Lawrence TS, Robertson JM, Anscher MS, Jirtle RL, Ensminger WD, Fajardo LF (1995) Hepatic toxicity resulting from cancer treatment. Int J Radiat Oncol Biol Phys 31(5):1237–1248
23. Marzola P, Maggioni F, Vicinanza E, Dapra M, Cavagna FM (1997) Evaluation of the hepatocyte-specific contrast agent gadobenate dimeglumine for MR imaging of acute hepatitis in a rat model. J Magn Reson Imaging 7(1):147–152
24. Mohnike K, Wieners G, Schwartz F, Seidensticker M, Pech M, Ruehl R, Wust P, Lopez-Hanninen E, Gademann G, Peters N, Berg T, Malfertheiner P, Ricke J (2010) Computed tomography-guided high-dose-rate brachytherapy in hepatocellular carcinoma: safety, efficacy, and effect on survival. Int J Radiat Oncol Biol Phys 78(1):172–179
25. Pascolo L, Cupelli F, Anelli PL, Lorusso V, Visigalli M, Uggeri F, Tiribelli C (1999) Molecular mechanisms for the hepatic uptake of magnetic resonance imaging contrast agents. Biochem Biophys Res Commun 257(3):746–752
26. Pastor CM, Planchamp C, Pochon S, Lorusso V, Montet X, Mayer J, Terrier F, Vallee JP (2003) Kinetics of gadobenate dimeglumine in isolated perfused rat liver: MR imaging evaluation. Radiology 229(1):119–125
27. Reed GB Jr, Cox AJ Jr (1966) The human liver after radiation injury A form of veno-occlusive disease. Am J Pathol 48(4): 597–611
28. Ricke J, Mohnike K, Pech M, Seidensticker M, Ruhl R, Wieners G, Gaffke G, Kropf S, Felix R, Wust P (2010) Local response and impact on survival after local ablation of liver metastases from colorectal carcinoma by computed tomography-guided high-dose-rate brachytherapy. Int J Radiat Oncol Biol Phys 78(2):479–485
29. Ricke J, Seidensticker M, Ludemann L, Pech M, Wieners G, Hengst S, Mohnike K, Cho CH, Lopez Hanninen E, Al-Abadi H, Felix R, Wust P (2005) In vivo assessment of the tolerance dose of small liver volumes after single-fraction HDR irradiation. Int J Radiat Oncol Biol Phys 62(3):776–784
30. Rohlfing T, West JB, Beier J, Liebig T, Taschner CA, Thomale UW (2000) Registration of functional and anatomical MRI: accuracy assessment and application in navigated neurosurgery. Comput Aided Surg 5(6):414–425
31. Rubbia-Brandt L, Audard V, Sartoretti P, Roth AD, Brezault C, Le Charpentier M, Dousset B, Morel P, Soubrane O, Chaussade S, Mentha G, Terris B (2004) Severe hepatic sinusoidal obstruction associated with oxaliplatin-based chemotherapy in patients with metastatic colorectal cancer. Ann Oncol 15(3):460–466
32. Sangro B, Gil-Alzugaray B, Rodriguez J, Sola I, Martinez-Cuesta A, Viudez A, Chopitea A, Inarrairaegui M, Arbizu J, Bilbao JI (2008) Liver disease induced by radioembolization of liver tumors: description and possible risk factors. Cancer 112(7):1538–1546
33. Schmoll HJ, Van Cutsem E, Stein A, Valentini V, Glimelius B, Haustermans K, Nordlinger B, van de Velde CJ, Balmana J, Regula J, Nagtegaal ID, Beets-Tan RG, Arnold D, Ciardiello F, Hoff P, Kerr D, Kohne CH, Labianca R, Price T, Scheithauer W, Sobrero A, Tabernero J, Aderka D, Barroso S, Bodoky G, Douillard JY, El Ghazaly H, Gallardo J, Garin A, Glynne-Jones R, Jordan K, Meshcheryakov A, Papamichail D, Pfeiffer P, Souglakos I, Turhal S, Cervantes A (2012) ESMO consensus guidelines for management of patients with colon and rectal cancer. A personalized approach to clinical decision making. Ann Oncol 23(10):2479–2516
34. Schuhmann-Giampieri G, Schmitt-Willich H, Frenzel T, Schitt-Willich H (1993) Biliary excretion and pharmacokinetics of a gadolinium chelate used as a liver-specific contrast agent for magnetic resonance imaging in the rat. J Pharm Sci 82(8): 799–803
35. Schuhmann-Giampieri G, Schmitt-Willich H, Press WR, Negishi C, Weinmann HJ, Speck U (1992) Preclinical evaluation of Gd-EOB-DTPA as a contrast agent in MR imaging of the hepatobiliary system. Radiology 183(1):59–64
36. Seidensticker M, Seidensticker R, Mohnike K, Wybranski C, Kalinski T, Luess S, Pech M, Wust P, Ricke J (2011) Quantitative in vivo assessment of radiation injury of the liver using Gd-EOB-DTPA enhanced MRI: tolerance dose of small liver volumes. Radiat Oncol 6:40
37. Seidensticker R, Denecke T, Kraus P, Seidensticker M, Mohnike K, Fahlke J, Kettner E, Hildebrandt B, Dudeck O, Pech M, Amthauer H, Ricke J (2012) Matched-pair comparison of radioembolization plus best supportive care versus best supportive care alone for chemotherapy refractory liver-dominant colorectal metastases. Cardiovasc Intervent Radiol 35(5):1066–1073
38. Sempoux C, Horsmans Y, Geubel A, Fraikin J, Van Beers BE, Gigot JF, Lerut J, Rahier J (1997) Severe radiation-induced liver disease following localized radiation therapy for biliopancreatic carcinoma: activation of hepatic stellate cells as an early event. Hepatology 26(1):128–134
39. Shin NY, Kim MJ, Lim JS, Park MS, Chung YE, Choi JY, Kim KW, Park YN (2012) Accuracy of gadoxetic acid-enhanced magnetic resonance imaging for the diagnosis of sinusoidal obstruction syndrome in patients with chemotherapy-treated colorectal liver metastases. Eur Radiol 22(4):864–871
40. Shulman HM, McDonald GB, Matthews D, Doney KC, Kopecky KJ, Gauvreau JM, Thomas ED (1980) An analysis of hepatic veno occlusive disease and centrilobular hepatic degeneration following bone marrow transplantation. Gastroenterology 79(6): 1178–1191

41. Spinazzi A, Lorusso V, Pirovano G, Kirchin M (1999) Safety, tolerance, biodistribution, and MR imaging enhancement of the liver with gadobenate dimeglumine: results of clinical pharmacologic and pilot imaging studies in nonpatient and patient volunteers. Acad Radiol 6(5):282–291
42. Watanabe H, Kanematsu M, Goshima S, Kondo H, Onozuka M, Moriyama N, Bae KT (2011) Staging hepatic fibrosis: comparison of gadoxetate disodium-enhanced and diffusion-weighted MR imaging–preliminary observations. Radiology 259(1):142–150
43. Wybranski C, Seidensticker M, Mohnike K, Kropf S, Wust P, Ricke J, Ludemann L (2009) In vivo assessment of dose volume and dose gradient effects on the tolerance dose of small liver volumes after single-fraction high-dose-rate 192Ir irradiation. Radiat Res 172(5):598–606
44. Yuan Y, Andronesi OC, Bortfeld TR, Richter C, Wolf R, Guimaraes AR, Hong TS, Seco J (2013) Feasibility study of in vivo MRI based dosimetric verification of proton end-of-range for liver cancer patients. Radiother Oncol 106(3):378–382

RADIATION ONCOLOGY

RESEARCH Open Access

Radiobiological restrictions and tolerance doses of repeated single-fraction hdr-irradiation of intersecting small liver volumes for recurrent hepatic metastases

Ricarda Rühl*[1], Lutz Lüdemann[2], Anna Czarnecka[3], Florian Streitparth[2], Max Seidensticker[1], Konrad Mohnike[1], Maciej Pech[1], Peter Wust[2] and Jens Ricke[1]

Abstract

Background: To assess radiobiological restrictions and tolerance doses as well as other toxic effects derived from repeated applications of single-fraction high dose rate irradiation of small liver volumes in clinical practice.

Methods: Twenty patients with liver metastases were treated repeatedly (2 - 4 times) at identical or intersecting locations by CT-guided interstitial brachytherapy with varying time intervals. Magnetic resonance imaging using the hepatocyte selective contrast media Gd-BOPTA was performed before and after treatment to determine the volume of hepatocyte function loss (called pseudolesion), and the last acquired MRI data set was merged with the dose distributions of all administered brachytherapies. We calculated the BED (biologically equivalent dose for a single dose d = 2 Gy) for different α/β values (2, 3, 10, 20, 100) based on the linear-quadratic model and estimated the tolerance dose for liver parenchyma D_{90} as the BED exposing 90% of the pseudolesion in MRI.

Results: The tolerance doses D_{90} after repeated brachytherapy sessions were found between 22 - 24 Gy and proved only slightly dependent on α/β in the clinically relevant range of α/β = 2 - 10 Gy. Variance analysis showed a significant dependency of D_{90} with respect to the intervals between the first irradiation and the MRI control ($p < 0.05$), and to the number of interventions. In addition, we observed a significant inverse correlation ($p = 0.037$) between D_{90} and the pseudolesion's volume. No symptoms of liver dysfunction or other toxic effects such as abscess formation occurred during the follow-up time, neither acute nor on the long-term.

Conclusions: Inactivation of liver parenchyma occurs at a BED of approx. 22 - 24 Gy corresponding to a single dose of ~10 Gy (α/β ~ 5 Gy). This tolerance dose is consistent with the large potential to treat oligotopic and/or recurrent liver metastases by CT-guided HDR brachytherapy without radiation-induced liver disease (RILD). Repeated small volume irradiation may be applied safely within the limits of this study.

Background

Irradiation of liver malignancies has been shown beneficial for patients with both primary and secondary intrahepatic tumors under specific oncological conditions, e.g. oligotopic metastases. Both stereotactic irradiation and image-guided brachytherapy have been described recently with promising results [1-6].

A dose-response relationship exists with an association between the delivery of a higher dose and improved clinical outcome [7] but since the liver is a radiosensitive organ there is an increasing risk of radiation-induced liver disease (RILD) when the whole organ is exposed to moderate doses, e.g. 30 Gy [8,9]. RILD, the most common liver toxicity after radiation therapy, is a clinical syndrome of anicteric hepatomegaly, ascites, and elevated liver enzymes occurring typically between 2 weeks to 3 months after completion of radiation therapy [10].

* Correspondence: ricarda.ruehl@med.ovgu.de
[1] Universitätsklinikum Magdeburg, Klinik für Radiologie und Nuklearmedizin, Otto-von-Guericke-Universität Magdeburg, Germany
Full list of author information is available at the end of the article

For this reason, external total liver irradiation plays a very limited role in the treatment of intrahepatic tumors. However, treatment of parts of the liver with higher radiation doses is possible without clinical consequences as long as an adequate volume of normal liver is spared.

Hepatic toxicity due to radiation therapy has been extensively investigated. Robertson et al. reported 12 of 26 patients with primary hepatobiliary cancers and measurable treatment-related toxicity. Doses ranged from 36 Gy (whole liver) to 72.6 Gy (focal liver). Two patients were diagnosed with nonfatal radiation hepatitis [11]. Cheng et al reported 12 out of 68 patients developing RILD after three-dimensional conformal radiotherapy (3D-CRT) of hepatocellular carcinoma with radiation portals designed to include the gross hepatic tumor on CT scan with 1.5-2 cm margins. No patient was given radiation to the whole liver. The mean dose was 50.2 Gy in daily fractions of 1.8-2 Gy [12]. Our own workgroup has previously published 2 papers on human hepatic dose tolerance after single small volume irradiation treatments employing the brachytherapy model and hepatocyte selective contrast agent to determine focal liver function loss. Whereas the mean dose threshold for lasting focal hepatic dysfunction was 15 Gy for all lesions. We found a considerable dose volume effect up to a threshold of 18 Gy favouring very small irradiation volumes [13,14]. However, no human in vivo data on dose tolerance or late toxic effects of repeated treatments of hepatic parenchyma is available today. The aim of the study described herein was to determine hepatic threshold doses for repeated small volume irradiation e.g. in case of tumor recurrence after previous radiation treatment of liver metastases, and to rule out the occurrence of any other toxic effects.

Methods

General methodology

Patients eligible for this study had received at least 2 applications of computed tomography (CT)-guided brachytherapy of adjacent liver areas with intersecting dose distributions with time intervals of more than 4 weeks between radiation treatments. We sought to determine safety and clinical consequences of multiple applications of single-fraction irradiation of small liver volumes. We utilized a methodology previously described in a study on the tolerance dose of hepatic parenchyma after singular single-fraction HDR irradiation [13,14]. A fluoroscopy CT was used for catheter positioning and 3D-CT data sets are acquired for dose planning (Figure 1, 2). During follow-up to irradiation-therapy, magnetic resonance imaging (MRI) with the hepatocyte-directed contrast agent gadobenate dimeglumine (Gd-BOPTA) was selected to identify the function loss of liver parenchyma, hereinafter referred to as "cumulative pseudolesion". Gadobenate dimeglumine is an octadentate chelate of the paramagnetic ion gadolinium. Its kinetic properties resemble those of conventional iodinated contrast media and comprises a distribution phase and an elimination phase [15]. Studies have shown that this agent differs from other available gadolinium chelates in selectively being taken up only by functioning hepatocytes and excreted into the bile by the so-called canalicular multispecific organic anion transporter shared with bilirubin [15-17]. Changes in uptake of a hepatocyte specific contrast media illuminate the final path of the radiation injury, i.e. visualize areas of a dysfunctional hepatic system [18] (Figure 3). The histological appearance of radiation induced liver damage indicates that endothelial injury and subsequent obstruction of centrilobular venules and sinusoids are the key events in the pathogenesis of radiation injury of the liver. The pathological lesion resembles veno-occlusive disease [19-21] (Figure 4).

Figure 1 Image-fusion: Contrast-enhanced computed tomography (CT) after CT-guided positioning of brachytherapy catheters (arrows) in a liver metastasis of a colorectal carcinoma, merged with the last magnetic resonance imaging of the liver acquired after all interventions (grey delineation). The hypointensity area shows the impairment of hepatocyte function in the left liver lobe.

After image fusion, the isodose lines calculated for interstitial irradiation were projected onto the respective MRI scans. In the study described herein, we employed these techniques to assess the biologically equivalent tolerance dose of the irradiated volumes of liver parenchyma after repeated applications of single-fraction high-dose rate (HDR) brachytherapy. The LQ-model, established to predict late effects for different fractionation schemes, was adopted for the HDR-brachytherapy approach. The sensitivity of a tissue for a specific late effect was described by the critical dose α/β in Gy.

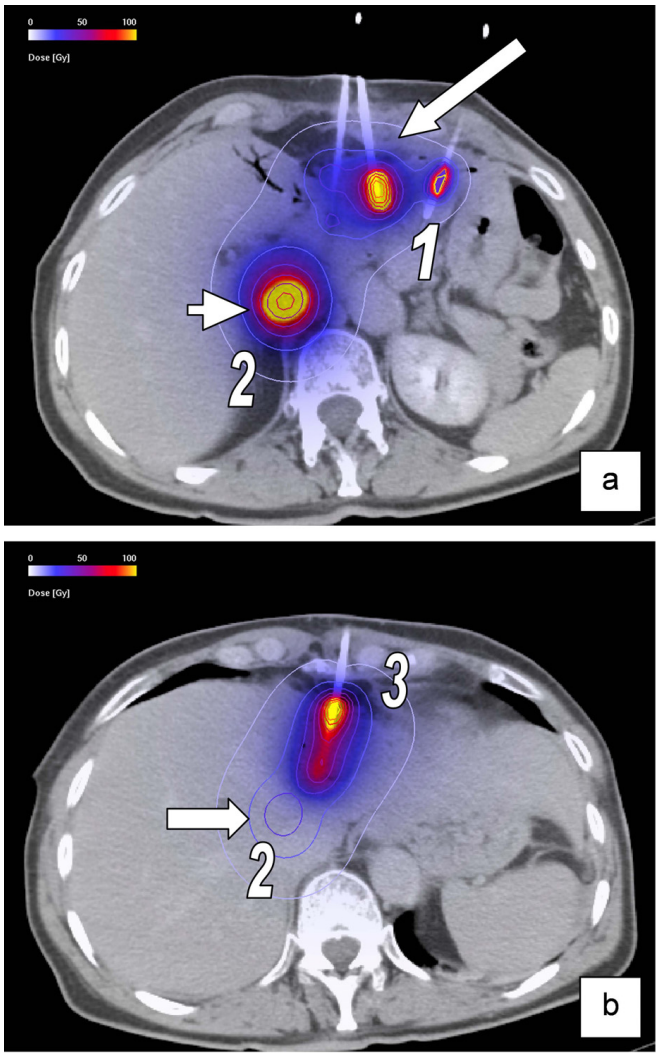

Figure 2 Image fusion of CT-data set with the accumulated 3-D dosimetry of three different irradiation sessions. (a) Contrast-enhanced CT after first (No.1) CT-guided positioning of brachytherapy catheters (long arrow) in metastases of a colorectal carcinoma. The short arrow shows the 3-D dosimetry of another lesion, irradiated in session No.2. (b) Contrast-enhanced CT after third intervention (No.3) in the same patient. The arrow shows the upper boundary of the 3-D dosimetry of the lesion irradiated in session No.2. Physical doses are shown in the colour map.

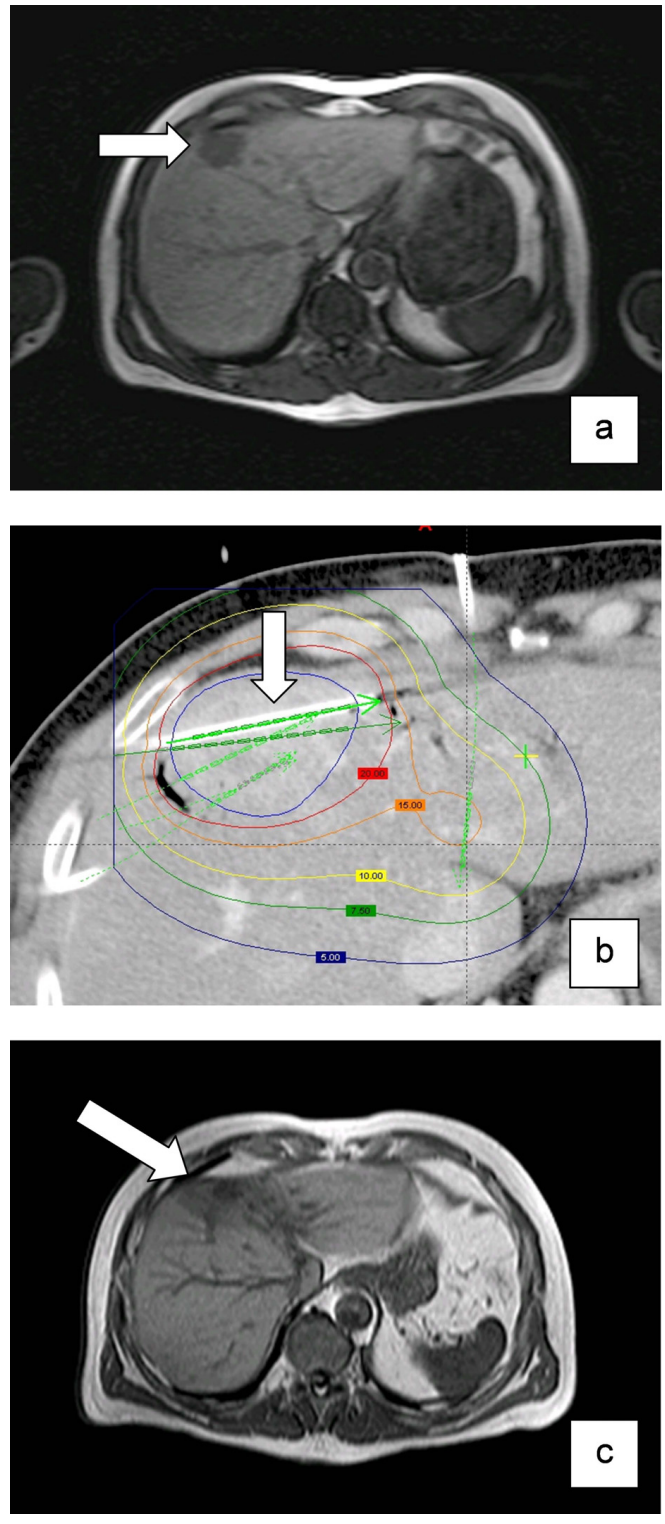

Figure 3 Development of radiation injury of the liver after HDR brachytherapy: (a) Colorectal metastasis in liver segment IV (arrow), T1w-GRE 20 minutes after application of Gd-BOPTA. (b) Contrast-enhanced planning-CT and dosimetry after insertion of brachytherapy catheters (arrow) in the metastasis. The coloured lines indicate different isodoses. Applicated dose at the tumor margin was 20 Gy. (c) MRI after 3 months with a decreased uptake (arrow) of Gd-BOPTA around the irradiated and shrunken metastasis (T1w-GRE 20 minutes after application of Gd-BOPTA).

Study population

We retrospectively analyzed the dose distributions of twenty patients. All patients received between two and four applications of CT-guided HDR brachytherapy either of the same liver lesion or in close proximity due to local tumor recurrence or growth of a satellite lesion. Written informed consent was obtained from all patients.

The patient population comprised of 10 men and 10 women; mean age was 64 years (51-84 years). Primary malignancies were colorectal carcinoma (n = 18), cholangiocellular carcinoma (n = 1) and breast carcinoma (n = 1). Karnofsky performance score was higher than 80%. Nineteen patients had received systemic anticancer treatments before brachytherapy, terminated at least 4 weeks

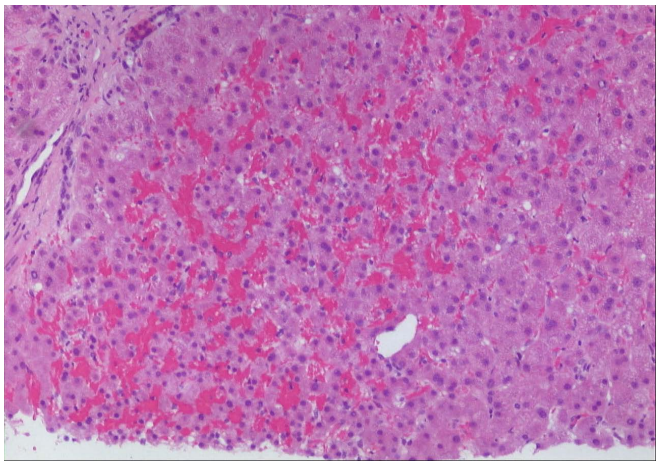

Figure 4 Liver biopsy. Biopsy was performed to rule out a suspected local recurrence. Tissue had been exposed to approximately 20 Gy two months ago. Heterogenous congestion of the sinusoids with beginning atrophy of liver cells. Hematoxylin-eosin, original magnification: ?100.

before tumor ablation. Some of these drugs cause specific toxic effects in the liver as steatosis and steatohepatis, hyperbilirubinaemia and vascular changes, sinusoidal obstruction or dilatation syndrome. Patients received in particular irinotecan (n = 8), fluorouracil (n = 15), capecitabine (n = 2), oxaliplatin (n = 5), epirubicine (n = 1) and gemcitabine (n = 1) before intervention. In between the interventions and during postinterventional surveillance 7 patients received again irinotecan, 5 patients received fluorouracil and oxaliplatine respectively, capecitabine (n = 3), avastine (n = 2) and UFT (n = 1).

Treatment was carried out consecutively without selection or randomisation. There was a minimum interval of 4 weeks and a maximum of 14 months between sequential applications (table 1). The decision to treat or re-treat any lesion was taken individually following oncological considerations.

Only patients who underwent more than one application of CT-guided HDR-brachytherapy with intersecting dose distributions were included. Normal liver function based on laboratory parameters as well as clinical examination was acquired before CT-guided brachytherapy.

We excluded patients with any clinical or laboratory sign of liver function degradation before therapy.

Interventional technique and irradiation

The technique of CT-guided brachytherapy has been described in detail elsewhere [22]. Positioning of the brachytherapy applicators was performed with a fluoroscopy CT (Siemens, Erlangen, Germany). After catheter placement a spiral CT of the liver (slice thickness: 5 mm, increment: 5 mm), enhanced by i.v. application of iodide contrast media (100 mL Ultravist 370, flow: 1 mL/s; start delay: 80s), was acquired using the breath-hold technique for treatment planning purposes.

The HDR afterloading system (GammaMed, Varian, Charlottesville,VA) used a ^{192}Iridium source of 10Ci. The source diameter was <1 mm and dwell positions were located every 5 mm. Dwell times were corrected automatically according to the actual source strength.

Treatment planning and dosimetry analysis

Treatment planning employed BrachyVision (Varian Medical Systems, Palo Alto, CA). A radiation oncologist and radiologist jointly performed the planning process, i.e. delineation of the clinical target volume CTV (gross tumor volume GTV plus safety margin of a few mm) according to clinical considerations. The prescribed dose to enclose the CTV ranged from 15 to 25 Gy (mean 20 Gy, average 18.27 Gy) (table 1). In organs at risk (intestine, stomach) $D_{1\ ml}$ was prescribed to be < 15 Gy. The volume dose to the liver ($D_{15\ Gy}$, $D_{10\ Gy}$, $D_{7\ Gy}$) was kept as small as reasonable.

All applications were performed as a single dose employment.

Follow-Up

MRI examinations were performed in 20 patients 1 day before, 3 days, 6 weeks and following every 12 weeks after irradiation. The MRI protocol was comprised of the following sequences: T2-w breathing-triggered UTSE (TE/TR 90/2,100 ms), T1-w breath-hold gradient echo (GRE) (TE/TR 5/30 ms, flip angle 30°) precontrast, 20 s and 2 h post i.v. application of 15 mL Gd-BOPTA (Multihance; Bracco, Princeton, NJ). The slice thickness was 8 mm, acquired in interleafed mode with no gap applied.

At the same control dates we also assessed the following laboratory parameters: bilirubin, aspartate aminotransferase, alanine aminotransferase, alkaline phosphatase, albumin, ammonia and C-reactive protein to assess treatment-related toxicity using Radiation Therapy Oncology Group (RTOG) toxicity score.

Image registration

All 3D-dosimetry data calculated by BrachyVision during all CT-guided brachytherapies were merged with the last MRI-data set which had been acquired during a period of ≤12 months after the last intervention. All data were processed by anisoscalar image registration (Figure. 1, 2). By reducing the images to contain liver parenchyma and a small surrounding margin (approx. 1 cm), anisotropic image fusion was sufficient to achieve accuracy better than 5 mm for the liver surface and prominent anatomic structures (e.g. large vessels) [14].

The registration routine of the algorithm was based on normalized mutual information and has been described by Studholme et al. [23]. We employed a modified inde-

Table 1: The extent of the irradiation effects ("cumulative pseudolesion" in cm³) and calculated D_{90} (for α/β = 2 Gy) with respect to the minimal prescribed dose inside of the clinical target volume (CTV) in the different irradiation sessions.

Pat.	$D_{90\ (2\ Gy)}$	Cum. Pseudo-lesion Volume (cm³)	Fractions (n)	Interval between inter-ventions (months)	Interval between first irradiation & last MRI (months)	Interval between last irradiation & last MRI (months)	Minimal prescribed dose inside CTV (Gy)	Liver Volume (cm³)
1	18.80	289	3	3/3	17	11	20/20/20	1960
2	16.20	327	2	7	14	7	25/15	2184
3	35.20	135	4	7/1/8	31	3	15/20/20/20	1123
4	25.30	172	3	4/3	18	11	20/20/15	1548
5	17.20	710	2	12	5	4	15/15	2077
6	25.15	381	2	13	13	12	15/20	1357
7	16.40	239	2	7	18	11	25/15	1847
8	14.35	803	2	6	13	7	15/20	1463
9	31.90	92	4	4/4/8	24	7	15/15/20/20	1424
10	23.65	425	2	14	18	4	20/15	2054
11	28.35	178	2	5	10	4	15/20	1662
12	21.64	668	3	4/6	16	6	20/15/20	2165
13	21.70	207	2	10	12	3	15/15	1439
14	15.90	529	3	1/5	9	4	15/15/15	1441
15	16.30	238	2	11	14	3	20/15	2025

Table 1: The extent of the irradiation effects ("cumulative pseudolesion" in cm^3) and calculated D_{90} (for $\alpha/\beta = 2$ Gy) with respect to the minimal prescribed dose inside of the clinical target volume (CTV) in the different irradiation sessions. (Continued)

16	21.75	244	3	1/7	10	3	20/20/15	1604
17	33.20	476	4	1/10/1	19	9	25/15/25/25	1951
18	20.55	227	2	1	5	4	20/20	1387
19	14.90	319	2	11	10	8	15/15	1428
20	29.60	75	2	9	12	3	20/20	1246
Mean	22.40	336.7	3	5	14	6	20	1669.16

The different time intervals between the interventions and the different time intervals between the interventions and acquisition of MRI examinations are shown.

pendent implementation of this algorithm within the 3D visualization software Amira version 3.1 (Mercury Computer Systems, Inc, San Diego, USA). The accuracy of the implemented algorithm was verified by Rohlfing et al. [24].

Quantitative analysis

For every patient, we calculated the cumulative biologically equivalent dose BED in every voxel over the whole liver for different α/β-values (2, 3, 10, 20, 100) by the following equation [25]:

$$\sum_k D_k\left(\frac{\alpha}{\beta}+D_k\right)=\left(\frac{\alpha}{\beta}+2\right)D_{tot} \qquad (1)$$

where D_K is the dose per voxel deposited during the intervention k = 1,...,n and D_{tot} is the BED per voxel with respect to conventional fractionation.

Every lesion was the result of repetitive single interventions with different dose distributions. On the T1-w late Gd-BOPTA enhanced images of the last MRI acquired after the last therapy, two experienced GI-radiologists evaluated the fused images of MRI and dose distributions by delineating the border of hypointensity in the irradiated liver area in consensus. In liver regions with no detectable uptake of Gd-BOPTA (hypointensity) we assumed radiation-induced damage of liver tissue [13,14].

Based on the total 3D D_{90}-data set, Amira software calculated the dose-volume histograms for a set of α/β values (2, 3, 10, 20, 100) (Figure 5) to determine the D_{90} (α/β) for every cumulative pseudolesion, i.e. the BED exposing 90% of the pseudolesion in MRI.

Statistical analysis

Standard Pearson correlation coefficients were determined to perform an univariate correlation analysis with following variables used: D_{90} (for α/β = 2), number of interventions, interval between first irradiation and last MRI, interval between last irradiation and last MRI, mean interval between several interventions and volume of the cumulative pseudolesion. Kendall's W-test for related samples was used to test the difference with respect to various α/β-values.

We compared 2 groups of patients with pseudolesion volumes of ≤200 mL (n = 5) or >200 mL (n = 15). The comparison between the $D_{90(2\ Gy)}$ of the two groups was performed by using an unpaired *t*- test.

Analyses were performed using the Statistical Package for the Social Sciences, version 13.0.0 (SPSS for Windows, Chicago, Illinois, USA). A p-value < 0.05 was considered statistically significant.

Results

The volumes of radio-affected liver tissue (pseudolesion) are presented in Table 1 in dependency on the time intervals between the interventions and the time intervals from interventions to MRI examinations. The lesion size overall ranged from 75 cm^3 to 803 cm^3 (median 266.5 cm^3), the whole liver volume ranged from 1123 cm^3 to 2184 cm^3 (median 1576 cm^3). The time interval from the first brachytherapy to the last MRI ranged from 5 to 31 months (median 13.5 months), and from the last brachytherapy to the last MRI from 3 to 12 months (median 5 months), respectively. The MRI-data we used was the latest MRI acquired during a period of median 5 months after the last intervention.

Table 2 shows the calculated D_{90} covering the inactivated liver tissue corresponding to variable α/β values. The mean tolerance doses ranged from 22.40 Gy for α/β = 2 to 23.34 Gy for α/β = 10, and 24.08 Gy for α/β = 20 to 26.17 Gy for α/β = 100, respectively. The differences in the D_{90} were statistically significant, but the differences for clinical relevant α/β-values between 2 and 10 were smaller than 1 Gy (table 2, Figure 5, 6).

The D_{90} (for α/β = 2) and the interval between the first irradiation and the last MRI correlated significantly (p = 0.005) as a result of ongoing repair or regeneration. A correlation was also shown between the D_{90} and the number of interventions, likely as a result of better recovery in case of a smaller number of irradiation treatments (p = 0.004) (table 3). There was a trend for a positive correlation (p = 0.092) between D_{90} and the mean interval between the whole series of several interventions. The time interval between repeated interventions did increase the $D_{90(2\ Gy)}$, indicating that the time available for regeneration influenced the dose tolerance. Conversely, a significant inverse relationship (p = 0,037) between the volume of the pseudolesion and D_{90} was found (table 3).

After definition of three groups with different pseudolesion volumes (1: up to 199 mL (30.1 Gy), 2: 200-399 mL (19.1 Gy) and 3: ≥400 mL (21 Gy)), the Bonferroni-test revealed a significant difference for the $D_{90(2\ Gy)}$ between group 1 and both other groups, while there was no difference between group 2 and 3. However, there was a cut off at 200 mL and the comparison of the two groups regarding patients with different pseudolesion volumes showed a difference between the $D_{90(2\ Gy)}$ (30.1 Gy vs. 19.1 Gy) (p = 0.01) (table 4).

There was no significant correlation with all the other variables tested: a) the interval from last irradiation to MRI did not correlate with the $D_{90(2\ Gy)}$ (p = 0.834); b) the intervals between repeated irradiations and MRI did not correlate with the mean interval between all interven-

Table 2: The D90 for impairment of hepatocyte function ("cumulative pseudolesion") calculated for different α/β-values (2, 3, 10, 20, 100).

D90 (Gy) for impairment of hepatocyte function for different α/β-values					
Patient	**α/β = 2**	**α/β = 3**	**α/β = 10**	**α/β = 20**	**α/β = 100**
1	18.80	19.00	19.99	20.90	23.60
2	16.20	16.40	16.65	17.30	18.80
3	35.20	35.70	36.50	36.90	38.10
4	25.30	25.40	26.20	27.00	29.60
5	17.20	17.30	18.00	18.65	20.45
6	25.15	25.20	25.65	26.15	27.85
7	16.40	16.60	17.50	18.45	20.70
8	14.35	14.45	15.20	15.87	17.55
9	31.90	32.60	33.40	34.00	36.80
10	23.65	23.80	24.75	25.78	28.80
11	28.35	28.40	29.90	30.90	34.70
12	21.64	21.70	22.65	23.48	26.10
13	21.70	21.80	22.45	23.10	25.00
14	15.90	16.10	17.10	17.90	20.10
15	16.30	16.40	16.95	17.70	19.45
16	21.75	21.90	22.10	22.90	25.20
17	33.20	34.10	34.90	35.60	37.10
18	20.55	20.60	20.85	21.35	22.50
19	14.90	15.10	16.00	16.80	19.00
20	29.60	29.90	30.00	30.80	31.90
Mean	22.40	22.62	23.34	24.08	26.17
Stand. deviation	6.47	6.62	6.64	6.61	6.68

tions. Next to that, the number of interventions did not negatively influence hepatocyte function recovery at specific dose levels.

All patients included in this study demonstrated normal liver function parameters before CT-guided brachytherapy. There was no Grade 2 or above hematologic toxicity according RTOG toxicity scale. No patient developed symptoms of acute or late chronic liver dysfunction in between the interventions or during follow up, which could be related to irradiation.

Discussion

The tolerance doses of the entire liver or large portions of the liver to external irradiation have been described previously in the literature. A $TD_{5/5}$ of 30 Gy is given for the whole liver, while one-third to two-third of the liver tolerate higher doses of 35 Gy to 50 Gy, respectively [19,26]. Small volume effects have been described for both stereotactic radiation as well as CT-guided brachytherapy treatments [1,5,14]. Promising results with sustained local control rates have been achieved.

Ricke et al. reported a median survival of 23.4 months after image-guided high dose rate brachytherapy (minimal tumor-enclosing doses of 15 Gy, 20 Gy, or 25 Gy as D100) of seventy-three patients with 199 colorectal liver metastases [5].

Lee et al. showed a median survival of 17.6 months in sixty-eight patients with inoperable liver metastases being treated with individualized stereotactic body radiotherapy (SBRT) with a median SBRT dose of 41.8 Gy in six fractions over two weeks [2]. No RILD or other grade 3 - 5 liver toxicity was seen. Also Rusthoven et al. demonstrated in a multi-institutional trial with forty-seven patients (with one to three liver metastases) that high-dose liver SBRT is safe and effective with a median survival of 20.5 months with only one patient presenting with grade 3 toxicity [6]. Localablative irradiation therapies of liver malignancies are of great value especially for patients who are not suitable for surgical interventions.

In this study we sought to determine threshold doses for hepatic dysfunction as well as toxic effects e.g. after repeated irradiation treatments of liver metastases due to local failure. As a result we found that repeated sessions of high dose rate, single fraction irradiation at very high dose levels targeting identical or intersecting liver volumes were safe.

In our trial we did not observe any acute or long term toxicity despite hepatic dysfunction in areas of high dose accumulation.

One relevant factor for the tolerance to irradiation is the critical single dose α/β in Gy, which describes the sensitivity to the dose per fraction and/or dose rate of a particular tissue, either tumor or organ. The ratio α/β describes the initial form of the curvature of the underlying cell survival curves [27-29]. Small α/β-ratios are associated with a broader shoulder of the dose-response curve indicating a large dependency of the radiation effect on the dose per fraction, while large values of α/β indicate only minor fractionation sensitivity. These individual endpoints for specific tissues were first described in animal studies [30] and have been confirmed by numerous clinical data [29].

In our study we calculated the D_{90} of the pseudolesions for different α/β-values (2, 3, 10, 20 and 100) and did not find clinically relevant differences. The BED (biologically

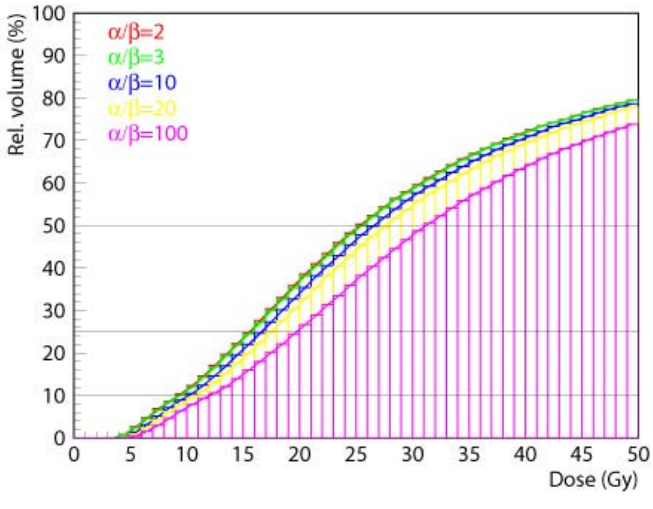

Figure 5 Based on the total 3D-D_{tot}-data set, Amira software calculated dose-volume histograms for all different α/β-values.

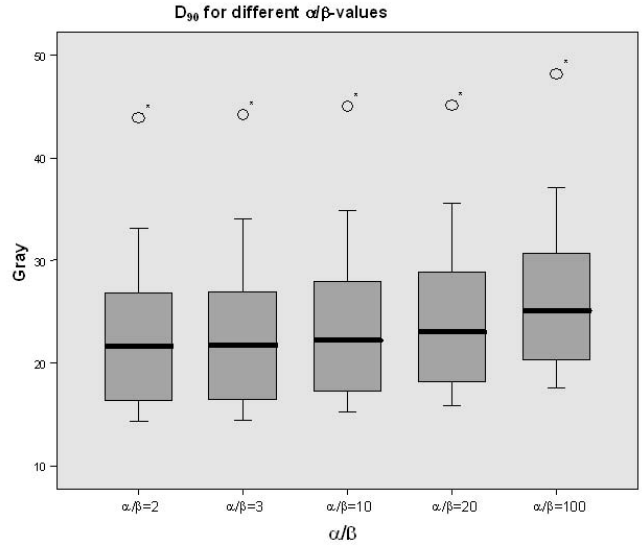

Figure 6 Mean D_{90} for different α/β-values (2, 3, 10, 20, 100) of all patients. Statistically there was a significant difference in the D_{90} results but the differences for clinical α/β-values were less than 1 Gy and therefore of no clinical. The star (*) represents one outlier in the series of calculation.

Table 3: D90 (for α/β = 2) tested against various variables for correlation analysis.

PEARSON CORRELATION	D90 (α/β = 2)
Interventions (n)	p = 0.004
Cumulative Pseudolesion (cm^3)	p = 0.037
Interval: first irradiation - MRT (months)	p = 0.005
Interval: last irradiation - MRT (months)	p = 0.745
Mean interval between several interventions (ΣT/n)	p = 0.092

The D90 (for α/β = 2) correlated significantly positive with the number of interventions and the interval between the first irradiation and the last MRI ($p < 0.05$). There was a significant negative correlation between the D90 (for α/β = 2) and the volume of the cumulative pseudolesion (p = 0,037). There was a trend for a positive correlation (p = 0.092) between the D90 (for α/β = 2) and the mean interval between several interventions (ΣT/n).

equivalent dose) causing injury to 90% of liver parenchyma was approximately 23 Gy (table 2). Obviously, the superposition of dose distributions with large gradients reduces the dependency on α/β.

Time factors (describing repair kinetics) had no or negligible influence in our study since the interval between two applications (between 4 weeks and 14 months, mean 5 months, table 1) was long enough to ensure sufficient repair [31,32]. We additionally propose that the dose rate variability as a result of the distance relative to the catheters had no relevant influence on repair capacity.

However, we observed a trend to a correlation of the D_{90} and the time intervals between the interventions as a result of regeneration or recovery of the irradiated liver tissue. This is in accordance with 2 previous trials performed by our own group, where the greatest volume of function loss after single applications of CT-guided HDR brachytherapy occurred after 6 weeks to 3 months [13,14]. Six months after irradiation, the volume with dysfunctional liver tissue had decreased significantly. We deduced a mean tolerance dose for irreversible damage above a dose level of 15 Gy (D_{90}) applied as a single radiation dose. At a dose exposure between 10 and 15 Gy, hepatic dysfunction proved to be reversible [13]. These results are somewhat contrary to a trial performed by Lawrence et al. who demonstrated just minor recovery of liver cell plates after six months and up to 6 years [19].

Table 4: The comparison between the two groups of different cumulative pseudolesion volumes (≤200 mL; >200 mL) showed a statistically significant difference in the D90 (α/β = 2).

Critical irradiation volume	D90 (α/β = 2)
Cum. Pseudolesion ≤200 mL (n = 5)	30.1 Gy
Cum. Pseudolesion >200 mL (n = 15)	19.1 Gy
t-test	p = 0.01

The statistically significant level was set at p-value ≤ 0.05.

In our present trial, MRI was acquired between 3 and 31 months (median 10 months) after irradiation and we expected liver regeneration in the irradiated areas between 10 - 18 Gy. Nevertheless, we still found a significant dependency between the D_{90} and the time interval from the first irradiation to the last MRI. In addition, we found a trend to a correlation of the D_{90} and the time intervals between the different irradiation sessions (table 3). Therefore, a long-term regeneration potential probably exists. With respect to the clinical endpoint liver failure we wish to add that even after multiple applications of HDR-brachytherapy in adjacent liver areas the (cumulative) volume of radiation injury did never exceed 803 mL (mean 336.7 mL). We therefore never reached a treatment volume critical for the overall liver function, i.e. >60 - 70% of the whole liver volume (mean 1669.16 mL).

On the other hand an inverse correlation between the overexposed (i.e. damaged) volume size and the equivalent tolerance dose (isoeffect-isodose for the impairment of hepatocyte function) was found. A volume threshold was found at 200 mL (table 4). For volumes <200 mL the tolerance dose increased up to 30 Gy. These results are in line with the previously published dose-volume effect of hepatic repair [14]. The tolerance dose of D_{90} (single dose) as determined in a previous study for a single HDR application was ~ 15 Gy [13]. A re-calculation of the BED from 15 Gy (single) for different α/β to conventional fractionation would result in a BED (α/β = 3) of 54 Gy, BED (α/β = 5) of 42 Gy, or BED (α/β = 10) of 31 Gy. In comparison, the tolerated D_{90} (2 Gy) of BED ~ 23 Gy in our study proved to be surprisingly low and suggests in particular that α/β for liver tissue might be higher than 5 Gy. The first (and most important) reason for this contradictory result probably is the small liver volume exposed to a single high dose in the referenced trial [13]. Under these circumstances a higher potential for regeneration might exist. For larger volumes (>200 mL) and repeated HDR applications, the tolerance doses were even below the limits for whole liver irradiation of approximately 30 Gy

as described in the literature. However it has to be mentioned that most of the patients have been treated with potentially hepatotoxic cytotoxics or new biological agents before or between the interventions, which may cause specific toxic effects in the liver and potentially lead to a reduced tolerance of the liver although most adverse reactions are idiosyncratic and are due to individual patient differences in susceptibility to drug-induced liver injury or inability to recover from the injury. Most patients tolerate the agent, or can adapt to it [33]. Clinically one-third or even two-thirds of the liver can be inactivated with no symptomatic liver function degradation. This is not clearly stated in the Emami report in 1991, which established baseline partial liver tolerances [26]. Dawson et al. further adjusted the Lyman model parameters in 2002 and derived the TD5/5 (in 1.5 Gy BID) for 1/3 of the liver volume = 107 Gy (~94 Gy in 2 Gy/fx), for 2/3 = 54 Gy (~48 Gy in 2 Gy/fx). They calculated a 5% risk of RILD for whole liver radiation therapy (3/3) with 32 Gy in 2 Gy/fx [7].

In our study the tolerance doses of liver parenchyma fell in the range of 22 - 24 Gy (conventional fractionation), which is clearly below the data in the literature. This might be a result of chemotherapy pretreatments in almost all our patients. However, even a BED of 22 - 24 Gy as determined in this study implies large clinical potential for irradiation of liver metastases if the hepatic radiation injury is limited to moderate volumes (table 1). Furthermore, we did not find clinically relevant late toxicity in any patient undergoing multiple applications of high-dose-rate brachytherapy. In none of our imaging studies fibrotic changes or considerable hypertrophy of the uninvolved liver was documented. All patients demonstrated normal liver function parameters before and after CT-guided brachytherapy.

Conclusion

We conclude that repeated high dose rate single fraction irradiation of intersecting liver volumes is safe. Very high tumor doses and repeated applications of brachytherapy and potentially stereotactic irradiation are possible for liver metastases treatments without an increased risk of liver failure. In our opinion caution is warranted in whole liver irradiation applying external techniques.

Our data suggests that the tolerance dose in a pretreated liver might not be < 30 Gy using fractions of 2 Gy as stated in the literature but as low as 22 - 24 Gy.

Competing interests

The authors declare that there is no actual or potential conflicts of interest, sources of financial support, corporate involvement, patent holdings, etc. for each author to report.

Authors' contributions

RR participated in the study's design and coordination, performed acquisition of data and the analysis of images, performed the statistical analysis and draft the manuscript. LL participated in the study's design, performed the statistical analysis and helped to draft the manuscript. AC and FS performed acquisition of data and the analysis of images. MS and KM participated in the study's coordination and helped to draft the manuscript. JR and PW conceived of the study, and participated in its design and coordination and helped to draft the manuscript. All authors read and approved the final manuscript.

Author Details

[1]Universitätsklinikum Magdeburg, Klinik für Radiologie und Nuklearmedizin, Otto-von-Guericke-Universität Magdeburg, Germany, [2]Charité Universitätsmedizin Berlin, Campus Virchow-Klinikum, Klinik für Strahlentherapie, Berlin, Germany and [3]Wroclaw Medical University, Department of Neuroradiology, Wroclaw, Poland

Received: 18 March 2010 Accepted: 27 May 2010
Published: 27 May 2010

References

1. Herfarth KK, Debus J, Lohr F, Bahner ML, Rhein B, Fritz P, *et al.*: **Stereotactic single-dose radiation therapy of liver tumors: results of a phase I/II trial.** *J Clin Oncol* 2001, **19:**164-170.
2. Lee MT, Kim JJ, Dinniwell R, Brierley J, Lockwood G, Wong R, *et al.*: **Phase I study of individualized stereotactic body radiotherapy of liver metastases.** *J Clin Oncol* 2009, **27:**1585-1591.
3. Mohnike K, Wieners G, Schwartz F, Seidensticker M, Pech M, Ruehl R, *et al.*: **Computed Tomography-Guided High-Dose-Rate Brachytherapy in Hepatocellular Carcinoma: Safety, Efficacy, and Effect on Survival.** *Int J Radiat Oncol Biol Phys* 2010.
4. Ricke J, Wust P, Stohlmann A, Beck A, Cho CH, Pech M, *et al.*: **CT-guided interstitial brachytherapy of liver malignancies alone or in combination with thermal ablation: phase I-II results of a novel technique.** *Int J Radiat Oncol Biol Phys* 2004, **58:**1496-1505.
5. Ricke J, Mohnike K, Pech M, Seidensticker M, Ruhl R, Wieners G, *et al.*: **Local Response and Impact on Survival After Local Ablation of Liver Metastases from Colorectal Carcinoma by Computed Tomography-Guided High-Dose-Rate Brachytherapy.** *Int J Radiat Oncol Biol Phys* 2010.
6. Rusthoven KE, Kavanagh BD, Cardenes H, Stieber VW, Burri SH, Feigenberg SJ, *et al.*: **Multi-institutional phase I/II trial of stereotactic body radiation therapy for liver metastases.** *J Clin Oncol* 2009, **27:**1572-1578.
7. Dawson LA, Normolle D, Balter JM, McGinn CJ, Lawrence TS, Ten Haken RK: **Analysis of radiation-induced liver disease using the Lyman NTCP model.** *Int J Radiat Oncol Biol Phys* 2002, **53:**810-821.
8. Ingold JA, Reed GB, Kaplan HS, Bagshaw MA: **Radiation Hepatitis.** *Am J Roentgenol Radium Ther Nucl Med* 1965, **93:**200-208.
9. Wharton JT, Delclos L, Gallager S, Smith JP: **Radiation hepatitis induced by abdominal irradiation with the cobalt 60 moving strip technique.** *Am J Roentgenol Radium Ther Nucl Med* 1973, **117:**73-80.
10. Dawson LA, Ten Haken RK: **Partial volume tolerance of the liver to radiation.** *Semin Radiat Oncol* 2005, **15:**279-283.
11. Robertson JM, Lawrence TS, Dworzanin LM, Andrews JC, Walker S, Kessler ML, *et al.*: **Treatment of primary hepatobiliary cancers with conformal radiation therapy and regional chemotherapy.** *J Clin Oncol* 1993, **11:**1286-1293.
12. Cheng JC, Wu JK, Huang CM, Liu HS, Huang DY, Cheng SH, *et al.*: **Radiation-induced liver disease after three-dimensional conformal radiotherapy for patients with hepatocellular carcinoma: dosimetric analysis and implication.** *Int J Radiat Oncol Biol Phys* 2002, **54:**156-162.
13. Ricke J, Seidensticker M, Ludemann L, Pech M, Wieners G, Hengst S, *et al.*: **In vivo assessment of the tolerance dose of small liver volumes after single-fraction HDR irradiation.** *Int J Radiat Oncol Biol Phys* 2005, **62:**776-784.
14. Wybranski C, Seidensticker M, Mohnike K, Kropf S, Wust P, Ricke J, *et al.*: **In vivo assessment of dose volume and dose gradient effects on the tolerance dose of small liver volumes after single-fraction high-dose-rate 192Ir irradiation.** *Radiat Res* 2009, **172:**598-606.
15. de Haen C, Lorusso V, Luzzani F, Tirone P: **Hepatic transport of the magnetic resonance imaging contrast agent gadobenate dimeglumine in the rat.** *Acad Radiol* 1995, **2:**232-238.
16. Kirchin MA, Pirovano GP, Spinazzi A: **Gadobenate dimeglumine (Gd-BOPTA). An overview.** *Invest Radiol* 1998, **33:**798-809.
17. de Haen C, Gozzini L: **Soluble-type hepatobiliary contrast agents for MR imaging.** *J Magn Reson Imaging* 1993, **3:**179-186.

18. Planchamp C, Gex-Fabry M, Becker CD, Pastor CM: **Model-based analysis of Gd-BOPTA-induced MR signal intensity changes in cirrhotic rat livers.** *Invest Radiol* 2007, **42:**513-521.
19. Lawrence TS, Robertson JM, Anscher MS, Jirtle RL, Ensminger WD, Fajardo LF: **Hepatic toxicity resulting from cancer treatment.** *Int J Radiat Oncol Biol Phys* 1995, **31:**1237-1248.
20. Fajardo LF, Colby TV: **Pathogenesis of veno-occlusive liver disease after radiation.** *Arch Pathol Lab Med* 1980, **104:**584-588.
21. Reed GB Jr, Cox AJ Jr: **The human liver after radiation injury. A form of veno-occlusive disease.** *Am J Pathol* 1966, **48:**597-611.
22. Ricke J, Wust P, Wieners G, Beck A, Cho CH, Seidensticker M, *et al.*: **Liver malignancies: CT-guided interstitial brachytherapy in patients with unfavorable lesions for thermal ablation.** *J Vasc Interv Radiol* 2004, **15:**1279-1286.
23. Studholme C, Hill DL, Hawkes DJ: **Automated three-dimensional registration of magnetic resonance and positron emission tomography brain images by multiresolution optimization of voxel similarity measures.** *Med Phys* 1997, **24:**25-35.
24. Rohlfing T, West JB, Beier J, Liebig T, Taschner CA, Thomale UW: **Registration of functional and anatomical MRI: accuracy assessment and application in navigated neurosurgery.** *Comput Aided Surg* 2000, **5:**414-425.
25. Fowler JF: **The linear-quadratic formula and progress in fractionated radiotherapy.** *Br J Radiol* 1989, **62:**679-694.
26. Emami B, Lyman J, Brown A, Coia L, Goitein M, Munzenrider JE, *et al.*: **Tolerance of normal tissue to therapeutic irradiation.** *Int J Radiat Oncol Biol Phys* 1991, **21:**109-122.
27. Thames HD, Bentzen SM, Turesson I, Overgaard M, Van den BW: **Fractionation parameters for human tissues and tumors.** *Int J Radiat Biol* 1989, **56:**701-710.
28. Thames HD, Hendry JH, Moore JV, Ang KK, Travis EL: **The high steepness of dose-response curves for late-responding normal tissues.** *Radiother Oncol* 1989, **15:**49-53.
29. Thames HD, Bentzen SM, Turesson I, Overgaard M, Van den BW: **Time-dose factors in radiotherapy: a review of the human data.** *Radiother Oncol* 1990, **19:**219-235.
30. Thames HD Jr, Withers HR, Peters LJ, Fletcher GH: **Changes in early and late radiation responses with altered dose fractionation: implications for dose-survival relationships.** *Int J Radiat Oncol Biol Phys* 1982, **8:**219-226.
31. teel GG, Deacon JM, Duchesne GM, Horwich A, Kelland LR, Peacock JH: **The dose-rate effect in human tumour cells.** *Radiother Oncol* 1987, **9:**299-310.
32. Dale RG: **The application of the linear-quadratic dose-effect equation to fractionated and protracted radiotherapy.** *Br J Radiol* 1985, **58:**515-528.
33. Field KM, Dow C, Michael M: **Part I: Liver function in oncology: biochemistry and beyond.** *Lancet Oncol* 2008, **9:**1092-1101.

doi: 10.1186/1748-717X-5-44
Cite this article as: Rühl *et al.*, Radiobiological restrictions and tolerance doses of repeated single-fraction hdr-irradiation of intersecting small liver volumes for recurrent hepatic metastases *Radiation Oncology* 2010, **5**:44

Original Paper

Digestive Diseases

Dig Dis 2009;27:189–199
DOI: 10.1159/000218352

Hepatocellular Carcinoma and Liver Cirrhosis: Assessment of the Liver Function after Yttrium-90 Radioembolization with Resin Microspheres or after CT-Guided High-Dose-Rate Brachytherapy

Ricarda Rühl[a] Max Seidensticker[a] Nils Peters[a] Konrad Mohnike[a]
Jan Bornschein[b] Kerstin Schütte[b] Holger Amthauer[a] Peter Malfertheiner[b]
Maciej Pech[a] Jens Ricke[a]

[a]Klinik für Radiologie und Nuklearmedizin und [b]Klinik für Gastroenterologie, Hepatologie und Infektiologie, Universitätsklinikum Magdeburg AöR, Magdeburg, Germany

Key Words
Yttrium-90 radioembolization · High-dose-rate brachytherapy · Radiation-induced liver disease · Hepatocellular carcinoma

Abstract
Purpose: To identify changes of liver function after single-fraction irradiation or yttrium-90 radioembolization (^{90}Y-RE) of hepatocellular carcinoma associated with liver cirrhosis on the basis of laboratory data. ***Methods and Materials:*** 24 patients with primary liver carcinoma and liver cirrhosis classified Child-Pugh A or B were treated either by image-guided high-dose-rate brachytherapy (HDR-BT) (12 patients) or by ^{90}Y-RE (12 patients). The following laboratory parameters were assessed 1 day before and 3 days, 6 weeks and 3 months after the intervention: total bilirubin and γ-glutamyl transpeptidase (GGTP) as parameters of detoxification function, albumin and cholinesterase (ChE) as direct synthesis parameters, alanine aminotransferase (ALT), aspartate aminotransferase (AST) and alkaline phosphatase (AP) as indicators of liver tissue damage. Preinterventional values were taken as baseline, following values were calculated as percentage changes from the baseline value. Statistical analysis was performed using the Wilcoxon-matched pairs test, comparing postinterventional with preinterventional values. Differences were considered statistically significant with a p value <0.05. ***Results:*** In all patients the median bilirubin, ALT, AP and albumin values remained within normal limits at any time of follow-up. AST levels in the RE group and GGTP in both groups have been already elevated over a normal range before the intervention, and in both groups both parameters showed a slight increase after interventions. ChE activity was lowered already in the baseline values and showed a further decrease 3 days after BT as well as 3 days and 6 weeks after RE, with final reconstitution to baseline values. All liver function test parameters showed mild changes shortly after radiation therapy but floating laboratory values recovering within 12 weeks to baseline values. Radiation or RE-induced liver disease was recorded in no patient. ***Conclusions:*** Liver function parameters show only mild changes shortly after intervention with recovery within 6–12 weeks to baseline values.

Introduction

Hepatocellular carcinoma (HCC) is the most common primary neoplasm of the liver. It is the sixth most common malignancy worldwide and the third most frequent

KARGER

Fax +41 61 306 12 34
E-Mail karger@karger.ch
www.karger.com

0257–2753/09/0272–0189$26.00/0

Accessible online at:
www.karger.com/ddi

Ricarda Rühl, MD
Klinik für Radiologie und Nuklearmedizin, Universitätsklinikum Magdeburg AöR
Leipzigerstrasse 44, DE–39120 Magdeburg (Germany)
Tel. +49 391 671 3030
E-Mail Ricarda.ruehl@med.ovgu.de

cause of cancer-related death in the world [1, 2]. Image-guided tumor ablation such as transarterial chemoembolization (TACE), radiofrequency ablation (RFA), CT- or MR-guided brachytherapy (BT) and RE with yttrium-90 (^{90}Y-RE) have proven not only as palliative therapeutic options, but also to bridge patients to liver transplantation in limited disease [3–6].

The majority of microtherapeutic procedures are performed by applying thermal ablation, either by radiofrequency or laser. Thermoablation of liver malignancies yields good therapeutic results [4, 7, 8]; nevertheless, thermoablative techniques are limited to a maximum tumor size of <4–5 cm and are sensitive to cooling effects of hyperperfused tumors or large neighboring vessels. In addition, they may not be used in lesions close to the liver hilum [7–9].

Novel approaches combining BT with modern interventional techniques have overcome these limitations [10–13]. The use of conformal radiotherapy (RT) and the follow-up of patients for radiation liver toxicities have led to a quantitative understanding of partial liver RT tolerance. The most common adverse event is radiation-induced liver disease (RILD), a syndrome of anicteric ascites, hepatomegaly and impaired liver function tests characterized by either elevation of alkaline phosphatase level (in the range of 3–10 times above normal) and elevation of transaminases in the range of twofold above upper limit of the normal or pretreatment level [14]. Sangro et al. [15] described the development of REILD (radioembolization-induced liver disease) in 20% of patients undergoing ^{90}Y-RE, characterized by jaundice and ascites as a form of sinusoidal obstruction syndrome. With better knowledge of the partial liver tolerance, safer dose escalation and an individualized therapeutic approach, RT could possibly be applied to more patients with liver cancer and other liver malignancies.

In this article we report on changes of liver function after ^{90}Y-RE and high-dose-rate BT (HDR-BT) of HCC based on laboratory data of a 3-month follow-up.

Patients and Methods

Patient Cohort

24 patients with unresectable HCC receiving RT were included in this retrospective study. 12 patients were scheduled to receive HDR single-fraction BT (Group BT), 12 patients underwent ^{90}Y-RE (Group RE). The patient population in the BT group was comprised of 11 men and 1 woman with a mean age of 69 (54–81) years, in the RE group of 10 men and 2 women, the mean age was 68 (44–80) years.

None of the patients presented with prognostic relevant extrahepatic tumor spread at preinterventional staging. All patients demonstrated a Karnofsky performance index >70%. All patients were further diagnosed with liver cirrhosis, presenting a Child-Pugh class A in all patients, except in 3 patients of the BT group classified as Child-Pugh B at enrollment. Patients who developed hepatic tumor progression associated with elevation of liver function parameters and/or ascites or those who were deficient at follow-up (≥1 missing value) were not eligible for this analysis. Written informed consent was obtained from all subjects.

Preinterventional Therapy

Four out of 12 patients (33%) in the BT group and 6 out of 12 patients (50%) in the RE group had undergone previous therapies before hepatic RT. Details are displayed in tables 1 and 2. All previous therapies had been terminated at least 3 months before intervention.

Preinterventional Evaluation

All patients underwent pretreatment assessment that consisted of the clinical history, appropriate laboratory workup (complete blood count, liver function tests, creatinine, serum albumin and prothrombin activity) and imaging studies (CT, MRI). All patients were classified according to the Child-Pugh classification system [16].

Indications for image-guided BT or ^{90}Y-RE were based on the consensus of a multidisciplinary team. In the cohort of patients presented herein, we chose BT for patients with <4 tumors irrespective of the individual size. RE was chosen in patients with (a) >4 nodules or (b) if lesions were not clearly demarcated in CT. Patients should present with preserved liver function including bilirubin <30 μmol/l (1.75 mg/dl). The total liver volume, the tumor volume and the irradiated liver volume (only for patients undergoing image-guided BT) were determined by volumetry before therapy.

^{90}Y-RE

All patients underwent mapping angiography before treatment to determine vascular anatomy and to detect possible arterial variants [17]. Prophylactic embolization of non-targeted vessels was performed in order to prevent irradiation of extrahepatic organs. A scintigraphy using macroaggregates of technetium-99m labeled human serum albumin was performed to assess the lung shunt fraction, any possible splanchnic shunting and the relative distribution of radioactivity between tumor manifestation and non-tumoral liver tissue. RE was performed by delivering ^{90}Y-labeled resin microspheres by catheterization of the liver artery supplying the tumor (SIR-Spheres®, Sirtex Medical Europe, Bonn, Germany). ^{90}Y is a pure β-emitter with a half-life of 64 h. The resin microspheres range from 20 to 40 μm in diameter. The dose applied to the target site was calculated applying the following equation:

$$\text{Dose (Bq)} = [\text{body surface area (m}^2) - 0.2 + \text{tumor volume (\%)}]/100$$

Applied doses ranged from 0.8 to 1.95 GBq (median 1.43 GBq) (whole liver dose). The technical details of RE of liver tumors have been described elsewhere [18]. In our institution, RE is performed in a sequential lobar approach to preserve liver function usually within an interval of 4–8 weeks between both interventions. In 11 out of 12 patients (91%) the interval between RE of the first liver lobe and RE of the second liver lobe was between 4

Table 1. Disease and therapy characteristics of patients undergoing HDR-BT

Patient	Gender	Age years	Interventions before BT	Child-Pugh status	Irradiated 5-Gy volume % of whole liver	Total liver volume, ml	Clinical target volume, ml	Irradiated 5-Gy volume, ml	Applied dose, Gy
1	f	65	–	A	3	1,730	5.1	53.2	15.00
2	m	75	Partial hepatectomy, 3 × PEI, RFA	A	18	1,132	72.5	208	15.00
3	m	71	–	A	9	2,142	14.37	194	15.00
4	m	75	–	A	14	1,666	76	227	15.00
5	m	62	–	B	13	2,200	18.2	296	15.00
6	m	81	–	A	20	708	2.05	141	15.00
7	m	72	Intraoperative RFA	A	18	2,100	56.4	370	15.00
8	m	64	–	A	10	1,745	6.58	171	15.00
9	m	70	4 × TACE	A	9	1,830	14.8	158	15.00
10	m	66	–	A	5	2,268	13.7	123	15.00
11	m	74	–	B	4	1,327	3.11	53.9	15.00
12	m	55	3 × TACE, BT	B	3	1,070	3.15	27.6	15.00

Table 2. Disease and therapy characteristics of patients undergoing ^{90}Y-RE

Patient	Gender	Age years	Interventions before RE	Child-Pugh status	Tumor volume % of whole liver	Total liver volume, ml	Therapeutic approach	Interval between REs weeks	Dose delivered GBq
1	m	56	Syst. CTX doxorubicin	A	20	1,742	sequential lobar	6	1.60
2	m	69	–	A	40	2,525	sequential lobar	8	1.25
3	m	74	–	A	40	2,720	sequential lobar	6	1.40
4	m	68	–	A	20	2,091	sequential lobar	6	1.55
5	f	64	2 × TACE	A	20	2,155	sequential lobar	6	1.00
6	m	73	Partial hepatectomy	A	25	2,023	sequential lobar	9	1.65
7	m	60	–	A	15	1,851	sequential lobar	5	1.95
8	m	67	Partial hepatectomy, sorafenib	A	30	2,055	sequential lobar	4	1.70
9	m	71	–	A	12	1,718	sequential lobar	5	1.80
10	f	67	–	A	60	3,322	unilobar	0	1.20
11	m	80	Partial hepatectomy	A	10	1,562	sequential lobar	8	0.80
12	m	44	6 × TACE	A	25	2,886	sequential lobar	6	1.24

and 9 weeks (median 6 weeks). In 1 case only the right liver lobe was treated since there was no tumor manifestation in the left liver lobe.

Image-Guided BT

The technique of CT-guided BT has been described elsewhere [10]. The placement of the BT applicators was performed with a fluoroscopy CT (Aquilion 16, Toshiba Medical Systems, Tokyo, Japan) or open high-field MRI (Panorama HFO MRI, Philips, Best, The Netherlands). For treatment planning purposes, a spiral CT of the liver (slice thickness 5 mm, increment 5 mm), enhanced by intravenous application of iodide contrast media (100 ml Ultravist 300; flow 1 ml/s, start delay 80 s) was acquired in breath-hold technique after positioning of BT catheters in the tumor.

The HDR afterloading system MicroSelectron V3 (Nucletron, Veenendaal, The Netherlands) employed an iridium-192 source of 10 Ci. The source diameter was <1 mm. Dwell positions were located every 2.5 mm.

Treatment planning was performed using Oncentra Masterplan (Nucletron, Veenendaal, The Netherlands). The radiation therapist and radiologist jointly performed the treatment planning, i.e. delineation of the clinical target volume (gross tumor volume + safety margin of five millimeters) according to clinical considerations. A reference dose of 15 Gy, which was aimed to enclose the lesion (clinical target volume), was prescribed in our patients and applied as a single dose. To preserve liver function, we prescribed a dose of <5 Gy to one-third of the liver parenchyma. The irradiation time was typically 20–60 min.

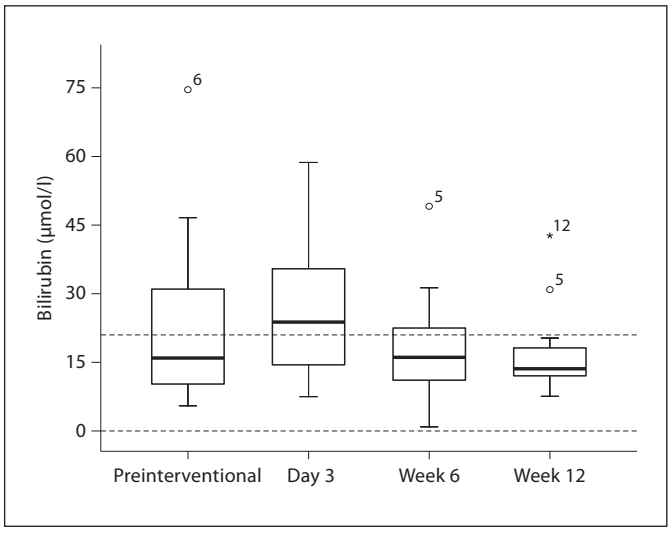

Fig. 1. Bilirubin values 1 day before, 3 days, 6 weeks and 3 months after image-guided BT (standard values between dashed lines).

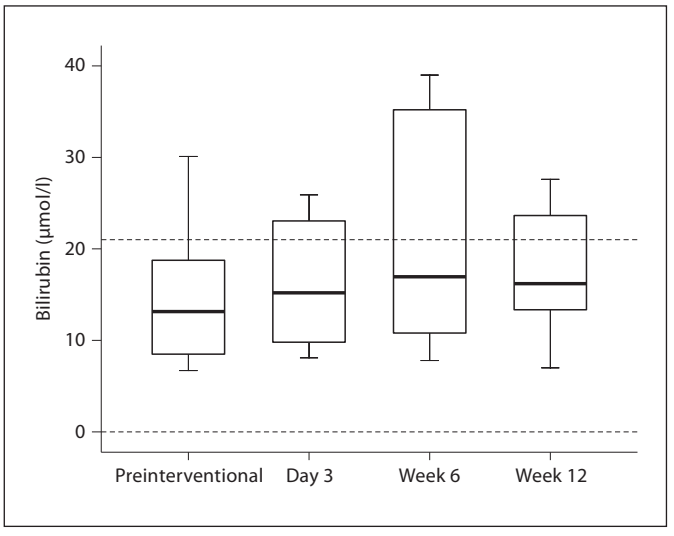

Fig. 2. Bilirubin values 1 day before, 3 days, 6 weeks and 3 months after ^{90}Y-RE (standard values between dashed lines).

Follow-Up

Follow-up schedules after treatment included physical examination, blood tests and MRI of the liver at 3 days, 6 and 12 weeks after intervention. Blood tests comprised total bilirubin and γ-glutamyl transpeptidase (GGTP) as parameters of detoxification function, albumin and cholinesterase (ChE) as direct synthesis parameter (all values in median), alanine aminotransferase (ALT), aspartate aminotransferase (AST) and alkaline phosphatase (AP) as indicators of liver tissue damage.

Statistical Analysis

Preinterventional values were taken as baseline and the follow-up values were calculated as percentage changes from baseline. We used the Wilcoxon-matched pairs test to compare postinterventional with preinterventional values. Differences were considered statistically significant with a p value <0.05.

Results

Characteristics of the Study Population

24 patients with irresectable HCC were included in this study. In the BT group, liver volume was 708 to 2,268 cm^3 (mean 1,565 cm^3). The clinical target volume (gross tumor volume + safety margin of 5 mm) ranged from 3.1 to 72.5 cm^3 (mean 21 cm^3). The irradiated liver volume (without tumor) exposed to >5 Gy ranged from 27 to 370 cm^3 (2.6–20.3%; mean 168 cm^3, 11%). In the RE group, the total liver volume ranged from 1,562 to 3,322 cm^3 (mean 2,221 cm^3). The percentage of tumor volume in the RE group ranged from 10 to 40% (mean 26%). An exact dosimetry including the normal liver parenchyma exposed to >5 Gy cannot be estimated in RE patients.

Indirect Bilirubin (Normal Value <17 µmol/l)

In all patients the median bilirubin values were within normal limits at baseline. Serum levels increased 3 days after the interventions in both groups, descending again to the initial values during further follow-up (fig. 1, 2).

Patients with HDR-BT

The preinterventional values for total bilirubin were 15.95 µmol/l (range 5.5–46.6). Values on day 3 after the procedure increased to 23.80 µmol/l (range 7.5–58.7), slightly exceeding the standard value before decreasing to 16.10 µmol/l (range 9.3–136.1) 6 weeks after the procedure and to 13.60 µmol/l (range 7.6–42.7) 3 months after the intervention. Statistically significant differences were observed between preinterventional and 3-day follow-up values ($p < 0.05$) as well as between the 3-day and 12-week follow-up values ($p < 0.05$). The changes in percentage based upon the preinterventional values were on day 3 +49.21%, after 6 weeks +0.94%, and after 3 months –14.73%. One patient was lost to follow-up after 3 months.

Patients with ^{90}Y-RE

The median preinterventional values for total bilirubin were 13.15 µmol/l (range 6.7–30.1). Median values on day

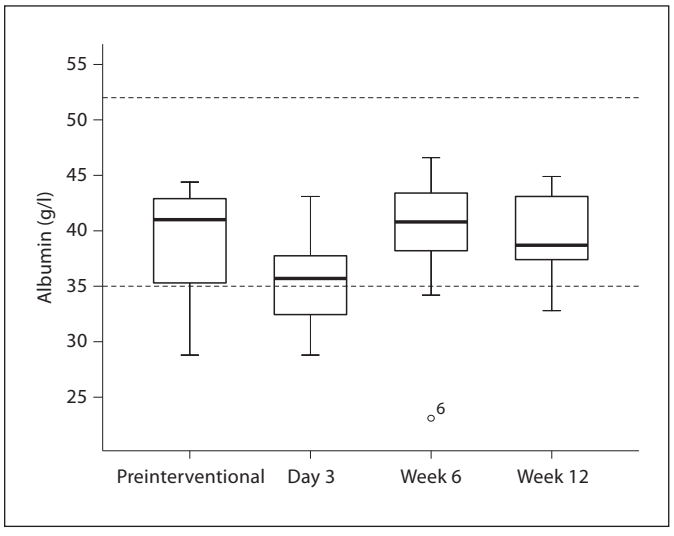

Fig. 3. Albumin values 1 day before, 3 days, 6 weeks and 3 months after image-guided BT (standard values between dashed lines).

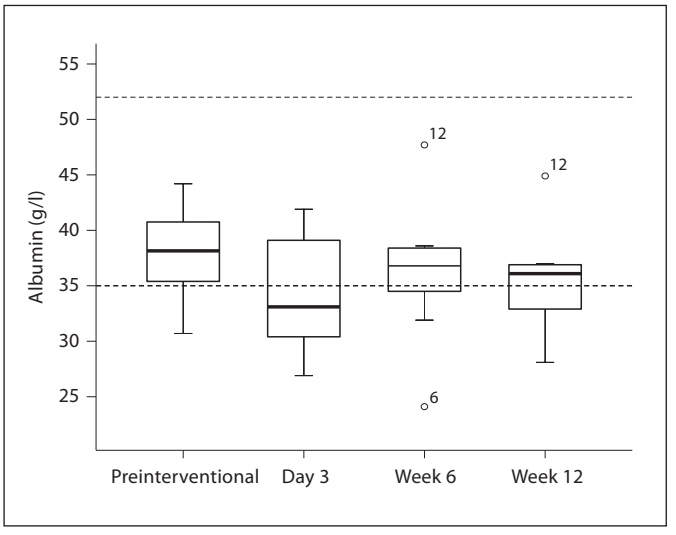

Fig. 4. Albumin values 1 day before, 3 days, 6 weeks and 3 months after ^{90}Y-RE (standard values between dashed lines).

3 after the procedure were 15.20 μmol/l (range 8.1–25.9), 6 weeks after the procedure 16.95 μmol/l (range 7.8–25.6), and 3 months after the intervention 16.20 μmol/l (range 7.0–27.6), slightly increasing over time but within the limits of standard values. The changes in percentage based upon the preinterventional values were on day 3 +15.58%, after 6 weeks +28.89%, and after 3 months +23.19%. Two patients were lost to follow-up after 6 weeks and 4 patients were lost to follow-up after 3 months.

Albumin (Normal Value 35–52 g/l)

The median albumin values in both groups declined considerably 3 days after the interventions indicating decreased liver function but recovered in the next follow-up examinations. All data except the 3-day control after RE were within the normal limits (fig. 3, 4).

Patients with HDR-BT

Preinterventional albumin values were within normal limits (28.8–44.4 g/l, median 41.0 g/l). On day 3 after the procedure, mean albumin decreased significantly to 35.7 g/l (range 28.8–43.1) ($p < 0.05$). After 6 weeks the results were 40.8 g/l (range 23.1–46.6) with a significant increase compared to the 3-day values ($p < 0.05$), and after 3 months 38.7 g/l (range 32.8–44.9). The changes in percentage based upon the preinterventional values on day 3 were –12.92%, after 6 weeks +0.48%, and after 3 months –5.60%. One patient was lost to follow-up after 3 days, after 6 weeks, and after 3 months, respectively.

Patients with ^{90}Y-RE

The preinterventional values for albumin were 38.1 g/l (range 30.7–44.2). Values on day 3 after the procedure decreased to 33.1 g/l (range 26.9–41.9) ($p < 0.05$). Six weeks after the procedure values increased again to 36.80 g/l (range 24.1–47.7). Three months after the intervention mean albumin was 36.1 g/l (range 28.1–44.9) with statistically significant differences between preinterventional and day-3 values, between preinterventional and week-6 values and between preinterventional and week-12 values ($p < 0.05$). Except for data at 3 days after RE, all values were within the normal limits, although 2 patients were lost to follow-up after 6 weeks and 4 patients were lost to follow-up after 3 months. The changes in percentage based upon the preinterventional values were on day 3 –13.23%, after 6 weeks –3.53%, and after 3 months –5.37%.

ChE/Pseudo-ChE (Normal Value 88–215 μmol/s·l)

The level of serum ChE (also termed pseudo-ChE) activity follows the pattern of protein metabolism, falling in catabolism and rising in anabolism. In hepatocellular disease ChE activity is typically lowered as shown in the baseline values of all our patients. Three days after the BT as well as 3 days and furthermore 6 weeks after RE, ChE values decreased further, but finally increased to the initial values in both groups (fig. 5, 6).

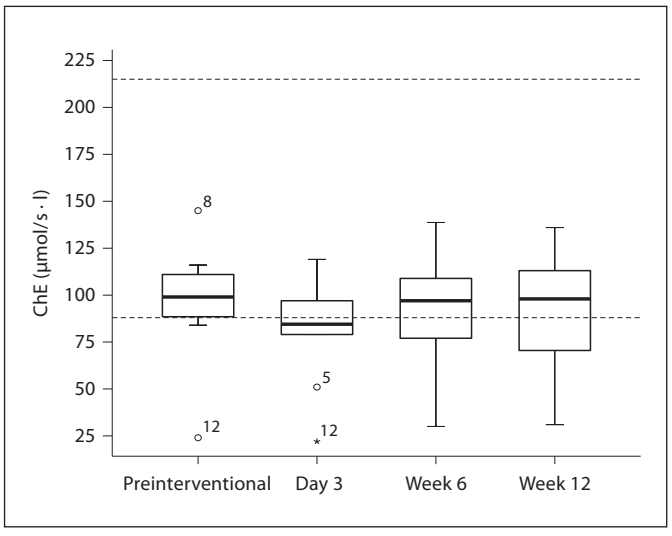

Fig. 5. ChE values 1 day before, 3 days, 6 weeks and 3 months after image-guided BT (standard values between dashed lines).

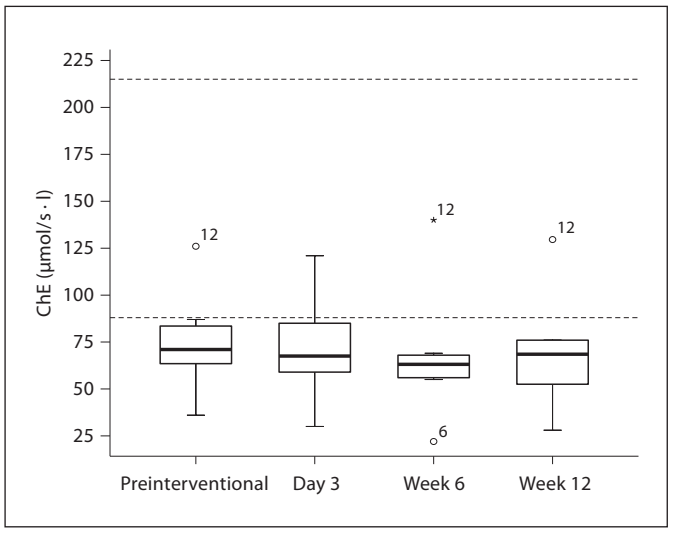

Fig. 6. ChE values 1 day before, 3 days, 6 weeks and 3 months after ^{90}Y-RE (standard values between dashed lines).

Patients with HDR-BT

The ChE values before the intervention were 99.0 µmol/s·l (range 24–145) being in the normal laboratory limits. Three days after the intervention, ChE decreased to 84.5 µmol/s·l, ranging from 22 to 119 µmol/s·l ($p < 0.05$). Six weeks and 3 months after the procedure the median ChE values increased to 97.0 µmol/s·l (range 34–138.7; $p < 0.05$) and 98.0 µmol/s·l (range 31–136) after the HDR-BT according to the baseline values. Two patients were lost to follow-up after 3 days, 1 patient after 6 weeks and as well as after 3 months. Calculated percentage changes of ChE based upon the preinterventional ChE values showed on day 3 after the procedure a decrease of –14.64%. Six weeks and 3 months after the intervention, ChE changed –2.02 and –1.01%, respectively.

Patients with ^{90}Y-RE

The preinterventional values for ChE in the group of patients undergoing RE were 71.0 µmol/s·l (range 36–126). Values on day 3 after the procedure were 67.5 µmol/s·l (range 30–121; $p < 0.05$), 6 weeks after the procedure 63.1 µmol/s·l (range 22–140), and 3 months after the intervention 68.50 µmol/s·l (range 28–130). For all tests, ChE was below the standard value but did not intelligibly deviate from the baseline data as shown in the changes in percentage based upon the preinterventional values: on day 3 –4.92%, after 6 weeks –11.10%, and after 3 months –3.52%. Two patients were lost to follow-up af-ter 6 weeks and 4 patients were lost to follow-up after 3 months.

ALT (Normal Value 0.17–0.83 µmol/s·l)

ALT is often increased in conditions in which hepatocytes are damaged or undergo apoptosis. The level of ALT may correlate roughly with the degree of cell death or inflammation. However, in our analysis the ALT level just increased 3 days after HDR-BT and decreased again to the baseline value after 6 weeks and 3 months. The median was within the standard values (0.17–0.83 µmol/s·l) during the whole time of observation, in the group of patients undergoing BT as well as in the group of patients undergoing ^{90}Y-RE. In the group of patients undergoing ^{90}Y-RE, ALT values did not change significantly over the whole time of observation (fig. 7, 8).

Patients with HDR-BT

The preinterventional values for ALT were 0.56 µmol/s·l (range 0.37–0.84), being in the normal laboratory limits for ALT. Median values 3 days and 6 weeks after the procedure were 0.74 µmol/s·l (range 0.37–1.07) and 0.59 (range 0.27–1.11) and after 3 months 0.5 µmol/s·l (range 0.25–1.02). Data did not exceed the limits of standard values at any point of time of follow-up and the changes in percentage based upon the preinterventional values were on day 3 +33.33%, after 6 weeks +5.4%, and after 3 months –9.9%. Statistically significant differences existed between preinterventional values and values after 3 days ($p < 0.05$) and between day-3 values and 3 months ($p < 0.05$). One patient was lost to follow-up after 3 days and 1 patient was lost to follow-up after 3 months.

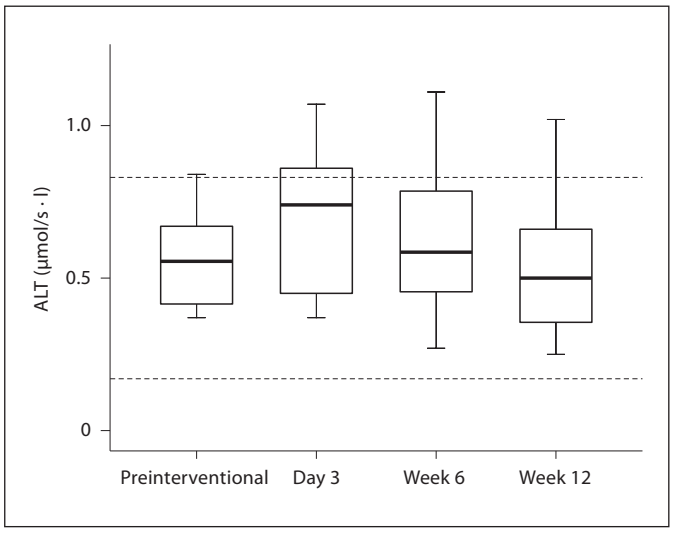

Fig. 7. ALT values 1 day before, 3 days, 6 weeks and 3 months after image-guided BT (standard values between dashed lines).

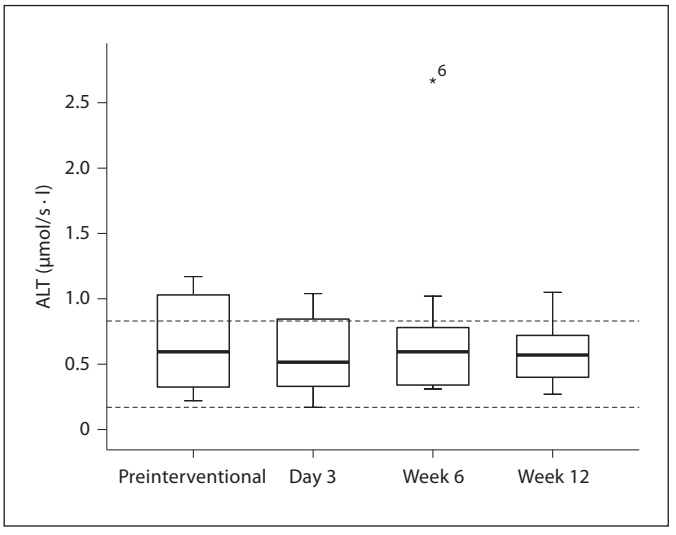

Fig. 8. ALT values 1 day before, 3 days, 6 weeks and 3 months after ^{90}Y-RE (standard values between dashed lines).

Patients with ^{90}Y-RE

The preinterventional median values for ALT within the group of patients undergoing ^{90}Y-RE were 0.6 µmol/s·l (range 0.3–13.69). Values on day 3 after the procedure were 0.52 µmol/s·l (range 0.28–13.22), 6 weeks after the procedure again 0.6 µmol/s·l (range 0.31–2.67), and 3 months after the intervention 0.57 µmol/s·l (range 0.27–1.05), all within the limits of standard values. Statistically significant differences existed between preinterventional values and values after 3 days ($p < 0.05$). The changes in percentage based upon the preinterventional values were on day 3 –13.44%, after 6 weeks without any changes, and after 3 months –4.20%. One patient was lost to follow-up after 6 weeks and 6 patients were lost to follow-up after 3 months.

AST (Normal Value 0.17–0.83 µmol/s·l)

In many cases of liver inflammation, the AST and ALT activities are elevated roughly in a 1:1 ratio. In some conditions, such as alcoholic hepatitis or shock liver, the elevation in the serum AST level may be higher than the elevation in the serum ALT level, as also shown in our analysis where AST levels slightly increase after intervention in both groups over the whole time whereas the AST level in the RE group has been already elevated over a normal range before the intervention. In that group the maximum ascent occurred at week 12 after RE with a 22% gain compared to the baseline data (fig. 10).

Patients with HDR-BT

The median value for AST before the procedure was 0.74 µmol/s·l (range 0.41–2.21). On day 3 after the intervention the AST rose to 0.81 µmol/s·l (range 0.36–2.16). After 6 weeks AST was 0.87 µmol/s·l (range 0.25–1.19), and after 3 months 0.90 µmol/s·l (range 0.46–2.24), only slightly exceeding the standard values (0.17–0.83 µmol/s·l) without statistically significant differences (fig. 9). Percentage changes with preinterventional AST as baseline were on day 3 +9.45%, after 6 weeks +16.89%, and after 3 months +21.62%. One patient was lost to follow-up after 3 days, 2 patients after 6 weeks, and 1 patient after 3 months.

Patients with ^{90}Y-RE

The median AST value within the group of patients undergoing ^{90}Y-RE was 0.91 µmol/s·l (range 0.56–5.17) before the intervention. Three days after the intervention, AST decreased to 0.86 µmol/s·l, ranging from 0.52 to 4.37 µmol/s·l. Six weeks and 3 months after the procedure the AST value increased to 0.96 µmol/s·l (range 0.57–3.99) and to 1.17 µmol/s·l (range 0.85–1.86), respectively. Only the values obtained 3 days and 12 weeks after RE show statistically significant differences ($p < 0.05$). Two patients were lost to follow-up after 6 weeks and 4 patients after 3 months. Calculated percentage change of AST based upon the preinterventional AST values on day 3 after the procedure was –4.97%. Six weeks and 3 months after the intervention, AST changed –6.07 and –28.72%, respectively.

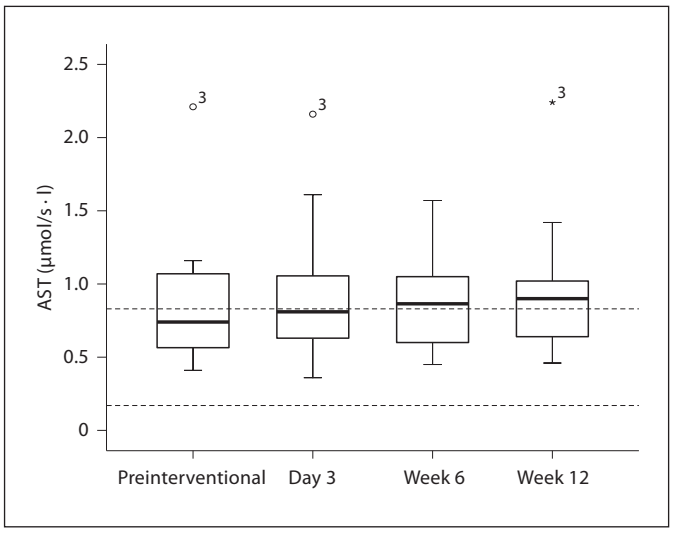

Fig. 9. AST values 1 day before, 3 days, 6 weeks and 3 months after image-guided BT (standard values between dashed lines).

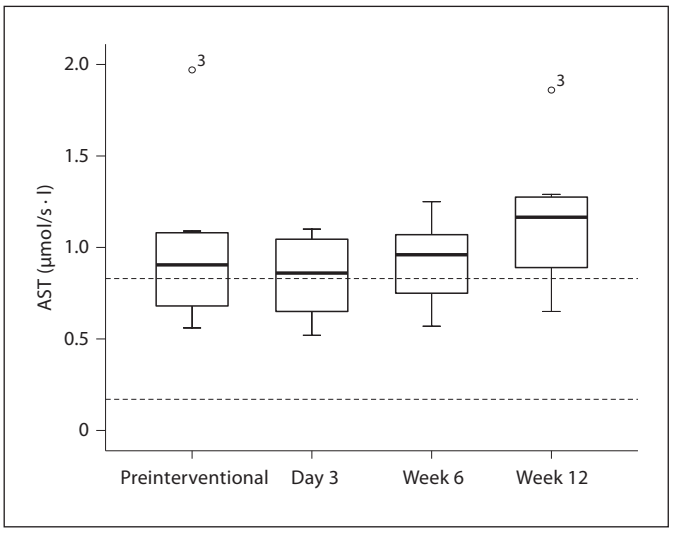

Fig. 10. AST values 1 day before, 3 days, 6 weeks and 3 months after ^{90}Y-RE (standard values between dashed lines).

AP (Normal Value 0.67–2.15 µmol/s·l)

AP is an enzyme, or more precisely a family of related enzymes, produced amongst others in the bile ducts. In the RE group the median AP level is initially reduced and then increased to the baseline value after 6 and 12 weeks, being in the upper limits of standard values. In the BT group an elevation in the level of serum alkaline is shown 3 days and 6 weeks after the intervention but does not exceed the standard limits (fig. 11, 12).

Patients with HDR-BT

Preinterventional median AP was 1.45 µmol/s·l (range 0.7–2.76); on the third postinterventional day, 6 weeks and 3 months after the intervention AP was 1.70 µmol/s·l (range 0.55–2.46), 1.88 µmol/s·l (range 0.78–5.65), and 1.59 µmol/s·l (range 0.6–3.42). Median data are within the standard values slightly increasing in the short term with changes in percent from baseline values with an increase of 16.89% on day 3, 29.65% after 6 weeks, and 9.65% after 3 months. Statistically significant are only the differences between 3 days and 6 weeks and differences between 3 days and 12 weeks. Two patients were lost to follow-up after 3 days, 1 patient after 6 weeks, and 1 patient after 3 months.

Patients with ^{90}Y-RE

The preinterventional values for AP within the group of patients undergoing ^{90}Y-RE were 2.17 µmol/s·l (range 0.9–4.12). Values on day 3 after the procedure were 1.84 µmol/s·l (range 0.88–3.64), 6 weeks after the procedure 2.23 µmol/s·l (range 0.96–4.56), and 3 months after the intervention 2.19 µmol/s·l (range 1.43–5.53). Two patients were lost to follow-up after 6 weeks and 4 patients were lost to follow-up after 3 months. The changes in percentage based upon the preinterventional values were on day 3 –15.43%, after 6 weeks +2.53%, and after 3 months +0.69%.

GGTP (Normal Value 0.17–1.19 µmol/s·l)

GGTP is an enzyme produced in the bile ducts which was elevated in all patients at all times of follow-up examinations. However, it may be elevated in virtually any liver disease and even sometimes in healthy individuals. GGTP is also induced by many drugs, including alcohol, and its serum activity may be increased in heavy drinkers even in the absence of liver damage or inflammation. Interestingly, GGTP values after RE remained almost unchanged while they continuously increased after HDR-BT (fig. 13, 14).

Patients with HDR-BT

Median GGTP values were elevated at all points of time during the analysis where preinterventionally GGTP was 3.31 µmol/s·l, ranging from 0.98 to 18.75 µmol/s·l. On day 3 after the intervention, GGTP increased to 4.48 µmol/s·l (range 0.8–11.14), 6 weeks and 3 months postinterventionally GGTP was 4.65 µmol/s·l (range 1.36–15.6) and 5.38 µmol/s·l (range 0.82–12.72). One patient was

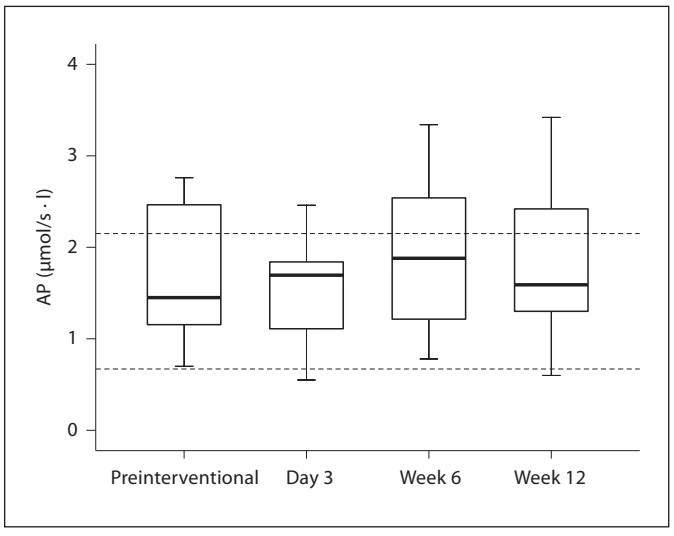

Fig. 11. AP values 1 day before, 3 days, 6 weeks and 3 months after image-guided BT (standard values between dashed lines).

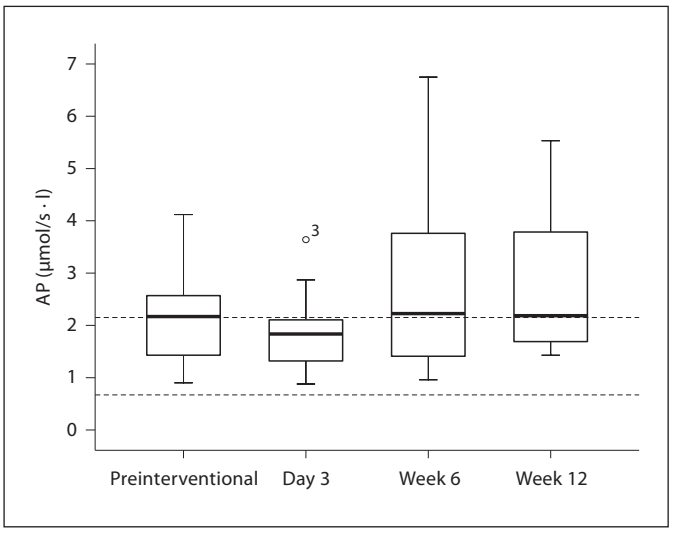

Fig. 12. AP values 1 day before, 3 days, 6 weeks and 3 months after ^{90}Y-RE (standard values between dashed lines).

lost to follow-up after 3 days and 1 patient after 3 months. Calculating the percentage changes with the preinterventional GGTP as a baseline on the third postinterventional day, GGTP increased by 35.55%. After 6 weeks and 3 months, GGTP changed by +40.54 and +62.78%, respectively.

Patients with ^{90}Y-RE

Also within the group of patients undergoing ^{90}Y-RE the median GGTP values exceed the standard values: the preinterventional value was 2.12 µmol/s·l (range 0.83–5.91). Values on day 3 after the procedure were 1.91 µmol/s·l (range 0.81–5.94; $p < 0.05$), 6 weeks after the procedure 2.64 µmol/s·l (range 0.72–10.77), and 3 months after the intervention 2.40 µmol/s·l (range 1.55–10.11). The changes in percentage based upon the preinterventional values were on day 3 –9.92%, after 6 weeks +24.82%, and after 3 months +13.47%. Two patients were lost to follow-up after 6 weeks and 4 patients were lost to follow-up after 3 months.

Discussion

With the integration of radiation therapy into multimodality treatment for liver malignancies, the issues of dose escalation and risk reduction of treatment-related complications became more important. Liver irradiation has been associated with poor tolerance and a high risk of RILD, probably related to a lack of compensation by the untreated part of the liver [14].

In recent years, major advances in the use of RT for liver malignancies have been obtained. Increased understanding of the relationship between radiation dose and volume and the risk of hepatic toxicity has allowed delivery of high-dose focal liver radiation while minimizing damage to normal tissues and organs. The results of such therapy reported to date are encouraging – especially among patients with HCC where ^{90}Y-RE led to significant tumor growth control [19, 20].

In this cohort study, we assigned laboratory parameters in a 3-month follow-up in patients suffering from irresectable HCC undergoing either single-fraction image-guided HDR-BT or sequential lobar ^{90}Y-RE to report on changes of liver function and to evaluate hepatic toxicity.

Despite liver cirrhosis graded Child A or B, no patient presented evidence of distinctive liver function degradation. Preinterventional abnormal values were elevated AST (median 0.91 µmol/) and lowered values for ChE (median 71.0 µmol/) in the patient group undergoing ^{90}Y-RE. Median values for GGTP had been elevated preinterventionally in both groups (BT group: median 3.31 µmol/; RE group: 2.12 µmol/). Interventions were well tolerated by all patients, with no major complication observed in this series. We were able to demonstrate that liver irradiation by image-guided BT or ^{90}Y-RE in patients suffering from HCC is feasible even if patients pre-

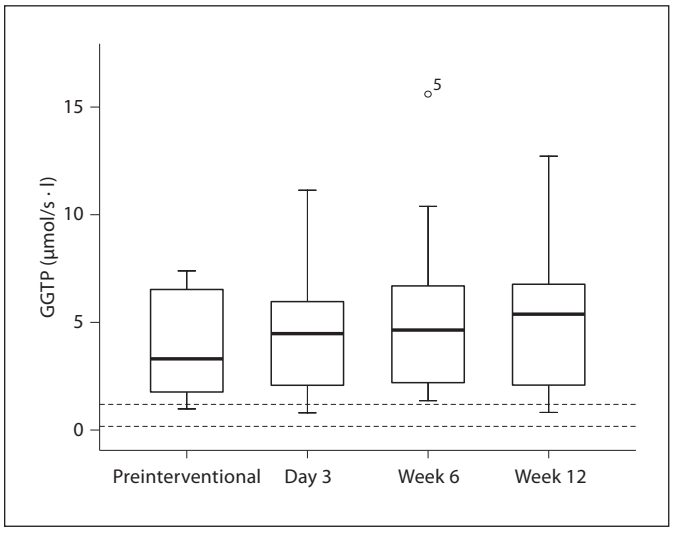

Fig. 13. GGTP values 1 day before, 3 days, 6 weeks and 3 months after image-guided BT (standard values between dashed lines).

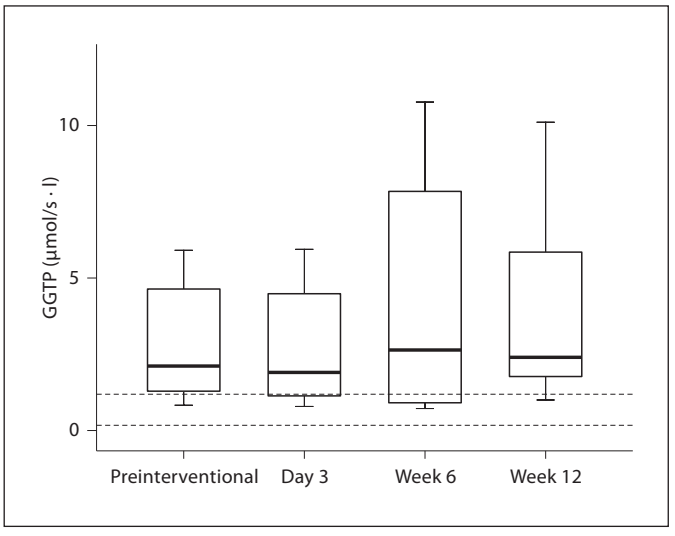

Fig. 14. GGTP values 1 day before, 3 days, 6 weeks and 3 months after ^{90}Y-RE (standard values between dashed lines).

sent with mild impairment of liver tests (including Child A or B cirrhosis) before therapy.

There are some limitations of the study presented. Our major outcome measures were based solely on laboratory abnormalities to identify patients with liver function changes, since other clinical parameters, such as jaundice, ascites or hepatic encephalopathy did not occur. Liver biopsy to prove veno-occlusive disease-similar features were not obtained since there was no suspicion of RILD or REILD. These syndromes usually occur 4–8 weeks after liver irradiation. RILD causes rapid weight gain due to ascites and a strong elevation in serum AP levels that is in proportion with that of other liver enzymes [14]. REILD may demonstrate weight gain, jaundice, ascites and elevation of bilirubin with only mild elevation of transaminases and AP [15].

In our institution, ^{90}Y-RE is performed as a sequential lobar treatment. Especially non-cirrhotic patients with colorectal cancer after treatment with oxaliplatin or capecitabine present a high risk of RILD or REILD [19] due to the fact that these agents may similarly cause hepatic sinusoidal obstruction syndrome as well [21]. By splitting the radiation dose and treating just one liver lobe at one time while the other one is treated after an interval of 4–8 weeks, liver parenchyma may regenerate to keep up as functional reserve for contralateral treatment. According to our data, this kind of treatment schedule may help to preserve liver function and may improve patient tolerance in case of comorbidities, as well as in patients previously treated with other hepatotoxic therapeutic regimens.

Another limitation is the relatively small number of patients evaluated in this study due to narrow inclusion criteria. Patients who developed image-proved hepatic tumor progression within the first 3 months after intervention were not eligible for this analysis. Patients receiving additionally other local ablative therapies or combined therapy modalities (e.g. RE of one liver lobe and subsequent RFA of a small nodule in the other liver lobe) were excluded. Furthermore, we also included patients who had undergone various pretreatments at the time of enrolment (40%). These patients had already undergone partial hepatectomy and/or local ablative therapies such as RFA, BT and TACE, whereas most of them did not show previous exposure to chemotherapeutic agents (except for 1 patient pretreated with systemic doxorubicin and 1 patient pretreated with sorafenib until 3 months before RE). Liver function remained substantially stable independently of whether patients had undergone previous treatments.

Impairment of liver function due to underlying liver cirrhosis was moderate in all cases (all patients were classified Child-Pugh class A except 3 patients in the BT group classified as Child-Pugh B before therapy). At discharge as well as after 3 months of follow-up, no considerable changes in the patient's clinical status occurred and Child-Pugh scores did not change in any patient.

In conclusion, our data suggest that in patients suffering from HCC, classified Child-Pugh A or B undergoing ^{90}Y-RE or HDR-BT, mild changes in liver function parameters such as total bilirubin and GGTP, albumin, ChE and ALT, AST and AP are common shortly after radiation therapy. Floating laboratory values recover within 6 weeks to baseline values. Clinical syndromes such as RILD or REILD are very uncommon under circumstances and preventive measures as described. Rigorous patient selection on the basis of tumor characteristics and clinical conditions is decisive for low complication rates in both BT and RE. However, in light of the aggressive nature of both treatments as well as the extensive tumor loads treated in this series, the functional tolerance of the liver seems to be very high.

References

1 Parkin DM, Bray F, Ferlay J, Pisani P: Global cancer statistics, 2002. CA Cancer J Clin 2005;55:74–108.

2 Bosch FX, Ribes J, Diaz M, Cleries R: Primary liver cancer: worldwide incidence and trends. Gastroenterology 2004;127(suppl 1): S5–S16.

3 Kulik LM, Atassi B, van Holsbeeck L, Souman T, Lewandowski RJ, Mulcahy MF, et al: Yttrium-90 microspheres (TheraSphere®) treatment of unresectable hepatocellular carcinoma: downstaging to resection, RFA and bridge to transplantation. J Surg Oncol 2006;94:572–586.

4 Lu DS, Yu NC, Raman SS, Limanond P, Lassman C, Murray K, et al: Radiofrequency ablation of hepatocellular carcinoma: treatment success as defined by histologic examination of the explanted liver. Radiology 2005;234:954–960.

5 Ruhl R, Ricke J: Image-guided microtherapy for tumor ablation: from thermal coagulation to advanced irradiation techniques. Onkologie 2006;29:219–224.

6 Dick EA, Taylor-Robinson SD, Thomas HC, Gedroyc WM: Ablative therapy for liver tumours. Gut 2002;50:733–739.

7 Galandi D, Antes G: Radiofrequency thermal ablation versus other interventions for hepatocellular carcinoma. Cochrane Database Syst Rev 2004:CD003046.

8 Curley SA, Izzo F: Radiofrequency ablation of primary and metastatic hepatic malignancies. Int J Clin Oncol 2002;7:72–81.

9 Pech M, Werk M, Beck A, Stohlmann A, Ricke J: System continuity and energy distribution in laser-induced thermo therapy (in German). Rofo 2002;174:754–760.

10 Ricke J, Wust P, Stohlmann A, Beck A, Cho CH, Pech M, et al: CT-guided interstitial brachytherapy of liver malignancies alone or in combination with thermal ablation: phase I–II results of a novel technique. Int J Radiat Oncol Biol Phys 2004;58:1496–1505.

11 Ricke J, Wust P, Wieners G, Beck A, Cho CH, Seidensticker M, et al: Liver malignancies: CT-guided interstitial brachytherapy in patients with unfavorable lesions for thermal ablation. J Vasc Interv Radiol 2004;15:1279–1286.

12 Salem R, Lewandowski RJ, Atassi B, Gordon SC, Gates VL, Barakat O, et al: Treatment of unresectable hepatocellular carcinoma with use of ^{90}Y microspheres (TheraSphere®): safety, tumor response, and survival. J Vasc Interv Radiol 2005;16:1627–1639.

13 Geschwind JF, Salem R, Carr BI, Soulen MC, Thurston KG, Goin KA, et al: Yttrium-90 microspheres for the treatment of hepatocellular carcinoma. Gastroenterology 2004; 127(suppl 1):S194–S205.

14 Lawrence TS, Robertson JM, Anscher MS, Jirtle RL, Ensminger WD, Fajardo LF: Hepatic toxicity resulting from cancer treatment. Int J Radiat Oncol Biol Phys 1995;31: 1237–1248.

15 Sangro B, Gil-Alzugaray B, Rodriguez J, Sola I, Martinez-Cuesta A, Viudez A, et al: Liver disease induced by radioembolization of liver tumors: description and possible risk factors. Cancer 2008;112:1538–1546.

16 El Serag HB, Marrero JA, Rudolph L, Reddy KR: Diagnosis and treatment of hepatocellular carcinoma. Gastroenterology 2008; 134:1752–1763.

17 Covey AM, Brody LA, Maluccio MA, Getrajdman GI, Brown KT: Variant hepatic arterial anatomy revisited: digital subtraction angiography performed in 600 patients. Radiology 2002;224:542–547.

18 Salem R, Thurston KG: Radioembolization with yttrium-90 microspheres: a state-of-the-art BT treatment for primary and secondary liver malignancies. Part 1. Technical and methodologic considerations. J Vasc Interv Radiol 2006;17:1251–1278.

19 Sangro B, Bilbao JI, Boan J, Martinez-Cuesta A, Benito A, Rodriguez J, et al: Radioembolization using ^{90}Y-resin microspheres for patients with advanced hepatocellular carcinoma. Int J Radiat Oncol Biol Phys 2006;66: 792–800.

20 Lau WY, Ho S, Leung TW, Chan M, Ho R, Johnson PJ, et al: Selective internal radiation therapy for nonresectable hepatocellular carcinoma with intraarterial infusion of yttrium-90 microspheres. Int J Radiat Oncol Biol Phys 1998;40:583–592.

21 Rubbia-Brandt L, Audard V, Sartoretti P, Roth AD, Brezault C, Le Charpentier M, et al: Severe hepatic sinusoidal obstruction associated with oxaliplatin-based chemotherapy in patients with metastatic colorectal cancer. Ann Oncol 2004;15:460–466.

OPEN ACCESS Freely available online

PLOS ONE

Prospective Randomized Trial of Enoxaparin, Pentoxifylline and Ursodeoxycholic Acid for Prevention of Radiation-Induced Liver Toxicity

Max Seidensticker[1,2]*, Ricarda Seidensticker[1,2], Robert Damm[1,2], Konrad Mohnike[1,2], Maciej Pech[1,2,7], Bruno Sangro[3], Peter Hass[4], Peter Wust[5], Siegfried Kropf[6], Günther Gademann[4], Jens Ricke[1,2]

1 Universitätsklinik Magdeburg, Klinik für Radiologie und Nuklearmedizin, Magdeburg, Germany, **2** International School of Image-Guided Interventions, Deutsche Akademie für Mikrotherapie, Magdeburg, Germany, **3** Clinica Universidad de Navarra, Liver Unit, Department of Internal Medicine, Pamplona, Spain, **4** Universitätsklinik Magdeburg, Klinik für Strahlentherapie, Magdeburg, Germany, **5** Charité Universitätsmedizin Berlin, Klinik für Radioonkologie und Strahlentherapie, Berlin, Germany, **6** Universitätsklinik Magdeburg, Institut für Biometrie und Medizinische Informatik, Magdeburg, Germany, **7** Medical University of Gdansk, 2nd Department of Radiology, Gdansk, Poland

Abstract

Background/Aim: Targeted radiotherapy of liver malignancies has found to be effective in selected patients. A key limiting factor of these therapies is the relatively low tolerance of the liver parenchyma to radiation. We sought to assess the preventive effects of a combined regimen of pentoxifylline (PTX), ursodeoxycholic acid (UDCA) and low-dose low molecular weight heparin (LMWH) on focal radiation-induced liver injury (fRILI).

Methods and Materials: Patients with liver metastases from colorectal carcinoma who were scheduled for local ablation by radiotherapy (image-guided high-dose-rate interstitial brachytherapy) were prospectively randomized to receive PTX, UDCA and LMWH for 8 weeks (treatment) or no medication (control). Focal RILI at follow-up was assessed using functional hepatobiliary magnetic resonance imaging (MRI). A minimal threshold dose, i.e. the dose to which the outer rim of the fRILI was formerly exposed to, was quantified by merging MRI and dosimetry data.

Results: Results from an intended interim-analysis made a premature termination necessary. Twenty-two patients were included in the per-protocol analysis. Minimal mean hepatic threshold dose 6 weeks after radiotherapy (primary endpoint) was significantly higher in the study treatment-group compared with the control (19.1 Gy versus 14.6 Gy, $p = 0.011$). Qualitative evidence of fRILI by MRI at 6 weeks was observed in 45.5% of patients in the treatment versus 90.9% of the control group. No significant differences between the groups were observed at the 12-week follow-up.

Conclusions: The post-therapeutic application of PTX, UDCA and low-dose LMWH significantly reduced the extent and incidence fRILI at 6 weeks after radiotherapy. The development of subsequent fRILI at 12 weeks (4 weeks after cessation of PTX, UDCA and LMWH during weeks 1–8) in the treatment group was comparable to the control group thus supporting the observation that the agents mitigated fRILI.

Trial Registration: EU clinical trials register 2008-002985-70 ClinicalTrials.gov NCT01149304

Citation: Seidensticker M, Seidensticker R, Damm R, Mohnike K, Pech M, et al. (2014) Prospective Randomized Trial of Enoxaparin, Pentoxifylline and Ursodeoxycholic Acid for Prevention of Radiation-Induced Liver Toxicity. PLoS ONE 9(11): e112731. doi:10.1371/journal.pone.0112731

Editor: Vincent Wong, The Chinese University of Hong Kong, Hong Kong

Received August 6, 2014; **Accepted** September 30, 2014; **Published** November 13, 2014

Data Availability: The authors confirm that all data underlying the findings are fully available without restriction. All relevant data are within the paper and its Supporting Information files.

Funding: This study was funded in full by Sirtex medical (http://www.sirtex.com.au/eu/), funding received by university hospital of Magdeburg. The writing of this paper was funded in part by Sirtex medical. Writing support was provided by Rae Hobbs and was funded by Sirtex medical. Apart from that, the funders had no role in study design, data collection and analysis, decision to publish, or preparation of the manuscript.

Competing Interests: M. Seidensticker has served as a speaker for Bayer Healthcare and Sirtex medical, and has received research funding from Sirtex medical. R. Seidensticker has served as a speaker for Bayer Healthcare and Sirtex medical, and has received research funding from Sirtex medical. J. Ricke has served as a speaker for Bayer Healthcare and Sirtex medical, and has received research funding from Sirtex medical, Bayer Healthcare and Siemens. M. Pech has served as a speaker for Sirtex medical. B. Sangro has served as a speaker and an advisory board member for Sirtex medical. The authors state herewith that the competing interest as listed above do not alter their adherence to PLOS ONE policies on sharing data and materials.

* Email: max.seidensticker@med.ovgu.de

Introduction

Highly targeted radiotherapy of liver malignancies has found to be effective in selected patients. Stereotactic radiotherapy, radioembolization using yttrium-90 (^{90}Y) microspheres as well as image-guided brachytherapy (BT) have been described in the literature with promising results [1,2,3]. A key limiting factor of these therapies is the relatively low tolerance of the liver parenchyma to radiation leading to either subclinical focal or generalized injury of the liver parenchyma. When the intensity or the extent of

radiation-induced liver injury (RILI) exceeds the functional reserve, clinical complications appear in the form of radiation (radioembolization) induced liver disease (RILD or REILD) [4,5,6,7]. Prior exposure or concomitant chemotherapy is thought to increase the risk of RILD (or REILD), and as a consequence is a relatively common complication, for example, after conditioning therapy prior to bone marrow transplantation (BMT) [5,8,9,10]. Liver damage whether associated with whole body irradiation or liver-directed radiotherapy have the same pathology, i.e. veno-occlusive disease (VOD) [5,11,12,13].

Medication designed to reduce RILI could improve the safety as well as enable more aggressive radiotherapy. Clinical studies have shown with varying strength of evidence that VOD/RILD after BMT can be ameliorated by pentoxifylline (PTX), ursodeoxycholic acid (UDCA) and low molecular weight heparin (LMWH) [14,15,16,17,18,19,20,21,22] (see Table 1). However, the equivocal nature of the results from most studies probably reflect the heterogeneous study populations (including patients who have received prior chemotherapy or had underlying liver disease) [23]. Thus, a more standardized clinical model is needed to evaluate the protective effects of prophylactic regimens against VOD/RILD.

Image-guided, single-fractioned, high-dose-rate BT of liver malignancies is associated with a well-characterized focal RILI (fRILI), which can be visualized and quantified using functional hepatobiliary magnetic resonance imaging (MRI) (see Figure 1) [6,7]. Importantly, the histopathological evidence of fRILI (i.e. sinusoidal congestion with hepatocyte atrophy and increased reticulin deposits) correlates well with the absence of the hepatocyte uptake of hepatolbiliary MRI contrast media [24]. We have previously found that development of areas of fRILI were maximal at 6–8 weeks post-BT which correlates to the peak incidence of RILD/REILD after conditioning therapy/radioembolization througout the first 2 months post-intervention [5,6,7,25]. We conducted a prospective study to quantify fRILI in patients who were randomized to BT with and without prophylactic PTX, UDCA and low-dose LMWH. To minimize the confounding effects of prior chemotherapy on radiation tolerability, only patients with liver metastases from colorectal cancer (mCRC) were included because these patients tend to have a more consistent pattern of prior exposition to chemotherapy. The cumulative effect of three drugs over a period of 8 weeks [26,27,28] was assessed and patients followed-up at 6 and 12 weeks.

Materials and Methods

The protocol for this trial and supporting CONSORT checklist are available as supporting information; see Checklist S1 and Protocol S1.

Study design

This was a prospective, randomised phase II, parallel-group, open-label study conducted at a single centre. The study was approved by the competent authorities (Federal Institute for Drugs and Medical Devices (in german: Bundesinstitut für Arzneimittel und Medizinprodukte - BfArM)) and the local ethics committee (Ethikkommission der Otto-von-Guericke-Universität der Medizinischen Fakultät). Trial registration: Eudra-CT: 2008-002985-70; ClinicalTrials.gov-identifier NCT01149304. Written informed consent was obtained from all patients prior to study entry. Group allocation approach was unrestricted randomization.

Patient characteristics

Consecutive patients (18–80 years) with liver metastases from mCRC, who were scheduled for local ablation with computed-tomography (CT)/MRI-guided BT between 2009 and 2012, were screened (Figure 2). (BT is the local standard ablative treatment in patients ineligible for surgical or all other appropriate intervention).

Women who were pregnant, lactating or of childbearing potential were excluded as were patients with liver cirrhosis, hepatitis B or C, severe coronary artery disease, autoimmune diseases, acute bacterial endocarditis, active major bleedings or high-risk of uncontrolled hemorrhage; severe or moderate renal impairment (GFR <60 mL/min), or known contraindication or hypersensitivity to any of the study treatments or procedures.

Treatment and follow-up

Patients received a single-fraction, CT- or MRI-guided BT of CRC liver metastases (see details below). In those randomized to prophylaxis, the following treatment was initiated during the evening of the day of BT: sc injection of 40 mg q.d. enoxaparin (Clexane, Sanofi Aventis, Paris, France) [20], oral 400 mg t.i.d. PTX (Trental, Sanofi Aventis) [16] and oral 250 mg t.i.d. UDCA (Ursofalk, Falk Pharma, Freiburg, Germany) [17,19]. Patients were discharged usually on the third day post-BT and continued to take study medication at home for 8 weeks. All patients were followed-up on day 3, week 6 and 12 with an optional follow-up at week 24. Within 24 hours of the procedure and at each subsequent visit, blood samples were taken for liver-specific and inflammatory/hemostatic laboratory parameters, and patients were assessed for ECOG-performance status and health-related quality-of-life (using the EQ5D-questionnaire). All adverse reactions related to the study medication or BT were recorded.

Compliance to the prophylactic regimen was evaluated during a dialogue at each visit and the evaluation of anti-Xa-activity at 6 weeks. Insufficient compliance was determined by: either anti-Xa-activity <0.1 IU/mL measured up to 4 hours after last enoxaparin injection, or two dose interruptions of the prophylactic regimen for more than 1 day/week. Non-compliant patients were withdrawn from the per-protocol analysis and study-specific medication stopped.

Image-guided interstitial brachytherapy

The technique of image-guided BT has been described previously [2]. Briefly, the placement of the introducer sheaths (6F Radiofocus, Terumo, Tokyo, Japan) with the BT applicators (Lumencath, Nucletron/Elekta, Veenendaal, The Netherlands) was performed using CT or MRI fluoroscopy. For treatment planning purposes, a spiral CT or T1-weighted MRI of the liver (reconstructed slice thickness: 3 mm) enhanced by intravenous application of iodine contrast media (CT) or Gd-EOB-DTPA (MRI) was acquired.

The high-dose-rate afterloading system (Microselectron, Nucletron/Elekta, Veenendaal, The Netherlands) employed an iridium-192 source with a nominal activity of 10Ci (i.e. 370GBq); decay correction was performed daily. Relative coordinates (x, y, z) of the catheters were determined in the CT/MRI-data set and transferred to the treatment planning system (Oncentra, Nucletron/Elekta). Using these coordinates, the clinical target volume and the predefined minimum dose (20 Gy, delivered as a single fraction [2]), the software calculated a dosimetry and the duration of the iridium-192 source inside the BT catheters. A planning CT with dosimetry is displayed in Figure 1B and F.

Table 1. Summary of published studies on drug treatments for the prevention of VOD/RILD.

Reference	Study design	N	Treatment regimen	Incidence of VOD	p-value*	Bilirubin (μmol/L)	p-value*
Attal et al. 1993 [14]	Prospective RCT	70	**Pentoxifylline** 1,600 mg/d day −8 to day+100 post-BMT	4%	NS	26.4 (mean max)	NS
		70	Control	3%		24.4 (mean max)	
Clift et al. 1993 [22]	Prospective RCT	44	**Pentoxifylline** 2,400 mg/d day −3 to day+70 post-allogeneic BMT	-		26.6 (mean max)	0.62
		44	Control	-		23.47 (mean max)	
Bianco et al. 1991 [16]	Phase 1–2	30	**Pentoxifylline** 1,200, 1,600, and 2,000 mg/d; day −10 to day+100 post-BMT	10%	0.001	-	-
		20	Control (retrospective)	65%		-	
Attal et al 1992 [15]	Prospective RCT	81	**Unfractionated heparin** 100 U/kg/d cont. infusion; day −8 to day+30 post-BMT	2.5%	0.01	7.4% exceeding 34	<0.05
		80	Control	14%		18.7% exceeding 34	
Forrest et al. 2003 (18)	Prospective single-arm	40	**LMWH**: dalteparin 2500 anti-Xa i.u; day −1 to day +30 post-BMT or hospital discharge	22.5%, 2.5% severe			
Or et al. 1996 [20]	Prospective RCT, pilot	61	**LMWH**: enoxaparin 40 mg/day; day+1 to day+40 post-BMT or hospital discharge		0.01	(duration of elevated levels)	0.01
		33	Control				
Essel et al. 1998 [17]	Prospective RCT	34	**UDCA** 600–1200 mg/d; day at least −1 to day +80 post-BMT	15%	0.03	102.6 (mean max)	0.13
		32	Control	40%		188.1 (mean max)	
Ohashi et al. 2000 [19]	Prospective RCT	67	**UDCA** 600 mg/d; day −21 to day+80 post-BMT	3%	0.004	Not reported in detail	NS
		65	Control	18.5%		Not reported in detail	

Table 1. Cont.

Reference	Study design	N	Treatment regimen	Incidence of VOD	p-value*	Bilirubin (µmol/L)	p-value*
Park et al. 2002 [28]	Prospective RCT	82	**UDCA** 600 mg/d **+ unfractionated heparin** 5–50 U/kg/d adjusted aPTT of 50 s; day +1 to day +30 post-BMT or hospital discharge (but a minimum of 15d)	16%	0.348	148.8 (mean max)	0.725
		83	**Unfractionated heparin** 5–50 U/kg/d adjusted aPTT of 50 s; day +1 to day +30 post-BMT or hospital discharge (but a minimum of 15d)	19%		173.6 (mean max)	

*Group comparison; LMWH: Low molecular weight heparin; BMT: Bone marrow transplantation; Max: Maximum; NS: Not significant; VOD: Veno-occlusive disease; RCT: Randomized controlled trial; UDCA: ursodeoxycholic acid (ursodiol); aPTT: activated Partial Thromboplastin Time.

doi:10.1371/journal.pone.0112731.t001

Magnetic resonance imaging

MRI (Achieva 1.5T, Philips, Best, The Netherlands) using the hepatobiliary contrast medium Gd-EOB-DTPA (Primovist, Bayer Healthcare, Leverkusen, Germany) was performed 1 day before and 6 and 12 weeks post-BT. MR-sequence of events was as follows: axial 3D T1-weighted (T1-w) gradient echo THRIVE (T1-High-Resolution-Isotropic-Volume-Excitation) (Time-to-Echo/Time-to-Repetition 4/10 ms, flip-angle 10°) with fat-suppression pre-contrast, at 20 s, 60 s and 120 s and 20 minutes after iv 0.1 mL/kg bodyweight Gd-EOB-DTPA. The slice thickness was 3 mm. For the study-specific MRI volumetry, dynamic THRIVE at 60 s (for the exclusion of tumor progression/local recurrence) and hepatobiliary phase THRIVE 20 min after application of Gd-EOB-DTPA (for the determination of area of fRILI) were mandatory.

Identification of the radiation isodose (minimal hepatic threshold dose) that demarcated the border between the fRILI and functioning liver tissue (as defined by non-uptake and uptake of Gd-EOB-DTPA enhanced MRI, respectively) was performed as follows in a blinded matter.

The hepatobiliary phase THRIVE was transferred to the BT-planning software. Image registration of the hepatobiliary phase THRIVE to the contrast-enhanced planning CT/MRI (including the dosimetry) was performed by an isoscalar local semi-automated point-based 3D-3D image registration using predefined match points (3 or 4 corresponding landmarks restricted to liver structures). Registration was only accepted if the target area merged perfectly by visual assessment. As a result of this procedure, the software simultaneously displayed the treatment dosimetry and anatomical structures/fRILI of the hepatobiliary phase THRIVE. The volume of the liver parenchyma with radiation-induced impaired uptake of Gd-EOB-DTPA (i.e. fRILI) was determined. The isodose of the dosimetry encircling this volume was determined at five different axial levels and the mean of these values recorded. This dose resembles the dose which was formerly applied at the now demarcated rim of the fRILI, corresponding to the assumed minimal hepatic tolerance dose. To ensure a negligible registration error, the volume of fRILI was inserted into the dose-volume-histogram of the dosimetry. The corresponding isodose was stored. Results of the two methods showed a high correlation of 0.899 and 0.562 ($p<0.001$ and $p = 0.006$) for 6 and 12 weeks, respectively. To minimize methodological errors, the mean isodose value of the two methods was taken. In case of more than one treated lesion, the mean of the determined isodoses was used. If no detectable fRILI was seen in follow-up, the minimal mean hepatic threshold dose was defined as the dose which was previously administered at the tumor margin (since an effect on the liver parenchyma above this dose level cannot be excluded). Figure 1 illustrates the development and appearance of the fRILI in hepatobiliary phase THRIVE.

Endpoints and statistical analyses

The aim of the study was to assess if a combination regimen of PTX, UDCA and low-dose LMWH for 8 weeks provided a preventive effect regarding irradiation damage to liver parenchyma (as resembled by the minimal mean threshold dose of the fRILI volume) at 6 weeks (primary endpoint) and at 12 weeks (secondary endpoint) after BT.

As additional descriptor, detectable fRILI in Gd-EOB-DTPA MRI (yes/no) was recorded at each follow-up. Further secondary objectives included the safety of the study treatment after BT including changes in bilirubin and albumin which were graded according to Common Terminology Criteria for Adverse Events version 3 (CTCAE3.0).

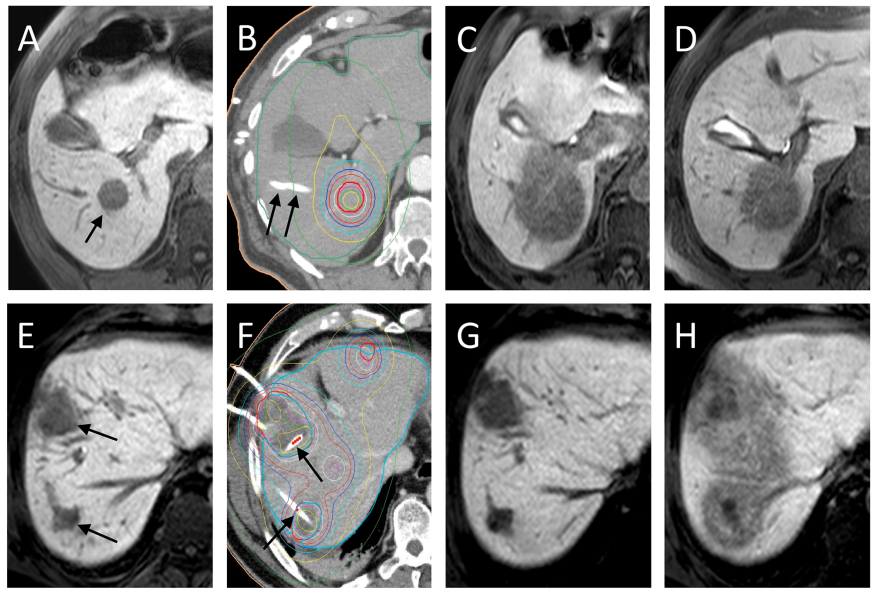

Figure 1. T1w-axial THRIVE 20 min after application of Gd-EOB-DTPA (A, C–E and G, H) and BT planning CT with dosimetry (B and F). A–D, control group. A: pre-treatment MRI displaying a metastasis scheduled for BT treatment (black arrow). B: Planning-CT after introduction of the brachytherapy catheters (black arrows). Clinical target volume (CTV) represented by bold red circle and dosimetry by coloured lines (red: 20 Gy-, blue: 12 Gy-isodose). C: MRI at 6 weeks showing substantial reduction in Gd-EOB-DTPA uptake by liver parenchyma adjacent to treated metastases (i.e. focal radiation-induced liver injury, fRILI). Note: The area of fRILI matches the geometry of the dosimetry (B). Determined threshold dose: 9.75 Gy. D: MRI at 3 months showing shrinkage of the fRILI. Determined threshold dose: 11.9 Gy. E–H, treatment group. E: pre-treatment MRI displaying two metastases (black arrow); two more treated lesions are not displayed in the plane. F: Planning-CT (annotations: see B). G: MRI at 6 weeks showing no fRILI. H: MRI at 3 months after radiotherapy (and 1 month after finishing study treatment) showing a substantial region of fRILI. Determined threshold dose: 15.8 Gy.
doi:10.1371/journal.pone.0112731.g001

The relation between hepatocyte dysfunction and changes in the following liver-specific and inflammatory/hemostatic laboratory values were analysed: fibrinogen, factor-VIII-activity, interleukin-6, protein-C-activity, protein-S-activity, von-Willebrand-factor-activity and antithrombin-III-activity [29].

Determination of sample size was based on the expected minimum between-group difference of 2.1 Gy (SD 2.3 Gy) for minimal mean hepatic threshold dose at 6 weeks after BT (from 9.9 Gy to 12 Gy) [7]. A sequential test with 2 stages according to the Pocock-design was used which yielded a total of 22 observations per group with a scheduled interim analysis after 11 observations per group when $a = 0.025$ and power $1\text{-}b = 0.8$. Interim-analysis showed a significant difference between the groups regarding the primary variable with a one-sided p-value of 0.011. A one-sided p of <0.0148 was necessary to terminate the study prematurely.

Statistical analysis was performed using SPSS (SPSS21, IBM, Chicago, Il, USA). Descriptive analysis of patient characteristics and laboratory findings was performed. The primary analysis was evaluated in the per protocol cohort and repeated in the intention-to-treat population as sensitivity analysis. Between-group differences in minimal mean hepatic threshold after BT at 6 and 12 weeks were compared using a two-sample *t*-tests, and evidence of detectable fRILI were compared using the Fisher's-exact-test. Possible confounding factors were evaluated using the Mann-Whitney-*U*-test for metric variables and the Fisher's-exact-test for categorical variables, and then between-group differences for the primary endpoint were evaluated with inclusion of the covariables (ANOVA and ANCOVA). The relationship between the minimal mean hepatic threshold dose and laboratory values was tested by Pearson's correlation and ANCOVA. Group comparison regarding ECOG and EQ5D was made by Mann-Whitney-*U*-test. Median overall survival was estimated by Kaplan-Meier (group comparison by log-rank test). A p-value of <0.05 was statistically significant.

Results

Of 129 patients screened with liver metastases from colorectal cancer scheduled for BT, 30 patients were included in the study and 22 patients (11 per group) in the primary analyses of the per-protocol group (see CONSORT diagram, Figure 2). Demographic characteristics of randomized patients at screening are summarized in Table 2 and the baseline liver function and other laboratory parameters are presented in Table 3. Group comparison revealed a similar distribution of possible confounders. A tendency towards a larger volume of significantly radiation exposed liver parenchyma (>10 Gy) in the study treatment group (Table 2) may have potentially lowered the hepatic tolerance dose in this group instead of increase it [25].

The minimal mean hepatic threshold dose at 6 weeks after BT (primary endpoint) was significantly higher in the study treatment group than the control (19.1 Gy versus 14.6 Gy, $p = 0.011$, Table 4) with comparable results with the intention-to-treat analysis (Table 4). Correspondingly, fewer patients in the study treatment group than the control had evidence of fRILI at 6 weeks (45.5% versus 90.9%); this difference was also significant in the intention-to-treat analysis (Table 4). However at 12 weeks after BT (and 4 weeks after cessation of study treatment), these between-group differences were not observed (in neither the per-protocol nor intention-to-treat analyses) for the minimal mean hepatic threshold dose and the proportion of patients with fRILI (Table 4). Results from the optional follow-up at 24 weeks after BT continually showed no between-group differences for the minimal

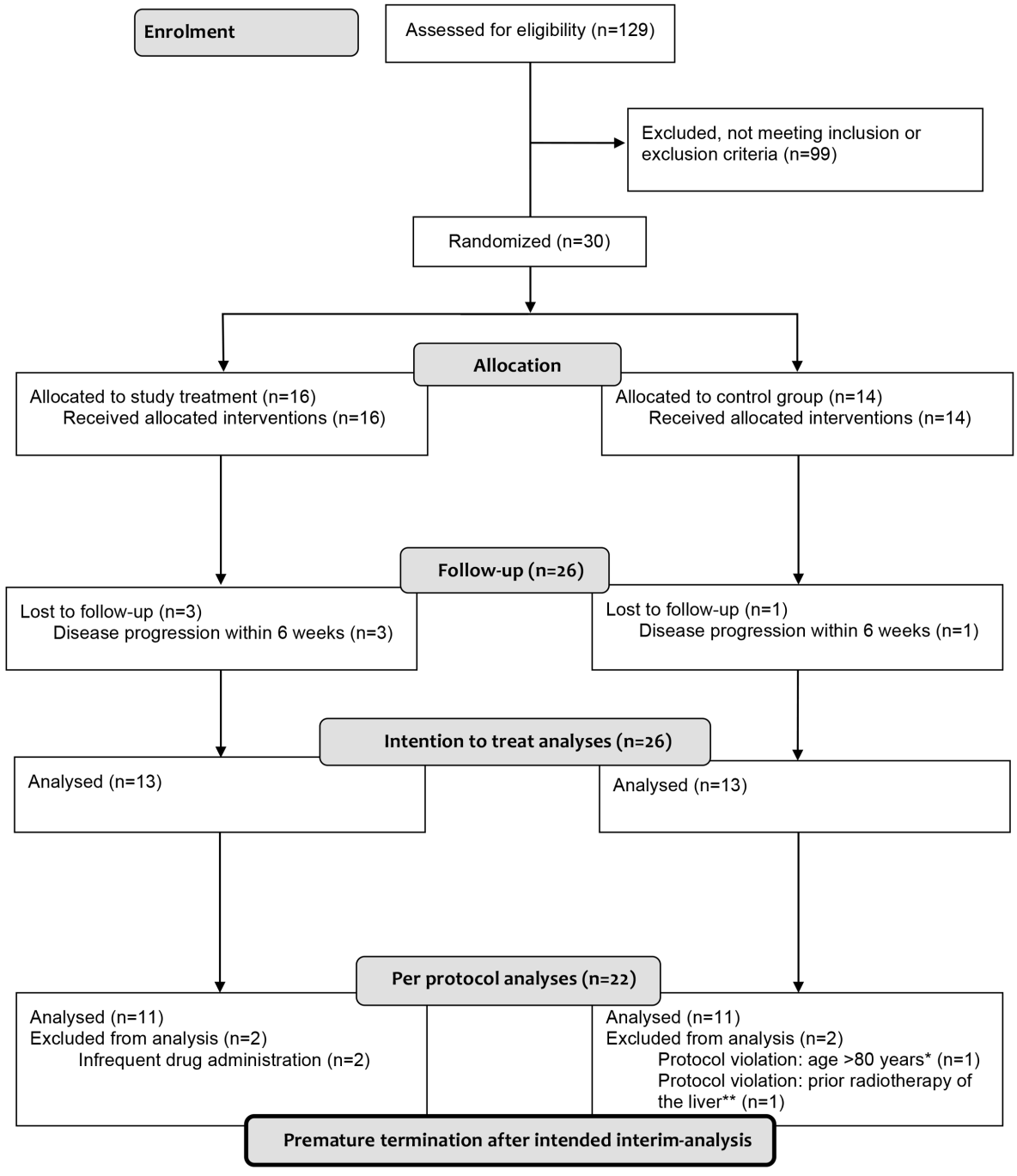

Figure 2. CONSORT-diagram. *Exclusion criterion age was initially disregarded by error in this patient (aged 82). **Exclusion criterion prior radiotherapy was initially disregarded by error in this patient (prior radiotherapy was performed 2 years earlier with location in the contralateral liver lobe).
doi:10.1371/journal.pone.0112731.g002

mean hepatic threshold dose and the proportion of patients with fRILI (no change of the proportion of patients with fRILI as compared to 12 weeks follow-up; the minimal mean hepatic threshold dose for treatment group was 20.1 Gy (1 patient missing) and for the control group 21.0 Gy; $p>0.05$, per-protocol analysis (with comparable results with the intention-to-treat analysis)).

Covariate analyses also showed no influence of recorded covariables on the primary endpoint; only group allocation was significant (Table 5).

EQ5D (as a descriptor of quality of life) and distribution of ECOG performance status were not significantly different at baseline (Table 2) or at any follow-up visit (Table S1). Median overall survival from time of BT on was not different between the groups with 30.0 months (95%CI: 8.7–51.3) in the treatment group and 39.5 months (27.5–51.5) in the control group ($p = 0.430$).

Safety analyses were conducted in all 30 patients who received BT. The following mild-to-moderate adverse events CTCAEv3 grade 1–2 were reported (in the treatment/control groups) on day

Table 2. Patient characteristics (per protocol analysis).

Variable	Treatment group (n = 11)	Control (n = 11)	p-value (between group)*
Sex (m/f)	9/2	8/3	1.000
Age (years)	71.09±5.47	65.09±12.55	0.408
Weight (kg)	84.64±11.68	83.91±12.89	0.592
Height (cm)	174.09±6.79	172.64±6.90	0.834
ECOG at baseline (0/1/2)	6/4/1	4/5/2	0.370
EQ5D visual analogue score	72.36±14.56	76.36±13.02	0.446
History of liver surgery	45.5%	45.5%	1.000
Steatosis hepatis	36.4%	18.2%	0.635
Diabetes mellitus	18.2%	27.3%	1,000
Chemotherapy pretreatment			
Applied lines	1.00±0.63	1.00±0.45	1.000
no chemotherapy	18.2%	9.1%	NA
1 line	63.6%	81.8%	0.672
2 lines	18.2%	9.1%	NA
Prior chemotherapy			
Oxaliplatin	63.6%	63.6%	1.000
Irinotecan	36.4%	36.4%	1.000
Biologicals	54.5%	54.5%	1.000
Number of treated metastases	1.91±1.04	1.45±0.52	0.382
Maximum diameter of metastases (mm)	37.18±12.91	29.45±11.79	0.146
Clinical target volume (cm^3)	42.82±29.26	31.36±37.14	0.156
Number of used brachytherapy catheters	3.18±1.78	2.27±1.74	0.079
Liver volume (cm^3)	1296.1±226.6	1451.3±278.6	0.401
Interval between BT and 6 weeks FU (days)	43.91±4.76	45.09±4.68	0.757
Interval between BT and 3 months FU (days)	87.34±4.52	89.55±6.15	0.505
Liver volume with a dose exposure >10 Gy (%)	22.55±14.45	11.95±10.43	0.056
Chemotherapy during follow-up	18.2%	9.1%	1.000

Continuous data: mean ± standard deviation, frequencies: counts or percent.
*Group comparison, continuous data compared by Mann-Whitney U test, frequency data compared by Pearson's chi square test.
doi:10.1371/journal.pone.0112731.t002

3 after BT: pain (1 patient/1 patient) and fatigue (0/1); at week 6: pain (2/0), fatigue (0/1), nausea (1/0) and diarrhea (2/0); nausea and diarrhea was probably related to PTX or UDCA. One grade 3 subacute bleeding episode from the bile duct, related to BT, occurred in the study treatment group which was successfully managed by endoscopic coagulation.

Analysis of the laboratory data revealed no grade 3/4 changes in bilirubin or albumin. One grade 1 reduction of albumin in the treatment group at 6 weeks was unchanged at week 12. One patient in control group with elevated (grade 1) bilirubin at baseline remained stable throughout follow-up. RILD was not observed on either group.

Laboratory analysis regarding liver-specific and inflammatory/hemostatic parameters found no relevant findings at baseline (Table 3). At week 6, slightly higher gamma-glutamyl-transferase levels and protein-S-activity were recorded in the control group compared with the treatment group. At 6 and 12 weeks, there was slight but significant mean decrease from baseline in cholinesterase in the treatment group. Additionally, mean fibrinogen and von-Willebrand-factor-activity increased significantly from baseline in the treatment group at 6 and 12 weeks; while significant increases from baseline were recorded with mean fibrinogen, factor-VIII-activity and aspartate-transaminase in the control group at 6 weeks.

No correlation between the minimal mean hepatic threshold and liver-specific and inflammatory/hemostatic laboratory values was found at either week 6 or 12 (data not shown).

Discussion

In this prospective study, we were able to show a significant reduction in fRILI (as measured by hepatobiliary MRI) at 6 weeks after BT of colorectal liver metastases in patients who received low-dose LMWH, PTX and UDCA. Re-assessment of patients at 12 weeks (4 weeks after cessation of study treatment) found that the extent and incidence of fRILI was comparable to the control group, thereby supporting the reliability of our findings. This is further authenticated by the results of the (optional) 24 weeks follow-up. According to our results we believe that we were able to mitigate rather than delay the fRILI by the prophylactic regimen. The finding that the positive effect of the medication to the liver parenchyma as seen at the 6 weeks follow-up vanished after discontinuation of the medication (after 8 weeks) in the 3 months

Table 3. Laboratory parameters at baseline and follow-up (per protocol analysis).

Variable (normal range)		Treatment group (n = 11)	Control (n = 11)	p-value (between group)*	p-value (baseline *vs.* follow-up)**
Bilirubin	baseline	8.27±2.92	8.39±5.61	0.594	
(<21.0 μmol/L)	6 weeks	9.58±9.94	9.56±7.18	0.641	0.182 (0.350)
	12 weeks	8.71±4.27	8.75±5.95	0.735	0.594 (0.505)
Albumin	baseline	44.21±3.46	44.05±2.45	0.833	
(35.0–52.0 g/L)	6 weeks	42.49±5.16	42.67±3.17	0.743	0.197 (0.060)
	12 weeks	42.84±4.94	43.66±2.31	0.743	0.212 (0.332)
Cholinesterase	baseline	149.26±47.97	144.73±21.73	0.718	
(88–215 μmol/s.L)	6 weeks	136.27±51.65	143.82±29.10	0.433	**0.023** (0.929)
	12 weeks	132.94±49.22	153.36±30.96	0.088	**0.010** (0.423)
Aspartate transaminase	baseline	0.56±0.18	0.46±0.17	0.211	
(0.17–0.83 μmol/s.L)	6 weeks	0.59±0.17	0.55±0.23	0.533	0.373 (**0.016**)
	12 weeks	0.63±0.47	0.54±0.17	0.974	0.563 (0.056)
Alanine transaminase	baseline	0.44±0.20	0.51±0.36	1,000	
(0.17–0.83 μmol/s.L)	6 weeks	0.50±0.18	0.62±0.45	0.742	0.443 (0.109)
	12 weeks	0.53±0.43	0.52±0.27	0.718	0.508 (0.722)
Gamma glutamyltransferase	baseline	1.61±2.62	1.49±1.21	0.189	
(0.17–1.19 μmol/s.L)	6 weeks	0.82±0.83	2.21±1.71	**0.011**	0.100 (0.050)
	12 weeks	1.25±1.17	1.97±1.49	0.139	0.722 (0.306)
Glutamate dehydrogenase	baseline	104.36±91.47	108.82±94.84	0.844	
(<120 nmol/s.L)	6 weeks	67.55±31.43	123.27±105.88	0.490	0.328 (0.308)
	12 weeks	128.11±108.79	126.09±95.19	0.849	0.674 (0.374)
International normalized	baseline	93.9±3.03	95.55±2.98	0.053	
ratio (0.85–1.27)	6 weeks	94.11±2.71	94.8±2.44	0.399	0.438 (0.502)
	12 weeks	94.63±2.50	95.33±3.61	0.732	0.334 (0.498
Interleukin 6	baseline	4.54±3.31	3.71±3.09	0.245	
(<7.0 pg/mL)	6 weeks	8.44±8.53	7.62±4.41	0.809	0.266 (0.038)
	12 weeks	10.50±9.24	4.06±2.42	0.229	0.139 (0.515)
Fibrinogen	baseline	3.72±0.53	3.99±0.46	0.377	
(1.50–4.00 g/L)	6 weeks	4.50±1.17	4.77±0.84	0.365	**0.014** (**0.017**)
	12 weeks	4.65±1.04	4.23±0.49	0.416	**0.037** (0.214)
Factor VIII activity	baseline	169.09±41.51	160.60±42.12	0.756	
(70–150%)	6 weeks	195.45±61.02	218.91±60.77	0.490	0.130 (0.093)
	12 weeks	199.7±67.26	257.09±150.23	0.360	0.169 (**0.017**)
Protein C activity	baseline	107.36±33.99	109.70±12.46	0.145	
(>70%)	6 weeks	108±32.68	106.55±18.67	0.767	0.799 (0.475)
	12 weeks	101.5±27.26	114±19.76	0.084	0.113 (0.540)
Protein S activity	baseline	85.36±12.26	86.80±12.55	0.848	
(>60%)	6 weeks	82.18±15.16	104.36±27.09	**0.036**	0.266 (0.086)
	12 weeks	87.3±14.54	91±10.6	0.549	0.799 (0.507)
von Willebrand factor	baseline	164.09±42.81	174.90±71.14	0.973	
activity (70–130%)	6 weeks	222.27±59.75	201.73±71.76	0.554	**0.013** (0.075)
	12 weeks	209.5±77.35	215.27±75.31	0.883	**0.013** (0.333)
Antithrombin III activity	baseline	92.73±13.72	98.90±11.50	0.191	
(>80%)	6 weeks	96.73±15.31	98.2±9.78	0.944	0.082 (0.779)
	12 weeks	96.4±12.08	96.73±9.51	0.751	0.407 (0.681)

*Between group comparison, Mann-Whitney U test;
**Comparison versus baseline (in brackets p-value of control group), Wilcoxon test.
doi:10.1371/journal.pone.0112731.t003

Table 4. Minimal mean hepatic tolerance dose (Gy) and evidence of detectable focal radiation-induced liver injury (fRILI) after BT, group comparison.

Variable	Group			p-value (between groups)
Minimal mean hepatic tolerance dose (primary endpoint)		**Dose (Gy)**	**SD**	
At 6 weeks	Control	14.64 [14.15]	4.01 [3.93]	
	Treatment	19.06 [18.46]	3.35 [3.59]	**0.011** [**0.007**]
At 12 weeks	Control	16.38 [16.10]	3.57 [3.60]	
	Treatment	19.04 [18.50]	2.88 [3.11]	0.069 [0.082]
Detectable fRILI		**Counts**	**Frequency**	
At 6 weeks	Control	10 [12]	90.9% [92.3%]	
	Treatment	5 [7]	45.5% [53.8%]	**0.022** [**0.027**]
At 12 weeks	Control	10 [12]	90.9% [92.3%]	
	Treatment	10 [12]	90.9% [92.3%]	1.000 [1.000]

Per protocol analysis (n = 22); Intention-to-treat analysis (n = 26) in square brackets.
doi:10.1371/journal.pone.0112731.t004

follow-up, make us believe that the fRILI was in fact mitigated in that period. Further on, the extent of the fRILI at 6 weeks in the treatment group and at 3 months (and 6 months) in both groups was less in size compared to the fRILI in the control group at 6 weeks (the peak of the fRILI in our study). Thus, the maximum extent of the fRILI at 6 weeks was skipped in the treatment group as compared to the control group. However, the radiation damage could not be suppressed completely by the prophylactic regimen with a rebound after cessation of the treatment to the level of the control group in later follow-ups. Thus, it is possibly right to assume additionally a delay on the development of the fRILI by the prophylactic regimen. This delay is considered to be advantageous as well since a rapid formation of the fRILI can be delayed (and mitigated) allowing the liver remnant to compensate for the fRILI. However, although appropriately powered, the study should be understood as a pilot due to the small sample size. To compensate for the rebound of the fRILI after cessation of the prophylactic regimen and for a better understanding of the dynamics of the fRILI, a study concept with a prolonged course for the prophylactic regimen is planned.

RILI remains a challenge in the treatment of liver malignancies by radiotherapy (whether percutaneous, interstitial or by radio-embolization) because it may eventually translate into RILD or REILD. Further on, life-threatening VOD associated with combined-modality induced liver disease occurs in 5–60% of patients undergoing BMT [18,23,26]. For this reason, the potentially protective effects of a number of treatments including low-dose LMWH, PTX and UDCA have been evaluated. Although the efficacy appears equivocal in some studies [14,15,16,17,18,19,20,21,28] (Table 1), we determined that the combination of low-dose LMWH, PTX and UDCA appeared to be the most promising option for further evaluation with BT. We believe that our success in showing a benefit in ameliorating fRILI with this combination is based on the following factors: a highly homogeneous patient cohort; attention to patient compliance to the prophylactic regimen; and direct measurement of damage to the liver parenchyma rather than clinical endpoints.

The treatment course of 8 weeks for the medication was determined on the assumption that occurrence of RILD and fRILI peaks around 2 months after radiation-exposure [5,6,7,25]. However, our findings suggest that the radiation-induced injury to the liver structures and cell endothelial continues beyond 8 weeks and that discontinuation of the medication at this time allows the development of a veno-occlusive state/liver cell dysfunction. Endothelial cell damage, which triggers local thrombotic mechanisms, leading to microvascular flow insufficiency, production of cytotoxic substances, and ultimately hepatocellular necrosis, has been thought to be an early event in the development of RILD/VOD [5,10,11,30,31]. The current evidence indicates that PTX, low-dose LMWH and UDCA may act through a variety of mechanisms to alleviate these effects. PTX, for example, down regulates tumor-necrosis factor-α (TNF-α), a prime suspect in either the initiation or amplification of tissue injury following radiation. PTX also stimulates vascular endothelial production of non-inflammatory prostaglandins of the E- and I-series, enhancing loco-regional blood flow and promoting thrombolysis [16].

LMWHs are assumed to prevent subsequent thrombosis of hepatic venules after endothelial damage and therefore decrease the risk of VOD/RILD [18].

By oral administration of UDCA the concentration of potentially liver toxic hydrophobic bile acids can be reduced [32]. Several *in vitro* studies suggest that potential attenuating effects of UDCA on the pathogenesis of VOD is achieved through the down-regulation of inflammatory cytokine such as TNF-α and interleukin-1 [33]. These cytokines not only induce and amplify liver damage but are also associated with apoptosis in endothelial cells [34] and the development of VOD. UDCA also appears to have a direct effect on programmed-cell death, inhibiting apoptosis and protecting against the membrane damaging effects associated with hydrophobic bile acids in both hepatocytes and non-liver cells [35].

The rationale for this combined treatment approach is based on the assumption that LMWH, PTX and UDCA, which act through a variety of different mechanisms, may act synergistically or in a complimentary fashion to protect the liver [26,27,28]; although further study is needed to fully evaluate this hypothesis. However, based on the low toxicity profile of these medications, we believe

Table 5. Covariate analysis of minimal mean hepatic tolerance dose 6 weeks after BT (per protocol, n = 22).

Covariate*	p-value (group influence)	p-value (co-variate influence)
Sex (m/f)	**0.015**	0.458
Age (y)	**0.016**	0.864
Weight (kg)	**0.010**	0.117
Height (cm)	**0.011**	0.485
ECOG at baseline (0 and 1 vs 2)	**0.008**	0.310
EQ5D visual analogue score	**0.015**	0.868
History of liver surgery	**0.007**	0.064
Steatosis hepatis	**0.014**	0.845
Diabetes mellitus	**0.015**	0.627
Chemotherapy pre treatment	**0.012**	0.373
Used chemotherapeutic agents		
Oxaliplatin	**0.013**	0.991
Irinotecan	**0.011**	0.327
Biologicals	**0.012**	0.459
Number of treated metastases	**0.013**	0.681
Maximum diamter of metastases (mm)	**0.023**	0.669
Clinical target volume (cm^3)	**0.013**	0.815
Liver volume (cm^3)	**0.018**	0.937
Interval from BT to 6 weeks FU (days)	**0.008**	0.258
Liver volume with a dose exposure >10 Gy (%)	**0.013**	0.598
Chemotherapy during follow-up	**0.015**	0.191
Bilirubin baseline	**0.030**	0.401
Albumin baseline	**0.020**	0.784
Aspartate transaminase baseline	**0.025**	0.263
Alanine transaminase baseline	**0.006**	0.092
Cholinesterase baseline	**0.013**	0.425
Gamma glutamyltransferase baseline	**0.012**	0.317
Glutamate dehydrogenase baseline	**0.011**	0.352
International normalized ratio baseline	**0.008**	0.783
Interleukin 6 baseline	**0.030**	0.401
Fibrinogen baseline	**0.002**	0.232
Factor VIII activity baseline	**0.005**	0.615
Protein C activity baseline	**0.004**	0.868
Protein S activity baseline	**0.004**	0.831
von Willebrand factor activity baseline	**0.004**	0.763
Antithrombin III activity baseline	**0.008**	0.261

*Two-way ANOVA for categorical factors, ANCOVA for metric covariables.
doi:10.1371/journal.pone.0112731.t005

that this initial approach can be justified. Although the patient numbers are small, the absence of severe toxicities acccords with experience of other published data [15,16,17,19,20,21,28].

Regarding changes of laboratory values, no clinically relevant (grade 3/4) toxicities were observed. The observed slight increases (varying over time and group) of fibrinogen, factor-VIII-activity, protein-S-activity and von-Willebrand-factor-activity correspond most likely to an unspecific increase in acute-phase proteins after radiotherapy or/and to a consequence of radiation-induced endothelial damage of the hepatic veins and sinuses with subsequent platelet aggregation. Regarding the course of liver specific laboratory paramters after BT, it might be argued that the induced fRILI was possibly too small to induce a significant overall increase of these parameters. However, the slight but significant increase of aspartate transaminase in the control group indicates a parenchymal damage. Interestingly, this increase was not seen in the treatment group, indicating a decreased parenchymal damage under preventive medication.

The primary endpoint in our analysis is based on a surrogate i.e. fRILI visualized and quantified using hepatobiliary contrast agent (Gd-EOB-DTPA)-enhanced MRI. Hepatobiliary contrast agents differ from other gadolinium chelates in that they are selectively taken up by functioning hepatocytes through an organic-anion-transporter-polypeptide (mainly OATP1B1 and 3) and excreted

into the bile by the multidrug-resistance-protein-2. For Gd-EOB-DTPA, the biliary excretion rate is approximately 50% in humans [36,37]. Regardless of the mechanism of damage to liver, the hepatobiliary contrast media in functionally altered liver parenchyma is significantly reduced [38]. This is also true for fRILI since a loss of uptake of hepatobiliary contrast media is clearly evident in the liver parenchyma adjacent to the clinical target volume after local radiotherapy (Figure 2) [6,7]. Importantly, an agreement has been found between the histopathological evidence of fRILI/VOD and loss of hepatocellular uptake of hepatobiliary contrast agent [24].

Unlike the reduced uptake of hepatobiliary contrast agents in sinusoidal-obstruction-syndrome observed after platinum-containing chemotherapy (which is reticular in geometry and generalized all over the liver) [39], the reduced uptake of hepatobiliary contrast media after BT is focal, homogenous and circumferential around the clinical target volume (Figure 1) [6,7]. Thus, we believe that we can exclude underlying sinusoidal-obstruction-syndrome as a confounder of our results. Additionally, the history of platinum-containing chemotherapy was equal between the groups and without influence on the endpoint.

We suggest that our study results can be transferred to other established radiation treatment methods of liver malignancies such as ^{90}Y-radioembolization. According to conversion calculations, the dose ranges in the liver parenchyma associated with ^{90}Y-radioembolization and BT are comparable, if re-calculated with respect to the standard fractionation. We therefore hypothesize that preventive treatment approaches against RILD/REILD should be equally effective for both ^{90}Y-radioembolization and BT.

Conclusions

In summary, our results show a highly significant reduction in fRILI after BT of colorectal liver metastases in patients who received low-dose LMWH, PTX and UDCA. Further on, we believe that these findings can be adopted for the prevention of radiation-induced liver damage after other radiotherapeutic approaches as ^{90}Y-radioembolization and that further clinical studies in this area are warranted.

Supporting Information

Table S1 ECOG, EQ5D dimensions and EQ5D VAS, baseline and follow-up; group comparison (per-protocol only).
(DOCX)

Checklist S1 Consort Checklist regarding the present study.
(DOCX)

Protocol S1 Study protocol as submitted to the competent authorities.
(PDF)

Author Contributions

Contributed to the writing of the manuscript: MS PW JR. Statistical planning and analysis: SK RD MS. Conceived and designed the experiments: MS RS RD BS JR. Performed the experiments: MS RS RD PH GG JR. Analyzed the data: MS RD KM MP RS SK. Contributed reagents/materials/analysis tools: PH GG SK.

References

1. Boda-Heggemann J, Dinter D, Weiss C, Frauenfeld A, Siebenlist K, et al. (2012) Hypofractionated image-guided breath-hold SABR (stereotactic ablative body radiotherapy) of liver metastases–clinical results. Radiation oncology 7: 92.
2. Ricke J, Mohnike K, Pech M, Seidensticker M, Ruhl R, et al. (2010) Local response and impact on survival after local ablation of liver metastases from colorectal carcinoma by computed tomography-guided high-dose-rate brachytherapy. International journal of radiation oncology, biology, physics 78: 479–485.
3. Seidensticker R, Denecke T, Kraus P, Seidensticker M, Mohnike K, et al. (2012) Matched-pair comparison of radioembolization plus best supportive care versus best supportive care alone for chemotherapy refractory liver-dominant colorectal metastases. Cardiovascular and interventional radiology 35: 1066–1073.
4. Emami B, Lyman J, Brown A, Coia L, Goitein M, et al. (1991) Tolerance of normal tissue to therapeutic irradiation. International journal of radiation oncology, biology, physics 21: 109–122.
5. Lawrence TS, Robertson JM, Anscher MS, Jirtle RL, Ensminger WD, et al. (1995) Hepatic toxicity resulting from cancer treatment. International journal of radiation oncology, biology, physics 31: 1237–1248.
6. Ricke J, Seidensticker M, Ludemann L, Pech M, Wieners G, et al. (2005) In vivo assessment of the tolerance dose of small liver volumes after single-fraction HDR irradiation. International journal of radiation oncology, biology, physics 62: 776–784.
7. Seidensticker M, Seidensticker R, Mohnike K, Wybranski C, Kalinski T, et al. (2011) Quantitative in vivo assessment of radiation injury of the liver using Gd-EOB-DTPA enhanced MRI: tolerance dose of small liver volumes. Radiation oncology 6: 40.
8. McDonald GB, Sharma P, Matthews DE, Shulman HM, Thomas ED (1985) The clinical course of 53 patients with venocclusive disease of the liver after marrow transplantation. Transplantation 39: 603–608.
9. Sangro B, Gil-Alzugaray B, Rodriguez J, Sola I, Martinez-Cuesta A, et al. (2008) Liver disease induced by radioembolization of liver tumors: description and possible risk factors. Cancer 112: 1538–1546.
10. Farthing MJ, Clark ML, Sloane JP, Powles RL, McElwain TJ (1982) Liver disease after bone marrow transplantation. Gut 23: 465–474.
11. Fajardo LF, Colby TV (1980) Pathogenesis of veno-occlusive liver disease after radiation. Archives of pathology & laboratory medicine 104: 584–588.
12. Reed GB, Jr., Cox AJ, Jr (1966) The human liver after radiation injury. A form of veno-occlusive disease. The American journal of pathology 48: 597–611.
13. Shulman HM, Gown AM, Nugent DJ (1987) Hepatic veno-occlusive disease after bone marrow transplantation. Immunohistochemical identification of the material within occluded central venules. The American journal of pathology 127: 549–558.
14. Attal M, Huguet F, Rubie H, Charlet JP, Schlaifer D, et al. (1993) Prevention of regimen-related toxicities after bone marrow transplantation by pentoxifylline: a prospective, randomized trial. Blood 82: 732–736.
15. Attal M, Huguet F, Rubie H, Huynh A, Charlet JP, et al. (1992) Prevention of hepatic veno-occlusive disease after bone marrow transplantation by continuous infusion of low-dose heparin: a prospective, randomized trial. Blood 79: 2834–2840.
16. Bianco JA, Appelbaum FR, Nemunaitis J, Almgren J, Andrews F, et al. (1991) Phase I-II trial of pentoxifylline for the prevention of transplant-related toxicities following bone marrow transplantation. Blood 78: 1205–1211.
17. Essell JH, Schroeder MT, Harman GS, Halvorson R, Lew V, et al. (1998) Ursodiol prophylaxis against hepatic complications of allogeneic bone marrow transplantation. A randomized, double-blind, placebo-controlled trial. Annals of internal medicine 128: 975–981.
18. Forrest DL, Thompson K, Dorcas VG, Couban SH, Pierce R (2003) Low molecular weight heparin for the prevention of hepatic veno-occlusive disease (VOD) after hematopoietic stem cell transplantation: a prospective phase II study. Bone marrow transplantation 31: 1143–1149.
19. Ohashi K, Tanabe J, Watanabe R, Tanaka T, Sakamaki H, et al. (2000) The Japanese multicenter open randomized trial of ursodeoxycholic acid prophylaxis for hepatic veno-occlusive disease after stem cell transplantation. American journal of hematology 64: 32–38.
20. Or R, Nagler A, Shpilberg O, Elad S, Naparstek E, et al. (1996) Low molecular weight heparin for the prevention of veno-occlusive disease of the liver in bone marrow transplantation patients. Transplantation 61: 1067–1071.
21. Ruutu T, Eriksson B, Remes K, Juvonen E, Volin L, et al. (2002) Ursodeoxycholic acid for the prevention of hepatic complications in allogeneic stem cell transplantation. Blood 100: 1977–1983.
22. Clift RA, Bianco JA, Appelbaum FR, Buckner CD, Singer JW, et al. (1993) A randomized controlled trial of pentoxifylline for the prevention of regimen-related toxicities in patients undergoing allogeneic marrow transplantation. Blood 82: 2025–2030.
23. McDonald GB, Sharma P, Matthews DE, Shulman HM, Thomas ED (1984) Venocclusive disease of the liver after bone marrow transplantation: diagnosis, incidence, and predisposing factors. Hepatology 4: 116–122.
24. Seidensticker M, Burak M, Kalinski T, Garlipp B, Koelble K, et al. (2014) Radiation-Induced Liver Damage: Correlation of Histopathology with Hepatobiliary Magnetic Resonance Imaging, a Feasibility Study. Cardiovascular and interventional radiology.

25. Wybranski C, Seidensticker M, Mohnike K, Kropf S, Wust P, et al. (2009) In vivo assessment of dose volume and dose gradient effects on the tolerance dose of small liver volumes after single-fraction high-dose-rate 192Ir irradiation. Radiation research 172: 598–606.
26. Shulman HM, Hinterberger W (1992) Hepatic veno-occlusive disease–liver toxicity syndrome after bone marrow transplantation. Bone marrow transplantation 10: 197–214.
27. Lakshminarayanan S, Sahdev I, Goyal M, Vlachos A, Atlas M, et al. (2010) Low incidence of hepatic veno-occlusive disease in pediatric patients undergoing hematopoietic stem cell transplantation attributed to a combination of intravenous heparin, oral glutamine, and ursodiol at a single transplant institution. Pediatric transplantation 14: 618–621.
28. Park SH, Lee MH, Lee H, Kim HS, Kim K, et al. (2002) A randomized trial of heparin plus ursodiol vs. heparin alone to prevent hepatic veno-occlusive disease after hematopoietic stem cell transplantation. Bone marrow transplantation 29: 137–143.
29. Lee JH, Lee KH, Kim S, Lee JS, Kim WK, et al. (1998) Relevance of proteins C and S, antithrombin III, von Willebrand factor, and factor VIII for the development of hepatic veno-occlusive disease in patients undergoing allogeneic bone marrow transplantation: a prospective study. Bone marrow transplantation 22: 883–888.
30. Catani L, Gugliotta L, Vianelli N, Nocentini F, Baravelli S, et al. (1996) Endothelium and bone marrow transplantation. Bone marrow transplantation 17: 277–280.
31. Geraci JP, Mariano MS (1993) Radiation hepatology of the rat: parenchymal and nonparenchymal cell injury. Radiation research 136: 205–213.
32. Kowdley KV (2000) Ursodeoxycholic acid therapy in hepatobiliary disease. The American journal of medicine 108: 481–486.
33. Neuman MG, Shear NH, Bellentani S, Tiribelli C (1998) Role of cytokines in ethanol-induced cytotoxicity in vitro in Hep G2 cells. Gastroenterology 115: 157–166.
34. Lindner H, Holler E, Ertl B, Multhoff G, Schreglmann M, et al. (1997) Peripheral blood mononuclear cells induce programmed cell death in human endothelial cells and may prevent repair: role of cytokines. Blood 89: 1931–1938.
35. Rodrigues CM, Fan G, Ma X, Kren BT, Steer CJ (1998) A novel role for ursodeoxycholic acid in inhibiting apoptosis by modulating mitochondrial membrane perturbation. The Journal of clinical investigation 101: 2790–2799.
36. Pascolo L, Cupelli F, Anelli PL, Lorusso V, Visigalli M, et al. (1999) Molecular mechanisms for the hepatic uptake of magnetic resonance imaging contrast agents. Biochemical and biophysical research communications 257: 746–752.
37. Schuhmann-Giampieri G, Schmitt-Willich H, Press WR, Negishi C, Weinmann HJ, et al. (1992) Preclinical evaluation of Gd-EOB-DTPA as a contrast agent in MR imaging of the hepatobiliary system. Radiology 183: 59–64.
38. Watanabe H, Kanematsu M, Goshima S, Kondo H, Onozuka M, et al. (2011) Staging hepatic fibrosis: comparison of gadoxetate disodium-enhanced and diffusion-weighted MR imaging–preliminary observations. Radiology 259: 142–150.
39. Shin NY, Kim MJ, Lim JS, Park MS, Chung YE, et al. (2012) Accuracy of gadoxetic acid-enhanced magnetic resonance imaging for the diagnosis of sinusoidal obstruction syndrome in patients with chemotherapy-treated colorectal liver metastases. European radiology 22: 864–871.

Strahlenther Onkol (2019) 195:265–273
https://doi.org/10.1007/s00066-018-1404-1

ORIGINAL ARTICLE

Biliary duct stenosis after image-guided high-dose-rate interstitial brachytherapy of central and hilar liver tumors

A systematic analysis of 102 cases

Maciej Powerski[1] · Susanne Penzlin[1] · Peter Hass[2] · Ricarda Seidensticker[3] · Konrad Mohnike[4] · Robert Damm[1] · Ingo Steffen[5] · Maciej Pech[1] · Günther Gademann[2] · Jens Ricke[3] · Max Seidensticker[3]

Received: 17 July 2018 / Accepted: 13 November 2018 / Published online: 23 November 2018

Abstract

Objective Image-guided high-dose-rate interstitial brachytherapy (iBT) with iridium-192 is an effective treatment option for patients with liver malignancies. Little is known about long-term radiation effects on the bile duct system when central hepatic structures are exposed to iBT. This retrospective analysis investigates the occurrence of posthepatic cholestasis (PHC) and associated complications in patients undergoing iBT.

Materials and methods We identified patients who underwent iBT of hepatic malignancies and had point doses of ≥1 Gy to central bile duct structures. Patients with known bile duct-related diseases or prior bile duct manipulation were excluded.

Results 102 patients were retrospectively included. Twenty-two patients (22%) developed morphologic PHC after a median of 17 (3–54) months; 18 of them were treated using percutaneous transhepatic cholangiopancreatography drainage or endoscopic retrograde cholangiopancreatography. The median point dose was 24.8 (4.4–80) Gy in patients with PHC versus 14.2 (1.8–61.7) Gy in those without PHC ($p = 0.028$). A dose of 20.8 Gy (biological effective dose, $BED_{3/10} = 165/64.1$ Gy) was identified to be the optimal cutoff dose ($p = 0.028$; 59% sensitivity, 24% specificity). Abscess/cholangitis was more common in patients with PHC compared to those without (4 of 22 vs. 2 of 80; $p = 0.029$). Median survival did not differ between patients with and without PHC (43 vs. 36 months; $p = 0.571$).

✉ Maciej Powerski, MD
maciej.powerski@med.ovgu.de

Susanne Penzlin, MD
s.penzlin@web.de

Peter Hass, MD
peter.hass@med.ovgu.de

Ricarda Seidensticker, MD
ricarda.Seidensticker@med.uni-muenchen.de

Konrad Mohnike, MD
konrad.mohnike@berlin-dtz.de

Robert Damm, MD
robert.damm@med.ovgu.de

Ingo Steffen, MD
ingo.steffen@charite.de

Maciej Pech, MD
maciej.pech@med.ovgu.de

Günther Gademann, MD
guenther.gademann@med.ovgu.de

Jens Ricke, MD
jens.ricke@med.uni-muenchen.de

Max Seidensticker, MD
max.Seidensticker@med.uni-muenchen.de

[1] Klinik für Radiologie und Nuklearmedizin, Otto-von-Guericke University, Leipziger Straße 44, 39120 Magdeburg, Germany

[2] Klinik für Strahlentherapie, Otto-von-Guericke University, Leipziger Straße 44, 39120 Magdeburg, Germany

[3] Klinik und Poliklinik für Radiologie, Klinikum der Universität München, Marchioninistraße 15, 81377 München, Germany

[4] Diagnostisch Therapeutisches Zentrum Berlin, Kadiner Straße 23, 10243 Berlin, Germany

[5] Klinik für Nuklearmedizin, Charité Universitätsmedizin Berlin, Campus Virchow Klinikum, Augustenburger Platz 1, 13353 Berlin, Germany

Conclusion iBT of liver malignancies located near the hilum can cause PHC when the central bile ducts are exposed to high point doses. Given the long latency and absence of impact of iBT-induced PHC on median survival, the rate of cholestasis and complications seen in our patients appears to be acceptable.

Keywords Local ablation · Interstitial brachytherapy · Bile duct stenosis · Extrahepatic cholestasis · Central and hilar liver tumors

Gallengangstenosen nach bildgeführter interstitieller Hochdosis-Brachytherapie zentraler und hilusnaher Lebertumore

Eine systematische Analyse von 102 Fällen

Zusammenfassung

Zielsetzung Die bildgestützte interstitielle Hochdosis-Brachytherapie (iBT) mit Iridium-192 ist eine effektive Methode zur Ablation hepatischer Malignome. Unklar ist die Langzeitauswirkung auf das Gallengangsystem bei Bestrahlung zentraler Leberstrukturen. Die vorgestellte retrospektive Studie eruiert den Einfluss der iBT auf die Entstehung posthepatischer Cholestasen (PHC) und vergesellschafteter Komplikationen.

Material und Methoden Eingeschlossen wurden Patienten mit iBT hepatischer/hilusnaher Malignome mit Punktdosen ≥1 Gy an zentralen Gallengangstrukturen. Ausschlusskriterien waren gallengangassoziierte Erkrankungen oder vorherige Manipulationen an den Gallenwegen.

Ergebnisse In die Studie konnten 102 Patienten eingeschlossen werden. Von diesen entwickelten 22 (22 %) nach im Median 17 Monaten (Spanne 3–54 Monate) eine morphologische PHC, die in 18 Fällen (18 %) mit perkutaner transhepatischer Cholangiodrainage oder endoskopischer retrograder Cholangiopankreatikographie abgeleitet werden musste. Die Punktdosis der Patienten mit PHC lag im Median bei 24,8 Gy (Spanne 4,4–80 Gy), derjenigen ohne PHC bei 14,2 Gy (Spanne 1,8–61,7 Gy; $p = 0{,}028$). Bei 20,8 Gy (biologische effektive Dosis, $BED_{3/10} = 165/64{,}1$ Gy) konnte ein optimaler Cut-off-Wert (Schwellendosis) ermittelt werden ($p = 0{,}028$; Sensitivität 59 %, Spezifität 24 %). Abszesse/Cholangitiden traten bei Patienten mit PHC signifikant häufiger auf als ohne (4 von 22 vs. 2 von 80; $p = 0{,}029$). Im medianen Überleben zwischen Patienten mit und ohne PHC zeigte sich kein Unterschied (43 vs. 36 Monate; $p = 0{,}571$).

Schlussfolgerung Die iBT hilusnaher Lebertumore kann bei hohen Punktdosen an zentralen Gallengängen zu einer klinisch relevanten PHC führen. In Anbetracht der langen Latenzzeit und der fehlenden Auswirkung iBT-assoziierter PHC auf das mediane Überleben halten wir die ermittelte Rate an Strikturen und Komplikationen für akzeptabel.

Schlüsselwörter Lokale Ablation · Interstitielle Brachytherapie · Gallangangsstenose · Extrahepatische Cholestase · Zentrale und hilusnahe Lebertumore

Introduction

Treatment of hepatic malignancies located centrally or near the hilum continues to be a clinical challenge regardless of the tumor entity [1, 2]. The natural history of such lesions is characterized by obstructive bile duct complications and reduced overall survival [3]. For most types of malignant liver lesion, the effect of systemic treatments is moderate and/or short. Moreover, for technical, oncologic, or medical reasons, most patients with central or hilar liver tumors are not candidates for surgery [1–4]. Local thermal ablation techniques such as radiofrequency ablation (RFA) or microwave ablation are limited by reduced effectiveness due to the heat-sink effect near large blood vessels in the hilar region and a high rate of bile duct-related complications (up to 46%) [5, 6]. Other thermal approaches such as cryoablation, while having low biliary toxicity in animal experiments, have been shown to achieve only moderate local tumor control in the clinical setting [7, 8].

Radiotherapy, applied either percutaneously or interstitially (as catheter-based radiotherapy, iBT), has evolved into an effective and also safe local therapy for central liver tumors [9, 10]. Safety data derive mainly from theoretic estimates and observational case series [11]. However, there is evidence of varying strength to support the assumption that even significant radiation exposure will not have an effect on the main bile ducts: Collettini et al. reported one biliary complication (biliary abscess in a pancreatic cancer patient with hepaticojejunostomy) after catheter-based radiotherapy of 34 central liver metastases from various primaries (target dose of 15–20 Gy) located within 5 mm of the common bile duct or hepatic bifurcation. A remarkable local control rate of 88.2% was achieved during a mean follow-up of 18.75 months [9]. Comparable results were

published by Ricke et al. after catheter-based radiotherapy of 20 central lesions in unfavorable location for RFA. They achieved a local control rate of up to 93% after 12 months and saw only one biliary complication (transient obstructive jaundice) [10]. Data on radiation exposure of the main bile ducts were not provided in these two studies. Studies of percutaneous radiotherapy of liver tumors typically focus on efficacy and rarely investigate the relationship between radiation exposure and biliary duct complications. Two studies of hepatobiliary adverse events after stereotactic body radiation therapy (SBRT) reported an overall rate of 18.8–26% of ≥ grade 3 toxicities according to CTCAE v4.03 [12] (including lab values) for the treatment of hepatic tumors in any location. Unfortunately, these studies did not provide satisfactory data on dose-related bile duct vulnerability [13, 14].

To the best of our knowledge, systematic clinical trials including dosimetric analysis of the radiation sensitivity of central bile ducts are currently not available. Therefore, we retrospectively identified 102 patients who underwent image-guided high-dose-rate interstitial brachytherapy (iBT) for liver malignancies located centrally or near the hilum to systematically analyze the occurrence of stenotic cholestasis and related complications and the impact on outcome and survival. The aim was to identify a safe cutoff dose for radiation exposure of biliary structures. To allow comparison of the doses identified in our study with doses published for fractionated radiotherapy regimens, we converted relevant doses to biological effective doses (BED) using the linear quadratic formula published by Fowler in 1989 [15, 16].

Materials and methods

Patient population

Patients who underwent image-guided high-dose-rate interstitial brachytherapy (iBT) of hepatic malignancies located centrally or near the hilum were retrospectively identified for inclusion in this retrospective analysis when they had a point dose of at least 1 Gy to a central bile duct. For the purpose of this analysis, the central bile ducts included all bile ducts that were clearly visible in computed tomography (CT) and magnetic resonance imaging (MRI) datasets obtained before radiotherapy for diagnosis and planning (common hepatic duct [CHD], left and right bile duct, and visible first-order branches). Exclusion criteria were bile duct malignancy, cancer of unknown primary (CUP) syndrome, primary sclerosing/chronic cholangitis, and status post biliary manipulation (liver transplant, papillary splitting, bile duct stenting, biliodigestive anastomosis), prior radiotherapy of the liver, no follow-up, and low point dose

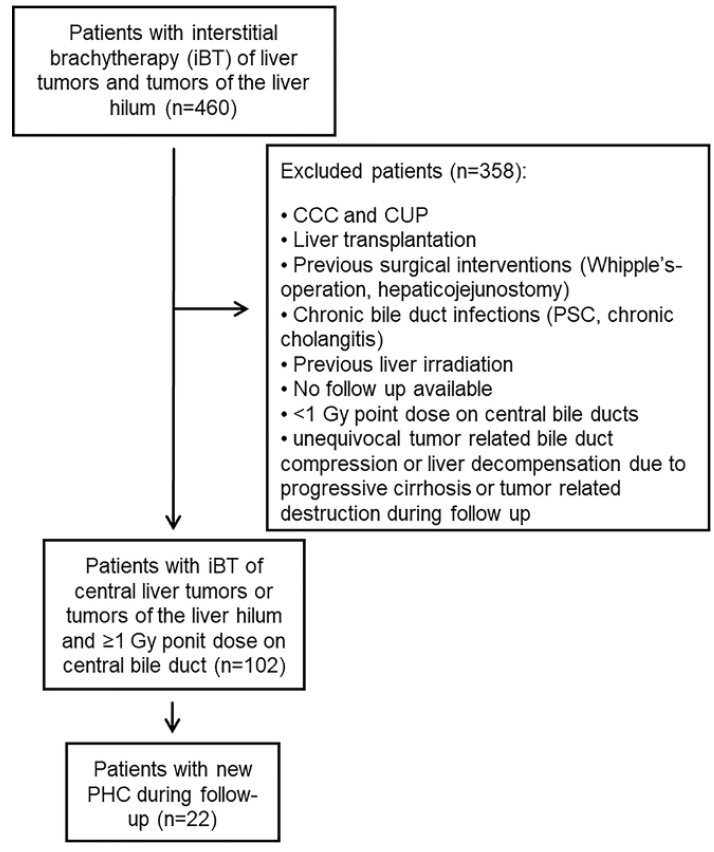

Fig. 1 Consort diagram of inclusion and exclusion criteria and the final study population. *CCC* cholangiocellular carcinoma, *CUP* cancer of unknown primary, *PSC* primary sclerosing cholangitis, *PHC* post-hepatic cholestasis

of <1 Gy to central bile ducts (Fig. 1). The indication for iBT was established by an interdisciplinary tumor board. Criteria were nonresectable malignant liver lesion (unfavorable location, poor liver function, small liver remnant), medical/oncologic contraindication to surgery, and patient refusal of surgery. Our retrospective analysis was approved by the local ethics committee.

Intervention/iBT catheter placement

The technique of image-guided placement of the catheters for iBT has been described before [17, 18]. In brief, the catheters were placed using CT fluoroscopy (Aquilion Prime, Toshiba, Japan) or in an open MRI scanner (1.0 T Panorama HFO, Philips Healthcare, Best, The Netherlands). Following puncture of the target lesion with an 18-G coaxial needle, a stiff angiography wire (Amplatz, Boston Scientific, Boston, MA, USA, for CT interventions or Radiofocus Guide Wire Stiff Type, Terum, Tokyo, Japan, for MR interventions) was introduced for placement of a 6-F introducer sheath (Radiofocus, Terumo) in Seldinger technique, through which the brachytherapy catheter (Nucletron, Elektra AB, Stockholm, Sweden) was inserted. For radiotherapy planning, catheter placement was followed by

contrast-enhanced CT (Immeron 300, Braco, Milano, Italy; 2 ml/kg body weight, maximum dose of 150 ml, delay of 120s, 3 mm slice thickness) or MRI (T1-weighted 3D turbo field echo sequences). Sedation, analgesia, and monitoring of the patients and removal of brachytherapy catheters were performed as described by Ricke et al. [17].

Radiation properties, treatment planning

Radiotherapy was planned using Oncentra software (Nucletron, Elektra AB, Stockholm, Sweden). First, the clinical target volume was delineated in the planning CT/MRI dataset in a slice-by-slice fashion. Next, the relative coordinates (x, y, z) of the catheter tips in relation to the tumor margin were transferred to the planning system. The anticipated minimum D99.9 per clinical target volume was a single dose of 15–25 Gy, depending on the tumor type [19, 20], and was adjusted to spare structures at risk (threshold dose of 15 Gy/ml for stomach and duodenum) [21]. The high-dose-rate (HDR) afterloading system used in our study (Nucletron, Elektra AB, Stockholm, Sweden) has an iridium-192 source with a nominal activity of 10 Ci. To identify patients eligible for our analysis, we outlined the contours of the central bile ducts (i. e., ducts clearly visible on pretherapeutic and planning imaging) and the Oncentra software calculated the maximum bile duct point dose (Gy) for each individual. To ensure comparability with published data, doses are additionally provided as biological effective doses (BED), which were calculated using the linear square model [15, 16]. BED were calculated for $\alpha/\beta = 3$ (late-responding tissues, abbreviated to BED_3) and $\alpha/\beta = 10$ (early-responding tissues, abbreviated to BED_{10}).

Follow-up

After iBT, all patients underwent follow-up MRI of the liver at 3-month intervals. Minimum requirement for the MRI protocol included T2-weighted sequences with and without fat saturation, T1-weighted sequences before and during gadolinium contrast agent administration (dynamic sequences), and—if performed at our hospital—T1-weighted sequences acquired 20 min after IV administration of 0.1 ml/kg Gd-EOB-DTPA (Primovist, Bayer, Leverkusen, Germany). Patients with contraindications to MRI underwent abdominal CT scans with three-phase liver imaging after IV contrast (at our hospital: Imeron 300; 2 ml/kg, maximum dose of 150 ml; Bracco, Milan, Italy) administration. In addition, follow-up included clinical examinations with documentation of adverse effects, serology, hematology, and liver function parameters: aspartate transaminase (AST), alanine transaminase (ALT), alkaline phosphatase (AL), gamma-glutamyltransferase (GGT), bilirubin, albumin, and clotting.

Definition of posthepatic cholestasis

New-onset posthepatic cholestasis was diagnosed when there was bile duct dilatation peripheral to the site of maximum radiation exposure. Dilatation was assumed when the bile duct diameter was over 5 mm or when there was an increase in diameter of at least 2 mm on follow-up CT or MRI compared with the pretherapeutic diameter. Patients with a concomitant first-time bilirubin level above 21 µmol/l (>1.2 mg/dl) were treated using percutaneous transhepatic cholangiopancreatography drainage/endoscopic retrograde cholangiopancreatography (PTCD/ERCP). Patients with disease progression leading to unequivocal tumor-related bile duct compression as well as patients with liver decompensation (e. g., due to progressive cirrhosis or tumor-related liver parenchyma destruction) were secondarily excluded from the analysis.

Statistical analysis

All study data were compiled retrospectively. Statistical analysis was performed using SPSS version 24 (IBM, Armonk, NY, USA). The group comparisons presented in Table 1 were conducted using either Fischer's exact test, the U test, or the log-rank test. The Kaplan–Meier method was used to calculate overall survival rates. Receiver operating characteristic (ROC) curve analysis was performed to identify an optimal radiation dose cutoff. Statistical significance was assumed at p-values <0.05.

Results

We identified 460 patients who underwent iBT of primary or secondary liver malignancies at our department from 2007 through 2014; 102 of them met our criteria and were included in this retrospective analysis (Fig. 1 and Materials and Methods). Median follow-up of all enrolled individuals was 31 months (range 3–69). Twenty-two patients (22%) developed PHC distal to radiation-exposed bile ducts after a median of 17 months (range 3–54). In these 22 patients, PHC was apparent on CT or MRI, and 18 of them had increased bilirubin levels and underwent PTCD or ERCP for drainage of bile (Table 1). Fig. 2 shows an example of PHC after iBT of metastatic lymph nodes near the hilum.

There were six instances of abscess or cholangitis in the total study population (6%). This complication was significantly more common in patients with PHC than in those without (4 of 22 [18%] vs. 2 of 80 [3%]; $p = 0.029$). No effect of PHC or its complications on median survival (43_{PHC} vs. $36_{no\ PHC}$ months; $p = 0.571$) or on the course of survival curves (Fig. 3) was noted.

Table 1 Patients with iBT of central liver tumors and tumors of the liver hilum

	Enrolled patients, $n = 102$		*p*-value
	PHC during follow-up $n = 22$ (22%)	No PHC during follow-up $n = 80$ (78%)	
Male/female (*n*)	11/11	50/30	0.689
Age (years; median; range)	69 (50–84)	66 (35–89)	0.625
Tumor entity (n)			
Colorectal cancer	11	36	0.834
Hepatocellular carcinoma	4	25	0.437
Breast cancer	2	12	0.731
Other ($n \leq 3$)	5	7	0.152
Liver (n)			
Steatosis	3	5	0.379
Cirrhosis	5	22	1.000
Cholecystectomy	12	19	0.064
Bilirubin (µmol/l) before iBT[a]	8.1 (4.9–30.9)	7.9 (2.8–40.4)	0.935
Additional treatment (n)			
Previous chemotherapy	18	53	0.586
Chemotherapy during FU	12	43	1.000
Ablation/Embolization during FU	3	17	0.763
Dosimetric calculation (Gy)			
Point dose[a]	24.8 (4.4–80)	14.2 (1.8–61.7)	*0.028
Point dose BED_3[a,b]	229.8 (10.9–2213.3)	81.4 (2.9–1330.7)	n.a.
Point dose BED_{10}[a,b]	86.3 (6.3–720)	34.4 (2.1–442.4)	n.a.
Optimal cutoff	20.8	–	–
Optimal cutoff BED_3[b]	165	–	–
Optimal cutoff BED_{10}[b]	64.1	–	–
Further characteristics			
Follow-up after iBT (months)[a]	31 (3–69)	26 (3–73)	0.456
Time between iBT and PHC (months)[a]	17 (3–54)	–	–
PHC in CT/MRI only (*n*)	4 (18%)	–	–
PHC requiring ERCP/PTCD (*n*)	18 (82%)	–	–
Bilirubin when PHC was detected (µmol/l)[a]	42.7 (4.7–370.8)	–	–
Abscess/cholangitis (*n*)	4 (18%)	2 (3%)	*0.029
Median survival (month)	43	36	0.571

[a]median (range)
[b]calculated dose
*statistically significant *p*-value
PHC posthepatic cholestasis, *CT* computed tomography, *MRI* magnetic resonance imaging, *ERCP* endoscopic retrograde cholangiopancreatography, *PTCD* percutaneous transhepatic cholangiography drainage, *BED* biological effective dose, *BED_3* BED calculation for $\alpha/\beta = 3$ (late responding tissues), *BED_{10}* BED calculation for $\alpha/\beta = 10$ (early responding tissues)

The median point dose to central bile ducts was 24.8 (4.4–80) Gy in patients with PHC versus 14.2 (1.8–61.7) Gy in those without PHC ($p = 0.028$; see Table 1 for BED). ROC analysis ($p = 0.028$) identified 20.8 Gy as the optimal cutoff ($BED_{3/10} = 165/64.1$ Gy; 59% sensitivity, 24% specificity; Fig. 4).

Comparability of the two groups was tested for sex, age, liver disease, gallbladder resection, baseline bilirubin level, and prior ablation and systemic therapies: no significant differences were identified (Table 1).

Discussion

The results presented here suggest that the risk of radiation-induced bile duct stenosis increases with the point dose to which structures-at-risk are exposed. In our analysis, patients who developed cholestasis after iBT had a significantly higher point dose exposure of central bile ducts than patients without PHC. Nevertheless, there is scatter and overlap in point doses between the two groups, resulting in poor discriminatory power despite a significant area under the curve (AUC) in ROC analysis. The best

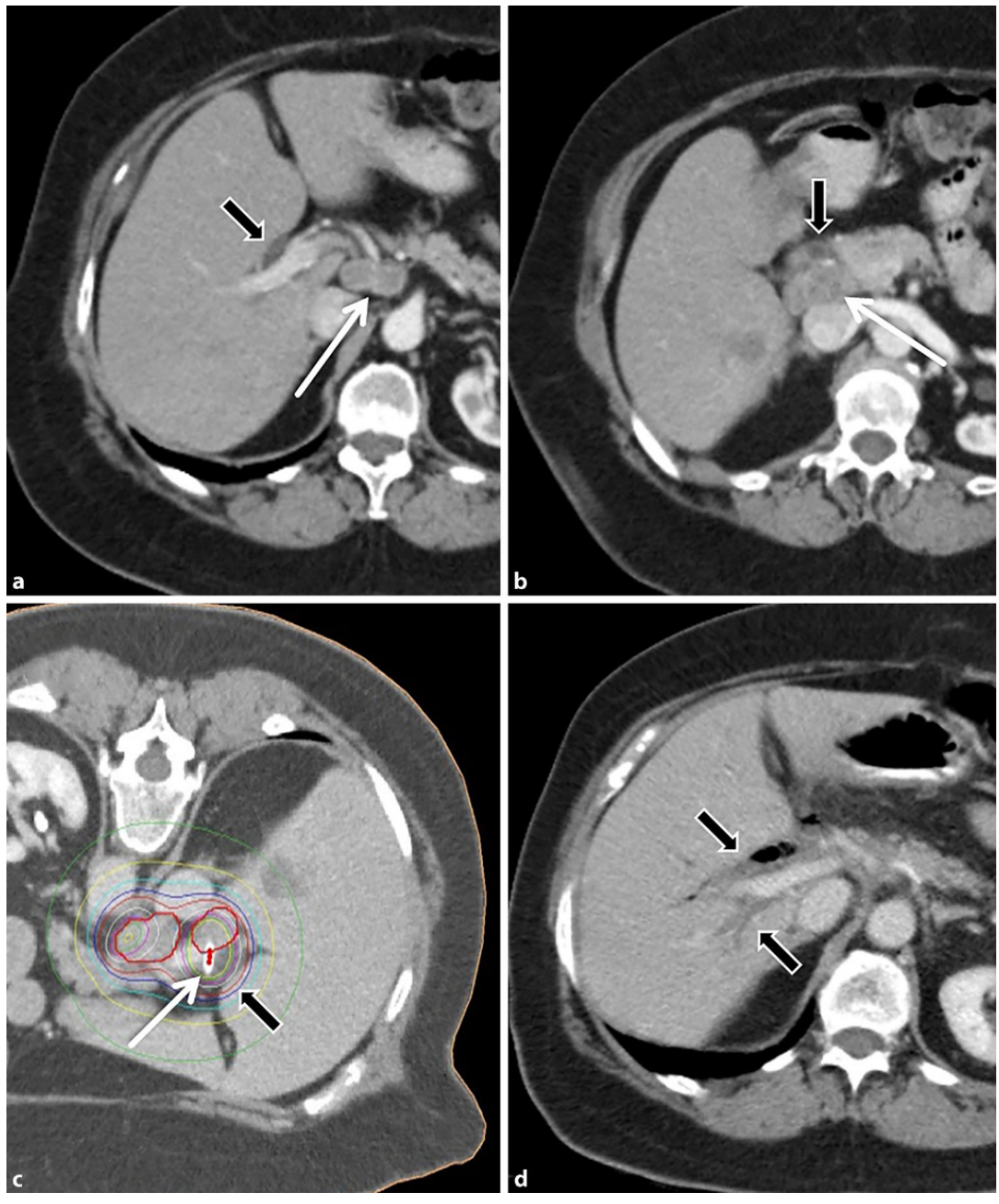

Fig. 2 Example of posthepatic cholestasis after image-guided high-dose-rate interstitial brachytherapy (iBT). **a**, **b** *Black arrows* indicate the course of the right bile duct (**a**) and of the choledochal duct (**b**). *White arrows* indicate lymph node metastases from colorectal cancer with hepatic metastatic spread. **c** Irradiation planning with isodoses. Brachytherapy catheters were advanced into the lymph nodes (*white arrow*) with the patient in prone position. The 25 Gy isodose cuts across the right bile duct (*black arrow*). **d** 12 months after iBT, the patient developed right-hepatic cholestasis (*black arrows*) which was successfully treated by endoscopic retrograde cholangiopancreaticography and metal stent placement (aerobilia)

cutoff (threshold dose) based on our results turned out to be 20.8 Gy ($BED_{3/10}$ = 165/64.1 Gy); however, this cutoff has only 59% sensitivity, and 41% of patients with PHC had a dose below 20.8 Gy. Calculations predict that if the threshold dose identified here is not exceeded, the rather high PHC rate of 22% should drop to approximately 9%. While only few data are available in the literature on biliary dosimetry, the available data at least allow a plausibility check of the threshold dose identified in our analysis. Tselis et al. treated 59 central liver tumors in 41 patients using iBT [22]. The total dose was applied in four fractions (4 × 8 Gy=32 Gy; $BED_{3/10}$ = 117.3/57.6 Gy; 19 patients) or as a single dose (1 × 14 Gy; $BED_{3/10}$ = 79.3/33.6 Gy, 22 patients). No biliary toxicity was observed by Tselis et al. during a median follow-up period of 12.4 months. In a study of 50 patients who underwent stereotactic body radiation therapy (SBRT), Eriguchi et al. reported one case of cholestasis 12 months after the last radiotherapy session [23]. In this patient, overlapping fields in metachronic treatment of two lesions, each with 5 × 8 Gy = 40 Gy, resulted in a total dose of 10 × 8 Gy = 80 Gy ($BED_{3/10}$ = 293.33/144 Gy) in the area where the patient later developed bile duct stenosis. None of the 14 patients with a biliary dose of 5 × 8 Gy = 40 Gy ($BED_{3/10}$ = 146.7/72 Gy) or any of the remaining patients with lower doses developed any symptoms during a median follow-up period of 18.2 months. The results of both studies allow derivation of presumably safe dose levels (Tselis et al.: $BED_{3/10}$ = 117.3/57.6 Gy; Erigutchi et al.: $BED_{3/10}$ = 146.7/72 Gy—no PHC in either study) for the central bile ducts which are approximately on the order of the cutoff identified in our study ($BED_{3/10}$ = 165/64.1 Gy; 9 PHC in 102 patients). The fact that no cholestasis was

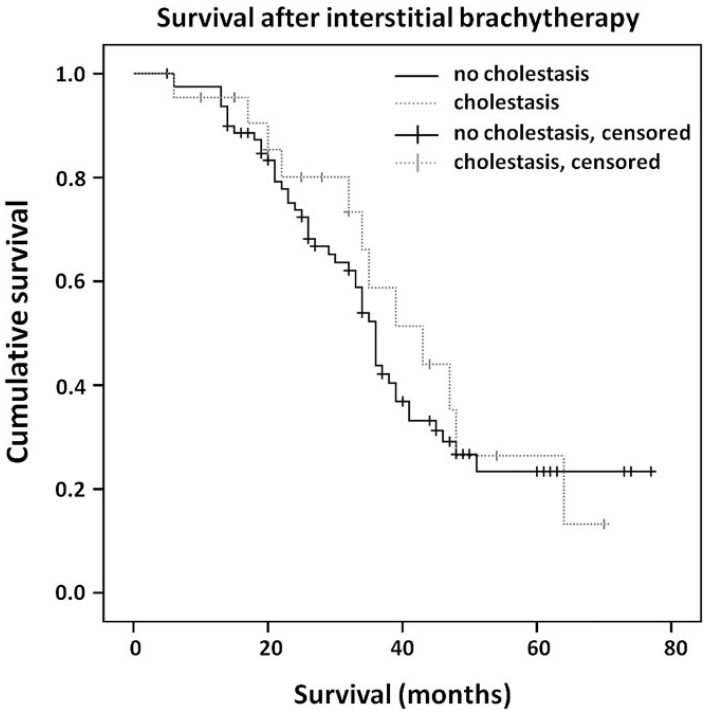

Fig. 3 Comparison of survival curves of patients with posthepatic cholestasis (PHC; *interrupted gray line*; $n=22$) and patients without PHC (*black line*; $n=80$) following image-guided high-dose-rate brachytherapy of central or hilar malignant liver lesions ($p=0.571$)

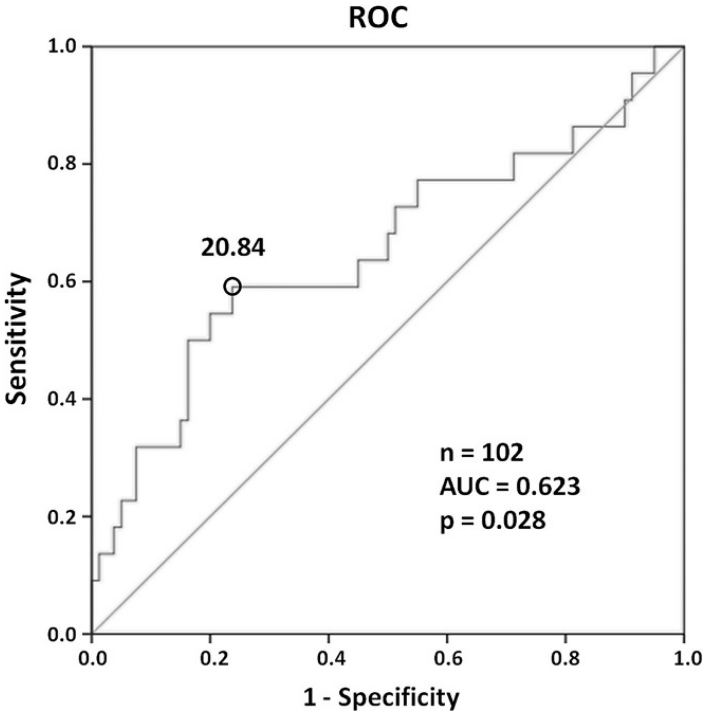

Fig. 4 Receiver operating characteristic (ROC) curve analysis for determining the optimal cutoff dose (in Gy) tolerated by the central bile ducts without the risk of inducing cholestasis. *AUC* area under the curve

observed by either Tselis et al. or Eriguchi et al. might be attributable to the short follow-up (12.4 and 18.2 months, respectively), especially in light of the observation that it took a median of 17 months (range 3–54) before bile duct stenoses occurred in our patient population. Overall, though, we think that the results derived from the two studies just quoted are consistent with the threshold dose determined in our study, at the same time confirming that our dose is plausible. Threshold dose volumes of the central biliary tract after SBRT were also evaluated by Osmundson et al. and Toesca et al. [13, 14]. However, these investigators primarily assessed the predictive power of dose exposure for the occurrence of hepatobiliary grade 2+ and 3+ toxicity, and their data say little about the radiation vulnerability of central bile ducts. Osmundson et al., for instance, show that irradiation of an area >21 cm^3 with 72 Gy_{BED10} or of >24 cm^3 with 66 Gy_{BED10} of a volume defined as the central biliary tract significantly increases the likelihood of grade 3+ hepatobiliary toxicities. It is not clear from the article how many instances of toxicity were attributable to obstructive cholestasis developing in patients with radiation doses above this threshold. Moreover, the 13 PHCs in the 96 study patients were nearly exclusively observed in patients with cholangiocellular carcinoma (11 PHC in 20 CCA patients). In these cases, PHC may not be attributable to radiation damage alone.

Biliary congestion is among the most common causes of spontaneous cholangitis and biliogenic abscess [24]. The results in our population are consistent with this pathomechanism, as we typically observed complications in patients with PHC. Rapid management of cholestasis (ERCP/PTCD plus stenting as needed), IV antibiotic treatment, and transcutaneous abscess drainage are the therapeutic measures of first choice and can reduce the mortality rate of acute cholangitis far below 5% [25]. This explains the absence of a difference in median survival or the total survival curve between patients with and without PHC in our population (Fig. 3). The fact that it takes a median of 17 months before bile duct stenosis becomes apparent has important implications in a population mostly including patients with a reduced life expectancy due to their underlying conditions such as hepatocellular (HCC) and colorectal cancer (CRC). Patients with HCC considered for ablation generally have a poor BCLC A or good BCLC B stage of disease, with a median survival of 20 to 60 months [26]. Patients with hepatic metastasis from CRC are typically awaiting second- or third-line chemotherapy and have a median survival of approximately 11 months [27]. Thus, the remaining life expectancy, in conjunction with the radiosensitivity of the target lesions in the liver (HCC: local control >90% after >12 months for iBT with 15 Gy [20]; CRC: >80% local control after >40 months for irradiation with 25 Gy [19]), justifies the application of an ablative radiation dose

in most cases. For instance, when the dose of D100 15 Gy is adhered to in patients with HCC, only poor catheter positioning will lead to point doses to the bile ducts that exceed the threshold dose of 20.8 Gy identified here. Options in patients with central metastasis from CRC include administration of a lower dose (local control on the order of 60–80% for 20 Gy after 12 months [19]) and/or use of more ablation catheters to achieve a steeper decrease in dose at the border. Furthermore, it should be noted that for selected cases, a fractionated regime can be considered (to reduce BED_3), were ablation catheters stay in place and irradiation is repeated, e. g., twice a day. However, this demands a strict organization and a great amount of discipline from the patient to lay still for a time span of 1–2 days (2–4 fractions). When life expectancy is shorter than the time it takes for stenotic complications to develop, the biliary threshold dose can be ignored. Consequently, the overall clinical situation must be considered to decide on the best approach for each patient. Finally, it should be pointed out here that despite high bile duct exposure in some of the patients and related complications in our study population, median overall survival was high at 43 months with PHC and 36 months without PHC. Such survival rates are difficult to achieve without local ablation, given the mechanical complications (portal vein and bile duct compression) facing patients with central liver tumors.

Our study has some limitations including the retrospective design and the fact that it is a single-center analysis. The threshold dose we determined here might be affected, for example, by scar formation with bile duct narrowing following iatrogenic injury of the bile ducts during ablation catheter placement. Note also that we did not include patients with cholangiocellular carcinoma and/or chronic bile duct disease (or chronic pathogen colonization of bile ducts after surgical or other medical manipulation). Therefore, it remains open whether our results also apply in patients with prior damage or diseases of the bile ducts.

Conclusion

In conclusion, our findings suggest that in most patients, the radiation sensitivity of central bile ducts does not limit image-guided interstitial high-dose-rate brachytherapy of malignant liver lesions located centrally or in the hilar area. While there is a dose-dependent vulnerability of central bile ducts, the threshold dose identified in our analysis is high, and there is a long median interval before patients are likely to develop posthepatic cholestasis. In addition, with adequate laboratory and radiologic follow-up and timely intervention, bile duct-related complications have no effect on median survival.

Conflict of interest M. Powerski, S. Penzlin, P. Hass, R. Seidensticker, K. Mohnike, R. Damm, I. Steffen, M. Pech, G. Gademann, J. Ricke, and M. Seidensticker declare that they have no competing interests.

References

1. Kuo I-M, Huang S-F, Chiang J-M et al (2015) Clinical features and prognosis in hepatectomy for colorectal cancer with centrally located liver metastasis. World J Surg Oncol 13:92. https://doi.org/10.1186/s12957-015-0497-6
2. Schmoll HJ, Van Cutsem E, Stein A et al (2012) ESMO consensus guidelines for management of patients with colon and rectal cancer. A personalized approach to clinical decision making. Ann Oncol 23:2479–2516. https://doi.org/10.1093/annonc/mds236
3. Fukasawa M, Takano S, Shindo H et al (2017) Endoscopic biliary stenting for unresectable malignant hilar obstruction. Clin J Gastroenterol 10:485–490. https://doi.org/10.1007/s12328-017-0778-4
4. Cho Y, Kim TH, Seong J (2017) Improved oncologic outcome with chemoradiotherapy followed by surgery in unresectable intrahepatic cholangiocarcinoma. Strahlenther Onkol 193:620–629. https://doi.org/10.1007/s00066-017-1128-7
5. Kim Y, Rhim H, Cho OK et al (2006) Intrahepatic recurrence after percutaneous radiofrequency ablation of hepatocellular carcinoma: analysis of the pattern and risk factors. Eur J Radiol 59:432–441. https://doi.org/10.1016/j.ejrad.2006.03.007
6. Ohnishi T, Yasuda I, Nishigaki Y et al (2008) Intraductal chilled saline perfusion to prevent bile duct injury during percutaneous radiofrequency ablation for hepatocellular carcinoma. J Gastroenterol Hepatol 23:e410–e415. https://doi.org/10.1111/j.1440-1746.2007.05091.x
7. Kahlenberg MS, Volpe C, Klippenstein DL et al (1998) Clinicopathologic effects of cryotherapy on hepatic vessels and bile ducts in a porcine model. Ann Surg Oncol 5:713–718
8. Huang Y-Z, Zhou S-C, Zhou H, Tong M (2013) Radiofrequency ablation versus cryosurgery ablation for hepatocellular carcinoma: a meta-analysis. Hepatogastroenterology 60:1131–1135. https://doi.org/10.5754/hge121142
9. Collettini F, Singh A, Schnapauff D et al (2013) Computed-tomography-guided high-dose-rate brachytherapy (CT-HDRBT) ablation of metastases adjacent to the liver hilum. Eur J Radiol 82:e509–e514. https://doi.org/10.1016/j.ejrad.2013.04.046
10. Ricke J, Wust P, Wieners G et al (2004) Liver malignancies: CT-guided interstitial brachytherapy in patients with unfavorable lesions for thermal ablation. J Vasc Interv Radiol 15:1279–1286. https://doi.org/10.1097/01.RVI.0000141343.43441.06
11. Grimm J, LaCouture T, Croce R et al (2011) Dose tolerance limits and dose volume histogram evaluation for stereotactic body radiotherapy. J Appl Clin Med Phys 12:3368
12. National Cancer Institute (2009) CTCAE v4.03. https://ctep.cancer.gov/protocolDevelopment/electronic_applications/ctc.htm#ctc_50. Accessed 17 July 2018
13. Osmundson EC, Wu Y, Luxton G et al (2015) Predictors of toxicity associated with stereotactic body radiation therapy to the central hepatobiliary tract. Int J Radiat Oncol Biol Phys 91:986–994. https://doi.org/10.1016/j.ijrobp.2014.11.028
14. Toesca DAS, Osmundson EC, von Eyben R et al (2017) Central liver toxicity after SBRT: an expanded analysis and predictive nomogram. Radiother Oncol 122:130–136. https://doi.org/10.1016/j.radonc.2016.10.024
15. EQD2 and BED calculator. http://eqd2.com. Accessed 17 July 2018
16. Fowler JF (1989) The linear-quadratic formula and progress in fractionated radiotherapy. Br J Radiol 62:679–694. https://doi.org/10.1259/0007-1285-62-740-679

17. Ricke J, Wust P, Stohlmann A et al (2004) CT-guided brachytherapy. A novel percutaneous technique for interstitial ablation of liver metastases. Strahlenther Onkol 180:274–280. https://doi.org/10.1007/s00066-004-1179-4
18. Mohnike K, Neumann K, Hass P et al (2017) Radioablation of adrenal gland malignomas with interstitial high-dose-rate brachytherapy : efficacy and outcome. Strahlenther Onkol 193:612–619. https://doi.org/10.1007/s00066-017-1120-2
19. Ricke J, Mohnike K, Pech M et al (2010) Local response and impact on survival after local ablation of liver metastases from colorectal carcinoma by computed tomography-guided high-dose-rate brachytherapy. Int J Radiat Oncol Biol Phys 78:479–485. https://doi.org/10.1016/j.ijrobp.2009.09.026
20. Mohnike K, Wieners G, Schwartz F et al (2010) Computed tomography-guided high-dose-rate brachytherapy in hepatocellular carcinoma: safety, efficacy, and effect on survival. Int J Radiat Oncol Biol Phys 78:172–179. https://doi.org/10.1016/j.ijrobp.2009.07.1700
21. Streitparth F, Pech M, Böhmig M et al (2006) In vivo assessment of the gastric mucosal tolerance dose after single fraction, small volume irradiation of liver malignancies by computed tomography-guided, high-dose-rate brachytherapy. Int J Radiat Oncol Biol Phys 65:1479–1486. https://doi.org/10.1016/j.ijrobp.2006.02.052
22. Tselis N, Chatzikonstantinou G, Kolotas C et al (2013) Computed tomography-guided interstitial high dose rate brachytherapy for centrally located liver tumours: a single institution study. Eur Radiol 23:2264–2270. https://doi.org/10.1007/s00330-013-2816-z
23. Eriguchi T, Takeda A, Sanuki N et al (2013) Acceptable toxicity after stereotactic body radiation therapy for liver tumors adjacent to the central biliary system. Int J Radiat Oncol Biol Phys 85:1006–1011. https://doi.org/10.1016/j.ijrobp.2012.09.012
24. Ahmed M (2018) Acute cholangitis—an update. World J Gastrointest Pathophysiol 9:1–7. https://doi.org/10.4291/wjgp.v9.i1.1
25. Sun Z, Zhu Y, Zhu B et al (2016) Controversy and progress for treatment of acute cholangitis after Tokyo Guidelines (TG13). Biosci Trends 10:22–26. https://doi.org/10.5582/bst.2016.01033
26. Llovet JM, Brú C, Bruix J (1999) Prognosis of hepatocellular carcinoma: the BCLC staging classification. Semin Liver Dis 19:329–338. https://doi.org/10.1055/s-2007-1007122
27. Bennouna J, Sastre J, Arnold D et al (2013) Continuation of bevacizumab after first progression in metastatic colorectal cancer (ML18147): a randomised phase 3 trial. Lancet Oncol 14:29–37. https://doi.org/10.1016/S1470-2045(12)70477-1

Strahlenther Onkol (2016) 192:288–296
DOI 10.1007/s00066-016-0957-0

ORIGINAL ARTICLE

Radioablation of liver malignancies with interstitial high-dose-rate brachytherapy

Complications and risk factors

Konrad Mohnike[1] · Steffen Wolf[1] · Robert Damm[1] · Max Seidensticker[1] · Ricarda Seidensticker[1] · Frank Fischbach[1] · Nils Peters[2] · Peter Hass[2] · Günther Gademann[2] · Maciej Pech[1] · Jens Ricke[1]

Received: 5 October 2015 / Accepted: 3 February 2016 / Published online: 29 February 2016

Abstract
Background To evaluate complications and identify risk factors for adverse events in patients undergoing high-dose-rate interstitial brachytherapy (iBT).
Material and methods Data from 192 patients treated in 343 CT- or MRI-guided interventions from 2006–2009 at our institution were analyzed. In 41 %, the largest tumor treated was ≥5 cm, 6 % of the patients had tumors ≥10 cm. Prior to iBT, 60 % of the patients had chemotherapy, 22 % liver resection, 19 % thermoablation or transarterial chemoembolization (TACE). Safety was the primary endpoint; survival data were obtained as the secondary endpoints. During follow-up, MRI or CT imaging was performed and clinical and laboratory parameters were obtained.
Results The rate of major complications was below 5 %. Five major bleedings (1.5 %) occurred. The frequency of severe bleeding was significantly higher in patients with advanced liver cirrhosis. One patient developed signs of a nonclassic radiation-induced liver disease. In 3 patients, symptomatic gastrointestinal (GI) ulcers were detected. A dose exposure to the GI wall above 14 Gy/ml was a reliable threshold to predict ulcer formation. A combination of C-reactive protein ≥165 mg/l and/or leukocyte count ≥12.7 Gpt/l on the second day after the intervention predicted infection (sensitivity 90.0 %; specificity 92.8 %.) Two patients (0.6 %) died within 30 days. Median overall survival after the first liver treatment was 20.1 months for all patients and the local recurrence-free surviving proportion was 89 % after 12 months.
Conclusions Image-guided iBT yields a low rate of major complications and is effective.

Keywords Liver neoplasms · Treatment efficacy · Local ablation · Hepatocellular carcinoma · Adverse events

Radioablation von Lebermalignomen mit interstitieller High-dose-rate-Brachytherapie

Komplikationen und Risikofaktoren

Zusammenfassung
Hintergrund Evaluierung der Komplikationsrate und Identifizierung von Risikofaktoren für Komplikationen und Nebenwirkungen bei Patienten mit Lebermalignomen, die mit der hochdosierten interstitiellen Brachytherapie (iBT) behandelt wurden.
Material und Methoden Von 2006 bis 2009 wurden 192 Patienten in 343 CT- oder MRT-geführten Interventionen behandelt und deren Daten ausgewertet. Der größte behandelte Tumor war in 41% der Fälle ≥5 cm, 6% der Patienten hatten Tumoren ≥10 cm. Vor Behandlungsbeginn hatten 60% der Patienten eine Chemotherapie, 22% eine Leberesektion und 19% eine Thermoablation oder transarterielle Chemoembolisation (TACE). Primärer Endpunkt war die Behandlungssicherheit, als sekundäre Endpunkte wurden Überlebensdaten ausgewertet. Die Nachsorge umfasste ne-

✉ Dr. med. Konrad Mohnike
konrad.mohnike@med.ovgu.de

[1] Klinik für Radiologie und Nuklearmedizin, Universitätsklinikum Magdeburg A.ö.R., Otto-von-Guericke-Universität, Leipziger Straße 44, 39120 Magdeburg, Germany

[2] Klinik für Strahlentherapie, Universitätsklinikum Magdeburg A.ö.R., Otto-von-Guericke-Universität, Leipziger Straße 44, 39120 Magdeburg, Germany

ben klinischen und paraklinischen Parametern MRT- und CT-Untersuchungen.
Ergebnisse Die Rate an Major-Komplikationen lag unter 5%. Es traten 5 behandlungsbedürftige Blutungen auf (1,5%). Die Häufigkeit schwerer Blutungen war bei Patienten mit Leberzirrhose im fortgeschrittenen Stadium signifikant höher. Ein Patient entwickelte Zeichen einer nichtklassischen Strahlenhepatitis. Bei 3 Patienten zeigten sich symptomatische Magen-Darm-Ulzera. Eine Dosisexposition der Magen- bzw. Duodenalschleimhaut von mehr als 14 Gy/ml Einzeitdosis war mit dem Risiko von radiogen bedingten Ulzera verbunden. Eine CRP-Erhöhung auf mehr als ≥165 mg/l und/oder ein Anstieg der Leukozytenzahl auf mehr als ≥12,7 Gpt/l am 2. postinterventionellen Tag wies auf eine Infektion hin (Sensitivität 90,0%; Spezifität 92,8%). Die 30-Tage-Mortalität betrug 0,6%. Das mediane Gesamtüberleben nach der ersten Leberbehandlung betrug 20,1 Monate, die Lokalrezidivfreiheit nach 12 Monaten lag bei 89%.
Schlussfolgerung Die bildgeführte iBT hat eine niedrige Komplikationsrate und ist effektiv.

Schlüsselwörter Leberneoplasien · Behandlungswirksamkeit · Lokale Ablation · Hepatozelluläres Karzinom · Nebenwirkungen

Introduction

The diagnosis and treatment of primary and secondary liver malignancies have recently improved [1, 2]. Liver transplantation and surgical resection in patients with hepatocellular carcinoma (HCC) can potentially lead to cure in the minority of patients for whom these options are feasible [3]. In patients with small colorectal liver metastases (CRLM), 5-year survival rates between 7 and 58% are achieved [4, 5]. However, fewer than 25% of patients with CRLM are candidates for a potential curative treatment [6].

Thermoablative techniques have evolved for more than a decade; particularly, radiofrequency ablation (RFA) yields promising rates of tumor control and survival in small tumors [7–9]. However, RFA is of limited value in tumor lesions exceeding 3 cm in diameter, located close to the hepatic hilum or close to large vessels [10].

Precise radiotherapeutic techniques like stereotactic body radiotherapy (SBRT) has proven excellent local control, also after single-dose irradiation of liver tumors [11].

There is also experience with proton beam therapy, especially from Japan [12, 13]. Nonetheless, SBRT has demonstrated limitations in previous studies, such as a limited number of reasonably treatable metastases or a safe lesion diameter up to 4–5 cm [14, 15]. Beyond that size threshold, local tumor control rates after SBRT tend to decrease significantly [16, 17]. This has prompted the use of percutaneous image-guided interstitial high-dose-rate brachytherapy (iBT) [18]. Local control rates of up to 90% after 12 months and a prognostic impact in advanced and even very large HCC and CRLM have been found with a median overall survival (OS) of 19.4 and 23.4 months, respectively [19–21].

In liver malignancies of other primaries and in very large tumors, iBT has also been proven to be effective [22–26].

As iBT in the liver is an invasive procedure with an inhomogeneous dose distribution in contrast to percutaneous radiotherapy, and radiation is the tumor cell killing agent in contrast to conventional minimally invasive radiological techniques like radiofrequency ablation, a specific "complications spectrum" can be assumed with an exclusive impact on clinical practice. Therefore, its specific interventional and radiotherapeutic complication rate in a large patient cohort was the major goal of this study. To our knowledge, this is the largest study which thoroughly evaluates complications and risk factors for adverse events in patients with liver neoplasms treated with iBT.

Materials and methods

Study design

Patients treated at our institution with iBT from March 2006 to December 2007 were included in this study (group A, $N=144$). Treatment and safety data were documented prospectively in a dedicated database tailored to record treatment data and acute and chronic adverse events for later analysis. The frequency and quality of adverse events served as the primary endpoint. To address somatic discomfort more specifically, a second cohort of patients was recruited from December 2008 to March 2009 (group B, $N=48$) based on the same inclusion criteria, more closely monitored especially during the hospital stay with structured interviews to cover minor and more subjective side effects like mild pain and nausea more precisely.

Prior interventional therapies (e.g., RFA) were to have been completed at least 4 weeks before iBT; prior iBT had to be completed 3 months and yttrium90 radioembolization 6 months before iBT. Principal preconditions were a Child–Pugh score ≤8 points, a platelet count above 50 Gpt/l, and a prothrombin time of at least 50%. Ascites was not an exclusion criterion if controlled or minimal.

In general, we set a limit of liver involvement in a single session of not more than 5 Gy in two-thirds of the liver volume. In rare cases in patients with excellent liver function, this limit was exceeded.

Every 3 months, MRI or CT imaging was performed. Overall, progression-free and local recurrence-free survival

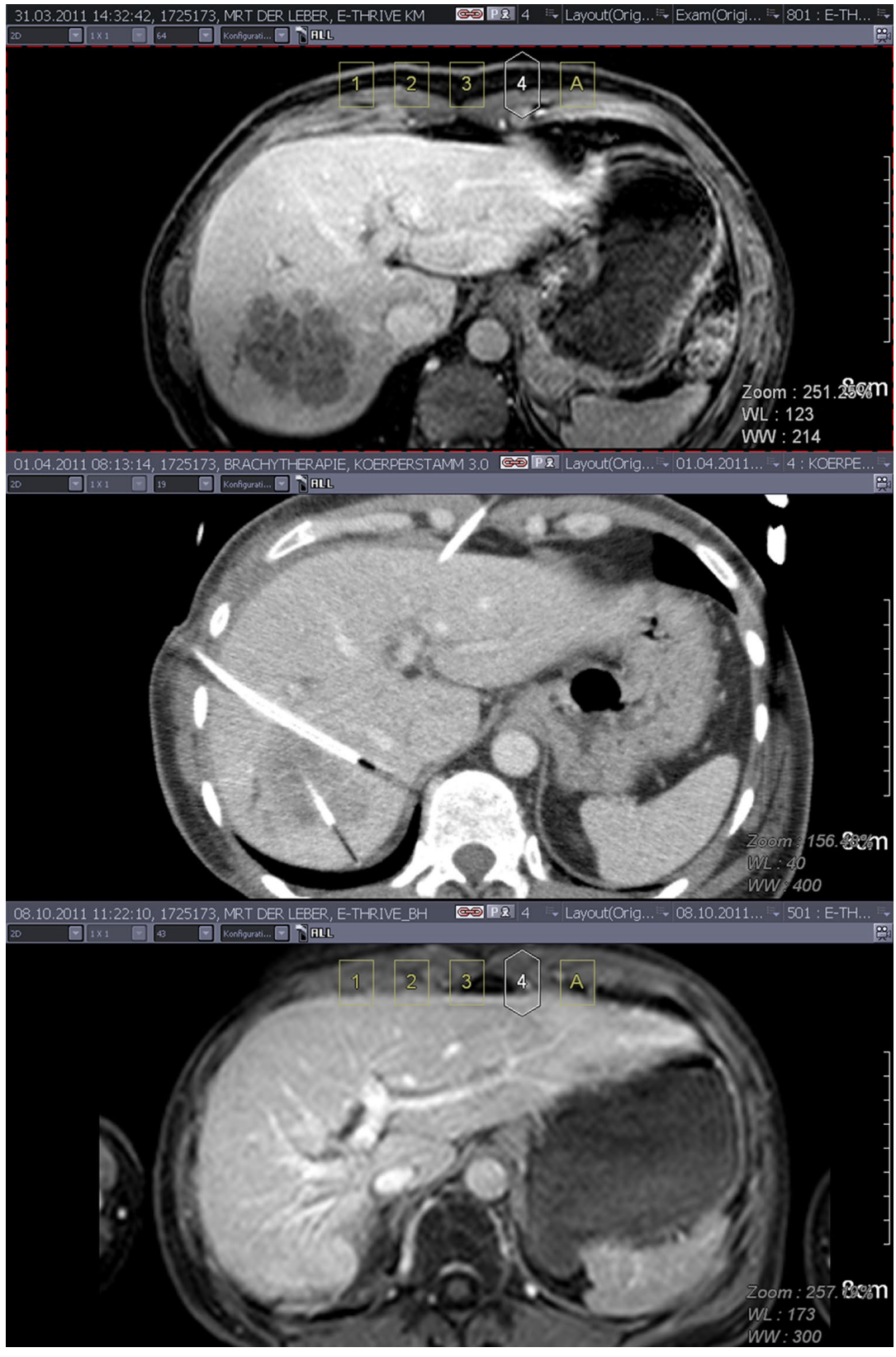

Fig. 1 A 42-year-old woman with breast cancer and hepatic metastasis. *Top* Pretherapeutic contrast-enhanced MRI. *Middle*: Contrast-enhanced CT after fluoroscopy-guided insertion of the iBT applicators. *Bottom* Contrast-enhanced MRI 6 months after iBT

were secondary endpoints. All patients provided written informed consent, and the study was approved by the local ethics committee.

Data acquisition

Postprocedural imaging was performed within the first 3 days. All patients treated at our institution were monitored closely with clinical examinations, laboratory, and CT or MRI imaging 6 and 12 weeks and then every 3 months for signs of adverse events or tumor progression (Fig. 1). Every

follow-up visit took place in our institution and the respective findings were documented in the mentioned database. In patient cohort A, this documentation was supplemented by thorough chart reviews, external documents, and telephone interviews (if events in the follow-up required such), whereas patient cohort B was additionally more closely monitored especially during the hospital stay with structured interviews to cover side effects regarding somatic discomfort such as pain and nausea more precisely.

Intervention and irradiation technique

Irradiation by the iBT technique, using an afterloading 10Ci iridium192 source system (Nucletron, the Netherlands) was performed. Positioning of the brachytherapy catheters was accomplished percutaneously either by fluoroscopy CT (Fig. 1, Toshiba Aquilion, Tokyo, Japan) or by real-time MRI (Panorama 1.0 T open MR system, Philips Healthcare) under a mild analgosedation, usually with midazolam and fentanyl. The catheter position, the tumor margin, and anatomic risk structures were verified by contrast-enhanced images sent to the treatment planning unit (Fig. 2 and 3, Oncetra-MasterPlan, Nucletron, the Netherlands; treatment characteristics: Tab. 1).

The target was defined as the gross tumor volume (GTV) on CT or MRI adding a safety margin of 2–3 mm in axial and craniocaudal directions. The prescribed dose at the tumor margin depended on the primary tumor based on findings from previous trials (e.g., hepatocellular carcinoma 15 Gy, and colorectal carcinoma 20 Gy) [20, 21]. Inhomogeneity of dose distribution was accepted with dose peaks in centrally located tumor regions, assumed that the prescribed dose at the tumor margin was reached.

Tab. 1 Interventional/radiotherapeutic characteristics and follow-up ($N=343$ interventions)

Variable	Value	Available data, *n* (%)
Guiding imaging		343 (100)
CT [*n* (%)]	284 (82.8)	
MRI [*n* (%)]	59 (17.2)	
Number of catheters [*n* (IQR; maximum)]	4.0 (2.0–5.0; 9)	342 (99.7)
Target dose per lesion [in Gy (±SD)]	17.3 (±3.1)	337 (98.3)
CTV [in cm^3 (IQR; maximum)]	36.7 (13.0–78.8; 796.0)	317 (92.4)
LV [in cm^3 (±SD)]	1352.3 (±413.5)	295 (86.0)
(CTV/LV) × 100 [% (IQR; maximum)]	2.7 (1.1–6.1; 61.2)	291 (84.8)
(5 Gy/LV) × 100[a] [% (IQR; maximum)]	22.5 (13.8–34.7; 87.9)	293 (85.4)

CTV clinical target volume, *LV* liver volume, *IQR* interquartile range, *SD* standard deviation.

[a]5 Gy-volume of total tumor-free liver volume.

Attendance for follow-up was as follows: nominally 3 days (actually 2.9±0.9 days, appointments kept by patients representing 343/343 interventions); 6 weeks (42±12 days, appointments kept by patients representing 269/288 interventions); 3 months (85±12 days, 139/196); 6 months (147±29 days, 113/144); 9 months (215±34 days, 85/106); 12 months (293±33 days, 56/60); 15 months (386±39 days, 42/45); 18 months (484±41 days, 37/37); 21 months (611±49 days, 20/20); 24 months (712±58 days, 9/9)

Fig. 2 iBT planning based on interventional contrast-enhanced CT

Analysis and statistical methods

Adverse events were graded according to the 3rd version of the National Cancer Institute's Common Terminology Criteria for Adverse Events [27]. Furthermore, liver function was assessed according to the criteria for radiation-induced liver disease (RILD) [28]. Time to progression (TTP) and overall survival (OS) were estimated by the Kaplan–Meier method and compared by employing the log-rank, Breslow, and Tarone–Ware tests. Calculations were performed with SPSS® software, version 15 (SPSS Inc., Chicago, IL, USA).

Results

Patients and procedures

A total of 192 patients with primary and secondary malignancies of the liver were treated in 343 interventions, in which 1275 brachytherapy catheters were placed [patients with colorectal liver metastases (LM), $n=84$; hepatocellular carcinoma, $n=50$; cholangiocellular carcinoma, $n=16$; breast cancer LM, $n=13$; lung cancer LM, $n=8$; and 21 patients with LM of other origin]. The average clinical target volume (CTV) was 36.7 ml [interquartile range (IQR) 13–78.8 ml]. The mean number of lesions treated per patient was 1.5 (range 1–5).

Of 296 lesions, 277 were treated in a single session (median 16.4 Gy, range 5.9–31.2 Gy). The corresponding median biologically effective dose (BED) was 43.3 (range 9.4–128.5); the equivalent dose in 2 Gy fractions (EQD2) was 36.1 (range 7.8-107.1).

A total of 19 large to very large lesions were treated in 2 or 3 sessions dividing the tumor in different CTV for each single session (median 2 fractions, range 2–3, e.g., upper part and lower part). The median dose/fraction was 10.0 Gy (range 3.5–15.9 Gy). The corresponding median total BED was 50.3 (range 31.4–141.4), the EQD2 was 41.9 (range 26.1–117.8). If new lesions were treated with iBT during follow-up and the inclusion criteria were met, these interventions were included in the analysis. The proportion of the total liver volume exposed to at least 5 Gy (V5) in a single irradiation session was 22.5 % on average (max. 88 %). Treatment decisions were based on interdisciplinary consensus. Detailed information regarding tumor treatment are shown in Table 1 and baseline characteristics of the study population are shown in Table 2. Of the 192 patients, 111 received more than one iBT.

Complications

Overall, the proportion of patients with major complications was below 5 % (15/343). Full details are given in Table 3.

Tab. 2 Baseline patient characteristics. ($N=192$ patients; number of patients (%) are shown except where otherwise stated)

Age, years (mean ± SD)	66.08 (± 10.2)
Male	111 (57.8)
Tumor entity	
Colorectal carcinoma	84 (43.8)
Hepatocellular carcinoma	50 (26.0)
Cholangio carcinoma	16 (8.3)
Mammary carcinoma	13 (6.7)
Lung carcinoma	8 (4.2)
Others[a]	21(10.9)
Diameter of the largest lesion	
< 5 cm	105 (54.7)
5-–10 cm	66 (34.4)
> 10 cm	12 (6.3)
Diffuse tumor spread	9 (4.7)
More than one lesion to treat	79 (41.1)
Previous chemotherapy	114 (59.4)
First line	38 (33.3)
Second line or more	76 (66.7)
Previous liver resection	52 (22.4)
Previous tumor ablation[b]	51 (26.6)
RFA or LITT	23 (45.1)
TACE	13 (25.5)
iBT	15 (29.4)
Stereotactic radiation	1 (2.0)
Previous other therapies[c]	12 (6.3)
Liver cirrhosis	50 (26.0)
Child–Pugh class A (76 interventions)	44 (88.0)
B (12 interventions)	6 (12.0)
Portal vein thrombosis (30 interventions)[d]	15 (7.8)
Karnofsky index ≥ 70 %	188 (97.9)

[a]Leiomyosarcoma of the vena cava, urinary bladder cancer, gastric cancer, renal cell cancer, jejunal cancer, adenocarcinoma of unknown primary (2 each) and esophageal cancer, pancreatic cancer, gastrointestinal stroma tumor, cervical cancer, thyroid cancer, anal cancer, hypopharyngeal cancer, choroidal melanoma, prostate cancer (1 each).

[b]*RFA* radiofrequency ablation, *LITT* Laser Induced Thermo Therapy, *TACE* transarterial chemoembolization, *iBT* interstitial HDR brachytherapy.

[c]Additional hormone or tyrosine-kinase inhibitor therapy.

[d]Thrombosis in the main, right or left hemiliver portal vein.

Bleeding CTCAE grade ≥ III

The mean preinterventional platelet count differed significantly between patients with and without postinterventional bleeding [160.0 Gpt/l (range 87.5–256.0 Gpt/l) vs. 244.3 Gpt/l (range 165.0–303.3 Gpt/l); $p=0.043$], but not for age, the number of catheters placed [5.0 (range 2.5–6.0) vs. 4.0 (2.0–5.0); $p=0.410$], the incidence of portal vein thrombosis (20.0 vs. 9.4 %; $p=0.390$), and the preinterventional prothrombin time. Major bleeding occurred exclusively in patients with liver cirrhosis (5/89 'with' vs. 0/254

Tab. 3 Complications after iBT and subsequent treatments

Complication	Cases, *n* (%)[a]	Therapy[b]	Interval[c]
Major			
Bleeding CTCAE IV	1 (0.29)	Surgery, resolved	24 h
Bleeding CTCAE III	4 (1.17)	DSA and/or PRBC, resolved	24 h
Ascites CTCAE III	1 (0.29)[e]	Drainage and diuretics, resolved	48 h
Ulcer, GI	3 (0.87)	Endoscopic intervention, resolved	5 weeks–8 months
Non-classic RILD	1 (0.5)[h]	Symptomatic, UDC, resolved	7 weeks
Liver abscess	4 (1.17)[g]	Drainage and antibiotics, resolved	4 days–8 months
Bile duct occlusion[d]	1 (0.29)	Endoscopic stenting, resolved	1 week
30-day mortality	2 (1.0)[h]		
Minor			
Bleeding CTCAE I	9 (3.21)	None, resolved	24 h
Pleural effusion CTCAE I	31 (10.8)	None, resolved	24–72 h
Pleural effusion CTCAE II	4 (1.40)[f]	Thoracentesis, resolved	24–72 h
Pneumothorax CTCAE I	4 (1.40)	None, resolved	24 h
Pneumothorax CTCAE II	1 (0.35)	Chest tube, resolved	24 h
Ascites CTCAE I	2 (0.71)	None, resolved	24–72 h

iBT interstitial brachytherapy, *DSA* digital subtraction angiography with embolization, *PBRC* packed red blood cells, *CTCAE* Common Terminology Criteria for Adverse Events, *GI* gastrointestinal, *UDC* ursodeoxycholic acid, *RILD* radiation-induced liver disease.

[a]Percentages for major complications: based on total of 343 iBT procedures; for minor complications: based on the number of imagings performed 3 days after intervention (abdomen: 280, chest: 286).

[b]Therapy to treat given event.

[c]Usual time after iBT that event was observed. Some cases of hematoma/hemorrhage, pneumothorax occurred during the procedure.

[d]Edema related occlusion of a central bile tract.

[e]Increased from preinterventional grade I.

[f]Two increased from preinterventional grade I.

[g]One abscess was related to percutaneous transhepatic cholangio drainage.

[h]Percentage: patient-based.

'without'; $p=0.001$). In particular, the incidence was much higher in patients with severe liver dysfunction ['Child B/C' 3/13 vs. 'no cirrhosis or Child A': 2/330, with odds ratio (OR) 49.20 and 95 % confidence interval (CI) 7.38–327.83; $p<0.001$].

Gastrointestinal ulcers

Seventy-two interventions in 57 patients were associated with exposure of the upper GI tract to >1 Gy in the cubic centimeter subjected to the greatest exposure. Three symptomatic postinterventional GI ulcers occurred in the gastric wall, the duodenal wall and the gastroduodenal junction, respectively (3/72; 4.2 %). Interventions associated with GI ulcers showed a higher minimum dose applied to 1 ml (D_{1CC}) of the GI mucosa than interventions without ulcers (15.8 ± 2.5 vs. 10.0 ± 4.1 Gy; $p=0.020$). A dose exposure of the GI wall above 14 Gy was a reliable threshold to predict postinterventional ulcer formation (3/15 vs. 0/57, $p=0.008$) and this dose was less frequently (and not significantly) associated with ulcer formation when the patient received mucosal protection by the intake of a proton pump inhibitor (PPI; 2/5 [40 %] vs. 1/10 [10 %]; $p=0.242$).

Liver function

Transient elevation of bilirubin and liver enzymes without a clinically relevant impact was frequent. No case of classic RILD was found. However, one patient suffered from liver dysfunction after several treatments without any evidence of hepatic tumor progression. That patient with a relapsed hepatocellular carcinoma 22 months after resection of the left liver lobe and hepatitis C with steatohepatitis and preprocedural preserved liver function (Child A) developed ascites and an icteric elevation of liver enzymes with a 5fold elevation of bilirubin, a >5fold elevation of alkaline phosphatase, and a 3fold elevation of transaminases 7 weeks after the last of four brachytherapy sessions. The close chronological link to repeated iBT, the underlying hepatitis C, and the subsequent course makes this likely to have been a case of nonclassic RILD. Under symptomatic and diuretic treatment and administration of ursodeoxycholic acid these values reverted to almost normal levels within 7 months. The patient died 27 months after the last brachytherapy.

Postinterventional infection

Overall, ten postprocedural infections (10/343, 2.92 %), including four liver abscesses, were diagnosed. Further septic complications comprised of three cases of cholangitis and one of pneumonia. On the basis of clinical presentation, laboratory results, and response to antibiotic therapy, two infections without a specific focus were diagnosed. Eight infections were diagnosed after discharge from hospital.

Fever (>38 °C) occurred in approximately 10 % of interventions but was not significantly associated with infection ($p=0.260$). Serum levels of postinterventional C-reactive protein (CRP) positively correlated with the clinical target volume (CTV; $r=0.473$; $p<0.001$; $n=312/343$). Patients

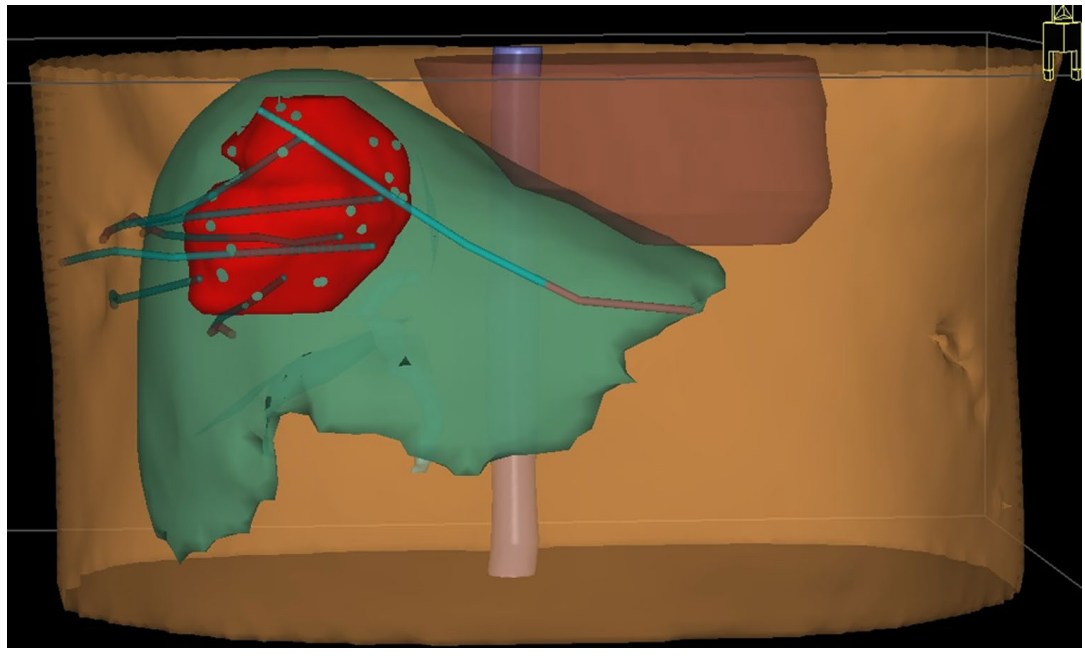

Fig. 3 The 3D tumor volume with the labeled catheter position

with postinterventional infection showed a higher level of CRP on the second postinterventional day than did patients without infection [129.8 mg/l (range 69.1–197.4) vs. 51.1 mg/l (range 24.1–90.6); $p<0.001$; $n=333/343$] and the mean leukocyte count was higher in these patients (12.8±4.1 Gpt/l vs. 7.4±2.9 Gpt/l; $p<0.001$, $n=337/343$). Univariate binary logistic regression analysis indicated that the postinterventional level of plasma leucocytes and the CRP (both on the second day) were predictive for septic events after iBT ($p<0.001$). In a binary regression analysis, prediction of postinterventional infection was even stronger when both variables were included ($p<0.001$).

Postinterventional CRP (2nd day after iBT) ≥165 mg/l *and/or* leukocyte count ≥12.7 Gpt/l revealed a sensitivity of 90.0% and a specificity of 92.8% for diagnosis of postprocedural infection.

30-day mortality

Two patients died within 30 days after a single brachytherapy not directly related to the intervention: One patient with Child–Pugh B liver cirrhosis died of severe esophageal bleeding 27 days after the procedure. Another patient died of neutropenic sepsis during chemotherapy after 29 days. This corresponded to 1.04% of all patients and 0.58% of all interventions.

Nausea/vomiting

Fifty-one events of nausea and/or vomiting were documented in 274 interventions (group A: 18.6%; vomiting: 19 grade I, 14 grade II; nausea: 35 grade I, 11 grade II). In group B ($n=69$), 26 (37%) were associated with nausea and/or vomiting (vomiting, 6 grade I and 10 grade II; nausea, 23 grade I and 2 grade II). In female patients, nausea and/or vomiting were more frequent (OR 2.89 with 95% CI 1.05–7.94; $p=0.049$).

Somatic discomfort

Severe pain (7/343, 2.0%) was associated with major bleeding or its management (3/5 vs. 4/338; $p<0.001$). In female patients, pain was more frequent (OR 3.53 with 95%CI 1.31–9.52; $p=0.016$).

Survival

Median follow-up time for survival was 20.5 months. Median OS after the first liver brachytherapy (not necessarily identical with the first intervention at our institution) for all patients was 20.1 months. Specifically, this was 27.9 months for breast cancer patients, 21.5 and 21.2 months for patients with colorectal liver metastases and hepatocellular carcinoma, 16.3 months for patients with cholangiocellular carcinoma, 8.7 months for lung cancer patients, and 24.1 months for patients with other malignancies. Eighty-three (43.2%) of patients also had extrahepatic disease [OS 22.3 (liver only) and 18.3 months (extrahepatic disease), respectively, $p<0.05$]. Median time to progression was 5.5 months, ranging from 11.7 months in patients with hepatocellular carcinoma to 2.2 months in patients with lung cancer.

Local recurrences (LR) were defined as any tumor growth, at any time point after iBT, adjacent to the field of administered radiation. Forty-four lesions (14.9%) of 296 treated developed a local recurrence (LR) with a 12-month local control rate (LCR) of 89% for all lesions (ranging from 97% in HCC lesions to 84% in colorectal liver metastases). A multivariate Cox regression including tumor diameter,

clinical target volume (CTV) and dose covering 100 % of the CTV (D100) revealed the significant influence of D100 upon LR-free survival only in colorectal liver metastases ($p = 0.03$), while this was not the case for lesions of other origin. Neither tumor diameter nor CTV had a significant effect on LR-free survival.

Discussion

Data from this study suggest that the safety of iBT compares to that of other minimally invasive ablation methods such as RFA. This is remarkable because iBT is predominantly conducted in patients unsuitable for RFA because of a high-risk location and/or the size of the lesion. The interventional major complication rate of 4.1 % in iBT is equivalent to that reported for RFA (4.1 %) and below the surgical complication rate [29, 30].

The greater complication rate in cirrhotic than in non-cirrhotic patients was also found in an earlier trial of iBT in HCC [19, 20]. Interestingly, beside cirrhosis no bleeding risk factors other than the platelet count were identified. This might also be due to catheter channel closing by gelaspone particles.

Streitparth et al. [31] showed in a small patient group that a dose exposure of the upper GI mucosa of 15.5 Gy (D1CC) was predictive of gastric ulceration after a single iBT. This finding is supported by our data, with a threshold of 14 Gy. Therefore, we now routinely start patients on PPI, when the dose exceeds 5 Gy to the highest exposed mucosal area.

The frequency of severe to irreversible liver toxicity is very low irrespective of single doses of up to 25 Gy, and of repetitive high-dose radiotherapies, as supported by findings of Ruehl et al. [32]. Only one patient (with diminished liver function and liver cirrhosis) developed reversible signs and symptoms of a nonclassic RILD after repetitive iBT (0.5 %). Bujold et al. [33] reported a rate of fatal liver failures of 5 % in patients receiving SBRT for HCC. In a trial of Kawashima et al. [34], 11 of 60 patients (18,3 %) with HCC treated with PBT developed a radiation-induced liver disease (RILD, or proton-induced hepatic insufficiency, PHI), of whom 7 patients (11 %) died of PHI. Two distinctive features might be responsible for the obvious high liver resistance to brachytherapeutic radiotherapy. First, the steep dose gradient results at least in a sharply defined and predictable scar, comparable to surgical tumor enucleation or atypical resection [35]. This also minimizes unnecessary exposure of the uninvolved parenchyma. Second, a part of the highly exposed liver parenchyma recovers over time [36, 37]. This is also in concordance with the findings of Brinkhaus et al. [38]. Facultative or obligate preventive medication to avoid RILD is established in ^{90}Y radioembolization, and a recent report by Seidensticker et al. has proven the effectiveness in iBT [39, 40].

A postinterventional (2nd day after iBT) CRP of ≥ 165 mg/l and/or leukocyte count ≥ 12.7 Gpt/l was considered to be a reliable threshold for distinguishing reactive elevations from inflammatory complications.

In this trial, 41 % of the lesions treated exceeded 5 cm in diameter but the 12 months local control rate ranged from 97 % in hepatocellular carcinoma to 84 % in colorectal liver metastases despite the fact that patients with limited disease were included, receiving a more or less “curative” intended high dose as well as patients with an advanced stage of disease with palliative treatment and lower doses.

Overall, our results indicate that iBT is a safe and effective procedure in heavily pretreated patients.

Financial support This work was funded exclusively by the University of Magdeburg.

Compliance with ethical standards

Conflict of interest K. Mohnike, S. Wolf, R. Damm, M. Seidensticker, R. Seidensticker, F. Fischbach, N. Peters, P. Hass, G. Gademann, M. Pech, and J. Ricke state that there are no conflicts of interest.

The study was conducted in accordance with the protocol, the ethical principles that have their origin in the Declaration of Helsinki and ICH-GCP. The study protocol and all study-related documentation were approved by all relevant authorities.

References

1. Deshpande R, O’Reilly D, Sherlock D (2011) Improving outcomes with surgical resection and other ablative therapies in HCC. Int J Hepatol 2011:686074
2. Pawlik TM, Assumpcao L, Vossen JA et al (2009) Trends in non-therapeutic laparotomy rates in patients undergoing surgical therapy for hepatic colorectal metastases. Ann Surg Oncol 16:371–378
3. Dhir M, Lyden ER, Smith LM, Are C (2012) Comparison of outcomes of transplantation and resection in patients with early hepatocellular carcinoma: a meta-analysis. HPB (Oxford) 14:635–645
4. Jones RP, Jackson R, Dunne DF et al (2012) Systematic review and meta-analysis of follow-up after hepatectomy for colorectal liver metastases. Br J Surg 99:477–486
5. Smith MD, McCall JL (2009) Systematic review of tumour number and outcome after radical treatment of colorectal liver metastases. Br J Surg 96:1101–1113
6. Khatri VP, Petrelli NJ, Belghiti J (2005) Extending the frontiers of surgical therapy for hepatic colorectal metastases: is there a limit? J Clin Oncol 23:8490–8499
7. Cirocchi R, Trastulli S, Boselli C et al. Radiofrequency ablation in the treatment of liver metastases from colorectal cancer. Cochrane Database Syst Rev 6:CD006317
8. Ruers T, Punt C, Van Coevorden F et al (2012) Radiofrequency ablation combined with systemic treatment versus systemic treatment alone in patients with non-resectable colorectal liver metastases: a randomized EORTC Intergroup phase II study (EORTC 40004). Ann Oncol 23:2619–2626

9. Sutherland LM, Williams JA, Padbury RT, Gotley DC, Stokes B, Maddern GJ (2006) Radiofrequency ablation of liver tumors: a systematic review. Arch Surg 141:181–190
10. Tanis E, Nordlinger B, Mauer M et al (2014) Local recurrence rates after radiofrequency ablation or resection of colorectal liver metastases. Analysis of the European Organisation for Research and Treatment of Cancer #40004 and #40983. Eur J Cancer 50:912–919
11. Herfarth KK, Debus J, Lohr F et al (2001) Stereotactic single-dose radiation therapy of liver tumors: results of a phase I/II trial. J Clin Oncol 19:164–170
12. Bush DA, Kayali Z, Grove R, Slater JD (2011) The safety and efficacy of high-dose proton beam radiotherapy for hepatocellular carcinoma: a phase 2 prospective trial. Cancer 117:3053–3059
13. Kawashima M, Furuse J, Nishio T et al (2005) Phase II study of radiotherapy employing proton beam for hepatocellular carcinoma. J Clin Oncol 23:1839–1846
14. Dawson LA (2011) Overview: where does radiation therapy fit in the spectrum of liver cancer local-regional therapies? Semin Radiat Oncol 21:241–246
15. Scorsetti M, Arcangeli S, Tozzi A et al. Is stereotactic body radiation therapy an attractive option for unresectable liver metastases? A preliminary report from a phase 2 trial. Int J Radiat Oncol Biol Phys 2013;86:336–342
16. Dawood O, Mahadevan A, Goodman KA (2009) Stereotactic body radiation therapy for liver metastases. Eur J Cancer 45:2947–2959
17. Kirkpatrick JP, Kelsey CR, Palta M et al (2014) Stereotactic body radiotherapy: a critical review for nonradiation oncologists. Cancer 120:942–954
18. Ricke J, Wust P, Wieners G et al (2004) Liver malignancies: CT-guided interstitial brachytherapy in patients with unfavorable lesions for thermal ablation. J Vasc Interv Radiol 15:1279–1286
19. Mohnike K, Wieners G, Pech M et al (2009) Image-guided interstitial high-dose-rate brachytherapy in hepatocellular carcinoma. Dig Dis 27:170–174
20. Mohnike K, Wieners G, Schwartz F et al. (2010) Computed tomography-guided high-dose-rate brachytherapy in hepatocellular carcinoma: safety, efficacy, and effect on survival. Int J Radiat Oncol Biol Phys 78:172–179
21. Ricke J, Mohnike K, Pech M et al. (2010) Local response and impact on survival after local ablation of liver metastases from colorectal carcinoma by computed tomography-guided high-dose-rate brachytherapy. Int J Radiat Oncol Biol Phys 78:479–485
22. Collettini F, Poellinger A, Schnapauff D et al (2011) CT-guided high-dose-rate brachytherapy of metachronous ovarian cancer metastasis to the liver: initial experience. Anticancer Res 31:2597–2602
23. Collettini F, Schnapauff D, Poellinger A et al (2012) Hepatocellular carcinoma: computed-tomography-guided high-dose-rate brachytherapy (CT-HDRBT) ablation of large (5–7 cm) and very large (> 7 cm) tumours. Eur Radiol 22:1101–1109
24. Tselis N, Chatzikonstantinou G, Kolotas C, Milickovic N, Baltas D, Zamboglou N (2013) Computed tomography-guided interstitial high dose rate brachytherapy for centrally located liver tumours: a single institution study. Eur Radiol 23:2264–2270
25. Wieners G, Mohnike K, Peters N et al (2011) Treatment of hepatic metastases of breast cancer with CT-guided interstitial brachytherapy - a phase II-study. Radiother Oncol 100:314–319
26. Wieners G, Pech M, Hildebrandt B et al (2009) Phase II feasibility study on the combination of two different regional treatment approaches in patients with colorectal "liver-only" metastases: hepatic interstitial brachytherapy plus regional chemotherapy. Cardiovasc Intervent Radiol 32:937–945
27. Trotti A, Colevas AD, Setser A et al (2003) CTCAE v3.0: development of a comprehensive grading system for the adverse effects of cancer treatment. Semin Radiat Oncol 13:176–181
28. Lawrence TS, Robertson JM, Anscher MS, Jirtle RL, Ensminger WD, Fajardo LF (1995) Hepatic toxicity resulting from cancer treatment. Int J Radiat Oncol Biol Phys 31:1237–1248
29. Bertot LC, Sato M, Tateishi R, Yoshida H, Koike K (2011) Mortality and complication rates of percutaneous ablative techniques for the treatment of liver tumors: a systematic review. Eur Radiol 21:2584–2596
30. Cheung TT, Poon RT, Yuen WK et al (2013) Long-term survival analysis of pure laparoscopic versus open hepatectomy for hepatocellular carcinoma in patients with cirrhosis: a single-center experience. Ann Surg 257:506–511
31. Streitparth F, Pech M, Bohmig M et al (2006) In vivo assessment of the gastric mucosal tolerance dose after single fraction, small volume irradiation of liver malignancies by computed tomography-guided, high-dose-rate brachytherapy. Int J Radiat Oncol Biol Phys 65:1479–1486
32. Ruhl R, Seidensticker M, Peters N et al (2009) Hepatocellular carcinoma and liver cirrhosis: assessment of the liver function after Yttrium-90 radioembolization with resin microspheres or after CT-guided high-dose-rate brachytherapy. Dig Dis 27:189–199
33. Bujold A, Massey CA, Kim JJ et al (2013) Sequential phase I and II trials of stereotactic body radiotherapy for locally advanced hepatocellular carcinoma. J Clin Oncol 31:1631–1639
34. Kawashima M, Kohno R, Nakachi K et al (2011) Dose-volume histogram analysis of the safety of proton beam therapy for unresectable hepatocellular carcinoma. Int J Radiat Oncol Biol Phys 79:1479–1486
35. Seidensticker M, Seidensticker R, Mohnike K et al (2011) Quantitative in vivo assessment of radiation injury of the liver using Gd-EOB-DTPA enhanced MRI: tolerance dose of small liver volumes. Radiat Oncol 6:40
36. Ricke J, Seidensticker M, Ludemann L et al (2005) In vivo assessment of the tolerance dose of small liver volumes after single-fraction HDR irradiation. Int J Radiat Oncol Biol Phys 62:776–784
37. Ruhl R, Ludemann L, Czarnecka A et al (2010) Radiobiological restrictions and tolerance doses of repeated single-fraction hdr-irradiation of intersecting small liver volumes for recurrent hepatic metastases. Radiat Oncol 5:44
38. Brinkhaus G, Lock JF, Malinowski M et al (2014) CT-guided high-dose-rate brachytherapy of liver tumours does not impair hepatic function and shows high overall safety and favourable survival rates. Ann Surg Oncol 21:4284–4292
39. Sangro B, Gil-Alzugaray B, Rodriguez J et al (2008) Liver disease induced by radioembolization of liver tumors: description and possible risk factors. Cancer 112:1538–1546
40. Seidensticker M, Seidensticker R, Damm R et al (2014) Prospective randomized trial of enoxaparin, pentoxifylline and ursodeoxycholic Acid for prevention of radiation-induced liver toxicity. PLoS One 9:e112731

Clinical Investigations

Original paper

First report on extended distance between tumor lesion and adjacent organs at risk using interventionally applied balloon catheters: a simple procedure to optimize clinical target volume covering effective isodose in interstitial high-dose-rate brachytherapy of liver malignomas

Peter Hass, MD[1,2], Ingo G. Steffen, MD[3], Maciej Powerski, MD[2,4], Konrad Mohnike, MD[2,5], Max Seidensticker MD[2,6], Frank Meyer, MD[7], Thomas Brunner, MD[1], Robert Damm, MD[4], Christoph Willich, MD[1], Mathias Walke, PhD[1], Efstratios Karagiannis, MD[8], Jazan Omari, MD[4], Jens Ricke, MD[2,6]

[1]Department of Radiation Oncology, University Hospital, Magdeburg, Germany, [2]International School of Image-Guided Interventions, Magdeburg, Germany, [3]Department of Nuclear Medicine, University Medical Center Charité, Berlin, Germany, [4]Department of Radiology and Nuclear Medicine, University Hospital, Magdeburg, Germany, [5]DTZ am Frankfurter Tor, Center for Radiology, Berlin, Germany, [6]Department of Clinical Radiology, Ludwig-Maximilians-University (LMU), Munich, Germany, [7]Department of General, Abdominal, Vascular, and Transplant Surgery, University Hospital, Magdeburg, Germany, [8]Department of Radiation Oncology, German Oncology Center, Limassol, Cyprus

Abstract

Purpose: Organs at risk (OARs), which are very close to a clinical target volume (CTV), can compromise effective tumor irradiation. The present study investigated the feasibility and safety of a novel approach, in particular, the extent of the dosimetric effect of distancing CTV from adjacent OARs by means of interventionally applied balloon catheters.

Material and methods: Patients with peripheral hepatic malignancies, in whom the critical proximity of an OAR to the CTV in the assessment by contrast-enhanced magnetic resonance imaging (MRI) scans and the preplanning process were included. Additionally, patients underwent placement of an interventional balloon catheter during computed tomography (CT)-guided application of interstitial brachytherapy (iBT) catheters inserted into the tissue between hepatic capsule and adjacent OAR. The virtual position of an OAR without balloon catheter was anticipated and contoured in addition to contouring of CTV and OAR. The calculated dose values for CTV as well as 1 cc of the relevant OAR (D_{1cc}) with and without balloon were recorded. The D_{1cc} of the realized irradiation plan was statistically compared to the D_{1cc} of the virtually contoured OARs.

Results: In 31 cases, at least one balloon catheter was administered. The mean D_{1cc} of the OAR in the group with balloon(s) was 12.6 Gy compared with 16 Gy in the virtual cohort without the device, therefore significantly lower ($p < 0.001$). Overall, there were no acute complications. Severe (> 2 CTCAEv4.03) late complications observed in 3/31 (9.6%) patients during follow-up period after brachytherapy were most certainly not due to the balloon application. Side effects were probably associated with pre-existing serious diseases and potentially additional local late effects of the irradiation in general rather than with the balloon catheters.

Conclusions: The distancing of the adjacent OARs allows a higher D_{100} value of CTV, therefore allowing for more efficient local control.

J Contemp Brachytherapy 2019; 11, 2: 152–161
DOI: https://doi.org/10.5114/jcb.2019.84798

Key words: balloon catheters, clinical target volume (CTV), dose per 1 cc (D_{1cc}), dose volume histogram (DVH), interstitial high-dose-rate (HDR) brachytherapy (iBT), liver malignancies, organ at risk (OAR).

Address for correspondence: Peter Hass, MD, Department of Radiation Oncology, University Hospital at Magdeburg, Leipziger Strasse 44, 39120 Magdeburg, Germany, phone: +49 391 6715795, fax: +49 391 6715324, ✉ e-mail: peter.hass@med.ovgu.de

Received: 05.09.2018
Accepted: 01.04.2019
Published: 29.04.2019

Purpose

The concept of oligo-metastasis [1] based on surgical studies [2,3,4] that was discussed for the first time in the 1990s, differs from the rigid scheme of palliation vs. curation. There is a cohort of oligo-metastasized patients, which is not yet clearly definable that benefits from a consequent local ablation in terms of an improvement in the overall prognosis [5]. The gold standard of local treatment is surgical procedure [6]. However, since a high proportion of hepatic oligo-metastases is not resectable, alternative ablation procedures have been successfully tested [7]. The "toolbox of ablative treatments" is now a part of the current "ESMO (European Society for Medical Oncology) guidelines for the management of patients with metastatic colorectal cancer" [8].

In this study, radio-ablative methods are particularly investigated.

The development of high-performance software for calculation and application of prescribed irradiation dose and device-based hardware, currently allow for very precise implementation of hypo-fractionated and radio-surgical approaches [9,10]. Therefore, in no resectable patient, primary and secondary liver malignancies can often be treated very effectively with radiotherapy [11]. The key for effective and sustainable radio-ablation is to provide adequate clinical target volume doses [12,13], taking into account the dose limits of adjacent organs at risk (OARs). Particularly, in the case of marginal liver tumor, compromises cannot often be avoided at the expense of a potentially reduced chance of local control.

The aim of the present analysis was to investigate the feasibility and safety of a novel approach, in particular, to examine whether an increase in the distance between the target volume and the structure at risk is technically possible without severe complications and to what extent a dosimetric advantage is generated.

Material and methods

Patients

As a rule, all patients who might be eligible for brachytherapy of the liver are considered by a tumor board prior to the initial presentation at our department. A standard operating procedure (SOP) defines the inclusion and exclusion criteria for performing interstitial brachytherapy (iBT) of the liver. All patients sign a written informed consent prior to planning a computed tomography (CT)- or magnet resonance imaging (MRI)-guided interstitial brachytherapy. From April 2009 to June 2016, 2,082 patients with primary or secondary liver tumors were treated with interstitial high-dose-rate (HDR) brachytherapy; 137 cases (6.6%) had subcapsular liver tumors near the stomach, duodenum, or large intestine (OAR).

From this cohort, 31 patients were included in the study and received one or two additional balloon catheter(s) to increase the distance between the hepatic margin/surface and adjacent OAR, as part of single stage CT-guided iBT (recorded dose-volume histogram (DVH) parameters, Table 1 and Figure 1).

The prescribed dose related to D_{100} depends on the histology of the primary tumor lesion (GIST [gastrointestinal stromal tumor] = 12 Gy, breast cancer, renal cell carcinoma, hepatocellular carcinoma = 15 Gy, other histologies = 20 Gy). The dose was applied as a single fraction targeted on the complete tumor ablation.

Method

Methodology and course of single-dose interstitial HDR brachytherapy was already described in detail elsewhere [12,14].

Briefly, HDR-brachytherapy catheters (Primed, Halberstadt, Germany) and angiographic occlusion balloon catheters (Equalizer™ Occlusion Balloon Catheter, 20 and 27 mm, Boston Scientific, Marlborough, USA) were placed in a similar way using CT fluoroscopy (Aquilion Prime, Canon Medical Systems, Neuss, Germany). Following the puncture of the target lesion (for brachytherapy catheters) or between the liver capsule with the adjacent target lesion and the OAR (for balloon catheters) with an 18-G coaxial needle, a stiff angiography wire (Amplatz Super Stiff™, Boston Scientific, Boston, MA, USA) was introduced for placement of a 6 F (for brachytherapy catheters) or 12 F (for balloon catheters) introducer sheath (Radifocus®, Terumo, Tokyo, Japan), using the Seldinger technique, through which the brachytherapy or balloon catheter was inserted. When in the correct position, the balloon catheter was inflated (with contrast medium) to dissociate the OAR from the target volume (Figure 2). After placement of brachytherapy and balloon catheters, a contrast agent-enhanced (intravenously, iodine-based, 80 ml) spiral CT in breath-holding-technique (slice thickness, 3 mm) of the liver was acquired. The catheter position, the tumor margin, and anatomic risk structures verified by contrast-enhanced images were sent to the treatment planning unit (Oncentra Brachy, Elekta AB, Stockholm, Sweden).

The decision to insert a balloon catheter was made after the evaluation of liver specific MRI scans (slice thickness, 3 mm; MRI protocol included: T2-weighted ultra-turbo spin echo sequences with and without fat saturation, diffusion-weighted imaging, a T1-weighted gradient echo sequence, T1-weighted dynamic sequences, and sequences acquired 20 min after IV administration of 0.1 ml/kg Gd-EOB-DTPA [Primovist®, Bayer Vital, Leverkusen, Germany] performed on an 1.5-tesla MRI scanner [Intera 1.5T, Philips Healthcare, Hamburg, Germany], if within the framework of a virtual catheter application, the calculated clinical target volume (CTV) enclosing prescription dose (D_{100}) did not seem to be feasible under consideration of the institutional OAR dose limits concerning D_{1cc} and V_5 [13,15,16], and outstanding publications and reviews, inter alia, by Timmermann, Herfarth *et al*. and Sterzing *et al*. [17,18,19] (Table 2).

The time for insertion of one balloon catheter corresponds approximately to the application time of two BT catheters (mean, 16 min). In case of an implant with one BT catheter tripling the intervention time and in case of more advanced liver lesions with 8 catheters, the duration time of the intervention increases by approximately 25%.

Table 1. Recorded dose-volume histogram (DVH) parameters

Patient study number	Prescribed single-dose for D_{100} CTV (Gy)	Calculated dose for D_{100} CTV with balloon (Gy)	Adjacent OAR	Accepted calculated dose for OAR $D1_{cc}$ with balloon (Gy)	Calculated dose for anticipated OAR without balloon
1	20	10.560	Stomach	15.720	16.195
2	12	6.700	Stomach	13.500	21.798
3	15	7.740	Duodenum	12.250	12.420
4	20	8.750	Stomach	14.250	15.610
5	20	9.330	Stomach	13.938	16.501
6	15	15.117	Large intestine	16.540	25.130
7	20	11.010	Stomach	13.880	14.440
8	15	14.250	Stomach	12.980	15.460
9	20	20.300	Stomach	9.320	13.924
10	15	12.050	Stomach	14.010	15.456
11	20	20.580	Duodenum	13.510	16.160
12	20	20.930	Stomach	14.220	15.625
13	20	20.670	Stomach	11.390	14.310
14	20	20.830	Stomach	13.560	14.290
15	20	15.886	Stomach	14.350	15.964
16	15	15.130	Stomach	8.970	21.030
17	12	12.310	Stomach	11.290	13.390
18	15	15.240	Stomach	14.280	23.787
19	15	13.140	Stomach	11.160	13.910
20	20	20.827	Stomach	9.200	11.130
21	20	15.440	Stomach	12.310	14.700
22	15	9.940	Stomach	13.685	14.957
23	15	15.146	Stomach	10.230	13.389
24	25	27.420	Stomach	9.920	16.870
25	25	25.300	Stomach	13.430	17.220
26	20	15.150	Stomach	14.810	14.920
27	25	25.290	Stomach	13.640	17.688
28	20	20.700	Stomach	12.220	15.497
29	25	27.560	Stomach	8.890	18.160
30	15	13.900	Stomach	10.437	11.300
31	20	22.530	Stomach	13.710	15.459

Prescribed and calculated dose for D_{100}-CTV, accepted calculated dose for OAR-D_{1cc} with balloon, calculated dose for OAR-D_{1cc} regarding anticipated OAR-contour without balloon.

In addition to CTV, liver and adjacent OAR (predominantly stomach) as well as virtual OAR volume without a balloon were contoured; the virtual position of the OAR could be anticipated by assessing the pre-interventional MRI scans and additionally, with the interventional CT scans with BT catheter only (Figure 1).

Dose calculation was performed in strict accordance with institutional OAR limits (Table 2). The relevant parameters for this analysis such as prescription dose, D_{100}-CTV, D_{1cc}-OAR with and without a balloon were recorded. The values for the $D1_{cc}$-OAR with and $D1_{cc}$-OAR without balloon were distinguished as two groups and statistically evaluated.

The values for $D1_{cc}$-OAR with and $D1_{cc}$-OAR without balloon were assigned to two groups. These two cohorts were compared statistically.

Interstitial HDR brachytherapy was performed using an ^{192}Ir source with an afterloading device from Elekta (MicroSelectron HDR V3, Oncentra Brachy, Elekta AB, Stockholm, Sweden).

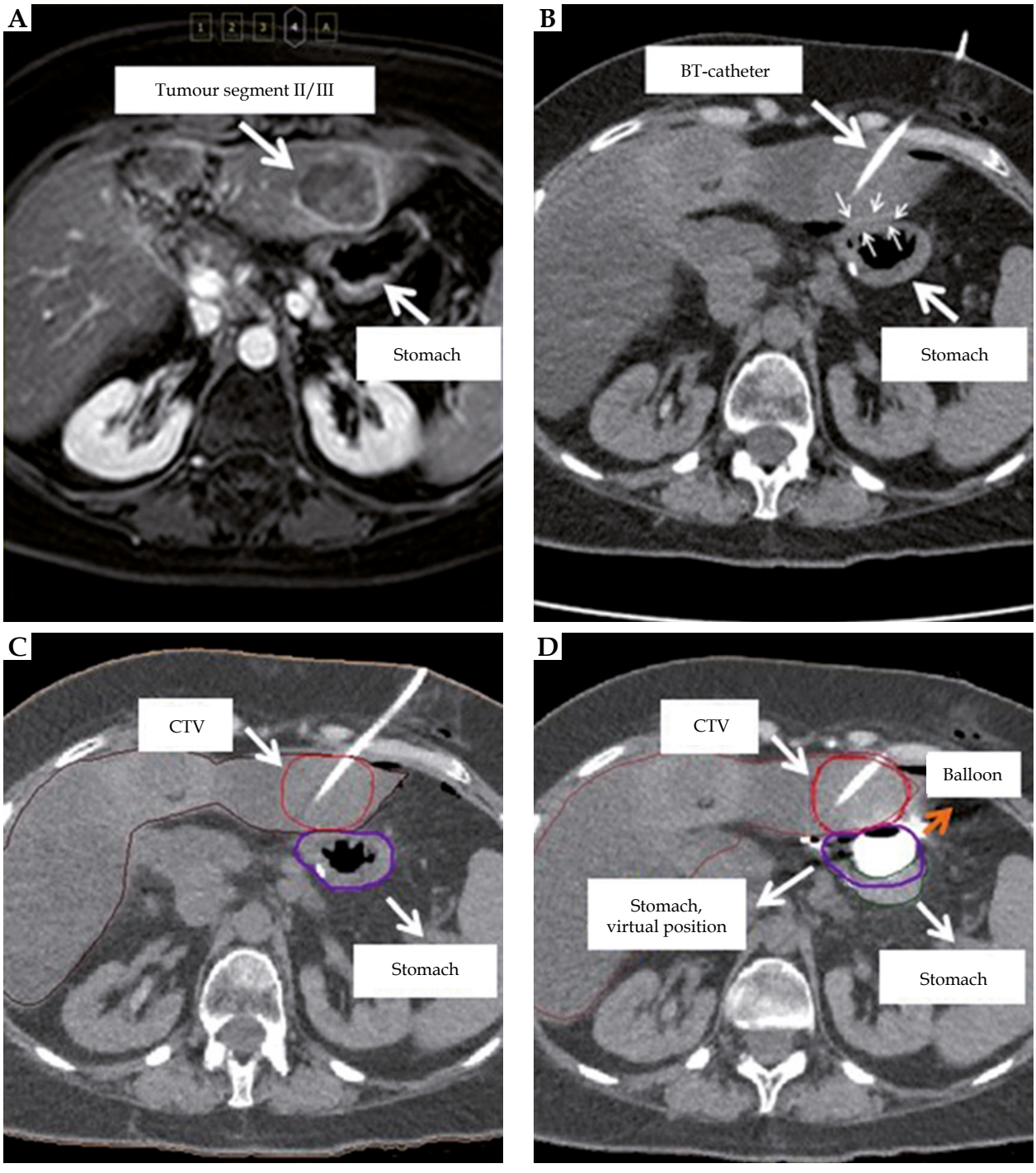

Fig. 1. Tomography imaging: **A**) Transversal MRI-scan: tumor lesion with marginal enhancement of contrast media, no BT, catheter; distinctly adjacent stomach; **B**) Corresponding transversal CT-scan with stomach position without balloon; one BT, catheter inserted; **C**) Corresponding transversal CT-scan; CTV and stomach contoured; **D**) Corresponding transversal CT-scan with additional balloon; CTV, stomach and stomach, virtual position without balloon contoured

Statistics

Statistics were collected with R (version 3.1.3; the R Foundation for Statistical Computing, Vienna, Austria).

Due to small sample size, non-parametric distribution of data was assumed, and data were described by median, interquartile range (IQR, 25^{th}-75^{th} percentiles), and minimum and maximum. Boxplots were used for visualization of data. Correlation of data was analyzed with Spearman's rho rank correlation coefficient and agreement of methods was described using Bland-Altman analysis [20]. Paired groups (with/without balloon) were compared with Wilcoxon signed rank test, and optimal cut-off was determined using receiver operating characteristics (ROC) curves [21] and Youden index as appro-

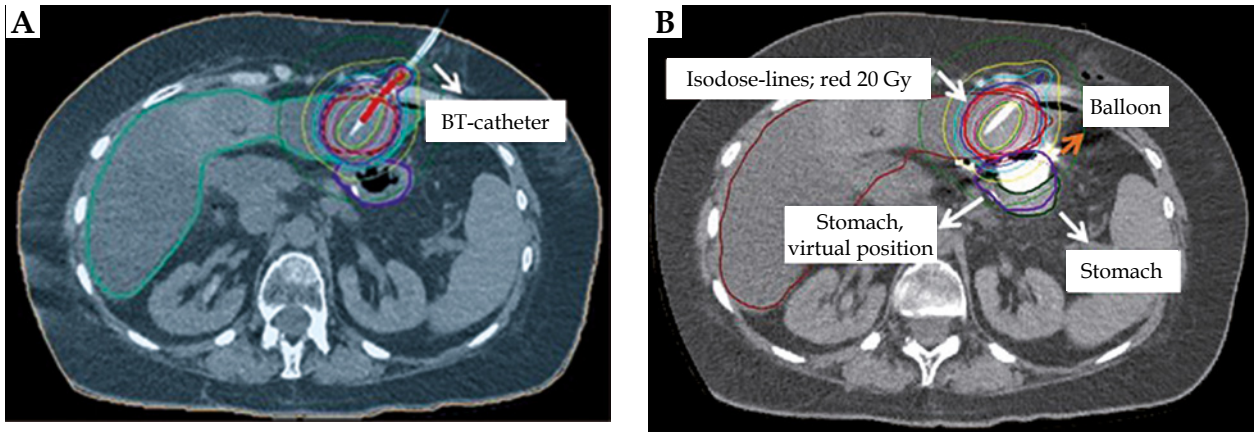

Resulting $D1_{cc}$	Dose (%)	Dose (Gy)	Volume (%)	Volume (ccm)
Stomach without balloon	113.09	22.6184	0.10	0.10
Liver without balloon	–	–	0.01	0.10
Stomach with balloon	89.84	17.9685	0.10	0.10
Liver with balloon	–	–	0.01	0.10
Stomach without balloon	86.23	17.2459	0.97	1.00
Liver without balloon	–	–	0.06	1.00
Stomach with balloon	69.65	13.9301	1.01	1.00
Liver with balloon	–	–	0.06	1.00

Fig. 2. Planning transversal CT scan with isodoses, prescribed dose to D_{100} CTV 20 Gy: **A**) CT-scan without balloon, one BT-catheter inserted; **B**) CT-scan with BT-catheter and one balloon-catheter inserted

priate. All tests were two-sided, and the significance level was set as 0.05.

Statement

The study was performed according to the guidelines of the Declaration of Helsinki for Biomedical Research from 1964 and its further amendments, and the procedures of "Good Research Practice". The analysis was designed as a retrospective study with approval of the local ethics committee. Each patient signed a written consent form prior to the planned intervention after an adequate patient-physician talk on the intervention and the frequency, severity, and profile of its complications.

Results

Patients

Thirty-one patients (17 females, 14 males; median age, 65.3 [range, 38-85] years), 22% of those with subcapsular liver tumors, were enrolled in the study. In 25 cases, one in 6 cases, two balloon catheters were inserted.

In 74% of the patients, primary lesions outside the liver were histologically confirmed (colorectal carcinoma, 45%; others, 29%), 26% had primary liver malignancies.

The marginal hepatic lesions were located within the liver segments 2/3 in 29 cases (93.5%), 2 patients had lesions within the right hepatic lobe, near large

Table 2. Dose constraints regarding organs at risk for single dose

Organ at risk	Timmermann SBRT constraints [17]		Herfarth, Sterzing, SBRT constraints [18,19]		Institutional constraints due to prospective and retrospective analysis of the XX/YY study-group [13,15,16]	
	DVH-parameter	Limit (Gy)	DVH parameter	Limit (Gy)	DVH parameter	Limit (Gy)/(%)
Stomach	D_{10cc}	< 13.0	D_{max}	12.0	D_{1cc}	14 (15*)
Duodenum	D_{5cc}	< 8.8	D_{max}	12.0	D_{1cc}	14 (15*)
Colon	D_{20cc}	< 11.0	Not specified	Not specified	D_{1cc}	18
Liver	D_{700cc}	9.1	D_{50}	4.0-7.0	V_5	/66

**The original values based on Streitparth's work [13] were decreased to 14 Gy from 2012 to further reduce the risk of late toxicity.*

Table 3. Patients' characteristics

Patient study number	Age (yr) at time of treatment	Gender	OAR	Primary tumor diagnosis	CTV volume (ccm)	Number (*n*) of balloon catheters
1	78	Male	Stomach	Colorectal cancer	23.75	1
2	68	Male	Stomach	Gastrointestinal stromal tumor	3.34	1
3	44	Female	Duodenum	Leiomyosarcoma	3.74	1
4	67	Male	Stomach	Colorectal cancer	191.7	2
5	57	Female	Stomach	Colorectal cancer	143.3	1
6	63	Male	Large intestine	Renal cell cancer	22.3	1
7	54	Female	Stomach	Colorectal cancer	87.95	2
8	64	Female	Stomach	Cholangiocellular carcinoma	336.0	2
9	69	Male	Stomach	Cholangiocellular carcinoma	10.3	1
10	77	Male	Stomach	Hepatocellular cancer	10.36	1
11	70	Male	Duodenum	Cholangiocellular carcinoma	62.7	1
12	74	Female	Stomach	Colorectal cancer	40.68	2
13	69	Female	Stomach	Colorectal cancer	18.75	1
14	48	Female	Stomach	Pancreatic cancer	31.48	1
15	56	Female	Stomach	Colorectal cancer	134.0	2
16	38	Female	Stomach	Breast cancer	3.54	1
17	73	Male	Stomach	Gastrointestinal stromal tumor	32.35	1
18	74	Male	Stomach	Cancer of unknown primary	9.37	1
19	46	Female	Stomach	Breast cancer	43.76	1
20	71	Female	Stomach	Colorectal cancer	28.81	1
21	75	Female	Stomach	Colorectal cancer	101.6	1
22	80	Male	Stomach	Colorectal cancer	135.2	1
23	84	Female	Stomach	Hepatocellular cancer	1.7	1
24	56	Female	Stomach	Cholangiocellular carcinoma	2.96	1
25	60	Male	Stomach	Colorectal Cancer	50.54	1
26	85	Male	Stomach	Colorectal Cancer	74.0	1
27	47	Male	Stomach	Colorectal cancer	9.3	1
28	74	Female	Stomach	Gallbladder cancer	3.1	1
29	70	Female	Stomach	Cancer of unknown primary	35.53	2
30	62	Male	Stomach	Hepatocellular cancer	12.3	1
31	71	Female	Stomach	Colorectal cancer	35.42	1

intestine. Patients' characteristics are presented in Table 3.

Application time for the whole implant depended on the number of inserted BT catheters and additional balloons. Median application time was 12.5 min (range, 7.5-30 min).

Organs at risk (stomach/duodenum, large intestine) D_{1cc}

D_{1cc} of the OAR with balloon (mean, 12 Gy; deviation, 8.9 to 16.5 Gy; median, 13.5 Gy; IQR, 11.2 to 14.0 Gy) were significantly ($p < 0.001$) lower compared to virtual antic-

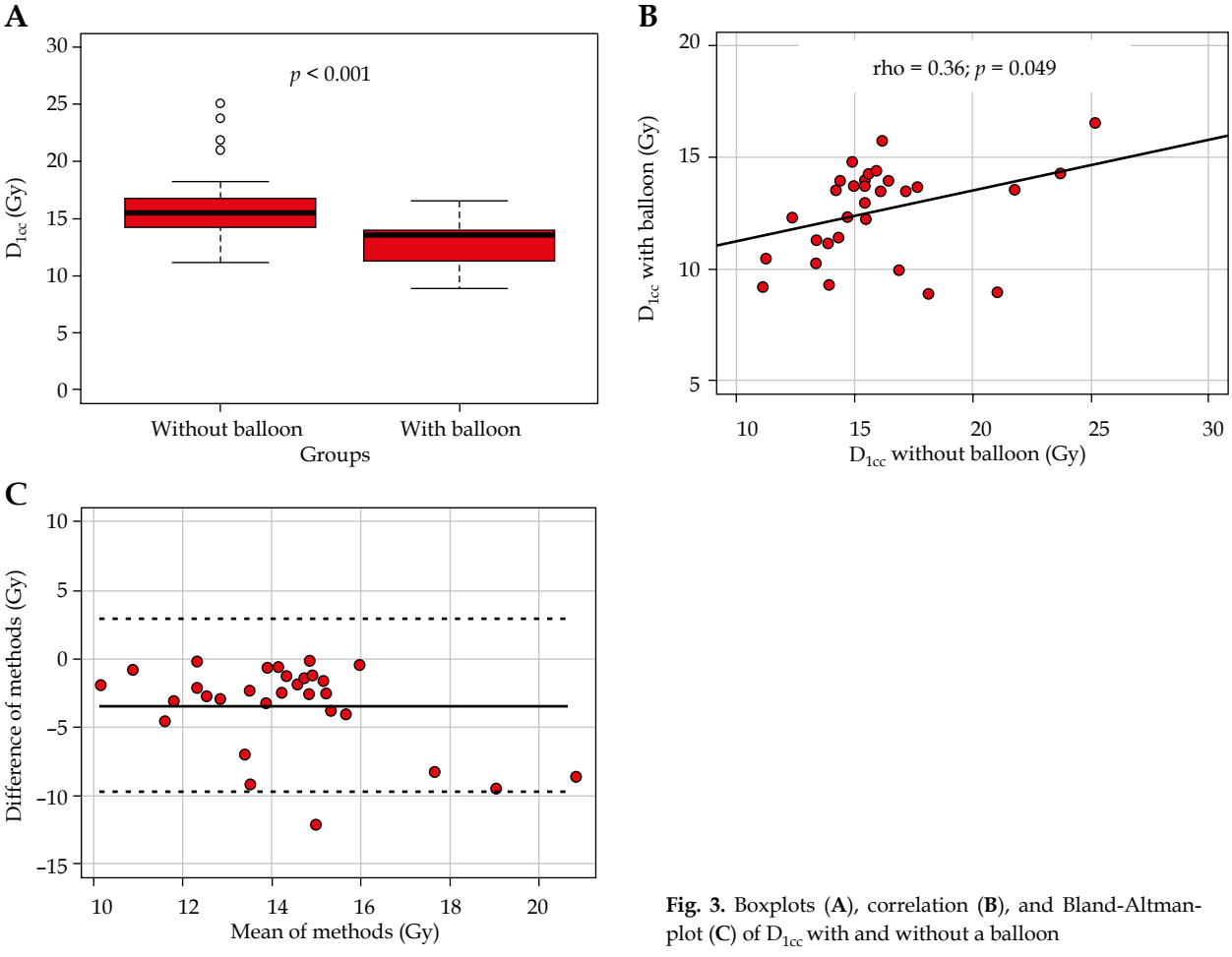

Fig. 3. Boxplots (**A**), correlation (**B**), and Bland-Altman-plot (**C**) of D_{1cc} with and without a balloon

ipated OAR without a balloon (mean, 16 Gy; deviation, 11.1 to 25.1 Gy; median, 15.5 Gy; IQR, 14.3 to 16.7 Gy; Figure 3A). The corresponding median relative difference was –16.3% (IQR, –23.2 to –8.9%), ranging from –57.3% to –0.7% (Table 4). Figures 3A and 3B shows the correlation of D_{1cc} with and without a balloon, with a Spearman's correlation coefficient of 0.36 (p = 0.049). Comparing both methods with Bland-Altman, analysis revealed 95% limits of agreement of –9.6 Gy to 2.9 Gy, with a mean of –3.4 Gy (Figure 3C).

Acute side effects and late morbidity

The additional balloon catheter was tolerated very well by all patients. Serious acute complications (e.g., bleeding) did not occur in any case. During the further course, 4 late complications in 3 patients (1 × abscess, 2 × gastric ulcers, 1 × non-classic radiation-induced liver disease [RILD]) were observed. Complications are described in detail in Table 5.

Thus, formally the rate of significant late effects was 12.9% (> 2) and 6.45% (> 3), respectively. Of these, only

Table 4. Statistics: organ at risk (OAR) D_{1cc} with and without a balloon as well as absolute and relative differences

Parameter	OAR without balloon D_{1cc} (Gy)	OAR with balloon D_{1cc} (Gy)	Difference absolute (Gy)	Difference relative (%)
Mean	16.0	12.6	–3.4	–19.4
SD	3.2	2.0	3.1	14.5
Median	15.5	13.5	–2.5	–16.3
25th percentile	14.3	11.2	–3.9	–23.2
75th percentile	16.7	14.0	–1.4	–8.9
Minimum	11.1	8.9	–12.1	–57.3
Maximum	25.1	16.5	–0.1	–0.7

Table 5. Side effects

Acute and late side effects according to CTCAE# v. 4.03 [1-5]	Number of cases (*n*/%)	Patient study number	Treatment/outcome	Interval between iBT and side effect
Temporarily increase of bilirubin [°1]	1/3	7	No treatment/resolved	24 h
Shivering [°1]	1/3	15	No treatment/resolved	1 h
Nausea/vomiting [°2]	2/6	29	Antiemetic drugs/resolved	1 h
Abscess [°3]	1/3	20	Drainage and antibiotics/resolved	8 weeks
Non classic RILD## (previous SIRT*) [°3]	1/3	7	Ursodeoxycholic acid/resolved	12 weeks (18 weeks after radioembolization)
Ulcus ventriculi** [°4]	1/3	20	Gastrectomy/resolved	14 weeks
Ulcus ventriculi*** [°5]	1/3	11	Gastrectomy/death	15 weeks

*#common terminology criteria for adverse events, ##radiation-induced liver disease (RILD), *selective interne radiotherapy (SIRT), **patient with significantly increased cumulative exposition of gastric mucosa, ***patient with pre-existing chronic gastritis, long-term avastin-based and/or anticoagulation treatment, severe diabetes mellitus*

in one case (3.22%, patient no. 20) a severe adverse event (SAE) can be suspected due to repeated radiation exposure of the gastric mucosa. Patient no. 11 suffered from diabetes mellitus and pre-existing chronic gastritis, and received long-term treatment with Avastin® (Bevacizumab, Roche Pharma AG, Grenzach-Wyhlen, Germany) and anticoagulation, whereas patient no. 7 underwent a radio-embolization 18 weeks prior to RILD.

Discussion

The data of this study demonstrate that the interventional application of one or two balloon catheter(s) into the connective tissue layer between the hepatic capsule and adjacent OAR generates a distance between subcapsular tumor lesion of the liver and OAR, resulting in a significant median reduction of dosage exposition of the adjacent OAR of about 16%. This effect enlarges the therapeutic "window" and consecutively, the CTV can be treated with a higher, thus presumably more efficient irradiation dose.

The current ESMO guideline for the treatment of metastatic colorectal cancer (CRC) [8] indicates the growing acceptance of minimally invasive methods for the treatment of oligo-metastases. The so-called "toolbox of minimally invasive methods" is particularly important because a significant proportion of patients with oligo-metastases are not resectable for various reasons [22]. However, in addition to the indisputable role of systemic treatment [23], local control is the key to potentially sustained improvement in the overall prognosis.

Modern irradiation techniques (e.g., stereotactic body radiotherapy [SBRT], iBT) enable precise application of very high single doses. In this regard, in addition to the tumor cell destruction mechanisms based on DNA damage, further effective radiobiological effects can be initiated [24,25]. Though, even the most accurate dose application can be limited by the proximity of sensitive OAR. Chang *et al*. [26] reported a rate of ≥ 3 toxicity of 10% (mainly gastrointestinal [GI] ulceration) after 25 Gy single fraction SBRT for unresectable pancreatic adenocarcinoma, within adjacent stomach and further GI structures.

The concept of simultaneously integrated protection (SIP) could be a conceivable strategy to avoid high doses to an OAR [27]. Whether this is associated with an increased rate of local recurrences is yet to be seen. This question is currently being examined by a prospective clinical study. Therefore, the possibility of increasing distance of the CTV to surrounding OAR appears promising.

In recent years, various groups [28,29,30] have tested feasibility, safety, and application effect of absorbable polyethylene glycol (PEG) to increase the distance between the prostate and the rectal wall. In fact, by applying PEG, a dosimetrically effective distancing can be achieved.

Thus, higher irradiation doses in patients with prostate cancer can be accomplished without an increased risk of chronic side effects onto the rectal wall. Considering this successful principle of distancing, the analysis presented here verified the feasibility, tolerability, safety, and efficacy of a balloon catheter-based approach.

As a limitation, direct comparison of both approaches, with regard to acute side effects and late toxicities is difficult, since the affected OAR within the pelvis region on one hand and the abdominal cavity on the other have different tolerance doses and, moreover, the total and single doses of the irradiation concepts are not comparable.

In addition, in recent years, numerous studies have been published regarding interstitial brachytherapy of the liver [12,13,30,31,32,33,34,35,36]. The rate of side effects ≥ 3 listed in these studies was approximately 5%.

In contrast, the rate of late toxicities ≥ 3 (12.9%) in this study appears to be higher in comparison to the cited studies. Can one or two additionally applied balloon catheter(s) cause this difference? This is rather unlikely because in the affected patients, the pre-treatment modes

(selective internal radiotherapy, surgical procedures, chemotherapy, repeated irradiation) as well as severe co-morbidities (insulin-dependent diabetes mellitus, chronic gastritis etc.) must be taken into consideration. Moreover, the intraoperative situs of the second (gastrectomized) patient (no. 11) also showed a recurrent liver metastasis, which had infiltrated and damaged a large area of the wall of the reconstructed upper GI tract.

Thus, the iBT (plus balloon)-related complication rate summarizing all side effects ≥ 3 (according to CTCAE v. 4.0) would be formally 3% (patient no. 20 with ulcer 4).

A further limitation of the study is the moderate number of cases and the retrospective and monocentric character of the analysis. In addition, the balloon catheters used are not optimal because they cannot distance the adjacent OARs in large space, only in very circumscribed areas. However, as far as known, there is currently no report on increasing the distance between tumor lesion and adjacent OAR by balloon catheter(s).

For optimization, reusable balloon catheters should be designed to be inflated and deflated when in position. In order to avoid selection bias, the results of this analysis should be examined in a prospective, possibly multicenter study.

Conclusions

Insertion of balloon catheters to increase the distance between subcapsular liver malignomas and adjacent OAR is feasible, low-risk (i.e., safe), and minimally invasive to significantly reduce the radiation dose exposure of the affected OAR due to iBT. This distancing of the adjacent OAR allows a higher D_{100} value of the CTV, therefore allowing for more efficient local control. Consequently, efficacy and sustainability of radio-ablative procedures can be increased.

During a short-term single-fraction iBT, an additional balloon catheter is well tolerated. Whether the insertion of such a catheter would also be possible for a longer period of several days within a fractional SBRT (several days) is currently still not investigated by a systematic study approach.

Thus, the insertion of a balloon catheter in cases with close-fitting OAR, which also overcomes the limitations of percutaneous, non-interventional SBRT, should be further discussed and more extensively proven as an additional option.

Addendum

This work has been conducted without research support.

Results of an interim analysis of this study with 20 patients were presented at the DEGRO-Congress (Hamburg) in 2015, final results at the ESTRO-Congress in Barcelona 2018.

Disclosure

Authors report no conflict of interest.

Dr. Hass reports personal fees from Merck Serono and BMS outside the submitted work.

Dr. Seidensticker reports personal fees from Bayer, grants and personal fees from SIRTEX Medical, personal fees from Cook Medical, personal fees from BTG, outside the submitted work.

References

1. Hellmann S, Weichselbaum RR. Oligometastases. *J Clin Oncol* 1995; 13: 8-10.
2. Hughes KS, Rosenstein RB, Songhorabodi S et al. Resection of the liver for colorectal carcinoma metastases: a multi-institutional study of long-term survivors. *Dis Colon Rectum* 1988; 31: 1-4.
3. Pawlik TM, Scoggins CR, Zorzi D et al. Effect of surgical margin status on survival and site of recurrence after hepatic resection for colorectal metastases. *Ann Surg* 2005; 241: 715-722.
4. House MG, Ito H, Gönen M et al. Survival after hepatic resection for metastatic colorectal cancer: trends in outcomes for 1,600 patients during two decades at a single institution. *J Am Coll Surg* 2010; 210: 744-752.
5. Weichselbaum RR, Hellmann S. Oligometastases revisited. *Nat Rev Clin Oncol* 2011; 190: 378-382.
6. Simmonds PC, Primrose JN, Colquitt JL et al. Surgical resection of hepatic metastases from colorectal cancer: a systematic review of published studies. *Br J Cancer* 2006; 10: 982-999.
7. Hass P, Mohnike K. Extending the frontiers beyond thermal ablation by Radiofrequency Ablation: SBRT, Brachytherapy, SIRT. *Visc Med* 2014; 30: 245-252.
8. Van Cutsem E, Cervantes A, Adam R et al. ESMO consensus guidelines for the management of patients with metastatic colorectal cancer. *Ann Oncol* 2016; 27: 1386-1422.
9. Dawson LA. Overview: Where does radiation therapy fit in the spectrum of liver cancer local-regional therapies? *Semin Radiat Oncol* 2011; 21: 241-246.
10. Schefter TE, Kavanagh BD. Radiation therapy for liver metastases. *Semin Radiat Oncol* 2011; 21: 264-270.
11. Rusthoven KE, Kavanagh BD, Gardenes H et al. Multi-institutional phase I/II trial of stereotactic body radiation therapy for liver metastases. *J Clin Oncol* 2009; 27: 1572-1578.
12. Ricke J, Wust P, Stohlmann et al. CT-guided interstitial brachytherapy of liver malignancies alone or in combination with thermal ablation: Phase I-II results of a novel technique. *Int J Radiat Oncol Biol Phys* 2004; 58: 1496-1505.
13. Ricke J, Mohnike K, Pech M et al. Local response and impact on survival after local ablation of liver metastases from colorectal carcinoma by computed tomography-guided high-dose-rate brachytherapy. *Int J Radiat Oncol Biol Phys* 2010; 78: 479-485.
14. Bretschneider T, Ricke J, Gebauer B et al. Image-guided high-dose-rate brachytherapy of malignancies in various inner organs – technique, indications, and perspectives. *J Contemp Brachytherapy* 2016; 8: 251-261.
15. Streitparth F, Pech M, Bohmig M et al. In vivo assessment of the gastric mucosal tolerance dose after single fraction, small volume irradiation of liver malignancies by computed tomography-guided, high-dose-rate brachytherapy. *Int J Radiat Oncol Biol Phys* 2006; 65: 1478-1486.
16. Wieners G, Mohnike K, Peters N et al. Treatment of hepatic metastases of breast cancer with CT-guided interstitial brachytherapy – a phase II-study. *Radiother Oncol* 2011; 100: 314-319.
17. Timmermann RD. An overview of hypofractionation and introduction to this issue of seminars in radiation oncology. *Semin Radiat Oncol* 2008; 18: 215-222.
18. Herfarth KK, Debus J, Lohr F et al. Stereotactic single-dose radiation therapy of liver tumors: results of a phase I/II trial. *J Clin Oncol* 2001; 19: 164-170.

19. Sterzing F, Brunner TB, Ernst I et al. Stereotactic body radiotherapy for liver tumors. *Strahlenther Onkol* 2014; 190: 872-881.
20. Hanley JA, McNeil BJ. The meaning and use of the area under a receiver operating characteristic (ROC) curve. *Radiology* 1982; 143: 29-36.
21. Bland JM, Altman DG. Statistical methods for assessing agreement between two methods of clinical measurement. *Lancet* 1986; 1: 307-310.
22. Misiakos EP, Karidis NP, Kouraklis G. Current treatment for colorectal liver metastases. *World J Gastroenterol* 2011; 17: 4067-4075.
23. Stein A, Schmoll HJ. Systemic treatment of liver metastases from colorectal cancer. *Ther Adv Med Oncol.* 2013; 5: 193-203.
24. Brown JM, Koong AC. High-dose single-fraction radiotherapy: exploiting a new biology? *Int J Radiat Oncol Biol Phys* 2008; 71: 324-325.
25. Murray D, McBride WH, Schwartz JL. Radiation biology in the context of changing patterns of radiotherapy. *Radiat Res* 2014; 182: 259-272.
26. Chang DT, Schellenberg D, Shen J et al. Stereotactic radiotherapy for unresectable adenocarcinoma of the pancreas. *Cancer* 2009; 115: 665-672.
27. Brunner TB, Nestle U, Adebahr S et al. Simultaneous integrated protection: A new concept for high-precision radiation therapy. *Strahlenther Onkol* 2016; 192: 886-894.
28. Song DY, Herfarth KK, Uhl M et al. A multi-institutional clinical trial of rectal dose reduction via injected polyethylene-glycol hydrogel during IMRT for prostate cancer: Analysis of dosimetric outcomes. *Int J Radiat Oncol Biol Phys* 2013; 87: 81-87.
29. Uhl M, van Triest B, Eble MJ et al. Low rectal toxicity after dose escalated IMRT treatment of prostate cancer using an absorbable hydrogel for increasing and maintaining space between the rectum and prostate: Results of a multi-institutional phase II trial. *Radiother Oncol* 2013; 106: 215-219.
30. Pinkawa M, Berneking V, König L et al. Hydrogel injection reduces rectal toxicity after radiotherapy for localized prostate cancer. *Strahlenther Onkol* 2017; 193: 22-28.
31. Mohnike K, Wolf S, Damm R et al. Radioablation of liver malignancies with interstitial high-dose-rate brachytherapy: Complications and risk factors. *Strahlenther Onkol* 2016; 192: 288-296.
32. Tselis N, Chatzikonstantinou G, Kolotas C et al. Computed-tomography-guided interstitial high dose rate brachytherapy for centrally located liver tumour: a single institution study. *Eur Radiol* 2013; 23: 2264-2270.
33. Mohnike K, Wieners G, Schwartz F et al. Computed tomography-guided high-dose-rate brachytherapy in hepatocellular carcinoma: Safety, efficacy and effect on survival. *Int J Radiat Oncol Biol Phys* 2010; 78: 172-179.
34. Bretschneider T, Mohnike K, Hass P et al. Efficacy and safety of image-guided interstitial single fraction high-dose-rate brachytherapy in the management of metastatic malignant melanoma. *J Contemp Brachytherapy* 2015; 2: 154-160.
35. Sharma DN, Thulkar S, Sharma S et al. High-dose-rate interstitial brachytherapy for liver metastases: first study from India. *J Contemp Brachytherapy* 2013; 5: 70-75.
36. Sharma DN, Thulkar S, Kumar R et al. Interstitial brachytherapy for liver metastases and assessment of response by positron emission tomography: a case report. *J Contemp Brachytherapy* 2010; 2: 114-116.

Strahlenther Onkol (2019) 195:982–990
https://doi.org/10.1007/s00066-019-01501-1

ORIGINAL ARTICLE

Prospective evaluation of CT-guided HDR brachytherapy as a local ablative treatment for renal masses: a single-arm pilot trial

R. Damm[1,6] · T. Streitparth[2] · P. Hass[3] · M. Seidensticker[2] · C. Heinze[1] · M. Powerski[1] · J. J. Wendler[4] · U. B. Liehr[4] · K. Mohnike[5] · M. Pech[1] · J. Ricke[2]

Received: 8 April 2019 / Accepted: 11 July 2019 / Published online: 25 July 2019

Abstract

Purpose In this pilot trial, we investigate the safety of CT-guided high-dose-rate brachytherapy (HDR-BT) as a local ablative treatment for renal masses not eligible for resection or nephrectomy.

Methods We investigated renal function after irradiation by HDR-BT in 16 patients (11 male, 5 female, mean age 76 years) with 20 renal lesions (renal cell carcinoma $n=18$; renal metastases $n=2$). Two patients had previous contralateral nephrectomy and two had ipsilateral partial nephrectomy. Six lesions had a hilar localization with proximity to the renal pelvis and would have not been favorable for thermal ablation. Renal function loss was determined within 1 year after HDR-BT by renal scintigraphy and laboratory parameters. Further investigations included CT and MRI every 3 months to observe procedural safety and local tumor control. Renal function tests were analyzed by Wilcoxon's signed rank test with Bonferroni–Holm correction of *p*-values. Survival and local tumor control underwent a Kaplan–Meier estimation.

Results Median follow-up was 22.5 months. One patient required permanent hemodialysis 32 months after repeated HDR-BT and contralateral radiofrequency ablation of multifocal renal cell carcinoma. No other patient developed a significant worsening in global renal function and no gastrointestinal or urogenital side effects were observed. Only one patient died of renal tumor progression. Local control rate was 95% including repeated HDR-BT of two recurrences.

Conclusion HDR-BT is a feasible and safe technique for the local ablation of renal masses. A phase II study is recruiting to evaluate the efficacy of this novel local ablative treatment in a larger study population.

Keywords Renal cell cancer · Brachytherapy · Local-ablative treatment · Renal tumors · Renal function

Prospektive Evaluation der CT-gesteuerten HDR-Brachytherapie als lokalablative Behandlung von Nierenraumforderungen: eine einarmige Pilotstudie

Zusammenfassung

Ziel In dieser Pilotstudie wurde die Sicherheit der computertomographie-(CT-)geführten „High-dose-rate"-Brachytherapie (HDR-BT) bei der lokalablativen Behandlung von nichtresektablen Nierenraumforderungen untersucht.

Availability of data and materials All relevant data regarding the study conclusion are displayed in the publication. Raw data used and/or analyzed during the study are available from the corresponding author on reasonable request.

✉ Dr. R. Damm
robert.damm@med.ovgu.de

[1] Department of Radiology and Nuclear Medicine, Otto-von-Guericke University, Magdeburg, Germany

[2] Department of Radiology, Ludwig-Maximilians-University Munich, Munich, Germany

[3] Department of Radiation Oncology, Otto-von-Guericke University, Magdeburg, Germany

[4] Department of Urology, Otto-von-Guericke University, Magdeburg, Germany

[5] Diagnostic and Therapeutic Center am Frankfurter Tor, Berlin, Germany

[6] Klinik für Radiologie und Nuklearmedizin, Universitätsklinikum Magdeburg, Leipziger Str. 44, 39120 Magdeburg, Germany

Methoden Es wurde die Nierenfunktion von 16 Patienten (11 männlich, 5 weiblich, mittleres Alter 76 Jahre) mit 20 Nierenläsionen (Nierenzellkarzinom $n=18$; Nierenmetastasen $n=2$) nach Bestrahlung mittels HDR-BT untersucht. Jeweils 2 Patienten hatten eine vorangegangene kontralaterale Nephrektomie bzw. ipsilaterale Teilresektion. Sechs Läsionen lagen zentral am Nierenbecken und waren technisch nicht suffizient durch eine thermische Ablation behandelbar. Die Nierenfunktion wurde innerhalb eines Jahres nach HDR-BT durch Nierensequenzszintigraphien sowie Laborwerte bestimmt. Weitere Untersuchungen beinhalteten CT und Magnetresonanztomographie (MRT) alle 3 Monate zur Beobachtung der Sicherheit und Tumorkontrolle. Die Nierenfunktionstests wurden mit dem Wilcoxon-Test mit Bonferroni-Holm-Korrektur der p-Werte analysiert. Überleben und lokale Tumorkontrolle wurden mit der Kaplan-Meier-Schätzung ausgewertet.
Ergebnisse Das mediane Follow-up betrug 22,5 Monate. Ein Patient benötigte permanente Hämodialyse 32 Monate nach wiederholter HDR-BT und kontralateraler Radiofrequenzablation bei multifokalem Nierenzellkarzinom. Keine weiteren Patienten zeigten eine signifikante Verschlechterung der globalen Nierenfunktion. Es wurden keine gastrointestinalen oder urogenitalen Nebenwirkungen beobachtet. Ein Patient verstarb durch lokale Tumorprogression. Die lokale Kontrollrate betrug – einschließlich wiederholter HDR-BT von zwei Rezidiven – 95%.
Schlussfolgerung Die HDR-BT ist eine technisch machbare und sichere Technik zur lokalen Ablation von Nierentumoren. Momentan rekrutiert eine Phase-II-Studie eine größere Patientenpopulation, um die Effektivität dieser neuen Anwendung genauer zu untersuchen.

Schlüsselwörter Nierenzellkarzinom · Brachytherapie · Lokalablative Behandlung · Nierentumore · Nierenfunktion

Introduction

Patients with locally confined renal masses will most likely undergo partial or total nephrectomy if clinically eligible [1]. However, up to 25% percent of patients might present with a contraindication to surgery [2]. In these cases, local therapies such as radiofrequency ablation (RFA), cryoablation (CA), or microwave ablation (MWA) are an alternative option with less treatment-associated morbidity [3, 4].

Computed tomography-guided interstitial high-dose-rate brachytherapy (HDR-BT) is an ablation technique utilizing single-fraction irradiation by an iridium-192 source which is inserted in the tumor via percutaneously applied catheters. In contrary to thermal ablation techniques, HDR-BT has no technical restriction in terms of tumor size or proximity to larger vessels or heat-vulnerable structures [5–7].

The most common application of CT-guided HDR-BT today is the radioablation of primary and secondary liver malignancies, especially hepatocellular carcinoma and colorectal liver metastases [8, 9]. A recent study also investigated the application of HDR-BT to adrenal gland malignancies [10].

To our knowledge, this new local ablative technique has not yet been thoroughly evaluated for the ablation of renal masses. Thus, we initiated a phase I trial to report the feasibility and safety of HDR-BT applied for renal masses in patients not eligible for surgery.

Patients and methods

Patient cohort

The institutional review board approved the study prior to recruitment and all patients gave oral and written informed consent.

Our study comprises 16 patients with 20 renal masses (11 male, 5 female, mean age 76 years) treated by HDR-BT at the Department of Radiology. Prior clinical evaluation was conducted by the Department of Urology and feasibility to undergo surgery was omitted in all patients (inadequate clinical performance status $n=6$; imminent hemodialysis after surgery $n=5$; metastatic disease $n=5$). Tumor entities include renal cell carcinoma (RCC; $n=18$) and metastases of colorectal carcinoma (CRC; $n=1$) or hepatocellular carcinoma (HCC; $n=1$). Bilateral and multifocal RCC were present in one patient. Two patients had prior contralateral nephrectomy and ipsilateral partial nephrectomy, respectively. Concomitant kidney diseases were polycystic kidney disease ($n=1$) and horseshoe kidney ($n=1$).

In summary, inclusion criteria were:

i. renal masses with indication for local treatment (renal metastases and histologically proven or suspected renal cell cancer),
ii. ineligibility to undergo surgical treatment (see above)
iii. sufficient performance status to safely undergo interventional treatment under conscious sedation,
iv. written informed consent,

Table 1 Characteristics for all 16 patients treated on 20 renal masses

	N (%)	Mean ± SD	Range
Patient data (N = 16)			
Sex			
Male	*N* = 11 (69)	–	–
Female	*N* = 5 (31)	–	–
Age (years)	–	75.7 ± 13.0	(52–92)
Prior surgery/renal diseases	*N* = 6 (37.5)	–	–
Horseshoe kidneys	*N* = 1 (6.3)	–	–
Polycystic kidney disease	*N* = 1 (6.3)	–	–
Contralateral total nephrectomy	*N* = 2 (12.6)	–	–
Ipsilateral partial nephrectomy	*N* = 2 (12.6)	–	–
Treatment data (N = 20)			
Etiology of renal masses			
Renal cell cancer	*N* = 18 (90)	–	–
Colorectal cancer	*N* = 1 (5)	–	–
Hepatocellular Carcinoma	*N* = 1 (5)	–	–
Tumor size and location			
T1a (<4 cm)	*N* = 15 (75)	–	–
T1b (>4 cm)	*N* = 5 (25)	–	–
Cortical/parenchymal localization	*N* = 14 (70)	–	–
Central/hilar localization	*N* = 6 (30)	–	–
Tumor size	–	3.5 ± 2.1 cm	(1.2–9.4 cm)
No. of irradiation catheters	–	2.2 ± 1.0	(1–5)
Clinical target volume	–	34.8 ± 40.3 cm^3	(3.5–163.3 cm^3)
D100	–	16.37 ± 2.18 Gy	(13.44–21.6 Gy)
Primary local tumor control	*N* = 17 (85)	–	–
Secondary local tumor control	*N* = 19 (95)	–	–

Exclusion criteria included:

i. life expectancy <6 months,
ii. estimated dose exposure to organs at risk (OAR) above local clinical standards (see below)
iii. insufficient laboratory parameters for interventional treatment (hemoglobin <6.0 mmol/l, thrombocyte count <50 Gpt/l, international normalized ratio >1.5, partial thromboplastin time >50 s)

The patient characteristics are displayed in Table 1.

Radioablation by HDR brachytherapy

To place brachytherapy catheters in a renal mass, the following procedure was performed under conscious sedation using midazolam and fentanyl: The tumor was punctured percutaneously by an 18 G coaxial needle under CT fluoroscopy (Aquillion, Canon Medical Systems, Neuss, Germany). Then, a 6F angiographic catheter sheath (Terumo Radifocus® Introducer II, Terumo Europe, Leuven, Belgium) was inserted through a guide wire (Amplatz SuperStiff™, Boston Scientific, Marlborough, USA). In a last step, a 6F irradiation catheter (afterloading catheter, Primed® medical GmbH, Halberstadt, Germany) was placed inside the catheter sheath. For the treatment of larger or complex-shaped lesions, multiple catheter placements were required for a sufficient geometry of the ablation zone while reducing the radiation exposure of adjacent organs. Twenty lesions were ablated in the study, requiring a total of 43 catheter placements in 16 patients and a median of 2 catheters per lesion (range 1–5). Typical time for the interventional procedure was 10 to 40 min depending on the complexity of the lesions and percutaneous access. Pretreatment medication included an antiemetic prophylaxis consisting of 8 mg dexamethasone and 8 mg odansetron administered intravenously. A routine antibiotic prophylaxis was not required.

After catheter placement, a multi-slice CT visualized the catheter position(s) in the renal mass and the imaging data (axial slices with 3 mm thickness) was transferred to the irradiation planning system (Oncentra® Brachy, Elekta Instrument AB, Stockholm, Sweden). The gross tumor volume (GTV) was delineated in a 3D treatment plan by hand and an automated algorithm generated a 5 mm safety margin to define the clinical target volume (CTV). As the brachytherapy catheters were fixed within the tumor eliminating inaccuracy of respiratory movement, the CTV was directly adopted as the planning target volume (PTV). Ra-

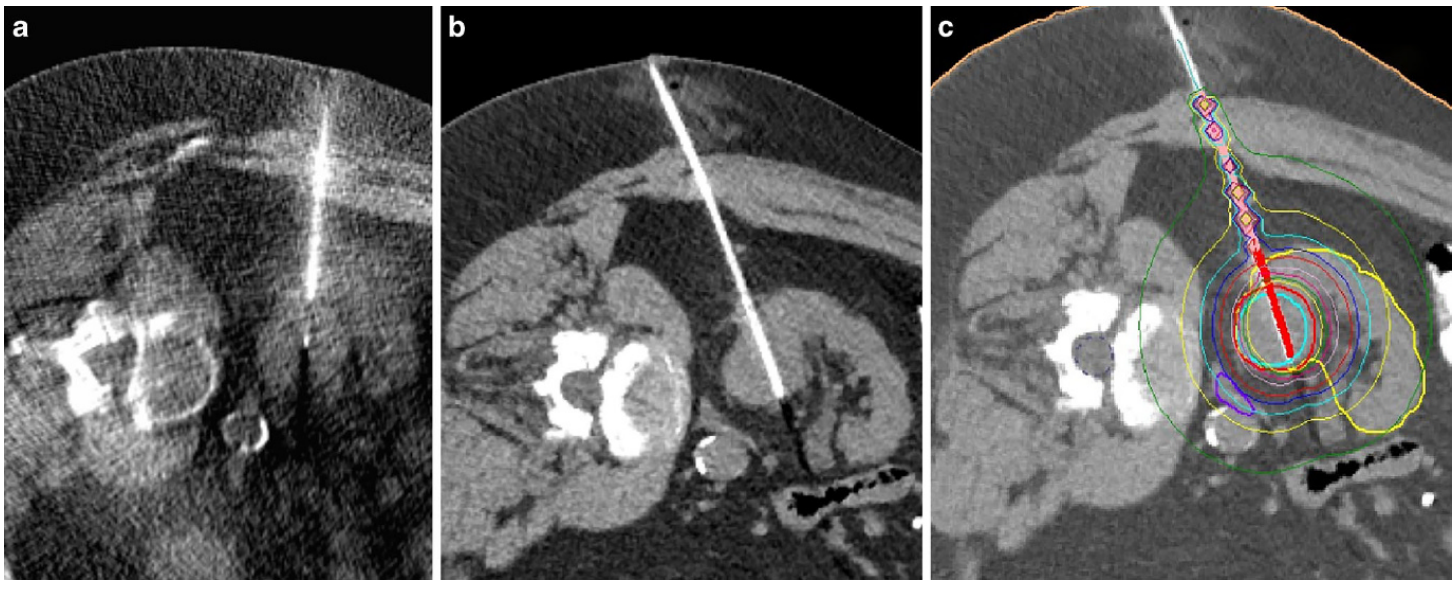

Fig. 1 Image data set of Computed tomography-guided brachytherapy for a renal cell carcinoma: **a** Computed tomography fluoroscopy, image-guided insertion of a coaxial needle for biopsy and subsequent catheter placement; **b** diagnostic computed tomography displaying the catheter sheath within the renal mass; **c** irradiation plan depicting the tip of the iridium-192 source (*red line*) and corresponding isodoses for radioablation

dioablation was then achieved by a single fraction of 15 Gy prescribed to the PTV [11]. In local recurrences of a previously irradiated lesion, a dose escalation for the PTV with 20 Gy was applied [12]. Dose constraints for organs at risk (OAR) were D_{1CC} ≤14 Gy for stomach and small bowel, D_{1CC} ≤18 Gy for large bowel and V_{5Gy} ≤66% for the liver, referring to contemporary literature [13–15].

After completion of the irradiation procedure, catheters and sheaths were removed, leaving a gelatin sponge in the catheter path to prevent bleeding. Patients continued fasting and bed rest for at least 4 h. To exclude early complications, ultrasonography of the treatment area was conducted 1 to 2 h after catheter removal. Scheduled hospitalization was 2 days after treatment. Post-treatment workup included standard laboratory evaluation prior to discharge. Interventional complications were recorded and assessed by the Clavien–Dindo classification [16], radiation-induced adverse events were classified by the Common Terminology Criteria for Adverse Events (CTCAE 4.02).

A typical imaging data set for HDR brachytherapy is depicted in Fig. 1.

Imaging

Pretreatment planning was performed by magnetic resonance imaging (MRI) of the kidneys comprising high resolution T1 and T2 sequences (with and without fat saturation) as well as dynamic contrast-enhanced studies. Additional tumor sites were assessed by contrast-enhanced computed tomography (CT) of the thorax and abdomen.

During follow-up, all patients were scheduled for MRI of the kidneys every 3 months and additional CT if necessary. All imaging datasets were then reviewed for local and locoregional recurrences.

Renal function tests

Primary endpoint of the study was renal function loss within 1 year after HDR-BT.

Laboratory evaluations were conducted prior to CT-guided HDR-BT as well as 3 days, 3 months, 6 months, and 12 months after treatment, including creatinine serum levels with calculation of the estimated glomerular filtration rate (eGFR) according to the Chronic Kidney Disease Epidemiology Collaboration (CKI-EPI) formula. Furthermore, patients underwent dynamic renal scintigraphy with technetium-99 mercaptoacetyltriglycine (Tc99m-MAG3) for determination of the tubular extraction rate (TER) at baseline and 3 months, 6 months, and 12 months after HDR-BT. The tracer extraction was quantified separately for both kidneys to assess the ipsilateral and contralateral effects of radiation exposure by HDR-BT on renal function.

Statistical analysis

Statistical analysis of all data was performed using IBM SPSS Statistics 22.0® (IBM Corp., Armonk, NY, USA). Measures for safety (e.g., acute and chronic adverse events) and efficacy (e.g., technical success) underwent descriptive statistics. Survival and local tumor control were calculated by the Kaplan–Meier estimation. All renal function tests were processed as non-parametric variables and testing was performed utilizing Wilcoxon's signed rank test with Bonferroni-Holm correction. All tests were carried out two-

sided. In data interpretation, $p \leq 0.05$ was determined as statistically significant.

Results

Treatment characteristics

Besides two renal metastases (CRC $n=1$; HCC $n=1$), all incidental lesions were proven histologically by prior or concomitant core needle biopsy as renal cell carcinomas (RCC $n=18$). Local tumor stage was T1a (<4 cm) in 15 lesions and T1b and greater (>4 cm) in 5 lesions. Six lesions had a central localization in or close to the renal hilum and were not eligible for thermal ablation.

Mean tumor size was 3.5 cm (range 1.2–9.4 cm), requiring a mean number of 2 catheters for sufficient dose application (range 1–5). Including a 5 mm safety margin, a mean effective tumor-surrounding dose (CTV/D100) of 16.37 ± 2.18 Gy was achieved. Mean irradiation time was 1325 ± 858 s (22.1 ± 14.3 min).

Concomitant treatments were Y90 radioembolization for liver-dominant metastatic colorectal cancer ($n=1$) or synchronous liver metastases of RCC ($n=1$). One patient underwent prior HDR-BT for multifocal hepatocellular carcinoma in liver cirrhosis.

A summary of patient and treatment characteristics is given in Table 1.

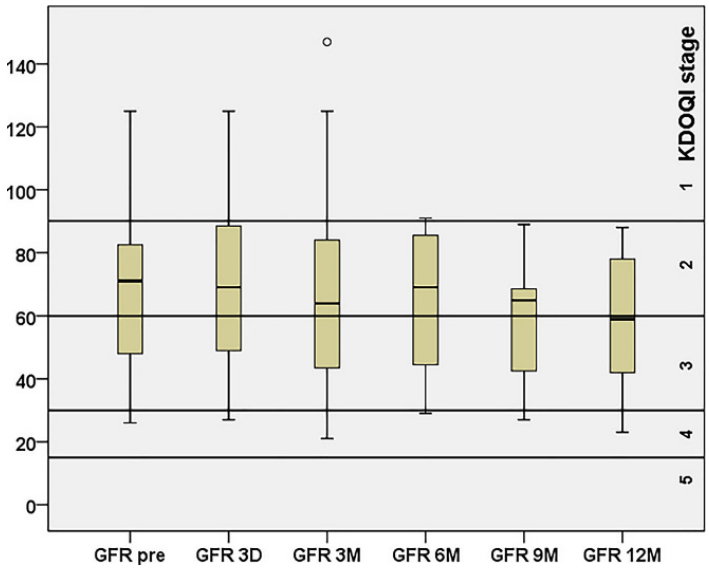

Fig. 2 Boxplots representing eGFR (ml/min) at baseline (*GFR pre*) and 3 days (*GFR 3D*), 3 months (*GFR 3M*), 6 months (*GFR 6M*), 9 months (*GFR 9M*), and 12 months (*GFR 12M*) after HDR-BT; *reference lines* depict corresponding KDOQI stages

Renal function analysis

The glomerular filtration rate was assessed by laboratory evaluation of serum creatinine (eGFR, estimated GFR according to the CKI-EPI formula) at baseline and 3 days after CT-guided brachytherapy, as well as every 3 months during follow-up. Medians of eGFR demonstrated a decrease from 71 ml/min (range 26–125 ml/min) at baseline to 58 ml/min (23–88 ml/min) after 12 months as demonstrated by the boxplot in Fig. 2. The reduction of eGFR after HDR-BT did not meet statistical significance at any time point (Wilcoxon signed rank test with Bonferroni–Holm correction). The corresponding KDOQI stages had a median of 2 from baseline to 9 months follow. At 12 months, the median KDOQI stage decreased to 3 without statistical significance ($p=0.315$). An overview of eGFR and KDOQI stages is given in Fig. 2.

Tubular excretion rate was determined by renal scintigraphy (TER) at baseline and 3 months, 6 months, and 12 months after HDR-BT. Medians for TER decreased from 156 ml/min (range 97–340 ml/min) at baseline to a minimum of 108 ml/min (range 108–142 ml/min) at 12 months

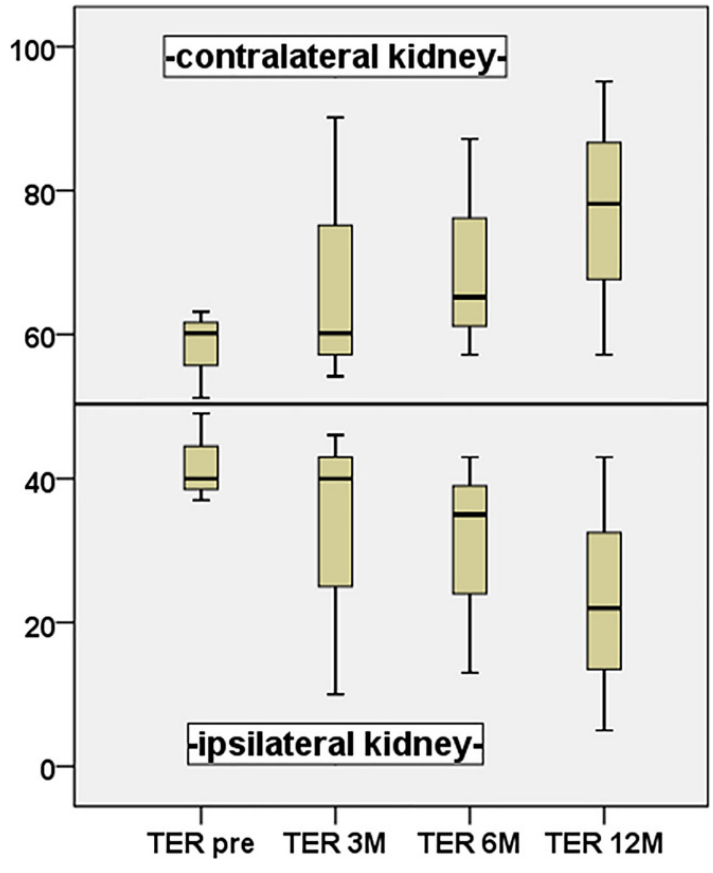

Fig. 3 Boxplots representing TER (ml/min) at baseline (*TER pre*), 3 months (*TER 3M*), 6 months (*TER 6M*), and 12 months (*GFR 12M*) after HDR-BT separated by ipsilateral (HDR-BT of renal mass) and contralateral kidney. *Reference line* represents 50 ml/min to visualize the stepwise decrease in ipsilateral kidney function after HDR-BT and compensatory increase of contralateral kidney function

follow-up. Correspondingly, median ipsilateral TER was reduced from 52 ml/min (range 37–100 ml/min) at baseline to 33 ml/min (range 5–100 ml/min) at 12 months follow-up ($p = 0.285$). The median contralateral TER demonstrated an increase from 51 ml/min (range 38–63 ml/min) to a maximum of 95 ml/min (range 57–95 ml/min) 12 months after HDR-BT ($p = 0.285$). A summary of ipsilateral and contralateral TER measurements is depicted in Fig. 3.

Clinical risk assessment

In our cohort, one puncture-related adverse event was observed in a patient suffering hematothorax from bleeding of an intercostal artery. The patient underwent subsequent ligation and was monitored for 24 h at the intensive care unit (ICU). The patient received 600 ml of packed red blood cells during surgery and antibiotic prophylaxis with ampicillin/sulbactam for 7 days. This single event was rated as grade IIIb according to the Clavien–Dindo classification and results in a patient-based risk of 6.3% and lesion-based risk of 5% for 30-day morbidity. No 30-day mortality or re-hospitalization was observed. Median duration of hospitalization was 2 days (range 2–9 days). Chronic adverse events occurred in one patient requiring permanent hemodialysis 32 months after HDR-BT with prior RFA of the contralateral kidney and a baseline eGFR of 26 ml/min. All other patients retained sufficient renal function and did not require hemodialysis during follow-up. Furthermore, no significant gastrointestinal or urogenital side effects (CTCAE grade 3/4 events) or infectious complications were observed after treatment. Overall, the patient-based risk of chronic adverse events was 6.3%.

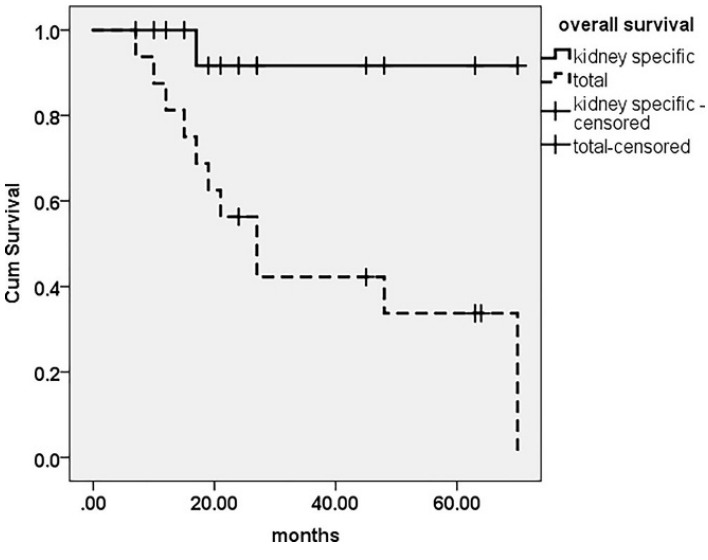

Fig. 4 Kaplan–Meier estimation for overall survival; *lines* represent any causes of death: *dotted line* including extra-renal causes, e.g., cardiovascular events, versus kidney-related causes of death (*solid line*), e.g., tumor progression of renal cell carcinoma. Median follow-up for survival was 22.5 months

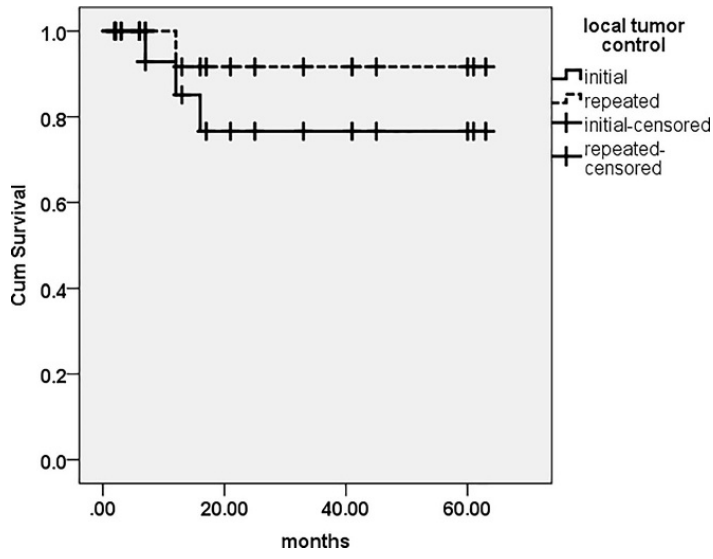

Fig. 5 Local tumor control for initial HDR-BT (85%) and additional HDR-BT in 2 cases of local recurrences (95%). Median follow-up for imaging was 14.5 months

Survival and local tumor control

Median overall survival was 27.0 months. Censoring extrarenal causes of death (malignant disease in other organs $n = 4$; aftermath of a fall in elderly patients $n = 2$; cardiopulmonary events $n = 1$; intracranial bleeding $n = 1$), the median of overall survival was not reached and mean overall survival accounted for 65.6 months. The Kaplan–Meier chart for survival is displayed in Fig. 4.

Local tumor control after CT-guided HDR-BT was reviewed throughout a median imaging follow-up of 14.5 months. Local recurrence was defined as tumor growth from baseline imaging. We observed a total of 3 local recurrences in 20 tumors, equaling a primary tumor control rate (pLTC) of 85%. Two of these recurrences were successfully treated by repeated HDR-BT, with dose escalation from 15 to 20 Gy yielding a secondary local tumor control rate of 95% (sLTC).

Figure 5 depicts the Kaplan–Meier estimation for local tumor control.

Discussion

The primary endpoint of this prospective observational trial was to assess renal function loss after CT-guided HDR-BT as a local ablative treatment for renal masses. As a secondary endpoint, we investigated procedural safety and local tumor control in HDR-BT.

Early and late adverse events

Neither acute radiation-induced effects on renal function nor any gastrointestinal side effects were observed within 30 days after HDR-BT. One heavily pretreated patient with known risk factors (treatment of bilateral tumors and severe kidney dysfunction at baseline [17]) required hemodialysis more than 2.5 years after brachytherapy. All other patients retained renal function without requiring hemodialysis during follow-up and without significant deterioration of eGFR—a benefit previously described for thermal ablation techniques [18]. In contrast, a decline in global kidney function of approximately 10% is commonly seen after partial nephrectomy and typically attributed to perioperative ischemia and nephron loss [19]. In the surgical setting, an ipsilateral decrease in renal function of up to 24.4% was reported, while contralateral compensation accounted for only 2.3% after partial nephrectomy. Correspondingly, the increase in contralateral volume was marginal [20, 21]. Our results suggest a functional hypertrophy in the contralateral kidney after CT-guided HDR-BT of ipsilateral renal masses as indicated by scintigraphic measurement of the tubular excretion rate (Fig. 3). Although these changes obviously originate from ipsilateral function loss, little is known about the specific etiology of radiation-induced nephropathy especially in single-fraction brachytherapy [22]. However, we hypothesize that the underlying mechanisms may contribute to a favorable safety profile of radioablation by HDR-BT in the kidney and our clinical follow-up implies that HDR-BT is safe in terms of global renal function.

Procedural complication rates in percutaneous radiofrequency ablation or cryoablation range from 13.0 to 23.0%, while major complications are reported in 4.3 and 4.5% of patients in larger cohorts, respectively [3, 23, 24]. Acute morbidity by CT-guided catheter placement was comparably low, including one case of puncture-associated bleeding (Clavien–Dindo grade IIIb; 6.3%).

HDR-BT compared to other ablation techniques

In our study population, one quarter of all renal masses exceeded the recommendations for thermal ablation (T1b; >4 cm) according to the recent guideline of the European Association of Urology (EAU) and nearly one third had a hilar localization that would prohibit radiofrequency ablation. Including these cases not favorable for thermal ablation techniques due to size or location, HDR-BT could demonstrate a primary local tumor control (pLTC) of 85%, and secondary tumor control (sLTC) increased to 95% after treatment of recurrences by repeated HDR-BT. In summary, local recurrence was comparable to radiofrequency ablation and cryoablation, as meta-analyses report local tumor control of 87.1 to 94.8% in small renal masses (T1a; <4 cm) and thermal ablation techniques [2, 25]. Inferior outcomes in radiofrequency ablation or cryoablation are reported for larger or central lesions [24, 26]. The LTC achieved in our study is also consistent with results of phase I/II trials investigating stereotactic body radiotherapy (SBRT) as another form of high-dose conformal irradiation in renal cell cancer (LTC ranging from 83 to 98%) [27]. Excellent results in SBRT were seen in T1a as well as T1b tumors, while toxicities were limited to grade 1 or 2 events in 18 to 78% of patients [28–30].

Advantages of SBRT include its noninvasiveness compared to the interventional approach in thermal ablation and interstitial brachytherapy, unless fiducial markers need to be placed for tumor tracking. Although procedural morbidity in interventional techniques is generally low, most reports of ablative treatments are restricted to lesions in favorable localizations, as complication rates rise with proximity to the renal pelvis [31–33]. Comparing both irradiation techniques, dose fall-off and elimination of respiratory motion by catheter fixation in single-fraction HDR-BT might reduce the impairment of healthy renal tissue while fractionating and dose distribution in SBRT might decrease radiation damage to adjacent bowel structures (comparative data only available for treatment planning in other abdominal organs) [34–36]. As HDR-BT and SBRT are not standardized in terms of dosage and fractionation, evaluation of study results is difficult.

In summery, these findings underline the potential of HDR-BT, as many technical restrictions known for thermal ablation techniques (e.g., heat-sink effect) do not apply for radioablation and no radiation-induced side effects on the renal pelvis and ureter were observed in our study. Given these technical restrictions of thermal ablation, irradiation by HDR-BT (as well as SBRT) might not only be a substitute for the ablation of small renal masses (T1a), but may present a favorable treatment for the local ablation of central or large renal tumors (T1b) compared to radiofrequency ablation or cryoablation [37, 38].

Limitations

Our study comprises only a small cohort of patients with predominantly higher age and pre-existing renal morbidity in more than one third. Furthermore, two patients underwent treatment for renal metastases as a part of systemic dissemination in advanced tumors. Hence, our study population might have been more susceptible to adverse events. Thus, safety seems to be favorable in CT-guided HDR-BT based on the presented clinical data. As tumor control might not last in all patients and statistical analysis of cofactors (e.g., tumor stage) cannot be conducted in our small cohort, upcoming investigations should focus on long-term follow-

up and a dedicated analysis of efficacy depending on tumor size (T1a vs. T1b).

Conclusion

CT-guided HDR-BT is a feasible technique for the local ablation of renal masses with encouraging results for safety and local tumor control, even in masses not eligible for thermal ablation. A phase II study is currently recruiting to evaluate the efficacy of this novel local ablative treatment in a larger study population.

Compliance with ethical guidelines

Conflict of interest R. Damm, T. Streitparth, P. Hass, M. Seidensticker, C. Heinze, M. Powerski, J.J. Wendler, U.B. Liehr, K. Mohnike, M. Pech, and J. Ricke state that there are no competing interests and that this work has not received any funding.

Ethical standards The study was conducted in accordance with the Declaration of Helsinki. All patients included were treated at a single institution, prospective data collection and analysis was approved by the local ethics committee. All patients gave written informed consent for the collection of their medical data for scientific purposes. No personal information is included in the publication, thus no dedicated approval was required.

References

1. Kim DY, Wood CG, Karam JA (2014) Treating the two extremes in renal cell carcinoma: management of small renal masses and cytoreductive nephrectomy in metastatic disease. Am Soc Clin Oncol Educ Book e214–21. https://doi.org/10.14694/EdBook_AM.2014.34.e214
2. Thompson RH, Atwell T, Schmit G, Lohse CM, Kurup AN, Weisbrod A et al (2015) Comparison of partial nephrectomy and percutaneous ablation for cT1 renal masses. Eur Urol 67:252–259
3. Rivero JR, De La Cerda J 3rd, Wang H, Liss MA, Farrell AM, Rodriguez R et al (2018) Partial nephrectomy versus thermal ablation for clinical stage T1 renal masses: systematic review and meta-analysis of more than 3,900 patients. J Vasc Interv Radiol 29:18–29
4. Sung HH, Park BK, Kim CK, Choi HY, Lee HM (2012) Comparison of percutaneous radiofrequency ablation and open partial nephrectomy for the treatment of size- and location-matched renal masses. Int J Hyperthermia 28:227–234
5. Collettini F, Schnapauff D, Poellinger A, Denecke T, Schott E, Berg T et al (2012) Hepatocellular carcinoma: computed-tomography-guided high-dose-rate brachytherapy (CT-HDRBT) ablation of large (5–7 cm) and very large (⟩7 cm) tumours. Eur Radiol 22:1101–1109
6. Collettini F, Singh A, Schnapauff D, Powerski MJ, Denecke T, Wust P et al (2013) Computed-tomography-guided high-dose-rate brachytherapy (CT-HDRBT) ablation of metastases adjacent to the liver hilum. Eur J Radiol 82:e509–14
7. Vollherbst D, Bertheau R, Kauczor HU, Radeleff BA, Pereira PL, Sommer CM (2017) Treatment failure after image-guided percutaneous radiofrequency ablation (RFA) of renal tumors—a systematic review with description of type, frequency, risk factors and management. Rofo 189:219–227
8. Mohnike K, Wieners G, Schwartz F, Seidensticker M, Pech M, Ruehl R et al (2010) Computed tomography-guided high-dose-rate brachytherapy in hepatocellular carcinoma: safety, efficacy, and effect on survival. Int J Radiat Oncol Biol Phys 78:172–179
9. Ricke J, Mohnike K, Pech M, Seidensticker M, Ruhl R, Wieners G et al (2010) Local response and impact on survival after local ablation of liver metastases from colorectal carcinoma by computed tomography-guided high-dose-rate brachytherapy. Int J Radiat Oncol Biol Phys 78:479–485
10. Mohnike K, Neumann K, Hass P, Seidensticker M, Seidensticker R, Pech M et al (2017) Radioablation of adrenal gland malignomas with interstitial high-dose-rate brachytherapy: Efficacy and outcome. Strahlenther Onkol 193:612–619
11. Wieners G, Pech M, Rudzinska M, Lehmkuhl L, Wlodarczyk W, Miersch A et al (2006) CT-guided interstitial brachytherapy in the local treatment of extrahepatic, extrapulmonary secondary malignancies. Eur Radiol 16:2586–2593
12. Geisel D, Collettini F, Denecke T, Grieser C, Florcken A, Wust P et al (2013) Treatment for liver metastasis from renal cell carcinoma with computed-tomography-guided high-dose-rate brachytherapy (CT-HDRBT): a case series. World J Urol 31:1525–1530
13. Mohnike K, Wolf S, Damm R, Seidensticker M, Seidensticker R, Fischbach F et al (2016) Radioablation of liver malignancies with interstitial high-dose-rate brachytherapy: Complications and risk factors. Strahlenther Onkol 192:288–296
14. Streitparth F, Pech M, Bohmig M, Ruehl R, Peters N, Wieners G et al (2006) In vivo assessment of the gastric mucosal tolerance dose after single fraction, small volume irradiation of liver malignancies by computed tomography-guided, high-dose-rate brachytherapy. Int J Radiat Oncol Biol Phys 65:1479–1486
15. Wieners G, Mohnike K, Peters N, Bischoff J, Kleine-Tebbe A, Seidensticker R et al (2011) Treatment of hepatic metastases of breast cancer with CT-guided interstitial brachytherapy—a phase II-study. Radiother Oncol 100:314–319
16. Dindo D, Demartines N, Clavien PA (2004) Classification of surgical complications: a new proposal with evaluation in a cohort of 6336 patients and results of a survey. Ann Surg 240:205–213
17. Huang WC, Levey AS, Serio AM, Snyder M, Vickers AJ, Raj GV et al (2006) Chronic kidney disease after nephrectomy in patients with renal cortical tumours: a retrospective cohort study. Lancet Oncol 7:735–740
18. Raman JD, Jafri SM, Qi D (2016) Kidney function outcomes following thermal ablation of small renal masses. World J Nephrol 5:283–287
19. Mir MC, Ercole C, Takagi T, Zhang Z, Velet L, Remer EM et al (2015) Decline in renal function after partial nephrectomy: etiology and prevention. J Urol 193:1889–1898
20. Choi KH, Yoon YE, Kim KH, Han WK (2015) Contralateral kidney volume change as a consequence of ipsilateral parenchymal atrophy promotes overall renal function recovery after partial nephrectomy. Int Urol Nephrol 47:25–32
21. Takagi T, Mir MC, Sharma N, Remer EM, Li J, Demirjian S et al (2014) Compensatory hypertrophy after partial and radical nephrectomy in adults. J Urol 192:1612–1618
22. Stewart FA, Te Poele JA, Van der Wal AF, Oussoren YG, Van Kleef EM, Kuin A et al (2001) Radiation nephropathy—the link between functional damage and vascular mediated inflammatory and thrombotic changes. Acta Oncol 40:952–957
23. Atwell TD, Schmit GD, Boorjian SA, Mandrekar J, Kurup AN, Weisbrod AJ et al (2013) Percutaneous ablation of renal masses measuring 3.0 cm and smaller: comparative local control and complications after radiofrequency ablation and cryoablation. Ajr Am J Roentgenol 200:461–466
24. Caputo PA, Zargar H, Ramirez D, Andrade HS, Akca O, Gao T et al (2017) Cryoablation versus partial nephrectomy for clinical

T1b renal tumors: a matched group comparative analysis. Eur Urol 71:111–117
25. Kunkle DA, Uzzo RG (2008) Cryoablation or radiofrequency ablation of the small renal mass: a meta-analysis. Cancer 113:2671–2680
26. Psutka SP, Feldman AS, McDougal WS, McGovern FJ, Mueller P, Gervais DA (2013) Long-term oncologic outcomes after radiofrequency ablation for T1 renal cell carcinoma. Eur Urol 63:486–492
27. Panje C, Andratschke N, Brunner TB, Niyazi M, Guckenberger M (2016) Stereotactic body radiotherapy for renal cell cancer and pancreatic cancer: literature review and practice recommendations of the DEGRO working group on stereotactic radiotherapy. Strahlenther Onkol 192:875–885
28. Pham D, Thompson A, Kron T, Foroudi F, Kolsky MS, Devereux T et al (2014) Stereotactic ablative body radiation therapy for primary kidney cancer: a 3-dimensional conformal technique associated with low rates of early toxicity. Int J Radiat Oncol Biol Phys 90:1061–1068
29. Siva S, Pham D, Kron T, Bressel M, Lam J, Tan TH et al (2017) Stereotactic ablative body radiotherapy for inoperable primary kidney cancer: a prospective clinical trial. BJU Int 120:623–630
30. Staehler M, Bader M, Schlenker B, Casuscelli J, Karl A, Roosen A et al (2015) Single fraction radiosurgery for the treatment of renal tumors. J Urol 193:771–775
31. Filippiadis DK, Gkizas C, Chrysofos M, Siatelis A, Velonakis G, Alexopoulou E et al (2018) Percutaneous microwave ablation of renal cell carcinoma using a high power microwave system: focus upon safety and efficacy. Int J Hyperthermia 34:1077–1081
32. Su MZ, Memon F, Lau HM, Brooks AJ, Patel MI, Woo HH et al (2016) Safety, efficacy and predictors of local recurrence after percutaneous radiofrequency ablation of biopsy-proven renal cell carcinoma. Int Urol Nephrol 48:1609–1616
33. Dai Y, Covarrubias D, Uppot R, Arellano RS (2017) Image-guided percutaneous radiofrequency ablation of central renal cell carcinoma: assessment of clinical efficacy and safety in 31 tumors. J Vasc Interv Radiol 28:1643–1650
34. Fukuda S, Seo Y, Shiomi H, Yamada Y, Ogata T, Morimoto M et al (2014) Dosimetry analyses comparing high-dose-rate brachytherapy, administered as monotherapy for localized prostate cancer, with stereotactic body radiation therapy simulated using CyberKnife. J Radiat Res 55:1114–1121
35. Pennington JD, Park SJ, Abgaryan N, Banerjee R, Lee PP, Loh C et al (2015) Dosimetric comparison of brachyablation and stereotactic ablative body radiotherapy in the treatment of liver metastasis. Brachytherapy 14:537–542
36. Siva S, Pham D, Gill S, Bressel M, Dang K, Devereux T et al (2013) An analysis of respiratory induced kidney motion on four-dimensional computed tomography and its implications for stereotactic kidney radiotherapy. Radiat Oncol 8:248
37. Dib RE, Touma NJ, Kapoor A (2009) Review of the efficacy and safety of radiofrequency ablation for the treatment of small renal masses. Can Urol Assoc J 3:143–149
38. Kapoor A, Touma NJ, Dib RE (2013) Review of the efficacy and safety of cryoablation for the treatment of small renal masses. Can Urol Assoc J 7:E38–44

European Journal of Radiology 112 (2019) 22–27

Contents lists available at ScienceDirect

European Journal of Radiology

journal homepage: www.elsevier.com/locate/ejrad

Research article

Efficacy and safety of CT-guided high-dose-rate interstitial brachytherapy in primary and secondary malignancies of the pancreas

Jazan Omari[a,*], Constanze Heinze[a], Antje Wilck[a], Peter Hass[b], Max Seidensticker[d], Ricarda Seidensticker[d], Konrad Mohnike[e], Jens Ricke[d], Maciej Pech[a,c], Maciej Powerski[a]

[a] Department of Radiology and Nuclear Medicine, University Hospital Magdeburg, Germany
[b] Department of Radiotherapy, University Hospital Magdeburg, Germany
[c] 2nd Department of Radiology, Medical University of Gdansk, Poland
[d] Department of Radiology, University Hospital Munich, Germany
[e] Diagnostisch Therapeutische Zentrum (DTZ), Berlin, Germany

ARTICLE INFO

Keywords:
Pancreatic cancer
Metastases
Image-guided intervention
Radiation therapy/oncology
Interstitial brachytherapy

ABSTRACT

Purpose: To evaluate efficacy and safety of CT-guided iBT in patients with primary and secondary malignancies of the pancreas.

Material and methods: 13 patients with 13 lesions of the pancreatic corpus and tail were included: 8 secondary malignancies (metastatic lesions = ML) and 5 primary malignancies, including 3 primary tumors (PT) and 2 isolated locoregional recurrences (ILR) after surgical resection were treated with image-guided iBT using a 192iridium source (single fraction irradiation). Every 3 months after treatment clinical and imaging follow-up were conducted to evaluate efficacy. Peri- and postinterventional complications were assessed descriptively.

Results: The median diameter of the gross tumor volume (GTV) was 3 cm (range 1–6.5 cm), treated with a median D100 (minimal enclosing tumor dose) of 15.3 Gy (range 9.2–25.4 Gy). Local tumor control (LTC) was 92.3% within a median follow-up period of 6.7 months (range 3.2–55.7 months). Cumulative median progression free survival (PFS) was 6.2 months (range 2.8–25.7 months; PFS of primary and secondary malignancies was 5.8 and 6.2 months, respectively). Cumulative median over all survival (OS) after iBT was 16.2 months (range 3.3–55.7 months; OS of primary and secondary malignancies was 7.4 months and 45.6 months, respectively). 1 patient developed mild acute pancreatits post iBT, spontanously resolved within 1 week. No severe adverse events (grade 3+) were recorded.

Conclusion: Image-guided iBT is a safe and particularly effective treatment in patients with primary and secondary malignancies of the pancreas and might provide a well-tolerated additional therapeutic option in the multidisciplinary management of selected patients.

1. Introduction

Treatment of advanced or metastatic disease is challenging and best approached by a multidisciplinary team with an increasing tendency towards an individually tailored anticancer therapy to achieve the best possible outcomes. In this context the significance of local ablative techniques is constantly rising. Out of the toolbox of local ablation techniques high-dose-rate interstitial Brachytherapy (HDR-iBT = iBT) is a well-tolerated catheter-based afterloading method and it has been shown to provide high tumor control rates in primary and secondary malignancies of the liver, such as hepatocellular carcinoma and particularly in metastatic colorectal carcinoma, demonstrating local tumor control (LTC) rates of 95% and 88.3% after 12 months, respectively [1–3].

Furthermore, favorable LTC rates have also been achieved in the ablation of primary and secondary lung malignancies with a LTC rate of 91% at 12 months [4,5].

Pancreatic ductal adenocarcinoma (PDAC) is a highly lethal disease with a varying 5-year survival rate of 0.5–9% [6]. Complete resections remains the only potential cure, however, more than 80% of the

* Corresponding author.
E-mail addresses: jazan.omari@med.ovgu.de (J. Omari), constanze.heinze@med.ovgu.de (C. Heinze), antje.wilck@googlemail.com (A. Wilck), peter.hass@med.ovgu.de (P. Hass), max.seidensticker@med.uni-muenchen.de (M. Seidensticker), ricarda.seidensticker@med.uni-muenchen.de (R. Seidensticker), konrad.mohnike@berlin-dtz.de (K. Mohnike), jens.ricke@med.uni-muenchen.de (J. Ricke), maciej.pech@med.ovgu.de (M. Pech), maciej.powerski@med.ovgu.de (M. Powerski).

https://doi.org/10.1016/j.ejrad.2018.12.020
Received 5 September 2018; Received in revised form 12 December 2018; Accepted 26 December 2018

patients are diagnosed with locally advanced or metastatic PDAC and therefore are not suitable for resection [7]. Furthermore, despite advances in surgical techniques and postoperative management pancreatic resection is still associated with substantial morbidity and mortality [8,9]. Additionally, about one third of the patients undergoing pancreaticoduodenectomy develop isolated locoregional recurrence (ILR) [10]. However, despite many therapeutic developments only moderate achievements regarding outcome and survival have been made over the last decades and especially in patients with locally advanced/unresectable or recurrent disease treatment options are scarce [11–13].

Apart from numerous studies considering therapy of PDAC little data exists regarding secondary malignancies of the pancreas; the estimated incidence of clinical occurrence of isolated metastatic lesions (ML) to the pancreas is about 2–5 % of all pancreatic neoplasm and in the majority of cases the represented primary tumor are renal, lung, colorectal or breast cancer and sarcoma [14,15]. Therapeutic options including resection depend on the type of primary tumor, location and number/volume of metastatic lesions and the patient's performance status.

In contrast, local ablative techniques, such as iBT provide a safe and minimal invasive approach and might offer an additional therapeutic option in the management of pancreatic neoplasms. To our knowledge no data has been published so far evaluating safety and efficacy of iBT in the ablation of primary and secondary malignancies of the pancreas. In this study we retrospectively analyzed a cohort of 13 patients with 13 inoperable lesions of the pancreas who underwent image-guided iBT.

2. Material and methods

2.1. Eligibility criteria and patients characteristics

Patient recruitment took place in a German university clinic, between October 2009 and February 2018. Indication for iBT was determined in an interdisciplinary tumor conference.

Principal inclusion criteria were: (a) unresectable neoplastic lesion of the pancreatic corpus or tail (including primary tumor = PT, ILR and ML), assessed by a surgeon with expertise in pancreatic malignancies, who considered them unresectable either due to tumor extent or medical comorbidities, (b) refusal of surgery, (c) East Coast Oncology Group (ECOG) performance status below 2. An upper limit was neither placed upon the number of lesions nor on the maximum tumor diameter. Contraindications to local ablation were (a) peritoneal carcinomatosis (b) prognosis limiting, widespread systemic disease (c) uncorrectable coagulation defects (target values: platelet count > 50,000/nl, Quick > 50%, partial thromboplastin time > 5 s) (d) lack of consent. The study was approved by the ethics committee of XXXXX (BLINDED).

In consideration of these criteria we included 13 patients (5 female and 8 male; median age 70 range 44–81) with one inoperable pancreatic lesion per patient (10 lesions of the pancreatic body and 3 lesions of the pancreatic tail). In detail: 3 PT (1 PDAC, 2 neuroendocrine tumors = NET), 2 ILR (PDAC) and 8 ML were treated, the latter comprised of 1 metastasis of gastric cancer, 1 breast cancer lesion and 6 renal cancer metastases. Out of these 8 patients with secondary malignancies 7 were presented with metachrone metastases. 11/13 patients had resection of the primary tumor, including 2 pylorus-preserving pancreaticoduodenectomy, followed by ILRs. 9/13 patients received palliative chemotherapy before iBT, including immune-checkpoint-inhibitors. Furthermore, 8/13 patients had additionally local ablative treatments of extrapancreatic metastases or the primary tumor prior to iBT; in detail: 1 iBT of lymphnode metastasis, 2 iBT of adrenal gland lesions, ablation of renal lesions (1 radiofrequency ablation, 3 iBTs) and 1 radioembolisation of the liver (for detailed patient characteristics see Table 1).

Prior to iBT all patients received a full clinical status evaluation with

Table 1
Patient characteristics.

Patient	Gender	Age	Location and Type of pancreatic neoplasm	Primary Tumor	Pathologic Subtypes	Maximum Diameter of the GTV (cm)	Administered D100 (Gy)	Local Recurrence (months after iBT)
1	m	75	ML of the corpus	gastric cancer	squamous cell carcinoma	4.3	12.0	6.7
2	m	77	ILR of the Corpus	pancreatic cancer	ductal adenocarcinoma	3	15.3	–
3	m	76	ILR of the Corpus	pancreatic cancer	ductal adenocarcinoma	3	9.2	–
4	m	69	PT of the cauda	pancreatic cancer	ductal adenocarcinoma	3	25.4	–
5	m	81	PT of the corpus	pancreatic cancer	neuroendocrine tumor	6.5	11.3	–
6	f	52	ML of the corpus	breast cancer	neuroendocrine tumor	4.5	17.4	–
7	f	44	PT of the corpus	pancreatic cancer	neuroendocrine tumor	2.5	10.3	–
8	f	73	ML of the corpus	renal cancer	clear cell renal cell carcinoma	1.3	15.8	–
9	m	73	ML of the caput	renal cancer	clear cell renal cell carcinoma	2.3	16.0	–
10	m	64	ML of the cauda	renal cancer	clear cell renal cell carcinoma	6.5	15.7	–
11	m	54	ML of the cauda	renal cancer	clear cell renal cell carcinoma	2.5	14.8	–
12	f	54	ML of the corpus	renal cancer	clear cell renal cell carcinoma	2.3	15.2	–
13	f	70	ML of the corpus	renal cancer	clear cell renal cell carcinoma	1	15.4	–

ML metastatic lesion, ILR isolated locoregional recurrence PT primary tumor.

a physical examination, laboratory assessment, whole body contrast-enhanced CT and Gb-EOB-DTPA-enhanced MRI (Primovist ®, Bayer, Pharma, Leverkusen, Germany) of the liver. Every 3 months after iBT clinical, laboratory and image-based follow-up (contrast-enhanced whole body CT) were performed.

2.2. Interventional procedure

The applied technique has been described elsewhere in detail [1,16,17]. Under guidance of a fluoroscopy-CT (Toshiba, Aquilion, Japan) an 18-gauge trocar puncture needle was inserted into the target lesions and a stiff angiography guide wire was exchanged for a flexible 6-F catheter sheath (Radifocus, Terumo™, Tokyo, Japan) using Seldinger's-technique followed by the placement of a 6-F afterloading catheter (Afterloadingkatheter, Primed® Medizintechnik GmbH, Halberstadt, Germany). The described intervention was performed under analgosedation (midazolam and fentanyl) and local anesthesia (lidocaine). The number and arrangement of the catheters was determined by the size, shape and anatomic location of the target. After catheter positioning a contrast-enhanced CT scan in breath-holding technique was acquired to document catheter positioning and for the purpose of irradiation planning. On these images the target lesion was carefully outlined as gross tumor volume (GTV), additionally, clinical target volume (CTV) and organs at risk (=OAR; e.g. stomach, duodenum) were marked by the interventional radiologist and the radiooncologist. Dose calculation was performed using the acquired dataset and Oncentra Masterplan (Oncentra® Brachy treatment planning system, Elekta AB, Stockholm, Sweden). The calculated isodose lines -relative to margins of the CTV- were controlled and adapted slice by slice. All irradiations were administered as single fraction irradiations using an iridium-192 source with a nominal activity of 10 Ci. A reference dose of 15 Gy was prescribed in our patients, which was defined as the minimum dose enclosing the complete CTV (D100). Inside the tumor higher doses were permitted and not limited. Additionally, dose limitations were taken into account due to adjacent OAR, i.e. gastric or duodenal wall (< 15 Gy/ml). After irradiation the catheters were removed and the puncture channels were sealed using gelfoam or fibrin tissue glue (Fig. 1 A–C illustrates the interventional method) [18].

2.3. Study design and statistical analysis

We retrospectively collected the data from our internally database ASENA® (LoeScap Technology GmbH). Primary endpoints were local tumor control (LTC) and safety; secondary endpoints were over all survival (OS) and progression free survival (PFS). The results were analyzed in a non-randomized and retrospective approach. Response Evaluation Criteria In Solid Tumors (RECIST vs1.1) were used to assess LTC and PFS. OS was calculated from the day of ablation to death. LTC, OS and PFS were evaluated employing the Kaplan-Meier method with SPSS (IBM Corp. Released 2013. IBM SPSS Statistics for Windows, Version 22.0. Armonk, NY: IBM Corp). Adverse events were defined according to Common Terminology Criteria for Adverse Events (CTCAE vs 4.03).

Safety was evaluated descriptively. Diagnosis of acute pancreatitis (AP) was made on the base of the Revised Atlanta Classification: requiring 2 of the following features: (a) characteristic abdominal pain (acute onset, severe character, epigastric pain often radiating to the back), (b) elevated enzyme activity (lipase or amylase) at least 3 times > than the upper limit of normal and (c) characteristic findings on contrast-enhanced CT scan.

3. Results

3.1. Treatment characteristics

We treated a total of 13 pancreatic lesions, comprised of 8 secondary malignancies/ML (61.5%) and 5 primary malignancies: 3 PT (23.1%) and 2 ILR (15.4%). Median diameter of the target lesions was 3 cm (range 1.0–6.5 cm). All lesions were irradiated in a total of 13 sessions with an employed mean of 1.5 catheters (range 1–4). The median administered D100 was 15.3 Gy (range 9.2–25.4 Gy). No OAR were irradiated in excess of critical value during treatment. The median irradiation time was 10.1 min (range 4–33 min).

3.2. Local tumor control, progression free survival and overall survival

Within the median follow up of 6.7 months (range 3.2–55.6 months) 1 patient displayed local recurrence of the GTV, resulting in a LTC of 92.3% in the Kaplan-Meier analysis (Fig. 2). The treated lesion was a ML of gastric squamous cell carcinoma to the pancreatic corpus and was covered with a minimum tumor dose of 12 Gy at time of treatment. Additionally, this patient displayed needle track tumor seeding. Cumulative median PFS was 6.2 months and ranged from 2.8 to 25.7 months, for patients with primary and secondary malignancies PFS was 5.8 (2.9–6.7 months) and 6.2 months (range 2.8–25.7 months), respectively (Fig. 3). Within the follow up period 12/13 patients displayed a systemic progressive disease and out of these 12 patients 7 received specific tumor therapy in the timespan between iBT and systemic progression: in detail, palliative chemotherapy (5/7) and radioembolisation of the liver (2/7). The cumulative median OS was 16.2 months (range 3.3–55.7 months) for patients with primary and secondary malignancies OS was 7.4 (5.8–19.1 months) and 45.6 months (range 3.3–55.7 months), respectively (Fig. 4). At time of censoring 6 patients were still alive (5/8 secondary malignancies). Patient No.4 was

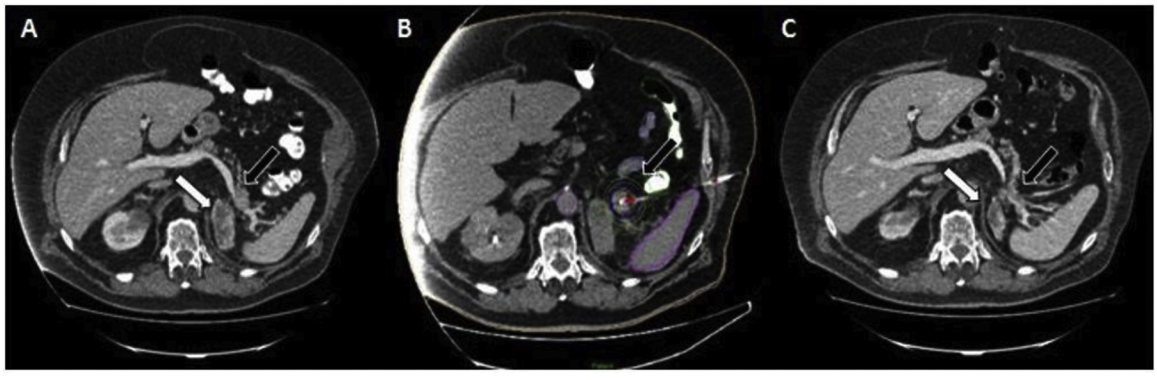

Fig. 1. (A): Pre-interventional contrast-enhanced CT slice showing a metastasis of NCC (black arrow) in the pancreatic tail. White arrow shows a metastasis of NCC of the left adrenal gland, previously treated with high dose rate brachytherapy (HDRBT). (B): Planning CT with indicated CTV (red line), catheter (marked in red) and isodose lines. (C): Follow up after 18 months: local control of treated lesion in the pancreatic tail (black arrow). Size reduction of the previously treated lesion in the left adrenal gland (white arrow).

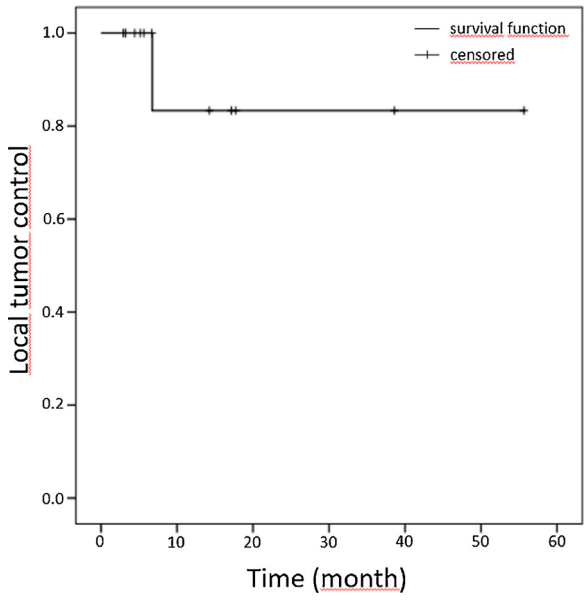

Fig. 2. Local tumor control after iBT of all treated pancreatic neoplasms.

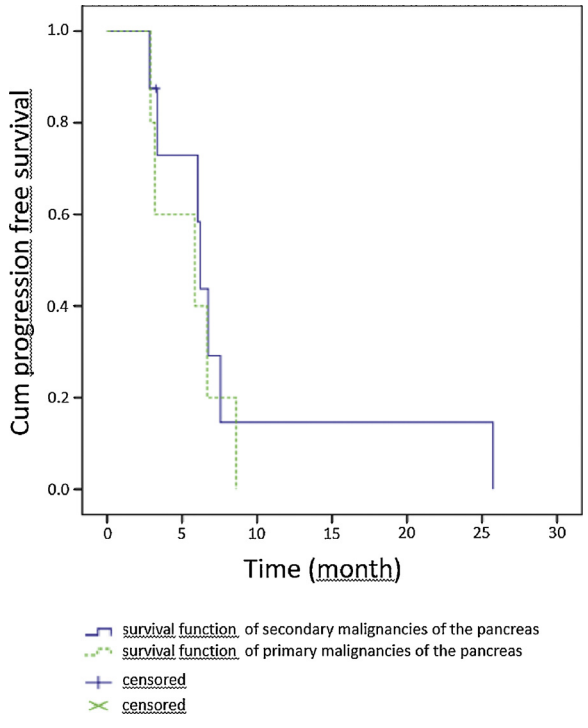

Fig. 3. Progression free survival of patients with primary (green line) and secondary malignancies (blue line) of the pancreas after iBT.

excluded from OS analysis due to lack of detailed information regarding the time point of death.

3.3. Safety and peri-and postinterventional complications

Median hospital stay was 4 days (range 4–11 days), whereby 1 patient underwent catheter positioning twice due to incorrect catheter placement in the first session. Patient No.6 was treated with iBT of the liver in the same hospital stay.

In 1 patient we observed increased level of systemic inflammation markers (C-reactive protein, leukocytosis) without fever or additional symptoms, administration of intravenous antibiotics (Ciproflaxacin and

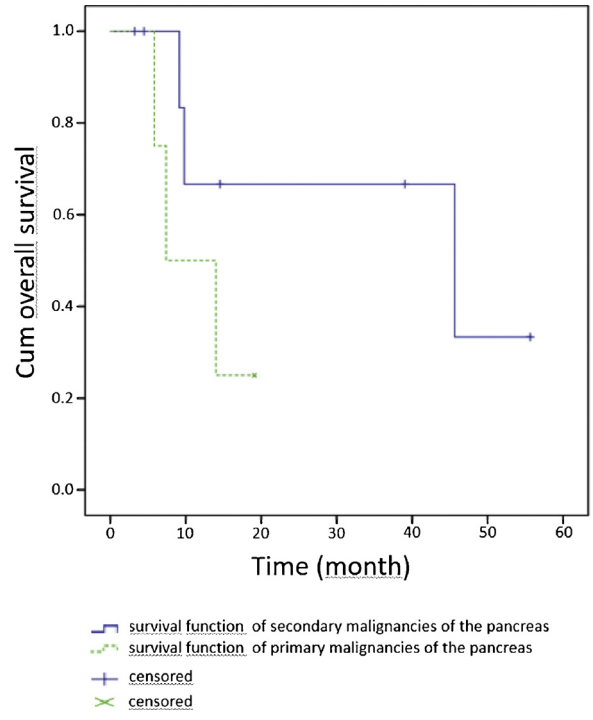

Fig. 4. Overall survival for patients with primary (green line) and secondary malignancies (blue line) of the pancreas after iBT. At the date of censoring 6 patients were still alive.

Metronidazole) led to rapid normalization. 1 patients reported unspecific nausea. With regard to the diagnosis of acute pancreatitis, 2 patients showed biochemical sign of a local injury of the pancreas, i.e. lipase elevated > 3times the upper limit of normal. Patient No.8 additionally experienced characteristic abdominal pain, an ultrasound and CT-scan did not show any sign of bleeding or early phase pancreatitis. The symptoms spontaneously resolved within the hospital stay (7days). However, this event was classified as mild acute pancreatitis, categorized as adverse event grade2. In patient No.9 we also observed critical enzyme elevation, but without any pain and therefore this patient did not received further radiologic examination. In conclusion, after iBT 12/13 patients did not show sufficient clinical features required for the diagnosis of acute pancreatitis on the base of the Revised Atlanta Classification. Furthermore, on the follow-up imaging no morphological features of acute pancreatitis, local complications (in terms of late toxicities) or following structural changes, including pancreatic strictures were observed.

4. Discussion

In selected patients with primary or secondary malignancies of the pancreas surgical resection remains the only possible cure or might achieve long-term survival, respectively [19]. In the literature pancreaticoduodenectomy is described to be associated with a substantial postoperative morbidity of 30–60% and in-hospital mortality rate of fewer than 5% [8,9]. However, Nimptsch et al. analyzed 58,003 inpatient episodes of pancreatic surgery between 2009 and 2013 in Germany and found a overall in-hospital mortality rate of 10.1%, including all surgical procedures of the pancreas; severe surgical complications occurred in 12.2–20.2% (i.e. peritonitis, sepsis, re-laparotomy, and > 6 blood transfusions) [20]. These findings suggest an underestimation of the mortality and morbidity rate due to publication bias, given the fact that low complication rates are mostly reported by single- and multiinstitutional studies of rather experienced hospitals with high caseloads.

However, only a minority of patients diagnosed with pancreatic

neoplasms are candidates for surgery, i.e. less than 20% of the patients diagnosed with PDAC are eligible for resection, likely a result of the tumor's invasiveness and propensity towards metastases [21]. Additionally, even after curative-intent surgery over 60% of patients will develop disease recurrence within 2 years resulting in a dismal prognosis [22], for instance after curative resection plus adjuvant chemotherapy median OS is reported to be 18.7–25 months for PDAC [23,24]. However, after complete pancreatic head resections for PDAC the surgical margin status has significant impact on further treatment an prognosis, with positive microscopic margin status (R1 resection) described to be as high as up to 76% [25]. This fact might explain that ILRs in the remnant pancreas or the locoregional structures are reported to occur in up to 30% after curative pancreatic surgery for PDAC [23,26].

Data is scarce for resection of secondary malignancies, however, Hung et al. found a 5-year survival rate of 61.1% after resection of 241 ML of the pancreas (73.9% renal cell carcinoma), suggesting that pancreatic resection should not be ruled out for ML [27].

In contrast, the presented study provides evidence that iBT achieves a high LTC rate of 92.3% in the ablation of primary and secondary pancreatic neoplasm. Within the median follow-up of 6.7 months 1 patient displayed local recurrence and needle track seeding after iBT of a ML of gastric squamous cell carcinoma, possibly caused by a relatively low administered D100 of 12 Gy regarding the pathologic subtype of the primary tumor.

However, in contrast to the reported surgery associated complication rates our findings demonstrate that iBT is a well-tolerated and safe procedure with no recorded severe adverse events (grade 3+). We report 1 case with mild acute pancreatitis post iBT that spontaneously resolved within 1 week (categorized as adverse event grade2). In the follow-up (including CT or MRI scans) no signs of acute pancreatitis (early or late phase), obstructive pancreatitis due to strictures or other late toxicities to adjacent organs were recorded.

About 30–40% of patients with PDAC are presented with borderline resectable or locally advanced unresectable disease and are -according to the current standard of care- treated with (neoadjuvant/palliative) chemotherapy depending on the patient's performance status [28]. Additionally, for this patient population subsequent local therapies, such as radiofrequency ablation (RFA), microwave ablation (MWA), irreversible electroporation (IRE) and cryoablation are available. These treatments are less evidence based and moreover seen in a palliative context with an emphasis on local tumor control and symptom relief. In general the techniques are delivered via laparotomy, again associated with surgical complications. Furthermore, to our knowledge no data regarding percutaneous ablation of secondary malignancies of the pancreas exists and even literature regarding percutaneous ablation of PDAC or NET is scarce.

RFA is a thermal ablative technique that uses heat generated from high frequency alternating current. The associated risk of thermal injuries to adjacent structures is relatively high, in surgical settings initially resulting in substantial morbidity (up to 40%) and mortality rates (up to 25%) due to massive gastrointestinal bleeding or duodenal injury, after technical adjustments the rates could be lowered to 24–28% and 1.8–3%, respectively [29–31]. To our knowledge, data regarding CT-guided RFA is only reported in cases studies. There are two studies concerning percutaneous, ultrasound-guided RFA, mainly focused on feasibility and safety: D'Onofrio et al treated 18 patients with PDAC with no described postprocedural complications, but efficacy regarding LTC was not assessed [32]; in the second study 7 patients with pancreatic NET were treated with a high complication rate of 3 grade3 adverse events [33]. IBT, in contrast, is independent of technical limitations concerning a potential cooling effect arising from large tumor masses (> 5 cm), resulting in a possible incomplete ablation, and even more importantly implies no potential thermal injury to adjacent OAR.

IRE is a non-thermal technique that uses short pulses of high voltage electrical current to create nanopores in the cell membrane causing apoptosis. In contrast to RFA IRE is thought to be able to destroy tumor tissue without the risk of thermal injuries to adjacent structures. Leen et al included 75 preteated patients with unresectable PDAC, median OS and PFS after CT-guided IRE was 27 and 15 months, respectively; local recurrence was reported to be 3% after 2–3 months [34]. Associated morbidity was 25%, mortality was nil. Although, one of the greatest technical restrictions of IRE is the need for general anesthesia with complete muscular paralysis, which provides additional risk and is a limiting factor for patient selection and procedural setting. IBT in contrast is performed under local anesthesia with analgosedation.

Data regarding percutaneous MWA and cryoablation is scarce and mainly concerning feasibility and safety in small case series [35–37].

Besides resection and percutaneous ablation of pancreatic neoplasms radiotherapy (including conventional radiotherapy and stereotactic bodyradiation = SBRT) provides another non-invasive approach. For patients treated with chemoradiation (gemcitabine plus radiotherapy: 1.8 Gy/fraction for a total of 50.4 Gy) for locally advanced PDAC early grade4 and 5 toxicities are described to occur in 41% and 9%, respectively [38]. SBRT has been studied with varying techniques and radiation doses applied, inducing morbidity rates up to 25% and especially late toxicities (grade2-4) up to 44% [39,40], i.e. adverse effects occurring at least 6 months post radiation of the pancreas, such as gastric/duodenal ulcer or perforation, gastrointestinal bleed, enteritis, colitis, intrapancreatic bile duct stricture. A phase-2-trail showed a LTC rate of 90% over a median follow-up of 13.5 months for 45 patients treated with SBRT for locally advanced PDAC (application of 45 Gy in 6 fractions); median PFS and OS was 8 and 13 months, respectively [41]. 49% of the population experienced grade1-2 toxicities, no grade 3+ events were reported, although, late toxicities occurred in 4% [41]. These results propose that SBRT permits precise irradiation, however, the varying rates for early and late toxicities suggest a significant exposure of normal surrounding tissue, resulting in gastrointestinal complications. Due to its percutaneous delivery iBT in contrast, allows the application of an effective, precise ablative dose in the CTV while saving adjacent OAR from potentially harmful exposure resulting in a low complication rate. Therefore iBT is not limited to the size or restrictions due to anatomic localization of the target. Moreover, in the presented study we did not report any early or late severe toxicities related to iBT.

From an oncological perspective our findings of a median PFS of 6.2 months (range 2.8–25.7 months) and an OS of 45.6 months (range 3.3–55.7 months) after iBT for patients with ML go in line with published outcome after resection. Hung et al, report a median OS of 20.0 months after resection of 241 ML, without the evaluation of LTC and PFS [27], and also Dar et al described a varying survival of 6–56 months for a case series of 5 patients [42]. Since, surgical risk is always one of the major concerns in consideration of any metastasectomy, iBT provides a particularly safe and effective alternative method.

For the patients presented with primary malignancies we found a median PFS of 5.8 months (2.9–6.7 months) and an OS of 7.4 months (5.8–19.1 months), however, our heterogeneous and rather small cohort is not comparable to the existing literature without restrictions, but for patients with locally advanced/unresectable or metastatic PDAC OS is reported to be similar with a median of 4–11 months under 1 st line chemotherapy [43,44]. Therefore, our findings might also suggest a potential additional survival benefit of selected patients treated with iBT, since the oncological impact of any local treatment is far from being answered.

Nevertheless, our study has several limitations: its retrospective nature and the low case number; moreover, the treated cohort was heterogeneous with respect to primary tumor, disease stage and previous treatment, resulting in a PFS and OS that is not beneficial from an oncological perspective. Therefore, a prospective trial with a higher caseload would be needed to investigate the effect of iBT with respect to the primary tumor and the previous treatment and also to possibly establish iBT in the toolbox of local ablative techniques for pancreatic

neoplasms located in the pancreatic body or tail.

However, despite these limitations our study demonstrates that iBT is a feasible alternative to resection of secondary malignancies and also provides a promising treatment for locally advanced/unresectable or recurrent primary malignancies of the pancreas. It offers treatment- and primary-tumor-independent effective LTC rates and accordingly, might offer a well-tolerated therapeutic option in the multidisciplinary management of selected patients.

In conclusion, for patients presented with primary or secondary malignancies of the pancreas located in the pancreatic body or tail iBT is a safe and particularly effective ablative technique that provides a promising alternative to surgery, SBRT and existing percutaneous ablation methods.

Conflicts of interest

The authors have no conflicts of interest to declare.

References

[1] J. Ricke, P. Wust, A. Stohlmann, A. Beck, C.H. Cho, M. Pech, G. Wieners, B. Spors, M. Werk, C. Rosner, E.L. Hanninen, R. Felix, CT-guided interstitial brachytherapy of liver malignancies alone or in combination with thermal ablation: phase I-II results of a novel technique, Int. J. Radiat. Oncol. Biol. Phys. 58 (5) (2004) 1496–1505.

[2] K. Mohnike, G. Wieners, F. Schwartz, M. Seidensticker, M. Pech, R. Ruehl, P. Wust, E. Lopez-Hanninen, G. Gademann, N. Peters, T. Berg, P. Malfertheiner, J. Ricke, Computed tomography-guided high-dose-rate brachytherapy in hepatocellular carcinoma: safety, efficacy, and effect on survival, Int. J. Radiat. Oncol. Biol. Phys. 78 (1) (2010) 172–179.

[3] F. Collettini, A. Lutter, D. Schnapauff, B. Hildebrandt, G. Puhl, T. Denecke, P. Wust, B. Gebauer, Unresectable colorectal liver metastases: percutaneous ablation using CT-guided high-dose-rate brachytherapy (CT-HDBRT), Rofo 186 (6) (2014) 606–612.

[4] N. Peters, G. Wieners, M. Pech, S. Hengst, R. Rühl, F. Streitparth, E. Lopez Hänninen, R. Felix, P. Wust, J. Ricke, CT-guided interstitial brachytherapy of primary and secondary lung malignancies, Strahlenther. Onkol. 184 (6) (2008) 296–301.

[5] J. Ricke, P. Wust, G. Wieners, S. Hengst, M. Pech, E.L. Hänninen, R. Felix, CT-guided interstitial single-fraction brachytherapy of lung tumors: phase I results of a novel technique, Chest 127 (6) (2005) 2237–2242.

[6] A. Carrato, A. Falcone, M. Ducreux, J.W. Valle, A. Parnaby, K. Djazouli, K. Alnwick-Allu, A. Hutchings, C. Palaska, I. Parthenaki, A Systematic Review of the Burden of Pancreatic Cancer in Europe: Real-World Impact on Survival, Quality of Life and Costs, J. Gastrointest. Cancer 46 (3) (2015) 201–211.

[7] M.A. Tempero, M.P. Malafa, S.W. Behrman, A.B. Benson, E.S. Casper, E.G. Chiorean, V. Chung, S.J. Cohen, B. Czito, A. Engebretson, M. Feng, W.G. Hawkins, J. Herman, J.P. Hoffman, A. Ko, S. Komanduri, A. Koong, A.M. Lowy, W.W. Ma, N.B. Merchant, S.J. Mulvihill, P. Muscarella, E.K. Nakakura, J. Obando, M.B. Pitman, S. Reddy, A.R. Sasson, S.P. Thayer, C.D. Weekes, R.A. Wolff, B.M. Wolpin, J.L. Burns, D.A. Freedman-Cass, Pancreatic adenocarcinoma, version 2.2014, J. Compr. Canc. Netw. 12 (8) (2014) 1083–1093.

[8] G. Malleo, C.M. Vollmer, Postpancreatectomy Complications and Management, Surg. Clin. North Am. 96 (6) (2016) 1313–1336.

[9] L. Maggino, C.M. Vollmer, Recent advances in pancreatic Cancer surgery, Curr. Treat. Options Gastroenterol. 15 (4) (2017) 520–537.

[10] V.P. Groot, H.C. van Santvoort, S.J.E. Rombouts, J. Hagendoorn, I.H.M. Borel Rinkes, M. van Vulpen, J.M. Herman, C.L. Wolfgang, M.G. Besselink, I.Q. Molenaar, Systematic review on the treatment of isolated local recurrence of pancreatic cancer after surgery; re-resection, chemoradiotherapy and SBRT, HPB (Oxford) 19 (2) (2017) 83–92.

[11] F.C. Passero, M.W. Saif, Second line treatment options for pancreatic cancer, Expert Opin, Pharmacother. 18 (15) (2017) 1607–1617.

[12] V. Chin, A. Nagrial, K. Sjoquist, C.A. O'Connor, L. Chantrill, A.V. Biankin, R.J.P.M. Scholten, D. Yip, Chemotherapy and radiotherapy for advanced pancreatic cancer, Cochrane Database Syst. Rev. (3) (2018).

[13] Y. Karakas, S. Lacin, S. Yalcin, Recent advances in the management of pancreatic adenocarcinoma, Expert Rev, Anticancer Ther. 18 (1) (2018) 51–62.

[14] S.L. Showalter, E. Hager, C.J. Yeo, Metastatic disease to the pancreas and spleen, Semin. Oncol. 35 (2) (2008) 160–171.

[15] M. Loi, A. Magallon-Baro, C. Papalazarou, M. Milder, J.J. Nuyttens, Robotic stereotactic treatment for malignant metastasis of solid tumour in the pancreas: A multiple case report and review of literature, CancerRadiothrapie 21 (8) (2017) 784–787.

[16] T. Bretschneider, J. Ricke, B. Gebauer, F. Streitparth, Image-guided high-dose-rate brachytherapy of malignancies in various inner organs - technique, indications, and perspectives, J. Contemp. Brachytherapy 8 (3) (2016) 251–261.

[17] J. Ricke, P. Wust, Computed tomography-guided brachytherapy for liver cancer, Semin. Radiat. Oncol. 21 (4) (2011) 287–293.

[18] P.A. Banks, T.L. Bollen, C. Dervenis, H.G. Gooszen, C.D. Johnson, M.G. Sarr, G.G. Tsiotos, S.S. Vege, Classification of acute pancreatitis—2012: revision of the Atlanta classification and definitions by international consensus, Gut 62 (1) (2013) 102.

[19] M. Wagner, C. Redaelli, M. Lietz, C.A. Seiler, H. Friess, M.W. Büchler, Curative resection is the single most important factor determining outcome in patients with pancreatic adenocarcinoma, BJS 91 (5) (2004) 586–594.

[20] U. Nimptsch, C. Krautz, G.F. Weber, T. Mansky, R. Grützmann, Nationwide in-hospital mortality following pancreatic surgery in Germany is higher than anticipated, Ann. Surg. 264 (6) (2016) 1082–1090.

[21] K.Y. Bilimoria, D.J. Bentrem, C.Y. Ko, A.K. Stewart, D.P. Winchester, M.S. Talamonti, National failure to operate on early stage pancreatic Cancer, Ann. Surg. 246 (2) (2007) 173–180.

[22] S.S. Griffin, Jewell W. JF, J.C. Paradelo, R.D. Reymond, R.E. Hassanein, R.G. Evans, Patterns of failure after curative resection of pancreatic carcinoma, Cancer 66 (1) (1999) 56–61.

[23] A. Van den broeck, G. Sergeant, N. Ectors, W. Van Steenbergen, R. Aerts, B. Topal, Patterns of recurrence after curative resection of pancreatic ductal adenocarcinoma, European Journal of Surgical Oncology (EJSO) 35 (6) (2009) 600–604.

[24] A. Pugalenthi, M. Protic, M. Gonen, T.P. Kingham, I.D. Angelica Michael, P. Dematteo Ronald, Y. Fong, R. Jarnagin William, J. Allen Peter, Postoperative complications and overall survival after pancreaticoduodenectomy for pancreatic ductal adenocarcinoma, J. Surg. Oncol. 113 (2) (2015) 188–193.

[25] I. Esposito, J. Kleeff, F. Bergmann, C. Reiser, E. Herpel, H. Friess, P. Schirmacher, M.W. Büchler, Most pancreatic Cancer resections are R1 resections, Ann. Surg. Oncol. 15 (6) (2008) 1651–1660.

[26] V.P. Groot, N. Rezaee, W. Wu, J.L. Cameron, E.K. Fishman, R.H. Hruban, M.J. Weiss, L. Zheng, C.L. Wolfgang, J. He, Patterns, Timing, and Predictors of Recurrence Following Pancreatectomy for Pancreatic Ductal Adenocarcinoma, Ann. Surg. 267 (5) (2018) 936–945.

[27] J.-H. Hung, S.-E. Wang, Y.-M. Shyr, C.-H. Su, T.-H. Chen, C.-W. Wu, Resection for Secondary Malignancy of the Pancreas, Pancreas 41 (1) (2012) 121–129.

[28] J. Kleeff, M. Korc, M. Apte, C. La Vecchia, C.D. Johnson, A.V. Biankin, R.E. Neale, M. Tempero, D.A. Tuveson, R.H. Hruban, J.P. Neoptolemos, Pancreatic cancer, Nat. Rev. Dis. Primers 2 (2016) 16022.

[29] R. Girelli, I. Frigerio, A. Giardino, P. Regi, S. Gobbo, G. Malleo, R. Salvia, C. Bassi, Results of 100 pancreatic radiofrequency ablations in the context of a multimodal strategy for stage III ductal adenocarcinoma, Langenbecks Arch. Surg. 398 (1) (2013) 63–69.

[30] A. Giardino, R. Girelli, I. Frigerio, P. Regi, M. Cantore, A. Alessandra, A. Lusenti, R. Salvia, C. Bassi, P. Pederzoli, Triple approach strategy for patients with locally advanced pancreatic carcinoma, HPB 15 (8) (2013) 623–627.

[31] M.G. Keane, K. Bramis, S.P. Pereira, G.K. Fusai, Systematic review of novel ablative methods in locally advanced pancreatic cancer, World J. Gastroenterol. 20 (9) (2014) 2267–2278.

[32] M. D'Onofrio, S. Crosara, R. De Robertis, G. Butturini, R. Salvia, S. Paiella, C. Bassi, R.P. Mucelli, Percutaneous Radiofrequency Ablation of Unresectable Locally Advanced Pancreatic Cancer: Preliminary Results, Technol. Cancer Res. Treat. 16 (3) (2016) 285–294.

[33] S. Rossi, F.T. Viera, G. Ghittoni, L. Cobianchi, L.L. Rosa, L. Siciliani, C. Bortolotto, L. Veronese, A. Vercelli, A. Gallotti, V. Ravetta, Radiofrequency ablation of pancreatic neuroendocrine tumors: a pilot study of feasibility, efficacy, and safety, Pancreas 43 (6) (2014) 938–945.

[34] E. Leen, J. Picard, J. Stebbing, M. Abel, T. Dhillon, H. Wasan, Percutaneous irreversible electroporation with systemic treatment for locally advanced pancreatic adenocarcinoma, J. Gastrointest. Oncol. 9 (2) (2018) 275–281.

[35] G. Carrafiello, A.M. Ierardi, F. Fontana, M. Petrillo, C. Floridi, N. Lucchina, S. Cuffari, G. Dionigi, A. Rotondo, C. Fugazzola, Microwave ablation of pancreatic head cancer: safety and efficacy, J. Vasc. Interv. Radiol. 24 (10) (2013) 1513–1520.

[36] A.M. Ierardi, P. Biondetti, A. Coppola, E.M. Fumarola, A.M. Biasina, S. Alessio Angileri, G. Carrafiello, Percutaneous microwave thermosphere ablation of pancreatic tumours, Gland Surg. 7 (2) (2018) 59–66.

[37] L. Niu, L. He, L. Zhou, F. Mu, B. Wu, H. Li, Z. Yang, J. Zuo, K. Xu, Percutaneous ultrasonography and computed tomography guided pancreatic cryoablation: feasibility and safety assessment, Cryobiology 65 (3) (2012) 301–307.

[38] P.J. Loehrer, Y. Feng, H. Cardenes, L. Wagner, J.M. Brell, D. Cella, P. Flynn, R.K. Ramanathan, C.H. Crane, S.R. Alberts, A.B. Benson, Gemcitabine alone versus gemcitabine plus radiotherapy in patients with locally advanced pancreatic cancer: an eastern cooperative oncology group trial, J. Clin. Oncol. 29 (31) (2011) 4105–4112.

[39] S.J.E. Rombouts, J.A. Vogel, H.C. van Santvoort, K.P. van Lienden, R. van Hillegersberg, O.R.C. Busch, M.G.H. Besselink, I.Q. Molenaar, Systematic review of innovative ablative therapies for the treatment of locally advanced pancreatic cancer, BJS 102 (3) (2014) 182–193.

[40] D. Schellenberg, K.A. Goodman, F. Lee, S. Chang, T. Kuo, J.M. Ford, G.A. Fisher, A. Quon, T.S. Desser, J. Norton, R. Greco, G.P. Yang, A.C. Koong, Gemcitabine chemotherapy and single-fraction stereotactic body radiotherapy for locally advanced pancreatic Cancer, Int. J. Radiat. Oncol. 72 (3) (2008) 678–686.

[41] T. Comito, L. Cozzi, E. Clerici, C. Franzese, A. Tozzi, C. Iftode, P. Navarria, G. D'Agostino, L. Rimassa, C. Carnaghi, N. Personeni, M.C. Tronconi, F. De Rose, D. Franceschini, A.M. Ascolese, A. Fogliata, S. Tomatis, A. Santoro, A. Zerbi, M. Scorsetti, Can stereotactic body radiation therapy be a viable and efficient therapeutic option for unresectable locally advanced pancreatic adenocarcinoma? Results of a phase 2 study, Technol. Cancer Res. Treat. 16 (3) (2017) 295–301.

[42] F.S. Dar, S. Mukherjee, S. Bhattacharya, Surgery for secondary tumors of the pancreas, HPB 10 (6) (2008) 498–500.

[43] H.A. Burris, M.J. Moore, J. Andersen, M.R. Green, M.L. Rothenberg, M.R. Modiano, M.C. Cripps, R.K. Portenoy, A.M. Storniolo, P. Tarassoff, R. Nelson, F.A. Dorr, C.D. Stephens, D.D. Von Hoff, Improvements in survival and clinical benefit with gemcitabine as first-line therapy for patients with advanced pancreas cancer: a randomized trial, J. Clin. Oncol. 15 (6) (1997) 2403–2413.

[44] T. Conroy, F. Desseigne, M. Ychou, O. Bouché, R. Guimbaud, Y. Bécouarn, A. Adenis, J.-L. Raoul, S. Gourgou-Bourgade, C. de la Fouchardière, J. Bennouna, J.-B. Bachet, F. Khemissa-Akouz, D. Péré-Vergé, C. Delbaldo, E. Assenat, B. Chauffert, P. Michel, C. Montoto-Grillot, M. Ducreux, FOLFIRINOX versus gemcitabine for metastatic pancreatic cancer, N. Engl. J. Med. 364 (19) (2011) 1817–1825.

Cardiovasc Intervent Radiol (2016) 39:1716–1721
DOI 10.1007/s00270-016-1423-1

CLINICAL INVESTIGATION INTERVENTIONAL ONCOLOGY

Haemorrhagic Complications and Symptomatic Venous Thromboembolism in Interventional Tumour Ablations: The Impact of Peri-interventional Thrombosis Prophylaxis

Konrad Mohnike[1] · Hanna Sauerland[1] · Max Seidensticker[1] · Peter Hass[2] · Siegfried Kropf[3] · Ricarda Seidensticker[1] · Björn Friebe[1] · Frank Fischbach[1] · Katharina Fischbach[1] · Maciej Powerski[1] · Maciej Pech[1] · O. S. Grosser[1] · Erika Kettner[1] · Jens Ricke[1]

Received: 17 June 2016 / Accepted: 9 July 2016 / Published online: 19 July 2016

Abstract
Aim The aim of this study was to assess the rates of haemorrhagic and thrombotic complications in patients undergoing interventional tumour ablation with and without peri-interventional low-molecular-weight heparin (LMWH) thrombosis prophylaxis.
Methods Patients presented with primary and secondary neoplastic lesions in the liver, lung, kidney, lymph nodes and other locations. A total of 781 tumour ablations (radiofrequency ablation, $n = 112$; interstitial brachytherapy, $n = 669$) were performed in 446 patients over 22 months; 260 were conducted under peri-interventional thrombosis prophylaxis with LMWH (H-group;) and 521 without this (NH-group, in 143 of these, LMWH was given post-interventionally).
Results Sixty-three bleeding events occurred. There were significantly more bleedings in the H-group than in the NH-group (all interventions, 11.66 and 6.26 %, $p = 0.0127$; liver ablations, 12.73 and 7.1 %, $p = 0.0416$). The rate of bleeding events Grade $\geq$ III in all procedures was greater by a factor of >2.6 in the H-group than in the NH-group (4.64 and 1.73 %, $p = 0.0243$). In liver tumour ablations, the corresponding factor was about 3.3 (5.23 and 1.54 %, $p = 0.028$). In uni- and multivariate analyses including covariates, the only factor constantly and significantly associated with the rate of haemorrhage events was peri-interventional LMWH prophylaxis. Only one symptomatic lung embolism occurred in the entire cohort (NH-group). The 30- and 90-day mortalities were significantly greater in the H-group than in the NH-group.
Conclusions Peri-interventional LMWH thrombosis prophylaxis should be considered with caution. The rate of clinically relevant thrombotic events was extremely low.

Keywords Ablation · Complications · Bleeding events · Heparin · LMWH · RFA · Brachytherapy

Introduction

In hospital patients, venous thromboembolism (VTE), including deep vein thrombosis (DVT) and pulmonary embolism (PE), is an important preventable cause of morbidity and mortality. Over the past decades this has led to the adoption of recommendations for VTE prophylaxis in current guidelines [1, 2, 5]. Cancer patients have twice the incidence of DVT compared with those without cancer [14]. Overall, the incidence of VTE was 2.0 and 0.6 % for PE among over 40 million cancer patients hospitalized in the United States from 1979 to 1999 [14]. There are large differences between the various types of cancer. One study [14] showed that patients with pancreatic cancer had the highest relative risk of 4.65 compared with non-cancer hospitalized controls, whereas patients with bladder cancer had a relative risk of 1.07, scarcely higher than that of the non-cancer control group. However, this study did not discriminate between invasive and non-invasive treatments

✉ Konrad Mohnike
konrad.mohnike@med.ovgu.de

[1] Klinik für Radiologie und Nuklearmedizin, Universitätsklinikum Magdeburg A.ö.R., Otto-von-Guericke-Universität, Leipziger Straße 44, 39120 Magdeburg, Germany

[2] Klinik für Strahlentherapie, Universitätsklinikum Magdeburg A.ö.R., Otto-von-Guericke-Universität, Leipziger Straße 44, 39120 Magdeburg, Germany

[3] Institut für Biometrie, Universitätsklinikum Magdeburg A.ö.R., Otto-von-Guericke-Universität, Leipziger Straße 44, 39120 Magdeburg, Germany

or procedures. Interestingly, and in contrast to current guidelines, a recent meta-analysis reached the conclusion that in over 16,000 patients the use of heparin-based VTE prevention did not lead to a significant reduction in symptomatic DVT, PE, fatal PE or total mortality, although the cohort included patients with and without cancer [13].

Over and above heparin-induced thrombocytopenia [4], peri-operative administration of low-molecular-weight heparin (LMWH) leads to an increased risk of haemorrhagic complications. In patients undergoing hepatopancreatobiliary surgery, the preoperative administration of LMWH led to a lower incidence of thromboembolic events (1.1 % with LMWH, 6.1 % without) but to a higher rate of bleeding episodes requiring intervention (10.9 % with LMWH, 3.1 % without) [6].

Owing to the inception of an interdisciplinary oncological gastrointestinal ward and the harmonization of the standard operating procedures with the surgical department, most of the cancer patients treated from March 2013 until November 2013 received peri-interventional thrombosis prophylaxis with LMWH. A higher rate of minor and major bleeding events was noticed, and therefore the relevant standard procedure was changed to a much more restrictive regimen regarding the use of LMWH. After this, all patients treated with or without peri-interventional LMWH from January 2013 to October 2014 were analysed for bleeding events and symptomatic VTE.

Patients and Methods

Patient Population and Eligibility Criteria

Data from 781 extracranial interstitial interventions in 446 patients treated either by high-dose-rate interstitial brachytherapy (iBT, $N = 669$) or by radiofrequency ablation (RFA, $N = 112$) from January 2013 to October 2014 were analysed for haemorrhagic complications and symptomatic venous thromboembolism events.

Patients presented with primary and secondary neoplastic lesions in the liver, lung, kidney, lymph nodes and other locations (for patients and treatment characteristics, see Table 1).

Two hundred and sixty interventions were conducted that included peri-interventional thrombosis prophylaxis with low-molecular-weight heparin (H-group), whereas 521 interventions were performed without this (NH-group). In 143 of these 521 interventions, LMWH was given post-interventionally. All patients were mobilized early (4 h after the intervention). Peri-interventional LMWH dosing was defined as any administration at least 24 h before intervention. For thrombosis prophylaxis, we usually prescribed Dalteparin (Fragmin P forte®) once a day for the entire hospital stay, starting from the preinterventional evening.

The study was approved by the local ethics committee (Ethics Committee of the Medical Faculty, University of Magdeburg, 185/14).

Ablation Methods

Patients were treated by either radiofrequency ablation (RFA) or interstitial brachytherapy (iBT) under guidance with magnetic resonance imaging (MRI) or computed tomography (CT). In RFA, thermoablation was performed with an AngioDynamics generator (Latham, NY) and correspondent RF-applicators (RITA Starburst). For iBT, between one and eight 6F-angiography sheaths were placed in the liver, the lung or other extracranial body regions harbouring 6F-brachytherapy catheters guiding the iridium-192 point source during the treatment session. This ablation method has been described in detail elsewhere [8–12].

The tracks of the radiofrequency applicators were coagulated during retreatment following the manufacturer's instructions. The tracks of the brachytherapy catheters were closed with Gelaspone plugs introduced over the sheaths during the retraction.

Interventions were performed under mild analgosedation and local anaesthesia.

Assessments and Statistical Methods

Events were recorded according to the Common Terminology Criteria for Adverse Events (version 4.0) with minor adaptations regarding Grade I and II bleeding events (Grade I, asymptomatic haematoma <1 cm; Grade II, symptomatic haematoma or haematoma ≥ 1 cm). The complete patient documentation, including admission and discharge diagnoses, discharge summary, the health and medical records of each patient and the peri- and post-interventional imaging (CT, MRI, sonography) were included in the evaluation. Therefore, haematoma or active bleeding was diagnosed with ultrasound and/or computed tomography and/or magnetic resonance imaging.

Peri- and post-interventional LMWH dosing was documented and correlated with bleeding events. Clinical and paraclinical parameters and cofactors such as bleeding or clotting disorders, coagulation status, the Padua Prediction Score for the risk of VTE were recorded [3].

The primary variables in this analysis were as follows: (i) the rate of bleeding events (any grade), (ii) the rate of bleeding events requiring intervention (Grade III and above) and (iii) the frequency of VTE. These were compared for the patients either with (H-group) or without (NH-group) peri-interventional LMWH administration. Secondary endpoints were the rate of bleeding events in

Table 1 Patients and treatment characteristics

Patients	$N = 446$
Interventions	$N = 781$ (100.0 %)
Primary cancer	$n = 308$ (39.4 %)
Colorectal cancer	$n = 104$ (13.3 %)
Hepatocellular carcinoma	$n = 96$ (12.3 %)
Cholangiocellular cancer	$n = 50$ (6.4 %)
Breast cancer	$n = 50$ (6.4 %)
Renal cell cancer	$n = 30$ (3.8 %)
Liver cancer	$n = 24$ (3.1 %)
Gastroenteropancreatic neuroendocrinal tumour	$n = 119$ (15.2 %)
Other	
Clotting disorders	$n = 22$ (2.9 %)
Thrombopenic	$n = 14$ (1.8 %)
Thrombophilic	$n = 8$ (1.0 %)
Cirrhosis	$n = 98$ (12.5 %)
Child–Pugh stage B	$n = 21$ (2.7 %)
Padua score <4	$n = 229$ (29.3 %)
Padua score ≥4	$n = 552$ (70.7 %)
RFA	$n = 112$ (14.3 %)
iBT	$n = 669$ (85.8 %)
Peri-interventional LMWH dosing	$n = 260$ (33.3 %)
Hospital stay	4.8 days (95 % CI 4.6–5.1, range 2–15)

liver interventions and the 30- and 90-day mortality. In order to address the fact that some of the patients had several treatments, generalised mixed linear models (software SAS, Version 9.4, Proc GLIMMIX) were used, with the number of bleeding events or bleeding events requiring intervention as the dependent variable, a random intercept for each patient, and the presence or absence of peri-interventional LMWH as fixed factor. In secondary analyses, additional covariates were considered in the model (only one at a time, because of the limited number of events). Furthermore, the analyses were repeated in the subgroup of liver interventions.

The 30- and 90-day mortality and survival times were analysed at the patient level (considering only the first treatment for each patient) by using the χ^2 test, log-rank tests and Cox regression as appropriate, comparing patients with and without bleeding events. These analyses were performed with the programme suite IBM SPSS Statistics 22.0.

p values below 0.05 were considered significant at an exploratory level of this study.

Results

In all 781 interventions, 63 haemorrhagic events of any severity occurred (8.1 %). In 33 of 521 interventions in patients without peri-interventional LMWH dosing (NH-group), bleeding of any grade occurred corresponding to a bleeding rate of 6.3 %. Compared with 30 interventions with haemorrhagic events of any grade in patients with peri-interventional LMWH dosing (H-group, 11.7 %), this difference was statistically significant ($p = 0.0127$). In liver interventions, there were 23 of 325 interventions in the NH-group (7.1 %) compared with 22 of 173 in the H-group (12.73 %; $p = 0.046$).

Severe bleeding (Grade III and above) occurred in 9 of 521 interventions (all sites) in the NH-group (1.7 %) compared with 12 of 260 interventions in the H-group (4.64 %, $p = 0.024$). In liver interventions, there were 5 of 325 interventions in the NH-group (1.54 %) compared with 9 of 173 in the H-group (5.23 %; $p = 0.028$).

The rate of bleeding events of any grade was higher after RFA (16 of 112 interventions, 14.29 %) than after iBT ablation (47 of 669 interventions, 7.03 %; $p = 0.0149$). In liver interventions, there were 11 such events (19.6 %) in 56 RFA interventions and 34 events (7.7 %) in 441 iBT interventions ($p = 0.0054$). No differences were seen in respect of the proportion of patients receiving peri-interventional LMWH dosing between the treatments RFA and iBT (iBT 33.0 %, RFA 34.8 %, $p = 0.710$). The frequency of severe bleeding events was not significantly different between the RFA and iBT patients ($p = 0.5351$).

Peri-interventional LMWH dosing was the only constantly and significantly contributing factor to increase both

the total and severe bleeding rate in a secondary analysis, including covariates known or suspected to increase, directly or indirectly, the bleeding rate (see Tables 2, 3). The treatment (RFA or iBT) proved to be an independent risk factor for the total bleeding rate. However, this was not the case for severe bleeding events. Thrombopenic disorders were more frequent in patients with haemorrhagic complications (5 % for those with complications, 1 % for those without; $p = 0.03$, Table 4).

No bleeding events occurred in patients with post-interventional LMWH dosing (143 interventions). Symptomatic VTE occurred in only one patient without peri-interventional LMWH dosing, diagnosed 2 months after the intervention.

The all-cause 30-day mortality rate was 1.2 % (5 of 431 patients) and the 90-day rate was 3.5 % (14 of 404 patients). In uni- and multivariate analysis, bleeding events of the Common Terminology Criteria for Adverse Events (CTCAE) Grade $\geq$ III were strongly associated with the 30-day mortality ($p < 0.0001$, odds ratio 53.4), whereas no significant association with age was found ($p = 0.162$ and 0.374 in uni- and multivariate analysis respectively). Therefore, the 30- and 90-day mortality rates among patients without, or with mild, bleeding events were 0.5 and 2.3 % (2 of 418 and 9 of 391 patients), while among patients with bleeding events of CTCAE Grade $\geq$ III it were 23.1 and 38.5 % (3 of 13 and 5 of 13 patients). These differences were significant ($p < 0.0001$). The specific causes of death in the group of patients with severe haemorrhagic complications were subsequent bleeding complications due to the following: (1) uncontrolled oozing in the pelvicocealiceal system after brachytherapy of a renal cell carcinoma, (2) a colon perforation distant from the liver irradiation zone after urgent embolisation of a large intrahepatic haematoma following brachytherapy of liver metastases, (3) an infected intrahepatic haematoma with subsequent sepsis and multiple organ failure after RFA of liver metastases, (4) an uncontrollable bleeding into the biliary tract despite angiography and endoscopy after iBT of the liver, (5) haematothorax after RFA of lung metastases, with pneumonia and sepsis after discharge.

Discussion

To our knowledge, this is the first study specifically addressing the correlation between bleeding events (and symptomatic VTE) and the administration of peri-operative LMWH in cancer patients undergoing interventional, image-guided tumour-directed treatments.

The analysis led to three principal results. First of all, the analysis of this large patient cohort proves the increased risk of bleeding (both 'all events' and 'severe events') associated with the peri-interventional administration of LMWH. The analysis showed a 2.7-fold increase in the frequency of such severe events after peri-interventional LMWH dosing in the entire patient cohort and a 3.4-fold increase in after liver interventions. This is comparable to

Table 2 Haemorrhagic complications of any severity

Covariate	Mean value (95 % CI)	Bleeding rate: Interaction between peri-interventional LMWH dosing and covariate, p value		Influence of peri-interventional LMWH dosing on bleeding rate adjusted for covariate, p value		Influence of covariate on bleeding rate adjusted for peri-interventional LMWH dosing, p value		Influence of covariate only, p value	
Interventions		All	Liver	All	Liver	All	Liver	All	Liver
Modality (RFA/iBT)	n.a.	0.4110	0.8294	**0.0137**	**0.0145**	**0.0172**	**0.0057**	**0.0149**	**0.0054**
Number of Catheters (iBT)	2.71 (1–9)	0.2001	0.1463	**0.0198**	**0.0422**	0.5421	0.5201	0.5075	0.5076
Thrombocytes (Gpt/l, 176–391)	212 (204–220)	0.6166	0.9062	**0.0120**	**0.0426**	0.4926	0.8879	0.5428	0.8025
Haemoglobin (mmol/l, 7.2–9.6)	8.04 (7.95–8.14)	0.8232	0.8904	**0.0138**	**0.0474**	0.4882	0.3768	0.4276	0.3168
Haematocrit (l/l, 0.35–0.45)	0.39 (0.39–0.39)	0.8838	0.7455	**0.0129**	**0.0434**	0.6889	0.5186	0.6607	0.4840
Prothrombin time (>70 %)	108 (106–109)	0.3096	0.8845	**0.0160**	**0.0405**	0.1335	0.3270	*0.0762*	0.2537
Creatinine (μmol/l)	89 (82–95)	0.6525	0.6234	**0.0074**	**0.0235**	0.2435	0.2899	0.3163	0.3779
Cirrhosis	n.a.	0.7009	0.7019	**0.0134**	**0.0388**	0.2696	0.3891	0.2487	0.4311
Cirrhosis CHILD–PUGH B	n.a.	0.6024	0.9234	**0.0135**	**0.0414**	0.3558	0.7461	0.3208	0.7576

Generalised linear mixed model. Interaction between peri-interventional LMWH dosing and different covariates. Influence of LMWH adjusted for covariates and vice versa and of covariates alone. p values <0.05 (bold letters) indicate statistical significance. p value at the border of significance ($p < 0.1$) is in italic

Table 3 Severe haemorrhagic complications

Covariate	Mean value (95 % CI)	Bleeding rate: Interaction between peri-interventional LMWH dosing and covariate, p value		Influence of peri-interventional LMWH dosing on bleeding rate adjusted for covariate, p value		Influence of covariate on bleeding rate adjusted for peri-interventional LMWH dosing, p value		Influence of covariate only, p value	
Interventions		All	Liver	All	Liver	All	Liver	All	Liver
Modality (RFA/iBT)	n.a.	0.4563	0.9079	**0.0248**	**0.0281**	0.5669	0.2469	0.5351	0.2357
Number of Catheters (iBT)	2.71 (1–9)	0.4867	0.8657	**0.0241**	**0.0281**	0.8403	0.8923	0.8041	0.8778
Thrombocytes (Gpt/l, 176–391)	212 (204–220)	0.2422	0.5330	**0.0216**	**0.0224**	0.1773	0.1658	0.1987	0.2095
Haemoglobin (mmol/l, 7.2–9.6)	8.04 (7.95–8.14)	0.6401	0.5974	**0.0247**	**0.0284**	0.8841	0.9593	0.8203	0.8552
Haematocrit (l/l, 0.35–0.45)	0.39 (0.39–0.39)	0.7044	0.7844	**0.0243**	**0.0279**	0.9896	0.9443	0.9902	0.9895
Prothrombin time (>70 %)	108 (106–109)	0.1718	0.2555	**0.0202**	**0.0168**	0.4277	0.8612	0.2738	0.9942
Creatinine (µmol/l)	89 (82–95)	0.8958	0.5906	**0.0146**	**0.0144**	0.7404	0.5808	0.8160	0.7184
Cirrhosis	n.a.	0.7635	0.7331	**0.0245**	**0.0287**	0.8350	0.7809	0.8083	0.7212
Cirrhosis CHILD–PUGH B	n.a.	0.7364	0.9234	**0.0262**	**0.0274**	*0.0871*	0.4657	*0.0707*	0.4853

Generalised linear mixed model. Interaction between peri-interventional LMWH dosing and different covariates. Influence of LMWH adjusted for covariates and vice versa and of covariates alone. p values <0.05 (bold letters) indicate statistical significance. p values at the border of significance ($p < 0.1$) are in italics

Table 4 Covariates across groups

Covariate	Peri-interventional LMWH dosing			Haemorrhagic complication			Severe haemorrhagic complication		
	Yes	No	p	Yes	No	p	Yes	No	p
Haematocrit [l/l, 0.35–0.45]	0.39	0.39	0.64	0.39	0.39	0.67	0.39	0.39	0.69
Haemoglobin [mmol/l, 7.2–9.6]	8.0	8.1	0.14	8.0	8.0	0.77	8.1	8.0	0.92
Thrombocytes (Gpt/l, 176–391)	213	212	0.84	205	213	0.36	204	212	0.56
Prothrombin time (>70 %)	107	108	0.79	106	108	0.17	107	108	0.97
Creatinine (µmol/l)	90	88	*0.07*	88	89	0.96	91	88	0.62
Cirrhosis	11 %	11 %	0.98	14 %	10 %	0.41	13 %	11 %	0.82
Child–Pugh stage B	3 %	2 %	0.77	4 %	2 %	0.39	8 %	2 %	0.16
Padua score ≥4	78 %	72 %	0.17	81 %	73 %	0.29	85 %	74 %	0.33
Thrombopenic disorder	–	–	–	5 %	1 %	**0.03**	7 %	1 %	*0.09*
Thrombophilic disorder	1.8 %	0.2 %	**0.037**	0.9 %	0.7 %	0.82	–	–	–

Estimators of marginal means from mixed linear models or estimates of percentages from generalized linear mixed models. p values <0.05 (bold letters) indicate statistical significance. p values at the border of significance ($p < 0.1$) are in italics

findings in hepatopancreatobiliary surgery [6]. In an earlier study addressing complications in interstitial brachytherapy of liver neoplasms, severe bleeding was linked to the advanced liver cirrhosis [9]. In that study, peri-interventional LMWH dosing was not a standard procedure and the number of interventions in patients with Child–Pugh B cirrhosis was higher than in our trial (3.5 vs 2.7 %). Nonetheless, we observed a trend towards an effect of Child–Pugh B cirrhosis on the severe bleeding rate in this trial too (see Table 3).

Secondly, only one symptomatic venous thromboembolic event (lung embolism) occurred in all 781 interventions (0.13 %). The low invasiveness of the therapeutic procedures and the early mobilization 3–4 h after the intervention as a standard operating procedure at our department may have been the contributing factors.

Thirdly, patients with severe bleeding rates showed very high 30- and 90-day mortality rates. Therefore, we attribute the peri- and short-term post-interventional mortality mainly to severe bleeding and its complications, leading to

a 46-fold increase in the 30-day mortality and to a 17-fold increase in the 90-day mortality. The mortality rates were higher than reported for upper gastrointestinal bleeding, even though a broad range among centres has been reported [7]. This is most probably due to the impact of cancer on the patient's general condition, and to cancer-related coagulopathies and other comorbidities in this elderly patient cohort, enhancing the negative impact of volume loss, anaemia and inflammation. The causes of death were uncontrollable, ooze bleedings that could not be embolised, infections most probably related to haematoma, and a colon perforation probably driven by ischaemia due to volume loss-related centralization effects. Therefore, and to reduce mortality, aggressive early interventions in these patients are indicated. Such interventions may include early blood transfusion, early angiography or surgery (if surgery appears promising and interventional embolisation fails). Furthermore, close monitoring of haematomas for signs of infections is necessary and urgent antibiotic/anti-inflammatory treatment should be provided.

However, in some patients, peri-interventional anticoagulation (e.g. as a bridging therapy in patients with vitamin K antagonists medication) cannot be evicted. In these patients, the indication to interstitial treatments and the conduction of such demand a comprehensive and prudent proceeding.

Conclusion

Our findings show that a "blanket" peri-interventional LMWH prophylaxis for all patients cannot be recommended in the cancer patients undergoing radiological interventions. On the contrary, it should be prescribed with caution, and those patients receiving it require particularly close monitoring for bleeding events. Patients with severe bleeding events need aggressive treatment to avoid, or to treat, a relevant volume loss or the development of large haematomas.

Funding This work was funded exclusively by the University of Magdeburg.

Compliance with Ethical Standards

Conflict of interest There are no conflicts of interest to state.

Ethical Standards The study was conducted in accordance with the protocol, with the ethical principles that have their origin in the Declaration of Helsinki and with ICH-GCP. The study protocol and all study-related documentation were approved by the relevant committee (Ethic Committee of the Medical Faculty, University of Magdeburg, 185/14).

References

1. Lowe GDO (Chairman of the THRIFT Consensus group). Risk of and prophylaxis for venous thromboembolism in hospital patients. Thromboembolic Risk Factors (THRIFT) Consensus Group. BMJ. 1992;305(6853):567–74.
2. Anderson FA Jr, Wheeler HB, Goldberg RJ, Hosmer DW, Forcier A, Patwardhan NA. Physician practices in the prevention of venous thromboembolism. Ann Intern Med. 1991;115(8):591–5.
3. Barbar S, Noventa F, Rossetto V, et al. A risk assessment model for the identification of hospitalized medical patients at risk for venous thromboembolism: the Padua Prediction Score. J Thromb Haemost: JTH. 2010;8(11):2450–7.
4. Battistelli S, Genovese A, Gori T. Heparin-induced thrombocytopenia in surgical patients. Am J Surg. 2010;199(1):43–51.
5. Clagett GP, Anderson FA Jr, Heit J, Levine MN, Wheeler HB. Prevention of venous thromboembolism. Chest. 1995;108(4 Suppl):312S–34S.
6. Doughtie CA, Priddy EE, Philips P, Martin RC, McMasters KM, Scoggins CR. Preoperative dosing of low-molecular-weight heparin in hepatopancreatobiliary surgery. Am J Surg. 2014;208(6):1009–15.
7. Jairath V, Martel M, Logan RF, Barkun AN. Why do mortality rates for nonvariceal upper gastrointestinal bleeding differ around the world? A systematic review of cohort studies. Can J Gastroenterol. 2012;26(8):537–43.
8. Mohnike K, Wieners G, Schwartz F, et al. Computed tomography-guided high-dose-rate brachytherapy in hepatocellular carcinoma: safety, efficacy, and effect on survival. Int J Radiat Oncol Biol Phys. 2010;78(1):172–9.
9. Mohnike K, Wolf S, Damm R, et al. Radioablation of liver malignancies with interstitial high-dose-rate brachytherapy: complications and risk factors. Strahlentherapie Onkol. 2016;192(5):288–96.
10. Peters N, Wieners G, Pech M, et al. CT-guided interstitial brachytherapy of primary and secondary lung malignancies: results of a prospective phase II trial. Strahlentherapie Onkol. 2008;184(6):296–301.
11. Ricke J, Mohnike K, Pech M, et al. Local response and impact on survival after local ablation of liver metastases from colorectal carcinoma by computed tomography-guided high-dose-rate brachytherapy. Int J Radiat Oncol Biol Phys. 2010;78(2):479–85.
12. Ricke J, Wust P, Wieners G, et al. Liver malignancies: CT-guided interstitial brachytherapy in patients with unfavorable lesions for thermal ablation. J Vasc Intervent Radiol JVIR. 2004;15(11):1279–86.
13. Spencer A, Cawood T, Frampton C, Jardine D. Heparin-based treatment to prevent symptomatic deep venous thrombosis, pulmonary embolism or death in general medical inpatients is not supported by best evidence. Intern Med J. 2014;44(11):1054–65.
14. Stein PD, Beemath A, Meyers FA, Skaf E, Sanchez J, Olson RE. Incidence of venous thromboembolism in patients hospitalized with cancer. Am J Med. 2006;119(1):60–8.

Clinical Investigations

Original paper

Needle track seeding in hepatocellular carcinoma after local ablation by high-dose-rate brachytherapy: a retrospective study of 588 catheter placements

Robert Damm, MD[1], Ingo Zörkler, MD[1], Bela Rogits, MD[2], Peter Hass, MD[3], Jazan Omari, MD[1], Maciej Powerski, MD, PhD[1], Prof. Sigrfried Kropf[4], Konrad Mohnike, MD[5], Prof. Maciej Pech, MD[1], Prof. Jens Ricke, MD[6], Prof. Max Seidensticker, MD[6]

[1]Department of Radiology and Nuclear Medicine, Otto-von-Guericke University, Magdeburg, [2]Pawlow Poliklinik, Radiologische Gemeinschaftspraxis, Magdeburg, [3]Department for Radiation Oncology, Otto-von-Guericke University, Magdeburg, [4]Institute for Biometry and Medical Informatics, Otto-von-Guericke University, Magdeburg, [5]Diagnostic and Therapeutic Center am Frankfurter Tor, Berlin, [6]Department of Radiology, Ludwig-Maximilians-University, Munich, Germany

Abstract

Purpose: Needle track seeding in the local treatment of hepatocellular carcinoma (HCC) is not yet evaluated for catheter-based high-dose-rate brachytherapy (HDR-BT), a novel local ablative technique.

Material and methods: We report a retrospective analysis of 100 patients treated on 233 HCC lesions by HDR-BT (using 588 catheters in total). No needle or catheter track irradiation was used. Minimum required follow-up with imaging was 6 months. In case of suspected needle track seeding (intra- and/or extrahepatic) in follow-up, image fusion of follow-up CT/MRI with 3D irradiation plan was used to verify the location of a new tumor deposit within the path of a brachytherapy catheter at the time of treatment.

Results: We identified 9 needle track metastases, corresponding to a catheter-based risk of 1.5% for any location of occurrence. A total of 7 metastases were located within the liver (catheter-based risk, 1.2%), and 2 metastases were located extrahepatic (catheter-based risk, 0.3%). Eight out of 9 needle track metastases were successfully treated by further HDR-BT.

Conclusions: The risk for needle track seeding after interstitial HDR-BT of HCC is comparable to previous reports of percutaneous biopsies and radiofrequency ablation (RFA), especially in case of extrahepatic needle track metastases. To compensate for the risk of seeding, a track irradiation technique similar to track ablation in RFA should be implemented in clinical routine.

J Contemp Brachytherapy 2018; 10, 6: 516–521
DOI: https://doi.org/10.5114/jcb.2018.80626

Key words: hepatocellular carcinoma, local ablative treatment, needle track seeding.

Purpose

Hepatocellular carcinoma (HCC) is a primary liver tumor most often found in patients with liver cirrhosis and/or viral hepatitis. Its incidence has increased over the last years worldwide [1]. Beneath surgical resection, local ablative (e.g., radiofrequency ablation – RFA, microwave ablation – MWA) and loco-regional (e.g., transarterial chemoembolization – TACE) treatments are favored for early to intermediate stage of HCC. However, these treatments may not be suitable for every patient due to technical restrictions [2,3,4]. Thermal ablation techniques have their limitations, especially in location close to vulnerable structures (e.g., bile ducts) and lesion size of 3.5 to 4 cm, while loco-regional techniques require sufficient, vascular access for the application of embolic agents, showing lack in local control if tumor nodules exceed a size of 5 to 7 cm [5,6]. Thus, computed tomography (CT)-guided high-dose-rate brachytherapy (HDR-BT) as a form of catheter-based radiotherapy is a promising treatment option for tumors not accessible for thermal ablation techniques as well as an alternative to TACE. By inserting an Iridium 192 source through percutaneously applied catheters, interstitial brachytherapy has no technical restrictions in lesion size to deliver potentially ablative doses, and can be employed close to central structures [7,8]. In a series of studies, the safety and effectiveness of HDR-BT has already been

Address for correspondence: Robert Damm, MD, Klinik für Radiologie und Nuklearmedizin, Universitätsklinikum Magdeburg, Leipziger Str. 44, 39120 Magdeburg, Germany, phone: +49 391 67 13030, fax: +49 391 67 13029, ✉ e-mail: Robert.Damm@med.ovgu.de

Received: 28.09.2018
Accepted: 12.11.2018
Published: 28.12.2018

demonstrated, suggesting a potential as a bridging therapy to liver transplantation in addition to radiofrequency ablation or transarterial chemoembolization [9].

The risk of spreading malignant cells during diagnostic and therapeutic methods have been reported for liver biopsy and thermal ablation with heterogeneous results, also varying by the utility of needle track ablation [10,11,12,13]. As the catheter placement for HDR-BT comprises an initial puncture (including possible corrections of the needle position) and insertion of catheter sheets in Seldinger's technique, a corresponding risk of dislocating tumor cells through manipulation should be assumed.

The risk of needle track seeding after HDR brachytherapy, particularly in case of the potential utility as a bridging treatment for liver transplantation in early stage HCC, should be further investigated. On the other side, patients with larger tumor volumes in intermediate stage of the disease might have an increased risk for needle track seeding, as more catheter placements are required for a sufficient dose distribution [14]. In this retrospective study, we report needle track seeding after HDR brachytherapy in a series of 100 patients, with a total of 588 catheter placements for local ablation of 233 HCC lesions. No catheter or needle track irradiation had been used in these patients.

Material and methods

Eligibility criteria and patient cohort

We retrospectively analyzed patients who underwent interstitial HDR brachytherapy for HCC between 2006 and 2012. All lesions were previously proven either by core needle biopsy or by matching the non-invasive criteria of HCC in CT or magnetic resonance imaging (MRI) [15], according to the Clinical Practice Guidelines of the European Association for the Study of the Liver (EASL) released in 2012 [16].

100 patients (83 males, 17 females), with 233 HCC nodules and a total of 588 catheter placements met the inclusion criteria (see section follow-up). The average age at the time of intervention was 68 ± 8.1 years (44-82 years). Nearly all patients had an underlying liver cirrhosis (n = 98), mainly caused by alcohol consumption (n = 28) or viral hepatitis (n = 22). Infrequent causes of cirrhosis were non-alcoholic steatohepatitis (n = 8) and hemochromatosis (n = 2). In all other cases, the etiology of cirrhosis was cryptogenic (n = 38).

Only a minority of patients presented with extrahepatic disease including lymphatic (n = 5) or distant metastases (n = 5). A summary of patient and treatment characteristics is presented in Table 1.

Table 1. Patient and treatment characteristics and analysis on influencing factors for needle track seeding

Variable	% (*N*) or mean ± SD	Patient-based *p*	Lesion-based *p*	Catheter-based *p*
Male/female	83% (83)/17% (17)	0.66	0.49	0.33
Age (years)	68.0 ± 8.1	0.26	0.21	0.37
Liver cirrhosis	98% (98/100)			
hemochromatosis	2% (2/98)	1.0		
viral hepatitis	22% (22/98)	1.0		
ASH	29% (28/98)	0.99		
NASH	8% (8/98)	0.99		
other	39% (38/98)			
HCC grading	62% (62/100)	0.54	0.23	0.3
well	39% (24/62)			
moderate	55% (34/62)			
poor	6% (4/62)			
Concomitant sorafenib treatment	22% (22/78)	0.6	0.96	0.62
Pseudo-capsular HCC	8% (18/233)	0.98		
Lesion size (cm)	3.3 ± 2.6	0.2	0.78	0.09
Ablation dose (Gy)	16.5 ± 11.6	0.65	0.7	0.59
Overpenetration (per catheter)	9% (53/588)	0.23	0.69	
Catheter insertion lengths (cm)				
/patient	74.8 ± 57.4	0.94		
/lesion	32.1 ± 37.4		0.78	
/catheter	12.7 ± 31.2			0.75

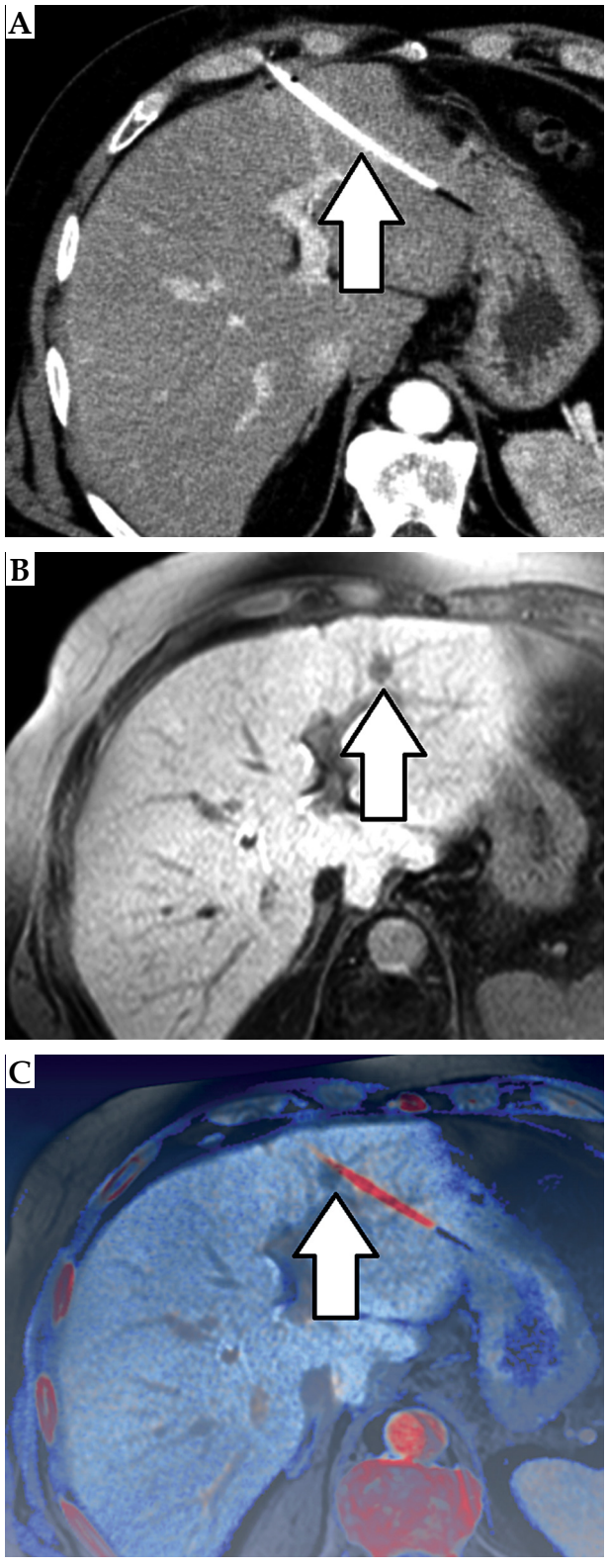

Fig. 1. Image fusion data set: peri-interventional CT showing HDR brachytherapy catheter (arrow, **A**), follow-up MRI suspecting a needle track lesion (arrow, **B**), axial image fusion of follow-up MRI and planning CT of HDR brachytherapy confirming the origin of the new lesion within the former path of the brachytherapy catheter (arrow, **C**)

HDR brachytherapy technique

In order to place an Iridium 192 source directly in the HCC lesions, irradiation catheters must be inserted into the tumor. The access for a soft catheter is accomplished by a percutaneous puncture with an 18 Ga coaxial needle under image guidance (CT or open MRI fluoroscopy) and subsequent insertion of an angiographic catheter sheet in Seldinger's technique. The irradiation catheter is then placed inside the catheter sheath and fixed by a single suture. For planning purposes, diagnostic imaging (e.g., contrast enhanced CT) is performed after complete catheter placement. Afterwards, a three-dimensional treatment plan is generated based on diagnostic imaging data acquired following catheter placement. Generally, the preferred surrounding dose for HCC is 15 Gy. After successful delivery of the desired dose in a single fraction, the catheters and sheaths are removed leaving absorbable gelatin sponge in the track. Concomitant conscious sedation is achieved by individual administration of fentanyl and midazolam. A further description of irradiation technique and concomitant treatment is presented elsewhere [17].

Follow-up

All eligible patients required a follow-up consisting of CT or MRI at least 3 and 6 months after therapy, with a dynamic contrast-enhanced scan protocol including arterial, portal venous, and late venous phase. Any new intrahepatic lesion with a diameter of at least 1 cm and arterial enhancement with venous wash out was defined as an intrahepatic recurrence of HCC, while clear tumor growth outside the liver was sufficient for the definition of extrahepatic lesions [16].

Subsequent therapies in the follow-up period included sorafenib (n = 22), transarterial chemoembolization (n = 18), Y90 radioembolization (n = 4), and radiofrequency ablation (n = 4).

Imaging analysis

We determined the primary tumor size, number and location of metastases, the total length of each catheter from the skin to the tip as well as 'over-penetration' of the tip beyond the HCC lesion.

As a first step, the available image data sets were evaluated for the probability of needle tract seeding according to the following definitions: 1) Temporal causality: needle track seeding should be diagnosed after therapy within a reasonable timeframe of 2 years; 2) Local causality: needle tract seeding had to be situated around a prior catheter track within a margin of 1 cm.

In a second step, the suspected needle track metastases had to be objectively verified. Amira® 3.x was applied for the fusion of CT/MRI and irradiation treatment plans. Overlay images were generated to determine the exact position of the suspected metastases in relation to the prior catheter location.

As a novel approach, we assessed both, extrahepatic and intrahepatic seeding. An example of an image fusion data set is provided in Figure 1.

Statistical analysis

We collected technical data of the irradiation plan and documented possible risk factors such as patient demographics, histological grading, and imaging features.

The statistical analysis of the data was conducted by using the statistical software SPSS® and SAS®. Differences between variables were examined using Student's *t*-test for metric variables and Chi-Square test for frequencies. The survival analysis was performed according to Kaplan-Meier method, the statistical significance was determined using log-rank test. The influence of potential risk factors on the occurrence of needle track metastases was calculated using a generalized linear mixed model. All tests were performed two-sided, a *p*-value of $p \leq 0.05$ was considered statistically significant.

Results

Patient and treatment characteristics

In our cohort of 100 patients, a total of 233 HCC lesions were treated. In 62 patients, histological reports were available with 38.7% ($n = 24$) being well differentiated, 54.8% ($n = 34$) being moderately differentiated, and 6.5% ($n = 4$) being poorly differentiated tumors. Pseudo-capsular HCC were present in 18 out of 233 lesions (7.7%). 22 patients (22%) received concomitant therapy with sorafenib.

In all patients, thermal ablation was technically not favorable related to either tumor size (exceeding 3 cm) or tumor location (proximity to liver hilum or adjacent gastrointestinal structures) of at least one lesion.

The median follow-up was 15.7 months (range, 6-70.2 months). Within the observation period, 67 patients developed a tumor progression with a median progression-free survival of 7.0 months. Median overall survival of all patients was 20.0 months. A summary of patient and treatment characteristics is presented in Table 1.

Catheter-based analysis

A total number of 588 catheters were placed within 100 patients. The mean insertion length of a single catheter was 12.7 ± 31.2 cm (range, 5.7-25.4 cm). Four catheters were too remote in relation to the target lesion and were not used for irradiation (0.7%). However, these lesions were treated in the same session with more precisely placed catheters. A total of nine needle track metastases were identified yielding an incidence of 1.5% per catheter placement. Seven out of nine seeding metastases were located within the liver (catheter-based risk for intrahepatic seeding, 1.2%). Two metastases occurred within the peritoneal cavity in the location of a former catheter path (catheter-based risk for extrahepatic seeding, 0.3%).

Lesion-based analysis

A total of 233 HCC lesions were treated. The mean diameter of HCC nodule was 3.3 ± 2.6 cm (range, 1.0-16.6 cm) requiring a mean number of 2.6 catheters per lesion to ensure a sufficient dose application. The mean applied radiation dose at the tumor rim was 16.5 ± 11.6 Gy. The mean sum of in-body catheter length per lesion was 32.1 ± 37.4 cm (range, 5.9-247.0 cm). Over-penetration of HCC nodule was found in 53 cases (9.0%), with a mean over-penetration length of 1.2 cm (range, 0.1-2.8 cm). The cumulative frequency of needle track metastases per treated tumor was 3.9% (intrahepatic location, 3.0%; extrahepatic location, 0.9%).

Patients-based analysis

In our cohort of 100 patients, an average number of 5.9 catheters were placed per patient leading to a mean total in-body catheter length of 74.8 ± 57.3 cm (range, 8.6-288.8 cm). Imaging analysis revealed needle track metastases in 9 patients. The mean time of occurrence of needle track seeding was 5.5 months (range, 4.8-6.2 months).

Risk assessment

Needle track seeding occurred in a median time interval of 5.5 months (range, 4.8-6.2 months). No increased risk was found for the tumor grading, age, and sex.

In a catheter-based analysis, we found more frequent seeding in smaller HCC lesions ($p = 0.09$). Liver cirrhosis and underlying etiology had no significant influence on the development of needle track seeding; the same was seen for pseudo-capsular HCC. Treatment-related parameters such as catheter insertion lengths, over-penetration of the lesion (i.e., with the possibility of dislocating tumor cells beyond the lesions into the liver parenchyma), and applied dose as well as concomitant treatment with sorafenib, demonstrated no significant influence.

Of note, 8 out of 9 seeding metastases were successfully treated by further HDR-BT directly after their occurrence. In one case, needle track metastasis occurred parallel to systemic progression at other sites and needed systemic therapy with sorafenib.

Median overall survival was 25.0 months in patients with needle track vs. 20.0 months in patients without ($p = 0.86$, log-rank test). The overall results of the risk factor analysis are included in Table 1.

Discussion

We were able to calculate the risk for tumor seeding after local ablation of HCC by catheter-based radiotherapy for both intrahepatic and extrahepatic locations, with an analysis of catheter-, lesion-, and patient adjusted frequencies. No track irradiation had been used in these patients.

Needle track seeding in local ablation

Needle track seeding in HCC is known to occur after diagnostic biopsies and local ablative procedures such as radiofrequency or microwave ablation. Stigliano *et al*. reported a meta-analysis of diagnostic and therapeutic interventions in 2007, with an overall frequency of 1.27% after liver biopsy and/or local ablation with extrahepatic needle track metastases [11].

Initial reports of seeding in up to 12.5% of patients after RFA illustrated the demand of track ablation tech-

niques [18]. Similarly, recent reports after RFA and MWA using track ablation depict low seeding rate of 0.61% to 1.6% [13,19]. However, all these studies have focused on extrahepatic seeding only; intrahepatic seeding was not evaluated to differentiate tumors seeding from *de novo* HCC due to technical limitations.

Our recent study identified a cumulative (extrahepatic and intrahepatic) catheter-based risk for seeding of 1.5% (without track ablation technique), which is comparable to reported seeding risk after thermal ablation using track ablation or even lower, considering that literature focusses on extrahepatic seeding only.

Due to the need of multiple catheters in larger HCC lesions (mean lesion diameter in our cohort: 3.3 ± 2.6 cm; range, 1.0-16.6 cm), the cumulative lesion-based seeding risk is as high as 3.9%. Theoretically, the seeding risk is still comparable to thermal ablation techniques, considering the need for multiple probes/multiple positions and in RFA or MWA ablation for the treatment of larger tumors.

Extrahepatic seeding

As stated above, our data indicates that the risk for extrahepatic seeding (0.2% per catheter) after HDR brachytherapy is comparable or even lower than after thermal-based ablative techniques (0.61-1.6%). Furthermore, our data supports findings previously published by Denecke *et al*. who utilized HDR brachytherapy in the pre-transplant setting and found no extrahepatic recurrence due to seeding in their smaller group of patients undergoing subsequent liver transplantation [9]. In fact, only a minority of seeding metastases occurred outside the liver in our cohort (0.2% per catheter). Assuming a tumor size and tumor number within transplant criteria for HCC, the lesion-based and patient-based risk should be equal or only slightly increased in those patients as compared to the catheter-based risk supporting the findings of Denecke *et al*. Both, the work of Denecke *et al*. and our results support the use of HDR brachytherapy as bridging for transplant, at least in tumors with an unfavorable location for RFA or TACE.

In case of larger or multilocular HCC outside transplant criteria, multiple catheter placements in HDR brachytherapy are usually necessary, resulting in a higher seeding rate (e.g., 0.9% in lesion-based analysis). Theoretically, several needle positions would have been required for a complex thermal ablation in those patients. Thus, the cumulative risk (i.e., lesion- and catheter-based risk) for track seeding seen in our study can be assumed to be comparable to a cumulative risk resulting from multiple ablation positions in RFA/MWA [11,20,21].

Intrahepatic seeding

Unfortunately, many studies still neglect the possibility of intrahepatic seeding, probably as the differentiation between intrahepatic seeding metastases and tumor progression is difficult [12]. We applied a novel approach of image fusion for the identification of intrahepatic seeding, leading to the confident identification of lesions, which most likely derive from track seeding. All these lesions are omitted by the extrahepatic definition of seeding in most studies. In fact, intrahepatic needle track metastases were more frequent as compared to extrahepatic needle track metastases with a catheter-based risk of 1.3%. This is easily explainable, since the penetration depth within the liver parenchyma is usually longer than the thickness of the abdominal wall.

The higher rate of intrahepatic seeding as compared to extrahepatic seeding in our analysis, along with the focus on extrahepatic-only seedings in literature, suggests that seeding (intrahepatic plus extrahepatic) after thermal ablation or biopsy might be more frequent, but data to further elucidate that matter is not available. However, this might pose a clinical impact for treatment decision making and should be a subject for further investigation. Furthermore, techniques to decrease the seeding rate after HDR brachytherapy were not applied in the study population. As a consequence of our analysis, we established a procedure similar to needle track ablation by radiation of the path of the catheter during the withdrawal of the Iridium 192 source, with a mean dose of 10 Gy in up to 2-3 mm depth. Taking RFA and MWA as an example, the introduction of track ablation techniques resulted in drastically lower rate of (extrahepatic) seeding (from 12.5% to 0.61-1.6%; see above), indicating a significant influence of track ablations techniques to control tumor seeding in local ablations of HCC. We believe that this applies also to HDR brachytherapy.

Beside this assumed influencing factor on track seeding, none of the evaluated variables within the study revealed a significant influence on the rate of track seeding on a catheter-, lesion-, and patient-based analysis, as these were in particular sex, age, etiology of liver disease, grading of the HCC, evidence of a tumor pseudo-capsular, size of the targeted lesion, in situ catheter length, over-penetration of the targeted lesion, ablation dose, and concomitant systemic treatment. Only the size of targeted lesion showed a tendency to significantly influence track seeding (in the patient-based analysis, $p = 0.09$), with a higher rate of track seeding in smaller lesions. It can be hypothesized that more manipulations (i.e., needle passes to enable a sufficient catheter placement) are needed in smaller lesions. Quantitative or semi-quantitative information on needle manipulations during the intervention were not available in this study making further clarification of this hypothesis impossible. However, since this finding was only evident on a patient-based analysis but not on a lesion- or catheter-based analysis, stochastic effects are the most probable cause.

Limitations

The limitations of this analysis are those inherent to a retrospective analysis. Although study format was retrospective, the data (clinical data, treatment-related data) were obtained from a prospectively managed database, in which all patients who undergo a local or loco-regional treatment at our department are electronically filed using standardized reporting forms for treatment and follow-up visits. Additionally, treated patient undergo

a standardized follow-up including imaging (at our institution) every three months, which diminishes a possible bias derived from inconsistent image follow-up intervals and inconsistent imaging protocols. However, a patient selection bias cannot be ruled out.

As pointed out in the section above, we were not able to evaluate systematically the incidence of needle manipulations during the interventions, which could have an influence on the risk of track seeding, since the number of possible tumors passes increases. However, misplacements of the needle during the intervention usually occur outside the tumor (i.e., in the liver parenchyma without risk for seeding), a believed position within the tumor (although position might not be perfect for treatment) entail the exchange to the brachytherapy catheter by standard operating procedure in order to prevent seeding. Thus, we believe that the possible influence of needle manipulations during the interventions is too small to neglect.

Finally, the differentiation between iatrogenic track seeding and de novo HCC is still a challenge that might influence the analysis. Since all possible track seeding metastases were verified in their origin by precise image registration of the follow-up imaging with the final imaging after placement of the brachytherapy catheters, we can rule out an underestimation of the frequency of treatment-associated track seeding. Only a risk for an overestimation of the frequency of new metastases related to the previously performed local ablation is possible but is regarded as acceptable from a clinical and scientific perspective.

Conclusions

The technique of percutaneous catheter placement for HDR brachytherapy in HCC is generally not associated with an elevated risk of needle track metastases as compared to biopsy or RFA/MWA, especially in extrahepatic seeding. In fact, data indicates a lower risk for track metastases after HDR brachytherapy as compared to biopsy and thermal-based ablation techniques, although HDR brachytherapy was conducted without a track ablation technique in this study.

To further reduce the risk of seeding along the catheter path, track irradiation in HDR brachytherapy should be implemented in daily practice.

Disclosure

Authors report no conflict of interest.

References

1. Schütte K, Kipper M, Kahl S et al. Clinical characteristics and time trends in etiology of hepatocellular cancer in Germany. *Digestion* 2013; 87: 147-159.
2. Han K, Kim JH. Transarterial chemoembolization in hepatocellular carcinoma treatment: Barcelona clinic liver cancer staging system. *World J Gastroenter* 2015; 21: 10327-10335.
3. Feng K, Ma KS. Value of radiofrequency ablation in the treatment of hepatocellular. *World J Gastroenterol* 2014; 20: 5987-5998.
4. Tanaka M, Ando E, Simose S et al. Radiofrequency ablation combined with transarterial chemoembolization for intermediate hepatocellular carcinoma. *Hepatol Res* 2014; 44: 194-200.
5. Terzi E, Piscaglia F, Forlani L et al. TACE performed in patients with a single nodule of hepatocellular carcinoma. *BMC Cancer* 2014; 14: 601.
6. Yang W, Yan K, Wu GX et al. Radiofrequency ablation of hepatocellular carcinoma in difficult locations: Strategies and long-term outcomes. *World J Gastroenterol* 2015; 21: 1554-1566.
7. Mohnike K, Wieners G, Schwartz F et al. Computed tomography-guided high-dose-rate brachytherapy in hepatocellular carcinoma: safety, efficacy, and effect on survival. *Int J Radiat Oncol Biol Phys* 2010; 78: 172-179.
8. Collettini F, Singh A, Schnapauff D et al. Computed-tomography-guided high-dose-rate brachytherapy (CT-HDRBT) ablation of metastases adjacent to the liver hilum. *Eur J Radiol* 2013; 82: e509-514.
9. Denecke T, Stelter L, Schnapauff D et al. CT-guided Interstitial Brachytherapy of Hepatocellular Carcinoma before Liver Transplantation: An Equivalent Alternative to Transarterial Chemoembolization? *Eur Radiol* 2015; 25: 2608-2616.
10. Cabibbo G, Craxi A. Needle track seeding following percutaneous procedures for hepatocellular carcinoma. *World J Hepatol* 2009; 1: 62-66.
11. Stigliano R, Marelli L, Yu D et al. Seeding following percutaneous diagnostic and therapeutic approaches for hepatocellular carcinoma. What is the risk and the outcome? Seeding risk for percutaneous approach of HCC. *Cancer Treat Rev* 2007; 33: 437-447.
12. Francica G. Needle track seeding after radiofrequency ablation for hepatocellular carcinoma: prevalence, impact, and management challenge. *J Hepatocell Carcinoma* 2017; 4: 23-27.
13. Yu J, Liang P, Yu XL et al. Needle track seeding after percutaneous microwave ablation of malignant liver tumors under ultrasound guidance: analysis of 14-year experience with 1,462 patients at a single center. *Eur J Radiol* 2012; 81: 2495-2499.
14. Collettini F, Schnapauff D, Poellinger A et al. Hepatocellular carcinoma: computed-tomography-guided high-dose-rate brachytherapy (CT-HDRBT) ablation of large (5-7 cm) and very large (> 7 cm) tumours. *Eur Radiol* 2012; 22: 1101-1109.
15. Bruix J, Sherman M, Llovet JM et al. Clinical management of hepatocellular carcinoma. Conclusions of the Barcelona-2000 EASL conference. European Association for the Study of the Liver. *J Hepatol* 2001; 35: 421-430.
16. European Association for The Study Of The L, European Organization For R, Treatment Of C. EASL-EORTC clinical practice guidelines: management of hepatocellular carcinoma. *J Hepatol* 2012; 56: 908-943.
17. Ricke J, Wust P. Computed tomography-guided brachytherapy for liver cancer. *Semin Radiat Oncol* 2011; 21: 287-293.
18. Llovet JM, Vilana R, Bru C et al. Increased risk of tumor seeding after percutaneous radiofrequency ablation for single hepatocellular carcinoma. *Hepatology* 2001; 33: 1124-1129.
19. Zhong-Yi Z, Wei Y, Kun Y et al. Needle track seeding after percutaneous radiofrequency ablation of hepatocellular carcinoma: 14-year experience at a single center. *Int J Hyperthermia* 2017; 33: 1-20.
20. Shirai K, Tamai H, Shingaki N et al. Clinical features and risk factors of extrahepatic seeding after percutaneous radiofrequency ablation for hepatocellular carcinoma. *Hepatol Res* 2011; 41: 738-745.
21. Silva MA, Hegab B, Hyde C et al. Needle track seeding following biopsy of liver lesions in the diagnosis of hepatocellular cancer: a systematic review and meta-analysis. *Gut* 2008; 57: 1592-1596.

Seidensticker et al. BMC Cancer (2015) 15:517
DOI 10.1186/s12885-015-1499-z

BMC Cancer

RESEARCH ARTICLE Open Access

Locally ablative treatment of breast cancer liver metastases: identification of factors influencing survival (the Mammary Cancer Microtherapy and Interventional Approaches (MAMMA MIA) study)

Max Seidensticker[1,2*†], Benjamin Garlipp[3†], Sophia Scholz[1], Konrad Mohnike[1,2], Felix Popp[3], Ingo Steffen[1], Ricarda Seidensticker[1,2], Patrick Stübs[3], Maciej Pech[1,2,4], Maciej Powerskl[1], Peter Hass[5], Serban-Dan Costa[6], Holger Amthauer[1,2], Christiane Bruns[2,3] and Jens Ricke[1,2]

Abstract

Background: Liver metastases from breast cancer (LMBC) are typically considered to indicate systemic disease spread and patients are most often offered systemic palliative treatment only. However, retrospective studies suggest that some patients may have improved survival with local treatment of their liver metastases compared to systemic therapy alone. In the absence of randomized trials, it is important to identify patient characteristics indicating that benefit from local treatment can be expected.

Methods: 59 patients undergoing radiofrequency ablation (RFA), interstitial brachytherapy (BT), or radioembolization (RE) of LMBC as a salvage treatment were studied. Potential factors influencing survival were analyzed in a multivariate Cox model. For factors identified to have an independent survival impact, Kaplan-Meier analysis and comparison of overall survival (OS) using the log-rank test was performed.

Results: Median OS following local interventional treatment was 21.9 months. Considering only factors evaluable at treatment initiation, maximum diameter of liver metastases (≥3.9 cm; HR: 3.1), liver volume (≥ 1376 mL; HR: 2.3), and history of prior chemotherapy (≥ 3 lines of treatment; HR: 2.5-2.6) showed an independent survival impact. When follow-up data were included in the analysis, significant factors were maximum diameter of liver metastases (≥ 3.9 cm; HR: 3.1), control of LMBC during follow-up (HR: 0.29), and objective response as best overall response (HR: 0.21). Neither the presence of any extrahepatic metastases nor presence of bone metastases only had a significant survival impact. Median OS was 38.7 vs. 16.1 months in patients with metastases < vs. ≥ 3.9 cm, 36.6 vs. 10.2 months for patients having objective response vs. stable/progressive disease, and 38.5 vs. 14.2 months for patients having controlled vs. non-controlled disease at follow-up.

(Continued on next page)

* Correspondence: max.seidensticker@med.ovgu.de
†Equal contributors
[1]Klinik für Radiologie und Nuklearmedizin, Universitätsklinik Magdeburg, Leipziger Strasse 44, 39120 Magdeburg, Germany
[2]International School of Image-Guided Interventions, Deutsche Akademie für Mikrotherapie, Magdeburg, Germany
Full list of author information is available at the end of the article

(Continued from previous page)

Conclusion: Local control of LMBC confers a survival benefit and local interventional treatment for LMBC should be studied in a randomized trial. Patients with small metastases and limited history of systemic LMBC treatment are most likely to benefit from local approaches. Limited extrahepatic disease should not lead to exclusion from a randomized study and should not be a contraindication for local LMBC treatment as long as no randomized data are available.

Keywords: Liver metastases, Breast cancer, Oligometastases, Locally ablative therapy, Liver surgery

Background

In the last two decades, the notion that formation of metastases of any malignant tumor indicates systemic spread of the disease and precludes benefit from local tumor treatment has been challenged by the observation that some patients remain disease-free after removal of their primary tumor and all visible metastatic lesions, indicating cure. As a result, surgical or locally ablative treatment of metastatic lesions is now an accepted, potentially curative modality in a variety of cancers for patients with limited metastatic burden (e.g., colorectal, renal cell, and non small-cell lung cancer) and has been integrated into treatment guidelines [1–3]. More recently, however, the distinction between "curable" and "non-curable" cancer has become less clear as some patients may continuously demonstrate controllable disease for many years and eventually die from causes unrelated to their cancer. The propensity of a cancer to develop rapid dissemination has been referred to as the disease's biology; however, it is likely that a complex pattern of interaction between the tumor cells and the host organism rather than specific properties of the tumor alone determine the metastatic potential [4]. These observations have led to the concept of a distinct "oligometastatic" disease state which incorporates patients who may derive benefit from local treatment (even repeatedly) despite the impossibility to achieve true cure [5, 6].

It is unknown if an oligometastatic subpopulation exists among patients with metastatic breast cancer (MBC). Generally, MBC is regarded as a systemic disease and these patients, in line with current European and American treatment guidelines which essentially reserve locally ablative or surgical treatment to lesions that are symptomatic or prone to cause local complications [7, 8], are mostly offered palliative systemic treatment regardless of their metastatic burden. This is particularly true for liver metastases (LMBC) that typically occur late in the course of breast cancer and are uncommon in the absence of extrahepatic disease [9, 10]. Despite this, there are a number of retrospective, non-randomized reports demonstrating superior survival in patients undergoing liver resection for LMBC [11–15] compared to patients receiving systemic treatment alone, with surgically treated patients achieving median survival of up to 5 years and 5 year overall survival of up to 60 %, whereas median survival in MBC patients treated with systemic therapy only is approximately 24 months and only 5-10 % are alive at 5 years [16, 17]. Survival figures reported for patients treated with locally ablative modalities (radiofrequency ablation (RFA) or interstitial CT-guided brachytherapy (BT)) are generally lower, probably in part owing to a selection bias. However, they still compare favorably to systemic treatment alone, demonstrating some benefit from local control of liver metastases in a disease that is assumed to be systemic by nature [18–22]. This is further complemented by the observation that, in chemorefractory patients not amenable to surgical or locally ablative treatment, encouraging survival was observed with locoregional intrahepatic therapies (^{90}Y radioembolization (RE) or intrahepatic chemotherapy) [23, 24].

As currently available data do not allow to determine if improved survival in patients undergoing locoregional therapy represents a true treatment benefit or must be regarded as an expression of favorable disease biology, with patients demonstrating relatively indolent disease preferably being selected for local treatment, it has repeatedly been suggested that these treatments be evaluated within a randomized trial comparing the combination of local and systemic therapy to systemic therapy alone. The exploratory data we present here is intended to help modelling such study concepts by identifying prognostic factors in a cohort of LMBC patients both with and without extrahepatic disease who were not amenable to radical surgery and received locally ablative (RFA or BT) or locoregional intrahepatic (RE) treatment either once or in combination as part of sequential treatment decisions.

Methods

Study design

This retrospective study explores prospectively collected data from patients with LMBC who were referred to our department for local interventional treatment of liver metastases between 2006 and 2010. The local ethics committee (Ethik-Kommission der Otto-von-Guericke-Universität in Magdeburg) was informed about the analyses, an approval was waived due to the retrospective nature of the study. Written informed consent for anonymized analysis of disease- and treatment-related

patient data for scientific purposes was obtained from all patients.

Patients undergoing either radiofrequency ablation (RFA), interstitial catheter-based radiotherapy (BT), or ^{90}Y Radioembolization (RE) for LMBC were included if: (i) imaging follow-up was available (computed tomography (CT) or magnetic resonance imaging (MRI), every 2-4 months), (ii) clinical follow-up data (including laboratory analyses) were available (every 2-4 months), (iii) a written informed consent for anonymized patient data analysis was available, (iv) no other active cancer was known.

Patient characteristics

59 patients (58 female, 1 male, mean age 57.4 years, range 32-80) were included in this analysis. Selection of patients for local interventional treatment was based on lack of further chemotherapeutic options (progression of LMBC on all standard chemotherapeutic protocols or patient refusal of further chemotherapy) as well as surgical non-resectability of all visible lesions (either technically or due to impaired patient tolerance for major liver surgery). Patients had to have liver-predominant disease; however, limited extrahepatic disease that was stable under systemic treatment or amenable to local ablation was allowed.

The median interval from diagnosis of LMBC to presentation for interventional treatment was 22 (1-294) months.

Tumors were hormone-receptor positive in 49 of 59 patients and Her2-neu positive in 20 of 59 patients.

Differentiation of liver metastases was graded as G1 (4 patients), G2 (26 patients), or G3 (21 patients). For 8 patients no information on tumor differentiation was available.

At presentation for interventional treatment of LMBC, the mean intrahepatic tumor load (mean cumulative volume of all liver metastases relative to total liver volume) was 8.2 % (range 0.1–51.4). Mean number of liver metastases was 13 (range 1-88). The diameter of the largest liver lesion ranged from 1-14 cm (mean 4.9 cm). The mean cumulative volume of the liver metastases was 129.6 mL (range 0.5-976), and mean total liver volume was 1445 mL (range 801-2202).

54 of 59 patients had a history of 1-8 (median 2) lines of systemic chemotherapy (without hormones) for their breast cancer prior to presentation for interventional treatment of LMBC. Bisphosphonates had been applied in 24 patients. Surgery and external beam radiation for breast cancer metastases had been performed in 19 and 20 patients, respectively.

29 of 59 patients had evidence of limited extrahepatic disease at the time of interventional LMBC treatment (bone metastases only, 19/59 patients; extrahepatic disease other than bone metastases, 5/59 patients; extrahepatic disease other than bone metastases and bone metastases, 5/59 patients).

Patient and treatment characteristics are summarized in Tables 1 and 2.

Table 1 Baseline Characteristics (59 patients)

Sex (f/m)		58/1
Mean age (y, range)		57.4 (32 - 80)
Age ≤ 60y		63 % ($n = 37$)
Hormone receptor positive		83 % ($n = 49$)
Her2 neu positive (triple)		34 % ($n = 20$)
Grading (1/2/3/ not available)		7 % ($n = 4$)/ 44 % ($n = 26$)/36 % ($n = 21$)/13 % ($n = 8$)
Median time from first BC diagnosis to diagnosis of liver metastases (mo, range)		45 (0 – 335.4)
Median time from diagnosis of liver metastases to first interventional treatment (mo, range)		22 (1 - 294)
Mean number of liver metastases (n, range)		13 (1 - 88)
Mean maximum diameter of liver metastases (cm, range)		4.9 (1 - 14)
Mean liver volume (mL, range)		1445 (801 - 2202)
Mean volume of liver metastases (mL, range)		129.6 (0.5 - 976)
Mean tumor load (%, range)		8.2 (0.1 - 51.4)
Extrahepatic metastases		49 % ($n = 29$)
	Bone only	$n = 19$
	Bone	$n = 24$
	Lung	$n = 6$
	Lymphatic nodes (others than axillary)	$n = 4$
	Peritoneum	$n = 1$

Table 2 Treatment characteristics (59 patients)

Chemotherapy prior to interventional LMBC treatment (without hormones)		92 % ($n = 54$)
	median number of applied lines (range)	2 (0 - 8)
Local treatment of breast cancer metastases prior to interventional LMBC treatment, overall		68 % ($n = 40$)
	surgery (for metastasis)[a]	$n = 19$
	radiotherapy[a]	$n = 20$
Bisphophonates prior to interventional LMBC treatment		$n = 24$
Concomitant or subsequent breast cancer therapy (after initiation of interventional LMBC treatment), overall		86 % ($n = 51$)
	chemotherapy[a]	$n = 40$
	hormones[a]	$n = 22$
	surgery[a]	$n = 7$
	radiotherapy[a]	$n = 14$
Total number of interventional procedures for LMBC[a]		$n = 97$
	interstitial brachytherapy (BT)	$n = 68$
	radioembolization (RE)	$n = 34$
	radiofrequency ablation (RFA)	$n = 5$
Number of interventional procedures per patient (1/2/3/4/5/6/7) (n)		(37/13/5/0/2/1/1)
First treatment per patient (BT/RE/RFA/combination) (n)		(29/22/3/5)
Treatment modalities per patient (first and all subsequent procedures)		
	RE only	$n = 17$
	BT only	$n = 25$
	RFA only	$n = 1$
	BT and RE	$n = 12$
	BT and RFA	$n = 3$
	RE and RFA	$n = 1$

[a]more than one treatment/site per patient possible

Locally ablative therapies

In general, BT or RFA was performed in case of no more than five hepatic metastases. RFA was preferred in patients with a maximum lesion diameter of 3 cm whereas BT was performed for lesions exceeding this limit and for lesions under 3 cm with an unfavorable location for RFA (i.e., close proximity to the liver hilum or other heat-vulnerable structures).

BT and RFA were performed under conscious sedation and analgesia using midazolam and fentanyl under continuous surveillance of vital parameters.

Image guided interstitial brachytherapy (BT)

The technique has been described previously [25]. Briefly, the placement of the introducer sheaths (6 F in size) with the brachytherapy applicators inside was performed under CT-fluoroscopy using Seldinger technique. For treatment planning purposes, a contrast enhanced CT of the liver was acquired. According to the defined course of the catheters, the clinical target volume and the predefined minimum dose at the tumor margin (15 Gy, delivered as a single fraction), the planning software (Oncentra, Nucletron, Veenendaal, The Netherlands) calculated a dosimetry and the dwell of the Iridium-192 source inside the brachytherapy catheters, respectively. The high-dose-rate afterloading system (Microselectron, Nucletron, Veenendaal, The Netherlands) employed an Iridium-192 source with a nominal activity of 10 Ci..

Radiofrequency ablation (RFA)

All RFA procedures were performed using multitined expandable electrodes (RITA Starburst; Angiodynamics, Latham, USA) that were placed under CT or MR fluoroscopy guidance. The RFA procedure was conducted according to the manufacturer's recommendations. To control the achieved coagulation zone instantaneously after completing the procedure, a postprocedural contrast-enhanced CT scan (or a fat saturated T2-weighted spinecho sequence in case of conduction under MRI guidance) with the electrode still in place was performed.

If needed, the electrode was repositioned to achieve a volume large enough to cover the entire metastasis including a safety margin.

Locoregional treatment

Radioembolization (RE)

In general, RE was performed if the number of hepatic metastases exceeded five. RE was performed employing Yttrium-90 resin microspheres (SIR-Spheres®, Sirtex Medical, Lane Cove, Australia). Treatment including pre-procedural diagnostic work-up was performed according to standard algorithm (detailed description in [26]). The activity of ^{90}Y resin microspheres was calculated by the body surface area (BSA) method. ^{90}Y resin microspheres were delivered selectively into the hepatic arteries (using a transfemoral approach) sequentially with an interval of 4-6 weeks between the treatments of each liver lobe (if a bilobar treatment was necessary). All patients received proton pump inhibitors (pantoprazole, 20 mg daily), low dose prednisolone (5 mg daily), and ursodeoxycholic acid (500 mg daily) for 8 weeks to ameliorate the effect of possibly migrated spheres in the gastric mucosa and the embolization effect to the liver parenchyma.

Treatments and combinations

Interventional LMBC treatment

The following interventional procedures were performed: BT only (29 patients), RFA only (3 patients), RE only (22 patients). 5 Patients had localized disease in one liver lobe accompanied by multilocular metastases in the contralateral lobe and were treated with both unilateral RE and RFA or BT of the solitary contralateral lesions. 22 patients were re-treated for progressive disease following the first interventional procedure (see Table 2).

Further treatment

Forty patients received subsequent chemotherapy and 22 patients received hormonal therapy following interventional LMBC treatment. Surgery and external beam radiotherapy for localized extrahepatic disease were performed in 7 and 14 patients, respectively. For detailed information see Table 2.

Imaging, volumetry and response analysis

For all patients a baseline Gd-EOB-DTPA (Primovist, Bayer Healthcare, Leverkusen, Germany, 0.025 mmol/kg/bodyweight) enhanced MRI of the liver was available. Baseline MRI (hepatobiliary phase T1- weighted imaging, 5 mm slice thickness) was used for volumetry of the liver and tumor volume as well as for measurement of the tumor diameters using the image processing software Osirix (Antoine Rosset, 2003-2011).

Follow-up imaging consisted of either MRI of the liver or CT of the abdomen (with or without thorax) every 2-4 months. MRI (1.5 Tesla system, Achieva 1.5 T, Philips, Best, The Netherlands) of the liver was conducted using Gd-EOB-DTPA as i.v. contrast agent. For response analysis hepatobiliary phase imaging (T1-weighted imaging, 5 mm slice thickness) was used. In case of inconclusiveness, other sequences (contrast dynamic, T2-weighted imaging) were taken into account. CT (multislice CT, either 16 (Toshiba Aquilion, Toshiba Medical, Tokyo, Japan) or 64 (Siemens Definition AS, Erlangen, Germany) row detector system) was conducted using 90 mL iodinated contrast media (Imeron 300, Iomeprol, Bracco, Princeton, USA) with a reconstructed slice thickness of 5 mm. For response analysis, venous phase imaging was used.

Response analysis according to RECIST 1.0 was performed separately for the liver only and overall. Analyses of response to treatment are based on best response recorded during follow-up.

As an additional efficacy descriptor beyond RECIST, control of LMBC by interventional treatment during follow-up was used, with patients demonstrating either overall objective response, stable disease, or limited disease progression amenable to repeat local ablation being regarded as having controlled disease. Disease progression not amenable to local intervention was defined as non-controlled.

Toxicity analysis

All patients underwent standard clinical and laboratory examination including liver-related parameters at first presentation and during follow up after interventional treatment. The Common Terminology Criteria for Adverse Events (CTCAE) version 4.02 (National Cancer Institute, USA) were used for toxicity assessments of laboratory values and clinical findings.

Statistics

Statistical analysis was performed using SPSS (SPSS 21, IBM, Chicago, Il, USA). Descriptive analysis of patient characteristics and findings was performed with continuous variables displayed as mean or median with standard deviation or range and frequency data displayed as counts.

Survival (from first diagnosis, first diagnosis of liver metastases, first interventional treatment of LMBC) was estimated according to the Kaplan-Meier method.

Possible factors influencing survival were included in a univariate Cox model. Continuous variables were dichotomized according to a ROC analysis using survival (longer vs. shorter than median overall survival) as the target variable. Optimal cut-off was determined according to the Youden index (see Additional file 1: Table S1).

Interactions of variables found to have significant influence on survival in the univariate analysis were evaluated by the Chi-square test/Fisher's exact test (see Additional file 2: Table S2). In case of interactions,

either the variable with the lower p-value in the univariate Cox model or the more practicable variable was chosen. To test the independent impact of each confounder identified at univariate analysis on survival, multivariate Cox models were created including all variables that were unevenly distributed between the groups of patients with shorter vs. longer than median survival and did not show significant interaction. This analysis was first performed excluding parameters that were not available prior to treatment and then repeated using all parameters (including those available at follow-up only). Additionally, due to interaction of these variables, separate models were created to analyze the survival impact of either overall extrahepatic disease or bone metastases as the sole extrahepatic tumor manifestation.

Factors found to have an independent impact on survival in the multivariate model were used as stratifying variables in a Kaplan-Meier analysis of survival after first interventional LMBC treatment. The log rank test was used for survival comparison.

A $p < 0.05$ was considered statistically significant.

Results

Median overall survival from first interventional treatment of LMBC was 21.9 months (95 % CI: 11.1-32.6), from first diagnosis of liver metastases, 56.3 months (44.5-67.9), and from first diagnosis of breast cancer, 127.9 months (87.1-168.7) (Table 3).

The ROC analysis used to dichotomize continuous variables with respect to median overall survival yielded the following significant results: number of liver metastases (optimal cut-off: </≥ 6 lesions), maximum diameter of liver metastases (</≥ 3.9 cm), volume of liver metastases (</≥ 27.9 mL), intrahepatic tumor load (</≥ 2 %), liver volume (</≥ 1376 mL), number of previous lines of chemotherapy (</≥ 3), CA 15-3 (</≥ 62.6U/mL), and CEA (</≥ 6.2U/mL) (see Additional file 1: Table S1). Dichotomized variables were used for further analyses. Although the ROC analysis was unable to dichotomize time from first breast cancer diagnosis to diagnosis of liver metastases, this variable was still considered a possible influencing factor for further analyses with a cut-off based on data reported in the literature (<2 years vs. ≥ 2 years; [27]).

Univariate Cox regression regarding overall survival from first interventional LMBC treatment of the LMBC yielded type of initial local treatment (BT/RFA vs. RE), presence of extrahepatic metastases, presence of bone metastases only, number of liver metastases, maximum diameter of liver metastases, volume of liver metastases, tumor load, liver volume, number of lines of chemotherapy applied prior to interventional LMBC treatment, CA 15-3, CEA, best response during follow-up (overall), best response during follow-up (liver only), and control of LMBC by interventional treatment during follow-up (according to the definition given in the methods section) as factors with a significant survival impact (Table 4). These variables were then tested for inter-variable interaction (see Additional file 2: Table S2) and the following non-interacting variables were extracted for inclusion into the multivariate Cox models: presence of extrahepatic metastases (and presence of bone metastases only, separate model), liver volume, maximum diameter of liver metastases, number of liver metastases, number of lines of chemotherapy applied prior to interventional LMBC treatment, control of LMBC by interventional treatment during follow-up, and best overall response to interventional treatment during follow-up. When only factors available at treatment initiation were included in the analysis, only maximum diameter of liver metastases (≥ 3.9 cm; HR: 3.1), liver volume (≥ 1376 mL; HR: 2.3), and history of prior chemotherapy (≥ 3 lines of treatment; HR: 2.5-2.6) showed a significant impact on

Table 3 Survival and Progression[a]

	months (median)		95 % CI		*p*-value
Follow-up	16.14				
Overall survival					
from first diagnosis	127.9		87.1- 168.7		
from first diagnosis liver metastases	56.3		44.5 - 67.9		
from first interventional treatment	21.9		11.1 - 32.6		
Maximum diameter of liver metastases (≥ vs. < 3.9 cm)	16.1	38.7	9.8 - 22.5	19.6 - 57.8	0.001
Best response overall (OR, RECIST)					
OR (CR + PR) ($n = 37$) vs. PD + SD ($n = 22$)	36.6	10.2	26.4 - 46.7	6.1 - 14.3	< 0.001
Disease controlled during follow-up (yes/no)[b]	38.5	14.2	27.1 - 39.7	9.4 - 18.9	0.002

Survival (from first diagnosis, first diagnosis of liver metastases, first interventional treatment of LMBC) estimated according to the Kaplan-Meier method. Factors found to have an independent impact on survival in the multivariate model (Table 5) were used as stratifying variables in a Kaplan-Meier analysis of survival after first interventional LMBC treatment. The log rank test was used for survival comparison

[a]Addressing overall survival data and significant influencing factors from multivariate cox regression

[b]Patients demonstrating either overall objective response, stable disease, or limited disease progression amenable to repeat local ablation were regarded as having controlled disease. Disease progression not amenable to local intervention was defined as non-controlled

Table 4 Univariate Cox Regression for Survival

Variable		Hazard ratio	95 % CI	*p*-value
Age		0.99	0.97 - 1.03	0.836
Age (>60y)		0.51	0.24 - 1.11	0.089
Hepatic progression in FU (yes)		0.8	0.37 - 1.73	0.566
Systemic progression in FU (yes)		1.57	0.78 - 3.17	0.209
Under local control in FU (yes)		0.31	0.14 - 0.68	0.004
Her2 neu (pos)		1.22	0.59 - 2.53	0.588
Hormone receptor (pos)		0.96	0.41 - 2.24	0.926
Grading (1-3)		0.93	0.5 - 1.73	0.826
Other prior therapies for metastastes (yes)		1.99	0.89 - 4.43	0.094
Extrahepatic metastases (yes)		2.86	1.39 - 5.87	0.004
	bones only	3.01	1.49 - 6.08	0.002
First local treatment				
	Brachytherapy (BT) or RFA	0.28	0.13 - 0.59	0.001
	Radioembolization (RE)	3.31	1.57 - 6.98	0.002
	Combination RE/BT or RE/RFA	1.14	0.40 - 3.26	0.813
Best response hepatic (OR, RECIST)		0.37	0.17 - 0.79	0.01
Best response overall (OR, RECIST)		0.15	0.07 - 0.34	< 0.001
Clinical and laboratory grade 3/4 toxicities (yes)		1.83	0.78 - 4.31	0.168
Number of liver metastases (≥ 6)		2.08	1.01 - 4.31	0.048
Maximum diameter of liver metastases (≥ 3.9 cm)		3.43	1.57 - 7.52	0.002
Liver volume (≥ 1376 mL)		2.27	1.11 - 4.64	0.024
Volume of liver metastases (≥ 27.9 mL)		4.33	1.91 - 9.79	< 0.001
Tumor load (≥ 2 %)		5.6	2.37 - 13.23	< 0.001
Lines of chemotherapy (≥ 3)		3.17	1.55 - 6.49	0.002
CA 15-3 (≥ 62.6U/mL)		2.42	1.10 - 5.36	0.029
CEA (≥ 6.2U/mL)		3.36	1.58 - 7.15	0.002
Time from first diagnosis to liver metastases (≥ 2y)		0.79	0.40 - 1.56	0.492
Concomitant or subsequent therapies for breast cancer metastases (yes)		0.43	0.16 - 1.16	0.094

Possible factors influencing survival were included in a univariate Cox model. Continuous variables were dichotomized according to a ROC analysis (see Additional file 1: Table S1)

survival (Table 5a). Analyzing all potential factors including those available at follow-up only, only maximum diameter of liver metastases (≥ 3.9 cm; HR: 3.1), control of LMBC by interventional treatment during follow-up (HR: 0.29), and objective response as best overall response during follow-up (HR: 0.21) demonstrated a significant influence on survival (Table 5b). Neither the presence of any extrahepatic metastases nor presence of bone metastases only had a significant impact on survival in any of the models (Table 5a and b).

Overall survival estimates stratified for the maximum diameter of liver metastases (</≥ 3.9 cm) were 38.7 vs. 16.1 months ($p = 0.001$), for best overall response during follow-up (objective response vs. SD and PD), 36.6 vs. 10.2 months ($p < 0.001$), and for control of LMBC by interventional treatment during follow-up (yes vs. no), 38.5 vs. 14.2 months ($p = 0.002$) (Table 3).

After interventional treatment of LMBC, 9 grade 3 and no grade 4 toxicities were recorded. This included elevation of alanine aminotransferase (1 patient), elevation of alkaline phosphatase and reduction of albumin (1 patient), liver decompensation (defined as ascites unrelated to disease progression; 5 patients), and i.v. port infection (1 patient). All reported toxicities occurred after radioembolization. Patients developing any grade 3 toxicity following treatment had a tendency towards decreased survival (median survival, 8.2 vs. 14.2 months with vs. without toxicity in patients receiving RE at any time during their treatment sequence); however, this was not significant ($p = 0.234$).

Table 5 Multivariate Cox Regression for Survival

a. Multivariate Cox Regression for Survival, Factors available at treatment initiation only			
Variable set	Hazard ratio	95 % CI	p-value
Extrahepatic metastases (yes)	2.13	0.97 - 4.64	0.058
Liver volume (≥ 1376 mL)	2.25	1.01 - 5.02	0.047
Maximum diameter of liver metastases (≥ 3.9 cm)	3.12	1.39 - 7.02	0.006
Number of liver metastases (≥ 6)	1.48	0.69 - 3.14	0.312
Lines of chemotherapy (≥ 3)	2.48	1.15 - 5.36	0.021
Bone metastases only (yes)	1.56	0.70 - 3.47	0.279
Liver volume (≥ 1376 mL)	2.01	0.93 - 4.36	0.076
Maximum diameter of liver metastases (≥ 3.9 cm)	3.1	1.37 - 7.02	0.007
Number of liver metastases (≥ 6)	1.51	0.72 - 3.20	0.278
Lines of chemotherapy (≥ 3)	2.6	1.14 - 5.92	0.023
b. Multivariate Cox Regression for Survival, All Factors (Pre- and Posttherapeutic)			
Variable set	Hazard ratio	95 % CI	p-value
Extrahepatic metastases (yes)	1.05	0.43 - 2.58	0.92
Liver volume (≥ 1376 mL)	2.17	0.90 - 5.22	0.084
Maximum diameter of liver metastases (≥ 3.9 cm)	3.1	1.31 - 7.36	0.01
Number of liver metastases (≥ 6)	1.13	0.49 - 2.59	0.782
Lines of chemotherapy (≥ 3)	1.81	0.83 - 3.97	0.138
Under local control in FU (yes)	0.29	0.11 - 0.73	0.009
Best response overall (OR, RECIST)	0.21	0.08 - 0.57	0.002
Bone metastases only (yes)	1.06	0.46 - 2.44	0.89
Liver volume (≥ 1376 mL)	2.16	0.92 - 5.03	0.075
Maximum diameter of liver metastases (≥ 3.9 cm)	3.05	1.22 - 7.61	0.017
Number of liver metastases (≥ 6)	1.12	0.48 - 2.59	0.796
Lines of chemotherapy (≥ 3)	1.8	0.80 - 4.01	0.154
Under local control in FU (yes)	0.29	0.12 - 0.70	0.006
Best response overall (OR, RECIST)	0.21	0.08 - 0.52	0.001

Multivariate cox models were created on the basis of significant and non-interacting factors from univariate analysis with one model exclusively analyzing factors available prior to treatment (5 a.) and a separate model including all factors including those available at follow-up only (5 b.). Additionally, due to interaction of these variables, separate models were created to analyze the survival impact of either overall extrahepatic disease or bone metastases as the sole extrahepatic tumor manifestation

Discussion

In the past, scientific workup of surgical treatment for patients with metastatic cancers has been hampered by the fact that surgery used to carry substantial risks which were considered to be non-justified in a disease that is unlikely to be cured. Nonetheless, with the continuing improvement of perioperative outcomes in liver surgery, there is now an increasing role for liver resection as part of a multidisciplinary treatment concept in many cancers, even outside of a curative approach [28, 29]. Minimally invasive local treatment modalities have been developed to further reduce periprocedural risks. Recent data referring to a variety of techniques demonstrates encouraging results regarding local tumor clearance, making them particularly attractive in patients in whom a more radical approach associated with higher morbidity may not be acceptable because a survival benefit cannot be reliably predicted. Among these treatments, RFA is the most widely accepted modality and is regularly used to ablate liver tumors of limited number and size (usually <3-5 cm) in a suitable location (i.e., outside the immediate vicinity of large vessels to minimize the heat-sink effect, or at some distance from the hepatic bifurcation) [30]. Image-guided, catheter-based, interstitial brachytherapy is employed by an increasing number of centers since it avoids the tumor size limitation applicable for RFA [20, 25, 31]. Finally, RE using ^{90}Y-labelled glass or resin microspheres is able to target multifocal lesions not amenable to RFA or interstitial BT due to its inherent locoregional effects. RE has

demonstrated impressive response rates in both primary and metastatic liver tumors [32].

No data is currently available on the outcome of single, combined or sequential use of such locally and locoregionally active devices. For the cohort described herein, treatment decisions were generally based on 2 dominant terms:

a) a therapeutic algorithm mirroring the individual patient situation, i.e., all disease except for (controlled) bone metastases was amenable to treatment using a minimally invasive technique; systemic chemotherapy was either not effective, not further applicable due to toxicity or refused by the patient.
b) the selection of the appropriate device followed the technical considerations described above; i.e., RFA for patients with up to 3 tumors up to 3 cm in diameter (if not adjacent to main portal vein or hepatic bifurcation); BT for patients with up to 5 tumors any size in any location; RE for diffuse disease with up to 50 % tumor load.

Due to its liberal inclusion criteria with no upper limit to the number and size of liver metastases, extensive prior chemotherapy in almost all patients, and inclusion of patients with controlled extrahepatic disease (both sceletal and extrasceletal), the present study represents a negatively selected cohort of patients. In this dismal patient selection with LMBC diagnosed almost 2 years (median 22 months) prior to presentation for local treatment, the observed median overall survival of 21.9 months compares favorably with literature results on patients with LMBC undergoing systemic treatments only [33]. Our patient cohort recruited between 2006 and 2010 did not benefit of advances in systemic treatments that were recently reported for the use of nab-Paclitaxel in patients with metastatic breast cancer [34], with approx. 80 % of the patients in that study having visceral metastases whereas the proportion of hepatic metastases (that are considered to confer a particularly poor prognosis [35]) was not specified. Hence, our results must be compared to studies employing anthracycline, taxanes or cyclophosphamide. Data available refers to first line patients (in contrast to our cohort in a salvage situation), and median overall survival ranged from 22.7 to 27.1 months in patients with liver metastases only and from 14-16.8 months in patients with liver-dominant and limited extrahepatic disease [10, 9, 36]. The beneficial effect of a local treatment approach is further complemented by the observation that local control of the liver metastases and objective response to locoregional treatment at follow-up were found to be the strongest factors indicating prolonged survival at multivariable analysis in our study (HR of 0.29 and 0.21, respectively). Thus, in contrast to the view held by some investigators that local control of liver metastases in breast cancer has no survival impact due to the generalized nature of the disease [37], our results (in line with other published research [38]) are rather suggestive of the existence of an oligometastatic subpopulation in LMBC patients whose prognosis is determined by the visible lesions rather than subclinical tumor dissemination which will cause rapid systemic progression regardless of local disease control. The observation that most patients developing recurrence following resection of LMBC have the liver as their first site of recurrence further underscores this view [39, 40].

There are currently no methods to reliably identify the oligometastatic subpopulation which may benefit from local surgical or image-guided treatment approaches. In the absence of established molecular biomarkers, the selection of metastatic breast cancer patients who are most likely to derive benefit relies on retrospective identification of prognostic factors in patients receiving these therapies. In published studies, patient characteristics most often reported to be associated with prolonged survival include long disease-free interval between the treatment of the primary cancer and the diagnosis of liver metastases [40, 41], small size and/or low number of liver metastases [14, 15, 21, 42], well-differentiated histopathology [14], and response to pre-interventional or preoperative chemotherapy [43]. In some studies, patients demonstrating extrahepatic disease were generally excluded from local or locoregional treatment [14, 42, 44]. In the studies that did include patients with tumor spread beyond the liver, presence of extrahepatic disease was identified as a poor prognostic factor by some [12, 13, 45] but not all investigators [21, 43]. In the study by Jakobs et al. [22], presence of extrahepatic disease in patients undergoing RFA of liver metastases was associated with poor prognosis; however, this did not apply to patients who had bone metastases as their only extrahepatic tumor site.

Since factors predictive for treatment benefit should be available before treatment is started, we first analyzed the survival impact of parameters prior to treatment only. Of these parameters, only large liver volume, tumor diameter of ≥ 3.9 cm, and at least 3 lines of chemotherapy prior to local treatment were associated with poor prognosis. Presence of extrahepatic disease showed a tendency towards a negative prognostic impact ($p = 0.058$) when only factors known prior to the therapeutic decision were included. The negative effect almost vanished if extrahepatic disease was limited to bone metastases only. To evaluate the survival benefit conferred by locally ablative treatment, parameters related to treatment outcome that were available at follow-up only were entered into a subsequent analysis.

Sustained local control of the liver lesions and objective treatment response were the strongest predictors of good outcome in this setting, whereas neither the presence of any extrahepatic disease, nor evidence of bone metastases as the only extrahepatic tumor site preserved their tendency towards a negative prognostic impact.. Interestingly, the impact of prior chemotherapy was also no longer significant, indicating that even heavily pretreated patients may derive benefit from locoregional treatment modalities if local control of the liver lesions is achieved.

The treatments used in our study appeared to be generally safe, with no grade 4 toxicities observed and only few grade 3 toxicities occurring exclusively among patients treated with RE. Although a tendency towards decreased survival in patients developing grade 3 toxicity was noted, this was not significant. A larger analysis is required to reliably establish the relationship between treatment toxicity and outcome, and to determine how toxicities occurring after locally ablative treatment impact patient's tolerance for further antineoplastic therapy.

In summary, our results indicate that patients most likely to derive benefit from local or locoregional LMBC treatment are those with a largest tumor diameter of < 4 cm and only limited history of systemic chemotherapy prior to treatment. According to our data, patients with controlled extrahepatic disease, and specifically patients with bone metastases as the only extrahepatic site, may be considered for local ablation. We postulate that this is the patient population that should be selected for future trial concepts designed to compare local tumor treatment plus systemic chemotherapy with standard chemotherapy alone.

Our study has several limitations. First, we have no sound explanation for the finding that liver volume ≥1376 ml was identified as an independent poor prognostic factor. Because liver volume included the volume of any intrahepatic tumor lesions, one might suspect that this was simply an expression of high tumor load being responsible for increased liver volume, thereby impairing survival. However, there was no correlation between liver volume and the volume of liver metastases (see Additional file 2: Table S2). For patients undergoing RE, a possible explanation could be that dose calculation according to the BSA method as in our study may lead to relative underdosing of ^{90}Y in patients whose liver volume to BSA ratio is elevated compared to the average population. Using our data, we were unable to test this hypothesis and any attempt at providing an explanation for this finding must remain speculative. Second, our selection of patients based on the criterion "no uncontrolled extrahepatic disease" was somewhat subjective. This represents clinical practice at our institution as well as in many other centers. It may be appropriate as long as neither a broadly accepted definition of "controllable disease" nor treatment guidelines exist. However, for a future prospective trial a clear definition of what extent of extrahepatic disease is acceptable must be adopted. According to our data, this should clearly include patients with bone metastases only. For extrasceletal metastases, a possible threshold could be sustained disease stabilization for at least 12 months prior to local treatment as in the study by Hoffmann et al. [40]. Third, with patients included in our study who underwent RFA, interstitial brachytherapy, and RE, a very heterogeneous spectrum of treatment modalities and tumor distribution within the liver was analyzed. Thermal (RFA) vs. non-thermal (BT and RE) treatments are based on different working principles, as are high-dose (BT) vs. low-dose (RE) radiation therapy. If high-dose, catheter-based brachytherapy or low-dose, microsphere-based radioembolization is more effective in terms of response as well as recurrence rate and survival will be an area of high interest for larger, future analyses. The aim of our study, however, was to obtain information on the general benefit of liver-directed local treatment in metastatic breast cancer and to identify predictive and prognostic factors to help modelling future research strategies. All of the treatments studied exclusively target intrahepatic disease; hence, we considered it appropriate for our exploratory purposes to perform a joint analysis of the results obtained with all of these treatments.

Conclusions

In conclusion, our results confirm that patients with hepatic metastases from breast cancer, despite being incurable in most cases, may have favorable survival outcomes from locoregional treatment of their liver disease. The exact role of such therapies must be established in a randomized trial. Our study supports the assumption that an "oligometastatic" subgroup exists among patients with breast cancer metastases and that, as long as no reliable biomarkers exist to predict disease behavior, even limited extrahepatic disease should not automatically exclude patients from being treated locally.

Additional files

Additional file 1: Table S1. ROC Analysis and Cut-off Values. In order to prepare continuous variables for the Cox model, the according variables were dichotomized by a ROC analysis using survival (longer vs. shorter than median overall survival) as the target variable. Optimal cut-off was determined according to the Youden index. Variables with no significant cut-off were not used for the cox model, except the variable time from first breast cancer diagnosis to diagnosis of liver metastases since this variable was still considered as a possible influencing factor according to literature (with a cut off <2 years vs. ≥ 2 years).

Additional file 2: Table S2. Chi-Square Test for Interactions. The Chi-Square test was used to identify interactions between variables with influence on survival according to the univariate cox model in order to build up a robust multivariate cox model without interacting variables.

Competing interests

Following financial and non-financial competing interests might exist outside the submitted work:
Max Seidensticker, Benjamin Garlipp, Ricarda Seidensticker and Jens Ricke report to receive lecture fees from SIRTEX Medical.
Max Seidensticker, Ricarda Seidensticker and Jens Ricke report to receive lecture fees from Bayer Healthcare and research grants from SIRTEX Medical.
Jens Ricke reports to receive research grants from Bayer Healthcare and Siemens.
Christiane Bruns reports to receive travel grants und lecture fees from SIRTEX Medical.
Holger Amthauer reports grants from GE Medical, Siemens, Covidien, Bayer Healthcare, SIRTEX Medical and 3-B-Phamramceuticals.

Authors' contributions

MS, BG, RS, SS, PH, KM, MP, JR performed the research and the related therapies; MS and SS collected and analysed the data; MS, BG, and JR designed the research study; MS, BG, MP and JR wrote the manuscript; HA, KM, JR,SC, CB, PS, and PF were involved in interdisciplinary care and selected appropriate patients for locally ablative treatment; IS and MS did the statistical analysis; all authors did the proofreading and provided input for final corrections of the manuscript. All authors approved the final version of the article, including the authorship list.

Author details

[1]Klinik für Radiologie und Nuklearmedizin, Universitätsklinik Magdeburg, Leipziger Strasse 44, 39120 Magdeburg, Germany. [2]International School of Image-Guided Interventions, Deutsche Akademie für Mikrotherapie, Magdeburg, Germany. [3]Universitätsklinik Magdeburg, Klinik für Allgemein, Viszeral- und Gefäßchirurgie, Magdeburg, Germany. [4]Second Department of Radiology, Medical University of Gdansk, Gdansk, Poland. [5]Institut für Strahlentherapie, Universitätsklinik Magdeburg, Magdeburg, Germany. [6]Universitätsklinik Magdeburg, Universitätsfrauenklinik, Magdeburg, Germany.

Received: 14 October 2014 Accepted: 18 June 2015
Published online: 14 July 2015

References

1. Peters S, Adjei AA, Gridelli C, Reck M, Kerr K, Felip E. Metastatic non-small-cell lung cancer (NSCLC): ESMO Clinical Practice Guidelines for diagnosis, treatment and follow-u. Ann Oncol. 2012;23 Suppl 7:vii56–64.
2. Escudier B, Eisen T, Porta C, Patard JJ, Khoo V, Algaba F, et al. Renal cell carcinoma: ESMO Clinical Practice Guidelines for diagnosis, treatment and follow-up. Ann Oncol. 2012;23 Suppl 7:vii65–71.
3. Schmoll HJ, van Cutsem E, Stein A, Valentini V, Glimelius B, Haustermans K, et al. ESMO Consensus Guidelines for management of patients with colon and rectal cancer. a personalized approach to clinical decision making. Ann Oncol. 2012;23:2479–516.
4. Gupta GP, Massagué J. Cancer metastasis: building a framework. Cell. 2006;127:679–95.
5. Jones RP, Stättner S, Sutton P, Dunne DF, McWhirter D, Fenwick SW, et al. Controversies in the oncosurgical management of liver limited stage IV colorectal cancer. Surg Oncol 2014;23(2):53–60.
6. Weichselbaum RR, Hellman S. Oligometastases revisited. Nat Rev Clin Oncol. 2011;8:378–82.
7. Cardoso F, Harbeck N, Fallowfield L, Kyriakides S, Senkus E. Locally recurrent or metastatic breast cancer: ESMO Clinical Practice Guidelines for diagnosis, treatment and follow-up. Ann Oncol. 2012;23 Suppl 7:vii11–9.
8. NCCN Clinical Practice Guidelines in Oncology - Breast Cancer. Version 3.2014 [http://www.nccn.org/professionals/physician_gls/f_guidelines.asp#breast]. Accessed April 20, 2014.
9. Er O, Frye DK, Kau SC, Broglio K, Valero V, Hortobagyi GN, et al. Clinical course of breast cancer patients with metastases limited to the liver treated with chemotherapy. Cancer J. 2008;14:62–8.
10. Atalay G, Biganzoli L, Renard F, Paridaens R, Cufer T, Coleman R, et al. Clinical outcome of breast cancer patients with liver metastases alone in the anthracycline-taxane era: a retrospective analysis of two prospective, randomised metastatic breast cancer trials. Eur J Cancer. 2003;39:2439–49.
11. Kim JY, Park JS, Lee SA, Kim JK, Jeong J, Yoon DS, et al. Does liver resection provide long-term survival benefits for breast cancer patients with liver metastasis? A single hospital experience. Yonsei Med J. 2014;55:558–62.
12. Mariani P, Servois V, de Rycke Y, Bennett SP, Feron JG, Almubarak MM, et al. Liver metastases from breast cancer: Surgical resection or not? A case-matched control study in highly selected patients. Eur J Surg Oncol. 2013;39:1377–83.
13. Dittmar Y, Altendorf-Hofmann A, Schüle S, Ardelt M, Dirsch O, Runnebaum IB, et al. Liver resection in selected patients with metastatic breast cancer: a single-centre analysis and review of literature. J Cancer Res Clin Oncol. 2013;139:1317–25.
14. Weinrich M, Weiß C, Schuld J, Rau BM. Liver resections of isolated liver metastasis in breast cancer: results and possible prognostic factors. HPB Surg. 2014;2014:893829.
15. van Walsum G, de Ridder J, Verhoef C, Bosscha K, van Gulik T, Hesselink E, et al. Resection of liver metastases in patients with breast cancer: Survival and prognostic factors. Eur J Surg Oncol. 2012;38:910–7.
16. Cheng YC, Ueno NT. Improvement of survival and prospect of cure in patients with metastatic breast cancer. Breast Cancer. 2012;19:191–9.
17. Pagani O, Senkus E, Wood W, Colleoni M, Cufer T, Kyriakides S, et al. International Guidelines for Management of Metastatic Breast Cancer: Can Metastatic Breast Cancer Be Cured? J Nat Cancer Inst. 2010;102:456–63.
18. Bortolotto C, Macchi S, Veronese L, Dore R, Draghi F, Rossi S. Radiofrequency ablation of metastatic lesions from breast cancer. J Ultrasound. 2012;15:199–205.
19. Taşçi Y, Aksoy E, Taşkın HE, Aliyev S, Moore H, Ağcaoğlu O, et al. A comparison of laparoscopic radiofrequency ablation versus systemic therapy alone in the treatment of breast cancer metastasis to the liver. HPB. 2013;15:789–93.
20. Wieners G, Mohnike K, Peters N, Bischoff J, Kleine-Tebbe A, Seidensticker R, et al. Treatment of hepatic metastases of breast cancer with CT-guided interstitial brachytherapy – A phase II-study. Radiother Oncol. 2011;100:314–9.
21. Meloni MF, Andreano A, Laeseke PF, Livraghi T, Sironi S, Lee FT. Breast cancer liver metastases: US-guided percutaneous radiofrequency ablation–intermediate and long-term survival rates. Radiology. 2009;253:861–9.
22. Jakobs TF, Hoffmann R, Schrader A, Stemmler HJ, Trumm C, Lubienski A, et al. CT-Guided Radiofrequency Ablation in Patients with Hepatic Metastases from Breast Cancer. Cardiovasc Intervent Radiol. 2009;32:38–46.
23. Nielsen D, Nørgaard H, Vestermark L, Pfeiffer P, Jensen B, Nelausen K, et al. Intrahepatic and systemic therapy with oxaliplatin combined with capecitabine in patients with hepatic metastases from breast cancer. Breast. 2012;21:556–61.
24. Cianni R, Pelle G, Notarianni E, Saltarelli A, Rabuffi P, Bagni O, et al. Radioembolisation with 90Y-labelled resin microspheres in the treatment of liver metastasis from breast cancer. Eur Radiol. 2013;23:182–9.
25. Ricke J, Wust P, Stohlmann A, Beck A, Cho CH, Pech M, et al. CT-guided interstitial brachytherapy of liver malignancies alone or in combination with thermal ablation: phase I-II results of a novel technique. Int J Radiat Oncol Biol Phys. 2004;58:1496–505.
26. Seidensticker R, Seidensticker M, Damm R, Mohnike K, Schütte K, Malfertheiner P, et al. Hepatic toxicity after radioembolization of the liver using (90)Y-microspheres: sequential lobar versus whole liver approach. Cardiovasc Intervent Radiol. 2012;35:1109–18.
27. Eichbaum MHR, Kaltwasser M, Bruckner T, de Rossi TM, Schneeweiss A, Sohn C. Prognostic factors for patients with liver metastases from breast cancer. Breast Cancer Res Treat. 2006;96:53–62.
28. Poon RT, Fan ST, Lo CM, Liu CL, Lam CM, Yuen WK, et al. Improving perioperative outcome expands the role of hepatectomy in management of benign and malignant hepatobiliary diseases: analysis of 1222 consecutive patients from a prospective database. Ann Surg. 2004;240:698–708. discussion 708-10.
29. Jarnagin WR, Gonen M, Fong Y, DeMatteo RP, Ben-Porat L, Little S, et al. Improvement in perioperative outcome after hepatic resection: analysis of 1,803 consecutive cases over the past decade. Ann Surg. 2002;236:397–406. discussion 406-7.
30. Ruers T, Punt C, van Coevorden F, Pierie JPEN, Borel-Rinkes I, Ledermann JA, et al. Radiofrequency ablation combined with systemic treatment versus systemic treatment alone in patients with non-resectable colorectal liver

metastases: a randomized EORTC Intergroup phase II study (EORTC 40004). Ann Oncol. 2012;23:2619–26.
31. Ricke J, Wust P, Wieners G, Beck A, Cho CH, Seidensticker M, et al. Liver malignancies: CT-guided interstitial brachytherapy in patients with unfavorable lesions for thermal ablation. J Vasc Interv Radiol. 2004;15:1279–86.
32. Kennedy A, Coldwell D, Sangro B, Wasan H, Salem R. Radioembolization for the Treatment of Liver Tumors. Am J Clin Oncol. 2012;35:91–9.
33. Pentheroudakis G, Fountzilas G, Bafaloukos D, Koutsoukou V, Pectasides D, Skarlos D, et al. Metastatic breast cancer with liver metastases: a registry analysis of clinicopathologic, management and outcome characteristics of 500 women. Breast Cancer Res Treat. 2006;97:237–44.
34. Gradishar WJ, Krasnojon D, Cheporov S, Makhson AN, Manikhas GM, Clawson A, et al. Phase II trial of nab-paclitaxel compared with docetaxel as first-line chemotherapy in patients with metastatic breast cancer: final analysis of overall survival. Clin Breast Cancer. 2012;12:313–21.
35. Llombart-Cussac A, Pivot X, Biganzoli L, Cortes-Funes H, Pritchard KI, Pierga J, et al.: A prognostic factor index for overall survival in patients receiving first-line chemotherapy for HER2-negative advanced breast cancer: An analysis of the ATHENA trial. Breast. 2014;23:656–62
36. Belfiglio M, Fanizza C, Tinari N, Ficorella C, Iacobelli S, Natoli C. Meta-analysis of phase III trials of docetaxel alone or in combination with chemotherapy in metastatic breast cancer. J Cancer Res Clin Oncol. 2012;138:221–9.
37. Veltri A, Gazzera C, Barrera M, Busso M, Solitro F, Filippini C, et al. Radiofrequency thermal ablation (RFA) of hepatic metastases (METS) from breast cancer (BC): an adjunctive tool in the multimodal treatment of advanced disease. Radiol Med. 2014;119:327–33.
38. Saxena A, Kapoor J, Meteling B, Morris DL, Bester L. Yttrium-90 Radioembolization for Unresectable, Chemoresistant Breast Cancer Liver Metastases: A Large Single-Center Experience of 40 Patients. Ann Surg Oncol. 2014;21:1296–303.
39. Bathe OF, Kaklamanos IG, Moffat FL, Boggs J, Franceschi D, Livingstone AS. Metastasectomy as a cytoreductive strategy for treatment of isolated pulmonary and hepatic metastases from breast cancer. Surg Oncol. 1999;8:35–42.
40. Hoffmann K, Franz C, Hinz U, Schirmacher P, Herfarth C, Eichbaum M, et al. Liver Resection for Multimodal Treatment of Breast Cancer Metastases: Identification of Prognostic Factors. Ann Surg Oncol. 2010;17:1546–54.
41. Caralt M, Bilbao I, Cortés J, Escartín A, Lázaro JL, Dopazo C, et al. Hepatic Resection for Liver Metastases as Part of the "Oncosurgical" Treatment of Metastatic Breast Cancer. Ann Surg Oncol. 2008;15:2804–10.
42. Lubrano J, Roman H, Tarrab S, Resch B, Marpeau L, Scotté M. Liver resection for breast cancer metastasis: Does it improve survival? Surg Today. 2008;38:293–9.
43. Adam R, Aloia T, Krissat J, Bralet M, Paule B, Giacchetti S, et al. Is Liver Resection Justified for Patients With Hepatic Metastases From Breast Cancer? Ann Surg. 2006;244:897–908.
44. Vlastos G, Smith DL, Singletary SE, Mirza NQ, Tuttle TM, Popat RJ, et al. Long-term Survival After An Aggressive Surgical Approach in Patients With Breast Cancer Hepatic Metastases. Ann Surg Oncol. 2004;11:869–74.
45. Sakamoto Y, Yamamoto J, Yoshimoto M, Kasumi F, Kosuge T, Kokudo N, et al. Hepatic Resection for Metastatic Breast Cancer: Prognostic Analysis of 34 Patients. World J Surg. 2005;29:524–7.

Seidensticker et al. BMC Cancer (2018) 18:882
https://doi.org/10.1186/s12885-018-4784-9

BMC Cancer

RESEARCH ARTICLE Open Access

Local ablation or radioembolization of colorectal cancer metastases: comorbidities or older age do not affect overall survival

Ricarda Seidensticker[1,6†], Robert Damm[2*†], Julia Enge[2], Max Seidensticker[1,6], Konrad Mohnike[3,6], Maciej Pech[2,6], Peter Hass[4], Holger Amthauer[5,6] and Jens Ricke[1,6]

Abstract

Background: Local ablative techniques are emerging in patients with oligometastatic disease from colorectal carcinoma, commonly described as less invasive than surgical methods. This single arm cohort seeks to determine whether such methods are suitable in patients with comorbidities or higher age.

Methods: Two hundred sixty-six patients received radiofrequency ablation (RFA), CT-guided high-dose rate brachytherapy (HDR-BT) or Y90-radioembolization (Y90-RE) during treatment of metastatic colorectal cancer (mCRC). This cohort comprised of patients with heterogenous disease stages from single liver lesions to multiple organ systems involvement commonly following multiple chemotherapy lines. Data was reviewed retrospectively for patient demographics, previous therapies, initial or disease stages at first intervention, comorbidities and mortality. Comorbidity was measured using the Charlson Comorbidity Index (CCI) and age-adjusted Charlson Index (CACI) excluding mCRC as the index disease. Kaplan-Meier survival analysis and Cox regression were used for statistical analysis.

Results: Overall median survival of 266 patients was 14 months. Age ≥ 70 years did not influence survival after local therapies. Similarly, CCI or CACI did not affect the patients prognoses in multivariate analyses. Moderate or severe renal insufficiency ($n = 12$; $p = 0.005$) was the only single comorbidity identified to negatively affect the outcome after local therapy.

Conclusion: Interventional procedures for mCRC may be performed safely even in elderly and comorbid patients. In severe renal insufficiency, the use of invasive techniques should be limited to selected cases.

Keywords: Colorectal cancer, Elderly patients, Comorbidities, Multimodal therapy

Background

Age is a major risk factor for colorectal cancer (CRC) and cancer in general [1]. Elderly patients often suffer from comorbidity and reduced organ function thus requiring particular considerations when making treatment decisions. Additionally elderly patients present a very heterogeneous group with chronological age being insufficient to describe individual resources and deficits. Contributing to these difficulties in decision making, elderly patients are underrepresented in cancer trials while they account for most of the actual patients [2]: When analyzing 495 NCI (National Cancer Institute) studies, Lewis et al. found that only 32% of cancer trial participants were age 65 years and older, in contrast to 61% in the US cancer population [3]. Other authors have published similar results, with an even greater difference for patients aged 70 years and older [4]. Although there is evidence that age should not be a reason to refrain from surgery and chemotherapy, most studies comprise a higher age and comorbidities as exclusion criteria [5–7]. In clinical practice, patients at higher age or with comorbidities often receive the recommended chemotherapies at reduced doses outside

* Correspondence: Robert.Damm@med.ovgu.de
†Ricarda Seidensticker and Robert Damm contributed equally to this work.
[2]Department of Radiology and Nuclear Medicine, Otto-von-Guericke-University Magdeburg, Leipziger Str. 44, 39120 Magdeburg, Germany
Full list of author information is available at the end of the article

the standard prescription [8–10]. Yet, the effectiveness of such adapted therapy regimen is unknown.

Local ablative treatments (LAT, e.g. radiofrequency/microwave ablation and interstitial HDR-brachytherapy) as well as locoregional therapies (e.g. Y90 radioembolization) offer local tumor control and extensive cytoreduction with low morbidity and mortality. In oligometastatic disease with few tumor sites and limited number of metastases, LAT can achieve long-term disease control by complete tumor ablation in patients not eligible for surgery [11]. In contrast, locoregional therapies such as Y90 radioembolization may contribute to the overall survival of selected patient by improving the local response in liver-dominant disease or by providing a salvage treatment in chemo-refractory liver metastases [12, 13]. Accordingly, the toolbox of local ablative treatments and locoregional therapies was included in the latest ESMO guideline for colorectal cancer with oligometastatic disease or liver dominant, chemo-refractory metastases [14]. In the context of elderly and comorbid patients, data on the efficacy of LAT is still rare.

This study aims to assess the influence or absence of negative effects of higher age or comorbiditieson the outcome after local therapies. We hypothesize that minimal-invasive local or locoregional techniques add further value by offering broader treatment options in elderly and comorbid patients with metastatic colorectal disease.

Methods

Patient cohort

We searched our institutional data base for all patients with mCRC receiving at least one radiofrequency ablation (RFA), high-dose-rate brachytherapy (HDR-BT) or Y90-radioembolization (Y90-RE) between 2006 and 2010. We included all patients with complete records on patient history and at least one follow up visit.

The study comprised a total of 266 patients (179 male, 87 female; mean age 66 years). One hundred ninety-six patients (73.7%) had synchronous metastases within 12 months after diagnosis of the primary tumor. Nearly all patients presented with hepatic metastases ($n = 251$, 94.4%). Further sites of dissemination included lung ($n = 77$, 28.4%), lymphatic ($n = 44$, 16.5%), osseous ($n = 10$, 3.8%) or other metastases ($n = 22$, 8.3%). Most of the patients failed at least one ($n = 79$, 29.7%) or two ($n = 160$, 60.2%) lines of chemotherapy compromising either irinotecan or oxaliplatin combined with 5-fluorouracil. Additionally, 169 patients (63.5%) received EGFR or VEGF inhibiting therapy. Prior surgical treatments included surgery for the primary tumor in 263 patients (98.9%), resection of hepatic metastases in 91 patients (34.2%) and resection of lung/other metastases in 34 patients (12.8%).

Throughout the observation period, nearly half of the patients developed further liver metastases ($n = 118$, 44.4%) followed by lung metastases ($n = 108$, 40.6%), lymphatic metastases ($n = 51$, 19.2%), osseous metastases ($n = 18$, 6.8%) and other ($n = 73$, 27.4%).

Patients were considered for local ablative treatment and Y90 radioembolization by a multidisciplinary team (MDT; including medical, surgical and radiation oncologists) depending on their stage of disease (e.g. size of tumor, number of lesions, tumor sites) as well as organ function and performance status. Local ablation was selected in potentially resectable metastases only if patients had an unfavorable performance status and/or severe comorbidities (resulting in a high risk of perioperative morbidity and mortality) or if patients refused surgery. Patients with single lesions up to 3 cm in diameter were preferably treated by radiofrequency ablation. If the localization and number of metastases or tumor size above 3 cm limited RFA, interstitial HDR brachytherapy was applied for oligometastatic disease. Patients with diffuse, liver-dominant involvement underwent Y90 radioembolization. In case of tumor progress during follow-up, patients were reassessed by the MDT for the next treatment step, i.e. further local treatment strategies and/or systemic therapy. In total, 732 interventions were performed.

Local and locoregional therapies

The following image guided techniques were considered by the MDT (if not eligible for systemic therapy only).

Radiofrequency ablation

Radiofrequency ablation induces a coagulation necrosis of tumor tissue by generating heat [15]. RFA is considered to be a safe and effective method with major complications occurring in 1–5% of patients. Beside limitations according to proximity to vulnerable organs, RFA underlies a heat-sink effect restricting the maximum size of the coagulation necrosis [16].

In our study, local ablation for smaller lung or liver metastases (< 3 cm) was performed using CT-guided radiofrequency ablation (LeVeen®, Boston Scientific, Natrick, United States or Starburst Semi-Flex®, AngioDynamics, Mountain View, Canada) according to manufacturer's specifications. A total of 21 liver and 77 lung RFA interventions were conducted.

CT guided high-dose rate brachytherapy

CT-guided HDR-BT is an ablative technique utilizing radiation from an Iridium-192 source in afterloading technique. Interstitial catheters were inserted by CT-guidance and subsequent 3D treatment planning was applied (Oncentra®, Nucletron, Veenendaal, The Netherlands). As the catheters are fixed within the tumor, the delivery of

irradiation is not affected by breathing motion. As a consequence, dose delivery to the tumor is highly accurate and exposure of healthy tissues or risk organs can be reduced to a minimum [17].

Since HDR-BT has no systematic restrictions for tumor size and location close to vessels, it was preferably indicated if multiple tumors were present as well as in larger (> 3 cm) liver or lung metastases or any lymphatic metastases [18–20]. To ensure a complete ablation, a target dose of 20Gy in a single session was subscribed [21]. HDR-BT was mainly used for liver ablations ($n = 422$), as well as for ablation of lung metastases ($n = 52$), lymphatic nodes ($n = 9$) and other tumor sites ($n = 8$).

Y90-radioembolization

If number, size or location of liver metastases exceeded the capabilities of local ablation by RFA or HDR-BT, patients were subsequently evaluated for loco-regional radioembolization using microspheres labeled with the beta-emitter Yttrium-90 (half-life 64 h; mean energy 0.96 MeV) administered through an angiographic catheter to the liver arteries [22, 23]. Multinodular liver metastases were treated in 96 cases by 142 radioembolizations using Y90 resin microspheres (SIR-Spheres®, Sirtex Medical, Lane Cove, Australia), the required dose was calculated previously according to the body-surface area method after an initial evaluation with Technecium-99 m macro-aggregated albumin (LyoMAA, Covidien, Neustadt, Germany).

Comorbidity measurement

To assess comorbidities, we used the Charlson Comorbidity Index (CCI) which is validated in older patients with the option to calculate an age adjusted index (Charlson Age Comorbidity Index, CACI) [24, 25] to predict mortality in a range of comorbid conditions. 19 comorbidity items were included and each condition was assigned a score of 1, 2, 3 or 6 (see Table 3), depending on the risk of death associated with each one. The sum of these items (between 0 and 30) formed the final comorbidity index (CCI, CACI) that has been established as a predictor of patient outcome and mortality in different settings and larger populations including cancer patients [26]. The index disease, metastatic colorectal cancer, was excluded when calculating the index. Additional information was assessed regarding typical cardiovascular risk factors not included within the CCI (e.g. hypertension, hyperlipidemia, obesity).

All information on comorbidity was recorded at baseline.

Statistical analysis

SPSS 21.0 (IBM®, New York, USA) was used for the complete analysis set. Comorbidity items including the summary within the CCI/CACI, patient age and key characteristics of disease and treatment underwent a stepwise Cox regression analysis. All baseline variables were initially analyzed in a univariate Cox regression. Any variable scoring a p-value < 0.1 was then included in a multivariate Cox proportional hazard model. Tables 3 and 4 give a summary of the main analysis with p-values, harzard ratios (HR) and 95% confidence intervals (95% CI). Statistical significance in the multivariate analysis was assumed for p-values < 0.05. Visualization was achieved by Kaplan-Meier charts.

Results

Treatment outcome

A total of 732 procedures were performed in all patients, an overview is given in Table 1. All survival data were

Table 1 Overview on procedures and outcome

			Median overall survival (months)[a]			
	Patients	Procedures	Patient age		Comorbidity	
	n	*n*	≥ 70 years	< 70 years	CCI ≥ 3	CCI < 3
RFA	60	99	26.7 m	24.3 m	24.0 m	26.2 m
liver	18	21		**($p = 0.76$)**		**($p = 0.16$)**
lung	42	77				
other	1	1				
HDR-BT	192	491	19.1 m	18.2 m	16.4 m	18.9 m
liver	176	422		**($p = 0.83$)**		**($p = 0.43$)**
lung	29	52				
lymph node	9	9				
other	8	8				
Y90-RE	96	142	6.9 m	6.5 m	5.3 m	6.9 m
				($p = 0.86$)		**($p = 0.21$)**

[a]statistics for overall survival according to Cox regression analysis; p-values (bold) refer to the comparison of survival between age/comorbidity groups

measured beginning with the first treatment at our institution.

RFA patients

Patients initially presenting with singular, small metastases (< 3 cm) confined to lung ($n = 42$) or liver ($n = 18$) were treated by radiofrequency ablation yielding a median survival of 26.7 months and 24.4 months (including further local ablative treatments and/or systemic therapies in case of disease progression). A single RFA treatment was used for the ablation of a vertebral metastasis. 50 out of 60 patients (83%) treated by RFA underwent multiple RFA sessions and/or further treatment by HDR-BT for recurrent metastases.

CT-guided HDR brachytherapy patients

Oligonodular and larger metastases were treated by HDR-BT. Patients with liver metastases eligible for HDR-BT at their first presentation in our department achieved a median survival of 18.1 months ($n = 176$). Initially applying HDR-BT to lung metastases, a median survival of 29.6 months was observed ($n = 29$). Lymphatic nodes and other infrequent localizations of metastases (e.g. adrenal glands, pancreas) were treated exclusively by HDR-BT with a corresponding median survival of 17.0 to 26.7 months. In patients with multiple tumor sites or disease progression during follow up, HDR-BT was repeated ($n = 143$) or Y90-RE performed ($n = 28$).

Radioembolization patients

Ninety- six patients with diffuse liver metastases underwent Y90-RE with a median survival of 6.7 months. 68 of these patients who had failed first and second line chemotherapy including variable treatment cycles with oxaliplatin, irinotecan and 5-fluorouracil demonstrated a significantly shorter median survival of 5.8 months in univariate and multivariate Cox regression analyses ($p < 0.001$). However, 19 salvage patients (28%) undergoing Y90 radioembolization had a survival of at least 9 months with long-term survivors reaching a survival of nearly 30 months. All salvage patients treated by Y90-RE in this cohort represent a majority of patients in a dedicated prognostic analysis which can be reviewed for supplementary information [27].

Impact of palliative chemotherapy after first interventional treatment

A total of 120 patients (45%) received further chemotherapy after the first local treatment. These patients demonstrated an improved survival of 22.0 vs. 16.1 months compared to patients without further systemic therapies ($p = 0.009$; HR 0.71; 95% CI 0.55–0.92).

Table 2 Patient characteristics

	n	%
All patients	266	100.00
Male	179	67.30
Female	87	32.70
First diagnosis		
Mean age (SD) in years	63.0 (+/− 9.7)	
Primary tumor		
located in Colon (C18)	151	56.77
Rectosigmoid junction (C19)	18	6.77
Rectum (C20)	98	36.84
T1,T2	29	10.90
T3,T4	227	85.30
T missing	10	3.80
N0	74	27.80
N1,2	179	67.30
N status missing	13	4.90
Synchronous metastases	166	62.41
Prior treatment		
Systemic chemotherapy	248	93.23
Median lines of chemotherapy (range)	2 (0–8)	
Radiochemotherapy	30	11.28
Surgery for colorectal primary	263	98.87
Radiation therapy for colorectal primary	21	7.89
Surgery for liver metastases	91	34.21
Other local treatment for liver metastases	40	15.04
Surgery for lung metastases	14	5.26
Surgery for other metastases	20	7.52
Local therapy for other metastases	5	1.88
First interventional treatment		
Mean age (SD) in years	66,5 (+/−9.6)	
Age > 70 years	89	33.5
Median Karnofsky index (range) in %	80 (50–100)	
Liver metastases	251	96.99
Liver metastases only	121	45.50
Liver involvement > 25%	45	16.92
Lung involvement	100	37.60
Other	83	31.20
≥ 2 organ systems involved	140	52.63

Outcome by patient characteristics

Overall patient characteristics are outlined in Table 2. Survival in all patients accounted for 14 months, survival analysis was conducted using a stepwise Cox regression analysis. Nearly all patients suffered from liver metastases ($n = 251$). Patients with an initial positive N stage (n

= 179) and metachronous lymph node metastases (n = 44) had a poorer prognosis (13.1 vs 17.0 months; 9.8 vs 16.1 months) after first interventional treatment in univariate analysis, yet multivariate regression analysis did not demonstrate a significant influence on overall survival (p = 0.25 and p = 0.17; respectively).

Synchronous metastases at first diagnosis (n = 166) only had significant influence in univariate analysis (p = 0.036) but not in multivariate analysis (p = 0.90). Metachronous pulmonary metastases had no impact on survival (p = 0.55).

Systemic therapy options after initiation of interventional therapy were stratified by previous failure of either oxaliplatin or irinotecan based combined regimen (second line, n = 79) or failure of both (third line, n = 160). Patients without prior chemotherapy were classified to first line (n = 27), including patients with contraindications to systemic therapy. A median survival of 13.2 vs. 16.6 months was observed in patients receiving third line therapy compared to patients in earlier lines of therapy without prognostic influence in multivariate analysis (p = 0.30).

If third line patients were still eligible for local-ablative techniques (RFA and/or HDR-BT), the median survival reached 17.5 months (n = 114).

The complete multivariate analysis is demonstrated in Table 4.

Age analysis

Our cohort included 89 patients (33.5%) 70 years or older. This patient group demonstrated no altered survival as compared to younger patients after first interventional therapy in a Cox regression analysis (p = 0.19; HR 0.84; 95% CI 0.64–1.10). Median survival in the subgroup of elder patients was 16.6 vs. 13.2 months as shown in Fig. 1.

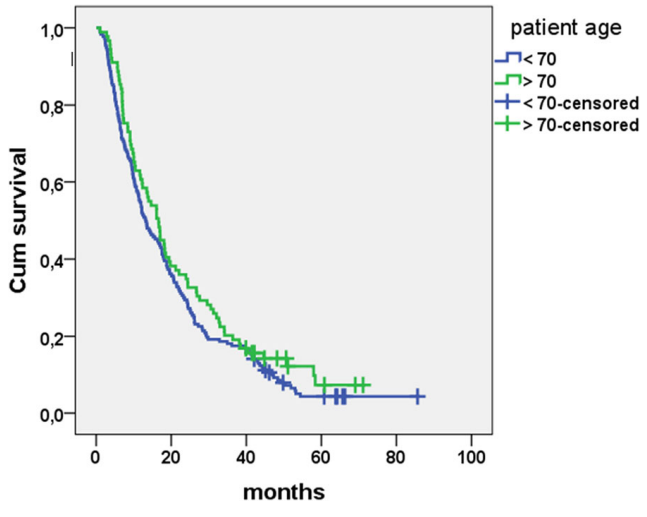

Fig. 1 Overall survival by age. Kaplan Meier estimation for overall survival after first treatment by age < 70 (13.2 months; n = 177) and age ≥ 70 (16.6 months; n = 89), no statistical difference between groups (p = 0.19; Cox regression analysis)

In patients older than 70 years initial or additional lymphatic metastases were of no prognostic value (p = 0.11; HR 1.24; 95% CI 0.95–1.61 and p = 0.23; HR 1.62; 95% CI 0.74–3.54), just as for heavily pretreated patients with at least three lines of systemic chemotherapy (p = 0.18; HR 1.23; 95% CI 0.91–1.67). Survival of elderly versus younger patients was similar regarding the first technique applied (RFA, HDR-BT or Y90-RE) in regression analysis, see Table 1.

Comorbidity analysis (CCI, CACI)

With a sum of 3 points or more for the CCI, 43 patients (16.2%) displayed severe comorbidities at baseline. These comorbidities were significantly more frequent in older patients ≥70 years (n = 21; 23.6%) than in younger patients < 70 years (n = 22; 12.4%; p = 0.023; Chi-Square test). According to the age adjusted CACI, a total of 112 patients (42.1%) were considered with severe comorbidities at first therapy. An overview of CCI/CACI in the patient cohort is given in Table 3.

In a univariate Cox regression, both CCI or CACI ranging from 0 to 7 and 0–8 had no significant impact on the patients prognosis (p = 0.82; p = 0.86), respectively. Comparison of patients with severe comorbidities (CCI ≥ 3) versus no or moderate comorbidities demonstrated no significant influence on overall survival either (18.8 months vs. 21.9 months; p = 0.41; see Fig. 2). Regression analysis of all single items summarized in the index (see Table 3) revealed a significant influence of moderate or severe renal disease in 12 patients (p = 0.005). Two patients with gastric or duodenal ulcer died after 3.7 and 5.7 months, respectively (p = 0.006). Patients with chronic pulmonary disease (n = 29) had a lower hazard ratio (p = 0.006; HR 0.61; 95 CI 0.38–0.99). No other comorbidity item had a considerable impact, despite 55 patients suffering from peripheral vascular disease and 36 patients with a history of myocardial infarction or coronary heart disease (p = 0.81 and p = 0.38). Multivariate regression analysis finally confirmed a statistical significant impact of moderate or severe renal disease in all patients (p = 0.005).

Apart from the conditions reflected in the CCI, 116 patients had been diagnosed with hypertension (43.6%), 18 patients with obesity (6.8%) and 20 with hyperlipidemia (7.5%). None of these factors demonstrated a significant influence on survival as demonstrated in Table 4.

Discussion

Interventional oncology in elderly patients

Metastatic colorectal cancer continues to be a major therapeutic challenge especially in elderly patients as prevalence of comorbidity is considered to be more frequent compared to the background population [28]. The corresponding interaction between cancer and comorbidity, and whether comorbidity leads to cancer

Table 3 Prevalence of comorbidities according to the Charlson Comorbidity index

CCI[a]	condition	*n*	%	*p*-value°	HR (95% CI)
1	myocardial infarction, coronary artery disease	36	13,5	0.38	0.85 (0.58–1.23)
	congestive heart failure	15	5,6	0.62	0.87 (0.51–1.50)
	peripheral vascular disease	55	20,7	0.81	0.96 (0.71–1.31)
	cerebrovascular disease	13	4,9	0.58	0.85 (0.48–1.52)
	dementia	0	0		
	chronic pulmonary disease	21	7,9	0.046	0.61 (0.38–0.99)
	connective tissue disorder	2	0,8	0.93	0.94 (0.23–3.78)
	peptic ulcer disease	2	0,8	0.006	7.40 (1.80–30.50)
	mild liver disease	10	3,8	0.26	1.44 (0.76–2.72)
	diabetes without complications	42	15,8	0.94	0.99 (0.70–1.40)
2	diabetes with end-organ damage	17	6,4	0.74	0.92 (0.55–1.52)
	hemiplegia	1	0,4	0.70	1.48 (0.21–10.61)
	moderate/severe renal disease	12	4,5	0.005	2.3 (1.29–4.13)
	any tumor without metastases (incl. Leukemia, lymphoma)	34	12,8	0.89	1.03 (0.71–1.50)
3	moderate/severe liver disease	3	1,1	0.33	1.77 (0.57–5.55)
6	metastatic solid tumor (mCRC excluded)	0	0		
	AIDS	0	0		
8	AIDS and any tumor	0	0		

[a]age adjusted index CACI adds 1 point for each decade after 40 years
°statistics for overall survival according to univariate Cox regression, variables with univariate p < 0.1 are processed in Table 4

diagnosis in earlier or later stages, is still object to ongoing discussions [29]. Furthermore, elderly and multimorbid patients are often not eligible for surgery or efficacious polychemotherapies [30].

In our group of metastatic CRC patients, about 62% had comorbidities according to the CCI. Adding conditions as hypertension, hyperlipidemia and obesity, 71% of patients were suffering from comorbidities, which is far more frequent than in other studies applying the CCI reporting a prevalence between 32 and 41% in metastatic or non-metastatic CRC patients [31].

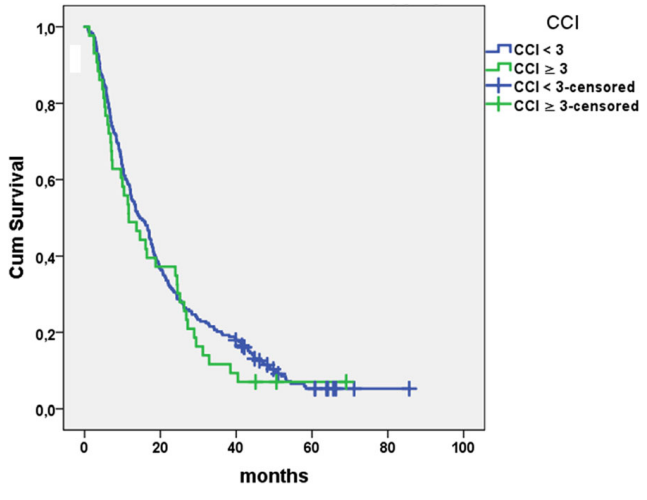

Fig. 2 Overall survival by CCI. Kaplan Meier estimation for overall survival after first treatment separated by Charlson Comorbidity Index < 3 (21.9 months; *n* = 223) and ≥ 3 (18.1 months; *n* = 43); no statistical difference between groups (*p* = 0.41; Cox regression analysis)

Median survival after RFA as first local treatment of liver metastases was 24.4 months in our patients, which is consistent with existing data ranging from 24 to 36 months [32].

As HDR-BT is usually applied in metastases exceeding the technical feasibility of RFA in size and number, thus adding an unfavorable prognosis bias, a corresponding median survival of 18.1 months was found in those patients. A retrospective analysis by Collettini et al. demonstrated a comparable median survival of 18 months after HDR-BT of colorectal liver metastases [33].

Most patients undergoing Y90-radioembolization had previously failed all accessible chemotherapies leading to a median survival of 5.8 months in this group. However, one quarter of these patients survived 9 or more months including a small group of long term survivors > 2 years indicating that patient selection is of utmost importance in a salvage population [34]. This could be shown by our group in a previous study regarding the prognostic value of Karnofsky index, tumor load and tumor markers in patients undergoing Y90-radioembolization to help selecting appropriate patients [27].

When applying CCI and CACI to measure the prognostic impact of comorbidities in our patients, we did not observe a relation of higher index values with overall

Table 4 Stepwise Cox regression analysis of key characteristics at baseline including CCI items with univariate $p < 0.1$ (all items of CCI are shown in Table 3)

Variable	Univariate *p*	HR (95% CI)	Multivariate *p**	HR (95% CI)
CCI items p < 0.1				
Chronic pulmonary disease	0.046*	0.61 (0.38–0.99)	0.30	0.76 (0.45–1.28)
Peptic ulcer disease	0.006*	7.40 (1.80–30.50)	0.17	2.75 (0.65–11.69)
Moderate/severe renal disease	0.005*	2.3 (1.29–4.13)	0.005	2.46 (1.32–4.57)
Comorbidities not included in CCI				
Hypertension	0.54	0.93 (0.72–1.20)		
Obesity	0.32	0.77 (0.47–1.28)		
Hyperlipidemia	0.48	0.84 (0.51–1.37)		
Patient and treatment characteristics				
Age > 70 years	0.19	0.84 (0.64–1.10)		
CCI ≥ 3	0.41	1.15 (0.82–1.62)		
Positive N stage of primary	0.004*	1.27 (1.08–1.50)	0.25	1.11 (0.93–1.33)
Synchronous metastases	0.036*	1.36 (1.02–1.81)	0.90	0.98 (0.71–1.35)
Metachronous lymph node metastases	0.032*	1.44 (1.03–2.00)	0.17	1.31 (0.89–1.91)
Metachronous pulmonary metastases	0.55	1.09 (0.83–1.43)		
1st/2nd Line vs. 3rd Line treatment	0.001*	0.83 (0.77–0.90)	0.30	0.89 (0.72–1.1)
Salvage treatment in Y90-RE	0.001*	2.17 (1.37–3.45)	< 0.001	4.35 (3.06–6.17)

*multivariate Cox regression analysis including all variables $p < 0.1$ in univariate analysis

survival. It should be noted that about 42% of all patients had severe comobidities according to the age-adjusted index (CACI≥3). This finding supports the assumption that local ablative therapies such as RFA or HDR-BT, or a locoregional treatment such as Y90 radioembolization, can be safely applied in risk patients with a moderate toxicity profile or adverse event rate, respectively.

A similar relationship was seen recently by Jehn et al. in patients undergoing systemic therapy for mCRC as CCI and age showed no influence on survival [35]. In this population, adverse events were not found to be more frequent in elderly patients, although a significantly higher CCI was observed. Also response rates and survival were balanced irrespective of age and comorbidity. Further studies even discuss inferior outcome in younger patients, most probably caused by more aggressive tumor biology as compared to elder patients [36, 37]. With regard to our patients treated by local therapies, we observed a similar trend potentially related to a more favorable tumor biology in the eldery.

Implications

Our study has demonstrated that older age or a higher rate of comorbidities with age (CCI and CACI) do not influence survival in metastatic colorectal cancer when patients are selected for local or loco-regional ablation by RFA, HDR-BT or Y90 radioembolization. A poorer survival was only seen in patients with moderate or severe renal impairment in our multivariate analysis. Renal disease in general is associated with a poor prognosis and has been reported to have a specifically negative impact on survival in different cancer populations [38].

Limitations

A possible source of error in our analysis may result from data being derived from discharge diagnoses or follow up documentation in our own medical hospital records. Conditions treated by the general practitioner or subsequently in other hospitals may not have been completely represented in our data as a result of the studies retrospective nature. Furthermore, our sample is not necessarily representative for all mCRC patients with a comparatively high frequency of comorbidities in our cohort as compared to other studies. However, we hypothesize that these finding exclude a positive selection in our cohort.

Conclusion

The tool box of image guided treatments proved to be safe and applicable even in patients of higher age or patients presenting with comorbidities. Our study results support offering ablative treatments to metastatic colorectal cancer patients even at advanced age or high Charlson indices.

Abbreviations

CACI: Charlson Age Comorbidity Index; CCI: Charlson Comorbidity Index; CT: Computed tomography; ESMO: European Society for Medical Oncology; HDR-BT: High-dose rate brachytherapy; mCRC: metastatic colorectal cancer; MRI: magnetic resonance imaging; RFA: Radiofrequency ablation; Y90-RE: Y90-radioembolization

Acknowledgements
Ricarda Seidensticker and Robert Damm contributed equally and share the first authorship.

Funding
The authors state that this work has not received any funding.

Availability of data and materials
All relevant data regarding the study conclusion are displayed in the publication. Raw data used and/or analysed during the study are available from the corresponding author on reasonable request.

Authors' contributions
RS and RD participated in the design of the study, carried out data analysis and statistical work, drafted the manuscript. JE helped in the organization of the study and performed data acquisition and interpretation. MS participated in the design of the study and helped to revise the manuscript. KM and PH participated in the data acquisition and data interpretation. MP and HA participated in the design of the study and performed data interpretation. JR participated in the design of the study, helped drafting the manuscript and carried out the final revision. All authors have given final approval for the manuscript and takes public responsibility.

Ethics approval and consent to participate
The study was conducted in accordance with the Declaration of Helsinki. All patients included were treated at a single institution, retrospective data collection and analysis was approved by the local ethics committee (Otto-von-Guericke University Magdeburg). All patients gave written informed consent for the collection of their medical data for scientific purposes.

Consent for publication
No personal information is included in the publication, thus no dedicated approval was required.

Competing interests
RS, MS, KM, HA, MP, JR have received lecture fees and/or travel grants from Sirtex Medical Europe.

Publisher's Note

Author details
[1]Department of Radiology, Ludwig-Maximilians-University Munich, Munich, Germany. [2]Department of Radiology and Nuclear Medicine, Otto-von-Guericke-University Magdeburg, Leipziger Str. 44, 39120 Magdeburg, Germany. [3]Diagnostic and Treatment Center Frankfurter Tor, Berlin, Germany. [4]Department of Radiation Oncology, Otto-von-Guericke-University Magdeburg, Berlin, Germany. [5]Department of Nuclear Medicine, Charite, Berlin, Germany. [6]Deutsche Akademie für Mikrotherapie e.V, Magdeburg, Germany.

Received: 26 June 2018 Accepted: 30 August 2018
Published online: 10 September 2018

References

1. Balducci L. Geriatric oncology: challenges for the new century. Eur J Cancer. 2000;36(14):1741–54.
2. Aapro MS, Kohne CH, Cohen HJ, Extermann M. Never too old? Age should not be a barrier to enrollment in cancer clinical trials. Oncologist. 2005;10(3):198–204.
3. Lewis JH, Kilgore ML, Goldman DP, Trimble EL, Kaplan R, Montello MJ, Housman MG, Escarce JJ. Participation of patients 65 years of age or older in cancer clinical trials. J Clin Oncol. 2003;21(7):1383–9.
4. Talarico L, Chen G, Pazdur R. Enrollment of elderly patients in clinical trials for cancer drug registration: a 7-year experience by the US Food and Drug Administration. J Clin Oncol. 2004;22(22):4626–31.
5. Basdanis G, Papadopoulos VN, Michalopoulos A, Fahantidis E, Apostolidis S, Berovalis P, Zatagias A, Karamanlis E. Colorectal cancer in patients over 70 years of age: determinants of outcome. Tech Coloproctol. 2004;8(Suppl 1):s112–5.
6. Etzioni DA, El-Khoueiry AB, Beart RWJ. Rates and predictors of chemotherapy use for stage III colon cancer: a systematic review. Cancer. 2008;113(12):3279–89.
7. Keating NL, Landrum MB, Klabunde CN, Fletcher RH, Rogers SO, Doucette WR, Tisnado D, Clauser S, Kahn KL. Adjuvant chemotherapy for stage III colon cancer: do physicians agree about the importance of patient age and comorbidity? J Clin Nutr. 2008;26(15):2532–7.
8. Daniele B, Croitoru A, Papandreou C, Bronowicki JP, Mathurin P, Serejo F, Stal P, Turnes J, Ratziu V, Bodoky G. Impact of sorafenib dosing on outcome from the European patient subset of the GIDEON study. Future Oncol. 2015;11(18):2553–62.
9. Nakayama G, Tanaka C, Uehara K, Mashita N, Hayashi N, Kobayashi D, Kanda M, Yamada S, Fujii T, Sugimoto H, et al. The impact of dose/time modification in irinotecan- and oxaliplatin-based chemotherapies on outcomes in metastatic colorectal cancer. Cancer Chemother Pharmacol. 2014;73(4):847–55.
10. Venderbosch S, Doornebal J, Teerenstra S, Lemmens W, Punt CJ, Koopman M. Outcome of first line systemic treatment in elderly compared to younger patients with metastatic colorectal cancer: a retrospective analysis of the CAIRO and CAIRO2 studies of the Dutch colorectal Cancer group (DCCG). Acta Oncol. 2012;51(7):831–9.
11. de Baere T, Tselikas L, Yevich S, Boige V, Deschamps F, Ducreux M, Goere D, Nguyen F, Malka D. The role of image-guided therapy in the management of colorectal cancer metastatic disease. Eur J Cancer. 2017;75:231–42.
12. Kennedy A, Cohn M, Coldwell DM, Drooz A, Ehrenwald E, Kaiser A, Nutting CW, Rose SC, Wang EA, Savin MA. Updated survival outcomes and analysis of long-term survivors from the MORE study on safety and efficacy of radioembolization in patients with unresectable colorectal cancer liver metastases. J Gastrointest Oncol. 2017;8(4):614–24.
13. Sangha BS, Nimeiri H, Hickey R, Salem R, Lewandowski RJ. Radioembolization as a treatment strategy for metastatic colorectal Cancer to the liver: what can we learn from the SIRFLOX trial? Curr Treat Options in Oncol. 2016;17(6):26.
14. Van Cutsem E, Cervantes A, Adam R, Sobrero A, Van Krieken JH, Aderka D, Aranda Aguilar E, Bardelli A, Benson A, Bodoky G, et al. ESMO consensus guidelines for the management of patients with metastatic colorectal cancer. Ann Oncol. 2016;27(8):1386–422.
15. Buscarini E, Savoia A, Brambilla G, Menozzi F, Reduzzi L, Strobel D, Hansler J, Buscarini L, Gaiti L, Zambelli A. Radiofrequency thermal ablation of liver tumors. Eur Radiol. 2005;15(5):884–94.
16. Lin ZY, Li GL, Chen J, Chen ZW, Chen YP, Lin SZ. Effect of heat sink on the recurrence of small malignant hepatic tumors after radiofrequency ablation. J Cancer Res Ther. 2016;12(Supplement):C153–8.
17. Peters N, Wieners G, Pech M, Hengst S, Ruhl R, Streitparth F, Lopez Hanninen E, Felix R, Wust P, Ricke J. CT-guided interstitial brachytherapy of primary and secondary lung malignancies: results of a prospective phase II trial. Strahlentherapie und Onkologie : Organ der Deutschen Rontgengesellschaft [et al]. 2008;184(6):296–301.
18. Collettini F, Singh A, Schnapauff D, Powerski MJ, Denecke T, Wust P, Hamm B, Gebauer B. Computed-tomography-guided high-dose-rate brachytherapy (CT-HDRBT) ablation of metastases adjacent to the liver hilum. Eur J Radiol. 2013;82(10):e509–14.
19. Ricke J, Wust P, Wieners G, Beck A, Cho CH, Seidensticker M, Pech M, Werk M, Rosner C, Hanninen EL, et al. Liver malignancies: CT-guided interstitial brachytherapy in patients with unfavorable lesions for thermal ablation. J Vasc Interv Radiol. 2004;15(11):1279–86.
20. Wieners G, Pech M, Rudzinska M, Lehmkuhl L, Wlodarczyk W, Miersch A, Hengst S, Felix R, Wust P, Ricke J. CT-guided interstitial brachytherapy in the local treatment of extrahepatic, extrapulmonary secondary malignancies. Eur Radiol. 2006;16(11):2586–93.
21. Ricke J, Mohnike K, Pech M, Seidensticker M, Ruhl R, Wieners G, Gaffke G, Kropf S, Felix R, Wust P. Local response and impact on survival after local ablation of liver metastases from colorectal carcinoma by computed tomography-guided high-dose-rate brachytherapy. Int J Radiat Oncol Biol Phys. 2010;78(2):479–85.
22. Jakobs TF, Hoffmann RT, Dehm K, Trumm C, Stemmler HJ, Tatsch K, La Fougere C, Murthy R, Helmberger TK, Reiser MF. Hepatic yttrium-90 radioembolization of chemotherapy-refractory colorectal cancer liver metastases. J Vasc Interv Radiol. 2008;19(8):1187–95.
23. Kennedy AS, Coldwell D, Nutting C, Murthy R, Wertman DE Jr, Loehr SP, Overton C, Meranze S, Niedzwiecki J, Sailer S. Resin 90Y-microsphere

brachytherapy for unresectable colorectal liver metastases: modern USA experience. Int J Radiat Oncol Biol Phys. 2006;65(2):412–25.
24. Charlson M, Szatrowski TP, Peterson J, Gold J. Validation of a combined comorbidity index. J Clin Epidemiol. 1994;47(11):1245–51.
25. Charlson ME, Pompei P, Ales KL, MacKenzie CR. A new method of classifying prognostic comorbidity in longitudinal studies: development and validation. J Chronic Dis. 1987;40(5):373–83.
26. Ouellette JR, Small DG, Termuhlen PM. Evaluation of Charlson-age comorbidity index as predictor of morbidity and mortality in patients with colorectal carcinoma. J Gastrointest Surg. 2004;8(8):1061–7.
27. Damm R, Seidensticker R, Ulrich G, Breier L, Steffen IG, Seidensticker M, Garlipp B, Mohnike K, Pech M, Amthauer H, et al. Y90 Radioembolization in chemo-refractory metastatic, liver dominant colorectal cancer patients: outcome assessment applying a predictive scoring system. BMC Cancer. 2016;16:509.
28. Jorgensen TL, Hallas J, Friis S, Herrstedt J. Comorbidity in elderly cancer patients in relation to overall and cancer-specific mortality. Br J Cancer. 2012;106(7):1353–60.
29. Sogaard M, Thomsen RW, Bossen KS, Sorensen HT, Norgaard M. The impact of comorbidity on cancer survival: a review. Clin Epidemiol. 2013;5(Suppl 1):3–29.
30. Lund CM, Vistisen KK, Dehlendorff C, Ronholt F, Johansen JS, Nielsen DL. The effect of geriatric intervention in frail elderly patients receiving chemotherapy for colorectal cancer: a randomized trial (GERICO). BMC Cancer. 2017;17(1):448.
31. Ostenfeld EB, Norgaard M, Thomsen RW, Iversen LH, Jacobsen JB, Sogaard M. Comorbidity and survival of Danish patients with colon and rectal cancer from 2000-2011: a population-based cohort study. Clin Epidemiol. 2013; 5(Suppl 1):65–74.
32. Solbiati L, Livraghi T, Goldberg SN, Ierace T, Meloni F, Dellanoce M, Cova L, Halpern EF, Gazelle GS. Percutaneous radio-frequency ablation of hepatic metastases from colorectal cancer: long-term results in 117 patients. Radiology. 2001;221(1):159–66.
33. Collettini F, Lutter A, Schnapauff D, Hildebrandt B, Puhl G, Denecke T, Wust P, Gebauer B. Unresectable colorectal liver metastases: percutaneous ablation using CT-guided high-dose-rate brachytherapy (CT-HDBRT). Rofo. 2014;186(6):606–12.
34. Seidensticker R, Denecke T, Kraus P, Seidensticker M, Mohnike K, Fahlke J, Kettner E, Hildebrandt B, Dudeck O, Pech M, et al. Matched-pair comparison of radioembolization plus best supportive care versus best supportive care alone for chemotherapy refractory liver-dominant colorectal metastases. Cardiovasc Intervent Radiol. 2012;35(5):1066–73.
35. Jehn CF, Boning L, Kroning H, Pezzutto A, Luftner D. Influence of comorbidity, age and performance status on treatment efficacy and safety of cetuximab plus irinotecan in irinotecan-refractory elderly patients with metastatic colorectal cancer. Eur J Cancer. 2014;50(7):1269-75.
36. Bakogeorgos M, Mountzios G, Kotsantis G, Economopoulou P, Fytrakis N, Kentepozidis N. Chemotherapy compliance, tolerance and efficacy in elderly and non-elderly patients with metastatic colorectal cancer: a single institution comparative study. J BUON. 2013;18(3):629–34.
37. Steele SR, Park GE, Johnson EK, Martin MJ, Stojadinovic A, Maykel JA, Causey MW. The impact of age on colorectal cancer incidence, treatment, and outcomes in an equal-access health care system. Dis Colon Rectum. 2014; 57(3):303–10.
38. Sarfati D, Gurney J, Lim BT, Bagheri N, Simpson A, Koea J, Dennett E. Identifying important comorbidity among cancer populations using administrative data: prevalence and impact on survival. Asia Pac J Clin Oncol. 2013;12(1):e47-56.

Cardiovasc Intervent Radiol (2019) 42:239–249
https://doi.org/10.1007/s00270-018-2127-5

CLINICAL INVESTIGATION INTERVENTIONAL ONCOLOGY

Radioablation by Image-Guided (HDR) Brachytherapy and Transarterial Chemoembolization in Hepatocellular Carcinoma: A Randomized Phase II Trial

Konrad Mohnike[1,11,12] · Ingo G. Steffen[2] · Max Seidensticker[3,12] · Peter Hass[4] · Robert Damm[1] · Nils Peters[11] · Ricarda Seidensticker[3,12] · Kerstin Schütte[5] · Jörg Arend[6] · Jan Bornschein[7] · Tina Streitparth[3] · Christian Wybranski[8] · Gero Wieners[3] · Patrick Stübs[9] · Peter Malfertheiner[10] · Maciej Pech[1,12] · Jens Ricke[3,12]

Received: 30 July 2018 / Accepted: 19 November 2018 / Published online: 28 November 2018

Abstract

Background and Aims The aim of this single-center, open-label phase II study was to assess the efficacy of image-guided high-dose-rate (HDR) brachytherapy (iBT) compared with conventional transarterial embolization (cTACE) in unresectable hepatocellular carcinoma.

Methods Seventy-seven patients were treated after randomization to iBT or cTACE, as single or repeated interventions. Crossover was allowed if clinically indicated. The primary endpoint was time to untreatable progression (TTUP). Eligibility criteria included a Child–Pugh score of ≤ 8 points, absence of portal vein thrombosis (PVT) at the affected liver lobe, and ≤ 4 lesions. Survival was analyzed by using the Cox proportional hazard model with stratification for Barcelona Clinic Liver Cancer (BCLC) stages.

✉ Konrad Mohnike
konrad.mohnike@berlin-dtz.de

Ingo G. Steffen
Ingo.Steffen@charite.de

Max Seidensticker
Max.Seidensticker@med.uni-muenchen.de

Peter Hass
Peter.Hass@med.ovgu.de

Robert Damm
Robert.Damm@med.ovgu.de

Nils Peters
nils.peters@berlin-dtz.de

Ricarda Seidensticker
Ricarda.Seidensticker@med.uni-muenchen.de

Kerstin Schütte
Kerstin.Schuette@mho.de

Jörg Arend
Joerg.Arend@med.ovgu.de

Jan Bornschein
janbornschein@ouh.nhs.uk

Tina Streitparth
tina.streitparth@med.uni-muenchen.de

Christian Wybranski
Christian.Wybranski@uk-koeln.de

Patrick Stübs
p.stuebs@drk-kliniken-berlin.de

Peter Malfertheiner
Peter.Malferthainer@med.ovgu.de

Maciej Pech
Maciej.Pech@med.ovgu.de

Jens Ricke
Jens.Ricke@med.uni-muenchen.de

[1] Department of Radiology and Nuclear Medicine, University of Magdeburg, Leipziger Str.44, 39120 Magdeburg, Germany

[2] Department of Radiology, Charité, Berlin, Germany

[3] Department of Radiology, Luwig-Maximilians-University Munich, Munich, Germany

[4] Department of Radiotherapy, University of Magdeburg, Magdeburg, Germany

[5] Nils-Stensen-Hospital, Osnabrueck, Germany

[6] Department of Surgery, University of Magdeburg, Magdeburg, Germany

[7] Translational Gastroenterology Unit, Oxford University Hospitals, Oxford, UK

[8] Department of Radiology, University Hospital of Cologne, Cologne, Germany

[9] DRK-Hospital Berlin-Koepenick, Berlin, Germany

Results Twenty patients were classified as BCLC-A (iBT/cTACE 8/12), 35 as BCLC-B (16/19), and 22 as BCLC-C (13/9). The 1-, 2-, and 3-year TTUP probabilities for iBT compared with cTACE were 67.5% versus 55.2%, 56.0% versus 27.4%, and 29.5% versus 11.0%, respectively, with an adjusted hazard ratio (HR) of 0.49 (95% confidence interval 0.27–0.89; $p = 0.019$). The 1-, 2-, and 3-year TTPs for iBT versus cTACE were 56.0% versus 28.2%, 23.9% versus 6.3%, and 15.9% versus 6.3%, respectively, with an adjusted HR of 0.49 (0.29–0.85; $p = 0.011$). The 1-, 2-, and 3-year OS rates were 78.4% versus 67.7%, 62.0% versus 47.3%, and 36.7% versus 27.0%, respectively, with an adjusted HR of 0.62 (0.33–1.16; $p = 0.136$).
Conclusions This explorative phase II trial showed a superior outcome of iBT compared with cTACE in hepatocellular carcinoma and supports proceeding to a phase III trial.

Keywords Ablation · Liver cancer · BCLC · HCC · RCT

Abbreviations

AASL	American Association for the Study of the Liver
BCLC	Barcelona Clinic Liver Cancer (staging system)
CI	Confidence interval
CLIP	Cancer of the Liver Italian Program
CT	Computed tomography
cTACE	Conventional transarterial chemoembolization
CTCAE	Common Terminology Criteria for Adverse Events
DEB-TACE	Drug-eluting beads transarterial chemoembolization
EASL	European Association for the Study of the Liver
HCC	Hepatocellular carcinoma
HDR	High dose rate
HR	Hazard ratio
iBT	Interstitial brachytherapy
OS	Overall survival
PVT	Portal vein thrombosis
RFA	Radiofrequency ablation
SBRT	Stereotactic body radiotherapy
TTP	Time to progression
TTUP	Time to untreatable progression

[10] Department of Gastroenterology, Hepatology and Infectiology, University of Magdeburg, Magdeburg, Germany

[11] Diagnostisch Therapeutisches Zentrum am Frankfurter Tor, Berlin, Germany

[12] Deutsche Akademie für Mikrotherapie e.V., Magdeburg, Germany

Introduction

In Europe, five-year survival rates of up to 51% have been shown for hepatocellular carcinoma (HCC) suitable for resection [1]. Unfortunately, 70–80% of patients are not candidates for resection, because of advanced cirrhosis, multiple lesions or diffuse tumor growth, and comorbidity. Liver transplantation is the only potentially curative option at present, with five-year post-transplantation survival rates of up to 70% for patients in early stages of disease [2]. The treatment of choice in the intermediate stage is transarterial chemoembolization ('conventional TACE' = cTACE; 'drug-eluting beads TACE' = DEB-TACE). In clinical practice, TACE is also applied in BCLC (Barcelona Clinic Liver Cancer stage)-A patients, often as an adjunct to radiofrequency ablation (RFA), and in BCLC-C patients, for whom sorafenib-only treatment is not considered appropriate [3–6]. However, effectiveness and feasibility of TACE are limited by factors such as advanced-stage cirrhosis, a hampered general condition and portal vein invasion. In ipsilateral complete portal vein thrombosis (PVT), TACE is known to be associated with a risk of ischemia and abscess formation. Thermal ablation is usually considered up to a tumor size of 3 cm. Beyond this limit, local recurrence rates increase [7, 8]. Some authors state the superiority of Gelaspon particles over Lipiodol for embolization purposes [9]. A recently invented method, CT (computed tomography)-guided interstitial HDR (high-dose-rate) brachytherapy (iBT), has successfully been used in various neoplasms of the liver and other sites [10–18]. As a unique feature, iBT is not restricted by tumor size or heat sink effect and PVT is not a contraindication [19–22].

A recent study encouraged us to address the clinical value of iBT as compared with standard treatment such as TACE in a future trial. A major intention of this explorative type II study was to investigate whether proceeding to phase III trial is supported [11].

Patients and Methods

Patient Population and Eligibility Criteria

Patient recruitment took place from October 2006 to September 2010. Patients with a diagnosis of HCC were randomized to receive either CT-guided HDR iBT or cTACE. Inclusion criteria were:

- Diagnosis of HCC by histopathology or according to the criteria of the Consensus Conference of the European Association for the Study of Liver Disease
- Unresectable HCC
- Karnofsky Index > 70
- Estimated life expectancy > 16 weeks
- Adequate bone marrow function
- Adequate contraception for female patients
- Informed consent

Exclusion criteria were as follows:

- PVT on the tumor side
- Extrahepatic spread
- Child C
- Other untreated malignant diseases
- General contraindication for chemotherapy
- Active infectious disease
- Neuropathy, platin-allergy
- Pregnancy

All patients were rated unresectable and not eligible for radiofrequency ablation owing to lesion size and/or location.

All patients received a full clinical status evaluation at inclusion, comprising a physical examination, extensive laboratory assessments, whole-body computed tomography, and MRI of the liver (Fig. 1).

Study Design

The study represents an exploratory randomized phase II approach comparing two interventional treatment arms. The study was registered at clinicaltrials.gov (NCT00807300), and the study protocol conformed with the Declaration of Helsinki. The institutional review board approved the study, and informed consent was obtained from all patients. This explorative phase II study analyzes the efficacy and safety of iBT in comparison with cTACE and aims to generate a hypothesis for a potential phase III study. A high type I error of 20% was allowed to keep patient numbers reasonable, and the sample size was set to 80 including a dropout rate of 10% [23]. Owing to slower patient accrual the trial was closed with a lower patient number than anticipated. However, the minimum target sample size (without dropouts) was achieved.

Patients meeting the inclusion criteria were randomly assigned to first treatment either with cTACE (control arm) or with iBT (experimental arm). Simple randomization was performed allocating patients sequentially to treatment groups using shuffled sealed opaque envelopes containing equal numbers of identifiers for treatment A and treatment B. After untreatable progression had been reached, any further treatment decisions were left to the investigator's judgment.

The primary endpoint was the time to untreatable progression (TTUP), defined as the time from the first treatment (either iBT or cTACE) to the time point when complete tumor ablation could not be repeated any further by applying the assigned method. The criteria for stopping the assigned treatment were as follows:

- No radiological response at follow-up/local failure
- Diffuse progression (> 3 new lesions)
- Chronic hepatic decompensation, as defined by a Child–Pugh score deterioration of $\geq$ 2 points
- Clinical conditions other than hepatic decompensation, permanently precluding further treatment (e.g., performance status).

Technique-associated no-go criteria possibly occurring during follow-up, such as failure of Lipiodol to accumulate in the lesion, missing angiographic visibility, development of ipsilateral PVT, development of an arterioportal shunt visible by angiography (all cTACE), or contraindications to a percutaneous interstitial approach (only iBT, including severe coagulopathy and uncontrolled ascites), were not counted, in order to ensure that the criteria for TTUP were the same in the two groups. The corresponding time points were censored.

Secondary endpoints were time to progression (TTP) and overall survival (OS).

Interstitial HDR Brachytherapy (iBT)

The technique of CT-guided brachytherapy has been described in detail elsewhere [18, 19]. We performed irradiation employing the HDR brachytherapy technique based on a 10-Ci Iridium-192 source. Positioning of the brachytherapy catheters was performed by fluoroscopy CT. For analgosedation, fentanyl and midazolam were used according to individual requirement.

The target dose was defined as the minimum dose taken up by the visible tumor margin. We prescribed a minimum target dose of 15 Gy, based on the results of two pilot studies [20, 21].

Transarterial Chemoembolization (cTACE)

After puncture of the right or left femoral artery, an angiography of the celiac artery and superior mesenteric artery via a 4F catheter was performed. Parasitic feeders to HCC lesions were searched for with the same catheter. Chemoembolization was conducted in a supraselective manner with a 3F microcatheter, applying the drug/oil emulsion over the feeding arteries of the tumor only. Typically, 30–50 mg/m^2 doxorubicin and cisplatin mixed

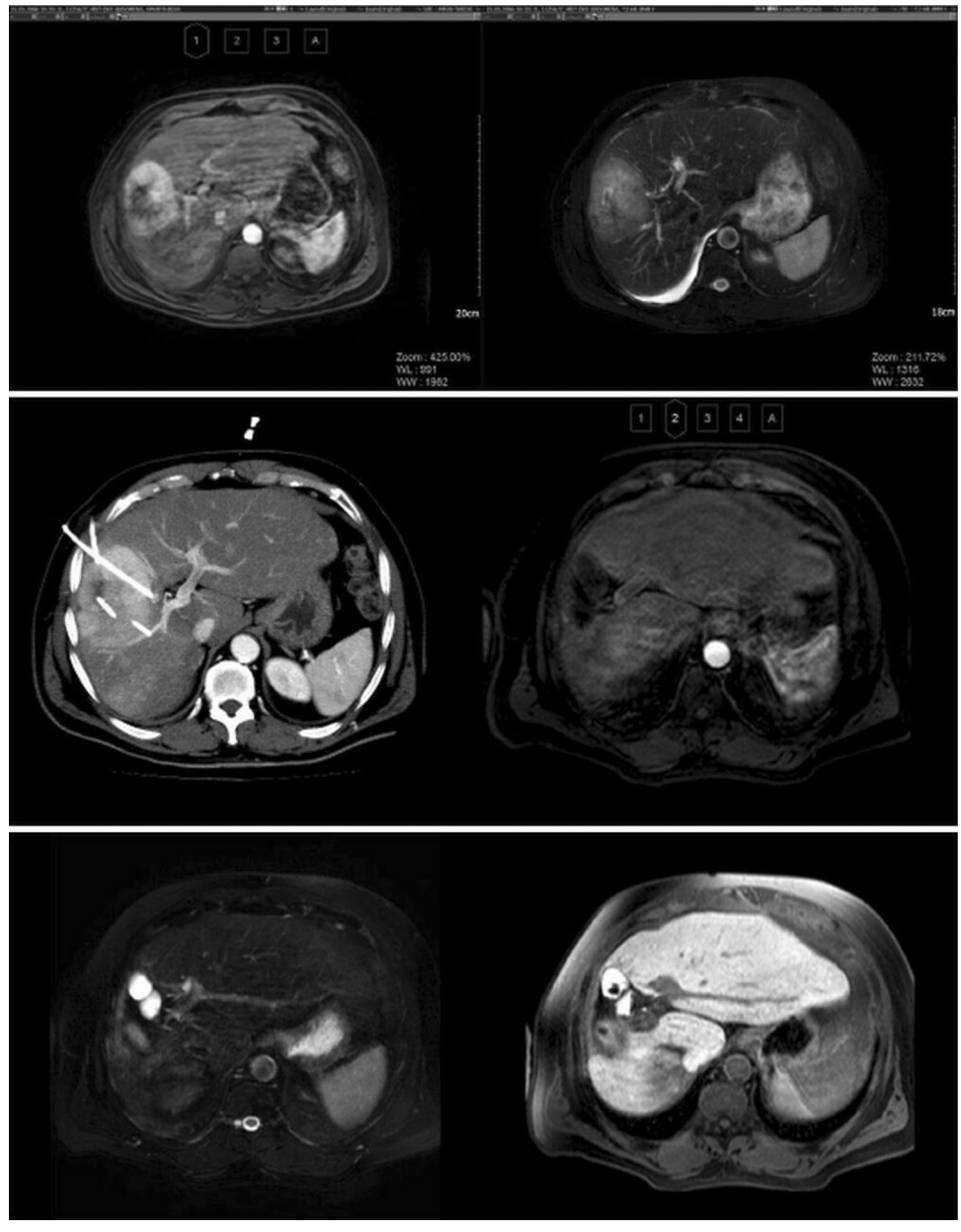

Fig. 1 Complete remission of a single hepatocellular carcinoma (8.3 cm) of the right liver lobe. The patient refused surgery. Upper row: before treatment, arterial phase (left) and T2 FS (right), May 2006. Middle row: Left: catheter placement during treatment. Right: arterial phase, June 2014. Bottom row: left: T2 FS. Right: T1 WATS late contrast phase (GD-EOB-DTPA). Note the completely ablated segment with prolapsed intestinal loops

with Lipiodol were administered. If the total tumor volume or tumor count could not be embolized in one session, the procedure was repeated after 6 weeks.

Assessments

Before therapy a physical examination, MRI and computed tomography (CT) scans, and laboratory tests were performed. These examinations were repeated every 3 months. Clinical evaluators (two experienced radiologists, consensus decision) were blinded to the chosen treatment.

Since the mRECIST criteria for tumor response had not been established for HCC in 2006, TTP was likewise assessed by following the recommendations of the European Association for the Study of the Liver (EASL) and American Association for the Study of the Liver (AASL) [24, 25].

Patients were censored at the time point of liver transplantation, liver resection, or crossover treatment. After untreatable progression (the primary endpoint TTUP) had been reached, any further treatment decisions were left to the investigator's judgment.

Statistical Methods

The program suite IBM SPSS Statistics 22.0 and R version 3.1.3 (The R Foundation for Statistical Computing, Vienna, Austria) were used for statistical analysis.

Metric parameters are described using median and interquartile range (25th–75th percentile), and the Mann–Whitney U test was used for analyzing differences between unpaired groups. Categorical variables were analyzed by using contingency tables, the Chi-square test and Fisher's exact test.

The observation period was 5 years. Patients were censored at crossover treatment, at loss to follow-up, and at the end of observation period. TTUP, TTP, and OS were estimated by the Kaplan–Meier (KM) method, and the Cox proportional hazard model was used to assess the association of TTUP, TTP, and OS with covariates. Parameters with p value ≤ 0.1 in univariate Cox regression were included in a multivariate Cox proportional hazard analysis. The multivariate model was optimized by using the Akaike information criterion with stepwise backward elimination. Analysis was performed on an intention-to-treat (ITT) basis (TTP, TTUP, and OS) and 'as treated' (safety). The Cox proportional hazard model was stratified for BCLC stages, as this parameter did not satisfy the proportional hazard assumption, which was assessed visually from log–log KM curves. Significance was assumed at a p value less than 0.05.

Results

Patients

In total, 392 patients were assessed for eligibility from October 2006 to September 2010. Of these patients 203 did not meet the inclusion criteria, 68 declined to participate, and 44 were excluded for other reasons. Of the remaining 77 patients 40 were randomly assigned to the cTACE group and 37 patients to the iBT group. Two patients allocated to receive cTACE were transferred to the iBT group for technical reasons. Thus, the per-protocol population comprised 38 patients in the cTACE group and 39 patients in the iBT group (Fig. 2).

Among the 77 enrolled patients (13 females and 64 males; mean age 68.5 years; range 43.4–82.7 years), in 34 patients, HCC was confirmed by biopsy (44%), whereas in 43 patients with cirrhosis, HCC was diagnosed on the basis of noninvasive criteria according to the EASL and AASL guidelines [24, 25]. Patient characteristics are summarized in Table 1.

Treatments and Follow-up

The number of treatments per patient was significantly lower in the iBT group (2.5 ± 1.6) compared with the cTACE group (4.0 ± 3.2, $p = 0.039$). Subsequent treatments after the end-of-study date are shown in Table 2.

In 8 of the 38 patients in the cTACE group, treatment had to be stopped for technique-related reasons such as AV shunts or ipsilateral PVT. Owing to missing visibility in CT or MRI, treatment had to be stopped in a patient with AFP recurrence in the iBT group. The difference was statistically significant (Chi-square test, $p = 0.012$).

During the 5-year observation period 52 patients died (iBT, $n = 31$; cTACE, $n = 21$) and 15 patients were censored because of crossover treatment after reaching

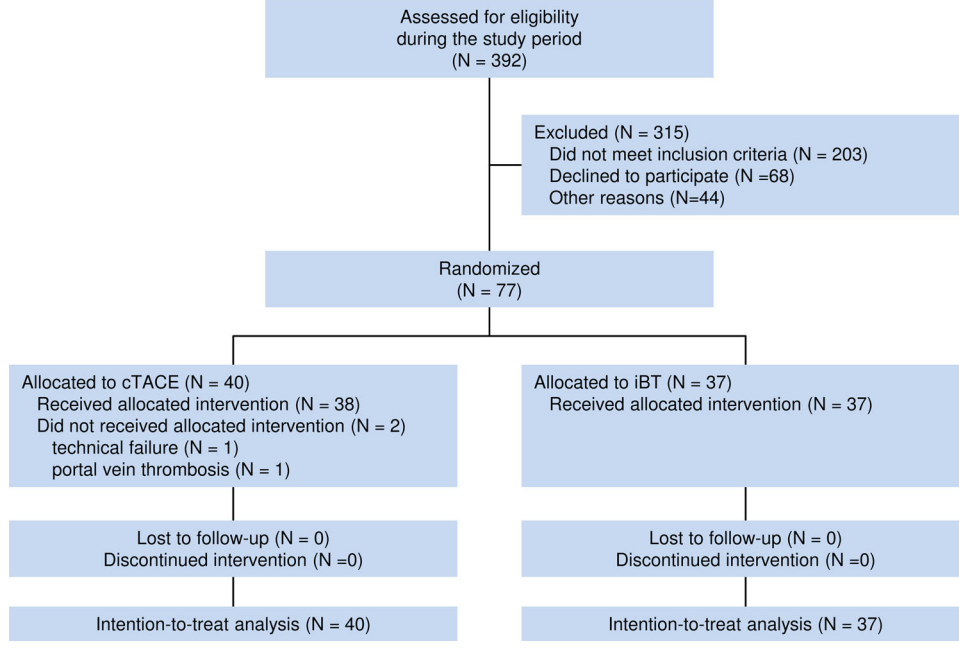

Fig. 2 CONSORT diagram for the trial

Table 1 Baseline patient characteristics

Characteristic	iBT (n = 37)	cTACE (n = 40)	p
Age at study inclusion (years), mean ± SD	69.3 ± 7.4	67.7 ± 9.0	0.419
Sex			0.881
Male	31 (84%)	33 (83%)	
Female	6 (16%)	7 (17%)	
Pretreatment AFP (ng/ml), median (IQR)	13 (4–258)	12 (5–83)	0.842
Pretreatment bilirubin (μmol/l), median (IQR)	12.2 (9.9–15.7)	18.9 (11.4–28.9)	**0.007**
Number of lesions, median (IQR)	2 (1–3)	2 (1–3)	0.466
Longest diameter (cm), median (IQR)	4.5 (3.0–6.5)	3.6 (2.1–6.6)	0.359
BCLC stage			0.434
A	8 (22%)	12 (30%)	
B	16 (43%)	19 (48%)	
C	13 (35%)	9 (22%)	
Child–Pugh class			0.194
A	36 (97%)	36 (90%)	
B	1 (3%)	4 (10%)	
Cirrhosis			0.388
Yes	32 (87%)	37 (93%)	
No	5 (13%)	3 (7%)	
HCC diagnosis			0.539
Biopsy	15 (40%)	19 (47%)	
Noninvasive	22 (60%)	21 (53%)	
Etiology			0.416
Alcohol abuse	13 (35%)	17 (42.5%)	
Nonalcoholic steatohepatitis	10 (27%)	7 (17.5%)	
Hepatitis C	7 (19%)	6 (15%)	
Hepatitis C + alcohol abuse	0	1 (2.5%)	
Hepatitis B	2 (5.5%)	0	
Hemochromatosis	0	2 (5%)	
Primary biliary cirrhosis	0	1 (2.5%)	
Cryptogenic	5 (13.5%)	6 (15%)	
Pretreatments			0.725
Untreated	31 (83.8%)	35 (87.5%)	
Resection	1 (2.7%)	2 (5%)	
Resection + sorafenib	1 (2.7%)	0	
Radiofrequency ablation	1 (2.7%)	1 (2.5%)	
Percutaneous ethanol installation	1 (2.7%)	0	
Sorafenib	1 (2.7%)	1 (2.5%)	
Resect. + percutaneous ethanol installation	1 (2.7%)	0	
Systemic therapy other than sorafenib	0	1 (2.5%)	

Bold value indicates $p < 0.05$

untreatable progression (14 patients of the cTACE arm received iBT and 1 patient in the iBT arm received cTACE) at a mean follow-up time of 15.5 months (SD 9.3 months; range 3.1–38.5 months). Of the remaining 10 patients 6 were still alive at the end of the 5-year observation period and the mean follow-up time was 41.2 months (SD 24.6 months; range 4.9–60 months).

Survival

The 1-, 2-, and 3 year TTUP survival rates for the iBT compared with the cTACE group were 67.5% versus 55.2%, 56.0% versus 27.4%, and 29.5% versus 11.0%, respectively, with an HR of 0.52 (0.30–0.90; $p = 0.021$; Fig. 3A). Stratifying by BCLC stages revealed an HR of 0.92 (95% CI 0.31–2.72; $p = 0.887$) for BCLC-A, 0.38 (95% CI 0.16–0.87; $p = 0.021$) for BCLC-B, and 0.51

Table 2 Treatment characteristics

	iBT (n = 37)	**cTACE** (n = 40)	p
Number of treatments before untreatable progression, mean ± SD	2.5 ± 1.6	4.0 ± 3.2	**0.039**
TTUP: dominant terminating events			
Diffuse progression	18 (48.6%)	13 (32.5%)	0.953
Hepatic decompensation	3 (8.1%)	4 (10.0%)	0.544
Performance status	3 (8.1%)	3 (7.5%)	0.699
Local failure	0	2 (5.0%)	0.267
Death	7 (18.9%)	6 (15%)	0.777
Subsequent therapies			
Liver transplantation	1 (2.7%)	4 (10%)	0.204
Resection	0	1 (2.5%)	0.519
Radiofrequency ablation (RFA)	1 (2.7%)	1 (2.5%)	0.772
Radioembolization	4 (10.8%)	5 (12.5%)	0.551
Systemic therapy with sorafenib	13 (35.1%)	13 (32.5%)	0.686
Crossover treatment	1 (2.7%)	14 (35%)	**< 0.001**

Bold values indicate $p < 0.05$

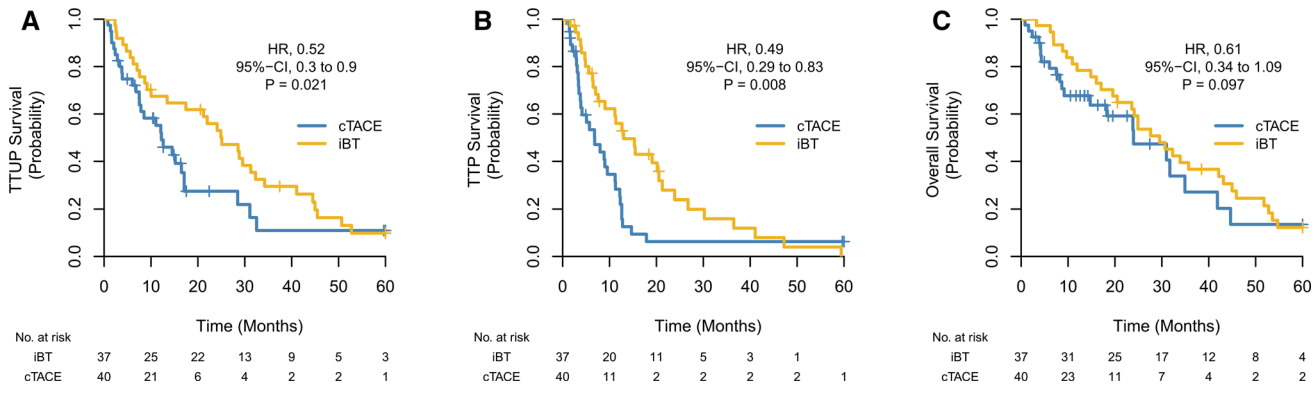

Fig. 3 Kaplan–Meier curves depicting time to untreatable progression (**A**), time to progression (**B**), and overall survival (**C**)

(95% CI 0.18–1.42; $p = 0.195$) for BCLC-C (Fig. 4). Further significant influencing factors were female gender (HR = 3.31; $p = 0.001$), AFP (unit: µg/ml; HR = 1.08; $p = 0.038$), Child–Pugh score B (HR = 3.91; $p = 0.018$), and pretherapeutic bilirubin > 19 µmol/l (HR = 2.03; $p = 0.024$). Near-significance was observed for lesion diameter > 5 cm (HR = 1.82; $p = 0.057$) and the number of lesions > 2 (HR = 1.77; $p = 0.056$). The multivariate Cox regression model included female gender (HR = 4.21, $p < 0.001$), iBT arm (HR = 0.49, $p = 0.019$), the number of lesions > 2 (HR = 1.80, $p = 0.069$), AFP (unit:µg/ml; HR = 1.13, $p = 0.001$), and Child–Pugh score B (HR = 3.81; $p = 0.036$).

The 1-, 2-, and 3-year TTP survival rates for iBT compared with cTACE were 56.0% versus 28.2%, 23.9% versus 6.3%, and 15.9% versus 6.3%, respectively, with a univariate HR of 0.49 (0.29–0.83; $p = 0.008$; Fig. 3B). Stratifying by BCLC stage revealed an HR of 0.68 (95% CI 0.26–1.77; $p = 0.430$) for BCLC-A, 0.46 (95% CI 0.21–1.00; $p = 0.051$) for BCLC-B, and 0.36 (95% CI 0.13–1.06; $p = 0.063$) for BCLC-C (Fig. 4). Further significant factors in univariate Cox regression were Child–Pugh score (HR = 3.33; $p = 0.031$) and pretherapeutic bilirubin > 19 µmol/l (HR = 1.86; $p = 0.042$). Near-significance was observed for age (unit: 10 years; HR = 0.74; $p = 0.070$), the number of lesions > 2 (HR = 1.73; $p = 0.060$), and AFP (unit: µg/mol; HR = 1.08; $p = 0.058$). The multivariate Cox regression model included age (unit: 10 years; HR = 0.78; $p = 0.130$), iBT (HR = 0.49, $p = 0.011$), AFP (unit: µg/mol; HR = 1.08; $p = 0.063$), and Child–Pugh score (HR = 3.12; $p = 0.045$).

The 1-, 2-, and 3-year overall survival rates in the iBT compared with the TACE group were 78.4% versus 67.7%, 62.0% versus 47.3%, and 36.7% versus 27.0%, respectively, with a univariate HR of 0.61 (0.34–1.09; $p = 0.097$; Fig. 3C). Stratifying by BCLC stage revealed an HR of

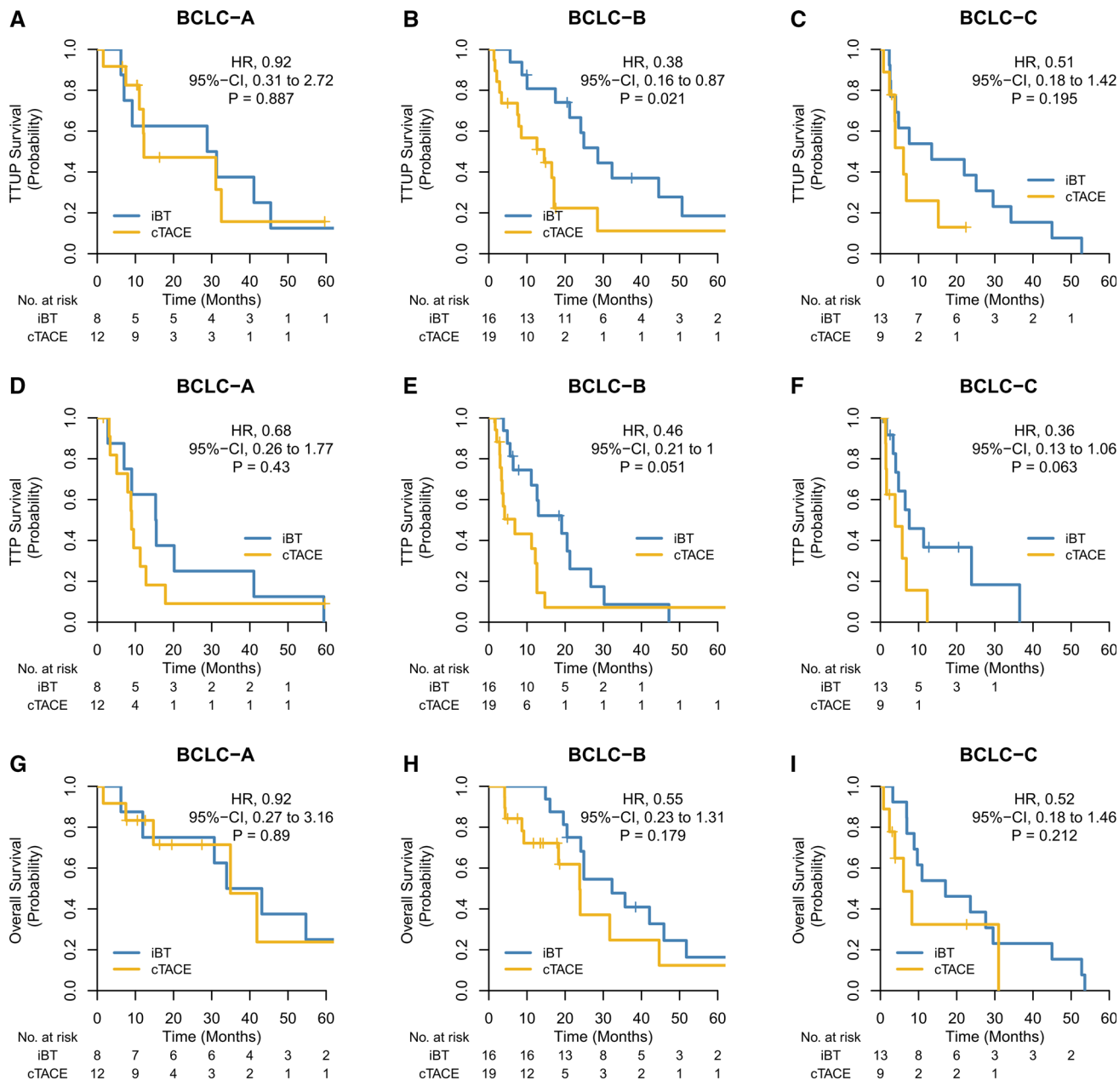

Fig. 4 Kaplan–Meier curves of time to untreatable progression (upper row), time to progression (middle row), and overall survival (lower row) stratified by BCLC (**A** left-hand column; **B** middle column; **C** right-hand column)

0.92 (95% CI 0.27–3.16; $p = 0.890$) for BCLC-A, 0.55 (95% CI 0.23–1.31; $p = 0.179$) for BCLC-B, and 0.52 (95% CI 0.18–1.46; $p = 0.212$) for BCLC-C. The univariate Cox regression model revealed female gender (HR = 2.88, $p = 0.006$), AFP (unit: µg/mol; HR = 1.12; p = 0.004), Child–Pugh score (HR = 6.19; $p = 0.002$), and pretherapeutic bilirubin > 19 µmol/l (HR = 3.33; $p < 0.001$) as significant factors and the number of lesions > 2 (HR = 1.68; $p = 0.089$) as a factor showing close significance. The multivariate Cox regression model for OS comprised female gender (HR = 3.46, $p = 0.002$), iBT (HR = 0.62; $p = 0.136$), the number of lesions > 2 (HR = 1.86; $p = 0.061$), AFP (unit: µg/mol; HR = 1.17; $p < 0.001$), and Child–Pugh score (HR = 5.76, $p = 0.006$; Table 3).

Safety (as Treated) and 30-day Mortality (as Treated)

For complications and 30-day mortality, see Table 4.

Table 3 Univariate and multivariate Cox regression for TTUP, TTP, and OS

Variable	Univariate			Multivariate		
	HR	95%-CI	*P*	HR	95%-CI	*p*
TTUP						
Age (unit: 10 years)	0.99	0.72–1.37	0.963			
Gender (female)	3.31	1.64–6.72	**0.001**	4.21	2.03–8.73	**<0.001**
ITT group (iBT)	0.52	0.30–0.90	**0.021**	0.49	0.27–0.89	**0.019**
Lesion diameter > 5 cm	1.82	0.98–3.39	*0.057*			
Number of lesions > 2	1.77	0.99–3.18	*0.056*	1.80	0.96–3.39	*0.069*
AFP (unit: µg/ml)	1.08	1.00–1.16	**0.038**	1.13	1.05–1.22	**0.001**
Child–Pugh score B	3.91	1.27–12.1	**0.018**	3.81	1.09–13.3	**0.036**
Bilirubin, pretherapeutic > 19 µmol/l[a]	2.03	1.10–3.74	**0.024**			
TTP						
Age (unit: 10 years)	0.74	0.53–1.03	0.070	0.78	0.56–1.08	0.130
Gender (female)	1.80	0.84–3.85	0.128			
ITT group (iBT)	0.49	0.29–0.83	**0.008**	0.49	0.29–0.85	**0.011**
Lesion diameter > 5 cm	1.11	0.60–2.07	0.730			
Number of lesions > 2	1.73	0.98–3.06	*0.060*			
AFP (unit: µg/ml)	1.08	1.00–1.16	*0.058*	1.08	1.00–1.16	*0.063*
Child–Pugh score B	3.33	1.11–10.0	**0.031**	3.12	1.02–9.53	**0.045**
Bilirubin, pretherapeutic > 19 µmol/l[a]	1.86	1.02–3.38	**0.042**			
OS						
Age (unit: 10 years)	1.13	0.79–1.60	0.506			
Gender (female)	2.88	1.35–6.12	**0.006**	3.46	1.59–7.54	**0.002**
ITT group (iBT)	0.61	0.34–1.09	0.097	0.62	0.33–1.16	0.136
Lesion diameter > 5 cm	1.51	0.78–2.93	0.226			
Number of lesions > 2	1.68	0.92–3.07	0.089	1.86	0.97–3.57	*0.061*
AFP (unit: µg/ml)	1.12	1.04–1.21	**0.004**	1.17	1.08–1.26	< 0.001
Child–Pugh score B	6.19	1.90–20.1	**0.002**	5.76	1.65–20.1	**0.006**
Bilirubin, pretherapeutic > 19 µmol/l[a]	3.33	1.72–6.44	**< 0.001**			

Bold values indicate $p < 0.05$

Italic values indicate $p > 0.05$ and $p < 0.07$

[a]Bilirubin was excluded from multivariate analysis because of significant association with Child–Pugh score

Discussion

The intention of this exploratory, randomized, phase II study was to assess the efficacy and safety of iBT in comparison with the standard treatment modality (cTACE) in order to decide whether a multicentric phase III study is justified.

The adjusted hazard ratio of 0.49, as observed both for the primary endpoint TTUP and for the secondary endpoint TTP, is convincing. The adjusted hazard ratio for OS was 0.62 for the entire study group, which also indicates a possible superiority of iBT compared with cTACE. A higher overall survival effect size was observed in patients with BCLC-B (HR = 0.55) and BCLC-C (HR = 0.52), whereas iBT showed no superiority in patients with BCLC-A (HR = 0.92).

In two reported randomized trials of TACE with positive outcome, repetitive TACE was found to have benefit in terms of OS [26, 27]. Consequently, recent TACE trials such as the TACE–sorafenib combination trial SPACE employed TTUP as a secondary endpoint [28]. Some of the conditions preventing TACE—such as the development of PVT or technical failure of TACE indicated by failed uptake of Lipiodol in hypoperfused tumors—do not influence the applicability or the therapeutic effect of iBT [26, 27]. However, these technique-inherent conditions did not apply in the final TTUP analysis.

Results of the PRECISION V study demonstrated better tolerability of DEB-TACE in comparison with conventional TACE [29]. However, since that study did not demonstrate any effect on survival or treatment duration by the choice of the TACE technique, we do not consider that any negative bias was introduced by the use of

Table 4 Adverse events (as treated)

	iBT (n = 120)	cTACE (n = 163)	p
CTCAE ≥ grade III			
BCLC-A	1 (0.8%)	1 (0.6%)	
BCLC-B	2 (1.7%)	5 (3.1%)	
BCLC-C	4 (3.3%)	3 (1.8%)	
Sum	7 (5.8%)	9 (5.5%)	1
CTCAE grade III/IV			
Liver decompensation	3 (2.5%)	3 (1.8%)	
Hepatic abscess treated with drainage and antibiotics	1 (0.8%)	1 (0.6%)	
Partial liver infarction with symptomatic treatment	0	1 (0.6%)	
Cholangitis	0	1 (0.6%)	
Subcapsular hematoma causing hemodynamic shock treated by blood transfusion	1 (0.8%)	0	
Aplastic anemia caused by perchlorate medication	1 (0.8%)	0	
Sum	6 (5.0)	6 (3.7%)	0.767
Mortality within 30 days			
Urinary tract infection and consecutive sepsis	1	0	
Hepatic decompensation	0	1	
Sepsis	0	1	
Brain metastasis leading to status epilepticus	0	1	
Sum	1 (0.8%)	3 (1.8%)	0.640

conventional, Lipiodol-based TACE in our trial (which had been designed before DEB-TACE was established).

In Europe, the recommended application criterion for TACE is BCLC-B with up to 7 points [30]. As outlined previously, favorable results of iBT in our study were evident in patients inside the established range of TACE indications (BCLC-B). In patients with BCLC-A the iBT treatment showed no clinically relevant effect compared with cTACE, with a hazard ratio of 0.83 for TTUP and 0.92 for overall survival. This may have been due to the relatively high efficacy and safety of cTACE in small tumors and small tumor numbers. In contrast, in patients with BCLC-B and BCLC-C a substantial benefit of iBT over cTACE can be assumed regarding the respective hazard ratios for TTUP, TTP, and OS. Assuming an effect size of 0.55, an event probability of 65%, an alpha error of 0.01, and the power to 90%, the sample size required for a phase III study would be 136 per group, respectively.

Because of the exploratory character of this study and the correspondingly small sample size, the confidence intervals of the observed hazard ratios are large and the level of significance was not reached for OS. However, it has to be emphasized that the type I error of a randomized phase II trial is typically high, in the range of 10–20%, to keep patient numbers reasonable, whereas the crucial parameter for a decision to proceed to a phase III trial is the observed effect size [23]. The stratification concerning BCLC stages was not planned prospectively, and thus, the subgroup analyses demonstrating a greater effect in BCLC-B/BCLC-C compared with BCLC-A have to be evaluated critically, especially on account of the small sample size in the subgroups. However, we consider that this stratification may be justified, as the proportional hazard assumption was not satisfied for BCLC stages.

Conclusion

This explorative phase II trial showed a superior outcome of iBT compared with cTACE in HCC, notably in patients with BCLC-B/ BCLC-C and supports proceeding to a phase III trial.

Funding This study was funded exclusively by the University of Magdeburg.

Compliance with Ethical Standards

Conflict of interest The authors declare that they have no conflict of interest.

Ethical Approval All procedures performed in studies involving human participants were in accordance with the ethical standards of the institutional and/or national research committee and with the 1964 Declaration of Helsinki and its later amendments or comparable ethical standards.

Informed Consent Informed consent was obtained from all individual participants included in the study.

Consent for Publication Consent for publication was obtained for every individual person's data included in the study.

Financial Support This work was funded exclusively by the University of Magdeburg.

Ethical Considerations The study was conducted in accordance with the protocol, the ethical principles that have their origin in the Declaration of Helsinki, and ICH-GCP. The study protocol and all study-related documentation were approved by all relevant authorities (Ethics Committee of the Medical Faculty, University of Magdeburg, 44/06).

References

1. Jaeck D, Bachellier P, Oussoultzoglou E, Weber JC, Wolf P. Surgical resection of hepatocellular carcinoma. Post-operative outcome and long-term results in Europe: an overview. Liver Transpl. 2004;10:S58–63.
2. Forner A, Reig M, Bruix J. Hepatocellular carcinoma. Lancet. 2018;391:1301–14.
3. Cheng BQ, Jia CQ, Liu CT, et al. Chemoembolization combined with radiofrequency ablation for patients with hepatocellular carcinoma larger than 3 cm: a randomized controlled trial. JAMA. 2008;299:1669–77.
4. Helmberger T, Dogan S, Straub G, et al. Liver resection or combined chemoembolization and radiofrequency ablation improve survival in patients with hepatocellular carcinoma. Digestion. 2007;75:104–12.
5. Llovet JM, Bruix J. Systematic review of randomized trials for unresectable hepatocellular carcinoma: chemoembolization improves survival. Hepatology. 2003;37:429–42.
6. Vogl TJ, Naguib NN, Nour-Eldin NE, et al. Review on transarterial chemoembolization in hepatocellular carcinoma: palliative, combined, neoadjuvant, bridging, and symptomatic indications. Eur J Radiol. 2009;72:505–16.
7. Cucchetti A, Piscaglia F, Cescon M, Ercolani G, Pinna AD. Systematic review of surgical resection vs radiofrequency ablation for hepatocellular carcinoma. World J Gastroenterol. 2013;19:4106–18.
8. Cucchetti A, Piscaglia F, Cescon M, et al. An explorative data-analysis to support the choice between hepatic resection and radiofrequency ablation in the treatment of hepatocellular carcinoma. Dig Liver Dis. 2014;46:257–63.
9. Takayasu K, Arii S, Ikai I, et al. Overall survival after transarterial lipiodol infusion chemotherapy with or without embolization for unresectable hepatocellular carcinoma: propensity score analysis. AJR Am J Roentgenol. 2010;194:830–7.
10. Collettini F, Schnapauff D, Poellinger A, et al. Hepatocellular carcinoma: computed-tomography-guided high-dose-rate brachytherapy (CT-HDRBT) ablation of large (5–7 cm) and very large (> 7 cm) tumours. Eur Radiol. 2012;22:1101–9.
11. Mohnike K, Wieners G, Schwartz F, et al. Computed tomography-guided high-dose-rate brachytherapy in hepatocellular carcinoma: safety, efficacy, and effect on survival. Int J Radiat Oncol Biol Phys. 2010;78:172–9.
12. Ricke J, Mohnike K, Pech M, et al. Local response and impact on survival after local ablation of liver metastases from colorectal carcinoma by computed tomography-guided high-dose-rate brachytherapy. Int J Radiat Oncol Biol Phys. 2010;78:479–85.
13. Ricke J, Thormann M, Ludewig M, et al. MR-guided liver tumor ablation employing open high-field 1.0T MRI for image-guided brachytherapy. Eur Radiol. 2010;20:1985–93.
14. Ricke J, Wust P, Stohlmann A, et al. CT-guided interstitial brachytherapy of liver malignancies alone or in combination with thermal ablation: phase I–II results of a novel technique. Int J Radiat Oncol Biol Phys. 2004;58:1496–505.
15. Ricke J, Wust P, Wieners G, et al. Liver malignancies: CT-guided interstitial brachytherapy in patients with unfavorable lesions for thermal ablation. J Vasc Interv Radiol. 2004;15:1279–86.
16. Tselis N, Chatzikonstantinou G, Kolotas C, Milickovic N, Baltas D, Zamboglou N. Computed tomography-guided interstitial high dose rate brachytherapy for centrally located liver tumours: a single institution study. Eur Radiol. 2013;23:2264–70.
17. Mohnike K, Neumann K, Hass P, et al. Radioablation of adrenal gland malignomas with interstitial high-dose-rate brachytherapy: efficacy and outcome. Strahlenther Onkol. 2017;193:612–9.
18. Mohnike K, Wolf S, Damm R, et al. Radioablation of liver malignancies with interstitial high-dose-rate brachytherapy: complications and risk factors. Strahlenther Onkol. 2016;192:288–96.
19. Hata M, Tokuuye K, Sugahara S, et al. Proton beam therapy for hepatocellular carcinoma with portal vein tumor thrombus. Cancer. 2005;104:794–801.
20. Lee SU, Park JW, Kim TH, et al. Effectiveness and safety of proton beam therapy for advanced hepatocellular carcinoma with portal vein tumor thrombosis. Strahlenther Onkol. 2014;190:806–14.
21. Sugahara S, Nakayama H, Fukuda K, et al. Proton-beam therapy for hepatocellular carcinoma associated with portal vein tumor thrombosis. Strahlenther Onkol. 2009;185:782–8.
22. Mohnike K, Sauerland H, Seidensticker M, et al. Haemorrhagic complications and symptomatic venous thromboembolism in interventional tumour ablations: the impact of peri-interventional thrombosis prophylaxis. Cardiovasc Intervent Radiol. 2016;39:1716–21.
23. Cannistra SA. Phase II trials in journal of clinical oncology. J Clin Oncol. 2009;27:3073–6.
24. Bruix J, Sherman M, Llovet JM, et al. Clinical management of hepatocellular carcinoma. Conclusions of the Barcelona-2000 EASL conference. European Association for the study of the liver. J Hepatol. 2001;35:421–30.
25. Bruix J, Sherman M. Practice Guidelines Committee AAftSoLD. Management of hepatocellular carcinoma. Hepatology. 2005;42:1208–36.
26. Llovet JM, Real MI, Montana X, et al. Arterial embolisation or chemoembolisation versus symptomatic treatment in patients with unresectable hepatocellular carcinoma: a randomised controlled trial. Lancet. 2002;359:1734–9.
27. Lo CM, Ngan H, Tso WK, et al. Randomized controlled trial of transarterial lipiodol chemoembolization for unresectable hepatocellular carcinoma. Hepatology. 2002;35:1164–71.
28. Lencioni R. Chemoembolization in patients with hepatocellular carcinoma. Liver Cancer. 2012;1:41–50.
29. Lammer J, Malagari K, Vogl T, et al. Prospective randomized study of doxorubicin-eluting-bead embolization in the treatment of hepatocellular carcinoma: results of the PRECISION V study. Cardiovasc Intervent Radiol. 2010;33:41–52.
30. Forner A, Gilabert M, Bruix J, Raoul JL. Treatment of intermediate-stage hepatocellular carcinoma. Nat Rev Clin Oncol. 2014;11:525–35.

CT-Guided Brachytherapy (CTGB) versus Interstitial Laser Ablation (ILT) of Colorectal Liver Metastases

An Intraindividual Matched-Pair Analysis

Maciej Pech[1], Gero Wieners[1], Rafal Kryza[1], Oliver Dudeck[1], Max Seidensticker[1], Konrad Mohnike[1], Ulf Redlich[1], Ricarda Rühl[1], Peter Wust[2], Günther Gademann[3], Jens Ricke[1]

Purpose: To compare local tumor control after percutaneous tumor ablation by interstitial laser therapy (ILT) or CT-guided brachytherapy (CTGB).
Patients and Methods: In a matched pair analysis including 18 patients with 36 liver metastases of colorectal primary, both ILT and CTGB were performed in different lesions. The following matching factors were considered: (i) tumor size ≤ 5 cm, and (ii) execution of chemotherapy after tumor ablation. Primary endpoint was local tumor control.
Results: Treated lesions were identical in terms of tumor size and all matching criteria were fulfilled in all patients except for the performance of adjuvant chemotherapy. Median follow-up was 14 months (3–24 months) for both groups. Only five of 18 patients (28%) demonstrated local tumor progression after CTGB, whereas in ten of 18 patients (56%) tumor progression was found after ILT. Differences encountered were significant for all patients ($p = 0.04$), whereas in those who fulfilled all matching criteria ($n = 14$) the level of statistical significance was not reached ($p = 0.23$).
Conclusion: CTGB demonstrated superior local tumor control compared to ILT in long-term follow-up.

Key Words: CT-guided brachytherapy · Interstitial laser therapy · Liver

Strahlenther Onkol 2008;184:302–6
DOI 10.1007/s00066-008-1815-5

Vergleich der CT-gestützten Brachytherapie mit der interstitiellen Laserablation von Lebermetastasen kolorektaler Karzinome. Matched-Pair-Analyse in demselben Patienten

Ziel: Intraindividueller Vergleich lokaler Kontrollraten nach perkutaner Tumorablation mit interstitieller Lasertherapie (ILT) oder CT-gestützter Brachytherapie (CTGB) von intrahepatischen Metastasen bei kolorektalem Karzinom.
Patienten und Methodik: Eine Matched-Pair-Analyse wurde bei 18 Patienten mit insgesamt 36 Lebermetastasen eines kolorektalen Karzinoms durchgeführt. Je eine Metastase wurde mit perkutaner Tumorablation mit ILT und je eine mit CTGB behandelt. Bei den Patienten mit identischer Tumorhistologie wurden folgende Faktoren betrachtet: 1. Tumorgröße ≤ 5 cm und 2. Durchführung oder Verzicht auf eine adjuvante Chemotherapie. Als primärer Endpunkt wurde die lokale Tumorkontrolle definiert.
Ergebnisse: Die Verteilung der Tumorgrößen war gleich, und alle Patienten erreichten volle Übereinstimmung bis auf den Vergleichsfaktor der adjuvanten Chemotherapie. Die mediane Beobachtungszeit betrug 14 Monate (3–24 Monate) für beide Gruppen. Fünf von 18 Patienten (28%) hatten eine lokale Tumorprogression nach CTGB und zehn von 18 Patienten (56%) nach ILT. Die Differenz zwischen den Gruppen war für alle Patienten signifikant ($p = 0,04$). Bei der Betrachtung der Patienten mit völliger Übereinstimmung wurde die Signifikanzgrenze nicht erreicht ($p = 0,23$).
Schlussfolgerung: Die CTGB zeigt in der Langzeitbeobachtung überlegene lokale Tumorkontrollraten im Vergleich zur ILT.

Schlüsselwörter: CT-gestützte Brachytherapie · Interstitielle Lasertherapie · Leber

[1] Clinic for Radiology and Nuclear Medicine, University of Magdeburg, Germany,
[2] Department of Radiology, Charité, Campus Virchow Clinic, University of Berlin, Germany,
[3] Clinic for Radiation Therapy, University of Magdeburg, Germany.

Received: November 11, 2007; accepted: March 26, 2008

Introduction

In recent years, percutaneous image-guided tumor ablation has evolved as a genuine alternative for the treatment of liver metastases of solid tumors [3, 9, 17, 26]. However, a size limitation of approximately 5 cm, adjacent large vessels or hyperperfusion of tumors responsible for adverse cooling effects, and location close to the liver hilum are disadvantages of thermal ablation [1]. CT-guided brachytherapy (CTGB) has overcome these limitations with promising results not only in liver tissue [6, 7, 10, 16, 20, 23–25, 28]. Currently, no clinical data is available comparing the effectiveness and local control (vs. time to progression) of these local tumor ablation techniques.

Patients and Methods

Patient Identification

18 patients (twelve men, six women, median age 66 years, range 49–82 years) with 36 metachronous liver metastases fulfilled the inclusion criteria with (i) solitary metastasis of colorectal primary at the time that each treatment was performed, and (ii) different time points for each treatment. 13 patients had received prior chemotherapy (first-line, n = 6, 33%; second-line, n = 5, 28%; third-line, n = 2, 11%). Twelve patients were treated with interstitial laser therapy (ILT) first and six with CTGB. The median time interval for the appearance of the second lesion was nearly equal for both groups (ILT = 10.6 months, CTGB = 8.9 months).

Interventional Technique

The technique of CTGB has been described in detail elsewhere [19] and was preferred for metastases located near large vessels or liver hilum. In short, the applicators were positioned under CT fluoroscopy followed by a single-dose irradiation of an iridium-192 source of 10 Ci using the high-dose-rate afterloading system.

The technique of ILT has also been described in detail [17, 26] and was preferred for metastases located in the liver periphery without contact to large vessels. In short, applicators were positioned under CT fluoroscopy followed by thermoablation with a neodymium-yttrium-aluminum garnet laser with a wavelength of 1,064 nm monitored with thermosensitive GRE MRI sequences (TE/TR 3.9/102; flip 70°).

Outcome Variables and Definitions

All patients received follow-up MRI 3 days, 6 weeks, and every 3 months after tumor ablation as described previously [15, 19]. Local control after CTGB or ILT was defined by (i) absence of symmetric lesion growth (≥ 25% of the tumor volume) at any time during follow-up, and (ii) absence of asymmetric tumor growth in the vicinity of the treated lesion at any time during follow-up. Any new tumor with a center of mass ≤ 10 mm apart from the contour of the formerly treated lesion was considered local recurrence.

Matching Factors

In addition to the criteria given above, we considered the following matching factors per individual patient: (i) tumor size ≤ 5 cm, and (ii) execution of chemotherapy after tumor ablation. Previous authors identified 5 cm as a threshold for successful thermal ablation, although CTGB has proven feasibility also in larger tumor volumes [18, 26].

Statistical Analysis

The Wilcoxon test was employed to compare both treatment groups. The Kaplan-Meier method along with the log-rank test was applied for local control curves. To avoid potential bias resulting from unequal follow-up time, all patients with local tumor control > 2 years were censored at this point.

Results

Patient Identification

Among all patients 14 of 18 fulfilled all matching criteria. In four patients tumor size exceeded 5 cm for either ILT or CTGB (Table 1). However, the distribution of tumor size among all tumors treated by ILT or CTGB was identical (p = 0.8; CTGB: 3.8 cm, 1.0–6.0 cm, median 4.0 cm; ILT: 3.4 cm, 1.8–5.8 cm, median 3.2 cm), and all patients demonstrated full match in terms of performance of adjuvant chemotherapy (Table 1). There was one metastasis > 5 cm treated by ILT (technical limitation) which showed no recurrence in the follow-up period.

Complications

Complications after CTGB comprised pain (n = 3), dyspnea (n = 1), nausea (n = 1), and pleural effusion (n = 1). No major complications were recorded. Minor complications after ILT comprised pleural effusion (n = 2), pain (n = 2), subcapsular liver hematoma (n = 1), nausea and vomiting (n = 1). Again, no major complications were observed.

Follow-up

The median follow-up after initial intervention was 14 months (3–24 months) for both ILT and CTGB. Five of 18 patients demonstrated local tumor progression after CTGB. According to the Kaplan-Meier method local tumor control was 87%, 80%, and 72% at 6, 9, and 12 months, respectively. Local tumor progression after ILT was observed in ten of 18 patients. According to the Kaplan-Meier method local tumor control was 73%, 44%, and 36% after 6, 9, and 12 months, respectively (Figure 1).

Statistical Analysis

Differences encountered between local control after CTGB or ILT were significant for all patients (Figure 1; p = 0.04). In patients displaying full match, a significance level was not reached (Figure 2; p = 0.23).

Discussion

Recently, a survival benefit for patients with colorectal liver metastases undergoing local tumor ablation compared with historical controls undergoing chemotherapy alone has been postulated [1, 26, 27]. Residual tumor after surgical resection has demonstrated to be an independent predictor of poor prognosis [5, 21]. To the best of our knowledge, no data has yet been published addressing the impact of tumor recurrence after tumor ablation. It thus remains unknown if incomplete tumor destruction has any impact on survival.

This retrospective matched-pair analysis was based on strict inclusion criteria. First, only patients with colorectal carcinoma were selected, in which ILT as well as CTGB have been performed, thus guaranteeing the treatment of histologically identical tumors and an intraindividual comparison. Second, only tumors of ≤ 5 cm were considered following recommendations of previous authors to ensure local tumor control by thermal ablation [1, 26]. Third, execution of adjuvant chemotherapy after local tumor ablation was included, which may well influence local tumor control even in salvage situations. As a result, the two cohorts matched well in terms of tumor entity, tumor size, and adjuvant systemic therapy.

In our study, local tumor control after ILT and CTGB was similar after 6 months (87% for CTGB vs. 73% for ILT). However, upon long-term follow-up of 12 months brachytherapy displayed a significant advantage over thermal ablation (72% for CTGB vs. 36% for ILT). Our results for ILT with a local tumor control were not in concordance with previously published results. Vogl et al. have published extensive data on ILT of liver metastases over the past years, with a local tumor control for colorectal tumors of > 95% at 6 months and no further local recurrences after 6 months [26]. We found less optimistic long-term results in a series of 191 liver metastases of various primaries treated with ILT at our institution with a local tumor control of 93% and 76% after 6 and 12 months, respectively [17]. In addition, data published for percutaneous radiofrequency ablation describe similar local tumor control rates between 60% and 65% after 12 months with a considerable number of local recurrences depicted between 6 and 12 months [8, 22]. Certainly, the categorization of tumor regrowth as local progression remains a matter of debate which may explain these differences in tumor control rates. In colorectal liver metastases, microsatellites beyond the macroscopic tumor border are frequently found in histopathologic specimen [14]. The presence of microsatellites as well as their distance to

Table 1. Patient outcome after local tumor ablation. CTGB: CT-guided brachytherapy; CTx: chemotherapy – 1: 5-fluorouracil/folinic acid, 2: 5-fluorouracil/folinic acid, irinotecan, 3: 5-fluorouracil/folinic acid, oxaliplatin, 4: tegafur-uracil/folinic acid, 5: capecitabine, A: hepatic artery infusion (5-fluorouracil/folinic acid, oxaliplatin), S: systemic chemotherapy (irinotecan); ILT: interstitial laser therapy. F: full match: meets all match criteria (adjuvant chemotherapy, size ≤ 5 cm); N: near match: meets one of two criteria (size or adjuvant chemotherapy).

Tabelle 1. Patientencharakteristika nach lokaler Tumorablation. CTGB: CT-gestützte Brachytherapie; Ctx: Chemotherapie – 1: 5-Fluorouracil/Folinsäure, 2: 5-Fluorouracil/Folinsäure, Irinotecan, 3: 5-Fluorouracil/Folinsäure, Oxaliplatin, 4: Tegafur-Uracil/Folinsäure, 5: Capecitabin, A: lokoregionäre Chemotherapie der Leber (5-Fluorouracil/Folinsäure, Oxaliplatin) S: systemische Chemotherapie (Irinotecan); ILT: interstitielle Laserablation. F: vollständige Übereinstimmung der Kriterien; N: ein Kriterium erfüllt (Größe oder adjuvante Chemotherapie).

Patient # (therapy sequence)	Time to second therapy (CTGB or ILT)	Lesion size ILT (mm)	Lesion size CTGB (mm)	Prior CTx	Adjuvant CTx	Local recurrence (technique, months)	Full match (F) Near match (N)
1 (ILT/CTGB)	7 months	44	35	1	–	ILT, 6	F
2 (CTGB/ILT)	9 months	18	41	–	–	No	F
3 (CTGB/ILT)	1 week	31	48	1, 2	A	ILT/CTGB, 3/6	F
4 (CTGB/ILT)	2 months	35	43	1, 4	S	CTGB, 6	F
5 (ILT/CTGB)	2 months	21	30	1	A	ILT, 13	F
6 (ILT/CTGB)	2 weeks	47	60	1	A	No	N
7 (ILT/CTGB)	3 weeks	50	55	–	A	ILT, 11	N
8 (ILT/CTGB)	5 months	32	10	–	A	No	F
9 (ILT/CTGB)	7 months	21	32	1, 5	–	ILT/CTGB, 6/6	F
10 (ILT/CTGB)	6 weeks	29	60	1, 2	A	ILT, 8	N
11 (CTGB/ILT)	2 weeks	33	20	–	A	No	F
12 (ILT/CTGB)	1 week	38	40	–	A	ILT/CTGB 6/12	F
13 (ILT/CTGB)	2 weeks	58	42	1, 3, 5	A	No	N
14 (CTGB/ILT)	1 week	34	24	1	A	No	F
15 (ILT/CTGB)	10 months	32	40	1	–	ILT, 7	F
16 (CTGB/ILT)	1 month	28	40	3, 5	–	No	F
17 (ILT/CTGB)	1 month	32	25	1	A	ILT/CTGB, 4/16	F
18 (ILT/CTGB)	3 weeks	32	35	1, 5, 4	A	ILT, 6	F

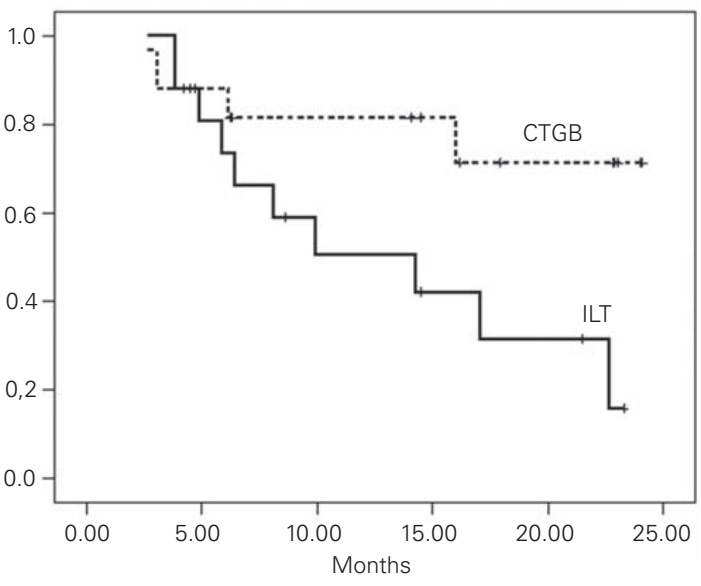

Figure 1. Local tumor control post ILT and CTGB (all patients; p = 0.041). Five of 18 patients (28%) demonstrated local tumor progression after CTGB, and ten of 18 patients (56%) after ILT.

Abbildung 1. Lokale Tumorkontrolle nach ILT und CTGB (alle Patienten; p = 0,041). Fünf der 18 Patienten (28%) zeigten einen lokalen Progress der behandelten Metastasen nach CTGB und zehn der 18 Patienten (56%) nach ILT.

the originating metastasis have been linked to the presence of a pseudocapsule, the extent of lymphocyte infiltration between the metastasis and the liver parenchyma, and the morphologic type of the lesion [12, 14, 29]. Nanko et al. described a mean distance of the microsatellites to the margin of the originating metastases of 7.5 mm ± 8 mm [12]. It remains unclear if, e.g., different definitions of local tumor recurrence versus new tumor manifestations adjacent to the ablated tumor volume may have contributed to the outcome variations after ILT in our study compared to the literature.

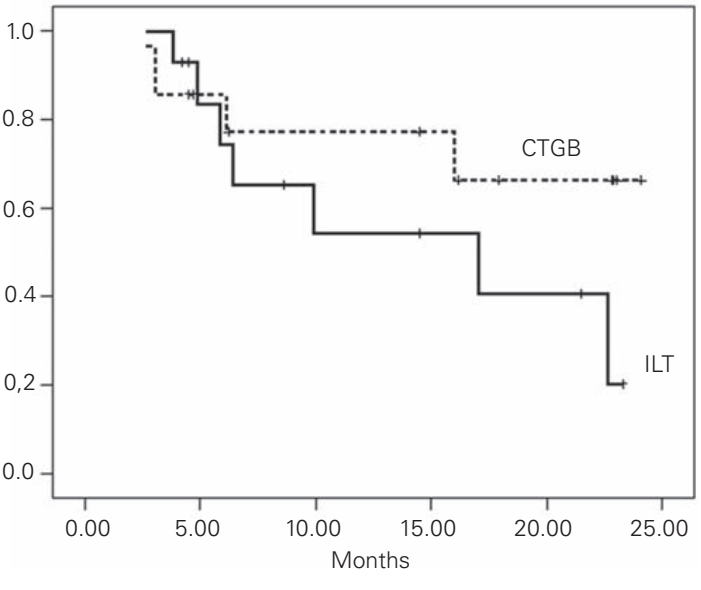

Figure 2. Local tumor control post ILT and CTGB (only patients meeting all match criteria; n = 14, nonsignificant).

Abbildung 2. Lokale Tumorkontrolle nach ILT und CTGB (nur bei Patienten mit allen zu erfüllenden Kriterien; n = 14, kein signifikanter Unterschied).

CTGB is a novel technique, and local tumor control rates have only been published for rather small populations yet. In these studies, local control after 12 months reached approximately 70% [18]. A recent, yet unpublished randomized study from our own group comprising 200 liver metastases of colorectal primaries treated by CTGB revealed a strong dose dependency of local tumor control. Whereas no local tumor recurrence was observed after 12 months in patients if > 23 Gy could be applied, patients receiving only 15 or 20 Gy minimal dose inside the tumor volume displayed local tumor control of 89% and 67% after 6 and 12 months, respectively.

Thermal ablation and brachytherapy differ considerably with respect to the underlying pathophysiology. While laser ablation induces a rather sharply defined thermal necrosis with the effect limited to the time of the actual treatment, brachytherapy displays a protracted, continuous effect on cells, which may lead to necrosis or apoptosis weeks to months after treatment [2, 4, 11]. In addition, the dose gradient beyond the target volume and thus the therapeutic effect decrease much slower compared to thermal ablation. Microscopic tumor spread beyond the radiologically detectable tumor involves a significantly reduced tumor cell density (by a factor of 10–100). For this lower cell number a reduced dose will be sufficient for local control. We presume that these favorable results for brachytherapy in this study result from the smoother decrease of radiation dose around the macroscopic lesions annihilating also the microscopic extension, an effect not applicable with thermal ablation. Moreover, Nikfarjam et al. showed thermal ablation to promote the progression of micrometastases to form macroscopically detectable neoplasm in treated regenerated liver [13].

Conclusion

CTGB displayed superior local tumor control over ILT during long-term follow-up, whereas both methods demonstrated equal results after 6 months. Advantage of thermal ablation remains the lower complexity of the technique, while CTGB is not limited by size or cooling effects from adjacent vessels. Furthermore, brachytherapy may as well be used in more risky areas such as the liver hilum [16, 20].

Acknowledgment

This work has been supported by the European Commission Leonardo da Vinci grant.

References

1. Berber E, Pelley R, Siperstein AE. Predictors of survival after radiofrequency thermal ablation of colorectal cancer metastases to the liver: a prospective study. J Clin Oncol 2005;23:1358–64.
2. Brenner DJ. Radiation biology in brachytherapy. J Surg Oncol 1997; 65:66–70.

3. Buscarini E, Savoia A, Brambilla G, et al. Radiofrequency thermal ablation of liver tumors. Eur Radiol 2005;15:884–94.
4. Dale RG, Jones B. The clinical radiobiology of brachytherapy. Br J Radiol 1998;71:465–83.
5. Fong Y, Fortner J, Sun RL, et al. Clinical score for predicting recurrence after hepatic resection for metastatic colorectal cancer: analysis of 1001 consecutive cases. Ann Surg 1999;230:309–18.
6. Imamura F, Ueno K, Kusunoki Y, et al. High-dose-rate brachytherapy for small-sized peripherally located lung cancer. Strahlenther Onkol 2006; 182:703–7.
7. Kolotas C, Tselis N, Sommerlad M, et al. Reirradiation for recurrent neck metastases of head-and-neck tumors using CT-guided interstitial ^{192}Ir HDR brachytherapy. Strahlenther Onkol 2007;183:69–75.
8. Livraghi T, Solbiati L, Meloni F, et al. Percutaneous radiofrequency ablation of liver metastases in potential candidates for resection: the "test-of-time approach". Cancer 2003;97:3027–35.
9. Mack MG, Straub R, Eichler K, et al. Percutaneous MR imaging-guided laser-induced thermotherapy of hepatic metastases. Abdom Imaging 2001; 26:369–74.
10. Major T, Fodor J, Takacsi-Nagy Z, et al. Evaluation of HDR interstitial breast implants planned by conventional and optimized CT-based dosimetry systems with respect to dose homogeneity and conformality. Strahlenther Onkol 2005;181:89–96.
11. Morrison PR, Jolesz FA, Charous D, et al. MRI of laser-induced interstitial thermal injury in an in vivo animal liver model with histologic correlation. J Magn Reson Imaging 1998;8:57–63.
12. Nanko M, Shimada H, Yamaoka H, et al. Micrometastatic colorectal cancer lesions in the liver. Surg Today 1998;28:707–13.
13. Nikfarjam M, Muralidharan V, Christophi C. Altered growth patterns of colorectal liver metastases after thermal ablation. Surgery 2006;139:73–81.
14. Okano K, Yamamoto J, Kosuge T, et al. Fibrous pseudocapsule of metastatic liver tumors from colorectal carcinoma. Clinicopathologic study of 152 first resection cases. Cancer 2000;89:267–75.
15. Pech M, Spors B, Wieners G, et al. Comparison of different MRI sequences with and without application of Gd BOPTA as follow-up after LITT. Rofo 2004;176:550–5.
16. Pech M, Wieners G, Fischbach F, et al. Synchronous CT-guided brachytherapy in patients at risk for incomplete interstitial laser ablation of liver malignancies. Med Laser Appl 2004;19:73–82.
17. Pech M, Wieners G, Freund T, et al. MR-guided interstitial laser thermotherapy of colorectal liver metastases: efficiency, safety and patient survival. Eur J Med Res 2007;12:161–8.
18. Ricke J, Wust P, Stohlmann A, et al. CT-guided brachytherapy. A novel percutaneous technique for interstitial ablation of liver metastases. Strahlenther Onkol 2004;180:274–80.
19. Ricke J, Wust P, Stohlmann A, et al. CT-guided interstitial brachytherapy of liver malignancies alone or in combination with thermal ablation: phase I–II results of a novel technique. Int J Radiat Oncol Biol Phys 2004; 58:1496–505.
20. Ricke J, Wust P, Wieners G, et al. Liver malignancies: CT-guided interstitial brachytherapy in patients with unfavorable lesions for thermal ablation. J Vasc Interv Radiol 2004;15:1279–86.
21. Scheele J, Stangl R, Altendorf-Hofmann A, et al. Indicators of prognosis after hepatic resection for colorectal secondaries. Surgery 1991;110:13–29.
22. Solbiati L, Livraghi T, Goldberg SN, et al. Percutaneous radio-frequency ablation of hepatic metastases from colorectal cancer: long-term results in 117 patients. Radiology 2001;221:159–66.
23. Takacsi-Nagy Z, Polgar C, Oberna F, et al. Interstitial high-dose-rate brachytherapy in the treatment of base of tongue carcinoma. Strahlenther Onkol 2004;180:768–75.
24. Tepel J, Niehoff P, Bokelmann F, et al. Feasibility and early results of interstitial intensity-modulated HDR/PDR brachytherapy (IMBT) with/without complementary external-beam radiotherapy and extended surgery in recurrent pelvic colorectal cancer. Strahlenther Onkol 2005;181:696–703.
25. Tselis N, Kolotas C, Birn G, et al. CT-guided interstitial HDR brachytherapy for recurrent glioblastoma multiforme. Long-term results. Strahlenther Onkol 2007;183:563–70.
26. Vogl TJ, Straub R, Eichler K, et al. Colorectal carcinoma metastases in liver: laser-induced interstitial thermotherapy – local tumor control rate and survival data. Radiology 2004;230:450–8.
27. Vogl TJ, Straub R, Zangos S, et al. MR-guided laser-induced thermotherapy (LITT) of liver tumours: experimental and clinical data. Int J Hyperthermia 2004;20:713–24.
28. Weitmann HD, Knocke TH, Waldhausl C, et al. Ultrasound-guided interstitial brachytherapy in the treatment of advanced vaginal recurrences from cervical and endometrial carcinoma. Strahlenther Onkol 2006;182:86–95.
29. Yasui K, Hirai T, Kato T, et al. A new macroscopic classification predicts prognosis for patient with liver metastases from colorectal cancer. Ann Surg 1997;226:582–6.

Address for Correspondence
Maciej Pech, MD
Clinic for Radiology and Nuclear Medicine
University of Magdeburg
Leipziger Straße 44
39120 Magdeburg
Germany
Phone (+49/391) 67-13030, Fax -13029
e-mail: maciej.pech@med.ovgu.de

ELSEVIER

BRACHYTHERAPY

Brachytherapy 18 (2019) 823–828

Gastrointestinal Oncology

Comparative analysis between interstitial brachytherapy and stereotactic body irradiation for local ablation in liver malignancies

Peter Hass[1], Konrad Mohnike[2], Siegfried Kropf[3], Thomas B. Brunner[1], Mathias Walke[1], Dirk Albers[4], Cordula Petersen[4], Robert Damm[7], Franziska Walter[5], Jens Ricke[6], Maciej Powerski[7], Stefanie Corradini[5,*]

[1]*Department of Radiation Oncology, University Hospital Magdeburg, Magdeburg, Germany*
[2]*Diagnostisch Therapeutisches Zentrum (DTZ), Berlin, Germany*
[3]*Institute of Biometry and Medical Informatics, University Hospital Magdeburg, Magdeburg, Germany*
[4]*Department of Radiation Oncology, University Hamburg-Eppendorf, Hamburg, Germany*
[5]*Department of Radiation Oncology, University Hospital, LMU Munich, Munich, Germany*
[6]*Department of Radiology, University Hospital, LMU Munich, Munich, Germany*
[7]*Department of Radiology and Nuclear Medicine, University Hospital Magdeburg, Magdeburg, Germany*

ABSTRACT

PURPOSE: Interstitial high-dose-rate brachytherapy (BT) is an alternative treatment option to stereotactic body radiotherapy (SBRT) for the ablative treatment of liver malignancies. The aim of the present comparative planning study was to reveal the possibilities and limitations of both techniques with regard to dosimetric properties.

METHODS AND MATERIALS: Eighty-five consecutive patients with liver malignancy diagnosis were treated with interstitial BT between 12/2008 and 09/2009. The prescription dose of BT varied between 15 and 20 Gy, depending on histology. For dosimetric comparison, virtual SBRT treatment plans were generated using the original BT planning CTs. Additional margins reflecting the respiratory tumor motion were added to the target volumes for SBRT planning.

RESULTS: The mean PTV_{BT} was 34.7 cm^3 (0.5–410.0 cm^3) vs. a mean PTV_{SBRT} of 73.2 cm^3 (6.1–593.4 cm^3). Regarding the minimum peripheral dose ($D_{99.9}$), BT achieved the targeted prescription dose of 15 Gy/20 Gy better without violating organ at risk constraints. The dose exposure of the liver was significantly influenced by treatment modality. The liver exposure to 5 Gy was statistically lower with 611 ± 43 cm^3 for BT as compared with 694 ± 37 cm^3 for SBRT plans (20-Gy group, $p = 0.001$), corresponding to 41.8% vs. 45.9% liver volume, respectively.

CONCLUSIONS: To the best of our knowledge, this is the first report on the comparison of clinically treated liver BT treatments with virtually planned SBRT treatments. The planning study showed a superior outcome of BT regarding dose coverage of the target volume and exposed liver volume. Nevertheless, further studies are needed to determine ideal applicability for each treatment approach.

Keywords: Interstitial brachytherapy; HDR; Liver; Ablation; Stereotactic body irradiation; SBRT

Introduction

To date, stereotactic body radiotherapy (SBRT) is the standard for local ablative treatments in radiation oncology (1). This advanced technology allows delivering high doses of radiation to small target volumes using 3–12 fractions. Due to the high conformality, SBRT provides a rapid dose falloff toward surrounding healthy tissues of organs at risk (OARs). Therefore, in the treatment of primary and secondary liver malignancies, SBRT has now been successfully integrated into clinical practice and achieves high local control rates with low toxicity (2, 3).

Received 27 May 2019; received in revised form 29 July 2019; accepted 7 August 2019.

Financial disclosures: C.S. received speaker fees and travel reimbursement from Nucletron Operations B.V. (ELEKTA AB). All other authors have no competing interests.

* Corresponding author. Department of Radiation Oncology, University Hospital, LMU Munich, Marchioninistraße 15, 81377 Munich, Germany. Tel.: +49-89-4400-74520; fax: +49-89-4400-74523.

E-mail address: stefanie.corradini@med.uni-muenchen.de (S. Corradini).

1538-4721/$ - see front matter
https://doi.org/10.1016/j.brachy.2019.08.003

Interstitial high-dose-rate brachytherapy can represent an alternative treatment option for the ablative treatment of liver malignancies. Although brachytherapy is a classical, long-standing, minimally invasive treatment method, it has not been broadly implemented for the ablation of liver lesions. Nevertheless, there is emerging evidence and the technique has recently been added to the "toolbox of ablative treatment options" of the European Society for Medical Oncology guidelines for metastatic colorectal carcinoma (4) and hepatocellular carcinomas (HCCs) (5). Brachytherapy is known to achieve comparable results to SBRT and radiofrequency ablation in the treatment of liver malignancies, with local tumor control rates of >80% at 12 months depending on tumor size (6, 7).

To date, some study groups evaluated the dosimetric comparison of SBRT to simulated "virtual" image-guided HDR brachytherapy of liver targets to evaluate the merits of each approach (8–10). The selection of the number and trajectory of simulated brachytherapy catheters was usually determined collaboratively between interventional radiologists and radiation oncologists experienced in brachytherapy. However, there are no reports addressing the dosimetric comparison between clinically applied BT plans and virtual SBRT plans in the treatment of liver malignancies. In our experience, it is challenging to predict the future position of a brachytherapy catheter because of several limitations, including respiratory motion. Moreover, it has been demonstrated, that with interstitial brachytherapy, it is possible to treat even very large liver lesions and extrahepatic malignancies (11).

The object of the present comparative planning study was to investigate the possibilities and limitations of both techniques with regard to dosimetric properties. SBRT is a noninvasive method that might have certain limitations in terms of size and number of treatable liver lesions. In contrast, BT may overcome these limitations in a number of patients. As a result, the outcome of this study may facilitate deciding whether a patient would benefit from BT rather than SBRT and vice versa.

Patients and methods

Study population and interstitial brachytherapy treatment

Inoperable patients (technically or due to severe comorbidities, as defined by a multidisciplinary tumor board) presenting with primary liver tumors or up to a maximum of six liver metastases (oligometastases) were included in this study. All patients had an Eastern Cooperative Oncology Group status of ≤2. A total of 85 consecutive patients with primary or secondary malignancies of the liver were included in the present planning study. All patients were treated at the University hospital Magdeburg, Germany with interstitial CT-guided brachytherapy between 12/2008 and 09/2009. The study was approved by the local ethics committee of the University of Magdeburg (No. 93-14 ex 07/2014) and was conducted in accordance with the ethical principles of the Declaration of Helsinki. Informed consent was obtained from all patients.

The placement of the brachytherapy catheters was performed under fluoroscopy-CT guidance (Toshiba, Japan) and local anesthesia. Midazolam and Fentanyl were given for sedation and analgesia as individually required by the respective patient. Hollow 17-gauge needles (KLS Martin, Freiburg, Germany) were placed into the lesions. Thereafter, an angiography sheath with a 6F diameter (Radifocus Introducer II, Terumo, Tokyo, Japan) was inserted over a stiff angiography guide wire (Amplatz Super Stiff, Boston Scientific, Boston) and the 6F brachytherapy catheters (Primed Halberstadt Medizintechnik GmbH, Halberstadt, Germany) were consecutively placed in the angiography sheaths (12).

After placement of the catheters, a contrast-enhanced planning CT was acquired using a breath-hold technique and a slice thickness of 3 mm. Treatment planning was performed using the Oncentra Brachy treatment planning system (Elekta AB, Stockholm, Sweden), which is based on the TG-43 algorithm. Target delineation included gross tumor volume (GTV) with an additional margin of 3–5 mm for the clinical target volume, depending on visualization quality of the GTV. There was no additional margin for the planning target volume (PTV) (clinical target volume = PTV), as there are less setup inaccuracies with BT as compared with external beam techniques and the BT catheters are fixed within the tumor. Moreover, OARs such as the liver, stomach, duodenum, colon, small intestines, and heart were delineated. After catheter reconstruction, treatment planning and dose optimization were performed. The prescription dose encompassing the entire PTV ($D_{99.9}$) varied between a single dose of 15 Gy (n = 23) or 20 Gy (n = 62), depending on histology. HCCs and breast cancer metastases were treated with 15 Gy, cholangiocellular carcinoma and nonbreast secondary liver malignomas, such as metastases of colorectal carcinoma, were treated with 20 Gy (6). Dose constraints for OARs (12, 13) are listed in Table 1. The dose distribution in liver brachytherapy usually is very heterogeneous, as only a few BT catheters are used to reduce the risk of bleeding complications through catheter insertion. In particular, patients with HCC often have preprocedural thrombocytopenia and therefore an elevated risk for major complications.

Brachytherapy was applied using an HDR afterloading system (microSelectron-HDR, Nucletron, Elekta AB, Stockholm, Sweden) with an Iridium-192 source. For catheter removal, gel foam was introduced through each brachytherapy sheath during removal to prevent bleeding.

Virtual stereotactic body radiotherapy treatment planning

Virtual SBRT treatment plans were calculated for every liver lesion. For tumor movement mitigation, standard patient positioning during CT imaging and treatment delivery

Table 1
OAR dose constraints for treatment planning of brachytherapy and SBRT

OAR	DVH parameter	Limit, Gy	Alpha/Beta (late effects)	EQD2 D1cc Gy
Esophagus	D1cc	15	4	47.5
Stomach	D1cc	15	4	47.5
Duodenum	D1cc	15	4	47.5
Small intestine	D1cc	18	4	66
Large intestine	D1cc	20	4	80
Gall bladder	D1cc	20	3	92
Spinal cord	D1cc	10	3	26
Skin	D1cc	9	3	21.6
Liver	V5Gy	66%		

OAR = organ at risk; DVH = dose-volume histogram; SBRT = stereotactic body radiotherapy.

of SBRT is usually achieved by using vacuum cushions in combination with abdominal compression (14). In addition, a respiratory correlated CT (4D-CT) is usually acquired, which allows to outline the GTV in different respiratory phases of a breathing cycle allowing for an internal target volume approach in treatment planning (15).

In the present planning study, SBRT plans were generated using the original brachytherapy planning CTs with the brachytherapy catheters in place. Therefore, no 4D-CT data sets were available, as brachytherapy planning CTs were performed using a breath-hold technique. To account for organ motion, additional margins reflecting the respiratory tumor motion had to be added to the target volumes. In the present analysis, a margin of 5 mm in lateral direction and 10 mm along the craniocaudal axis was added to the brachytherapy GTVs to generate virtual PTVs for SBRT treatment planning (16). The prescription dose (15 Gy/20 Gy in one fraction) of SBRT plans was the same as for brachytherapy plans and was prescribed to 99.9% of the PTV. Dose to the PTV was always tailored to fulfill the aimed prescription dose but was reduced if maximum dose limits of OARs were violated. The same OAR constraints for SBRT treatment planning were used as for brachytherapy planning (see Table 1). Treatments were planned for a TrueBeam (Varian Medical Systems, Palo Alto, CA) linac, equipped with a Millennium 120-leaf MLC. Beam energy was six or 15 MV. All plans were optimized by the use of a volumetric arc therapy technique. Dose distributions were computed with a 2.5-mm dose-grid step by an analytical anisotropic algorithm, based on superposition convolution principles, using Eclipse 10.0.42 (Varian Medical Systems, Palo Alto, CA).

Statistical analysis

Statistical analysis was conducted using IBM SPSS Statistics, version 24.0. Dosimetric variables (delivered dose to 90% of the PTV [D_{90}], delivered dose to 99.9% of the PTV [$D_{99.9}$], the liver volume receiving at least 5 Gy [V5Gy in cm^3], and the relative liver volume receiving at least 5 Gy [RV5Gy in %]) were derived from dose-volume histograms and compared between the two techniques (brachytherapy and SBRT). This comparison was made for the entire cohort, as well as for different prescription doses (15 and 20 Gy, respectively). In addition, the analysis included the evaluation of differences between the methods regarding the prescription dose. For V5Gy and RV5Gy, only one value was available per patient. Therefore, statistical analysis was performed using paired sample *t*-tests or a repeated measures analysis of variance with the treatment option (brachytherapy vs. SBRT) as the within-subject factor and the prescription dose as the between-subject factor. Mixed linear models were used for the two parameters D_{90} and $D_{99.9}$, in which several values per patient were available.

Results

Baseline patient characteristics

Eighty-five consecutive patients (male:female = 65:30) with primary or secondary malignancies of the liver were included in the present planning study (Table 2). The median age was 68 years (range: 40–89 years). Histology of liver malignancies included 24 primary liver lesions (HCC or cholangiocellular carcinoma) and 61 liver metastases of solid tumors. Lesions with a maximal diameter of <6 cm were included. The mean number of implanted BT catheter per patient was 3.66 (range: 1–8).

Dosimetric comparison

The mean brachytherapy PTV was 34.7 cm^3 (range: 0.5–410.0 cm^3) as compared to a mean SBRT PTV of 73.2 cm^3 (range: 6.1–593.4 cm^3). There were significant

Table 2
Patient characteristics

Variable	n (range)
Gender	
Male	65
Female	30
Age	
Median (range)	68 (40–89)
Primary liver tumors	24
HCC	16
CCC	8
Secondary liver tumors	61
CRC	49
Breast	4
Cancer of unknown primary (CUP)	4
Other entities	4
Prescribed dose	Patients
15 Gy	23
20 Gy	62
Median number of treated PTVs (range)	1 (1–6)
Median number of interstitial BT catheters (range)	3 (1–8)
Mean PTV_{BT} [cm^3] (range)	34.7 (0.5–410.0)
Mean PTV_{SBRT} [cm^3] (range)	73.2 (6.1–593.4)

BT = brachytherapy; HCC = hepatocellular carcinoma; CCC = cholangiocellular carcinoma; PTV = planning target volume; SBRT = stereotactic body radiotherapy; CRC = colorectal carcinoma.

Table 3
Dosimetric values of the different treatment modalities

	Overall			15-Gy prescription dose			20-Gy prescription dose			20 Gy vs. 15 Gy
	BT	SBRT	p	BT	SBRT	p	BT	SBRT	p	p
D_{90} (Gy)	27.9 ± 0.4	19.5 ± 0.3	<0.001	24.3 ± 0.8	16.5 ± 0.3	<0.001	29.2 ± 0.4	20.6 ± 0.3	<0.001	0.367
$D_{99.9}$ (Gy)	18.8 ± 0.4	16.8 ± 0.4	<0.001	16.0 ± 0.4	14.7 ± 0.4	0.003	19.9 ± 0.4	17.5 ± 0.5	<0.001	0.175
Liver V5 Gy (cm^3)	593 ± 36	671 ± 33	<0.001	544 ± 65	607 ± 71	0.098	611 ± 43	694 ± 37	0.001	0.674
Liver V5 Gy (%)	39.5 ± 2.0	43.6 ± 1.7	0.001	33.3 ± 2.7	37.3 ± 3.0	0.095	41.8 ± 2.5	45.9 ± 2.0	0.007	0.977

BT = brachytherapy; SBRT = stereotactic body radiotherapy.
All values are mean values (±standard error).

differences between dose coverage in BT and SBRT plans. Regarding the $D_{99.9}$, BT plans better approached the prescription dose of 15 Gy or 20 Gy, respectively, compared with SBRT plans. Especially in the 20-Gy group, BT plans reached a mean $D_{99.9}$ of 19.9 ± 0.4 Gy, whereas SBRT plans had a mean $D_{99.9}$ of 17.5 ± 0.5 Gy ($p < 0.001$). This might be influenced by the prescription of SBRT plans to the $D_{99.9}$. Results were comparable for the 15-Gy prescription group ($p = 0.003$). An overview is given in Table 3. Regarding the D_{90}, the effect was even more pronounced, underlining the heterogeneous dose distribution of interstitial BT as compared with SBRT treatment, with a rapid dose falloff. For the 15-Gy group, the mean D_{90} was 24.3 ± 0.8 Gy for BT as compared with 16.5 ± 0.3 Gy ($p < 0.001$) for SBRT. For the 20-Gy group, the mean D_{90} was 29.2 ± 0.4 for BT vs. 20.6 ± 0.3 for SBRT ($p < 0.001$).

The dose exposure of the liver was also significantly influenced by treatment modality. The V5Gy in SBRT was not statistically different for the 15-Gy prescription dose group with 544 ± 65 cm^3 vs. 607 ± 71 cm^3 ($p = 0.098$) corresponding to 33.3% ± 2.7 vs. 37.3% ± 3.0 of total liver volume, respectively ($p = 0.095$). In contrast, in the 20-Gy prescription dose group, the liver exposure was highly statistically different with 611 ± 43 cm^3 for BT as compared with 694 ± 37 cm^3 for SBRT plans ($p = 0.001$) corresponding to 41.8 ± 2.5% and 45.9 ± 2.0% of the liver volume ($p = 0.007$), respectively.

Discussion

Previous studies evaluated the dosimetric differences between BT and SBRT using clinically applied SBRT plans that were replanned for BT treatment using virtual catheters placed into the lesion (8–10). Pennington *et al.* (10) evaluated the dosimetric differences of BT and SBRT using data sets of 10 consecutive patients with hepatic metastases. BT was virtually replanned using five fractions of 12 Gy to the PTV of SBRT plans. Unfortunately, detailed dose prescription details, as for example, the exact PTV-encompassing isodose of SBRT plans, were not reported. They showed that the mean PTV receiving 100% of the prescribed dose was similar for BT and SBRT (94.1% vs. 93.9% of PTV, $p = 0.8$). In contrast, the mean volume receiving 150% of the prescribed dose was significantly higher for virtual BT plans (63.6% vs. 0%), indicating significant dose escalation within the PTV with BT. The study also reported on the minimum dose to the PTV, which was significantly lower for BT plans (65.8%) compared with SBRT plans (87.4%, $p = 0.0002$). The authors concluded that with BT, a higher target dose in the PTV can be applied with similar doses to OARs but potentially with lower target coverage compared with SBRT (10). This approach was different from the present study. As known from published studies on BT for liver malignancies, the minimum peripheral dose is the main criterion correlating with local control rates (6, 17). Therefore, liver BT in clinical reality is usually optimized with special emphasis on the minimum dose to the PTV, which should exceed 15 Gy for primary hepatic lesions (7, 18), and 20–25 Gy in metastatic disease (17, 19), taking into account BT-specific dose inhomogeneity with a high dose close to the BT catheters, which are positioned within the GTV. This concept has recently been adopted for SBRT (20). Lately, the importance of mean dose to the GTV for tumor control and outcome was observed for robotic and intensity-modulated SBRT techniques and emphasize the use of a mean GTV dose optimized treatment planning (21–24). To date, there are still a great number of differences and uncertainties in the dose prescriptions of liver SBRT. Different dose prescription approaches may include considerable dose inhomogeneity within the PTV, and PTV-encompassing isodose lines may range from 60% to 90%, allowing for considerable differences in dose distributions and dose to the GTV (24). The present study was conducted before the introduction of the ICRU 91 (20) and SBRT was prescribed to the $D_{99.9}$. Therefore, BT dose distributions did not mimic heterogeneity of certain SBRT techniques, because in virtual SBRT planning of the present study, a homogeneous dose distribution was used, which avoided central dose escalation. The much larger PTVs for SBRT and the prescription to $D_{99.9}$ might have influenced the results for SBRT, resulting in reduced dose coverage. Furthermore, a single-fraction SBRT (25) has not been widely adopted in clinical practice, as three- or five-fraction regimens to total doses of ≥50 Gy achieve better local control rates of 89–100% at 2 years of follow-up (26). Therefore, these limitations

should be addressed in future studies, and additional dosimetric endpoints (e.g. mean dose, near-minimum dose) should be evaluated. Furthermore, conformity indices and gradient-related indices should be evaluated (27).

Moreover, in SBRT, breathing-related motion adjacent or within the treatment volume is frequently associated with uncertainties in dose delivery and target coverage. Usually, this is compensated for by means of 4D-imaging–based GTV margin enlargement to create an internal target volume, which may result in higher doses to critical OARs (e.g. bowel) and increased liver dose exposure. Regarding dose to OARs, the study of Pennington *et al.* (10) observed no differences in liver volume receiving 15 Gy in five fractions or more, with 278 cm^3 for BT compared with 256 cm^3 in SBRT, $p = 0.3$. In contrast, the present study observed a significant difference for the V5Gy liver exposure of the 20-Gy prescription dose group, which is mainly attributable to the doubling of the median PTV. The liver exposure was highly statistically different with 611 ± 43 cm^3 for BT as compared to 694 ± 37 cm^3 for SBRT plans ($p = 0.001$) corresponding to 41.8 ± 2.5 and 45.9 ± 2.0, respectively ($p = 0.007$).

To the best of our knowledge, this is the first report on the comparison of clinically treated liver brachytherapy treatments with virtually planned SBRT treatments. A precise prediction of the position of brachytherapy catheters is challenging because of several limitations, including respiratory motion. In fact, of the 10 analyzed patients by Pennington *et al.* (10), it was not possible to develop a feasible virtual BT plan for one patient because of anatomical reasons. This patient was excluded from the analysis. Therefore, we decided to compare clinically applied BT plans to virtually applied SBRT plans, as BT seems to include more unpredictable variables.

To date, no randomized clinical data comparing SBRT to other local treatment options as BT are available. Because BT of liver lesions is not widely used, large randomized trials seem unlikely. Nevertheless, we can report from our extensive experience with both methods. The pros and cons of each method include the limited number and maximum diameter of treatable liver lesion of 4–6 cm for SBRT. BT also allows for treatment of lesions beyond this size threshold, with single doses of 15–20 Gy and excellent local control rates (>90%) in large primary or secondary hepatic lesions of up to 12–15 cm (6, 7, 28). Moreover, in contrast to thermoablative treatment approaches, it provides an effective treatment option for large and centrally located liver lesions (29, 30). When compared with most SBRT techniques, BT is less affected by uncertainties related to respiratory breathing motion, as the tumor is fixed by the implanted catheters. Another advantage of BT is the possibility of a repetitive approach (31), with the application of BT using hypofractionated fractionation schedules with two or three fractions to spare OARs or treat very large tumors, even in elderly patients (32). Regarding adverse events in BT, significant bleedings after the interventional catheter implantation occurred in 4% in HCC and 2.5% in colorectal liver metastases (6, 7). And the risk for radiation-induced liver disease seems to be very low, even after the treatment of very large liver tumors in livers with underlying cirrhosis (6, 7, 11). However, the main advantage of SBRT remains its noninvasive treatment character.

In conclusion, taking into account the aforementioned limitations, this dosimetric comparison of BT to virtually planned SBRT showed a superior outcome of BT regarding the dose coverage of the target volume (PTV: $D_{99.9}$, D_{90}) and exposed liver volume (V5Gy). Nevertheless, further work is needed to determine ideal suitability for each treatment approach.

References

[1] Alongi F, Arcangeli S, Filippi AR, *et al*. Review and uses of stereotactic body radiation therapy for oligometastases. *Oncologist* 2012;17:1100–1107.

[2] Gerum S, Heinz C, Belka C, *et al*. Stereotactic body radiation therapy (SBRT) in patients with hepatocellular carcinoma and oligometastatic liver disease. *Radiat Oncol* 2018;13:1–9.

[3] Wang PM, Chung NN, Hsu WC, *et al*. Stereotactic body radiation therapy in hepatocellular carcinoma: Optimal treatment strategies based on liver segmentation and functional hepatic reserve. *Rep Pract Oncol Radiother* 2015;20:417–424.

[4] Van Cutsem E, Cervantes A, Adam R, *et al*. ESMO consensus guidelines for the management of patients with metastatic colorectal cancer. *Ann Oncol* 2016;27:1386–1422.

[5] Vogel A, Cervantes A, Chau I, *et al*. Hepatocellular carcinoma: ESMO Clinical Practice Guidelines for diagnosis, treatment and follow-up. *Ann Oncol* 2018;29:iv238–iv255.

[6] Ricke J, Mohnike K, Pech M, *et al*. Local response and impact on survival after local ablation of liver metastases from colorectal carcinoma by computed tomography–guided high-dose-rate brachytherapy. *Int J Radiat Oncol* 2010;78:479–485.

[7] Mohnike K, Wieners G, Schwartz F, *et al*. Computed tomography–guided high-dose-rate brachytherapy in hepatocellular carcinoma: Safety, efficacy, and effect on survival. *Int J Radiat Oncol* 2010;78:172–179.

[8] Kamrava M, Loh C, Banerjee R, *et al*. Dosimetric comparison of image-guided high-dose-rate interstitial liver brachytherapy vs liver stereotactic body radiation therapy. *Brachytherapy* 2013;12:S18.

[9] Hrycushko BA, Meyer J, Sutphin P, *et al*. Dosimetric and economic comparison of interstitial high-dose-rate brachytherapy to stereotactic body radiation therapy for liver lesions. *Brachytherapy* 2013;14:S101.

[10] Pennington JD, Park SJ, Abgaryan N, *et al*. UCLA Authors Dosimetric comparison of brachyablation and stereotactic ablative body radiotherapy in the treatment of liver metastasis. *Brachytherapy* 2015;14:537–542.

[11] Hass P. Extending the frontiers beyond thermal ablation by radiofrequency Ablation: SBRT. *Brachytherapy* 2014;30:245–252.

[12] Bretschneider T, Ricke J, Gebauer B, *et al*. Image-guided high-dose-rate brachytherapy of malignancies in various inner organs-technique, indications, and perspectives. *J Contemp Brachytherapy* 2016;8:251–261.

[13] Streitparth F, Pech M, Bohmig M, *et al*. In vivo assessment of the gastric mucosal tolerance dose after single fraction, small volume irradiation of liver malignancies by computed tomography-guided, high-dose-rate brachytherapy. *Int J Radiat Oncol Biol Phys* 2006;65:1479–1486.

[14] Heinz C, Gerum S, Freislederer P, *et al*. Feasibility study on image guided patient positioning for stereotactic body radiation therapy of liver malignancies guided by liver motion. *Radiat Oncol* 2016;11:1−7.

[15] Heinz C, Reiner M, Belka C, *et al*. Technical evaluation of different respiratory monitoring systems used for 4D CT acquisition under free breathing. *J Appl Clin Med Phys* 2015;16:334−349.

[16] Goodman KA, Kavanagh BD. Stereotactic body radiotherapy for liver metastases. *Semin Radiat Oncol* 2017;27:240−246.

[17] Wieners G, Mohnike K, Peters N, *et al*. Treatment of hepatic metastases of breast cancer with CT-guided interstitial brachytherapy - a phase II-study. *Radiother Oncol* 2011;100:314−319.

[18] Mohnike K, Steffen IG, Seidensticker M, *et al*. Radioablation by image-guided (HDR) brachytherapy and transarterial chemoembolization in hepatocellular carcinoma: A Randomized phase II trial. *Cardiovasc Intervent Radiol* 2019;42:239−249.

[19] Omari J, Heinze C, Damm R, *et al*. Radioablation of hepatic metastases from renal cell carcinoma with image-guided interstitial brachytherapy. *Anticancer Res* 2019;39:2501−2508.

[20] Wilke L, Andratschke N, Blanck O, *et al*. ICRU report 91 on prescribing, recording, and reporting of stereotactic treatments with small photon beams: Statement from the DEGRO/DGMP working group stereotactic radiotherapy and radiosurgery. *Strahlenther Onkol* 2019;195:193−198.

[21] Andratschke N, Parys A, Stadtfeld S, *et al*. Clinical results of mean GTV dose optimized robotic guided SBRT for liver metastases. *Radiat Oncol* 2016;11:74.

[22] Zhao L, Zhou S, Balter P, *et al*. Planning target volume D95 and mean dose should be considered for optimal local control for stereotactic ablative radiation therapy. *Int J Radiat Oncol Biol Phys* 2016;95:1226−1235.

[23] Stera S, Balermpas P, Chan MKH, *et al*. Breathing-motion-compensated robotic guided stereotactic body radiation therapy: Patterns of failure analysis. *Strahlenther Onkol* 2018;194:143−155.

[24] Baumann R, Chan MKH, Pyschny F, *et al*. Clinical results of mean GTV dose optimized robotic-guided stereotactic body radiation therapy for lung tumors. *Front Oncol* 2018;8:171.

[25] Herfarth KK, Debus J, Lohr F, *et al*. Stereotactic single-dose radiation therapy of liver tumors: Results of a phase I/II trial. *J Clin Oncol* 2001;19:164−170.

[26] Rusthoven CG, Schefter TE. Rationale for ablation of oligometastatic disease and the role of stereotactic body radiation therapy for hepatic metastases. *Hepat Oncol* 2014;1:81−94.

[27] Milickovic N, Tselis N, Karagiannis E, *et al*. Iridium-Knife: Another knife in radiation oncology. *Brachytherapy* 2017;16:884−892.

[28] Collettini F, Schnapauff D, Poellinger A, *et al*. Hepatocellular carcinoma: computed-tomography-guided high-dose-rate brachytherapy (CT-HDRBT) ablation of large (5-7 cm) and very large (>7 cm) tumours. *Eur Radiol* 2012;22:1101−1109.

[29] Tselis N, Chatzikonstantinou G, Kolotas C, *et al*. Computed tomography-guided interstitial high dose rate brachytherapy for centrally located liver tumours: A single institution study. *Eur Radiol* 2013;23:2264−2270.

[30] Powerski M, Penzlin S, Hass P, *et al*. Biliary duct stenosis after image-guided high-dose-rate interstitial brachytherapy of central and hilar liver tumors: A systematic analysis of 102 cases. *Strahlenther Onkol* 2019;195:265−273.

[31] Gkika E, Strouthos I, Kirste S, *et al*. Repeated SBRT for in- and out-of-field recurrences in the liver. *Strahlenther Onkol* 2019;195:246−253.

[32] Seidensticker R, Damm R, Enge J, *et al*. Local ablation or radioembolization of colorectal cancer metastases: Comorbidities or older age do not affect overall survival. *BMC Cancer* 2018;18:882.

Strahlenther Onkol (2017) 193:612–619
DOI 10.1007/s00066-017-1120-2

ORIGINAL ARTICLE

Radioablation of adrenal gland malignomas with interstitial high-dose-rate brachytherapy

Efficacy and outcome

K. Mohnike[1,7] · K. Neumann[1] · P. Hass[2] · M. Seidensticker[1] · R. Seidensticker[1] · M. Pech[1] · S. Klose[3] · T. Streitparth[1] · B. Garlipp[4] · C. Benckert[4] · J. J. Wendler[5] · U. B. Liehr[5] · M. Schostak[5] · D. Göppner[6] · G. Gademann[2] · J. Ricke[1]

Received: 31 August 2016 / Accepted: 3 March 2017 / Published online: 24 March 2017

Abstract
Purpose To assess the efficacy, safety, and outcome of image-guided high-dose-rate (HDR) brachytherapy in patients with adrenal gland metastases (AGM).
Materials and methods From January 2007 to April 2014, 37 patients (7 female, 30 male; mean age 66.8 years, range 41.5–82.5 years) with AGM from different primary tumors were treated with CT-guided HDR interstitial brachytherapy (iBT). Primary endpoint was local tumor control (LTC). Secondary endpoints were time to untreatable progression (TTUP), time to progression (TTP), overall survival (OS), and safety. In a secondary analysis, risk factors with an influence on survival were identified.
Results The median biological equivalent dose (BED) was 37.4 Gy. Mean LTC after 12 months was 88%; after 24 months this was 74%. According to CTCAE criteria, one grade 3 adverse event occurred. Median OS after first diagnosis of AGM was 18.3 months. Median OS, TTUP, and TTP after iBT treatment were 11.4, 6.6, and 3.5 months, respectively. Uni- and multivariate Cox regression analyses revealed significant influences of synchronous disease, tumor diameter, and the total number of lesions on OS or TTUP or both.
Conclusion Image-guided HDR-iBT is safe and effective. Treatment- and primary tumor-independent features influenced survival of patients with AGM after HDR-iBR treatment.

Keywords Neoplasm metastases · Radiotherapy · Survival · Safety · Computed tomography

Radioablation von Nebennierenmalignomen mit interstitieller High-dose-rate-Brachytherapie

Wirkung und Outcome

Zusammenfassung
Zielsetzung Beurteilung der Effektivität, Sicherheit und Ergebnisse nach bildgeführter High-dose-rate-(HDR-)Brachytherapie bei Patienten mit Nebennierenmetastasen.
Material und Methoden Von Januar 2007 bis April 2014 wurden 37 Patienten (7 weiblich, 30 männlich; mittleres

✉ K. Mohnike
konrad.mohnike@berlin-dtz.de

1 Klinik für Radiologie und Nuklearmedizin, Universitätsklinikum Magdeburg A.ö.R., Otto-von-Guericke-Universität, Leipziger Straße 44, 39120 Magdeburg, Germany

2 Klinik für Strahlentherapie, Universitätsklinikum Magdeburg A.ö.R., Otto-von-Guericke-Universität, Leipziger Straße 44, 39120 Magdeburg, Germany

3 Klinik für Nieren- und Hochdruckkrankheiten, Diabetologie und Endokrinologie, Universitätsklinikum Magdeburg A.ö.R., Otto-von-Guericke-Universität, Leipziger Straße 44, 39120 Magdeburg, Germany

4 Klinik für Allgemein-, Viszeral- und Gefäßchirurgie, Universitätsklinikum Magdeburg A.ö.R., Otto-von-Guericke-Universität, Leipziger Straße 44, 39120 Magdeburg, Germany

5 Klinik für Urologie und Kinderurologie, Universitätsklinikum Magdeburg A.ö.R., Otto-von-Guericke-Universität, Leipziger Straße 44, 39120 Magdeburg, Germany

6 Klinik für Dermatologie, Universitätsklinikum Magdeburg A.ö.R., Otto-von-Guericke-Universität, Leipziger Straße 44, 39120 Magdeburg, Germany

7 DTZ am Frankfurter Tor, Kadiner Str.23, 10243 Berlin, Germany

Alter 66,8 Jahre, Spanne 41,5–82,5 Jahre) mit Nebennierenmetastasen verschiedener Primarien mit CT-gesteuerter interstitieller HDR-Brachytherapie (iBT) behandelt. Der primäre Endpunkt war die lokale Tumorkontrolle (LTC). Sekundäre Endpunkte umfassten die Zeit bis zum nicht mehr behandelbaren Progress (TTUP), die Zeit bis zum Progress (TTP), das Gesamtüberleben (OS) und die Sicherheit der Methode. In einer sekundären Analyse wurden Risikofaktoren ermittelt, die Einfluss auf das Überleben hatten.

Ergebnisse Die mediane biologische Äquivalenzdosis (BED) lag bei 37,4 Gy. Die mittlere LTC betrug nach 12 Monaten 88 % und nach 24 Monaten 74 %. Nach CTCAE-Kriterien trat ein Grad-3-Event auf. Das mediane OS nach Erstdiagnose der Nebennierenmetastasen ergab 18,3 Monate. Das mediane OS, TTUP und TTP nach CT-gesteuerter iBT betrug jeweils 11,4, 6,6 und 3,5 Monate. Uni- und multivariate Cox-Regressionsanalysen zeigten einen signifikanten Einfluss synchroner Nebennierenmetastasen, des Tumordurchmessers und der Gesamtanzahl neoplastischer Läsionen auf OS und/oder TTUP.

Schlussfolgerung Die bildgeführte HDR-iBT von Nebennierenmetastasen ist sicher und effektiv. Behandlungs- und primariusunabhängige Kofaktoren beeinflussten das Überleben von Patienten mit Nebennierenmetastasen nach der Behandlung mit HDR-iBR.

Schlüsselwörter Neoplasie, Metastasen · Radiotherapie · Überleben · Sicherheit · Computertomographie

Oligometastatic disease has been defined as a transitional state between localized and widespread systemic disease; thus, local control of oligometastases may yield improved systemic control or even cure [1, 2]. Almost all solid cancers have the potential to spread into the adrenal glands and up to 27% of metastasized malignancies eventually do so [3, 4]. However, little is known about the features of the oligometastatic state of disease in these patients. Although there is no precise definition of the oligometastatic state, most studies define "oligometastasis" as the presence of up to three or up to five metastatic lesions. Some authors have stated that the presence of adrenal metastases might be linked to poorer survival compared to other locations [5]. However, in isolated adrenal metastases, surgical cohort studies—not only from the recent past—have revealed long-term survival [6], raising the acceptance of local treatment in these patients.

For patients who are unfit for general anesthesia or have contraindications to surgery, stereotactic body radiotherapy (SBRT) seems to have the potential to provide benefit. A series of cohort studies have been published in recent years [7–11]. On thermal ablation, relatively few papers have been published [12–18]. However, evidence is scarce and heterogeneous for all local treatments, and a recent review revealed only 45 relevant studies from 1990 until 2012, with a total of 818 patients treated surgically, 178 patients treated by SBRT, and 51 patients treated by thermal ablation [19].

High-dose-rate (HDR) interstitial brachytherapy (iBT) of parenchymal organs with an iridium-192 source inserted directly into the tumor through interventionally implanted catheters is a technique that was invented in the early 2000s, allowing application of high doses of radioactivity within a well-defined and tightly confined target area [20, 21]. Independent of lesion size and location, this technique has proven its effectiveness in various cancer types, including even very large metastatic and primary locations such as liver, lung, and lymph nodes [22–26].

To the best of the authors' knowledge, this is the first report on the use of iBT in adrenal gland metastases of different primaries, apart from two reports of two cases each, in 2006 and 2012 [27, 28].

Materials and methods

Patient population and eligibility criteria

Patient recruitment took place from January 2007 to April 2014. Principal inclusion criteria were an East Coast Oncology Group (ECOG) performance status of 0–2, a platelet count above 50,000, and a prothrombin time of at least 50%. No upper limit was placed upon tumor diameter. All tumors were rated unresectable by visceral surgeons.

All patients received a full clinical status evaluation before treatment, comprising physical examination, extensive laboratory assessments, whole-body computed tomography (CT), and magnetic resonance imaging (MRI) of the liver.

Study design, endpoints, and statistical methods

The prospective database of a major German cancer center (University of Magdeburg), including all consecutive patients treated with iBT for AGM over 7 years, was reviewed. In the primary analysis, the efficacy and safety of iBT in the treatment of AGM was assessed. Therefore, the endpoint of the primary analysis was local tumor control (LTC). Secondary endpoints were time to untreatable progression (TTUP), time to progression (TTP), overall survival (OS), and safety variables.

Clinical and imaging follow-up were repeated every 3 months. TTP and TTUP were assessed by applying the Response Evaluation Criteria In Solid Tumors (RECIST) criteria, version 1.1. OS was defined as the timespan from the date of first treatment to the date of death.

TTUP was defined as the timespan from the first treatment to:

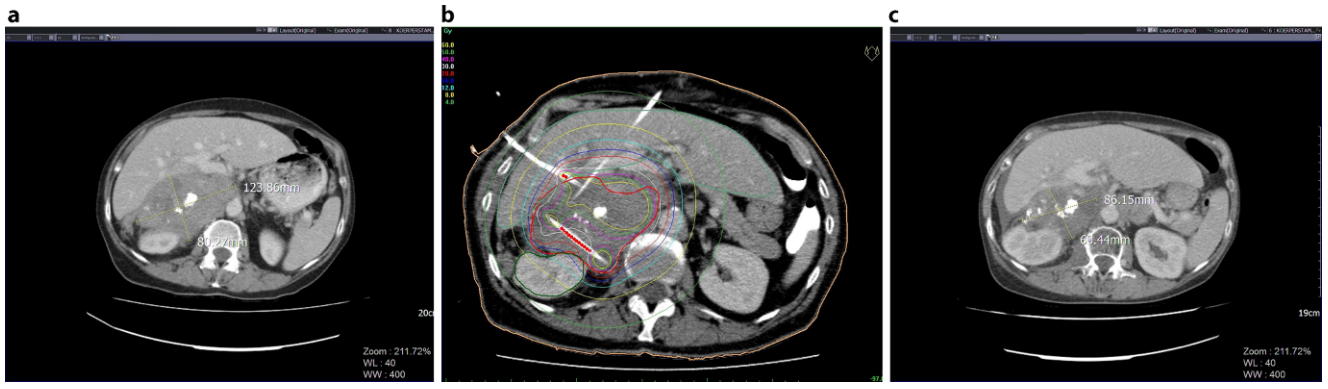

Fig. 1 63-year-old patient with cancer of unknown primary origin with hepatic metastases and a large adrenal gland metastasis (AGM). **a** Contrast-enhanced CT slice showing the large AGM. **b** Planning CT with indicated target volume (*red line*), catheters and isodose lines. **c** Contrast-enhanced CT-slice 11 months after interstitial brachytherapy showing partial remission

A. the time point at which diffuse systemic progression occurred with more than five new lesions or more than two new organ sites involved at follow-up imaging, precluding further local treatment,
   and/or
B. the time point at which a significant decrease in performance status (to ECOG 3 or higher) had to be recognized, precluding further treatment,
   or
C. the date of death, ultimately precluding further treatment.

In a Cox regression analysis, factors with an influence on survival were identified.

Toxicities were graded by the Common Terminology Criteria for Adverse Events (CTCAE), version 4.03. Grading was performed 3 days after treatment and every 3 months thereafter.

The program suite IBM SPSS Statistics 21.0 (IBM Corp. Armonk, NY, USA) was used for statistical analysis.

High-dose-rate interstitial brachytherapy

HDR-iBT is a radiation technique used in various locations *inside* the body, where a point source, e. g., iridium-192, is guided into the tumor through interventionally implanted catheters. The technique of CT-guided brachytherapy has been described in detail elsewhere [18, 19]. In this study, irradiation was performed by employing the HDR-iBT technique based on a 10 Ci iridium-192 source. Positioning of the brachytherapy catheters was achieved by fluoroscopy CT under a mild analgosedation, usually consisting of midazolam and fentanyl. After positioning the catheters, the ends were fixed at the skin by a suture. Hereafter, a three-dimensional (3D) contrast-enhanced CT dataset with a slice thickness of 3 mm was acquired and transferred to the treatment planning unit (Oncentra Brachy; Elekta/Nucletron B. V., Veenendaal, the Netherlands). The coordinates of the catheters in three dimensions and the tumor margin were determined on the basis of contrast-enhanced CT (Fig. 1).

The target dose was defined as the minimum dose taken up by the visible tumor margin. For treatment characteristics, see Table 1.

Results

A total of 37 patients (7 female, 30 male; mean age 66.8 years, range 41.5–82.52 years) with AGM from different primary tumors were treated by CT-guided HDR-iBT. While 8 (22%) of the patients presented with adrenal metastases only, 29 (78%) also had extraadrenal metastases. Systemic treatment was received by 6 of 37 patients after iBT (16%). For details of patient characteristics, see Table 1.

Within the cohort, 36 patients were treated for unilateral AGM and 1 was treated for bilateral AGM. Whereas 35 metastases were treated in a single treatment session, 3 required two sessions due to tumor size, with an interval of 2 weeks between the fractions. The median dose at the tumor margin was 15.5 Gy (95% confidence interval, 95% CI: 14.0–16.7; range 8.4–22.5 Gy), corresponding to a median biological equivalent dose (BED) of 37.4 Gy (range 15.5–73.0 Gy) assuming an α/β ratio of 10. The mean imaging follow-up time to assess LTC was 10.9 months; the follow-up time for OS was 12.1 months (range 8.6–15.6 months) on average. All patients ($N = 37$) were analyzed for OS and TTUP. Since 5 patients were lost to imaging follow-up, 32 patients (corresponding to 33 AGM procedures) were available for TTP and LTC.

Table 1 Patient and treatment characteristics

iBT patients, $N = 37$	Mean ± SD or *n* (%)
Age (years)	66.8 ± 9.9
Gender	
Male	30 (81)
Female	7 (18)
ECOG performance status	
0	3 (8)
1	13 (35)
2	21 (57)
Primary tumor entity	
Colorectal carcinoma	10 (27)
Lung cancer	7 (19)
Renal cell carcinoma	6 (16)
Hepatocellular carcinoma	5 (14)
Other origin[a]	9 (24)
Previous systemic treatment	28 (74)
First line (at least)	28 (74)
Second line (at least)	21 (18)
Third line (at least)	14 (38)
Previous surgical treatment	3 (8)
Treatment intention	
Ablation	34 (89)
Symptom relief	4 (11)
Concomitant cortisone treatment	3 (8)
Lesion diameter	5.4 ± 2.9
≤4 cm	18 (47)
>4 cm	20 (53)
Clinical target volume (cm^3)	100.7 ± 130.4
Dose (Gy)	15.4 ± 16.0
Biological equivalent dose (BED)	39.8 ± 16.0
Treatment-related toxicities (CTCAE)	12 (32)
Grade 1/2	11 (29)
Grade 3/4	1 (3)

iBT interstitial brachytherapy, *SD* standard deviation, *ECOG* East Coast Oncology Group, *CTCAE* Common Terminology Criteria for Adverse Events (version 4.03)
[a]Cancer of unknown primary, malignant melanoma, gastric cancer, esophageal cancer

Local tumor control and objective response

Mean LTC after 12 months was 88% and after 24 months this was 74%. In total, three local recurrences occurred after 6.5, 7.5, and 20.3 months. A univariate Cox regression analysis including BED, tumor diameter, and tumor volume failed to show a significant impact of any of these factors on LCT, but a tendency towards significance of BED (BED: $p = 0.080$, hazard ratio, HR = 0.769; tumor diameter $p = 0.776$, HR = 0.915; tumor volume $p = 0.750$, HR = 0.996) was revealed. The median BED for locally recurrent AGM was 27.4 Gy (standard deviation, SD, 4.5 Gy), while in the locally controlled AGM this was 39.7 Gy (SD = 15.7 Gy), with a trend towards a statistically significant difference ($p = 0.080$, χ^2 test). Best responses according to RECIST version 1.1 were complete response (CR) in 6 AGM cases, partial response (PR) in 25 AGM cases, and stable disease (SD) in 2 patients, corresponding to an objective response rate of 94% (of 33 AGM with imaging follow up).

Table 2 Univariate Cox regression for overall survival

Variable	Hazard ratio	95% CI	*p*-value*
Age (years)	1.004	0.962–1.0049	0.847
Gender (female)	0.635	0.264–1.525	0.309
Extraadrenal neoplastic disease	1.261	0.431–3.687	0.672
Diameter (cm)	1.163	1.038–1.301	**0.009**
Number of lesions	1.158	1.028–1.305	**0.016**
Interval to adrenal metastases	0.984	0.971–0.998	**0.022**
Multiple extraadrenal neoplastic sites	1.843	0.792–4.290	0.156
ECOG	1.397	0.739–2.639	0.303
Renal cell cancer	*n. a.*	*n. a.*	0.221
Cholangiocellular carcinoma	0.623	0.100–3.868	0.612
Colorectal cancer	0.493	0.211–1.151	0.102
Cancer of unknown primary	1.298	0.345–4.889	0.700
Esophageal cancer	2.033	0.325–12.721	0.448
Gastric cancer	1.698	0.448–6.445	0.436
Hepatocellular carcinoma	1.785	0.647–4.926	0.263
Lung cancer	0.884	0.343–2.277	0.799
Malign melanoma	2.728	0.706–10.544	0.146

n. a. not applicable, *ECOG* East Coast Oncology Group, *CI* confidence interval
p*-value of univariate Cox regression analysis, *p*-values <0.05 (bold** type) indicate statistical significance

Safety

Grade 1 or 2 toxicities occurred in 11 patients (29%), including pain, nausea, vomiting, and fatigue. One grade 3 event occurred (bleeding requiring angiographic embolization, 3%).

Ongoing cortisone substitution after treatment was required by 2 patients, while 1 patient required intermittent cortisone substitution for 1 month post treatment.

Table 3 Univariate Cox regression for time to untreatable progression

Variable	Hazard ratio	95% CI	*p*-value*
Age (years)	0.979	0.939–1.021	0.322
Gender (female)	0.848	0.537–1.341	0.482
Extraadrenal neoplastic disease	1.827	0.549–6.078	0.326
Diameter (cm)	1.201	1.055–1.367	**0.005**
Number of lesions	1.179	1.053–1.321	**0.004**
Interval to adrenal metastases	0.988	0.977–0.999	**0.030**
Multiple extraadrenal neoplastic sites	1.233	0.584–2.604	0.582
ECOG	1.238	0.675–2.272	0.491
Renal cell cancer	*n. a.*	*n. a.*	0.607
Cholangiocellular carcinoma	0.582	0.095–3.581	0.559
Colorectal cancer	0.751	0.348–1.618	0.464
Cancer of unknown primary	1.862	0.484–7.166	0.366
Esophageal cancer	1.535	0.250–9.423	0.644
Gastric cancer	1.572	0.416–5.947	0.505
Hepatocellular carcinoma	1.020	0.337–3.085	–
Lung cancer	0.836	0.334–2.094	0.702
Malign melanoma	2.010	0.528–7.651	0.306

n. a. not applicable, *ECOG* East Coast Oncology Group, *CI* confidence interval

p*-value from univariate Cox regression analysis; *p*-values <0.05 (bold** type) indicate statistical significance

Time to progression, time to untreatable progression, overall survival

Kaplan–Meyer estimates and multivariate analysis

Median OS from the first diagnosis of AGM was 18.3 months, with a survival rate of 80% after 12 months, 34% after 24 months, 20% after 36 months, and 13% after 60 months. Median OS, TTUP, and TTP after iBT treatment were 11.4, 6.6, and 3.5 months, respectively. A univariate analysis of cofactors for TTUP and OS indicated that only tumor diameter, the interval to occurrence of AGM, and the total number of lesions were factors contributing significantly to both endpoints; while this was not the case for age, number of extraadrenal neoplastic sites, or even the presence of multiple extraadrenal neoplastic sites, ECOG, patient's gender or primary tumor (see Table 2 and 3).

An additional multivariate Cox regression analysis of TTUP and OS with preexisting, primary independent covariates including tumor diameter, the total number of lesions, and the interval to the occurrence of AGM revealed a significant influence of the total number of lesions on TTUP and a tendency towards significance of the interval to the occurrence of AGM from diagnosis of the primary (see Table 4).

After subsequent subanalysis and under consideration of current evidence, cutoff values were defined for all three covariates :

1. synchronous disease (occurrence of AGM up to 6 months after diagnosis of the primary tumor);
2. longest diameter of AGM (a) up to 3.9 cm and (b) 4 cm and above;
3. total number of lesions (a) up to five or (b) more than five [29].

For these categorical covariates, the multivariate Cox regression revealed a significant influence on OS of synchronous disease and the dichotomized longest diameter of AGM, while there was a trend towards significance for the total number of lesions (Table 4).

The corresponding Kaplan–Meier estimates for OS were 16.2 and 3.8 months for metachronous and synchronous AGM ($p < 0.0001$, log-rank test), respectively, and 27.1 and 5.3 months for longest AGM diameter $\leq$3.9 and $\geq$4 cm ($p = 0.001$, log-rank test; Fig. 2), respectively.

Discussion

In AGM of different primaries, evidence is scarce for all local treatments, and a recent review revealed only 45 relevant studies from 1990 until 2012, with a total of 818 surgical patients, of whom 178 were treated by SBRT and 51 by thermal ablation [19]. The authors concluded that there is no evidence from randomized trials supporting the use of any adrenal metastasis-directed therapy, although, retrospectively, long-term survival has been achieved with both adrenalectomy and SBRT [19].

One question may arise: why was iBT used in the current study and not SBRT?

SBRT (like cranial stereotactic radiotherapy) permits precise irradiation. This enables the radiotherapist to lower the dose to adjacent risk structures or organs at risk (OAR) significantly compared to conventional 3D conformal radiotherapy, thus permitting ablative doses to the tumor. However, effective high doses go hand in hand with significant exposure of normal surrounding tissue. This results in relatively tight restrictions with respect to size, number of lesions, and location, and the balance between applying effective doses and safety concerns is sometimes difficult to find [10, 30]. Published data on the safety of abdominal SBRT describe grade 3 and 4 events in a wide range of up to 78 and 25%, respectively, including gastroduodenal ulcerations, hepatic toxicities, nausea/vomiting, esophagitis, and stenosis of the bile duct [31]. In a large study on iBT in liver neoplasms with 191 patients and 343 interventions,

Table 4 Multivariate Cox regression

Variable	TTUP			OS		
	Hazard ratio	95% CI	*p*-value*	Hazard ratio	95% CI	*p*-value*
A: Multivariate Cox regression for time to TTUP and OS, continuous variables						
Total number of lesions	1.143	1.012–1.291	**0.032**	1.111	0.972–1.270	0.122
Time from primary diagnosis to adrenal metastases	0.991	0.980–1.002	0.116	0.988	0.974–1.001	*0.072*
Max. diameter of AGM	1.123	0.977–1.291	0.104	1.069	0.942–1.212	0.301
B: Multivariate Cox regression for time to TTUP and OS, categorical variables						
Number of lesions >5 or ≤5	2.270	0.899–5.732	*0.083*	0.943	0.353–2.521	0.907
Synchronous disease	2.269	0.856–6.016	0.100	3.649	1.368–9.733	**0.010**
Max. diameter of AGM <4 or ≥4 cm	2.917	1.215–7.004	**0.017**	3.375	1.309–8.689	**0.012**

TTUP time to untreatable progression, *OS* overall survival, *CI* confidence interval
p*-value from univariate Cox regression analysis. **Bold type highlights $p < 0.05$, *italic* type $p < 0.1$

Table 5 Dose constraints for organs at risk

Organs at risk	α/β regarding late effects	1 fraction D_{1cc} (Gy)	BED D_{1cc} (Gy)	3 fractionsD_{1cc} (Gy)	BED (Gy)
Skin	3	9	36	4.7	36.19
Spinal cord	3	10	43	5.2	42.64
Stomach	4	14	63	7.3	61.86
Duodenum	4	14	63	7.3	61.86
Small intestine	4	18	99	9.7	99.66
Large intestine	3	18	126	9.8	125.44
Gall bladder	3	20	153	11	154
Organs at risk	α/β regarding late effects	1 fraction		3 fractions	
Liver	3	V_{5max}: 66%		V_{5max}: 40%	
Kidney	2	V_{20max}:32%			

BED biological equivalent dose, *D1cc* highest exposed ccm, V_{5max} Volume exposed to at least 5 Gy, V_{20max} Volume exposed to at least 20 Gy

the rate of major complications was below 5% (15/343) [32]. In the current study, the rate of grade 3 events was 3% (bleeding requiring intervention), and no grade 4 events occurred. There are some advantages of iBT compared to stereotactic radiotherapy, particularly in targets with a close proximity to OAR, such as the gastric or duodenal mucosa, the spinal cord, and others (Table 5). The technique allows delivery of ablative doses inside the target volume while saving adjacent structures from potentially harmful exposure due to favorable decay characteristics distant to the point source. It overcomes size limits and restrictions induced by tumor location.

In the present study, iBT was very effective, with local control rates of 88 and 74% after 12 and 24 months, respectively, with the number of local failures totaling 3/37. This can be compared to local control rates of 66 and 32% after 12 and 24 months, respectively, with a total of 13 local failures ($N = 34$) in the work of Scorcetti et al. [10].

From an oncological perspective, effectivity with respect to OS is of much more importance, and the impact on OS of any local treatment is far from having been answered. The cohorts described in the previous trials on surgery and SBRT were very inhomogeneous with respect to primary tumor and disease stage, and survival data can therefore hardly be compared. For example, the percentage of renal cell cancer in a given cohort must have an influence on survival, because of the well-known comparatively long OS of these patients compared with other cancers, particularly in an ipsilateral M1 situation with microscopic or small macroscopic disease. As a matter of fact, a patient group that is homogeneous in terms of cancer type and is of a statistically relevant size can hardly be achieved, even by tertiary cancer centers. Yet the question remains: what patients might benefit from local treatments including surgery, radiotherapy (SBRT and iBT), and thermal ablative techniques such as radiofrequency (RFA) or microwave ablation (MWA)?

The present analysis revealed an objective response rate of 82% for AGM of different primaries after HDR-iBR, with moderate to low toxicity.

In univariate analyses, neither tumor diameter nor volume influenced local recurrence-free survival, while the

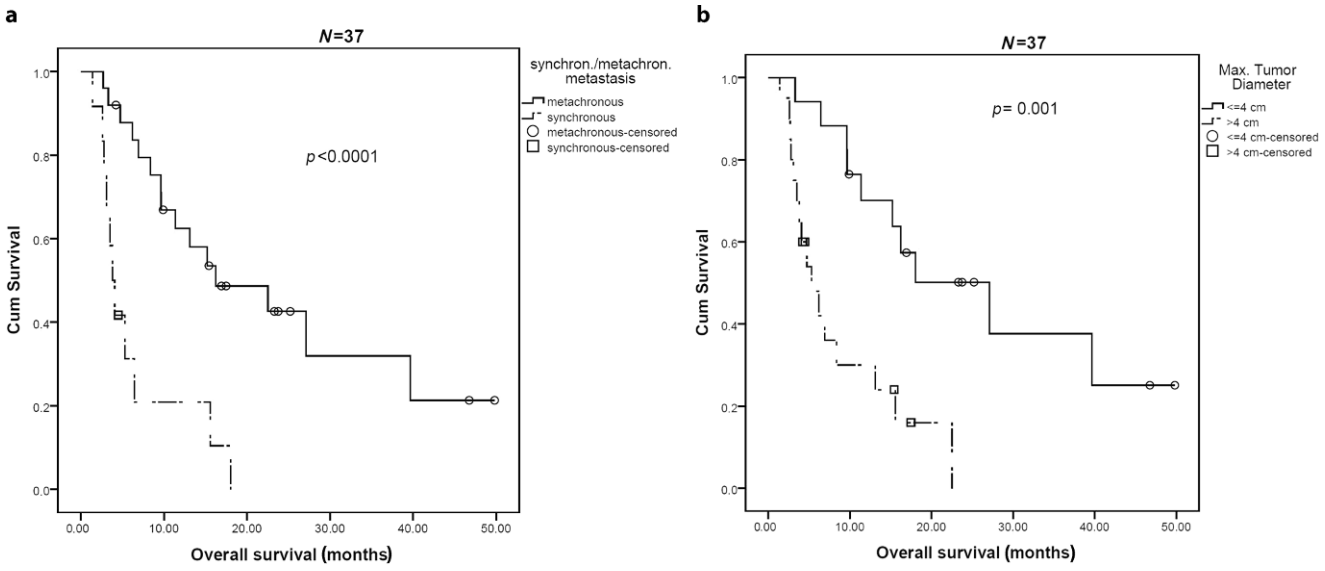

Fig. 2 Overall survival in synchronous versus metachronous disease (**a**) and in small (<4 cm) and larger (≥4 cm) adrenal gland metastases (**b**)

median BED showed a trend towards significance. However, OS—even after technically complete ablation—varied widely. Three variables existing pretreatment were found that significantly influenced OS, TTUP, or both in uni- and/or multivariate analyses: tumor size (in contrast to local-recurrence-free survival), synchronous disease, and the total number of lesions, while the type of primary tumor and other factors did not influence the outcome.

Finally, the present analysis indicates that treatment- and primary-independent features influenced the survival of patients with AGM after HDR-iBR, as also suggested in part by other authors [27, 33]. These characteristics will require confirmation in further studies, as a more detailed and accurate knowledge of these may be expected to contribute toward improving the comparability of different methods, which, in turn, will contribute to assessing the eligibility of patients for the various types of local treatment.

Conclusion

HDR-iBR is safe and effective. Treatment- and primary-tumor-independent features influenced the survival of patients with adrenal gland malignomas after HDR-iBR. These characteristics demand validation, as they could help to improve the comparability of different methods and selection of patients eligible for local treatments.

Funding This work was funded exclusively by the University of Magdeburg.

Compliance with ethical guidelines

Conflict of interest K. Mohnike, K. Neumann, P. Hass, M. Seidensticker, R. Seidensticker, M. Pech, S. Klose, T. Streitparth, B. Garlipp, C. Benckert, J.J. Wendler, U.B. Liehr, M. Schostak, D. Göppner, G. Gademann, and J. Ricke declare that they have no competing interests.

Ethical standards The study was conducted in accordance with the protocol and with the ethical principles that have their origin in the Declaration of Helsinki and ICH-GCP.

References

1. Hellman S, Weichselbaum RR (1995) Oligometastases. J Clin Oncol 13:8–10
2. Sterzing F, Brunner TB, Ernst I et al (2014) Stereotactic body radiotherapy for liver tumors: principles and practical guidelines of the DEGRO Working Group on Stereotactic Radiotherapy. Strahlenther Onkol 190:872–881
3. Glomset DA (1938) The incidence of metastasis of malignant tumors to the adrenals. Am J Cancer 32:57–61
4. Lenert JT, Barnett CC Jr., Kudelka AP et al (2001) Evaluation and surgical resection of adrenal masses in patients with a history of extra-adrenal malignancy. Surgery 130:1060–1067
5. Milano MT, Katz AW, Muhs AG et al (2008) A prospective pilot study of curative-intent stereotactic body radiation therapy in patients with 5 or fewer oligometastatic lesions. Cancer 112:650–658
6. Twomey P, Montgomery C, Clark O (1982) Successful treatment of adrenal metastases from large-cell carcinoma of the lung. JAMA 248:581–583
7. Ahmed KA, Barney BM, Macdonald OK et al (2013) Stereotactic body radiotherapy in the treatment of adrenal metastases. Am J Clin Oncol 36:509–513
8. Holy R, Piroth M, Pinkawa M, Eble MJ (2011) Stereotactic body radiation therapy (SBRT) for treatment of adrenal gland metastases from non-small cell lung cancer. Strahlenther Onkol 187:245–251

9. Rudra S, Malik R, Ranck MC et al (2013) Stereotactic body radiation therapy for curative treatment of adrenal metastases. Technol Cancer Res Treat 12:217–224
10. Scorsetti M, Alongi F, Filippi AR et al (2012) Long-term local control achieved after hypofractionated stereotactic body radiotherapy for adrenal gland metastases: a retrospective analysis of 34 patients. Acta Oncol (Madr) 51:618–623
11. Torok J, Wegner RE, Burton SA, Heron DE (2011) Stereotactic body radiation therapy for adrenal metastases: a retrospective review of a noninvasive therapeutic strategy. Future Oncol 7:145–151
12. Carrafiello G, Lagana D, Recaldini C et al (2008) Imaging-guided percutaneous radiofrequency ablation of adrenal metastases: preliminary results at a single institution with a single device. Cardiovasc Intervent Radiol 31:762–767
13. Haga H, Saito T, Okumoto K et al (2005) Successful percutaneous radiofrequency ablation of adrenal metastasis from hepatocellular carcinoma. J Gastroenterol 40:1075–1076
14. Kuehl H, Stattaus J, Forsting M, Antoch G (2008) Transhepatic CT-guided radiofrequency ablation of adrenal metastases from hepatocellular carcinoma. Cardiovasc Intervent Radiol 31:1210–1214
15. Lo WK, van Sonnenberg E, Shankar S et al (2006) Percutaneous CT-guided radiofrequency ablation of symptomatic bilateral adrenal metastases in a single session. J Vasc Interv Radiol 17:175–179
16. Wood BJ, Abraham J, Hvizda JL, Alexander HR, Fojo T (2003) Radiofrequency ablation of adrenal tumors and adrenocortical carcinoma metastases. Cancer 97:554–560
17. Yamakado K, Anai H, Takaki H et al (2009) Adrenal metastasis from hepatocellular carcinoma: radiofrequency ablation combined with adrenal arterial chemoembolization in six patients. Am J Roentgenol 192:W300–5
18. Wang Y, Liang P, Yu X, Cheng Z, Yu J, Dong J (2009) Ultrasound-guided percutaneous microwave ablation of adrenal metastasis: preliminary results. Int J Hyperthermia 25:455–461
19. Gunjur A, Duong C, Ball D, Siva S (2014) Surgical and ablative therapies for the management of adrenal 'oligometastases' – a systematic review. Cancer Treat Rev 40:838–846
20. Ricke J, Wust P, Wieners G et al (2004) Liver malignancies: CT-guided interstitial brachytherapy in patients with unfavorable lesions for thermal ablation. J Vasc Interv Radiol 15:1279–1286
21. Ricke J, Wust P, Wieners G et al (2005) CT-guided interstitial single-fraction brachytherapy of lung tumors: phase I results of a novel technique. Chest 127:2237–2242
22. Collettini F, Schippers AC, Schnapauff D et al (2013) Percutaneous ablation of lymph node metastases using CT-guided high-dose-rate brachytherapy. Br J Radiol 86:20130088
23. Mohnike K, Wieners G, Schwartz F et al (2010) Computed tomography-guided high-dose-rate brachytherapy in hepatocellular carcinoma: safety, efficacy, and effect on survival. Int J Radiat Oncol Biol Phys 78:172–179
24. Peters N, Wieners G, Pech M et al (2008) CT-guided interstitial brachytherapy of primary and secondary lung malignancies: results of a prospective phase II trial. Strahlenther Onkol 184:296–301
25. Ricke J, Mohnike K, Pech M et al (2010) Local response and impact on survival after local ablation of liver metastases from colorectal carcinoma by computed tomography-guided high-dose-rate brachytherapy. Int J Radiat Oncol Biol Phys 78:479–485
26. Collettini F, Schreiber N, Schnapauff D et al (2015) CT-guided high-dose-rate brachytherapy of unresectable hepatocellular carcinoma. Strahlenther Onkol 191:405–412
27. Kishi K, Tamura S, Mabuchi Y et al (2012) Percutaneous interstitial brachytherapy for adrenal metastasis: technical report. J Radiat Res 53:807–814
28. Wieners G, Pech M, Rudzinska M et al (2006) CT-guided interstitial brachytherapy in the local treatment of extrahepatic, extrapulmonary secondary malignancies. Eur Radiol 16:2586–2593
29. Lopez Guerra JL, Gomez D, Zhuang Y et al (2012) Prognostic impact of radiation therapy to the primary tumor in patients with non-small cell lung cancer and oligometastasis at diagnosis. Int J Radiat Oncol Biol Phys 84:e61–e67
30. Dawson LA (2011) Overview: where does radiation therapy fit in the spectrum of liver cancer local-regional therapies? Semin Radiat Oncol 21:241–246
31. Thomas TO, Hasan S, Small W Jr. et al (2014) The tolerance of gastrointestinal organs to stereotactic body radiation therapy: what do we know so far? J Gastrointest Oncol 5:236–246
32. Mohnike K, Wolf S, Damm R et al (2016) Radioablation of liver malignancies with interstitial high-dose-rate brachytherapy: complications and risk factors. Strahlenther Onkol 192:288–296
33. Oshiro Y, Takeda Y, Hirano S, Ito H, Aruga T (2011) Role of radiotherapy for local control of asymptomatic adrenal metastasis from lung cancer. Am J Clin Oncol 34:249–253